



PROGRAM OF TECHNICAL SESSIONS

FIFTIETH LUNAR AND PLANETARY SCIENCE CONFERENCE

MARCH 18–22, 2019

The Woodlands Waterway Marriott Hotel and Convention Center
The Woodlands, Texas

ABOUT LPSC

The Lunar and Planetary Science Conference brings together international specialists in petrology, geochemistry, geophysics, geology, and astronomy to present the latest results of research in planetary science. The four-and-a-half-day conference is organized by topical symposia and problem-oriented sessions.

LOGISTICAL INFORMATION

Venue Address and Phone Number

The conference is being held at The Woodlands Waterway Marriott Hotel and Convention Center, 1601 Lake Robbins Dr., The Woodlands TX 77380. LPSC conference staff can be reached by calling the hotel at 281-367-9797 and asking for the conference registration desk.

Please note that copy and printing services are not available at the conference registration desk, and must be arranged through the hotel business center. For your convenience, a minimal number of laptops with internet access and printers are available in Creekside Park.

Registration

The conference registration desk is open from 4:00 to 8:00 p.m. on Sunday and beginning at 8:00 a.m. each morning during the week (Monday through Friday). Conference badges provide access to all technical sessions, special events, and shuttle service.

Speaker-Ready Room/Presentation Check-In

Presentation validation is in the Alden Bridge Room. Those presenting on Monday morning should check in their presentations on Sunday evening when they register. Hours of Operation: Sunday, 4:00–8:00 p.m.; Monday through Thursday, 7:00 a.m. to 5:30 p.m.; Friday, 7:00 a.m. to noon.

Internet Access

Complimentary Wi-Fi service will be available throughout the conference venue.

Conference Shuttle Service

Conference shuttle service between the venue and the approved list of hotels is provided Sunday evening during the registration time and throughout the duration of the conference. Shuttle service will run before and immediately following all technical sessions. Detailed shuttle schedules are available in the registration area and on the LPSC website at <https://www.hou.usra.edu/meetings/lpsc2019/transportation/>. For onsite shuttle-related assistance contact Galveston Transportation at 409-744-5466 option #9. Galveston Transportation has a staffed table just outside the Town Center Exhibit Hall on the first floor.

Poster Printing Available

AlphaGraphics will have a staffed booth at The Woodlands Waterway Marriott, just outside the Town Center Exhibit Hall on the first floor. Poster presenters can pick up pre-ordered posters or place orders for posters beginning on Sunday, March 17. For more information, visit their website at www.txagprinting.com.

Personal Schedule

Create your own personal meeting schedule using the **Personal Schedule** tool found in the USRA Meeting Portal at https://www.hou.usra.edu/meeting_portal/schedule/. Select the sessions you want to attend or talks you want to hear, then create a shareable schedule that can be viewed on your smart phone or shared with a colleague.



INSTITUTIONAL SUPPORT

Lunar and Planetary Institute
Universities Space Research Association
National Aeronautics and Space Administration

CONFERENCE CO-CHAIRS

Louise Prockter, *USRA/Lunar and Planetary Institute*
Eileen Stansbery, *NASA Johnson Space Center*

PROGRAM COMMITTEE CHAIRS

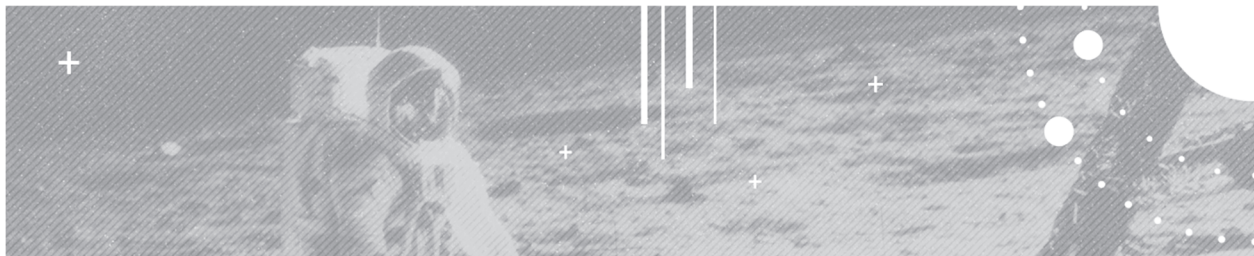
David Draper, *NASA Johnson Space Center*
Walter Kiefer, *USRA/Lunar and Planetary Institute*

PROGRAM COMMITTEE

Jessica Barnes, *ARES/NASA Johnson Space Center*
Erika Barth, *Southwest Research Institute*
Janice Bishop, *SETI Institute and NASA Ames*
Debra Buczkowski, *Johns Hopkins University Applied Physics Laboratory*
Paul Byrne, *North Carolina State University*
Nicholas Castle, *USRA/Lunar and Planetary Institute*
Roy Christoffersen, *Jacobs/NASA Johnson Space Center*
Ryan Ewing, *Texas A&M University*
Justin Filiberto, *USRA/Lunar and Planetary Institute*
Cyrene Goodrich, *USRA/Lunar and Planetary Institute*
Juliane Gross, *Rutgers University*
Sean Gulick, *University of Texas at Austin*
Jangmi Han, *USRA/Lunar and Planetary Institute*
Masatoshi Hirabayashi, *Auburn University*
Jonathan Kay, *USRA/Lunar and Planetary Institute*
Michelle Kirchoff, *Southwest Research Institute*
Steve Liu, *USRA/Lunar and Planetary Institute*
Alexander Morgan, *Smithsonian Institution*

Andrew Needham, *USRA/Science and Technology Institute*
Tabb Prissel, *USRA/Lunar and Planetary Institute*
Edgard Rivera-Valentín, *USRA/Lunar and Planetary Institute*
Katharine Robinson, *USRA/Lunar and Planetary Institute*
Paul Schenk, *USRA/Lunar and Planetary Institute*
Martin Schmieder, *USRA/Lunar and Planetary Institute*
Julia Semprich, *USRA/Lunar and Planetary Institute*
Andrew Shaner, *USRA/Lunar and Planetary Institute*
Elizabeth Silber, *Brown University*
Hannah Susorney, *University of British Columbia*
John Stansberry, *Space Telescope Science Institute*
Julie Stopar, *USRA/Lunar and Planetary Institute*
Driss Takir, *Jacobs/NASA Johnson Space Center*
Patrick Taylor, *USRA/Lunar and Planetary Institute*
Michelle Thompson, *Purdue University*
Allan Treiman, *USRA/Lunar and Planetary Institute*
Kathleen Vander Kaaden, *Jacobs/NASA Johnson Space Center*

Produced by the Lunar and Planetary Institute (LPI), 3600 Bay Area Boulevard, Houston TX 77058-1113, which is supported by NASA under Award No. NNX15AL12A. Logistics, administrative, and publications support for the conference were provided by USRA/LPI Meeting Planning Services.



LPSC WEEK AT A GLANCE

THE SESSION CODE APPEARS IN BOLD BRACKETS ABOVE EACH SESSION TITLE.

Day and Time	Waterway Ballroom 1	Waterway Ballroom 4	Waterway Ballroom 5	Waterway Ballroom 6	Montgomery Ballroom
Monday Morning, 8:30 a.m.	[M101] Lunar Basins, Impacts, and Regolith	[M102] Martian Crustal Column: Igneous, Metamorphic, and Hydrothermal Processes	[M103] Special Session: New Horizons at KBO 2014 MU69 (Ultima Thule)	[M104] Chondrites: Parent Body Processes	[M105] Titan: Releasing the Kraken
Monday Afternoon, 1:30 p.m.		[M150] Masursky Plenary Session			
Monday Afternoon, 2:30 p.m.	[M151] Lunar Polar Ices: Looking Over the Moon's Cold Shoulder	[M152] Special Session: Going Inside with InSight	[M153] Kuiper Belt Objects: From Pluto to Eris and Ultima Thule	[M154] Atmospheres Through the Solar System and Beyond	[M155] Habitability: Too Hot! Too Cold! Ah, Just Right!
Monday Evening, 5:30 p.m.		NASA Headquarters Briefing			
Tuesday Morning, 8:30 a.m.	[T201] Ice, Ice, Ice, followed at 10:15 a.m. by [T206] Lunar Impacts and Regolith Processes: New Exploration	[T202] Processes on Modern Mars	[T203] Special Session: OSIRIS-REx at Asteroid Bennu	[T204] Planetary Tectonics and Interior Dynamics	[T205] Mercury: Magnetism, Magma, and More
Tuesday Afternoon, 1:30 p.m.	[T251] Origin and Differentiation of the Moon	[T252] Martian Brines: Old Salts and New Views	[T253] Special Session: Hayabusa2 Unveiling Asteroid Ryugu	[T254] Ice Satellites: Dynamic Ice Shells followed at 3:15 p.m. by [T256] Planetary Aeolian Processes	[T255] Impacts: Target Earth I
Tuesday Evening, 6:00 p.m.	Town Center Exhibit Area Poster Session I				

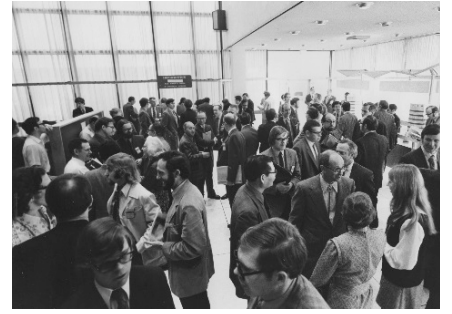
LPSC WEEK AT A GLANCE

THE SESSION CODE APPEARS IN BOLD BRACKETS ABOVE EACH SESSION TITLE.

Day and Time	Waterway Ballroom 1	Waterway Ballroom 4	Waterway Ballroom 5	Waterway Ballroom 6	Montgomery Ballroom
Wednesday Morning, 8:30 a.m.	[W401] Ryugu and Bennu: Diamond Asteroids are Forever <i>followed at 10:15 a.m. by [W406]</i> Chondrites: Organic Matter	[W402] Martian Aqueous Alteration: Tracing the Effects of Water Up Close and Far Away	[W403] Special Session: 50 Years of Lunar Science: The Legacy of "One Small Step"	[W404] Venus, or How I Stopped Worrying and Learned to Love the Second Planet	[W405] Space Weathering: From Samples to Spectra and Everything in Between
Wednesday Afternoon, 1:30 p.m.	[W451] Astrobiology: I Saw the Sign... of Life?	[W452] Water on Early Mars	[W453] Special Session: 50 Years of Planetary Science: "One Giant Leap for Mankind"	[W454] Ceres and Vesta	[W455] Chondrites: Refractory Components
Thursday Morning, 8:30 a.m.	[R501] New Lunar Science: A View from Apollo 50 Years Later	[R502] Martian Remote Sensing: Mineralogy, Morphology, and Chemistry	[R503] From Meteorites to Asteroids and Back Again!	[R504] Presolar, Interplanetary, and Cometary Dust	[R505] Impacts: Processes from Planetesimals to Planets
Thursday Afternoon, 1:30 p.m.	[R551] Lunar Petrology, Geochemistry, and Geochronology: from Surface to Interior	[R552] Martian Madness: Roving the Ridges <i>followed at 3:15 p.m. by [R556]</i> Martian Surface: Exposing Carbonates and Hydrothermal Alteration	[R553] Differentiation of Planets and Asteroids: From Cores to Late Veneers	[R554] Planetary Volcanism: A Song of Fire and Ice	[R555] Small Bodies: Observations from the Ground Up
Thursday Evening, 6:00 p.m.	Town Center Exhibit Area Poster Session II				
Friday Morning, 8:30 a.m.	[F701] Lunar Volcanism: Volcanic Features, Processes, and Magmatic Volatiles	[F702] Martian Polar Processes and Cryosphere	[F703] Impacts: Frontiers in Shock Metamorphism	[F704] Differentiated Meteorite Parent Asteroids and Their Provenance	[F705] Protoplanetary Disk Evolution and Chronology



**LUNAR AND PLANETARY
SCIENCE CONFERENCE**





AWARD WINNERS

2018 GSA Stephen E. Dworkin Award Winners

Graduate Oral

Xinting Yu, Johns Hopkins University

Where Does Titan Sand Come From: Insight from Mechanical Properties of Titan Organic Analogs

Honorable Mention – Graduate Oral

Erica Jawin, Brown University

Assessing the Volcanic History of the Prinz-Harbinger Region on the Moon Using Radar and Spectroscopy

Graduate Poster

Daniel Dunlap, Arizona State University

Pb-Pb Age of the Ungrouped Achondrite NWA 11119: Timing of Extraterrestrial Silica-Rich Volcanism

Honorable Mention – Graduate Poster

Ellen Leask, California Institute of Technology

New Possible CRISM Artifact at 2.1 Micrometers and Implications for Orbital Mineral Detections

Undergraduate Oral

Jordan Bretzfelder, University of Southern California

Divining the Lunar Mantle: Spectral Analysis of the Imbrium Basin

Honorable Mention – Undergraduate Oral

Aleksandra Gawronska, University of Notre Dame

Implications of Bimodal Olivine Compositions in VHK Basalts

Undergraduate Poster

Samuel Cartwright, Middlebury College

Geology of the Lunar Moscoviense Basin

Honorable Mention – Undergraduate Poster

Charlene Detelich, North Carolina State University

Investigating the Morphology of the Iapetus Equatorial Ridge

2019 Pierazzo International Student Travel Award Winner

Sammy Griffin, University of Glasgow

New Insights into the Magmatic and Shock History of the Naklite Meteorites from Electron Backscatter Diffraction

2019 LPI Career Development Award Winners

Enrica Bonato, Natural History Museum, United Kingdom

Frances Butcher, Open University, United Kingdom

Samuel Courville, Colorado School of Mines, United States

Ana Carolina De Souza Feliciano, Observatorio Nacional, Brazil

Ariel Deutsch, Brown University, United States

Houda El Kerni, University of Casablanca, Morocco

Al Emran, Auburn University, United States

Jordan Faltys, University of Alabama, United States

Keenan Golder, University of Tennessee-Knoxville, United States

Yuki Hibiya, University of Tokyo, Japan

Davitia James, Northern Colorado, United States

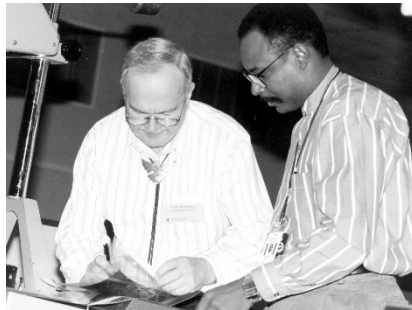
Laura Jenkins, Western University, Canada

Eleanor McIntosh, Scripps Institution for Oceanography, United States

Kaushik Mitra, Washington University, United States

Julia-Gabrielle Moreau, University of Helsinki, Finland

Kaitlyn Stacey, University of Texas, United States





LIST OF EXHIBITORS

Astrogeology Science Center, U.S. Geological Survey

<https://astrogeology.usgs.gov/>
2255 N. Gemini Drive
Flagstaff AZ 86001

The USGS Astrogeology Science Center serves the international planetary science community by (1) conducting innovative research that advances the fields of planetary spatial data infrastructure, geoscience, and remote sensing; (2) developing state-of-the-art software and techniques for the scientific and spatial analysis of planetary data; (3) producing accurate spatial data products, recognized internationally as benchmarks; (4) establishing data archive and mapping standards that foster international consistency; (5) archiving and distributing data and products for efficient access.

Cambridge University Press

<http://www.cambridge.org/academic>
1 Liberty Plaza, Floor 20
New York NY 10006

Cambridge University Press is a not-for-profit publisher that dates from 1534. We are part of the University of Cambridge and our mission is to unlock people's potential with the best learning and research solutions. Visit our stand to discuss publishing with us, browse our publications and get a 20% discount.

Centre for Planetary Science and Exploration (CPSX)

<http://cpsx.uwo.ca/>
1151 Richmond Street
London, Ontario N6A 3K7 Canada

The Centre for Planetary Science and Exploration (CPSX) at Western University is the leading organization for planetary science and exploration research and training in Canada. Our goal is to provide Canada and the global space program with the necessary expertise to design and support future planetary mission activities. Established in 2008, CPSX is home to the largest collection of graduate students and faculty in planetary science in the nation, with over 50 faculty and 30 graduate students from 11 different departments, and a growing number of alumni.

Exolith Lab

University of Central Florida
12354 Research Pkwy., Suite 211
Orlando FL 32826-2933

The Exolith Lab is a nonprofit extension of the Center for Lunar and Asteroid Surface Science (CLASS) at UCF, dedicated to regolith simulant production and applied research. Our high-fidelity mineral-based simulants allow users to address unique science questions, and serve as a testbed to mature technologies for future human exploration including *in situ* resource utilization.

GSA Planetary Geology Division

<https://community.geosociety.org/pgd/home>
1621 Cumberland Ave., Room 602
Knoxville TN 37917

Planetary Geology Division (PGD) of the Geological Society of America (GSA) was founded in May 1981, almost 100 years after the founding of GSA in 1888. We invite all interested persons to join the Planetary Geology Division of GSA as we provide a voice for planetary geoscience in the 21st century. At the Lunar and Planetary Science Conference, the PGD helps coordinate the Stephen E. Dworkin student presentation competition.

Jacobs

www.jacobs.com
2224 Bay Area Blvd.
Houston TX 77058

Jacobs is one of the world's largest and most diverse providers of technical, professional, and construction services, including all aspects of engineering and scientific services. With more than 65 years of experience supporting government and commercial clients across multiple markets and geographies, we have earned a reputation for excellence and outstanding technical and managerial achievements in quality, performance, and safety. Jacobs provides comprehensive planetary science research and analysis services for the NASA Johnson Space Center.

Johns Hopkins University Applied Physics Lab

<https://www.jhuapl.edu/>

11100 Johns Hopkins Rd.
Laurel MD 20723

The Space Exploration Sector of the Johns Hopkins Applied Physics Laboratory (APL) manages, builds, and operates NASA missions and conducts research on planetary, space physics, and Earth science. APL has built 70 spacecraft and nearly 300 instruments, including New Horizons, MESSENGER, Van Allen Probes, and Parker Solar Probe.

JMARS — Mars Space Flight Facility — Arizona State University

<https://jmars.mars.asu.edu/>

Arizona State University
P.O. Box 876305
Tempe AZ 85287-6305

JMARS (Java Mission-planning and Analysis for Remote Sensing) is a free, open-source, Java based geospatial information system developed by the Mars Space Flight Facility at Arizona State University. It is currently used for mission planning and scientific data analysis by several NASA missions, including Mars Odyssey, Mars Reconnaissance Orbiter, the Lunar Reconnaissance Orbiter, Dawn, and OSIRIS-REx.

Lockheed Martin Space — Deep Space Exploration

12257 S. Wadsworth Blvd.
Littleton CO 80125

Lockheed Martin Space designs, develops, manufactures, and operates spacecraft and systems in support of our military, civilian, and commercial customers worldwide. Our products include GPSIII, SBIRS, AEHF, and MUOS spacecraft for our military customers, commercial communications spacecraft for various domestic and international customers, GOES weather satellites for NOAA, the Orion Spacecraft in support of NASA Human Exploration and in support of NASA Science Mission Directorate, the Maven, MRO, Odyssey, Juno, OSIRIS-REx, InSight, and Lucy spacecrafts/lander.

Lunar and Planetary Institute

<https://www.lpi.usra.edu/>

3600 Bay Area Blvd.
Houston TX 77058

The Lunar and Planetary Institute (LPI), managed by the Universities Space Research Association (USRA), has a rich intellectual heritage in lunar and planetary science and exploration in support of NASA. LPI's mission is to advance understanding of the solar system by providing exceptional science, service, and inspiration to the world. Come to LPI's booth and learn about exciting opportunities and invaluable resources for scientists, postdoctoral fellows, educators, and students.

LPI-JSC Center for Lunar Science and Exploration

<https://www.lpi.usra.edu/exploration/>

3600 Bay Area Blvd.
Houston TX 77058

The LPI-JSC Center for Lunar Science and Exploration is one of the founding members of the Solar System Exploration Research Virtual Institute (SSERVI). At LPSC, the Center will help faculty find classroom resources, advise university students about future training opportunities, and distribute educational and public outreach materials.

Lunar Reconnaissance Orbiter Camera SOC

PO Box 873603
Tempe AZ 85287-3603

The Lunar Reconnaissance Orbiter Camera SOC operates the LROC NAC and WAC camera onboard LRO.

MAPCIS Research

danielconnelly@comcast.net

4815 Covered Bridge Rd.
Millville NJ 08332

An organization dedicated to the research of the Massive Australian Precambrian-Cambrian Impact Structure, also known as MAPCIS.

NASA JSC Astromaterials Research and Exploration Science (ARES) Division

<https://ares.jsc.nasa.gov/>
2101 E NASA Pkwy.
Houston TX 77058

Astromaterials Research and Exploration Science performs the physical science research at Johnson Space Center (JSC) and serves as the JSC focus for support to the HQ Science Mission Directorate. We perform research in Earth, planetary, and space sciences and the curatorial responsibility for all NASA-held extraterrestrial samples. ARES scientists and engineers support human and robotic spaceflight programs with expertise in orbital debris modeling, analysis of micrometeoroid/orbital debris risks to spacecraft, image analysis, and Earth observations.

NASA's Lunar Reconnaissance Orbiter

<https://lunar.gsfc.nasa.gov/>
8800 Greenbelt Road, Code 690
Greenbelt MD 20771

In 2019, NASA's Lunar Reconnaissance Orbiter will celebrate 10 years in orbit around the Moon. Come celebrate the scientific accomplishments enabled by this long-lived lunar mission, a mission that has reshaped our understanding of Earth's nearest celestial neighbor, built on the legacy of Apollo, and is paving the way for future exploration of the Moon and beyond.

NASA Planetary Data System

<https://pds.nasa.gov>
NASA/GSFC, Code 690.1
Building 34 Rm. S164X
Greenbelt MD 20772

The Planetary Data System (PDS) is a long-term archive of digital data products returned from NASA's planetary missions, and from other kinds of data acquisitions, including laboratory experiments. The archive is actively managed by planetary scientists to help ensure its usefulness and usability by the planetary science community. Archive submissions are prepared by researchers under the guidance of PDS personnel. All products are peer-reviewed, well-documented, and easily accessible via a system of online catalogs.

NASA Postdoctoral Program (NPP)/USRA

7178 Columbia Gateway Drive
Columbia MD 21046

The NASA Postdoctoral Program (NPP) offers unique research opportunities to highly-talented U.S. and non-U.S. scientists to engage in ongoing NASA research projects at a NASA Center, NASA Headquarters, or at a NASA-affiliated research institute. The NPP supports NASA's goal to expand scientific understanding of Earth and the universe in which we live. NPP Fellows engage in NASA research in Earth science, planetary science, heliophysics, astrophysics, aeronautics and engineering, human exploration and operations, space bioscience, and astrobiology.

NASA Radioisotope Power Systems Program

<https://rps.nasa.gov/>
21000 Brookpark Rd.
Cleveland OH 44135

Powering the Exploration of the Solar System: Building on a 50-year legacy, NASA is investing in technologies to expand our understanding of the universe. Stop by our booth and explore with us!

NASA Solar System Exploration Research Virtual Institute (SSERVI)

<https://sservi.nasa.gov>
NASA Ames Research Center
Moffett Field CA 94035

NASA created the Solar System Exploration Research Virtual Institute (SSERVI) to address basic and applied scientific questions fundamental to understanding the Moon, near-Earth asteroids, the martian moons Phobos and Deimos, and the near-space environments of these target bodies. As a virtual institute, SSERVI funds investigators at a broad range of domestic institutions, bringing them together along with international partners via virtual technology to enable new scientific efforts.

OpenSpace, American Museum of Natural History

<https://www.openspaceproject.com/>

Central Park West at 79th St.

New York NY 10024-5192

OpenSpace is a NASA supported open-source interactive data visualization software aimed primarily toward planetarium display to present and demonstrate a range of space science topics. Planetary science and space mission visualization has been a central focus of development in OpenSpace. Archives of surface data across spatial scales are capable of being displayed simultaneously for context. Large-scale multi-channel display as well as single-screen graphics accelerated machines can run OpenSpace, sharing basic mouse navigation.

Orbit Beyond, Inc.

<https://www.orbitbeyond.com/>

100 Menlo Park, Ste. 550

Edison NJ 8837

OrbitBeyond is a cislunar transportation company and an awardee of the NASA CLPS contract, providing global customers with reliable, repeated, and affordable services to the lunar surface. Our expandable spacecraft platform enables us to build lunar transportation capacity at a scale and cost that cannot be matched. This dramatic cost reduction will create new markets for discovering and utilizing resources in space, making in-space economy accessible and sustainable in the near future.

PROTO Manufacturing

www.protoxrd.com

12350 Universal Dr.

Taylor MI 48180-4070

PROTO Manufacturing's product line includes powder, Laue, and stress diffractometers, X-ray tubes, and custom XRD systems. For more than 30 years PROTO has provided solutions for laboratory, factory, and field environments. Our AXRD Benchtop powder diffractometer provides a low-cost alternative that can meet the challenges of even the most demanding X-ray diffraction material investigation — including temperature and humidity. The larger AXRD-Theta-Theta and AXRD-LPD systems are also available to accommodate more-demanding investigations.

Purdue University

www.eaps.purdue.edu/

550 West Stadium Ave.

HAMP Bldg, Room 2169

West Lafayette IN 47907

Purdue's Department of Earth, Atmospheric, and Planetary Sciences (EAPS) is dedicated to the scientific study of physical, chemical, and dynamic processes that include a broad range of phenomena from tectonics to asteroid impacts to severe weather. Come learn about the outstanding opportunities awaiting students interested in our department.

Smithsonian Astrophysical Observatory ADS

ads.harvard.edu

60 Garden Street, MS 83

Cambridge MA 2138

With over 13 million bibliographic records, the NASA Astrophysics Data System (ADS) is the primary index of scholarly content in Astronomy and Physics. During the meeting the ADS team will showcase the main features of its new search system and interface. Stop by to learn how to use the new ADS to search for people, papers, institutions, or topics and then use the system to generate visualizations showing collaborations or research subjects.

TRR 170

<https://www.trr170-lateaccretion.de/>

Malteserstrasse 74-100

Berlin 12249 Germany

Late Accretion Onto Terrestrial Planets (TRR 170) is a collaborative research center funded by the German Research Foundation. Our objective is to improve our current understanding of the late accretion history of Earth, its Moon, and other terrestrial planets. During the first funding phase, 15 research projects will provide new insights into timing, chemical budget, and geodynamic implications of late accretion. An integrated graduate program supports participating Ph.D. students. Funds for workshops and visitors are available.

VISIT
THE WOODLANDS
— T E X A S —

<https://visitthewoodlands.com/lpsc/>

*Welcome back to The Woodlands for the
50th Lunar and Planetary Science Conference!*

Whether you are coming from close by or from a country far away, our goal is to make this the best conference yet! The Woodlands offers numerous amenities – shopping and dining within walking distance; free trolley transportation along a 4.1-mile route connecting The Woodlands Mall, Market Street, The Woodlands Waterway, and Hughes Landing; and much more.

**WHILE YOU'RE HERE CHECK OUT OUR PARTICIPATING RESTAURANTS
TO RECEIVE 10%–20% OFF YOUR MEAL.
SHOW YOUR LPSC CONFERENCE BADGE TO QUALIFY!**

Visit The Woodlands is happy to partner once again with the Lunar and Planetary Institute in co-sponsoring the LPSC shuttles and catering.



The Universities Space Research Association (USRA) mission is to advance the space- and aeronautics-related sciences exploration through innovative research, technology, and education programs; promote space and aeronautics policy; and develop and operate premier facilities and programs by involving universities, governments, and the private sector for the benefit of humanity.

<https://www.usra.edu/>

USRA is pleased to co-sponsor LPSC catering and conference materials.

USRA has a storied heritage that traces back to the formation of the Lunar Science Institute by the National Academy of Sciences in 1968 at the height of the Apollo program.

USRA was founded in 1969, near the beginning of the Space Age, driven by the vision of two individuals, James Webb (NASA Administrator 1961-1968) and Frederick Seitz (National Academy of Sciences President 1962-1969). They recognized that the technical challenges of the exploration of space would require an ongoing and strong collaboration between NASA and the university research community. Together, they worked to create USRA to strengthen NASA's knowledge base as new areas of space research and technology were developed, and also to make it easier for university faculty and students to work with NASA to achieve mission objectives.



At the Manned Spacecraft Center in Houston, President Lyndon B. Johnson announces the establishment of the Lunar Science Institute, to be operated by the Rice Institute and the National Academy of Science.

USRA is dedicated to providing a networking forum for planetary scientists from across the globe.

Personal Recollections of the Lunar and Planetary Science Conference ***Pete Schultz, Brown University***

The first Lunar Science Conference in January 1970 was actually called the Apollo 11 Lunar Science Conference, at which more than 140 Principal Investigators (PIs) were asked to present the first results about the returned lunar samples in the Albert Thomas Convention and Exhibit Center in downtown Houston. Two of my thesis advisors (first J. Hoover Mackin and later Bill Muehlberger) at the University of Texas at Austin (UT Austin) were members of the Apollo Science Team. Even though Muehlberger would be the geology co-PI for the Apollo 16 and 17 missions, he couldn't get me into the first meeting since tickets were restricted to PIs and invited guests, not graduate students. But I was able to slip in through a "back door"; the mother of a friend at UT Austin (geology student Ruth Fruland) happened to work in the Public Affairs Office at the Manned Spacecraft Center (now the Johnson Space Center) and gave me the equivalent of a Willy Wonka Golden Ticket so I could attend the very first Lunar Science Conference. The conference also included a banquet at the Grand Ballroom of the historic Rice Hotel in downtown Houston. (Interestingly, in 1962 NASA's Astronaut Group 2 held its first meeting inside that same hotel to plan the next decade of space travel. Among that group was Neil Armstrong, Jim Lovell, and Pete Conrad.)



Swag from the Apollo 11 Lunar Science Conference. There was no official abstract volume handed out at the meeting, but PIs were encouraged to bring copies of one- or two-page abstracts to the meeting. Those were later collected and bound together with a cover. Credit: NASA.

I roomed with Muehlberger in downtown Houston (Mackin tragically passed away just one year before the landing). Filled with anticipation, I walked to the convention center from the hotel under one of those crisp January days with a deep blue sky. I had my camera with me, but thought it would be "unprofessional" if I took a bunch of photos, especially since I wasn't sure if I should be there anyway and wanted to maintain a low profile. Besides, I had loaded the camera with color film with a sensitivity that required time exposures in the meeting room. So, I took one photograph of the convention center from the outside and another of the registration desk inside. That was all.

The first Apollo results were presented in a single large room. All the big names were there. Some I had met at a Gordon Research Conference in 1968 or at Apollo team meetings (Don Gault, Mike Duke, Gene Shoemaker, Bill Quaide, Jim Head, and John Wood, to name just a few). But with my camera, I must have looked like a cub reporter. The first meeting naturally focused on sample analysis, but broad themes were already emerging, including Wood's lunar magma ocean model based on small light-colored particles (anorthosites) discovered in the lunar regolith at the Apollo 11 site. There were no formal abstracts at the first conference, but I picked up one- or two-page summaries that some speakers had left at the registration desk. Actually, NASA had issued a moratorium against publishing anything before the conference, in part because the journal *Science* would come out with the first results that same week.

The second conference in 1971 was again held downtown in January at the same venue. The moratorium against distributing results was lifted, and the first Lunar Science Conference abstract volume contained 241 contributions, a jump of 25% from the first year. Abstracts then ranged from a single long sentence to several pages (but without a table of contents or index), and revised abstracts were compiled with a pale yellow cover. This year also introduced the first Proceedings of the Lunar Science Conference, edited by the staff of the Lunar Science Institute later that year and published by MIT Press. In addition, 1971 was the year that Soviet scientists were invited to present their results from the Luna 16 automated sample return mission. I recall being really impressed by the tall, buffed Soviet "scientists" who accompanied A. P. Vinogradov in the meeting, not realizing that they must have been bodyguards (or perhaps KGB?).



The conference was moved to the Manned Spacecraft Center in 1972. Credit: NASA.

In 1972, the third Lunar Science Conference moved to the NASA Manned Spacecraft Center (MSC) in Clear Lake with sessions in Buildings 1, 17, and 30, and would remain at MSC for the next 30 years. [Note that the Space Center's name wouldn't be changed to NASA Johnson Science Center (JSC) until the following year.] The number of submissions had increased to 300 and remained relatively level for the next 5 years. The abstracts had generally expanded to two to three pages and were bound into two separate volumes with yellow covers (hence the references to the conference abstract volumes as the "Yellow Perils"). The fourth Lunar Science Conference in 1973 was again held in Clear Lake, with a "smoker" held in the Holiday Inn Ballroom up the street on NASA Road 1. [Editor's note: For you young whippersnappers, that's what cocktail hours were called back in the days when almost everyone smoked.]

The next year, the conference moved to the auditorium in Building 2 (later relabeled Building 1) and Rooms 104 and 206 of the Gilruth Center, which was actually a gym complex at the edge of the NASA JSC campus. In the first few years at the Gilruth Center, one of the gyms remained open during the conference, and you could actually hear basketballs bouncing during the science talks upstairs. The wooded setting of the Gilruth Center lent itself to casual discussions on picnic benches outside. Eventually, the Gilruth Center was essentially closed to athletic activities during the week of the conference, and all sessions were held there in two large halls (converted gyms) on the ground floor and three small rooms above (eventually four).

By then, the “smoker” had moved to the Nassau Bay Hotel (fondly called the “Nausea” Bay by some), which played an important role for many during the Apollo years. This is where Walter Cronkite gave his on-the-scene black-and-white television reports about the Apollo landings from the top floor, overlooking NASA JSC across the street. One of the most famous (or infamous) social scenes was the “Boom-Boom Room” in the back. This is the place where the Apollo astronauts (and lunar scientists!) let off steam during and after the Apollo missions. Some rooms in the hotel were carpeted from floor to ceiling and even had a glass-enclosed sitting pool. Such great history.



A conference attendee chats with Pamela (Jones) Solomon at the registration desk in 1977. Credit: NASA/Lunar and Planetary Institute.

During the late 1960s and early 1970s, the Lunar Science Conference was not the only “planetary” themed conference. In 1968, my primary thesis advisor (Harlan J. Smith) hosted the first meeting of the Division of Planetary Sciences of the American Astronomical Society (DPS) in Austin. I volunteered to be one of the slide-projector operators. However, the DPS meeting focused on planetary atmospheres, dynamics, solar system evolution, and spectrophotometry. I recall one talk that speculated about the surface of Mars. Although Mariner 4 images had captured a few images in 1965, they revealed only craters. One of the attendees (who shall remain nameless) stood up and proclaimed that this was not the conference at which to be talking about surfaces of planets. As a geologist, I thought this was a crushing comment! Conversely, there would be very few planetary astronomy talks at the early Lunar Science Conference, except those about multispectral imaging or photometry of the Moon. Even after the successful planetary missions (Mariner 6, 7, 9, and 10), the first six Lunar Science Conferences included few abstracts about planetary surfaces beyond the Moon, except a half dozen (each year) that placed the Moon in a broader context, such as lunar formation and solar system evolution.

This school of thought reflected three very distinct disciplines (and funding sources) of an emerging new research area: lunar geology, planetary astronomy, and planetary geology. Apollo funding covered the study of lunar geology, while traditional funding for planetary astronomy had a long history (e.g., atmospheres, dynamics, interiors). Funding for planetary geology, however, rode on the coattails of the manned mission program to the Moon, enabling the much cheaper Mariner missions (4, 6, 7, 9, 10). Even the Viking mission, which replaced a much more ambitious Voyager mission, was approved by Congress in 1968 at the peak of Apollo funding. Where were the conferences related to planetary surfaces beyond the Moon?



Tom McGetchin, conference co-chair (and Lunar Science Institute Director), is interviewed by the press during the 1977 conference. Credit: NASA/Lunar and Planetary Institute.

In 1969, one of my other advisors in geology (geochemist F. Earl Ingerson, known as “Dr. I” by his students) asked if I wanted to look at recently released images from Mariner 6 and 7 to Mars. At that time, NASA Headquarters was soliciting broader participation in planetary geology through small grants. Of course, I said yes. The astronomer Gerard de Vaucouleurs (of UT Austin’s astronomy department) had written books about Mars in the 1940s and published detailed observations. NASA funded him to compile the best photometric map of Mars based on the telescopic observations and photographs. I was asked to help but wanted to see actual features. Even the highest telescopic resolution revealed only irregular smudges and Mariner 4 did little to change this perception, other than to reveal a few craters on the surface, similar to the Moon. The first published reports about Mariner 6 and 7 seemed to support this conclusion, but others interpreted linear features as fault or joint systems. Using cross-correlations among images, I found these “faults” to be artifacts, coherent noise introduced during processing. Left over, however, were sinuous lines that I interpreted as narrow river-like valleys, broken-up terrains, and even portions of Valles Marineris (before seeing any Mariner 9 images). Dr. I asked if I would give a talk about my results at a PI meeting in Flagstaff, Arizona (my first professional talk). This 1969 meeting was the precursor to the Planetary Geology Principal Investigator’s (PGPI) conferences, which paralleled the Lunar Science Conference.

From the very beginning, then, I had my foot in all three “tribes” and enjoyed the very different perspectives and approaches, all the while observing science politics (and trying to stay out of them). This personal diversion is key for understanding and appreciating the later evolution of the Lunar Science Conference in the 1970s.

Apollo 17 would become the last human landing on the Moon at the end of 1972. Two upcoming landings were canceled; NASA’s budget was cut; and some funds were redirected toward international

cooperative programs, such as SkyLab (and later the Shuttle Program). It became apparent that new samples would not be coming back from the Moon, and there was a major shift in research emphasis that would transform future Lunar Science Conferences. Moreover, the Apollo program had ended in 1975, and some thought that lunar science should end as well. NASA Centers were told to identify their own role and mission (and avoid overlap). For example, the Planetary Geology Branch at NASA Ames was dissolved, and the Astrogeology Division at the U.S. Geological Survey redirected all its efforts to the upcoming Viking mission. I just happened to be on a train ride from San Jose to the Jet Propulsion Laboratory (NASA HQ asked me to select images for a planned Mercury Atlas) and was surprised to find acquaintances from Astrogeology at Menlo Park going to Flagstaff. They knew that this was more than a train ride: It represented the end of a 20-year journey of studying the Moon. In Flagstaff, they would be told to drop lunar research. I joined them for drinks in the upstairs glass-domed club on a gloomy ride before getting off the train in Pasadena.



Mike Duke, John Dietrich, Bill Quaide, and Doug Blanchard bravely volunteer as chili cook-off judges during the 1991 conference. Meeting organizer Pamela (Jones) Solomon is shown in the background on the right. Credit: Lunar and Planetary Institute.

NASA's funding shift resulted in a new emphasis on meteorites and terrestrial analog studies . . . along with new strategies to return samples from Mars. The outlook for a career in lunar science from 1973 through 1977, however, seemed grim. Yet the number of abstracts for the seventh and eighth Lunar Science Conferences (1976 and 1977) increased, along with just a few more dealing with objects other than the Moon. Lunar science was still holding on.



By the early 1990s, the three-volume LPSC abstract volumes, aka the "yellow perils," had grown so large that the LPI staff started putting them in boxes so attendees would be able to carry them. Credit: Lunar and Planetary Institute.

I moved from NASA Ames Research Center (as an NRC Post-Doc) to the Lunar Science Institute (now the Lunar and Planetary Institute) in Houston in 1976 (and ironically stayed in the Nassau Bay Hotel while waiting for our moving truck). That year, Robert (“Bob”) Pepin, then the Lunar Science Institute Director, initiated the Basaltic Volcanism Study Project (BVSP), which gathered a broad group of scientists to compare the nature, composition, and timing of volcanism on Earth, the Moon, Mercury, and Mars. This required a close look at lunar samples in a much broader planetary context. The next Lunar Science Institute Director (Tom McGetchin) in 1977 breathed life into the BVSP that stimulated new research at subsequent conferences.

In 1978, McGetchin formally changed the name of the Lunar Science Institute to the Lunar and Planetary Institute (LPI), and changed the name of the conference to the Lunar and Planetary Science Conference (LPSC). In addition, opportunities for post-Apollo research expanded through the Lunar Data Analysis and Synthesis Program (championed by Bill Quaide at NASA HQ), which was the first data analysis program at NASA and generated new funds for basic research starting in 1976. This new program contributed to a 26% jump in abstract submissions in 1978 (the ninth LPSC) from the previous year. While DPS and the PGPI meetings continued, LPSC was now the place to present the latest results and hypotheses about the compositions of the planets and the contrasting processes shaping their surfaces. Abstract submissions would remain between 445 and 490 for the next eight years.

For me, LPSC was about more than just giving and attending science presentations. My wife and I would regularly entertain as many as 15–20 visitors at our house for hors d’oeuvres. During one meeting, I arrived home a bit early to find my wife on top of the counter, scraping off food from the ceiling, while our guests arrived just a few minutes behind me. She had left a wooden spoon in the mixer that ballistically launched her cheese dip. There was a change in domestic procedures after that (including instructions to call ahead).



Conference attendees were given a “Taste of Texas” at the chili cook-off and barbecue dinner at the Pasadena Fairgrounds in 1993. Credit: Lunar and Planetary Institute.

The era of Willy Nelson and Mickey Gilley led to the famous (infamous?) LPSC Chili Cook-Off in 1981, first held on the LPI grounds and later at the Landolt Pavilion in a nearby park across from Clear Lake. There were some classic chili recipes, which I will just say were rather “interesting”: venison, frog legs, rattlesnake, eggs, and other unmentionable ingredients. The cook-offs encouraged great exchanges (i.e., trash talk) and swag (T-shirts, sweatshirts, hats, etc.). This transitioned into casual dining (from Mexican food to barbecue) and free beer at the Pasadena Fairgrounds for a number of years. I liked to sit down

at a random bench and make new acquaintances or meet up with colleagues dating back to some of the very first conferences. But free beer at a site far from the hotels raised liability issues, something we never used to think about.

These early science conferences included many strong personalities, which resulted in some intense “discussions.” For example, some argued that all the flows inside large lunar craters were simply debris flows, not impact melt. Other debates continued to focus on the origin of the highland plains on Mercury, citing lessons about the highland plains from the Apollo 16 mission. I recall chairing one session where two individuals argued about crater statistics (no names, but you can guess). The speaker had finished, but a person in the audience immediately rose to make a comment. As the speaker responded, the commenter answered back a bit more aggressively. The speaker then started moving off the podium while the audience member approached. I felt like a referee for the World Wrestling Association . . . although they both took their seats when the bell rang for the fourth time, my judo training almost came in handy.



At a special celebration in 1994, Bob Clayton, Gene Shoemaker, and George Wetherill cut the LPSC 25th anniversary cake, with conference co-chairs David Black and Doug Blanchard looking on.
Credit: Lunar and Planetary Institute.

There were only a handful of planetary missions during the 1980s, not counting every planet encountered by Voyager, which flew by Neptune in 1989, and the flotilla of non-U.S. missions to Comet Halley. The Challenger disaster in 1986 delayed several planned missions and put fiscal pressures on other programs. Nevertheless, LPSC remained a vibrant meeting because of new discoveries, including the global iridium layer at the K/T (K/Pg) boundary and the recognition of meteorites from Mars. As a result, I recall being in one of the Mars sessions in one of the small rooms in the Gilruth Center where only 20 people attended. In other years, only 15 people attended a session about the Moon. By 1981 (the twelfth LPSC), all oral sessions were held in the Gilruth Center.

After moving to Brown University in 1984, I no longer had the luxury of simply slipping my abstract under the door of the Publications Department on the day of the abstract deadline. Now, abstract-deadline day became an annual stressor. I would have to send any abstracts to Houston the day before. My students will confirm that we literally jogged down the hill to the downtown FedEx Office, sometimes with only minutes to spare. A couple of times, there was a car waiting outside to drive to the FedEx Center (near the airport), which stayed open later. One year, I actually flew down and delivered

my abstracts in person. (While this sounds like a great story, the trip actually coincided with the dedication of the new USRA/LPI building in 1992.)

In the 1980s, hotels in the vicinity of NASA JSC began to decline. But I thought it was important to give my students a sense of history by continuing to stay in the “Nausea” Bay Hotel. However, by 1986, there were only a few floors open in the hotel, and the Boom-Boom Room had closed. The “sense” of history (and the name “Nausea Bay”) became literal when sewage came up through the tub drain in one of our rooms. The following year, we chose a different hotel (and the Nassau Bay Hotel was demolished a few years later).



The author (far right) chats with another conference attendee during the 1994 poster session. Credit: Lunar and Planetary Institute.

Until 1991, the Planetary Geology Program still required its funded investigators to attend the PGPI meetings. In the beginning, their presentations actually contributed to their Progress Reports, somewhat similar to the very first Apollo 11 Lunar Science Conference. This program covered a broad range of disciplines, from the solar system formation to planetary mapping (and eventually was renamed to the Planetary Geology and Geophysics Program, or PGGPI). By the early 1990s, the line between topics in the PGGPI and LPSC meetings had blurred. As the PGGPI meetings ended, there was another surge in LPSC abstracts between 1990 and 1991, strengthening the role of the Houston conference as the key meeting where new findings about the planets, as well as the Moon, were presented.

In the early 1990s, striking new images of the surface of Venus resulted from the Magellan mission, and in the mid-1990s the Clementine mission returned new remote-sensing data about the Moon. But the number of abstract submissions remained relative constant (700–800) until 1999. In 1998, Lunar Prospector was launched, the Mars Global Surveyor first orbited Mars, and both Mars Pathfinder and Galileo mission (Galilean satellites) results were being reported. As a result, the 30th LPSC in 1999 featured a large increase in the number of abstracts (from 823 to 1075).

Until about 2002, most presentations used slide projectors or viewgraph projectors, eventually with dual screens. Some government presenters preferred viewgraphs because they were easier to create and display. In the large gyms, black curtains surrounded the platform with the slide projectors like a scene

from the Wizard of Oz. We all have stories of upside down or reverse slides, projectors that stuck, and blown bulbs that reduced our talks from 10 minutes to 5. During the transition from slides to digital presentations, I noticed that the power of the projectors dropped precipitously (and not because of the contrast between the old and new media). I suspect they used lower-wattage bulbs as a not-so-subtle way to encourage luddites to make the transition. I finally did.



Finding a suitable place for the LPSC poster session was one of the biggest challenges to remaining in the Clear Lake area. In 2000, the posters were displayed in the atria at the University of Houston-Clear Lake. But the poor lighting in that area, combined with the physical distance from the oral sessions, resulted in the decision to continue to look for other venues. Credit: Lunar and Planetary Institute.

In 2002, LPSC moved to the South Shore Harbor Hotel in League City, largely in response to security concerns after the September 11 attack the previous year. *[Editor's note: Security increased substantially at all NASA centers, and it was not clear whether the Gilruth Center would remain inside or outside the gates.]* This move still allowed satellite meetings either at the hotel, at the LPI, or even at NASA JSC before or after the meeting. In addition, attendees still could make visits to the NASA Visitor Center. But after seven years, this venue also became too small, and in 2009 LPSC moved to The Woodlands (north of Houston) for the 40th LPSC. Even though this venue was much farther away from NASA JSC, many researchers and students still headed down to the LPI or NASA JSC before and after the meetings.

The new millennium ushered in a flood of new data from both NASA and foreign missions (Mars Odyssey, Spirit/Opportunity, Mars Express, Rosetta, MESSENGER, Deep Impact, Mars Reconnaissance Orbiter, Phoenix, Kaguya, Dawn, Lunar Reconnaissance Orbiter, Chandrayaan-1, and LCROSS). By the end of the decade, the 41st LPSC had more than 1800 abstract submissions. These were the golden years of planetary exploration and discovery reflected in the flood of abstracts, which increased from

1100 at the 31st LPSC in 2000 to over 1800 at the 42nd LPSC in 2011. By the 44th LPSC, this number increased to over 2000, a level maintained at the 49th LPSC. Anyone with a broad interest had difficulty in deciding which session to attend. *[Editor's note: In spite of the partial government shutdown in the U.S., this year's 50th LPSC garnered a record number of abstract submissions: 2282.]*

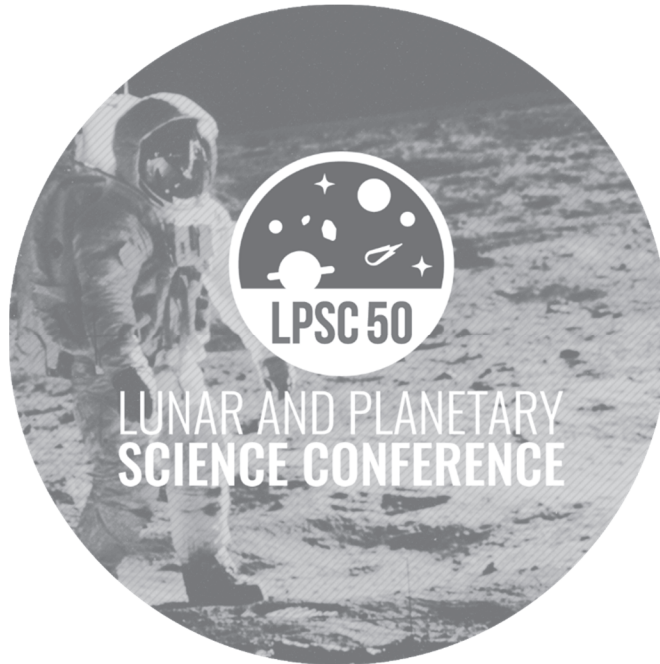


One of the most highly attended LPSC special sessions was the Mars session in 2004, at which science results from Mars Exploration Rovers Spirit and Opportunity were presented for the first time. Not only was every available chair taken, but attendees sat on the floor by the projection screen, stood along the walls in the front and back of the room, and stood outside the doors, straining to hear the talks. Credit: Lunar and Planetary Institute.

From the very beginning, the LSI/LPI arranged for the Galveston Limousine Service to shuttle conference goers between the LPSC venue and their hotels. Dominic Noto, who owned the service, is now one of the six remaining people who have been at all 50 meetings. Even after retiring and selling his service, Dominic still comes to the meeting and greets LPSC goers, simply because it is part of his legacy as well. If you see him at this year's conference, give him a "high-five."

This is my own reflection about the history of the Lunar and Planetary Science Conferences. I suspect that others would focus on different areas (e.g., the Hawaii or Arizona parties), and it would be great to hear their perspectives. The LPSC continues to include the latest results about planetary exploration while including fundamental research in lunar/planetary geology, exoplanets, exobiology, future mission planning, education, and public engagement with over 2000 abstract submissions from researchers around the world in 2018. What had started with coverage of just the Moon has now expanded to cover the entire solar system and beyond. This year marks my 50th conference, and I *have* to be there, just to be blown away by the latest results, whether from a mission or new interpretations of old data. Several years ago, I was not sure if I'd make it to the meeting (things happen). In the worst-case scenario, I asked my students to spread my ashes across certain seats at the 50th LPSC, just to leave my mark "behind." Rest assured that I'll be there one way or the other.

This article was originally published in Issue #155 of the Lunar and Planetary Information Bulletin (December 2018).



TECHNICAL PROGRAM

FIFTIETH LUNAR AND PLANETARY SCIENCE CONFERENCE

MARCH 18–22, 2019

The Woodlands Waterway Marriott Hotel and Convention Center
The Woodlands, Texas

Monday Morning, March 18, 8:30 a.m.

Room	Session	Session Title	Page
Waterway Ballroom 1	M101	Lunar Basins, Impacts, and Regolith	3
Waterway Ballroom 4	M102	Martian Crustal Column: Igneous, Metamorphic, and Hydrothermal Processes	4
Waterway Ballroom 5	M103	Special Session: New Horizons at KBO 2014 MU ₆₉ (Ultima Thule)	5
Waterway Ballroom 6	M104	Chondrites: Parent Body Processes	6
Montgomery Ballroom	M105	Titan: Releasing the Kraken	7

Monday Afternoon, March 18, 1:30 p.m.

Room	Session	Session Title	Page
Waterway Ballrooms 4 and 5	M150	Masursky Plenary Session	8

Monday Afternoon, March 18, 2:30 p.m.

Room	Session	Session Title	Page
Waterway Ballroom 1	M151	Lunar Polar Ices: Looking Over the Moon's Cold Shoulder	9
Waterway Ballroom 4	M152	Special Session: Going Inside with InSight	9
Waterway Ballroom 5	M153	Kuiper Belt Objects: From Pluto to Eris and Ultima Thule	10
Waterway Ballroom 6	M154	Atmospheres Through the Solar System and Beyond	11
Montgomery Ballroom	M155	Habitability: Too Hot! Too Cold! Ah, Just Right!	12

Monday Evening, March 18, 5:30 p.m.

Room	Session Title
Waterway Ballroom 4 and 5	NASA Headquarters Briefing
Town Center Exhibit Hall	Opening of Exhibits

ORAL SESSION

Monday, March 18, 2019

[M101]

LUNAR BASINS, IMPACTS, AND REGOLITH

8:30 a.m. Waterway Ballroom 1

Chairs: Barbara Cohen and Daniel Moriarty III

Times	Authors (*Denotes Presenter)	Abstract Title and Summary
8:30 a.m.	Bjonnes E. * Johnson B. C. Andrews-Hanna J. C.	<u><i>Exploring the Peak-Ring to Multiring Basin Transition on the Moon</i></u> [#2026] We simulate basin formation on the Moon to better understand the surface and interior conditions that affect formation.
8:45 a.m.	Jackson A. P. * Perera V. Elkins-Tanton L. T. Asphaug E.	<u><i>Puncturing Holes in the Early Lunar Crust with Re-Impacting Debris</i></u> [#2988] Impacts puncture crust / Exposing magma to space / But of what size and shape?
9:00 a.m.	Trowbridge A. J. * Johnson B. C. Freed A. M. Melosh H. J. Graves K.	<u><i>The Different Formation Evolution Between Mid-Sized and Large Basins</i></u> [#2468] Modeling the full evolution of South-Pole Aiken basin to understand the different formation mechanics between mid-sized and large lunar basins.
9:15 a.m.	White L. F. * Cernok A. Darling J. R. Whitehouse M. Joy K. H. et al.	<u><i>Crystallographic and Chronological Evidence for a Large Basin-Forming Lunar Impact at ~4.33 Ga</i></u> [#2787] A 4.33 Ga baddeleyite in lunar troctolite 76535 records phase heritage of a high temperature (>2300 C) cubic-ZrO ₂ precursor suggestive of origin in impact melt.
9:30 a.m.	Gleißner P. * Becker H.	<u><i>The Composition of Basin Forming Impactors and Large-Scale Impact Gardening in the Lunar Highlands</i></u> [#1093] New data on highly siderophile element abundances in lunar impactites will be discussed with respect to their crustal provenance and inferred time of formation.
9:45 a.m.	Moriarty D. P. III * Watkins R. N. Valencia S. N. Kendall J. D. Petro N. E.	<u><i>Mineralogy of Thorium-Enhanced Materials Within the South Pole-Aitken Basin: Possible Traces of the Lunar Upper Mantle</i></u> [#2874] Integrating remote sensing datasets, we evaluate the composition and geology of Th-enhanced materials within SPA. Conclusion: Exposure of stratified mantle.
10:00 a.m.	Venkatadri T. K. * Petro N. E.	<u><i>Analyzing Ejecta Thickness and Mixing in the Crisium and Nectaris Lunar Basins</i></u> [#1164] We modeled ejecta composition in the Crisium and Nectaris Basins to select possible future landing sites with abundant surface material from both basins.
10:15 a.m.	Poehler C. M. * Hiesinger H. van der Bogert C. H.	<u><i>The Light Plains of the Lunar Northern Region (45°–90°N)</i></u> [#2310] We determined the absolute model ages for light plains in the lunar northern region and studied their implications for the origin of light plains.
10:30 a.m.	Speyerer E. J. * Povilaitis R. Z. Robinson M. S. Martin A. C. Boyd A. et al.	<u><i>Examining the Impact Process and Regolith Maturation with Temporal and Photometric Observations</i></u> [#2878] Newly formed impacts discovered with LROC images provide new insight into the cratering process and the rate regolith matures on the surface of the Moon.
10:45 a.m.	Wang J. T. * Kreslavsky M. A. Liu J. Z. Head J. W. Kolenkina M. M.	<u><i>Quantitative Characterization of Impact Crater Materials on the Moon: Implications for Degradation Processes and Stratigraphic Age</i></u> [#1262] Topographic roughness and thermophysical properties of subunits of impact craters give insight into crater degradation and aid stratigraphic age estimation.
11:00 a.m.	Allen C. C. * Costello E. S. Hayne P. O. Paige D. A.	<u><i>A Time Horizon on the Aristarchus Plateau</i></u> [#1320] The gardening rate calculated from km-scale streaks on the Aristarchus plateau is closely comparable to rates estimated from impact modeling and Apollo cores.

11:15 a.m.	Hahn T. M. Jr. * Schonwald A. R. Robinson M. S.	Watkins R. N. Martin A. C. et al.	<u>Local Geology and Regolith at the Apollo 17 Landing Site from the Perspective of LROC NAC Photometric Analysis</u> [#1976] We examine outstanding Apollo 17 science questions through photometric investigation of the TLV using Apollo 17 soils and the Apollo 16 LISCT as ground-truth.
11:30 a.m.	Garvin J. B. * Sietins J. M. Green W. H.	Jones J. S. Kent R. et al.	<u>Volumetric Analysis of Micro-Craters in Apollo 16 Samples via X-Ray Computed Tomography and Laser Confocal Microscopy</u> [#1708] High resolution X-ray computed tomography of Apollo 16 samples reveals the topology and interior deformation of micro-craters at micron-scales.

Monday, March 18, 2019

[M102]

MARTIAN CRUSTAL COLUMN: IGNEOUS, METAMORPHIC, AND HYDROTHERMAL PROCESSES

8:30 a.m. Waterway Ballroom 4

Chairs: Christopher Herd and Julia Semprich

Times	Authors (*Denotes Presenter)	Abstract Title and Summary	
8:30 a.m.	Semprich J. * Filiberto J.	Treiman A. H. Schwenzer S. P.	<u>Low-Grade Metamorphic Phases on Mars as a Function of CO₂-H₂O Fluid Compositions</u> [#1437] Phase equilibria modeling is used to calculate low-grade metamorphic phases for likely martian compositions as a function of variations in fluid composition.
8:45 a.m.	Ott J. P. * Morris R. V.	Rampe E. B. Treiman A. H.	<u>Chemistry and Crystallography of Diagenetic, Authigenic, and Igneous Potassium Feldspar: Implications for Sedimentary Petrology in Gale Crater, Mars</u> [#1358] Sanidine on Mars / The question: how did it form? / Unit cells tell more.
9:00 a.m.	Nekvasil H. * Rogers A. D.	DiFrancesco N. D. King P. L.	<u>Martian Dust: Contributions of Condensates from Magmatic Gas</u> [#2652] Martian dust likely contains significant amounts of magmatic gas condensates (halides, oxides, sulfides) and secondary reaction products involving these phases.
9:15 a.m.	Rogaski A. * Yang S.	Ustunisik G. K. Humayun M.	<u>Volatilization of Germanium, Zinc, and Lithium in Martian Basalts and Associated Surface Alteration During Fumarolic Degassing</u> [#2864] Experimental determination of the behavior of Ge, Zn, and Li in the presence of various volatile loads and the associated alteration due to fumarolic degassing.
9:30 a.m.	Yang S. * Righter K. Zanda B.	Humayun M. Peslier A. H. et al.	<u>A Two Gigayear History of Germanium Outgassing from Shergottites</u> [#1908] LA-ICP-MS analyses of two ancient shergottites (NWA 7635 and NWA 8159) show a 2Ga year history of germanium degassing from shergottites.
9:45 a.m.	Payre V. * Dasgupta R.	Siebach K. L. Rampe E. B.	<u>Using Mineralchemistry in Gale Crater Sedimentary Rocks to Constrain Ancient Igneous Processes on Mars</u> [#2562] The chemistry of primary and detrital igneous minerals in Gale Crater, Mars, can be explained by fractional crystallization of shallow hydrated crustal melts.
10:00 a.m.	Phillips M. S. * Moersch J. E.	Viviano C. E.	<u>Plagioclase in Primary Mineralogy of Ancient Crust, Northern Hellas, Mars</u> [#2137] Ancient Hellas rocks / Reveal plagioclase in / Reflectance spectra.
10:15 a.m.	Liebske C. * Griffin S. *	Khan A. Daly L. Lee M. R. Piazolo S. Trimby P. W. et al.	<u>On the Principal Building Blocks of Mars</u> [#1870] We statistically mix chondritic and achondritic meteorites to reconcile geochemical signatures, geophysical properties, and redox characteristics of Mars.
10:30 a.m.	Griffin S. * Piazolo S.	Daly L. Lee M. R. Piazolo S. Trimby P. W. et al.	<u>New Insights into the Magmatic and Shock History of the Nakhilite Meteorites from Electron Backscatter Diffraction</u> [#1845] Large Area Electron Backscatter Diffraction (EBSD) has been applied to ten nakhilites to investigate their slip systems.
10:45 a.m.	Paquet M. * Udry A. Kumler B.	Day J. M. D. Hattingh R. et al.	<u>Fractionation of the Highly Siderophile Elements in Shergottite Sulfides</u> [#1456] Highly siderophile element abundances in shergottite sulfides seem to be controlled by petrogenetic processes such as fractional crystallization.

11:00 a.m.	Herd C. D. K. *	<u>Reconciling Redox: Making Spatial and Temporal Sense of Oxygen Fugacity Variations in Martian Igneous Rocks</u> [#2746] Oxygen fugit / Once molten rock travels space / Mars secrets revealed.
11:15 a.m.	Rahib R. R. Udry A. * Howarth G. H. Paquet M. Combs L. M. et al.	<u>Petrogenesis of Enriched and Intermediate Poikilitic Shergottites: From Magmatic Source to Emplacement</u> [#1428] Enriched and intermediate poikilitic shergottites have similar emplacement histories but were likely emplaced in different shallow sills in the martian crust.
11:30 a.m.	Balta J. B. * Castle N. Ennis M. E. McSween H. Y.	<u>Widespread Oxidation in Shergottite Magmas Recorded by Exsolved Spinel in Olivine</u> [#1707] Oxygen rises / Deep in martian olivine / Tiny chromites form.

Monday, March 18, 2019

[M103]

SPECIAL SESSION: NEW HORIZONS AT KBO 2014 MU₆₉ (ULTIMA THULE)

8:30 a.m. Waterway Ballroom 5

Chairs: Carly Howett and Kelsi Singer

Times	Authors (*Denotes Presenter)	Abstract Title and Summary
8:30 a.m.	Stern S. A. * Spencer J. R. Weaver H. A. Olkin C. B. Moore J. M. et al.	<u>Overview of Initial Results from the Reconnaissance Flyby of a Kuiper Belt Planetesimal: 2014 MU₆₉</u> [#1742] On 1 Jan 2019, NASA's New Horizons mission conducted a close flyby of KBO 2014 MU ₆₉ nicknamed Ultima Thule. Here we summarize the earliest results of that flyby.
8:45 a.m.	Moore J. M. * McKinnon W. B. Spencer J. R. Stern S. A. Binzel R. P. et al.	<u>The Geology of 2014 MU₆₉ ("Ultima Thule"): Initial Results from The New Horizons Encounter</u> [#2152] Overview of very preliminary limited-data geological analysis of MU ₆₉ , with the promise that many new, quite substantial results will be presented at the talk.
9:00 a.m.	Grundy W. M. * Binzel R. P. Britt D. T. Buie M. W. Cook J. C. et al.	<u>486958 2014 MU₆₉ Ultima Thule Surface Composition Overview</u> [#2473] Overview of compositional results from the New Horizons encounter with the small, Cold Cassical Kuiper belt object (486958) 2014 MU ₆₉ "Ultima Thule."
9:15 a.m.	McKinnon W. B. * Stern S. A. Weaver H. A. Spencer J. R. Buie M. W. et al.	<u>A Pristine "Contact Binary" in the Kuiper Belt: Implications from the New Horizons Encounter with 2014 MU₆₉ ("Ultima Thule")</u> [#2767] MU ₆₉ 's contact binary shape provides the clearest view to date of the accretion processes operative in the protosolar nebula and subsequent planetesimal disk.
9:30 a.m.	Buie M. W. * Porter S. B. Tamblyn P. Terrell D. Verbiscer A. J. et al.	<u>Stellar Occultation Results for (486958) 2014MU₆₉: A Pathfinding Effort for the New Horizons Flyby</u> [#3120] Four occultations were observed by 2014MU ₆₉ and the results were invaluable for mission planning and execution of the New Horizons flyby on 2019 Jan 1.
9:45 a.m.	Porter S. B. * Bierson C. J. Umurhan O. Beyer R. A. Lauer T. A. et al.	<u>A Contact Binary in the Kuiper Belt: The Shape and Pole of (486958) 2014 MU₆₉</u> [#1611] Two siblings hold hands / Spinning together in the void / Now visited.
10:00 a.m.	Schenk P. * Beyer R. Beddingfield C. Bierson C. J. Moore J. M. et al.	<u>Topography of Ultima Thule (2014 MU₆₉) at Local Scales: Surface Evolution of a Small Primitive Body</u> [#2934] Bi-lobed orb that rules the night / Ultima Thule is out of sight / Small-scale topography will shed some light.
10:15 a.m.	Zangari A. M. * Beddingfield C. B. Benecchi S. D. Beyer R. A. Bierson C. J. et al.	<u>The Mysterious Missing Light Curve of (486958) 2014 MU₆₉, a Bi-Lobate Contact Binary Visited by New Horizons</u> [#3007] Why no one found a / Rotation period / On spacecraft approach.
10:30 a.m.	Howett C. J. A. * Parker A. H. Olkin C. B. Protopapa S. Grundy W. et al.	<u>Colors of (486958) 2014 MU₆₉ as Observed by New Horizons' Multi-Spectral Visible Imaging Camera (MVIC)</u> [#1982] First results of 486958 MU ₆₉ are presented; it is shown to be red and bi-lobed. The two lobes have a consistent color, while the neck region is less red.

10:45 a.m.	Spencer J. R. * Showalter M. R. Lauer T. R. Buie M. W. Porter S. B. et al.	<u><i>The Search for Moons and Rings of 2014 MU₆₉ [#2737]</i></u> New Horizons conducted extensive searches for rings and moons during its flyby of 2014 MU ₆₉ . As of the time of writing, none have been found.
11:00 a.m.	Weaver H. A. * Stern S. A. Britt D. T. Buratti B. J. Cheng A. F. et al.	<u><i>Comparing (486958) 2014 MU₆₉ to Cometary Nuclei: Shapes and Surfaces [#2982]</i></u> MU ₆₉ vs. Cometary Nuclei: Comparisons of shapes and surfaces.
11:15 a.m.	Protopapa S. * Grundy W. M. Olkin C. B. Howett C. J. A. Parker A. H. et al.	<u><i>Comparing Ultima Thule with Comet Nuclei: Colors and Composition [#2732]</i></u> We compare the composition of 2014MU ₆₉ with that of comets to determine which features of comets are primitive and which have emerged because of their history.
11:30 a.m.	Singer K. N. * McKinnon W. B. Spencer J. R. Weaver H. A. Lauer T. R. et al.	<u><i>Impact Craters on 2014 MU₆₉: Implications for the Geologic History of MU₆₉ and Kuiper Belt Population Size-Frequency Distributions [#2239]</i></u> The craters on 2014 MU ₆₉ , or the lack thereof, will provide information on the evolution of the body itself and the size-distribution of Kuiper belt objects.

Monday, March 18, 2019

[M104]

CHONDRITES: PARENT BODY PROCESSES

8:30 a.m. Waterway Ballroom 6

Chairs: Neyda Abreu and Martin Lee

Times	Authors (*Denotes Presenter)	Abstract Title and Summary
8:30 a.m.	Jin Z. L. * Bose M.	<u><i>Hydrogen Isotope Systematics in Ordinary Chondrite Parent Bodies [#1576]</i></u> Orthopyroxenes from four ordinary chondrites have been measured for hydrogen isotope compositions and water contents using SIMS instruments.
8:45 a.m.	Shimizu K. * Alexander C. M. O'D. Hauri E. H. Sarafian A. R. Jacobsen S. D. et al.	<u><i>Hydrogen Abundances and Isotope Compositions of Chondrule Mesostases in Carbonaceous and Ordinary Chondrites [#2840]</i></u> Heavier H isotopic composition of mesostases in ordinary chondrites than in carbonaceous chondrites due to inheritance from D-rich ice or Fe oxidation by water.
9:00 a.m.	Greenwood R. C. * Howard K. T. King A. J. Lee M. R. Burbine T. H. et al.	<u><i>Oxygen Isotope Evidence for Multiple CM Parent Bodies: What Will We Learn from the Hayabusa2 and OSIRIS-REx Sample Return Missions? [#3191]</i></u> CM chondrites may originate from a diverse range of asteroids or alternatively the CM parent body was more isotopically heterogeneous than previously considered.
9:15 a.m.	Vacher L. G. * Piralla M. Piani L. Marrocchi Y.	<u><i>Monitoring the Thermal Evolution of the CM Parent Body(ies) with In Situ Oxygen Isotope Analyses [#1862]</i></u> We analyzed in situ O-isotopic compositions on calcite in the CM Murchison and Mukundpura in order to track the evolution temperature of CM parent body(ies).
9:30 a.m.	Donohue P. H. * Huss G. R. Nagashima K.	<u><i>Manganese-Chromium Systematics of Calcite in the CM Chondrites QUE 93005 and MET 01070 Determined Using a New Matrix-Matched Standard [#1949]</i></u> New synthetic manganese- and chromium-bearing carbonate standards allow us to re-investigate Mn-Cr systematics of carbonates in CM chondrites.
9:45 a.m.	Higashi K. * Mikouchi T. Zolensky M. E.	<u><i>Aqueous Alteration of Enstatite Chondrite Material in the Kaidun Meteorite [#2344]</i></u> We studied aqueously altered E chondrite clasts in Kaidun and found two types of altered materials and elongate calcite, suggesting separate alteration events.
10:00 a.m.	Abreu N. M. * Corrigan C. M. Keller L. P. Hezel D. C. Gross J. et al.	<u><i>Primary Nanocrystalline Anhydrous Chondrule Mesostasis: Limited Evidence of Secondary Alteration in Most CR Chondrites [#3097]</i></u> CR mesostases have primary crystalline nanophases, compositional differences between chondrules setting, and lack trends attributable to elemental mobilization.

10:15 a.m.	Brearley A. J. * Simon S. B.	<u><i>Behavior of Chromium in Type IIA Chondrule Olivine During the Earliest Stages of Thermal Metamorphism of CO₃ Carbonaceous Chondrites: Insights from Microstructural Studies of Kainsaz (CO3.2) [#1443]</i></u> TEM studies of a chromite-bearing vein in a ferroan olivine phenocryst in a type IIA chondrule in Kainsaz contain compositionally-zoned grains.
10:30 a.m.	Hellmann J. L. * Kruijer T. S. Van Orman J. A. Metzler K. Kleine T.	<u><i>A New Method for Simultaneously Constraining Cooling Rates and Ages of Ordinary Chondrites via Hf-W Chronometry [#2729]</i></u> Cooling rates and cooling ages of ordinary chondrites inversely correlate, indicating that the onion shell structure of their parent bodies was largely retained.
10:45 a.m.	Li Y. * Rubin A. E. Hsu W. Ziegler K.	<u><i>Early Impact Events on Ordinary-Chondrite Parent Asteroids: Insights from Northwest Africa (NWA) 11004, a Type-7 Breccia. [#2561]</i></u> The twice-shocked NWA 11004 OC has 4-mm poikilitic opx (as in acapulcoites but not type-6 OC); this indicates very high temp. At 4546 Ma, it cooled at <5°C/Ma.
11:00 a.m.	Nakanishi N. * Yokoyama T. Okabayashi S. Iwamori H.	<u><i>Thermal Histories of Metal Phases in a CH/CBb Chondrite Isheyevo: Implications from Siderophile Elements [#2253]</i></u> We discuss the thermal history of metal phases to understand physicochemical conditions in the early outer solar system where Isheyevo parent body has formed.
11:15 a.m.	Lunning N. G. * McCoy T. J. Schrader D. L. Nagashima K. Corrigan C. M. et al.	<u><i>Metal-Sulfide Segregates from a Carbonaceous Chondrite Impact Melt: The Ungrouped Irons Lewis Cliff 86211 and 86498 [#2763]</i></u> These sulfide-rich iron meteorites provide evidence of much larger scale impact melting on carbonaceous chondrite asteroids than previously recognized.
11:30 a.m.	Anzures B. A. * Parman S. W. Boesenberg J. S. Milliken R. E.	<u><i>Using Volatile (S, C, H, F, Cl) Contents of Enstatite in Reduced Meteorites to Estimate Oxygen Fugacity and Equilibrium Melt Compositions [#2179]</i></u> Reduced meteorites and experiments have trace S, H, C, and F in enstatite. Assuming saturation, S and C can be used to estimate f_{O_2} and volatile content of melt.

Monday, March 18, 2019

[M105]

TITAN: RELEASING THE KRAKEN

8:30 a.m. Montgomery Ballroom

Chairs: Morgan Cable and Donald Korycansky

Times	Authors (*Denotes Presenter)	Abstract Title and Summary
8:30 a.m.	Heslar M. F. * Barnes J. W. Dhingra R. D. Sotin C. Soderblom J. M.	<u><i>Latest Wave Detections in Titan's Kraken Mare as Seen by Cassini VIMS [#2266]</i></u> We discover consistent wave motion in Bayta Fretum, a narrow channel in Kraken Mare, in a dedicated survey of the T100-T126 flybys.
8:45 a.m.	Poggiali V. P. * Mastrogiuseppe M. M. Hayes A. G. H.	<u><i>The Bathymetry of Moray Sinus at Kraken Mare [#3148]</i></u> We present the bathymetry obtained from the analysis of radar altimeter data acquired during flyby T104 of Titan, during which Cassini observed the Kraken mare.
9:00 a.m.	Farnsworth K. * Chevrier V. Czaplinski E. Soderblom J. M.	<u><i>Freezing Points of Methane-Ethane-Nitrogen Mixtures Under Titan Surface Pressure [#2672]</i></u> This study experimentally explores the liquids viable to freezing on Titan's surface by investigating the solidus curve of methane-ethane-nitrogen mixtures.
9:15 a.m.	Hanley J. * Groven J. J. Grundy W. M. Dustrud S. Engle A. E. et al.	<u><i>Characterization of Possible Two Liquid Layers in Titan Seas [#1712]</i></u> Two liquid layers / Exist at depth in the seas / Of the moon Titan.
9:30 a.m.	Dhingra R. D. * Barnes J. W. Hedman M. H. Radebaugh J.	<u><i>Constraints on Titan Lake Similarities from their Shapes [#2898]</i></u> We use 'form follows process' to quantify shapes of Titan's lakes to hash out the probable formation scenarios.
9:45 a.m.	Czaplinski E. C. * Farnsworth K. K. Chevrier V. F.	<u><i>Experimental Study of Ethylene and Benzene Evaporites Under Titan Conditions [#1153]</i></u> Updated chamber / Gives new insights to Titan's / Evaporation.

10:00 a.m.	Cable M. L. * Vu T. H. Maynard-Casely H. E. Hodyss R.	<u><i>Molecular Minerals on Titan: A New Co-Crystal Between Acetylene and Butane</i> [#1477]</u> Around Titan's lakes / Butane and acetylene / A co-crystal make!
10:15 a.m.	Malaska M. J. * Lopes R. M. C. Hayes A. Schoenfeld A. Verlander T. et al.	<u><i>An Updated Organic Inventory Estimate for Titan</i> [#1711]</u> Organic airfall / Covering Titan's surface / How much is down there?
10:30 a.m.	Gregg T. K. P. * Sakimoto S. E. H.	<u><i>On the Evolution of Titan's Slot Canyons: Preliminary Analyses Using Fluid Dynamics</i> [#2743]</u> Titan's methane flows / Eroding and transporting / Sediment slowly.
10:45 a.m.	Matulka P. R. * Levy J. S. Burr D. M. Maue A. D.	<u><i>Rounding and Comminution Rates of Ice Clasts Using the Titan Tumbler: Fluctuating Roundness and Stepped Mass Loss</i> [#1490]</u> Tumbling clasts of ice / Comminution and rounding / Cryogenic cracks.
11:00 a.m.	Yu X. * Hörst S. M. He C. McGuiggan P.	<u><i>Direct Measurement of Single Particle Electrostatic Forces Between Titan Sand Analogs Using Atomic Force Microscopy</i> [#2042]</u> Organic sand on Titan / Contacting and rubbing / Could it produce electrostatic forces?
11:15 a.m.	Lalich D. E. * Hayes A. G.	<u><i>Classification and Degradation State of Mountainous Terrains on Titan from Cassini RADAR</i> [#2797]</u> Newly processed Cassini RADAR altimetry enables a fresh perspective on Titan's mountainous terrain.
11:30 a.m.	MacKenzie S. M. * Lorenz R. D. Lora J. M.	<u><i>A Thermal Inertia Map of Titan and the Effects on a Dry Climate</i> [#2999]</u> Some places heat fast / Some places heat slow — we think. / Dry atmosphere not.

Monday, March 18, 2019

[M150]

MASURSKY PLENARY SESSION

1:30 p.m. Waterway Ballrooms 4 and 5

Chairs: Louise Prockter and Eileen Stansbery



Harold Masursky
1923–1990

The History of the Masursky Lecture Series at LPSC

During his 20-year career in planetary science, Harold Masursky was a world-renowned pioneer in space exploration. He applied his many talents to the fields of economic, structural and planetary geology. In the 1960s he played a major role in the choice of Apollo landing sites. In the 1970s he headed the scientific team that first mapped the planet Mars, and he was actively involved in the selection of the Viking landing sites. Through the 1980s he was a key figure in Voyager Project. His work has resulted in over 200 publications. One of his major contributions was as president of the Working Group for Planetary System Nomenclature of the International Astronomical Union. He was the recipient of many honors from NASA, USGS, and other scientific organizations. His contributions to planetary geology, to the design of spacecraft instruments, and to international scientific cooperation will long be remembered.

As a tribute to his work, the Lunar and Planetary Science Conference has incorporated in the annual program a lecture series in his honor. The first lecture in this series was presented at the 23rd Lunar and Planetary Science Conference in 1992.

Monday, March 18, 2019

[M151]

LUNAR POLAR ICES: LOOKING OVER THE MOON'S COLD SHOULDER

2:30 p.m. Waterway Ballroom 1

Chairs: Anthony Colaprete and Kathy Mandt

Times	Authors (*Denotes Presenter)	Abstract Title and Summary
2:30 p.m.	Costello E. S. * Ghent R. R. Lucey P. G.	<u>Impact Gardening on the Moon and Mercury: The Source, Age, and Depth to Ice at the Poles</u> [#1991] Moon and Mercury / Icy poles so different / Broken by impacts.
2:45 p.m.	Kulchitsky A. V. * Hurley D. M. Johnson J. B.	<u>Discrete Element Monte Carlo Meso-Scale Volatile Thermo-Diffusion Model</u> [#2943] Study presents a model of water migration on meso-scale level to determine macro-scale mass transfer rates of water through regolith under different conditions.
3:00 p.m.	Patterson G. W. * Petro N. Keller J. Mandt K. E. McClanahan T. et al.	<u>The LRO Perspective on the Lateral and Depth Distribution of Water (Ice) at the Lunar Poles</u> [#3094] As LRO looks toward its next extended mission, the polar craters Cabeus and Amundsen stand out for their potential to address key lunar exploration questions.
3:15 p.m.	Luchsinger K. M. * Chanover N. J. Strycker P. D.	<u>Using Ground Based Observation of the LCROSS Impact Plume to Investigate Water Ice Stratification Within Permanently Shadowed Lunar Sediment</u> [#3035] We present an analysis of a family of permanently shadowed lunar sediment models, including water ice content, fit to the LCROSS ground-based observations.
3:30 p.m.	Williams J.-P. * Greenhagen B. T. Paige D. A. Schorghofer N. Aye K.-M. et al.	<u>Seasonal Variations in South Polar Temperatures on the Moon</u> [#2852] Seasonal temperature mapping of the south pole using LRO Diviner shows the amount of water cold-trapping area more than doubles between summer and winter.
3:45 p.m.	Kloos J. L. * Moores J. E. Sangha J. Nguyen T. G. Schorghofer N.	<u>The Temporal and Geographic Extent of Cold Trapping Regions at the North and South Pole of the Moon: Implications for Volatile Transport and the Seasonality of Polar Frost Distribution and Abundance</u> [#2471] We explore the influence of seasonal changes in cold trapping area on water transport, trapping and distribution within PSRs at the north and south pole.
4:00 p.m.	Wilson J. T. * Lawrence D. J. Miller R. S. Garrick-Bethell I. Siegler M. A.	<u>Constraining the Distribution of Hydrogen at the Lunar Poles Using Lunar Prospector Neutron Spectrometer Data and Ice Stability Models</u> [#3194] Via image reconstruction, we improved the resolution of the LP neutron data to better estimate the hydrogen abundance in areas hypothesized to contain excess H.
4:15 p.m.	Hayne P. O. * Siegler M. A. Paige D. A. Lucey P. G. Fisher E. A.	<u>Carbon Dioxide Frost at the Poles of the Moon: Thermal Stability and Observational Evidence from the Lunar Reconnaissance Orbiter</u> [#2628] Shadows in shadows / Collecting comet samples / Why don't we go see?
4:30 p.m.	Colaprete A. * Elphic R. C. Shirley M.	<u>Characterizing Lunar Polar Volatiles at the Working Scale: Going from Exploration Goals to Mission Requirements</u> [#1120] This paper provides an analysis of the number and distribution of observations needed to provide the necessary next steps in lunar volatile exploration.

Monday, March 18, 2019

[M152]

SPECIAL SESSION: GOING INSIDE WITH INSIGHT

2:30 p.m. Waterway Ballroom 4

Chairs: Katarina Miljkovic and Matthew Golombek

Times	Authors (*Denotes Presenter)	Abstract Title and Summary
2:30 p.m.	Banerdt W. B. * Smrekar S. Antonangeli D. Asmar S. Banfield D. et al.	<u>Insight — The First Three Months on Mars</u> [#3109] Status and summary of early results from the InSight mission: Trust my crystal ball? / Instruments remain healthy / Geophysics reigns!

MON ORAL

2:45 p.m.	Golombek M. * Warner N. H. Grant J. Hauber E. Ansan V. et al.	<u><i>Geology of the InSight Landing Site, Mars: Initial Observations</i></u> [#1694] InSight landed on a smooth, flat pebble rich surface with low rock abundance, impact craters in various stages of degradation, and eolian bed forms.
3:00 p.m.	Lognonné P. * Banerdt W. B. Pike W. T. Giardini D. Banfield D. et al.	<u><i>SEIS: Overview, Deployment, and First Science on the Ground</i></u> [#2246] This provides first scientific observations of SEIS for Mars micro-seismic noise, atmospheric-generated signals, and surface and subsurface elastic structure.
3:15 p.m.	Pike W. T. * Lognonne P. Banerdt W. B. Calcutt S. B. Standley I. M. et al.	<u><i>Results from the Short-Period (SP) Seismometers on the Mars InSight Mission: From Launch to Sol 40</i></u> [#2109] The dynamic environment at the InSight landing site has been observed with its short-period seismometers.
3:30 p.m.	Spohn T. * Grott M. Smrekar S. E. Knollenberg J. Hudson T. L. et al.	<u><i>The Heat Flow and Physical Properties Package HP3 on InSight — First Results</i></u> [#1344] The Heat Flow and Physical Properties Package on InSight is planned to measure the geothermal heat flow of Mars. First results after landing will be presented.
3:45 p.m.	Banfield D. * Spiga A. Newman C. Lorenz R. Forget F. et al.	<u><i>First Atmospheric Results from InSight APSS</i></u> [#2699] InSight sees weather / 'Round the clock and precisely / First results discussed.
4:00 p.m.	Newman C. E. * Viudez-Moreiras D. Baker M. M. Lewis K. W. Gomez-Elvira J. et al.	<u><i>The Observed Winter Circulation at InSight's Landing Site and Its Impact on Understanding the Year-Round Circulation and Aeolian Activity in Elysium Planitia and Gale Crater</i></u> [#2302] Comparing atmospheric model predictions for the InSight/MSL region with observed wind and aeolian features improves understanding of the key physical processes.
4:15 p.m.	Miljkovic K. * Collins G. S. Rajsic A. Wojcicka N. Neidhart T. et al.	<u><i>Numerical Investigation of Impact-Induced Seismic Signals in Martian Crust</i></u> [#1503] Simulations of meteoroid strikes on Mars using iSALE-2D code and connecting impact and target properties with properties of seismic waves generated by impacts.
4:30 p.m.	Plesa A.-C. * Padovan S. Tosi N. Breuer D. Grott M. et al.	<u><i>Using the InSight Measurements to Constrain Large-Scale Numerical Simulations of the Interior of Mars</i></u> [#3142] We present how thermal evolution models of interior dynamics of Mars can be improved by the measurements of the InSight mission.

Monday, March 18, 2019

[M153]

KUIPER BELT OBJECTS: FROM PLUTO TO ERIS AND ULTIMA THULE

2:30 p.m. Waterway Ballroom 5

Chairs: Jason Hofgartner and Andrew Poppe

Times	Authors (*Denotes Presenter)	Abstract Title and Summary
2:30 p.m.	Showalter M. R. * Buie M. W. Grundy W. M. Hamilton D. P. Kaufmann D. E. et al.	<u><i>Potential Implications of the Shape of 2014 MU₆₉ for Interpreting Other KBO Lightcurves</i></u> [#2132] The hypothesis that many KBOs are contact binaries (similar in shape to 2014 MU ₆₉) has testable implications for the distribution of KBO lightcurves.
2:45 p.m.	Verbiscer A. J. * Porter S. B. Benecchi S. D. Kavelaars J. J. Weaver H. A. et al.	<u><i>New Horizons Observations of Distant Kuiper Belt Objects: Rotational and Solar Phase Curves of (486958) 2014 MU₆₉ and Other Cold Classical KBOs</i></u> [#2959] Kuiper belt objects / Scatter feeble sunlight to / Show surface texture.
3:00 p.m.	Beyer R. A. * Weaver H. A. Porter S. B. Grundy W. M. Moore J. M. et al.	<u><i>Potential Mapping Schemes and Reference Systems for MU₆₉</i></u> [#2258] These are the New Horizons Team's initial thoughts about how to apply mapping schemes and cartographic reference systems to the bi-lobate contact binary MU ₆₉ .
3:15 p.m.	Keane J. T. * Bierson C. J. Lisse C. M. Showalter M. W. Stansberry J. A. et al.	<u><i>Gravity, Rotation, and Hill Slopes of 2014 MU₆₉</i></u> [#3145] MU ₆₉ / Little gravity, steep slopes / Good skiing at neck.

3:30 p.m.	Lisse C. M. * Singer K. N. Fernandez Y. R. Bauer J. M. Protopapa S. et al.	<u>Comets Sourced by KBOs — Comparison of SFDs Derived from Spitzer/Wise JFC Imaging and Pluto and Charon KBO Cratering Rates</u> [#2865] Spitzer/WISE JF comet and new NH Pluto/Charon KBO size-frequency distributions are similar; another piece of evidence that the populations are genetically linked.
3:45 p.m.	Burgener J. A. *	<u>The Influence of Dwarf Planets on the Stability of Objects in the Kuiper Belt</u> [#3163] Pluto and other dwarf planets can influence the stability of Classical Kuiper Belt objects causing them to be short period comets.
4:00 p.m.	Hofgartner J. D. * Buratti B. J. Hayne P. O. Young L. A.	<u>Eris: The Brightest (and Most Active?) Kuiper Belt Object</u> [#1608] Eris is anomalously bright; it is likely active. We test the hypothesis of atmospheric collapse for its albedo with a numerical model and find that it is unlikely.
4:15 p.m.	Poppe A. R. * Horányi M.	<u>Interplanetary Dust Delivery of Water to the Atmospheres of Pluto and Triton</u> [#1044] We use an interplanetary dust dynamics model and a dust ablation model to calculate the deposition of water at Pluto and Triton's atmospheres from dust.
4:30 p.m.	Buratti B. J. * Hicks M. D. Kramer E. Bauer J.	<u>Discovery of Remarkable Opposition Surges on Pluto and Charon</u> [#1723] We report on observations of Pluto and Charon when they are fully illuminated, a geometry that will not be repeated for 161 years. Both are anomalously bright.

Monday, March 18, 2019

[M154]

ATMOSPHERES THROUGH THE SOLAR SYSTEM AND BEYOND

2:30 p.m. Waterway Ballroom 6

Chairs: Edwin Kite and Erika Kohler

Times	Authors (*Denotes Presenter)	Abstract Title and Summary
2:30 p.m.	Mills F. P. * Marcq E. Yung Y. Parkinson C. D. Jessup K. L. et al.	<u>Atmospheric Chemistry on Venus: An Overview of Unresolved Issues</u> [#2374] This presentation discusses the current understanding of atmospheric chemistry on Venus and key outstanding issues.
2:45 p.m.	Korablev O. Montmessin F. * Fedorova A. Trokhimovskiy A. Ignatiev N. et al.	<u>Results from the Atmospheric Chemistry Suite (ACS) Experiment On Board the ExoMars Trace Gas Orbiter (TGO)</u> [#2838] Latest results from the ACS instrument onboard TGO over the period from the Science Phase start (04/2018) until the end of the 2018 dust event will be presented.
3:00 p.m.	Kite E. S. * Steele L. J. Mischna M. A.	<u>Aridity Enables Warm Climates on Mars</u> [#1360] A cold-start H ₂ O(i) cloud greenhouse can sustain T > 290K on early Mars for >>100yr in equilibrium with polar/mountain-top ice, but only if the planet is arid.
3:15 p.m.	Warren A. O. * Kite E. S.	<u>A New Martian Paleopressure Constraint Before 4 Ga from Crater Size-Frequency Distributions in Mawrth Vallis</u> [#1286] We present a new martain paleopressure estimate before 4 Ga and use this alongside existing constraints in a basic 2-component Mars atmosphere evolution model.
3:30 p.m.	Smith C. L. * Moores J. E. Guzewich S. D. Ellison D.	<u>Visibility and Line-of-Sight Extinction Measurements Within Gale Crater During the 2018/Mars Year 34 Global Dust Storm by Curiosity</u> [#1287] Global dust storm caused / Low visibility for / Curiosity.
3:45 p.m.	Corlies P. * Hayes A. G. Kelland J. Adamkovics M. Rodriguez S. et al.	<u>Ongoing Monitoring of Clouds on Titan</u> [#2776] We present an update on ongoing monitoring of clouds on Titan, as well as an analysis of Titan's clouds, including wind profiles of Titan's atmosphere.
4:00 p.m.	Kutsop N. W. * Hayes A. G. Sotin C. Lunine J. L. Corlies P. M. et al.	<u>Titan's Atmospheric Annuli as Observed by Cassini VIMS</u> [#3080] We report the detection of annular atmospheric features encircling Titan using observation from the Cassini-Huygens Visual and Infrared Mapping Spectrometer.

4:15 p.m.	Jackson B. * Sandidge W. Briggs J.	Adams E. R. Kreyche S.	<u><i>A Search for Variability in the Atmosphere of the Hot Jupiter Kepler-76 b</i></u> [#3167] Exo-Jupiters / Searing and turbulent worlds / Clouds whorl violently.
4:30 p.m.	Kohler E. * Marcum S.	Ferguson F.	<u><i>Measuring the Properties of Forsterite for Exoplanet Cloud Formation and Identification</i></u> [#2946] Experiments were conducted to directly measure the evaporation rate of forsterite for use in exoplanet cloud formation models.

Monday, March 18, 2019

[M155]

HABITABILITY: TOO HOT! TOO COLD! AH, JUST RIGHT!

2:30 p.m. Montgomery Ballroom

Chairs: Edgard Rivera-Valentín and Heather Smith

Times	Authors (*Denotes Presenter)	Abstract Title and Summary	
2:30 p.m.	Méndez A. *	<u><i>The Diversity and Distribution of Habitable Worlds</i></u> [#2981] We estimate that there are at least five major types of habitable worlds. Those more abundant are harder to detect and those similar to Earth are less common.	
2:45 p.m.	Abramov O. * Mojzsis S. J.	Brasser R.	<u><i>Comprehensive Modeling of Late Accretion Impacts on Earth</i></u> [#3181] This presentation will outline our current understanding of late accretion impact bombardment and discuss its thermal, geochemical, and biological effects.
3:00 p.m.	Moore C. A. * Moore J. E.	Smith C. L.	<u><i>Habitability of the Martian Subsurface: An Ultraviolet Perspective</i></u> [#2482] A theoretical exercise to assess the depth into the subsurface at which terrestrial radioresistant organisms can survive under martian insolation.
3:15 p.m.	Chevrier V. F. * Valentín E. G. Altheide T. S.	Rivera-Soto A. Melchiorri R.	<u><i>Existence of Martian Special Regions Based on the Stability and Distribution of Liquid Brines</i></u> [#2093] Deliquescence of brines only occurs for lowest eutectic salts and at high latitudes on Mars, putting strong limitations on the possibility of special regions.
3:30 p.m.	Stamenkovic V. * Mischna M.	Ward L. M. Fischer W. W.	<u><i>O₂ Solubility in Martian Near-Surface Environments and Implications for Aerobic Life on Mars</i></u> [#2784] We find that brines on Mars could contain enough oxygen for microbes to breathe.
3:45 p.m.	Smith H. D. * Schuerger A. C.	Duncan A. G. McKay C. P.	<u><i>Changes in Phospholipid Content of Hypersaline Crust After Exposure to Mars Simulated Conditions</i></u> [#2870] This study looked at the changes in PLFA content in a microbial community within a salt crust exposed to simulated martain conditions.
4:00 p.m.	Craig P. I. * Marnocha C. L.	Mickol R. L. Kral T. A.	<u><i>Clay Minerals: A Martian Microbe's Favorite Snack</i></u> [#2522] Methanogens can grow on Mars-relevant clay minerals without supplemental media, suggesting Noachian Mars could potentially have supported microbial life.
4:15 p.m.	Yazdani A. * Chevrier V. F.	Nepal S. Kumar P.	<u><i>Adaptive Evolution of Bacteria to High Concentrations of Magnesium Sulfate: Implications for Europa</i></u> [#3019] In this study we explore the adaptive evolution of bacteria to high concentrations of magnesium sulfate, which is the dominant salt in Jupiter's moon Europa.
4:30 p.m.	Hesse M. A. * Vance S. D.	Jordan J. S. McCarthy C.	<u><i>Oxidant Transport Through Europa's Ice Shell by Porosity Waves</i></u> [#1489] The habitability of Europa's interior ocean depends on the availability of redox gradients. We study oxidant transport by downward percolation of dense brines.

ORAL SESSION

Tuesday Morning, March 19, 8:30 a.m.

Room	Session	Session Title	Page
Waterway Ballroom 1	T201	Ice, Ice, Io	15
Waterway Ballroom 4	T202	Processes on Modern Mars	15
Waterway Ballroom 5	T203	Special Session: OSIRIS-REx at Asteroid Bennu	16
Waterway Ballroom 6	T204	Planetary Tectonics and Interior Dynamics	17
Montgomery Ballroom	T205	Mercury: Magnetism, Magma, and More	18

Tuesday Morning, March 19, 10:15 a.m.

Room	Session	Session Title	Page
Waterway Ballroom 1	T206	Lunar Impacts and Regolith Processes: New Exploration	19

Tuesday Afternoon, March 19, 1:30 p.m.

Room	Session	Session Title	Page
Waterway Ballroom 1	T251	Origin and Differentiation of the Moon	20
Waterway Ballroom 4	T252	Martian Brines: Old Salts and New Views	21
Waterway Ballroom 5	T253	Special Session: Hayabusa2 Unveiling Asteroid Ryugu	22
Waterway Ballroom 6	T254	Icy Satellites: Dynamic Ice Shells	23
Montgomery Ballroom	T255	Impacts: Target Earth I	24

Tuesday Afternoon, March 19, 3:15 p.m.

Room	Session	Session Title	Page
Waterway Ballroom 6	T256	Planetary Aeolian Processes	25

Tuesday, March 19, 2019

[T201]

ICE, ICE, IO

8:30 a.m. Waterway Ballroom 1

Chairs: Jonathan Kay and Tracy Gregg

Times	Authors (*Denotes Presenter)	Abstract Title and Summary
8:30 a.m.	Teodoro L. * Kegerreis J. Estrada P. Cuzzi J. Eke V. et al.	<u><i>The Origin of Saturn's Rings Revisited</i> [#2802]</u> Impact simulations of the Saturn's icy moons with unprecedented spatial resolution allow us to shed light on the Saturn's rings age.
8:45 a.m.	Asphaug E. * Emsenhuber A.	<u><i>Giant Impacts Around Saturn</i> [#1793]</u> We revisit a scenario for the formation of Saturn's middle-sized moons via giant impact by taking into account the presence of Saturn in the model.
9:00 a.m.	Gyalay S. * Dodds K. H. Nimmo F.	<u><i>Estimates for Moments of Inertia and Present Day Heat Fluxes of Tethys and Mimas from Their Long-Wavelength Topographies</i> [#1715]</u> We translate long-wavelength topography into spatial variations of tidal heating via isostasy. This reveals the interiors of Tethys and Mimas.
9:15 a.m.	Wong T. * Hansen U. Wiesehöfer T. Stellmach S. McKinnon W. B.	<u><i>Layer Formation and Evolution in Europa's Subsurface Ocean by Double-Diffusive Convection</i> [#1580]</u> Europa's subsurface ocean can be layered by the process of double-diffusive convection, which may affect heat and material transport through the ocean.
9:30 a.m.	Kiefer W. S. *	<u><i>Io's Heat Flux and Implications for the Distribution of Tidal Heating in its Interior</i> [#2311]</u> Galileo observations of Io's heat flux suggest that 50–75% of Io's tidal heating occurs in a shallow asthenosphere.
9:45 a.m.	Klimczak C. * Byrne P. K. Regensburger P. V. Bohnenstiehl D. R. Hauck, II S. A. et al.	<u><i>Strong Ocean Floors Within Europa, Titan, and Ganymede Limit Geological Activity There; Enceladus Less So</i> [#2912]</u> Lots of water makes / The floor strong and hard to break / So not much happens.
10:0 a.m.	Miller K. E. * Glein C. R. Waite J. H. Bolton S. J.	<u><i>Using D/H Ratio of Water and Volatile Organics to Constrain Thermoogenic Processes Inside Ice-Rock Bodies</i> [#3013]</u> Water, organics / H exchange in heated cores / Varies in extent.

TUES ORAL

Tuesday, March 19, 2019

[T202]

PROCESSES ON MODERN MARS

8:30 a.m. Waterway Ballroom 4

Chairs: Alfred McEwen and Lauren Mc Keown

Times	Authors (*Denotes Presenter)	Abstract Title and Summary
8:30 a.m.	McEwen A. S. * Schafer E. Sutton S. Chojnacki M.	<u><i>Abundant Recurring Slope Lineae (RSL) Following the 2018 Planet-Encircling Dust Event (PEDE)</i> [#1376]</u> We gonna rock down to electric RSL and then we'll take it higher.
8:45 a.m.	Tebolt M. * Schorghofer N. Goudge T. Levy J.	<u><i>Slope, Elevation, and Thermal Inertia Trends of Recurring Slope Lineae: RSL Initiation and Termination Points Fall Outside the Angle of Repose</i> [#1561]</u> We examine the possibility of various wet and dry formation processes of recurring slope lineae by analyzing the physical characteristics of 10,000+ RSL.
9:00 a.m.	Heyer T. * Kreslavsky M. Hiesinger H. Reiss D. Bernhardt H. et al.	<u><i>Slope Streaks on Mars: Seasonal Dependence of Formation Rates</i> [#1205]</u> Seasonal variations in slope streak activity were observed at intermediate latitudes as well as at the equator.
9:15 a.m.	Imamura S. * Sekine Y. Maekawa Y. Sasaki T.	<u><i>The Role of Salt Precipitation for Morphological Features Due to Brine Flow on Mars</i> [#2397]</u> Results of laboratory experiments suggest that due to salt precipitation within soils, brine flow forms elongated streaks on Mars even at a low flow rate.

9:30 a.m.	Guimpier A. * Mangeny A. Mangold N.	Conway S. J. Peruzzetto M.	<u><i>A Recent Mudflow in the Nili Fossae Region of Mars: Morphology and Numerical Simulations</i> [#1900]</u> Report on a landslide near the Nili Fossae region on Mars whose morphology resembles mudslides on Earth.
9:45 a.m.	Raack J. * Heyer T. Hiesinger H.	Conway S. J. Philippe M. et al.	<u><i>Contemporary Gully Activity in Sisyphi Cavi, Mars</i> [#1237]</u> Study of present-day active gullies in Sisyphi Cavi: Exact timings, thermal investigations, orientations, and presentation of a potential formation mechanism.
10:00 a.m.	Khuller A. R. *	Christensen P. R.	<u><i>Evidence of Water-Rich Snow Deposits Within Martian Gullies</i> [#3060]</u> We present novel visible, spectral, and thermal evidence of decameter-scale, water-rich snow deposits being exhumed within mid-latitude gully alcoves.
10:15 a.m.	Parsons R. A. * Miyamoto H.	Hemmi R. Kanzaki T.	<u><i>Cold-Based Glaciation and Moraine Deposition at Pavonis Mons, Mars</i> [#1762]</u> Obliquity-induced temperature variations influence the flow rate of an advancing equatorial ice sheet — facilitating ridge deposition on Tharsis Montes flanks.
10:30 a.m.	Soare R. J. * Williams J.-P. Mc Keown L. E.	Conway S. J. Gallagher C.	<u><i>Possible Pingo and Ice Wedge/Thermokarst Complexes in Utopia Planitia, Mars</i> [#1131]</u> We discuss martian mounds, whose shape, traits, scale, and spatially-associated landscape features would be expected were the mounds closed-system pingos.
10:45 a.m.	Grimm R. E. * Stillman D. E.	Michaels T.	<u><i>Multiphase Thermal Modeling of Martian Recurring Slope Lineae</i> [#1737]</u> RSL at five sites can initiate as liquid flows with the same ice-melting temperature near 250 K by considering differences in shallow subsurface structure.
11:00 a.m.	Knightly J. P. * Farnsworth K.	Fusco M. S. Chevrier V. F.	<u><i>Temporal Variations of Swiss Cheese Terrain</i> [#2187]</u> Observations of temporal variations and potential factors influencing the growth rate of Swiss Cheese Terrain on the south polar cap between Mars years 28–34.
11:15 a.m.	Hao J. * Adeli S. Portyankina G.	Michael G. G. Hauber E. et al.	<u><i>Variability of Araneiform Spatial Patterns at the Martian South Pole</i> [#2941]</u> Regional variation in the spiders' local spatial distribution was discussed. We tried to investigate possible constraints on spider spatial patterns.
11:30 a.m.	Mc Keown L. E. * McElwaine J. N. Patel M. R.	Bourke M. C. Sylvest M. E.	<u><i>An Investigation of the Physical Constraints on Araneiform Morphometry</i> [#2762]</u> We present the first laboratory observations of the formation of araneiforms by CO ₂ sublimation and the results of a survey of araneiform morphometry on Mars.

Tuesday, March 19, 2019

[T203]

SPECIAL SESSION: OSIRIS-REX AT ASTEROID BENNU

8:30 a.m. Waterway Ballroom 5

Chairs: Dante Lauretta and Erica Jawin

Times	Authors (*Denotes Presenter)	Abstract Title and Summary	
8:30 a.m.	Lauretta D. S. * Ballouz R. L. Bierhaus E. B.	Al Asad M. M. Barnouin O. S. et al.	<u><i>OSIRIS-REx Arrives at Asteroid (101955) Bennu: Exploration of a Hydrated Primitive Near-Earth Asteroid</i> [#2608]</u> We report the initial assessment of asteroid Bennu from data acquired during the Approach and Preliminary Survey phases of the OSIRIS-REx mission.
8:45 a.m.	Barnouin O. S. * Gaskell B. et al.	Palmer E. Weirich J. Daly M.	<u><i>Investigating the Shape of Bennu</i> [#1744]</u> We present results on the shape of Bennu, using newly acquired data by the OSIRIS-REx mission.
9:00 a.m.	Susorney H. C. M. * Johnson C. L. Daly M. G.	Barnouin O. S. Al Asad M. M. et al.	<u><i>The Global Surface Roughness of 101955 Bennu: First Results from the OSIRIS-REx Mission</i> [#1429]</u> Shape model studied / Surface roughness of Bennu / Boulders and craters.

9:15 a.m.	Al Asad M. M. * Johnson C. L. Barnoiun O. S. Daly M. Palmer E. et al.	<u><i>How Good are Our Efforts? Evaluating the Stereophotoclinometry (SPC)-Derived Shape Model of Asteroid Bennu</i></u> [#1495] We present a summary of our efforts for assessing and evaluating the shape models produced by stereophotoclinometric (SPC) models of asteroid Bennu.
9:30 a.m.	Scheeres D. J. * McMahon J. W. French A. S. Brack D. N. Leonard J. et al.	<u><i>The Gravity and Global Geophysical Environment of (101955) Bennu</i></u> [#1496] The global geophysical implications and interpretations of Bennu's estimated mass, shape, and spin state are discussed.
9:45 a.m.	Rizk B. * DellaGiustina D. N. Golish D. R. Bennett C. A. Drouet d'Aubigny C. et al.	<u><i>Results from Early Resolved Images of Asteroid Bennu</i></u> [#1717] The OSIRIS-REx Camera Suite (OCAMS) PolyCam and MapCam early images of Bennu reveal a fascinating small body.
10:00 a.m.	Walsh K. J. * Jawin E. R. McCoy T. Connolly H. C. Jr. Lauretta D. S. et al.	<u><i>Bennus' Global Geology</i></u> [#1898] A global overview of the geology of NEA Bennu, including its craters, boulders, linear features, and regolith.
10:15 a.m.	Ballouz R.-L. * Walsh K. J. Schwartz S. R. Baresi N. Barnouin O. S. et al.	<u><i>Crater Erasure on Small Bodies: Synthesizing Dynamical Surface Processes in Bennu's Journey to Near-Earth Space</i></u> [#1642] Impacts and spin-up / Move grains on Bennu's surface / Craters disappear.
10:30 a.m.	Jawin E. R. * Walsh K. J. Barnouin O. S. McCoy T. J. Ballouz R.-L. et al.	<u><i>The Geology of Bennu's Biggest Boulders</i></u> [#1577] The largest boulders on Bennu are diverse in their apparent lithology and local geologic setting.
10:45 a.m.	Molaro J. L. * Delbo M. Ballouz R.-L. Jawin E. Walsh K. et al.	<u><i>Fracture Formation Mechanisms on Bennu and Evidence of Thermally Driven Breakdown</i></u> [#1597] We relate numerical simulations to observations to explore the role that thermally induced stresses play in the development of fractures on Bennu's surface.
11:00 a.m.	Emery J. P. * Rozitis B. Christensen P. R. Hamilton V. E. Simon A. A. et al.	<u><i>Thermophysical Properties of (101955) Bennu from OSIRIS-REx Observations</i></u> [#2582] Full-disk thermal observations of Bennu from OSIRIS-REx are analyzed to derive thermophysical properties of Bennu's surface.
11:15 a.m.	Hamilton V. E. * Simon A. A. Christensen P. R. Reuter D. C. Della Giustina D. N. et al.	<u><i>VNIR and TIR Spectral Characteristics of (101955) Bennu from OSIRIS-REx Approach and Preliminary Survey Observations</i></u> [#1956] VNIR and TIR spectrometers onboard OSIRIS-REx have revealed evidence of hydrated phases across the surface of asteroid (101955) Bennu.
11:30 a.m.	Simon A. A. * Reuter D. C. Howell E. S. Clark B. E. Hamilton V. E. et al.	<u><i>Disk-Integrated Hydrated Mineral Features on (101955) Bennu with OVIRS</i></u> [#1244] Hello, small Bennu! / Hydration seen everywhere / What secrets await?

Tuesday, March 19, 2019

[T204]

PLANETARY TECTONICS AND INTERIOR DYNAMICS

8:30 a.m. Waterway Ballroom 6

Chairs: Robert Anderson and Debra Buczkowski

Times	Authors (*Denotes Presenter)	Abstract Title and Summary
8:30 a.m.	Anderson R. C. * Dohm J. M. Siwabessy A. Schroeder J. F.	<u><i>Unraveling the Complex Tectonic History of the Memnonia-Sirenum Region: A Window into the Early Formation of the Tharsis Rise</i></u> [#1907] A detailed reconstruction of the tectonic history of the Memnonia-Sirenum region of Mars is presented here through a new 1:5,000,000-scale USGS map.
8:45 a.m.	Citron R. I. * Manga M.	<u><i>Superplume Formation on Mars Following a Giant Impact</i></u> [#1322] We examine if following a giant impact on early Mars, a superplume could develop in the hemisphere opposite the impact.
9:00 a.m.	Broquet A. * Wieczorek M. A. Fa W.	<u><i>Geodynamic State of the Lithosphere Beneath the Northern Polar Cap of Mars</i></u> [#1892] Inversion of the present-day geodynamic state of Mars beneath the northern polar cap using elevation data from MOLA and radar data from MARSIS.

9:15 a.m.	Brennan M. C. * Fischer R. A. Irving J. C.	<u><i>Using Core Formation and Geophysical Modeling to Predict the Core Radius and Seismic Properties of Mars</i></u> [#1601] We modeled core formation and planetary structure to explore the parameters of importance for Mars' core size and the seismic properties observable by InSight.
9:30 a.m.	Schmerr N. C. * Kawamura T. Margerin L. van Driel M. Garcia R. et al.	<u><i>Measuring the Scattering and Attenuation of Seismic Waves in Mars with the Insight Seismometers</i></u> [#1644] Waves grow weak in Mars / What mechanisms drive this loss? / InSight will tell us!
9:45 a.m.	Andrews-Hanna J. C. *	<u><i>A Taxonomy of Wrinkle Ridges on Mars</i></u> [#2922] The topography of wrinkle ridges on Mars was analyzed, yielding three main ridge classes. Inversions of the profiles reveal the underlying geometry of faults.
10:00 a.m.	Clark J. D. * van der Bogert C. H. Hiesinger H. Watters T. R. Robinson M. S.	<u><i>Fault Slip Movement Along Wrinkle Ridge-Lobate Scarp Transitions in the Last 100 Ma</i></u> [#2084] Age determinations for wrinkle ridge-lobate scarp transitions reveal seismically induced resurfacing by fault slip events in the last 100 Ma.
10:15 a.m.	Martin E. S. * Watters T. R.	<u><i>Evaluating the Mascon Tectonic Model with High-Resolution Topography</i></u> [#2011] We evaluate two mechanisms for producing basin-centric graben on the Moon: (1) Extension due to lithospheric flexure, or (2) shallow-dike-induced dilation.
10:30 a.m.	Yu S. * Tosi N. Schulz F. Schwinger S. Breuer D. et al.	<u><i>Overturn of Ilmenite-Bearing Cumulates Activated by Non-Linear Mantle Rheology</i></u> [#2115] We check the rheological conditions needed for lunar magma ocean overturn in the context of non-linear mantle rheology.
10:45 a.m.	Weller M. B. * Fuchs L. Becker T. W. Soderlund K. M.	<u><i>Geodynamics of Icy Satellites: Effects of Latitudinal Surface Temperature Variations and Yielding in Thin Shells</i></u> [#2792] Icy shells ahoy / Solar insolation drives / Direction of flow.
11:00 a.m.	Chivers C. J. * Patterson G. W. Schmidt B. E.	<u><i>Europa's Tortured Ridges: A Case Study</i></u> [#2474] Europa's double ridges are generally considered nearly linear, but those that aren't may provide insight to other properties and processes in the shell.
11:15 a.m.	Kinczyk M. J. * Byrne P. K. Collins G. C. Patterson G. W. Bohnenstiehl D. R.	<u><i>Stress Risers in Enceladus' Cratered Terrain</i></u> [#1446] Enceladus cracks / Reoriented fractures / Are holes the culprit?
11:30 a.m.	Hay H. C. F. C. * Matsuyama I.	<u><i>Planet-Planet Tidal Heating in the TRAPPIST-1 System</i></u> [#1980] Planet pulls planet / Resulting dissipation / Rests on frequency.

Tuesday, March 19, 2019

[T205]

MERCURY: MAGNETISM, MAGMA, AND MORE

8:30 a.m. Montgomery Ballroom

Chairs: Karen Stockstill-Cahill and Edgar Steenstra

Times	Authors (*Denotes Presenter)	Abstract Title and Summary
8:30 a.m.	Bandfield J. L. * Osterloo M. M. Holsclaw G. M.	<u><i>Thermophysical Properties of Mercury: Revisiting Mariner 10 IRR Measurements</i></u> [#2653] Mariner 10 infrared measurements show evidence of regolith layering, rocky younger craters, and regions of low thermal inertia with similarities to Earth's Moon.
8:45 a.m.	Dong C. F. * Wang L. Hakim A. Bhattacharjee A. Slavin J. A. et al.	<u><i>A Novel High-Moment Two-Fluid Model for Mercury's Dynamic Magnetosphere: From the Planetary Interior to Interplanetary Space</i></u> [#3267] We studied Mercury's dynamic magnetosphere by using a novel high-moment two-fluid model that is capable of reproducing MESSENGER's observations beyond MHD model.

9:00 a.m.	Plattner A. M. * Johnson C. L.	<u><i>Large-Scale Non-Axisymmetric Internal Structure of Mercury's Magnetic Field</i></u> [#1645] We image the non-axisymmetric large-scale internal magnetic field of Mercury from longitudinal components and confirm its pattern using the radial component.
9:15 a.m.	Mouser M. D. * Dygert N. Grambling N. L. Anzures B. A. Kono Y. et al.	<u><i>Viscosity of the Mercurian Magma Ocean: Implications for Crystal Fractionation and Crustal Petrogenesis</i></u> [#2030] Viscometry experiments on a Mercurian composition constrain crystal fractionation and formation of the mantle during magma ocean solidification.
9:30 a.m.	Stockstill-Cahill K. R. * Peplowski P. N.	<u><i>Exploring the Geochemical Implications of Terranes Derived from Principal Components Analysis</i></u> [#2682] A PCA map / Heterogeneous surface / Mercury's story.
9:45 a.m.	James P. B. * Goossens S. Mazarico E.	<u><i>Crustal Density Estimation from Line-of-Sight Accelerations at Mercury</i></u> [#2458] We use Line-of-Sight (LOS) acceleration residuals from the lowest orbits of the MESSENGER spacecraft to estimate the bulk densities of Mercury's crust.
10:00 a.m.	Goossens S. * James P. B. Mazarico E. Genova A.	<u><i>Estimation of Crust and Lithospheric Properties for Mercury from High-Resolution Gravity Field Models</i></u> [#2202] We present a new, high-resolution gravity model for Mercury from line-of-sight data, and we use this new model to perform a localized admittance study.
10:15 a.m.	Du J. * Wieczorek M. A. Fa W.	<u><i>Lava Flow Thickness Estimation of the Northern Smooth Plains on Mercury Based on Partially Buried Craters</i></u> [#1836] We provide the first estimate of the lava flow thickness for the northern smooth plains on Mercury by modeling the degradation of partially buried craters.
10:30 a.m.	Wright J. * Conway S. J. Rothery D. A. Balme M. R.	<u><i>Long-Lived, Volatile-Driven Modification of Caloris Ejecta Blocks</i></u> [#1548] The circum-Caloris knobs (Caloris ejecta) encroach on craters and scarps that postdate Caloris. Their conical shape could arise from loss of volatiles.
10:45 a.m.	Zharkova A. Yu. Kreslavsky M. A. * Head J. W. III	<u><i>Rarity of Boulders on Mercury: Comparison with the Moon</i></u> [#1162] Boulders on Mercury are rare in comparison to the Moon (~30x). We discuss factors that decrease boulder production and increase obliteration rates on Mercury.
11:00 a.m.	Malliband C. C. * Conway S. J. Rothery D. A. Balme M. R.	<u><i>Potential Identification of Downslope Mass Movements on Mercury Driven by Volatile-Loss</i></u> [#1804] We have identified lineated mass movements on some young slopes. These features are not common and may be linked to volatile sublimation.
11:15 a.m.	Fei Y. * Tao R. Yang J.	<u><i>Constraint on Density Jump at the Inner Core Boundary from Silicon and Sulfur Partitioning Between Mercury's Inner and Outer Core</i></u> [#1617] We present data on melting relations in the Fe-Si-S system to the center pressure of Mercury. Partitioning data are used to constrain the density jumps at inner core boundary.
11:30 a.m.	Vander Kaaden K. E. * Blewett D. T. Byrne P. K. Chabot N. L. Ernst C. M. et al.	<u><i>Mercury Exploration: Looking to the Future</i></u> [#1105] Future of science / Enigmatic Mercury / We need a sample.

Tuesday, March 19, 2019

[T206]

LUNAR IMPACTS AND REGOLITH PROCESSES: NEW EXPLORATION

10:15 a.m. Waterway Ballroom 1

Chairs: Makiko Ohtake and Yang (Steve) Liu

Times	Authors (*Denotes Presenter)	Abstract Title and Summary
10:15 a.m.	Runyon K. D. * Moriarty D. Denevi B. W. Jozwiak L. M. Cohen B. A. et al.	<u><i>Yerkes Crater Central Peak as a Sample Site for Dating Crisium Basin</i></u> [#1854] Crisium Basin / How old are you, young or old? / Must date Yerkes' peaks.

10:30 a.m.	Liu T. * Michael G. Wünnemann K. Oberst O.	<u><i>Spatial Diffusion of Basin Melt by Impact Gardening: Implications for the Ejecta Source of Apollo Samples and Future Sampling</i></u> [#1241] We developed a numerical model to investigate diffusion of basin melt. The melt component of Apollo samples was estimated and compared with radiometric ages.
10:45 a.m.	Sargeant H. M. * Bickel V. T. Honniball C. I. Martinez S. N. Rogaski A. et al.	<u><i>Determining the Bearing Capacity of Permanently Shadowed Regions of the Moon Using Boulder Tracks</i></u> [#1792] This work uses lunar boulder tracks to calculate the bearing capacity of regolith in PSRs, and discusses the implications for future missions.
11:00 a.m.	Ohtake M. * Saiki K. Nakauchi Y. Shiraishi H. Ishihara Y. et al.	<u><i>Geology of the Crater Theophilus on the Moon: Landing Site of the Smart Lander for Investigating the Moon</i></u> [#2342] Analyses revealed that the central peak mainly consists of olivine-dominant unit (excavated from depth) with lesser amounts of PAN and Mg-spinel bearing units.
11:15 a.m.	Xiao L. * Qian Y. Q. Wang J. Huang J. Zhao J. N. et al.	<u><i>First and Historic Lunar Far Side Landing and Exploration of China's Chang'E-4 Mission</i></u> [#1538] The successful far side landing of China's Chang'e-4 lunar exploration mission is introduced.
11:30 a.m.	Ling Z. C. * Jolliff B. L. Liu C. Q. Qiao L. Cao H. J. et al.	<u><i>A Close View of Chang'E-4 Landing Site and Science Questions to be Answered by Yutu-2</i></u> [#2330] We report on the geological and compositional properties of the CE-4 landing site to place remote sensing observation constraints for Yutu-2 operations.

Tuesday, March 19, 2019

[T251]

ORIGIN AND DIFFERENTIATION OF THE MOON

1:30 p.m. Waterway Ballroom 1

Chairs: Amy Fagan and Nicholas Dygert

Times	Authors (*Denotes Presenter)	Abstract Title and Summary
1:30 p.m.	Budde G. * Burkhardt C. Kleine T.	<u><i>Molybdenum Isotopic Evidence for an Outer Solar System Origin of the Moon-Forming Impactor</i></u> [#2349] Earth's Mo isotope composition is intermediate between the CC and NC reservoirs, suggesting that the Moon-forming impactor is a CC embryo from beyond Jupiter.
1:45 p.m.	Lock S. J. * Stewart S. T. Petaev M. I. Jacobsen S. B.	<u><i>A Terrestrial Synestia: A New Environment for Formation of the Moon</i></u> [#1784] Synestias are / Very different from disks / Form a Moon like ours.
2:00 p.m.	Fischer R. A. * Nimmo F.	<u><i>Quantifying the Probability of the Earth and Moon Having the Same Tungsten Isotopic Composition</i></u> [#3173] It is possible, though unlikely, that the Earth and Moon inherited identical tungsten isotopic compositions by chance.
2:15 p.m.	Nielsen S. G. * Auro M. Kleine T.	<u><i>The Vanadium Isotope Composition of the Moon: Isotopic Test of the Giant Impact Hypothesis?</i></u> [#1612] We use vanadium isotope ratios measured in Apollo samples to test the giant impact hypothesis.
2:30 p.m.	Charnoz S. * Lee YN. Sossi P. Allibert L. Siebert J. et al.	<u><i>Efficient Early Moon Devolatilisation Just After Its Formation, Through Tidally Assisted Hydrodynamic Escape</i></u> [#2395] We explain the devolatilisation of the Moon material through degassing, aided by the Earth tidal field, just after its formation in a giant impact.
2:45 p.m.	Cano E. C. * Sharp Z. D. Shearer C. K.	<u><i>Oxygen Isotope Variation in the Moon and Implications for the Giant Impact</i></u> [#2927] Oxygen isotope variation found in lunar samples has a strong correlation with rock type and suggests a distinct isotopic difference between the Earth and Moon.
3:00 p.m.	Nie N. X. * Dauphas N.	<u><i>Rubidium Isotopic Compositions of the Earth and the Moon</i></u> [#2098] The Moon is enriched in heavy Rb isotopes compared with the Earth.

3:15 p.m.	Snape J. F. * Nemchin A. A. Whitehouse M. J. van Westrenen W.	<u><i>Lunar Magma Ocean Crystallisation: Constraints from Experimental and Analytical Studies</i> [#1529]</u> Here we use recent advances in Pb isotopic analyses of lunar samples and LMO models to place new constraints on the early magmatic evolution of the Moon.
3:30 p.m.	Boukaré C.-E. Parmentier E. M. * Parman S. W.	<u><i>Imposed Surface Heat Flux Does Not Necessarily Control Magma Ocean Solidification Timescale</i> [#2291]</u> The imposed surface heat flux dictates the MO solidification timescale only if heat convective transport in the MO can sustain this imposed heat flux.
3:45 p.m.	Evans A. J. *	<u><i>The Lunar Geochemical Asymmetry: Implications for KREEP and Magma Ocean Crystallization</i> [#2733]</u> Constraints are placed on the subsurface distribution and evolution of KREEP and other late-stage magma ocean cumulates throughout early lunar history.
4:00 p.m.	Dygart N. * Liang Y. Hirth G. Zhang N.	<u><i>Viscous Flow of Ilmenite-Bearing Cumulates During Lunar Magma Ocean Solidification: Consequences for Lunar Evolution</i> [#2798]</u> Dense ilmenite-bearing cumulates of the LMO sank as Rayleigh-Taylor instabilities during crystallization. We evaluate scenarios and implications for overturn.
4:15 p.m.	Prissel K. B. * Krawczynski M. J.	<u><i>Iron, Titanium, and Magnesium Isotopic Compositions of Lunar Ilmenite-Bearing Cumulates</i> [#1912]</u> Were mare basalt / Isotope compositions / Sourced from ilmenite?
4:30 p.m.	Brodsky H. F. * Brown S. M. Grove T. L.	<u><i>Origin of the High-Titanium Lunar Glasses: Constraints from Cumulate Remelting Experiments</i> [#2986]</u> Lunar magma ocean cumulate remelting experiments provide evidence for deep (> 800km) melting of overturned late stage ilmenite-bearing cumulates.

Tuesday, March 19, 2019

[T252]

MARTIAN BRINES: OLD SALTS AND NEW VIEWS

1:30 p.m. Waterway Ballroom 4

Chairs: Albert Yen and Katherine Primm

Times	Authors (*Denotes Presenter)	Abstract Title and Summary
1:30 p.m.	Hood D. R. * Karunatillake S. Gasnault O. Williams A. Dutrow B. et al.	<u><i>Contrasting Regional Soil Hydration Processes Across the Topographic Dichotomy of Mars</i> [#1887]</u> Mars soil chemistry / Principal components show / Widespread altered soils.
1:45 p.m.	Leask E. K. * Ehlmann B. L. Dundar M. M.	<u><i>Evidence for Chemically Distinct Waters Forming Sulphates and Chlorides in Terra Sirenum, Mars</i> [#2636]</u> Chloride and sulphate deposits in Terra Sirenum, Mars, appear to have formed independently, from chemically distinctive water reservoirs.
2:00 p.m.	Hill J. R. * Christensen P. R.	<u><i>Applying the THEMIS Quasi-Spectral Chloride Index to the Martian Southern Highlands</i> [#3213]</u> The THEMIS quasi-spectral chloride index has been validated against known deposits and is being applied to the southern highlands to find additional deposits.
2:15 p.m.	Primm K. M. * Stillman D. E.	<u><i>Investigating the Hysteretic Behavior of Mars-Relevant Salts</i> [#1291]</u> When freezing salt brines / Eutectic temps depend on / Maximum temp reached.
2:30 p.m.	Stillman D. E. * Primm K. P. Codd S. L. Seymour J. D. Lei P. et al.	<u><i>Magnetic Resonance and Dielectric Spectroscopy Investigations of Liquid Vein Networks Within Ice and Ice-Regolith Mixtures</i> [#2537]</u> Lab measurements of ice and ice-regolith to better understand the micro-structural properties of unfrozen liquid vein networks.
2:45 p.m.	Slank R. A. * Chevrier V. F. Rivera-Valentin E. G.	<u><i>Experimental Simulation of Calcium Perchlorate Liquid Brine Formation Through Deliquescence on Mars</i> [#1473]</u> It is known that perchlorates can deliquesce at the surface of Mars; now looking at the range in which they do experimentally.

3:00 p.m.	Nuding D. L. * Gough R. V. Toigo A. D. Guzewich S. Tolbert M. A.	<u><i>An Examination of Atmospheric Water Vapor as a Source for Recurring Slope Lineae on Mars</i></u> [#3113] Martian soil soaking / Up water and sun; does it / Change with the seasons? / Water vapor at / Recurring slope lineae / Potential trigger?
3:15 p.m.	Bishop J. L. * Toner J. D. Englert P. Gulick V. C. McEwen A. S. et al.	<u><i>Salty Solution to Slipping Soils on Martian Slopes</i></u> [#1188] Melting subsurface ice on Mars may have triggered dissolution of subsurface gypsum and Cl salts that could have led to surface flows including RSL and gullies.
3:30 p.m.	Nellessen M. A. * Baker A. M. Newsom H. E. Jackson R. S. Williams J. et al.	<u><i>Distribution and Analysis of Calcium Sulfate-Cemented Sandstones Along the MSL Traverse, Gale Crater, Mars</i></u> [#3031] Detection and distribution of calcium-sulfate cements found in Gale Crater bedrock by MSL Curiosity by ChemCam and their implications for martian history.
3:45 p.m.	Rapin W. * Ehlmann B. L. Dromart G. Schieber J. Thomas N. et al.	<u><i>High Salinity Recorded by Bedrock Sulfate Enrichments at Gale Crater</i></u> [#2147] Ca and Mg sulfate enrichments have been observed disseminated in the bedrock at Gale Crater and may hold important implications on paleoenvironments.
4:00 p.m.	Yen A. S. * Gellert R. Achilles C. N. Berger J. A. Blake D. F. et al.	<u><i>Sulfur Compounds in the Murray Formation, Gale Crater, Mars</i></u> [#2083] X-ray amorphous Mg-sulfates are present throughout the Murray formation. Fluids depositing Ca-sulfates also carried Mg and Cl.
4:15 p.m.	Rao M. N. * Nyquist L. E. Ross D. K. Wentworth S. J.	<u><i>Acid-Sulfate Weathering Environment at Shergottite Provenance on Mars</i></u> [#1950] The shergottite rocks were weathered by acid sulfate solution having moderate pH (~ 3 to 5) and moderate water/rock ratios after 180 Myr ago on Mars.
4:30 p.m.	Tabata H. * Sekine Y. Kanzaki Y. Sugita S.	<u><i>Effect of the Atmospherically Attenuated Solar Spectrum at the Surface for Acidification of Surface Water on Early Mars</i></u> [#2322] Acidification of surface water on early Mars may have been triggered by a change in the solar spectrum at the surface due to decrease of volcanic gas emission.

Tuesday, March 19, 2019

[T253]

SPECIAL SESSION: HAYABUSA2 UNVEILING ASTEROID RYUGU

1:30 p.m. Waterway Ballroom 5

Chairs: Deborah Domingue and Masatoshi Hirabayashi

Times	Authors (*Denotes Presenter)	Abstract Title and Summary
1:30 p.m.	Watanabe S. * Hirabayashi M. Hirata N. Hirata N. Shimaki Y. et al.	<u><i>High Porosity Nature of the Top-Shape C-Type Asteroid 162173 Ryugu as Observed by Hayabusa2</i></u> [#1265] Hayabusa2's initial observations of near-Earth C-type asteroid Ryugu revealed its high porosity (>50%) and top shape, indicating its rubble-pile nature.
1:45 p.m.	Sugita S. * Honda R. Morota T. Kameda S. Honda C. et al.	<u><i>The Evolution of Ryugu's Parent Body Constrained by Hayabusa2 Imaging Observations</i></u> [#2622] Spectral and geomorphologic observations suggest that Ryugu's parent body is Eulalia or Polana and may have experienced partial dehydration.
2:00 p.m.	Schroeder S. E. * Jaumann R. Schmitz N. Otto K. Stephan K. et al.	<u><i>Ryugu as Seen Close-Up by the MASCOT Camera</i></u> [#2450] We describe the surface of C-type asteroid Ryugu as seen close-up by the camera of the MASCOT lander, in particular the morphology and color of one rock.
2:15 p.m.	Riu L. * Kitazato K. Milliken R. Abe M. Ohtake M. et al.	<u><i>Global View of the Mineralogy and Surface Properties of the Asteroid Ryugu Using NIRS3 Near-Infrared Spectrometer on Board Hayabusa2</i></u> [#1154] We present here the main results of the NIRS3 spectrometer instrument onboard Hayabusa2, describing the mineralogy and surface properties of asteroid Ryugu.

2:30 p.m.	Okada T. * Tanaka S. et al.	Fukuhara T. Taguchi M. Arai T.	<u><i>Thermal Imaging of C-Type Near Earth Asteroid 162173 Ryugu by Thermal Infrared Imager TIR on Hayabusa2</i> [#1325]</u> Global and close-up thermal images of C-type asteroid 162173 Ryugu taken by TIR on Hayabusa2 and its derived thermophysical properties are briefly introduced.
2:45 p.m.	Namiki N. * Senshu H. Matusmoto K.	Mizuno T. Noda H. et al.	<u><i>Topography of Large Craters of 162173 Ryugu</i> [#2658]</u> Crater topography of Ryugu is examined using Hayabusa2/LIDAR data. Depth-to-diameter ratio is between 0.14 and 0.2, and is distinguished from Itokawa and Bennu.
3:00 p.m.	Sakatani N. * Honda R. Yamada M.	Sugita S. Morota T. et al.	<u><i>Surface Physical Condition of Asteroid Ryugu Using Close-up Optical and Thermal Images</i> [#1732]</u> This study investigates surface condition of asteroid Ryugu by integrating the optical and thermal images acquired during descending operations of Hayabusa2.
3:15 p.m.	Grott M. * Hamm M. Jaumann R.	Knollenberg J. Ogawa K. et al.	<u><i>In-Situ Determination of Thermal Inertia on Near Earth Asteroid (162173) Ryugu Using MARA — The MASCOT Radiometer</i> [#1267]</u> Thermal infrared data obtained by the MASCOT radiometer indicate that boulders on Ryugu have low thermal conductivity and are highly porous.
3:30 p.m.	Morota T. * Kanamaru M. Kameda S.	Cho Y. Honda R. et al.	<u><i>Timescale of Reddening Process of the Ryugu Surface Based on the Crater Size-Frequency Distribution</i> [#2833]</u> We performed the crater counts on the Ryugu surface to constrain the age of reddening event or the timescale of reddening process of the Ryugu surface.
3:45 p.m.	Honda R. H. * Tatsumi E. T. Barucci A. B.	Yokota Y. Y. Hayashi R. H. et al.	<u><i>Clustering Analysis of Visible Spectra of Asteroid Ryugu and Its Preliminary Global Spectrum Map</i> [#2901]</u> Spectral clustering analysis was conducted to extract representative reflectance spectra across asteroid Ryugu's surface using Hayabusa2's ONC-T images.
4:00 p.m.	Yokota Y. * Tatsumi E. Schröder S. E.	Honda R. Domingue D. et al.	<u><i>Disk-Resolved Photometry of Asteroid 162173 Ryugu Obtained by Hayabusa2 Visible Camera ONC</i> [#3195]</u> We investigate the disk-resolved photometric properties of the asteroid Ryugu using images obtained by the Optical Navigation Camera (ONC) onboard Hayabusa2.
4:15 p.m.	Parekh R. * Schmitz N. Otto K.	Jaumann R. Schroeder S. et al.	<u><i>Morphology and Measurement of Fractal Dimension of Boulders on Ryugu</i> [#2229]</u> This abstract discusses the diversity of boulders that has been analysed using MasCam high resolution images from Hayabusa2 mission, which landed on Ryugu.
4:30 p.m.	Nakamura T. * Amano K. Mita H.	Matsuoka M. Kobayashi S. et al.	<u><i>Possible Interpretations of Visible/Near-Infrared Spectra of Asteroid Ryugu Obtained by the Hayabusa2 Mission</i> [#1681]</u> Possible interpretations of Ryugu spectra are introduced based on the spectral comparison between Ryugu (ONC and NIRS3 data) and various carbonaceous chondrites.

Tuesday, March 19, 2019

[T254]

ICY SATELLITES: DYNAMIC ICE SHELLS

1:30 p.m. Waterway Ballroom 6

Chairs: Steven Vance and Sarah Morrison

Times	Authors (*Denotes Presenter)	Abstract Title and Summary
1:30 p.m.	Leonard E. J. * Howell S.	<u><i>Compositional Variations Within Europa's Ice Shell: Implications for Surface Geology</i> [#2631]</u> Europa's ice shell / Freezing, thawing, and deformed. / Salts reveal record.
1:45 p.m.	Buffo J. J. * Huber C.	<u><i>Entrainment and Dynamics of Ocean Derived Impurities Within Europa's Ice Shell</i> [#2191]</u> Quantifying material entrainment at ice-ocean interfaces using multiphase reactive transport modeling — geophysical and astrobiological implications.

2:00 p.m.	Craft K. L. * Walker C. C. Quick L. C. Lowell R. P.	<u>"Freckles," "Spots," and Domes on Europa and Ceres: Surface Features Driven by Subsurface Cryovolcanic Diking, and Surface Response? [#3102]</u> Spots on Europa / Ceres has them too — Salts? Ice? / Cryovolcanism!
2:15 p.m.	Noviello J. L. * Rhoden A. R.	<u>Global Microfeature Mapping on Europa: Constraining Microfeature Formation Models and the Presence of Liquid Water in the Ice Shell [#1461]</u> Europa's surface / Hidden by coarseness, can now / Reveal new constraints.
2:30 p.m.	Singh V. * Gudipati M. S. Rhoden A. R. Henderson B. L.	<u>What Lies on Europa's Surface? Microphysics and Spectroscopy of Ice Grains Under Radiation [#1464]</u> Bleak icy landscape / Spectra will reveal your truth / The lab man cometh.
2:45 p.m.	Hemingway D. J. * Manga M. Rudolph M. L. Jordan J.	<u>Cascading Parallel Fractures Due to Thinning Ice and Bending Stresses: Implications from Enceladus's Tiger Stripes [#2075]</u> Parallel and regularly spaced fractures, like the Tiger Stripes, can form through a repeating sequence of thinning ice, bending stresses, and tensile failure.
3:00 p.m.	Hammond N. P. * Parmentier E. M. Barr A. C.	<u>Slow Flow: The Migration of Ammonia-Rich Melt Through an Ice Shell and Implications for Cryovolcanism on Triton [#1915]</u> Ammonia-melt will flow through the ice shell but quite slow. It gets trapped in the ice, and before you look twice, you have a cryovolcano.

Tuesday, March 19, 2019

[T255]

IMPACTS: TARGET EARTH I

1:30 p.m. Montgomery Ballroom

Chairs: Sean Gulick and Anna Losiak

Times	Authors (*Denotes Presenter)	Abstract Title and Summary
1:30 p.m.	Gulick S. P. S. * Christeson G. L. Morgan J.	<u>Heterogeneity of Large Impact Structures as Illuminated by Chicxulub: A Terrestrial Analog While Placing IODP-ICDP Expedition 364 in Context [#1654]</u> We discuss heterogeneities of the Chicxulub structure deposits and melt rocks placing IODP site M0077. Controls on such heterogeneities yield insights.
1:45 p.m.	Huber M. S. * Kovaleva E.	<u>Was the Vredefort Melt Sheet Similar Composition to the Sudbury Melt Sheet? [#2396]</u> Big impacts make melt sheets / Does massive crustal melting generate similar compositions? / Modeling tells us it can.
2:00 p.m.	Hill P. J. A. * Osinski G. R. Banerjee N. R.	<u>Through the Impact Glass: Understanding the Origin and Evolution of Impact Melt from the Mistastin Lake Impact Structure [#1664]</u> Through the impact glass / Mistastin Lake's origin / A story revealed.
2:15 p.m.	Jaret S. J. * King D. T. Jr Tailby N. D. Adams M. C. Ebel D. S.	<u>Impact Melt Clasts from the Flynn Creek Impact Structure, Tennessee — Temperature Constraints from Titanium-in-Quartz Thermometry [#3170]</u> High titanium / In quartz tells that it formed at / High temperature.
2:30 p.m.	Pickersgill A. E. * Mark D. F. Lee M. R. Osinski G. R.	<u>A Refined Age for the Gow Lake Impact Structure [#2375]</u> Gow Lake age (million) / One hundred ninety-seven / Argh! Extra argon.
2:45 p.m.	McGregor M. * McFarlane C. R. M. Spray J. G.	<u>Multiphase U-Pb Geochronology and Shock Analysis of Apatite, Titanite, and Zircon from the La Moinerie Impact Structure, Canada [#2428]</u> First higher precision age constraints on the La Moinerie impact crater, Canada using multiphase U-Pb geochronology on apatite, titanite, and zircon.
3:00 p.m.	Lambert P. * Alwmark C. Baratoux D. Bouley S. Brack A. et al.	<u>The Rochechouart 2017-Cores Rescaled: Major Features [#2005]</u> Presenting and discussing the rescaled and correlated core/borehole wall observations for the cumulated 544 m cores recovered in the Rochechouart impact structure.
3:15 p.m.	Ormö J. * Sturkell E. Lambert P.	<u>Sedimentological Evidence for a Forceful Resurge at the Rochechouart Impact Crater, France: Implications for Target Environment [#1785]</u> The SC2 core suevite deposits suggest a shallow marine target environment. It is important for cratering mechanics and paleoenvironmental reconstruction.

3:30 p.m.	El Kerni H. * Chennaoui Aoudjehane H. Baratoux D. Kenkmann T. Wulf G. et al.	<u><i>The Size and the Center of the Agoudal Impact Structure (Central High Atlas, Morocco) [#1331]</i></u> In order to constrain the center and the size of Agoudal Crater, the natural neighbor interpolation technique and the Concentric Deviation Method were used.
3:45 p.m.	Losiak A. * Belcher C. Jöeleht A. Plado J. Szyszko M.	<u><i>Death from Space: Origin of Charcoal Found in Proximal Ejecta Blanket of Kaali Craters (Is NOT What We Think) [#2406]</i></u> Pieces of charcoal found in the proximal ejecta blanket of Kaali craters were most probably not formed by the radiative heat of the bolide.
4:00 p.m.	Simpson S. L. * Osinski G. R. Longstaffe F. J.	<u><i>Hydrothermal Clay Mineral Production in Meteorite Impacts: Lessons from $\delta^2\text{H}$ and $\delta^{18}\text{O}$ of Smectites from the Chicxulub Peak-Ring [#1663]</i></u> Crater clays preserve / Isotopic memoirs of / Hot, strange histories.
4:15 p.m.	Hildebrand A. R. *	<u><i>The Highly Oblique Source Impact of the Australasian Tektite Strewn Field in Champasak Province, Laos [#3116]</i></u> The Australasian tektite strewn field source impact is located in Champasak, Laos; this highly oblique impact produced a doublet of two elliptical craters.
4:30 p.m.	Schultz P. H. * Harris R. S. Peroud S. Blanco N. Tomlinson A. J. et al.	<u><i>Late Pleistocene Fireballs Over the Atacama Desert, Chile [#2893]</i></u> A series of intense fireballs during the Late Pleistocene generated widespread glasses through radiative and convective heating.

Tuesday, March 19, 2019

[T256]

PLANETARY AEOLIAN PROCESSES

3:15 p.m. Waterway Ballroom 6

Chairs: Cong Pan and James Zimbelman

Times	Authors (*Denotes Presenter)	Abstract Title and Summary
3:15 p.m.	Pan C. * Edwards C. S. Bennett K. A.	<u><i>Composition and Sources of Dark Aeolian Sediments within Martian Craters Associated with Central Mounds [#2249]</i></u> We investigate the composition of central mounds along with the dark aeolian sediments within craters, and constrain the sand sources.
3:30 p.m.	Wang A. * Yan Y. C. Houghton J. Jolliff B. L. Wang K.	<u><i>Plasma Chemistry Induced by Martian Dust Storms and Dust Devils [#2031]</i></u> We report the effect of plasma chemistry induced by martian dust storm and dust devils on surface materials, i.e., hydrous/anhydrous sulfates and sulfites.
3:45 p.m.	Roback K. P. * Runyon K. D. Avouac J. P. Newman C. E. Ayoub F.	<u><i>Understanding Ripple and Whole-Dune Motion at Active Martian Dune Fields [#3169]</i></u> We present measurements of sand fluxes associated with moving dunes and ripples at various sites on Mars, and discuss their potential significance.
4:00 p.m.	Silvestro S. * Chojnacki M. Vaz D. A. Cardinale M. Esposito F.	<u><i>First Evidence for Bright-Toned Megaripple Migration on Mars [#1800]</i></u> We show the first evidence for bright megaripple migration on Mars. These features can be used to track strong winds at the surface and test atmospheric models.
4:15 p.m.	Berger L. M. * Williams N. R. Golombek M. P.	<u><i>An Analysis of Aeolian Ripples in Western Jezero Crater, Mars [#1592]</i></u> Jezero Crater / Aeolian sand ripples / Do they move with time?
4:30 p.m.	Kremer C. H. * Bramble M. S. Mustard J. F.	<u><i>Lithologically Diverse Yardangs in the Circum-Isidis Region: Implications for Yardang Evolution Controls and In Situ Study at the Mars 2020 Landing Site [#1639]</i></u> Yardangs everywhere / At the 2020 site / So a fresh delta?

ORAL SESSION

Wednesday Morning, March 20, 8:30 a.m.

Room	Session	Session Title	Page
Waterway Ballroom 1	W401	Ryugu and Bennu: Diamond Asteroids are Forever	29
Waterway Ballroom 4	W402	Martian Aqueous Alteration: Tracing the Effects of Water Up Close and Far Away	29
Waterway Ballroom 5	W403	Special Session: 50 Years of Lunar Science: The Legacy of "One Small Step"	30
Waterway Ballroom 6	W404	Venus, or How I Stopped Worrying and Learned to Love the Second Planet	31
Montgomery Ballroom	W405	Space Weathering: From Samples to Spectra and Everything in Between	32

Wednesday Morning, March 20, 10:15 a.m.

Room	Session	Session Title	Page
Waterway Ballroom 1	W406	Chondrites: Organic Matter	33

Wednesday Afternoon, March 20, 1:30 p.m.

Room	Session	Session Title	Page
Waterway Ballroom 1	W451	Astrobiology: I Saw the Sign... of Life?	34
Waterway Ballroom 4	W452	Water on Early Mars	35
Waterway Ballroom 5	W453	Special Session: 50 Years of Planetary Science: "One Giant Leap for Mankind"	36
Waterway Ballroom 6	W454	Ceres and Vesta	37
Montgomery Ballroom	W455	Chondrites: Refractory Components	38

Wednesday, March 20, 2019

[W401]

RYUGU AND BENNU: DIAMOND ASTEROIDS ARE FOREVER

8:30 a.m. Waterway Ballroom 1

Chairs: Hannah Susorney and Seiji Sugita

Times	Authors (*Denotes Presenter)	Abstract Title and Summary
8:30 a.m.	Cho Y. * Morota T. Kanamaru M. Ernst C. M. Barnouin O. S. et al.	<u><i>Spatial Distribution and Morphology of Craters on Ryugu: Implications for Surface Processes on the C-Type Asteroid</i></u> [#1751] Morphology and spatial distribution of craters on Ryugu reveal the heterogeneous geology on this C-type asteroid.
8:45 a.m.	Bierhaus E. B. * Barnouin O. McCoy T. J. Connolly H. C. Jawin E. et al.	<u><i>Asteroid (101955) Bennu's Crater Population: Morphologies, Size-Frequency Distribution, and Consequences for Surface Age(s)</i></u> [#2496] We present observations and analysis of asteroid (101955) Bennu's crater population.
9:00 a.m.	Barucci M. A. * Honda R. Yokota Y. Sugita S. Morota T. et al.	<u><i>Statistical Analysis of Spectrophotometry and Spectral Variation on the Surface of (162173) Ryugu as Observed by JAXA Hayabusa2 Mission</i></u> [#1308] We used a multivariate statistical method to analyze ONC-T and NIRS3 data to characterize possible heterogeneities of Ryugu's surface composition.
9:15 a.m.	Kaplan H. H. * Hamilton V. E. Clark B. E. Howell E. S. Ferrone S. et al.	<u><i>Mineral and Chemical Map Production for the OSIRIS-REx Mission</i></u> [#1890] We describe the production and validation of compositional maps from spectral data collected by the OSIRIS-REx mission.
9:30 a.m.	Sasaki S. * Sugita S. Tatsumi E. Miyamoto H. Honda C. et al.	<u><i>Brightness and Morphology Variations on Surface Rocks of 162173 Ryugu: Space Weathering, Breccia Structure, and Meridional Cracks</i></u> [#1368] Space weathering darkened the rock surface and is responsible for brightness variation on Ryugu. Meridional cracks suggest that thermal stress may destroy rocks.
9:45 a.m.	Delbo M. * Molaro J. L. Walsh K. J. Ballouz R. L. Pajola M. et al.	<u><i>Distribution of Cracked Boulders on (101955) Bennu: Searching for Evidence of Solar-Induced Thermal Stress</i></u> [#1457] Preliminary data point to processes that can create cracked boulders on the surface of the asteroid Bennu with a non trivial spatial distribution.
10:00 a.m.		DISCUSSION

Wednesday, March 20, 2019

[W402]

MARTIAN AQUEOUS ALTERATION: TRACING THE EFFECTS OF WATER UP CLOSE AND FAR AWAY

8:30 a.m. Waterway Ballroom 4

Chairs: Nina Lanza and Rebecca Smith

Times	Authors (*Denotes Presenter)	Abstract Title and Summary
8:30 a.m.	Mittlefehldt D. W. * Arvidson R. E. Crumpler L. S. Farrand W. H. Gellert R. et al.	<u><i>Geochemistry of Noachian Bedrock and Alteration Events, Endeavour Crater, Mars</i></u> [#1100] Mars Exploration Rover Opportunity is providing details of the geology and geochemistry of the Noachian bedrock and alteration styles around Endeavour Crater.
8:45 a.m.	McCullom T. M. * Hynke B. M.	<u><i>Geochemical Data Indicate the Burns and Grasberg Formations at Meridiani Planum Had the Same Sediment Source (and the Source Was Probably Volcanic)</i></u> [#1139] Rocks of the Grasberg and Burns formations have nearly identical chemical compositions. Both probably derive from addition of SO ₃ to the same original basalt.
9:00 a.m.	Sutter B. * McAdam A. C. Rampe E. B. Archer P. D. Ming D. W. et al.	<u><i>Mineralogical and Geochemical Trends of the Murray Mudstones, Gale Crater: A Combined Sample Analysis at Mars-Evolved Gas Analyzer and Chemistry and Mineralogy Instrument Assessment</i></u> [#1355] SAM and CheMin analyses indicate that the Murray mudstones have been exposed to complex geochemical conditions of varying redox and pH.

WED ORAL

9:15 a.m.	Archer P. D. Jr * Ming D. W. Sutter B. Hogancamp J. V. Morris R. V. et al.	<u><i>Oxychlorine Detection in Gale Crater, Mars and Implications for Past Environmental Conditions</i> [#3041]</u> The Sample Analysis at Mars instrument on the MSL rover has detected variable oxychlorine, with implications for past environmental conditions.
9:30 a.m.	Martin P. E. * Farley K. A.	<u><i>A Reassessment of Perchlorate in Samples from Gale Crater, Mars</i> [#1445]</u> We reassess the evidence for perchlorate in Gale Crater in light of geochemical constraints and suggest alternative explanations for the observed data.
9:45 a.m.	Lanza N. L. * Fischer W. W. Lamm S. N. Gasda P. J. Meslin P.-Y. et al.	<u><i>Variable Redox Conditions in Gale Crater as Indicated by Manganese Abundance Along the Curiosity Traverse</i> [#3146]</u> Abundant Mn / Indicates strong oxidants / Have been present there.
10:00 a.m.	Mitra K. * Catalano J. G.	<u><i>Rates and Products of Fe(II) Oxidation by Chlorate: A Potential Oxidant on Mars</i> [#1296]</u> Experiments and modeling show Fe(II) oxidation by chlorate in Mars-relevant fluids forming Fe(III) minerals (e.g., jarosite, akaganeite) at temperatures down to 0 C.
10:15 a.m.	Thomas N. H. * Ehlmann B. L. Rapin W. Rivera-Hernandez F. Wiens R. C.	<u><i>Hydrogen Variability in the Murray Formation, Gale Crater, Mars</i> [#3079]</u> ChemCam measurements of Murray formation bedrock yield an average of 2.3–3.0 wt. % water. We examine high H points and correlations with sedimentology and chemistry.
10:30 a.m.	Hausrath E. M. * Ming D. W. Rampe E. B. Peretyazhko T.	<u><i>Interpreting Aqueous Alteration in the Murray Formation Using Reactive Transport Modeling</i> [#2050]</u> Reactive transport modeling of the Murray formation is most consistent with Mars observations under low pH conditions and increasing temperature with depth.
10:45 a.m.	Haber J. T. * Horgan B. Fraeman A. A. Johnson J. R. Wellington D.	<u><i>Mineralogy of an Ancient Lakeshore in Gale Crater, Mars, from Mastcam Multispectral Imagery</i> [#1871]</u> The Sutton Island member in Gale Crater formed in a lakeshore environment and may preserve mineralogical evidence of varying redox conditions.
11:00 a.m.	Fox V. K. * Bennett K. A. Bristow T. Ehlmann B. L. House C. et al.	<u><i>Exploring the Clay-Bearing Unit with the Curiosity Rover</i> [#2826]</u> Overview of the Curiosity rover's initial campaign in the clay-bearing unit.
11:15 a.m.	Weitz C. M. * Bishop J. L. Grant J. A.	<u><i>Analysis of Clay Deposits in and Around Ladon Basin and Ladon Valles</i> [#1929]</u> We have identified, mapped, and analyzed light-toned deposits, many of which are clay-bearing, in and around Ladon basin and Ladon Valles.
11:30 a.m.	Yen C. J.-K. * Milliken R. E. Fraeman A. A. Itoh Y. Parente M. et al.	<u><i>An Updated Orbital Analysis of Ancient Strata in Terby Crater, Mars: The Thickest Deltaic Sequence on Mars?</i> [#2215]</u> New data Terby / CRISM HiRISE DTMs / The thickest delta?

Wednesday, March 20, 2019

[W403]

SPECIAL SESSION: 50 YEARS OF LUNAR SCIENCE: THE LEGACY OF "ONE SMALL STEP"

8:30 a.m. Waterway Ballroom 5

Chairs: Louise Prockter and David Draper

Times	Authors (*Denotes Presenter)	Abstract Title and Summary
8:30 a.m.	Canup R. M. *	<u><i>Lunar Origin by Giant Impact: An Evolving Legacy of Apollo</i> [#2044]</u> Moon origin via impact dates back to Apollo, but the nature of this event is debated due to challenges in explaining dynamical and geochemical constraints.
8:45 a.m.	Elardo S. M. *	<u><i>The Lunar Magma Ocean is Dead,;Long Live the Lunar Magma Ocean!</i> [#2851]</u> The LMO hypothesis has been continuously challenged over the last 50 years, but even though it has grown enormously complex, the basic tenants hold true.

9:00 a.m.	Hiesinger H. *	<u><i>The Lunar Apollo Missions: Enabling Dating of Planetary Surfaces Throughout the Solar System</i></u> [#1328] The returned samples from the Apollo and Luna missions are key for understanding the history and evolution of the Moon and at least the inner solar system.
9:15 a.m.	Cohen B. A. *	<u><i>A Glimpse of Light on Broken Glass: Solar System Bombardment from Apollo Samples</i></u> [#1112] Apollo brought us / History in their gloved hands / Tiny rocky clocks.
9:30 a.m.	Gross J. * Prissel T. C.	<u><i>The Best Part of the Pie: The Crust; Old and New Views of the Moon from Apollo and Beyond</i></u> [#2072] Lunar crustal rocks / From Apollo long ago / Treasures everywhere.
9:45 a.m.	Shearer C. K. * Schmitt H. H. Jolliff B. L.	<u><i>An Apollo Legacy. Samples, the Gift that Keeps on Giving to Future Generations</i></u> [#1412] "New" Apollo samples that are available for study will broaden our fundamental understanding of magmatic, impact, regolith, and volatile reservoir processes.
10:00 a.m.	Zuber M. T. *	<u><i>Geophysics and Shallow Internal Structure of the Moon</i></u> [#1408] Highlighting how our understanding of the Moon's thermal and tectonic evolution has been transformed by global, high-resolution geophysical datasets.
10:15 a.m.	Weber R. C. *	<u><i>The Moon's Deep Interior: A Hotbed for Seismicity and the Question of Partial Melt</i></u> [#1095] The Moon is so close / And yet its inner secrets / Remain unresolved.
10:30 a.m.	Pieters C. M. *	<u><i>Global Composition of the Moon (As We're Learning to Know It)</i></u> [#1961] Still hidden events / Created crust of the Moon / That we strive to see.
10:45 a.m.	Hurley D. M. * Prem P. Benna M. Vondrak R. R. Farrell W. M. et al.	<u><i>Anatomy of the Lunar Water Exosphere</i></u> [#2547] We examine whether water migrates through the lunar exosphere to polar regions through comparing exospheric models to observations.
11:00 a.m.	McCubbin F. M. * Barnes J. J. Liu Y.	<u><i>Endogenous Lunar Volatiles: The View from 50 Years After Apollo 11</i></u> [#1061] One small step for man / An imprint upon our hearts / Must keep exploring.
11:15 a.m.	Denevi B. W. * Costello E. S. Ghent R. R. Glotch T. D. Greenhagen B. T. et al.	<u><i>The Lunar Regolith as Understood from Near and Far</i></u> [#1292] Over 50 years of lunar regolith studies have provided a detailed understanding of the processes that shape the Moon's surface, and how it continues to evolve.
11:30 a.m.	Petro N. E. * Keller J. W. Cohen B. A. McClanahan T. P.	<u><i>Ten Years of the Lunar Reconnaissance Orbiter (LRO): Advancing Lunar Science and Context for Future Lunar Exploration</i></u> [#2780] 50 years after Apollo 11 landed, and with lunar exploration again on the horizon, it is timely to review LRO accomplishments and look to science enabled by LRO.

Wednesday, March 20, 2019

[W404]

VENUS, OR HOW I STOPPED WORRYING AND LEARNED TO LOVE THE SECOND PLANET

8:30 a.m. Waterway Ballroom 6

Chairs: Jacob Richardson and Martha Gilmore

Times	Authors (*Denotes Presenter)	Abstract Title and Summary
8:30 a.m.	Richardson J. A. * Miller D. M. Gallant E.	<u><i>Erupted Volumes of Venus Low Shield Volcano Clusters</i></u> [#3009] Venus volcanoes / Too small to measure alone / Add up to a lot.
8:45 a.m.	Bethell E. M. * Ernst R. E. Samson C.	<u><i>Re-Evaluating the Structure of Thermuthis Corona Through Detailed Geological Mapping: The Second Largest Corona on Venus?</i></u> [#1462] Geological mapping of structures associated with Thermuthis Corona reveal its diameter (~1250 km) to be much larger than previously described (~330 km).
9:00 a.m.	Smrekar S. E. *	<u><i>New Constraints on the Elastic Thickness of Venus And Implications for Geodynamic Evolution</i></u> [#2929] New local estimates of high heat agree with regional values indicating heat flow of >95 mWm ² (similar to oceanic values), implying areas of active tectonics.

9:15 a.m.	Khawja S. * Kuiper Y. D.	Ernst R. E. Samson C.	<u><i>Structural Analysis of Salus Tessera, Venus: Interpreting Surface Lineament Sets Using Topographic Profiles</i> [#1967]</u> Interpretations of lineament sets on Salus Tessera, Venus.
9:30 a.m.	Perkins R. P. * Herrick R. R.	Gilmore M. S.	<u><i>A Reassessment of Venus' Tessera Crater Population and Implications for Tessera Deformation</i> [#2989]</u> Deformed by eons / CLFs tell us riddles / An answer: Strain rates?
9:45 a.m.	Ghail R. C. *		<u><i>Tesserae are Highly Eroded and Grow by Campus Accretion</i> [#2351]</u> Highland tesserae mainly comprise an ancient core surrounded by accreted plains material, many of which are much more eroded than previously realized.
10:00 a.m.	Whitten J. L. * Campbell B. A.		<u><i>Variations in the Radar Properties of Tesserae Across Venus as Observed with Magellan Data</i> [#2558]</u> We measure the backscatter coefficient of tesserae using Magellan data. Distinct variations are observed associated with craters and original tessera materials.
10:15 a.m.	Gilmore M. S. * Zalewski N.	Brossier J. F.	<u><i>Variations in the Radiophysical Properties of Venus Tesserae: Could be the Rocks? Could be the Climate?</i> [#2632]</u> Not all tesserae have the same radar emissivity patterns, requiring differences in rock types, atmospheric composition, and/or surface age.
10:30 a.m.	Brossier J. F. * Toner K.	Gilmore M. S.	<u><i>Radiophysical Behaviors of Venus' Plateaus and Volcanic Rises: Updated Assessment</i> [#2531]</u> Study of the variation of emissivity with elevation for venusian tesserae, mountains, and volcanoes to provide new insights on their composition and age.
10:45 a.m.	Port S. T. * Chevrier V. F.	Briscoe A. C. Fitting A. B.	<u><i>The Effects of Venusian Temperatures, Pressures, and CO₂ on Lead Minerals</i> [#1668]</u> Various lead minerals were tested at Venus temperature and pressure in CO ₂ to determine any changes to their structure and composition.
11:00 a.m.	Sruthi U. * Werner S. C.	Rolf T. Cramer F.	<u><i>The Role of Mantle Dynamics in the Rejuvenation of Venus' Surface: Insights from Numerical Modelling</i> [#2309]</u> To derive surface age distributions generated from numerical models featuring both volcanic and tectonic resurfacing.
11:15 a.m.	Ernst R. E. * Kuiper Y. D.	Samson C. Khawja S.	<u><i>Geological Testing of Climate Change Models on Venus</i> [#2382]</u> Given massive volcanism as the cause of hyper-warming on Venus, we consider geo-evidence for Earth-like conditions during tesserae time a early plains volcanism.
11:30 a.m.	O'Rourke J. G. * Tackley P. et al.	Gillmann C. Buz J. Fu R. R. et al.	<u><i>Detectability and Scientific Implications of Crustal Remanent Magnetism on the Surface of Venus</i> [#2222]</u> Venus has no internally generated magnetic field today. Proving it had one in the past would provide unique constraints on its formation and evolution.

Wednesday, March 20, 2019

[W405]

SPACE WEATHERING: FROM SAMPLES TO SPECTRA AND EVERYTHING IN BETWEEN

8:30 a.m. Montgomery Ballroom

Chairs: Jeffrey Gillis-Davis and Michelle Thompson

Times	Authors (*Denotes Presenter)	Abstract Title and Summary	
8:30 a.m.	Gillis-Davis J. J. * Góbi S. Frigge R.	Zhu C. Abplanalp M. J. et al.	<u><i>Laboratory Space Weathering Induced Formation of Sulfides in the Murchison (CM2) Meteorite</i> [#1282]</u> Hydrogen sulfide (H ₂ S) and hydrogen disulfide (H ₂ S ₂) are formed in the Murchison (CM2) meteorite upon exposure to energetic electrons and laser irradiation.
8:45 a.m.	Lacznia D. L. * Dukes C. A. Clemett S. J.	Thompson M. S. Morris R. V. et al.	<u><i>Coordinated Analysis of an Ion Irradiated Carbonaceous Chondrite Suggests Complex Space Weathering Effects</i> [#1972]</u> We present surface chemistry, reflectance, and organic functional group chemistry results from a H ²⁺ and He ⁺ irradiated section of the Murchison CM2 meteorite.

9:00 a.m.	Thompson M. S. * Loeffler M. J. Morris R. V. Clemett S. J. Trang D. et al.	<u>Coordinated Analysis of an Experimentally Space Weathered Carbonaceous Chondrite</u> [#2045] Laser shots show us / Changes in organics and / Nanoparticles.
9:15 a.m.	Matsumoto T. * Miyake A.	<u>An Impact Splash Melt Including Nanophase FeS Found in a Regolith Sample from S-Type Asteroid Itokawa</u> [#2183] We analyzed a splash melt on a regolith grain from Itokawa. The splash contains nanophase FeS in silicate melt, which may cause spectral change on Itokawa.
9:30 a.m.	Ohtaki K. K. * Bradley J. P. Gills-Davis J. J. Taylor G. J. Ishii H. A.	<u>Formation of Iron-Rich Nanoparticles Within Glassy Silicate Spherules in Lunar Soil</u> [#2156] Details of chemistry and distribution of Fe-rich inclusions observed in the interior of lunar glass spherules suggest they formed via impact melting.
9:45 a.m.	Utt K. L. * Ogliore R. C. Jolliff B. Bechtel H. A. Gillis-Davis J. J.	<u>Spatially-Resolved IR Spectral Effects of Space Weathering in Lunar Plagioclase</u> [#2867] We investigate space weathering in mature lunar soil using near-field synchrotron-based IR spectroscopy with nanoscale spatial resolution.
10:00 a.m.	McLain J. L. * Farrell W. M. Loeffler M. Keller J. W. Hudson R.	<u>Proton Induced Hydroxylation on Lunar Soil 78421.38</u> [#2831] Diffuse reflectance IR spectrometry is used to monitor the evolution of the OH band during proton irradiation of lunar soil 78421.38.
10:15 a.m.	Wohlfarth K. * Wöhler C. Grumpe A.	<u>How Does Space Weathering Affect the Detection of Lunar OH/H₂O? Insights from Ab-Initio Mie Modeling of Submicroscopic Iron</u> [#2584] We use ab-initio Mie modeling, Hapke theory, and M ³ data to simulate the effects of space weathering and how it affects the detection of lunar hydroxyl/water.
10:30 a.m.	Flom A. J. * Lucey P. Honniball C. I. Ferrari-Wong C. M.	<u>Water and Hydroxyl Features at Reiner Gamma</u> [#3189] Lunar swirls provide a natural laboratory for studying implanted H ₂ O/OH on the Moon. Using groundbased astronomy, we mapped the distribution of water at the Reiner Gamma swirl.
10:45 a.m.	McFadden J. A. * Garrick-Bethell I. Sim C. K. Kim S. S. Hemingway D.	<u>Dependence of Lunar Space Weathering on Soil Iron Content and the Brightness of Reiner Gamma Swirl</u> [#2251] The differential effects of solar wind weathering are reduced for high iron soils, implying they are saturated in nanophase iron at most lunar latitudes.
11:00 a.m.	Li S. * Lucey P. G. Sun V. Z. Fraeman A. A.	<u>Detection of A 850 nm Absorption Feature at High Latitudes on the Moon: Possible Presence of Hematite</u> [#2320] An absorption feature near 850 nm was detected at the lunar high latitudes, indicating the presence of hematite. Possible formation mechanisms were discussed.
11:15 a.m.	O'Brien P. * Byrne S. Zega T. J.	<u>Lunar Landscape Evolution and Space Weathering</u> [#2003] We compare maturities of lunar soils to surface residence times of tracer particles in a landscape evolution model to deduce the rate of space weathering.
11:30 a.m.	Nypaver C. * Thomson B. J. Burr D. M. Fassett C. I. Niesh C. D. et al.	<u>Constraining Degradation of Lunar Crater Ejecta Using Multiple Remote Sensing Datasets</u> [#2483] Crater ejecta / How fast does it disappear? / It's gone in the end.

Wednesday, March 20, 2019

[W406]

CHONDRITES: ORGANIC MATTER

10:15 a.m. Waterway Ballroom 1

Chairs: George Cody and Pierre Haenecour

Times	Authors (*Denotes Presenter)	Abstract Title and Summary
10:15 a.m.	Duprat J. * Augé B. Dartois E. Engrand C. Bardin N. et al.	<u>On the Origin of Organics in UltraCarbonaceous Antarctic MicroMeteorites (UCAMMs), Irradiation of N-Rich Ices in the Outer Solar System</u> [#2339] The precursors of the organic matter in UCAMMs can be produced by irradiation by Galactic Cosmic Rays of N ₂ -CH ₄ ices with initial heterogeneous D/H ratio.

10:30 a.m.	Kebukawa Y. * Zolensky M. E. Ito M. Goodrich C. A. Marcus M. A. et al.	<u><i>Investigation of Organic Matter in Carbonaceous Chondrite Lithologies of Almahata Sitta</i> [#1359]</u> We report STXM/C-XANES and NanoSIMS analyses of carbonaceous chondrite lithologies from a polymict ureilite, Almahata Sitta meteorite.
10:45 a.m.	Cody G. D. * Foustoukos D. I. Bullock E.	<u><i>Laboratory Synthesis of Chondritic Organic Solids (syn-IOM): Insights and Consequences</i> [#2692]</u> Formation of organic solids in planetesimal interiors generates potentially high gas pressures that could lead to extensive “hydro” fracturing of small bodies.
11:00 a.m.	Young J. M. * Glotch T. D.	<u><i>Reconstructing Ordinary Chondrite Parent Body Metamorphic Temperature Conditions from Raman Spectroscopy</i> [#1860]</u> A laser shows us / Carbon tells us, long ago / Things were really hot.
11:15 a.m.	Foustoukos D. I. * Cody G. D. Alexander C. O. M. 'D. Riebe M. E. I.	<u><i>Nitrogen Evolution During Thermal Alteration and Synthesis of Insoluble Organic Matter</i> [#1449]</u> An experimental study on the effects of synthesis, aqueous alteration, and thermal metamorphism on the N chemical and isotopic systematics in IOM.
11:30 a.m.	Bonato E. * King A. J. Schofield P. F. Kaulich B. Araki T. et al.	<u><i>In-Situ Carbon, Nitrogen, and Oxygen XANES Analysis of the Matrix in Pristine CO₃ Carbonaceous Chondrites</i> [#3047]</u> C N O with XANES / Are analysed in situ / In pristine COs.

Wednesday, March 20, 2019

[W451]

ASTROBIOLOGY: I SAW THE SIGN... OF LIFE?

1:30 p.m. Waterway Ballroom 1

Chairs: Erika Rader and Eric Parker

Times	Authors (*Denotes Presenter)	Abstract Title and Summary
1:30 p.m.	Garczynski B. J. * Horgan B. Kah L. C.	<u><i>Searching for Potential Biosignatures in Jezero Crater with Mars 2020 — An Investigation of Terrestrial Lacustrine Carbonate Analogs</i> [#2028]</u> A review of hydromagnesite analogs suggest marginal carbonates in Jezero are authigenic and biosignature preservation may be restricted to low energy shorelines.
1:45 p.m.	Goetz W. * Oehlke M. Li X. Danell R. M. Grubisic A. et al.	<u><i>How Do Minerals Affect the Search for Organics and Biosignatures on Mars by the Exomars-2020 Rover? Case Study on Magnetite and Gypsum</i> [#3207]</u> We examine how minerals do interfere with the detection of martian organics by the MOMA instrument.
2:00 p.m.	Barge L. M. * Flores E. Perl S. M. VanderVelde D. Baum M. M.	<u><i>Abiotic Organic Synthesis and Product Distributions in Mars Analogue Iron Mineral Systems</i> [#1439]</u> Amino acids and other organics form abiotically in iron mineral systems, with non-random distributions that are related to the geochemistry of the environment.
2:15 p.m.	Lewis J. M. T. * Eigenbrode J. L. McAdam A. C. Pavlov A. A. Li X. et al.	<u><i>The Preservation and Detection of Lipids in Mars-Relevant Sulfates and Chlorides</i> [#2021]</u> We are examining how lipids important for life can be trapped and preserved within minerals and whether we are able to detect them with flight instruments.
2:30 p.m.	Fox A. C. * Eigenbrode J. Freeman K. H.	<u><i>Radiolysis products of macromolecular organic matter in Mars-relevant matrices</i> [#1556]</u> We explored the radiolysis products of macromolecular organic matter exposed to high energy radiation. Implications for biosignature detection on Mars.
2:45 p.m.	Tan J. S. W. * Sephton M. A.	<u><i>Early Stage Diagenesis of Lipids from a Mars-Analogue Sulfur Stream — A Simulated Maturation Study</i> [#1089]</u> We attempt to understand the organic matter: Mineral interactions associated with post-burial diagenesis in iron-rich sulfur stream environments on Mars.

3:00 p.m.	Rader E. * Amador E. Cable M. L. Cantrell T. Cullen T. et al.	<u><i>The Effect of Grainsize, Temperature, Slope, and Chemical Composition on Biomass in Mars Analog Substrate for Sample Return, Iceland</i> [#2553]</u> We test how several conditions affect microbial communities in the martian analog, Iceland, like temperature, slope, composition and oxidation, and grainsize.
3:15 p.m.	Clark B. C. * Kolb V. M.	<u><i>Crater Lake Setting for Macrobionts on Mars: How and Where to Search</i> [#1300]</u> Crater lakes on Mars can create ancillary ponds that are candidate macrobionts, the settings under which prebiotic syntheses for the origin of life occur.
3:30 p.m.	O'Brien A. C. * Hallis L. J. Steele A. Daly L. Lee M. R.	<u><i>The Effects of Shock and Raman Laser Irradiation on the Maturity of Organics in Martian Meteorites</i> [#2376]</u> Look at falling sky / Rock from big red rock in black / Sky to find life signs.
3:45 p.m.	Parker E. T. * Aponte J. C. Alexander C. M. O'D. Foustoukos D. Dworkin J. P. et al.	<u><i>Investigating L-Amino Acid Enantiomeric Excess in CM and CR Carbonaceous Chondrites</i> [#2625]</u> In this work we are studying Antarctic meteorites including Y-791198, EET 96029, MIL 090657, LAP 02342, and GRA 95229 isovaline enantiomeric abundances.
4:00 p.m.	Simkus D. N. * Aponte J. C. Elsila J. E. McLain H. L. Dworkin J. P. et al.	<u><i>Amino Acid Analyses of Enstatite Chondrites</i> [#1651]</u> We discuss the distribution and potential origins of low abundances of amino acids detected in EH3 enstatite meteorite samples.
4:15 p.m.	Rios A. C. Cooper G. W. *	<u><i>Finding Evidence of a Prebiotic Pyruvate Reaction Network in Meteorites</i> [#2332]</u> The self-reactions of pyruvate lead to a network of possible pre-metabolic compounds. Such reactions may have been captured in carbonaceous chondrites.
4:30 p.m.	Bodnar R. J. Dolocan A. Zolensky M. E. * Lamadrid H. Kebukawa Y. et al.	<u><i>First Direct Measurements of Compositions of Early Solar System Aqueous Fluids</i> [#1142]</u> The fluid inclusions in Monahans halite contain a high concentration of organic species, as measured by TOF-SIMS.

Wednesday, March 20, 2019

[W452]

WATER ON EARLY MARS

1:30 p.m. Waterway Ballroom 4

Chairs: Robert Craddock and Mathieu Lapotre

Times	Authors (*Denotes Presenter)	Abstract Title and Summary
1:30 p.m.	Craddock R. A. * Rose T. Marsaglia K. M. Cawley J. Morgan A.	<u><i>Characteristics of Basaltic Sediments Reveal Depositional and Transport Processes</i> [#2627]</u> We report the characteristics of basaltic material can be used to diagnose transport distances and processes of surface material on Mars.
1:45 p.m.	Scuderi L. A. * Gallegos Z. E. Newsom H. E. Wiens R. C. Grant J. A. et al.	<u><i>An Amazonian Groundwater Springline at Peace Vallis Fan, Gale Crater; Implications for a Late Period of Surface Water Flow</i> [#2714]</u> Groundwater springlines of Amazonian age are observed on the Peace Vallis fan within Gale Crater and analyzed with MSL rover imagery and HiRISE orbital data.
2:00 p.m.	Denton C. A. * Head J. W.	<u><i>Fretted Channels and Closed Depressions in Northern Arabia Terra, Mars: Origins and Implications for Subsurface Hydrologic Activity</i> [#1082]</u> Analysis of the fretted channels and closed depressions of the Arabia Terra plateau indicates massive material removal facilitated by subsurface disruption.
2:15 p.m.	Smith I. B. * Viviano C. Chojnacki M. Putzig N. E. Quantin C. et al.	<u><i>Characterization of Hydrated, Layered Deposits at Valles Marineris Plateau, a Multidisciplinary Approach</i> [#2713]</u> Sediments on Mars / Full characterization / Many instruments.
2:30 p.m.	Cawley J. C. Irwin R. P. III *	<u><i>Variable Substrates and Morphology of Martian Valley Networks</i> [#2459]</u> Observations suggest that at presently resolvable levels, martian valley networks reflect geologic textures, substrate influences, and topographic control.

WED ORAL

2:45 p.m.	Grau Galofre A. * Jellinek M. A. Osinski G. R.	<u><i>Did Martian Valley Networks Form Under Ancient Ice Sheets? [#2574]</i></u> Channel networks draining massive ice sheets, forming rivers under the ice. Could those explain the puzzling characteristics of some martian valley networks?
3:00 p.m.	Bahia R. * Jones M. Covey-Crump S. Mitchell N.	<u><i>The Application of Hack's Law and Flint's Law to Martian Valley Networks and Its Implications for the Noachian Climate [#1197]</i></u> Hack's and Flint's Law allow inferences between valley network geometry and formation conditions to be made. We apply these laws to Noachian martian valleys.
3:15 p.m.	Cang X. * Luo W.	<u><i>Utilizing Valley Network Junction Angle to Estimate the Duration of "Warm" Mars [#1748]</i></u> We estimated the Noachian climatic condition and the duration of "warm" Mars by using the Mars junction angles data and the Earth streams and climatic data.
3:30 p.m.	Morgan A. M. * Craddock R. A.	<u><i>How Accurate are Paleodischarge Estimates for Martian Rivers? [#2695]</i></u> Ancient Mars rivers / How much water flowed within? / Uncertain! Use care.
3:45 p.m.	Lapotre M. G. A. * Ielpi A. Lamb M. P. Williams R. M. E. Knoll A. H.	<u><i>Single-Thread Rivers Without Land Plants: A Model to Interpret Martian Fluvial Deposits [#2519]</i></u> Red planet rivers / Meandered like Earth cousins / Yet, no plants to help.
4:00 p.m.	Cardenas B. T. * Swartz J. M. Mohrig D.	<u><i>The Length of Fluvial Sinuous Ridges on Mars [#1677]</i></u> Long ridges on Mars / Fluvial and sinuous / Tell us of the coast.
4:15 p.m.	Palumbo A. M. * Head J. W.	<u><i>Oceans on Mars: The Possibility of a Noachian Groundwater-Fed Ocean in a Sub-Freezing Martian Climate [#2024]</i></u> New climate and thermal model results show that a Noachian ocean could have formed in a cold climate, with global mean annual temperature at least 255 K.
4:30 p.m.	Rodriguez J. A. P. * Kargel J. S. Baker V. R. Robertson D. K. Komatsu G. et al.	<u><i>A NASA Spacecraft May Have Landed on an Early Mars Mega-Tsunami Deposit in 1976 [#2575]</i></u> Martian outwash plains are considered to comprise the Viking Lander 1 landing site. We reinterpret it as part of a Late Hesperian mega-tsunami deposit.

Wednesday, March 20, 2019

[W453]

SPECIAL SESSION: 50 YEARS OF PLANETARY SCIENCE: "ONE GIANT LEAP FOR MANKIND"

1:30 p.m. Waterway Ballroom 5

Chairs: Eileen Stansbery and Walter Kiefer

Times	Authors (*Denotes Presenter)	Abstract Title and Summary
1:30 p.m.	McKeegan K. D. *	<u><i>From a Sun-Kissed Moon to the Solar Nebula: Genesis Origins and Update [#2171]</i></u> Solar composition has been investigated by the capture of solar wind by the Genesis Discovery Mission.
1:45 p.m.	Bottke W. F. *	<u><i>Dynamical Evolution and Bombardment of the Early Solar System: A Few Highlights of the Last 50 Years [#1545]</i></u> The concept of planet migration has revolutionized our ideas about how our solar system formed. Early bombardment tells us the story of what took place.
2:00 p.m.	Solomon S. C. * Nittler L. R. Anderson B. J. Byrne P. K.	<u><i>First Rock from the Sun: 50 Years of Mercury Exploration [#1277]</i></u> First rock from the Sun / Dense, reduced, volatile rich / Magnetic, shrinking.
2:15 p.m.	Byrne P. K. * Ghail R. C. Gilmore M. S. Smrekar S. E. Treiman A. H. et al.	<u><i>The Exploration of Venus: Current Understanding and Open Questions [#2853]</i></u> For the second world / There is much left for us to / Learn; we must go back!
2:30 p.m.	Schmidt M. E. * Herd C. D. K. McCoy T. J. McSween H. Y. Rogers A. D. et al.	<u><i>Igneous Mars: Crust and Mantle Evolution as Seen by Rover Geochemistry, Martian Meteorites, and Remote Sensing [#2419]</i></u> Mars molten past is / Known from fallen stones, orbit / Robots, but unknowns.

2:45 p.m.	Rampe E. B. * Arvidson R. E. Edgar L. A. Edgett K. S. Fedro C. M. et al.	<u><i>The Sedimentary History of Mars as Observed by Rovers</i> [#1126]</u> We review ancient and modern depositional environments on Mars and evidence for diagenesis based on rover observations.
3:00 p.m.	Raymond C. A. * Russell C. T. Castillo-Rogez J. C.	<u><i>Ceres and Vesta: Diverse, Enigmatic Small Planets from the Dawn of the Solar System</i> [#3231]</u> Two protoplanets / From the early solar system / Shed light on its dawn.
3:15 p.m.	Bagenal F. *	<u><i>Exploration of Jupiter</i> [#1352]</u> Review of Jupiter after six spacecraft flybys, Galileo's and Juno's many orbits, summarizing what we have learned about the planet, satellites, and magnetosphere.
3:30 p.m.	Pappalardo R. T. *	<u><i>From the Moon to the Icy Galilean Satellites</i> [#2808]</u> Apollo lessons / Also pass legacy to / Far off icy moons.
3:45 p.m.	Lorenz R. D. *	<u><i>Titan Since Apollo</i> [#1215]</u> The last 50 years / Showed Titan is amazing / We want to go back.
4:00 p.m.	Waite J. H. Jr. * Glein C. Postberg F. Lunine J.	<u><i>Enceladus as Revealed by the Cassini-Huygens Mission</i> [#1290]</u> The Cassini-Huygens mission findings associated with establishing the habitability of Enceladus will be presented.
4:15 p.m.	Soderlund K. M. * Hofstadter M. D. Simon A. Atreya S. Banfield D. et al.	<u><i>Exploration of Uranus and Neptune: Looking into the Past and Towards the Future of Ice Giant Planets</i> [#1669]</u> Many mysteries / Within ice giant systems / New mission is key.
4:30 p.m.	Cruikshank D. P. * Stern S. A. Weaver H. A. Olkin C. B. Young L. A. et al.	<u><i>Fifty Years of Exploring Pluto: From Telescopes to the New Horizons Mission</i> [#2057]</u> The New Horizons encounter with Pluto in 2015 opened a new vista on this dwarf planet and its moons, and changed our perception of distant planetary icy bodies.

Wednesday, March 20, 2019

[W454]

CERES AND VESTA

1:30 p.m. Waterway Ballroom 6

Chairs: Thomas Prettyman and Julie Castillo-Rogez

Times	Authors (*Denotes Presenter)	Abstract Title and Summary
1:30 p.m.	Castillo-Rogez J. C. * Vinogradoff V. De Sanctis M. C. Hesse M. Marchi S. et al.	<u><i>Sources and Sinks of Carbon Inside Ceres</i> [#2264]</u> Organics in Ceres / Sink and float / Ceres crust is like / An ice cream sandwich.
1:45 p.m.	Cannon K. M. * Britt D. T.	<u><i>Into the Mire: The Behavior of Fines in a Mud Ocean on Ceres and Other Carbonaceous Bodies</i> [#2038]</u> Is the surface of Ceres a frozen mud ocean, or the seafloor left behind after an ice shell sublimated away? We performed experiments to test mud ocean models.
2:00 p.m.	Stein N. T. * Ehlmann B. L. Castillo-Rogez J. C. Raymond C. A.	<u><i>The Formation and Timing of Near-Surface Na-Carbonate Deposits on Ceres: Evidence for Diverse, Widespread, and Geologically Recent Emplacement</i> [#2150]</u> We investigate the timing of large shallow subsurface Na-carbonate deposits on Ceres and investigate mechanisms for their formation.
2:15 p.m.	Prettyman T. H. * Yamashita N. Landis M. E. Castillo-Rogez J. C. Ehlmann B. L. et al.	<u><i>Dawn's GRaND Finale: High Spatial-Resolution Elemental Measurements Reveal an Anomaly at Occator Crater</i> [#1356]</u> Occator's quirky / Subsurface composition / Tells crustal secrets.
2:30 p.m.	Scully J. E. C. * Schenk P. M. Williams D. A. Buczkowski D. L. Pasckert J. H. et al.	<u><i>The Evolution of Occator Crater and Its Faculae Revealed by Highest Resolution Observations of Ceres</i> [#1619]</u> Here we update our understanding of Ceres' Occator Crater and its bright faculae, based on spectacular, highest spatial resolution data returned from Dawn.
2:45 p.m.	Nathues A. * Thangjam G. Schmedemann N. Pasckert J. H. Cloutis E. et al.	<u><i>Revisiting the Geology of Occator Crater on Ceres: Recently Active Cryovolcanism?</i> [#1814]</u> The geology of the unique Occator Crater on (1) Ceres is revisited by using high resolution Dawn FC data.

WED ORAL

3:00 p.m.	Buczowski D. L. * Wyrick D. Y. Sizemore H. G. Schmidt B. E. Scully J. E. C. et al.	<u><i>Floor-Fractured Craters on Ceres and Implications for Interior Processes</i></u> [#1301] We explore potential formation mechanisms for floor-fractured craters on Ceres: Cryomagmatism, impact-derived cryomagmatism, and salt tectonics-like deformation.
3:15 p.m.	Duarte K. D. * Schmidt B. E. Sizemore H. G. Scully J. E. C. Hughson K. H. G. et al.	<u><i>From Landslides to Tholi: Ceres' Diverse Geomorphology and Its Implications for Ground-Ice</i></u> [#2070] Geologic features seen on Ceres are hypothesized to be influenced by the presence of ground-ice (Schmidt et al., 2017; Duarte et al., 2018).
3:30 p.m.	Zolotov M. Yu. *	<u><i>Ceres' Shape Agrees with an Organic-Rich Interior Structure</i></u> [#3064] An organic-rich interior is consistent with polar flattening, topography, and surface composition of Ceres. Water ice and/or high porosity are not required.
3:45 p.m.	Mao X. * McKinnon W. B.	<u><i>Spin Evolution of Ceres due to Impacts</i></u> [#1975] All asteroid spins evolve due to collisions, and Ceres is no exception. Its spin period could have varied \pm an hour or more, during its geological history.
4:00 p.m.	Ermakov A. I. * Park R. S. Raymond C. A. Castillo- Rogez J. C. Russell C. T.	<u><i>Using Effective Density Spectrum to Constrain Crustal Density Profile of Vesta and Ceres</i></u> [#2100] We use Dawn's gravity and shape data and compute effective density spectra of Vesta and Ceres in order to constrain their crustal density profiles.
4:15 p.m.	Steckloff J. K. * Goldstein D. Varghese P. Trafton L.	<u><i>The Origin of Vesta's Asymmetric Distribution of Hydrogen Signatures and Hydrated Minerals</i></u> [#1066] Water streaks Vesta / Too small for an exosphere / Water can't migrate.
4:30 p.m.	McSween H. Y. * Stolper E. M. Baker M. B. Lunning L. G. Raymond C. A.	<u><i>Distinguishing Intrusive and Extrusive Magmatism on Vesta</i></u> [#1220] The ratio of plutonic to volcanic rocks in Vesta's crust is Earth-like, suggesting a significant role for pluton emplacement in the asteroid's evolution.

Wednesday, March 20, 2019

[W455]

CHONDRITES: REFRACTORY COMPONENTS

1:30 p.m. Montgomery Ballroom

Chairs: Alexander Krot and Yogita Kadlag

Times	Authors (*Denotes Presenter)	Abstract Title and Summary
1:30 p.m.	Pravdivtseva O. * Tissot F. L. H. Dauphas N. Amari S.	<u><i>S-Process Noble Gas Enrichments in the Allende Fine-Grained CAIs: Case for a Presolar SiC Carrier</i></u> [#2006] Xe isotopic composition of five Type A Allende CAIs indicate presence of presolar SiC. The results are supported by Xe, Kr, and Ne data for the Curious Marie CAI.
1:45 p.m.	Torrano Z. A. * Rai V. K. Wadhwa M.	<u><i>Titanium Isotope Compositions of Refractory Inclusions: Implications for Nebular Mixing</i></u> [#1501] We report high-precision, mass-independent Ti isotope compositions for several CAIs and discuss the implications for nebular source reservoirs and mixing.
2:00 p.m.	Hu J. Y. * Dauphas N. Tissot F. L. H. Yokochi R. Ireland T. J.	<u><i>Insights into Evaporation/Condensation Processes in the Early Solar System from Mass-Dependent Fractionations of REEs in Type II CAIs</i></u> [#1938] We have analyzed the isotopic fractionations of seven REEs in type II CAIs. The REEs display behaviors inconsistent with the simple condensation snapshot scenario.
2:15 p.m.	MacPherson G. J. *	<u><i>CAIs Did Not Form in the Outer Solar System</i></u> [#3005] Isotopic and experimental data demonstrate unequivocally that CAIs formed in the inner, not outer, solar system; carbonaceous chondrites might have as well.

2:30 p.m.	Hertwig A. T. * Liu M.-C.	Dunham E. T. Wadhwa M.	<u>Mesquite: Petrography, Aluminum-26 Chronometry, and Be-B Systematics of an Unusually Large Melilite-Rich CAI from the Northwest Africa (NWA) 7892 CO3.0 Chondrite</u> [#2955] A melilite-rich CAI in the NWA 7892 CO3.0 chondrite is similar to most CAIs with respect to Al-Mg and Be-B systematics, but unique in size and texture.
2:45 p.m.	Krot A. N. * Simon S. B.	Nagashima K. Ma C.	<u>Grossite-Rich Refractory Inclusions in Carbonaceous Chondrites: Evidence for Early Generation of Different O-Isotope Reservoirs in the Protoplanetary Disk and O-Isotope Exchange During Fluid-Rock Interaction</u> [#1230] Grossite-rich CAIs recorded early generation of different O-isotope reservoirs in the protoplanetary disk and O-isotope exchange during fluid-rock interaction.
3:00 p.m.	Han J. *	Keller L. P.	<u>Fine-Grained, Spinel-Rich Ca-Al-Rich Inclusions from the Reduced CV3 Chondrite Efremovka: A Genetic Link to Wark-Lovering Rims?</u> [#2902] We present TEM analyses of pristine FGIs from the reduced CV3 chondrite Efremovka to characterize their primary textures and chemical compositions.
3:15 p.m.	Ebel D. S. *	Weisberg M. K.	<u>Amoeboid Olivine Aggregates Record Nebular Metal-Silicate Fractionation</u> [#2438] Many AOAs have metal nodules surrounded by Mg-olivine external to rimmed CAI nodules, recording metal/olivine separation at fine scales in chondrule precursors.
3:30 p.m.	Kadlag Y. * Frick D. A. Kühne P.	Tatzel M. Becker H.	<u>Chondrule-Matrix Complementarity in the Allende CV3 Chondrite — A Si Isotope Perspective</u> [#1092] Si isotopes are used to evaluate chondrule-matrix complementarity in carbonaceous chondrites and to shed a light on the chondrule formation processes.
3:45 p.m.	Weisberg M. K. * Fukuda K.	Kita N. T. Siron G. Ebel D. S.	<u>Microdistribution of Oxygen Isotopes in Unequilibrated Enstatite Chondrites</u> [#2461] High precision oxygen isotope analyses of chondrules and clasts from primitive EH3 and EL3 chondrites trend along the slope~1 Primitive Chondrule Mineral line.
4:00 p.m.	Ushikubo T. *	Kimura M.	<u>Oxygen Isotope Systematics of Chondrules and Isolated Olivine Grains from the Tagish Lake C2 Chondrite</u> [#1145] Oxygen isotope ratios of olivine grains from Tagish Lake (C2) are distributed along the PCM line. Their $\Delta^{17}\text{O-Mg\#}$ systematics is close to those of CR chondrules.
4:15 p.m.	Koefoed P. * Chen H. Wang K.	Pravdivtseva O. Gerritzen C.	<u>K Isotope Systematics of Individual Chondrules from the LL4 Chondrite Hamlet</u> [#1672] We present high-precision K isotope analyses of individual chondrules from the LL4 chondrite Hamlet and discuss their implications on chondrule formation.
4:30 p.m.	Schrader D. L. *	Davidson J.	<u>Olivine from the “Forbidden Triangle”: Evidence for Chondrule Migration to the Comet Forming Region?</u> [#1470] Chondrules, or chondrule fragments, from the UOCs may have migrated to the comet forming region.

ORAL SESSION

Thursday Morning, March 21, 8:30 a.m.

Room	Session	Session Title	Page
Waterway Ballroom 1	R501	New Lunar Science: A View from Apollo 50 Years Later	43
Waterway Ballroom 4	R502	Martian Remote Sensing: Mineralogy, Morphology, and Chemistry	44
Waterway Ballroom 5	R503	From Meteorites to Asteroids and Back Again!	45
Waterway Ballroom 6	R504	Presolar, Interplanetary, and Cometary Dust	46
Montgomery Ballroom	R505	Impacts: Processes from Planetesimals to Planets	47

Thursday Afternoon, March 21, 1:30 p.m.

Room	Session	Session Title	Page
Waterway Ballroom 1	R551	Lunar Petrology, Geochemistry, and Geochronology; from Surface to Interior	48
Waterway Ballroom 4	R552	Martian Madness: Roving the Ridges	49
Waterway Ballroom 5	R553	Differentiation of Planets and Asteroids: From Cores to Late Veneers	50
Waterway Ballroom 6	R554	Planetary Volcanism: A Song of Fire and Ice	51
Montgomery Ballroom	R555	Small Bodies: Observations from the Ground Up	52

Thursday Afternoon, March 21, 3:15 p.m.

Room	Session	Session Title	Page
Waterway Ballroom 4	R556	Martian Surface: Exposing Carbonates and Hydrothermal Alteration	53

Thursday, March 21, 2019

[R501]

NEW LUNAR SCIENCE: A VIEW FROM APOLLO 50 YEARS LATER

8:30 a.m. Waterway Ballroom 1

Chairs: Juliane Gross and Jessica Barnes

Times	Authors (*Denotes Presenter)	Abstract Title and Summary
8:30 a.m.	Zeigler R. A. * Mosie A. B. Kent J. J. Krysher C. H. Watts L. A. et al.	<u><i>The Apollo Sample Collection: 50 Years of Solar System Insight</i></u> [#3201] Apollo samples / Remarkably versatile / Let's go get more please.
8:45 a.m.	Greenhagen B. T. * Donaldson Hanna K. L. Yasanayake C. N. Bowles N. E. Pieters C. M. et al.	<u><i>Groundtruthing Diviner Lunar Radiometer Observations with Apollo Samples</i></u> [#2751] We use lunar soils, an enduring legacy of the Apollo missions, measured in a simulated lunar environment to groundtruth the Diviner compositional dataset.
9:00 a.m.	Strauss B. E. * Tikoo S. M. Gross J. Setera J. Turrin B.	<u><i>Intensity of the Lunar Dynamo Field at 3.0 Ga</i></u> [#3135] We determined that the lunar dynamo field had intensities below ~4–7 microtesla at ~3.0 Ga, confirming that the lunar high field epoch ceased before then.
9:15 a.m.	Guenther M. E. * Brown S. M. Grove T. L.	<u><i>Origin of the Apollo 14 Black Glasses: New Experimental Constraints on the Influence of Variable Oxygen Fugacity on the Depth of Multiple Saturation and Implications for Late-Stage Magma Ocean Cumulate Overturn</i></u> [#3242] New experimental data on the Apollo 14 ultramafic glass show that fO_2 has a big influence on liquidus phase relations and places depth of melting at 800 km.
9:30 a.m.	Füri E. * Zimmermann L. Deloule E. Saal A. E.	<u><i>The H-Noble Gas Signature of Single Apollo Volcanic Glass Beads</i></u> [#1778] Coupled H-noble gas analyses allow to understand the exposure history and volatile element signature of single Apollo 15 and 17 volcanic glass beads.
9:45 a.m.	Mikouchi T. * Yokoi N. Takenouchi A. Arai T.	<u><i>High Oxygen Fugacity of Lunar Anorthosites as Revealed by Iron Micro-XANES of Plagioclase</i></u> [#2341] Synchrotron Fe-XANES analysis of plagioclase in 12 lunar rocks suggests formation of anorthosites (FAN and MAN) at high fO_2 probably well above the IW buffer.
10:00 a.m.	Vanderliek D. M. * Becker H. Rocholl A.	<u><i>Large-Scale Redistribution of Heterogeneous PKT Material by the Imbrium Impact — Evidence from Petrology and U-Pb Zircon Dating of a Complex Apollo 16 Breccia</i></u> [#2379] Lithologies, zircon textures, and U-Pb and K-Ar ages of breccias from North Ray Crater (Apollo 16) are similar to heterogeneous Imbrium ejecta from Apollo 15.
10:15 a.m.	Gaffney A. M. * Borg L. E. Wimpenny J. B. N. Sio C. K. Cassata W. S. et al.	<u><i>Isotope Systematics of Mg-Suite Troctolite 14321,1847</i></u> [#2086] Rare earth element concentrations and Sm-Nd isotopic results reveal a complex history for an Mg-suite troctolite from the Apollo 14 site.
10:30 a.m.	Cernok A. * Anand M. Darling J. Zhao X. White L. et al.	<u><i>Lunar Apatite — A Reliable Shock-Resistant Hygrometer and Impact-Sensitive Pb-Pb Chronometer?</i></u> [#2232] Water abundance and its isotopic composition combined with Pb-Pb ages of variably shocked apatite reveal mineral's potential to retain important geochemical data.
10:45 a.m.	Prissel T. C. * Gross J.	<u><i>Establishing New Co-Magmatic Trends Among the Lunar Highlands</i></u> [#3106] Here, we challenge classical interpretations of the lunar highlands by establishing new co-magmatic trends among primitive igneous rock types.
11:00 a.m.	Fa W. * Liu T. Xie M. Du J.	<u><i>Regolith Thickness Over the Apollo Landing Sites from Morphology of Small Fresh Impact Craters</i></u> [#1765] We estimated regolith thickness over the Apollo landing regions from morphology of small impact craters and compared them with the seismic experiments.

THURS ORAL

11:15 a.m.	Nishiizumi K. * Welten K. C. Caffee M. W.	<u>Recent Deposition and Mixing History of the Apollo 17 Drill Core 70009–70001</u> [#2277] Depth profiles of cosmogenic nuclides from the Apollo 17 drill core were measured. Recent cratering and mixing history of the core were investigated.
11:30 a.m.	Jolliff B. L. * Korotev R. L.	<u>On the Importance of Apollo Regolith Samples for Scientific Exploration of the Moon</u> [#2706] Integration of Apollo soil and lunar meteorite regolith breccia compositional data with remote sensing continues to improve understanding of the lunar surface.

Thursday, March 21, 2019

[R502]

MARTIAN REMOTE SENSING: MINERALOGY, MORPHOLOGY, AND CHEMISTRY

8:30 a.m. Waterway Ballroom 4

Chairs: Mario Parente and Vivian Sun

Times	Authors (*Denotes Presenter)	Abstract Title and Summary
8:30 a.m.	Kamps O. M. * Hood D. Hewson R. H. van Ruitenbeek F. J. A. van der Meer F. D. et al.	<u>GRS Element Modelling with CRISM Summary Products</u> [#2543] Linear modelling of element concentration with spectral data. New method to understand the relation between geological processes and element distribution.
8:45 a.m.	Kaufman S. V. * Mustard J. F. Head J. W. III	<u>Valley Networks and Hydrous Mineralogy: Quantifying the Inverse Spatial Correlation Between Features Formed by Liquid Water</u> [#2207] Valley networks are / Against “warm and wet” due to / Lack of minerals.
9:00 a.m.	Stachurski F. * Liu Y.	<u>Water Content and Mineral Abundances at Gale Crater, Mars as Inferred from OMEGA and CRISM Observations</u> [#2616] We derive the water content at Gale Crater from OMEGA and mineral abundances of the region from CRISM, to compare with the ground truth data from Curiosity.
9:15 a.m.	Stack K. M. * Sun V. Z. Arvidson R. E. Fedo C. Bennett K. et al.	<u>Origin of Linear Ridges in the Clay-Bearing Unit of Mount Sharp, Gale Crater, Mars</u> [#1210] Linear ridges / In clay strata of Mount Sharp / Eroded bedrock.
9:30 a.m.	Powell K. E. * Arvidson R. E. Edwards C. S.	<u>Spectral Properties of the Layered Sulfate-Bearing Unit in Mount Sharp, Gale Crater, Mars</u> [#1455] Observations of the sulfate unit in Mt. Sharp and variations in its CRISM spectral signature due to differing textures and amounts of exposure.
9:45 a.m.	Tinker C. R. * Horgan B. Bennett K.	<u>Morphology and Occurrence of Dark Toned Diagenetic Features in the Vera Rubin Ridge, Gale Crater, Mars from MAHLI Color Images</u> [#1730] In this study, three kinds of dark toned diagenetic features are scrutinized through the eyes of MaHLI, citing possible origins from reducing fluvial activity.
10:00 a.m.	Parente M. * Arvidson R. E. Itoh Y. Lin H. Mustard J. F. et al.	<u>Convergence on Mineral Detections Over Gale Crater, NE Syrtis, and Jezero Crater Using Advanced Data Processing Techniques for CRISM Hyperspectral Imaging Data</u> [#3112] We compare mineral detections using several advanced data processing techniques to aid Curiosity traverse planning and to identify Mars 2020 science targets.
10:15 a.m.	Dundar M. * Ehlmann B. Leask E.	<u>Rare Phase Detections in CRISM Data at Pixel-Scale by Machine Learning Generate New Discoveries About Geology at Mars Rover Landing Sites: Jezero and NE Syrtis</u> [#3105] Using machine-learning techniques for processing CRISM data, we report new rare discoveries in significant locations for landed exploration with rovers.
10:30 a.m.	Zastrow A. M. * Glotch T. D.	<u>Probing Mineral Abundances in Olivine- and Carbonate-Bearing Units in Jezero Crater, Mars, with Linear Spectral Unmixing</u> [#2037] Spectral unmixing of Jezero Crater CRISM data reveals an interesting interplay between olivine, carbonate, and serpentine with carbonate abundances up to 35%.

THURS ORAL

10:45 a.m.	Sun V. Z. * Stack K. M.	<u><i>Understanding the Continuity of Regional Units in the Mars 2020 Jezero and Northeast Syrtis Regions: Implications for the Origin of the Mafic Unit(s)</i></u> [#2271] We propose that Jezero's mafic floor may be related to the regional NE Syrtis mafic cap unit, suggesting an airfall deposition origin rather than volcanic flow.
11:00 a.m.	Salese F. * Mangold N. Kleinhans M. G. de Haas T. Ansan V. et al.	<u><i>Estimated Minimum Lifespan of the Jezero Crater Delta, Mars</i></u> [#2107] We re-examine the delta-forming discharge and propose scenarios for a parameter range of grain size and other key variables.
11:15 a.m.	Tarnas J. D. * Mustard J. F. Lin H. Goudge T. A. Amador E. S. et al.	<u><i>Hydrated Silica in the Jezero Deltas</i></u> [#2551] We detect hydrated silica in the Jezero deltas and their source rock units, spanning a range of formation environments with different degrees of habitability.
11:30 a.m.	Fawdon P. * Balme M. R. Bridges J. Davis J. M. Gupta S. et al.	<u><i>The Ancient Fluvial Catchment of Oxia Planum: The Exomars 2020 Rover Landing Site</i></u> [#2356] The ExoMars rover landing site has a large catchment with evidence for several periods of fluvial and palaeolake activity post-dated by tectonic structures.

Thursday, March 21, 2019

[R503]

FROM METEORITES TO ASTEROIDS AND BACK AGAIN!

8:30 a.m. Waterway Ballroom 5

Chairs: Driss Takir and Monica Grady

Times	Authors (*Denotes Presenter)	Abstract Title and Summary
8:30 a.m.	Grady M. M. * Batty C. Farsang S. Rowden P.	<u><i>Identification of Organic Components in Carbonaceous Chondrites by UV Spectroscopy</i></u> [#2727] We have determined UV spectra (240–400 nm) of five C chondrites and several organic compounds to see if individual organic species can be identified.
8:45 a.m.	Izawa M. R. M. * Reddy V. Le Corre L. McGraw A. Sanchez J. A. et al.	<u><i>Discovery of a Possible CM2 Carbonaceous Chondrite Parent Body in the Near-Earth Asteroid Population</i></u> [#3174] We found a possible CM2 carbonaceous chondrite parent asteroid (1999 JV6) based on a strong spectral match with Mukundpura (CM2).
9:00 a.m.	Bates H. C. * Donaldson Hanna K. L. King A. J. Bowles N. E. Russell S. S.	<u><i>Spectrally Characterising the Effects of Thermal Metamorphism in CM2 and C2 Chondrites</i></u> [#1245] Features diagnostic of post aqueous alteration thermal metamorphism are identified in the thermal infrared spectra of some CM and C2 carbonaceous chondrites.
9:15 a.m.	Bramble M. S. * Milliken R. E. Patterson W. R. III Mustard J. F.	<u><i>Thermal Infrared Characterization of Ordinary Chondrite Analogs in a Simulated Asteroid Environment with Implications for the Remote Analysis of Asteroid Mineralogy</i></u> [#2101] How do you alter / Ye most common regolith / In space's cold void?
9:30 a.m.	Takir D. * Stockstill-cahill K. R. Hibbitts C. A. Nakauchi Y.	<u><i>3-μm Reflectance Spectroscopy of Carbonaceous Chondrites Under Asteroid-Like Conditions</i></u> [#2056] We present new analyses of 21 carbonaceous chondrites' 3- μ m reflectance spectra that were measured under asteroid-like condition.
9:45 a.m.	Cantillo D. C. * Reddy V. Pearson N. Sanchez J. A. Takir D. et al.	<u><i>Constraining Exogenic Carbonaceous Material Abundance on (16) Psyche from Laboratory Spectral Measurements</i></u> [#1703] We conducted laboratory experiments with mixtures of metal, silicates, and carbonaceous material to simulate the spectrum of asteroid (16) Psyche's regolith.
10:00 a.m.	Reddy V. * Pearson N. Agee C. B. Cantillo D. C. Le Corre L. et al.	<u><i>Spectral Investigation of Anomalous Metal-Rich Chondrite Northwest Africa (NWA) 12273: Implications for Asteroid (16) Psyche</i></u> [#2212] We collected spectra of metal-rich anomalous chondrite Northwest Africa (NWA) 12273 with 65% metal and 30% ordinary chondrite and compared it to (16) Psyche.

THURS ORAL

10:15 a.m.	Wakita S. * Genda H.	<u><i>Effect of Collisions on Dehydration of Hydrous Materials in Asteroids</i></u> [#1321] Our study found that hydrous materials in asteroids can avoid from dehydration during planetesimal collisions and might be origin for other asteroidal surface.
10:30 a.m.	Omura T. * Nakamura A. M.	<u><i>Experimental Study on the Primordial Porous Structure of Chondrite Parent Bodies Due to Self-Gravity</i></u> [#1324] We conducted compaction experiments using analogs of chondrite components to estimate internal porosity structure of chondrite parent bodies.
10:45 a.m.	Nichols K. D. * Scheeres D. J.	<u><i>New Electrostatic Charge Models Show Dust Lofting at Ryugu and Bennu</i></u> [#2136] This study applies new charge models to dust lofting on Ryugu and Bennu, finding it occurs frequently across a range of sizes for various surface conditions.
11:00 a.m.	Patel A. V. * Hartzell C. M.	<u><i>Cohesive Regolith Clump Size Prediction on Airless Bodies</i></u> [#1584] We present a model predicting the size of regolith clumps that are easier to detach than their constituent grains, as a function of grain and central body size.
11:15 a.m.	Fieber-Beyer S. K. * Gaffey M. J.	<u><i>The Family of Asteroid (6) Hebe: Initial Results</i></u> [#1047] Our research is a limited spectroscopic investigation of 35 asteroids in the dynamical region near Hebe to test for the presence of a small family of H-chondrite composition.
11:30 a.m.	Noonan J. W. * Reddy V. Harris W. M. Bottke W. F. Sanchez J. A. et al.	<u><i>Is Asteroid (3) Juno the Parent Body of H-Chondrite Meteorites?</i></u> [#1755] The near-infrared spectrum of (3) Juno observed by the NASA IRTF on Mauna Kea will make the case that the asteroid may be the source of the H chondrites.

Thursday, March 21, 2019

[R504]

PRESOLAR, INTERPLANETARY, AND COMETARY DUST

8:30 a.m. Waterway Ballroom 6

Chairs: Nan Liu and Thomas Zega

Times	Authors (*Denotes Presenter)	Abstract Title and Summary
8:30 a.m.	Schulte J. * Bose M. Young P. Vance G.	<u><i>Using Symmetric and Asymmetric Three-Dimensional Supernova Models to Constrain the Origins of Presolar SiC Grains</i></u> [#1746] Asymmetric 3-dimensional supernova models are a good fit to the presolar SiC X grain isotopic compositions.
8:45 a.m.	Shollenberger Q. R. * Brennecka G. A.	<u><i>Heavy Rare Earth Element Isotopics from Chemical Separates of the Murchison Meteorite: Implications for SiC Formation</i></u> [#1042] We report Dy, Er, and Yb isotope systematics of chemical separates from Murchison to understand SiC formation conditions and the presolar carriers of REEs.
9:00 a.m.	Liu N. * Stephan T. Cristallo S. Gallino R. Boehnke P. et al.	<u><i>Presolar Silicon Carbide Grains of Groups Y and Z: Their Strontium and Barium Isotopic Compositions and Stellar Origins</i></u> [#1349] We report Sr and Ba isotope data of a number of new Y and Z grains and discuss the inferred s-process efficiency and their stellar origins.
9:15 a.m.	Hoppe P. * Pignatari M. Amari S.	<u><i>Isotopic Signatures of Supernova Nucleosynthesis in Presolar SiC Grains of Type AB with Light Nitrogen</i></u> [#1547] We report C, N, Al-Mg, Si, and S isotope data of 22 presolar SiC grains of Type AB, which are discussed in the context of two supernova models.
9:30 a.m.	Zega T. J. * Bernal J. J. Howe J. Y. Haenecour P. Amari S. et al.	<u><i>In Situ Irradiation and Heating of Synthetic SiC and Implications for the Origins of C-Rich Circumstellar Materials</i></u> [#2127] In situ irradiation and heating of synthetic SiC can reproduce the microstructures observed in some C-rich circumstellar grains in primitive meteorites.
9:45 a.m.	Leitner J. * Hoppe P. Kodolányi J.	<u><i>Presolar Silicates with Unusual Magnesium-Isotopic Compositions</i></u> [#2090] We report two 25 Mg-poor Group 1 silicates that cannot be explained by standard low-mass AGB star models, suggesting incomplete mixing of precursor materials.

THURS ORAL

10:00 a.m.	Haenecour P. * Floss C. Brearley A. J. Howe J. Y. Zega T. J.	<u><i>A Large Donut-Shaped Presolar Silicate from the MIL 07687 Carbonaceous Chondrite</i></u> [#1683] We report on an unusually donut-shaped large presolar silicate grain that might show evidence of formation in multiple distinct environments.
10:15 a.m.	Taylor S. * Lever J. H. Alexander C. M. O'D. Bardyn A. Nittler L. R. et al.	<u><i>Sampling Interplanetary Dust Particles from Antarctic Air</i></u> [#2514] We built a collector that ran continuously for two years and collected IDPs from clean air at the South Pole. We found a few intact IDPs and ET particle fragments.
10:30 a.m.	Keller L. P. * Flynn G. J.	<u><i>A Kuiper Belt Source for Solar Flare Track-Rich Interplanetary Dust Particles</i></u> [#2002] Bullets from the Sun / Leave tracks in mineral grains / Are used as a clock.
10:45 a.m.	Gainsforth Z. * Butterworth A. L. Jilly- Rehak C. E. Westphal A. J.	<u><i>Evidence for Highly Variable, Pre-Accretionary Oxidation of GEMS</i></u> [#2278] GEMS have experienced oxidation and heating that cannot be ascribed solely to atmospheric entry.
11:00 a.m.	Noguchi T. * Ohashi N. Bradley J. P. Nakashima D. Nakamura T. et al.	<u><i>Chondrule-Like Objects and a Refractory Inclusion in GEMS-Bearing Antarctic Micrometeorites and Interplanetary Dust Particles</i></u> [#2392] We report chondrule-like objects and a refractory inclusion that are as large as those in the Stardust samples found in GEMS-bearing AMMs and IDP.
11:15 a.m.	Frank D. R. * Huss G. R. Nagashima K. Hellebrand E. Westphal A. J. et al.	<u><i>Rumuruti and Metamorphosed, Ordinary Chondrite Chondrule Fragments from Comet 81P/Wild 2</i></u> [#3281] We present combined chemical and Oxygen isotopic measurements of two new terminal particles from comet 81P/Wild2 and infer likely R chondrite and OC origins.
11:30 a.m.	Fukuda K. * Joswiak D. J. Brownlee D. E. Beard B. L. Spicuzza M. J. et al.	<u><i>The Relationship Between Oxygen and Magnesium Isotope Ratios in Olivine from the Comet 81P/Wild 2: A Comparison with AOAs in Primitive Meteorites</i></u> [#1989] Wild 2 olivine particles have near-chondritic Mg-isotope ratios, regardless of their different O-isotope ratios.

Thursday, March 21, 2019

[R505]

IMPACTS: PROCESSES FROM PLANETESIMALS TO PLANETS

8:30 a.m. Montgomery Ballroom

Chairs: Veronica Bray and Michael Poelchau

Times	Authors (*Denotes Presenter)	Abstract Title and Summary
8:30 a.m.	Stewart S. T. * Carter P. J. Davies E. J. Lock S. J. Kraus R. G. et al.	<u><i>Impact Vapor Plume Expansion and Hydrodynamic Collapse in the Solar Nebula</i></u> [#1250] Nebula displaced / By bow shock; plume unstable / Collapse makes a cloud.
8:45 a.m.	Emsenhuber A. * Asphaug E.	<u><i>Collision Chains Among the Terrestrial Planets</i></u> [#1856] We follow second remnants from giant impact, until they further collide. We determine whether there can be multiple collisions between the same or other bodies.
9:00 a.m.	Davison T. M. * Raducan S. D. Collins G. S. Bland P. A.	<u><i>Collisional Histories of Small Planetesimals: Implications for Constraining the Age of the Surface of OSIRIS-REx Target, Bennu</i></u> [#2385] How can we constrain / Bennu's surface age and strength? / Models of craters!
9:15 a.m.	Daly R. T. * Barnouin O. S. Light S. L. Cintala M. J. Hikosaka K. et al.	<u><i>Crater Morphometry and Scaling in Coarse, Rubble-like Targets: Insights from Impact Experiments</i></u> [#1647] Impact experiments reveal new clues to crater formation in rubble-like targets. We discuss implications for asteroids such as Itokawa, Ryugu, and Bennu.
9:30 a.m.	Elliott J. R. * Melosh H. J.	<u><i>The Role of Target Strength in High-Speed Ejecta Size Distributions</i></u> [#3123] We numerically simulate impacts into the martian surface with varying target materials and strengths. The resulting ejecta size distributions are reported.

THURS ORAL

9:45 a.m.	Hopkins R. T. * Osinski G. R.	<u><i>Transient Cavity Expansion and Collapse in Layered Sedimentary Versus Crystalline Targets</i></u> [#1885] We model crater formation in mixed targets to study the effect of sediment thickness and target layering on transient cavity expansion and collapse.
10:00 a.m.	Manske L. * Marchi S. Wuenemann K.	<u><i>Production and Provenience of Impact-Generated Melt by Large Scale Collisions on Mars</i></u> [#2753] In our numerical model series, we quantify impact-induced melt volumes, locate melt provenance and final distributions for large scale impactors on Mars.
10:15 a.m.	Sefton-Nash E. * Faes Z. Witasse O. Buchenberger B.	<u><i>Alignment of Mars Elongated Crater Azimuths with Orbit Planes Representing Paleo-Equators</i></u> [#3252] Do elongated craters on Mars align with paleo-equators such that impactors could have originated from a decaying debris disk?
10:30 a.m.	Pan L. * Quantin C. Michaut C. Breton S.	<u><i>An Impact Origin for Chryse Planitia on Mars?</i></u> [#2575] New evidence for an impact origin of Chryse Planitia is found through regional analysis of crater shape and statistics combined with gravity signature.
10:45 a.m.	Holo S. J. * Kite E. S.	<u><i>New Insights into Crater Obliteration in the Noachian Highlands of Mars</i></u> [#1649] Clustering analysis of Noachian craters constrains the crater obliteration process and demonstrates consistency with a crater SFD that changes through time.
11:00 a.m.	Scheller E. L. * Ehlmann B. L.	<u><i>Isidis Megabreccia Composition, Size, and Formation History</i></u> [#2033] We characterize pre-Isidis lithologies in megabreccia blocks associated with the western rim of Isidis basin and consider their possible formation mechanisms.
11:15 a.m.	Calef F. J. III * Wellington D. Newsom H. Gabriel T.	<u><i>Geology and Origin of Taconite Crater on the Vera Rubin Ridge</i></u> [#1983] Taconite Crater is the first small fresh crater investigated by the Curiosity rover in Gale Crater, Mars during its investigation along the Vera Rubin Ridge.
11:30 a.m.	Agarwal A. Poelchau M. H. * Kenkmann T.	<u><i>Kinked Biotite as a Strain Marker in Experimental Impact Craters in Gneiss</i></u> [#2540] Biotites shortened through shock-induced kinking were measured and mapped in the subsurface of experimental craters. Their use as strain markers is unique.

Thursday, March 21, 2019

[R551]

LUNAR PETROLOGY, GEOCHEMISTRY, AND GEOCHRONOLOGY; FROM SURFACE TO INTERIOR

1:30 p.m. Waterway Ballroom 1

Chairs: Tabb Prissel and Jed Mosenfelder

Times	Authors (*Denotes Presenter)	Abstract Title and Summary
1:30 p.m.	Thiessen F. * Nemchin A. A. Snape J. F. Whitehouse M. J.	<u><i>Magmatic Events Recorded in Apollo 14 Zircon</i></u> [#2294] U-Pb SIMS ages of zircon in four Apollo 14 breccias helped to identify different magmatic events between ~4.3 and ~3.9 Ga, and an impact event at ~3936 Ma.
1:45 p.m.	Barboni M. * Trail D. McKeegan K. D.	<u><i>Discovering Lost Lunar Magmas Using Apollo Zircons</i></u> [#3027] We propose a new approach to decipher lunar magmas' major element compositions using Aluminum contents of Apollo zircons.
2:00 p.m.	Robinson K. L. * Nagashima K. Huss G. R. Taylor G. J. Kring D. A.	<u><i>An Ancient KREEP-Poor, Chlorine-37-Rich Source Within the Moon</i></u> [#2063] New measurements of high ³⁷ Cl in KREEP-poor ~4.3 Ga lunar basalt from Miller Range 13317 suggest there may be multiple Cl reservoirs inside the Moon.
2:15 p.m.	Stephant A. * Anand M. Zhao X. Chan Q. H. S. Bonifacie M. et al.	<u><i>The Chlorine Isotopic Composition of the Moon as Revealed by Melt Inclusions</i></u> [#1857] ³⁷ Cl/ ³⁵ Cl of lunar melt inclusions are similar to apatite composition, implying that the Moon acquired its heavy signature during the earliest stages of LMO.

2:30 p.m.	Mosenfelder J. L. * Andrys J. L. Cseres J. R. Hirschmann M. M.	<u>Water in the Moon: The Perspective from Nominally Anhydrous Minerals</u> [#2506] If you want to put / Hydrogen in lunar plagioclase / Iron is the key.
2:45 p.m.	Simon S. B. * Sutton S. R.	<u>Valences of Ti and Cr in Lunar Crystalline Melt Breccias</u> [#1447] Valences of Cr and Ti and Ti coordination data for olivine and pyroxene from crystalline melt breccias are reported. Differences with basalt results are seen.
3:00 p.m.	Treiman A. H. * Semprich J.	<u>Dunite in Lunar Meteorite Northwest Africa 11421: Petrology and Origin</u> [#1225] From the Moon's mantle / Smear, cooked, thrown up in melt rock / It's been a rough ride.
3:15 p.m.	Stu Webb * Neal C. R.	<u>Quantitative Textural Analysis of Thin Sections Cut from the Interior and Exterior of Lunar Sample 14053</u> [#2534] Crystal size distribution profiles from the interior and exterior of lunar sample 14053.
3:30 p.m.	Nagaoka H. * Fagan T. J. Kayama M. Karouji Y. Hasebe N. et al.	<u>Mineralogic and Petrologic Characterization of a New Silicic Clast in Lunar Brecciated Meteorite, Northwest Africa 2727</u> [#2270] We report mineralogic and petrologic characters of the silicic clast in lunar meteorite NWA 2727, and discuss the petrogenesis by comparing with other samples.
3:45 p.m.	Valencia S. N. * Jolliff B. L. Korotev R. L.	<u>Apollo 12 Sample 12013: Petrogenesis by Silicate-Liquid Immiscibility or Bi-Modal Volcanism?</u> [#1433] We investigate possible formation mechanisms for Apollo 12 sample 12013, a lunar breccia composed of granitic, mafic, and REE-rich components.
4:00 p.m.	First E. C. * Rutherford M. J.	<u>Silicate Liquid Immiscibility in Evolved Lunar Magmas</u> [#2117] Experiments on silica-enriched lunar magmas show that immiscible liquids are encountered at depth and in the presence of small amounts (~3000 ppm) of H ₂ O.
4:15 p.m.	Fagan T. J. * Ohkawa S.	<u>Lunar Silica-Bearing Diorite: A Lithology from the Moon with Implications for Igneous Differentiation</u> [#2008] Silica-bearing igneous clast in lunar breccia found. What?! No correlative enrichment in incompatible elements or Fe?! Igneous mystery prevails.
4:30 p.m.	Christoffersen R. * Simon J. I. Mouser M. D. Ross D. K.	<u>First TEM Confirmation of Alkali Feldspar Cryptoperthite in Lunar Rocks: Implications for the Origin and Thermal History of Lunar Felsites</u> [#2131] TEM characterization of what appears to be the first well-documented lunar cryptoperthite provides clues to the thermal history of the host felsite.

Thursday, March 21, 2019

[R552]

MARTIAN MADNESS: ROVING THE RIDGES

1:30 p.m. Waterway Ballroom 4

Chairs: Abigail Fraeman and Nicholas Castle

Times	Authors (*Denotes Presenter)	Abstract Title and Summary
1:30 p.m.	Fraeman A. A. * Arvidson R. E. Horgan B. H. Jacob S. R. Johnson J. R. et al.	<u>Synergistic Orbital and In Situ Observations at Vera Rubin Ridge: Comparing CRISM and Curiosity Observations</u> [#2118] We synthesize Curiosity spectral data from the rover's traverse and orbital observations. Specific focus on results from Vera Rubin Ridge.
1:45 p.m.	Thompson L. M. * Fraeman A. A. Berger J. A. Rampe E. B. Boyd N. I. et al.	<u>Compositional Characteristics and Trends Within the Vera Rubin Ridge, Gale Crater, Mars as Determined by APXS: Sedimentary, Diagenetic, and Alteration History</u> [#3269] APXS derived chemistry of the VRR, Gale Crater, can elucidate depositional environment and diagenetic/alteration history.
2:00 p.m.	Morris R. V. * Bristow T. F. Rampe E. B. Yen A. S. Vaniman D. T. et al.	<u>Mineralogy and Formation Processes for the Vera Rubin Ridge at Gale Crater, Mars from CheMin XRD Analyses</u> [#1127] Mineralogy and formation process for the Vera Rubin Ridge in Gale Crater based on XRD analyses by the CheMin instrument on the MSL rover Curiosity.

THURS ORAL

2:15 p.m.	Johnson J. R. * Fraeman A. A. Wellington D.	Cloutis E. Bell J. F. III et al.	<u><i>Variations in Visible/Near-Infrared Hematite Spectra Related to Grain Size and Crystallinity</i></u> [#1314] Hematite VNIR spectral parameters vary with grain size and amorphous content, as seen in lab data of size separates and Mastcam spectra of hematite-rich targets.
2:30 p.m.	Turner S. M. R. * Schwenzer S. P. Bedford C. C. et al.	Bridges J. C. Rampe E. B. et al.	<u><i>Thermochemical Modelling of Fluid-Rock Reactions in Vera Rubin Ridge, Gale Crater, Mars</i></u> [#1897] Thermochemical modelling to investigate possible reaction pathways for the Fe-oxide rich mineral assemblage observed at Vera Rubin Ridge, Gale Crater, Mars.
2:45 p.m.	L'Haridon J. * Wiens R. C. David G.	Mangold N. Cousin A. et al.	<u><i>Iron Mobility During Diagenesis Deduced from ChemCam Observations at Gale Crater, Mars</i></u> [#1869] ChemCam onboard the Curiosity rover analyzed dark-toned Fe-rich diagenetic features indicative of redox processes in the sedimentary rocks of Gale Crater.
3:00 p.m.	Horgan B. * Johnson J. R. Jacob S.	Fraeman A. Thompson L. et al.	<u><i>Redox Conditions During Diagenesis in the Vera Rubin Ridge, Gale Crater, Mars, from Mastcam Multispectral Images</i></u> [#1424] End of the rainbow / No pot of gold on the ridge / Just water-bleached rocks.

Thursday, March 21, 2019

[R553]

DIFFERENTIATION OF PLANETS AND ASTEROIDS: FROM CORES TO LATE VENEERS

1:30 p.m. Waterway Ballroom 5

Chairs: Katherine Bermingham and Marc Hirschmann

Times	Authors (*Denotes Presenter)	Abstract Title and Summary
1:30 p.m.	Johnson B. C. * Evans A. J.	Sori M. M. <u><i>Ferrovolcanism, Pallasites, and Psyche</i></u> [#1625] Core material of a cooling planetesimal may be intruded into the rocky mantle of the planetesimal or even erupted onto its surface. #Pallasites #Psyche.
1:45 p.m.	Maurel C. * Weiss B. P. Ball M. R.	Bryson J. F. J. Lyons R. J. et al. <u><i>Partial Differentiation and Magnetic History of the IIE Iron Meteorite Parent Body</i></u> [#2049] We present new paleomagnetic evidence and impact simulations in favor of the partial differentiation of the IIE iron meteorite parent body.
2:00 p.m.	Ni P. * Ryan C. J.	Chabot N. L. Shahar A. <u><i>Iron Isotope Fractionation During Asteroidal Core Crystallization</i></u> [#3068] Equilibrium Fe isotope fractionation between liquid and solid metal has been determined to understand the heavy Fe isotopic composition for iron meteorites.
2:15 p.m.	Ray S. * Rai V. K.	Wadhwa M. <u><i>Iron Isotope Compositions of Large Metal Nodules from the Norton County Aubrite</i></u> [#1960] Insights into the origin of metal from Norton County aubrite using iron isotope composition.
2:30 p.m.	Righter K. * Rowland R. II Righter M.	Pando K. Ross D. K. et al. <u><i>Core-Mantle Partitioning of Silver and Bismuth from 0 to 20 GPa, with Application to Core Formation in Earth and Mars</i></u> [#1104] Core-mantle partitioning of Bi and Ag require a post-core formation removal mechanism — sulfide segregation/matte?
2:45 p.m.	Grewal D. S. * Holmes A. K. et al.	Dasgupta R. Costin G. Li Y. <u><i>The Fate of Nitrogen During Core-Mantle Separation</i></u> [#2189] New experimental data is used to discuss the fate of nitrogen during core-mantle separation for a wide range of accretion and differentiation scenarios.
3:00 p.m.	Steenstra E. S. * van Westrenen W. Klemme S.	Berndt J. Fei Y. <u><i>High-Temperature Partitioning of Volatile Elements in the Cores of Moon and Mars?</i></u> [#1071] High P-T experiments were used to study temperature effects on volatile element siderophile behavior. Results were applied to study volatiles in Moon and Mars.
3:15 p.m.	Young E. D. * Tang H.	<u><i>Isotopic Fractionation of Moderately Volatile Elements During Moon Formation</i></u> [#1941] We modeled MVE isotopic fractionation during Moon formation to interpret isotopic signature of MVE and lithospheric elements on the Moon relative to Earth.

THURS ORAL

3:30 p.m.	Dauphas N. *	<u><i>Reassessing the Depletions in K and Rb of Planetary Bodies</i> [#1466]</u> K and Rb show slightly different behaviors, providing a means of assessing the cause of their depletions in planets.
3:45 p.m.	Hirschmann M. M. * Li J. Bergin E. A. Ciesla F. J. Blake G. A.	<u><i>Origin of Major Volatiles (H,C,N,S) in the Bulk Earth: Insights from Moderately Volatile Elements, and from C/S vs. C Systematics of Chondritic and Achondritic Meteorites</i> [#2836]</u> Bulk Earth C and S estimated from moderately volatile depletions suggest accretion partly from partly degassed planetesimals akin to achondritic parent bodies.
4:00 p.m.	Walker R. J. * Bermingham K. R.	<u><i>Revisiting the Concept of Late Accretion</i> [#1385]</u> The concept of late accretion is supported by Os isotopes and dynamical modeling, but refuted by metal silicate partitioning of highly siderophile elements (HSE) at high pressure and temperature conditions.
4:15 p.m.	Bermingham K. R. * Walker R. J.	<u><i>Earth's Water Added During Late-Stage Primary Accretion?</i> [#1234]</u> Mo and Ru isotope compositions of meteorites and terrestrial materials indicate that water may have been delivered to Earth during late-stage primary accretion.
4:30 p.m.	Sharp Z. D. * Olson P. L.	<u><i>Nebular Ingassing of Water and Noble Gases</i> [#2555]</u> Nebular ingassing supplies an excess of light noble gases to Earth, and a deficit of heavy noble gases, explained by hydrodynamic escape and late addition.

Thursday, March 21, 2019

[R554]

PLANETARY VOLCANISM: A SONG OF FIRE AND ICE

1:30 p.m. Waterway Ballroom 6

Chairs: Susan Sakimoto and Paul Byrne

Times	Authors (*Denotes Presenter)	Abstract Title and Summary
1:30 p.m.	Besse S. * Barraud O. Doressoundiram A. Cornet T. Munoz C.	<u><i>Explosive Volcanism on Mercury: Latest Results from an In-Depth Analysis of the MASCs Observations</i> [#2451]</u> Explosive volcanism on Mercury appear to be larger in size than previously measured, with potential various eruptive mechanisms.
1:45 p.m.	Pegg D. L. * Rothery D. A. Balme M. R. Conway S. J.	<u><i>Explosive Vents on Mercury: Commonplace Multiple Eruptions and Their Implications</i> [#1273]</u> We have looked at all explosive volcanic vents on Mercury and have found that compound vents are common on the surface of the planet.
2:00 p.m.	Wilson L. * Head J. W. Morgan C. R.	<u><i>Factors Controlling the Dispersal of Lunar Pyroclasts</i> [#1342]</u> We show how the volatile contents of lunar magmas combine with pyroclast sizes to determine the distance to which they can be ejected in explosive eruptions.
2:15 p.m.	Gasplie L. M. * Bennett K. A. Gaddis L. R. Donaldson Hanna K. L. Horgan B. H. N. et al.	<u><i>Characterization of a Potential Compositional Halo Around Ina Irregular Mare Patch</i> [#2889]</u> Ina is haloed / It's shrouded in mystery / Where did it come from?
2:30 p.m.	Cataldo V. * Williams D. A. Schmeeckle M. W. Leone G.	<u><i>Vallis Schröteri, Moon: Results of First 3-D Model of Thermal Erosion by Turbulent Lava Reveal How Erosion Likely Shaped the Inner Rille</i> [#2297]</u> First 3-D model of thermal erosion by lava provides evidence for erosion at Vallis Schröteri and an estimate of the interplay of mechanical and thermal erosion.
2:45 p.m.	Sakimoto S. E. H. * Gregg T. K. P.	<u><i>On the Formation of Lunar Sinuous Rilles: Insights from Multiphysics Modeling Techniques</i> [#3108]</u> Moon's sinuous rilles / Turbulent or laminar? / Flow'd across the plains.
3:00 p.m.	Rodriguez Sanchez-Vahamonde C. D. * Neish C. D. Tornaberne L. L.	<u><i>Quantification of Surface Roughness of Lava Flows on Mars</i> [#2807]</u> We report RMS slope and Hurst exponent parameters for HiRISE DTMs of a variety of lava flows on Mars to constrain their surface roughness.
3:15 p.m.	Ganesh I. * Carter L. M. Smith I. B.	<u><i>SHARAD Mapping of the Caldera of Arsia Mons</i> [#1859]</u> We have modeled the SHARAD signal propagation using MCMC techniques to determine the dielectric properties of the subsurface media in the Arsia Mons caldera.

THURS ORAL

3:30 p.m.	Crown D. A. * Scheidt S. P. Berman D. C.	<u><i>Distribution and Morphology of Lava Tube Systems on the Western Flank of Alba Mons, Mars</i></u> [#1417] Geologic mapping studies are characterizing the distribution and morphology of the extensive lava tube systems on the western flank of Alba Mons.
3:45 p.m.	Whelley P. L. * Novak A. M. Richardson J. Bleacher J. A.	<u><i>Arabia Terra Layered Deposit Stratigraphy and Distribution: Evidence for Early Martian Explosive Volcanism?</i></u> [#1085] We are testing a provocative hypothesis that calderas in Arabia Terra produced wide spread ash deposits using topography and mineralogy observations.
4:00 p.m.	Horvath D. G. * Moitra P. Andrews-Hanna J. C.	<u><i>A Late-Amazonian Phreatomagmatic Tephra Deposit in Elysium Planitia, Mars</i></u> [#2517] We report on a low albedo feature in Elysium Planitia, interpreted as a recent pyroclastic deposit. The nature and formation of this deposit are discussed.
4:15 p.m.	Abrahams J. N. H. * Nimmo F.	<u><i>Ferrovulcanism: Iron Volcanism on Metallic Asteroids</i></u> [#1598] We predict iron volcanism to have occurred on metallic asteroids as they cooled and discuss implications for both the evolution and appearance of these bodies.
4:30 p.m.	McGovern P. J. * White O. L.	<u><i>Stress-Enhanced Ascent of Cryomagmas Through Pluto's Ice Shell from Nitrogen Ice Loading of a Sputnik Planitia Basin</i></u> [#2994] Loading of Pluto's icy outer shell from material filling the Sputnik Planum basin + impact-induced relief on the ice-ocean boundary can promote cryovolcanism.

Thursday, March 21, 2019

[R555]

SMALL BODIES: OBSERVATIONS FROM THE GROUND UP

1:30 p.m. Montgomery Ballroom

Chairs: Patrick Taylor and Amanda Hendrix

Times	Authors (*Denotes Presenter)	Abstract Title and Summary
1:30 p.m.	Walker J. D. * Chocron S. Grosch D. J. Durda D. D. Housen K. R.	<u><i>Momentum Enhancement Due to Hypervelocity Impacts into Various Rock Targets with Aluminum Impactor Sizes of 2.54 and 4.45 cm and Impact Speeds of 2 km/s</i></u> [#3214] Experimental work of aluminum spheres striking various rock materials and measuring the momentum enhancement with a ballistic pendulum. Size dependence occurs.
1:45 p.m.	Shober P. M. * Bland P. A. Jansen-Sturgeon T. Sansom E. K. Devillepoix H. A. R. et al.	<u><i>Detections of Mini-Moon Fireballs Within the Desert Fireball Network</i></u> [#1055] An orbital analysis of fireballs detected by the Desert Fireball Network (DFN) that were captured by the Earth prior to atmospheric impact.
2:00 p.m.	Rivera-Valentín E. G. * Taylor P. A. Reddy V. Jao J. S. Benner L. A. M. et al.	<u><i>Radar and Near-Infrared Characterization of Near-Earth Asteroid (163899) 2003 SD220</i></u> [#3016] Radar and IR / Reveal SD220 / Batatas for all!
2:15 p.m.	Kanamaru M. * Sasaki S. Wieczorek M.	<u><i>Density Distribution Estimation of Asteroid Itokawa Based on Distribution of Smooth Terrain</i></u> [#1414] We propose a new method to estimate interior density distribution within an asteroid using an inversion technique based on smooth terrain distribution.
2:30 p.m.	Kareta T. * Reddy V. Sanchez J. A. Linder T. Lauretta D. S. et al.	<u><i>Spectral Heterogeneity Among Geminid Complex Small Bodies</i></u> [#1710] We present the first NIR spectra of the "mini-Phaethon" (155140) 2005 UD, which reveals it to be different spectroscopically from its Geminid-creating cousin.
2:45 p.m.	Yu L. L. * Ip W. H. Spohn T.	<u><i>On the Active Mechanisms of the Geminids Parent (3200) Phaethon</i></u> [#1268] We proposed a "dust-ice" two-layer model to explain how Phaethon could provide the Geminids and the recent observed dust tails during its perihelion passages.

THURS ORAL

3:00 p.m.	Mainzer A. * Masiero J. Cutri R. M. Grav T. Kramer E. et al.	<u>Update on the NEOWISE Mission: Finding and Characterizing Minor Planets</u> [#3186] Reporting on NEOWISE mission results for minor planets.
3:15 p.m.	Usui F. * Hasegawa S. Ootsubo T. Onaka T.	<u>Exploring Hydrated Minerals on Asteroids with AKARI</u> [#1480] We report the spectroscopic survey of asteroids with the AKARI satellite for detecting the 3-micron absorption features attributed to hydrated minerals.
3:30 p.m.	Martin A. C. * Emery J. P. Lindsay S. S.	<u>Thermal-IR Spectral Analysis of Jupiter's Trojan Asteroids: Detecting Silicates</u> [#1238] Jupiter's Trojans / Where did they come from, and how? / We show spectral clues.
3:45 p.m.	Souza-Feliciano A. C. * De Prá M. N. Alvarez-Candal A. Pinilla-Alonso N. Fernández-Valenzuela E. et al.	<u>Visible Analysis of NASA's Lucy Mission Targets 3548 Eurybates, 15094 Polymele, 21900 Orus, and 52246 Donaldjohanson</u> [#1636] We perform rotationally resolved spectroscopy observations of some targets of the Lucy NASA mission looking for heterogeneities on the surface of these bodies.
4:00 p.m.	Bauer J. M. * Mainzer A. K. Kramer E. A. Grav T. Masiero J. R. et al.	<u>NEOWISE CO+CO₂ Observations of Active Centaurs: A Statistical Sample</u> [#3192] We will provide an overview of the reactivated mission comet CO+CO ₂ production rate analyses, with focus on the statistical sample of active Centaurs.
4:15 p.m.	EL-Maarry M. R. * Driver G. Jorda L. Gaskell R. Hviid S.	<u>Surface Changes on Comet 67P/Churyumov-Gerasimenko Following Outbursts as Observed by the Rosetta Mission</u> [#3020] We are conducting an investigation of surface changes on comet 67P following outbursts using Rosetta images. We report changes including a new cliff collapse.
4:30 p.m.	Birch S. P. D. * Hayes A. G. Umurhan O. M. Tang Y. Vincent J-B. et al.	<u>Migrating Scarps on Comet 67P</u> [#2106] We show observations of transient large-scale depressions that formed, and then evolved, on the surface of comet 67P as it approached perihelion in March 2015.

Thursday, March 21, 2019

[R556]

MARTIAN SURFACE: EXPOSING CARBONATES AND HYDROTHERMAL ALTERATION

3:15 p.m. Waterway Ballroom 4

Chairs: Adrian Brown and Elisabeth Hausrath

Times	Authors (*Denotes Presenter)	Abstract Title and Summary
3:15 p.m.	Viviano C. E. * Phillips M. S.	<u>Hydrothermal Alteration and Large Impact Basins on Mars</u> [#2824] Mineral mapping of CRISM data in the regions surrounding Isidis and Hellas basins reveal regional trends in hydrothermal alteration and metamorphic grade.
3:30 p.m.	Ramkissoon N. K. * Schwenzer S. P. Pearson V. K. Olsson-Francis K.	<u>Modelling Secondary Mineral Formation Within a Martian Impact-Generated Hydrothermal System</u> [#1380] We have modelled water-rock interactions that can form within impact-generated hydrothermal systems found on Mars, using sulfur and Fe ³⁺ -rich lithologies.
3:45 p.m.	Liu Y. * Goudge T. A. Salvatore M. R.	<u>Large Localized Carbonate Exposures in NE Tyrrhena Terra, Mars, and Possible Formation Mechanisms</u> [#2754] We identified a large Fe/Ca-carbonate exposures in NE Tyrrhena Terra on Mars and discussed their formation mechanisms.
4:00 p.m.	Ruff S. W. * Hamilton V. E. Rogers A. D. Edwards C. S. Horgan B.	<u>Olivine-Rich, Carbonate-Bearing Ash Deposits Link Jezero and Gusev Craters</u> [#2775] Rocks with Mg-rich olivine and carbonate in both the Nili Fossae region and Columbia Hills raises the possibility that they have a common formation history.

THURS ORAL

4:15 p.m.	Kissick L. E. * Tosca N. J.	<p><u>Carbonate Precipitation Kinetics in Anoxic Water-Rock Systems: Implications for the Martian "Missing Carbonates" [#1229]</u></p> <p>We attempted to synthesize FeCO₃ under Mars-like conditions. Even under 1 bar CO₂, they do not form. They may be harder to form on Mars than previously realized.</p>
4:30 p.m.	El-Shenawy M. I. * Niles P. B.	<p><u>Oxygen and Carbon Isotope Systematics in CO₂-H₂O-(Ca,Mg,Na)ClO₄ Brine System Below 0°C: Implications for Oxygen Isotope Composition of Water and Carbon Sequestration on Mars [#2244]</u></p> <p>The interaction between CO₂ and perchlorate brines was investigated using oxygen and carbon stable isotopes.</p>

ORAL SESSION

Friday Morning, March 22, 8:30 a.m.

Room	Session	Session Title	Page
Waterway Ballroom 1	F701	Lunar Volcanism: Volcanic Features, Processes, and Magmatic Volatiles	57
Waterway Ballroom 4	F702	Martian Polar Processes and Cryosphere	58
Waterway Ballroom 5	F703	Impacts: Frontiers in Shock Metamorphism	59
Waterway Ballroom 6	F704	Differentiated Meteorite Parent Asteroids and Their Provenance	60
Montgomery Ballroom	F705	Protoplanetary Disk Evolution and Chronology	61

Friday, March 22, 2019

[F701]

LUNAR VOLCANISM: VOLCANIC FEATURES, PROCESSES, AND MAGMATIC VOLATILES

8:30 a.m. Waterway Ballroom 1

Chairs: Debra Needham and Ali Bramson

Times	Authors (*Denotes Presenter)	Abstract Title and Summary
8:30 a.m.	McBride M. J. * Horgan B. H. N. Gaddis L. R. Bennett K. A.	<u><i>Moon Mineralogy Mapper Analysis of Volcanic Deposits in Schrödinger Basin</i></u> [#1985] Where the crust is thin / Explosive eruptions / Go collect the glass.
8:45 a.m.	Stopar J. D. * Gaddis L. R. Horgan B. H. N. McBride M. J. Lawrence S. J. et al.	<u><i>Outcrop-Scale Investigations of the Pyroclastic Deposits in J. Herschel Crater</i></u> [#1937] Relatively cool, localized eruptions begin gas-rich, but the plume's extent decreases over time, concentrating juvenile materials proximal to the vent.
9:00 a.m.	Bramson A. M. * Carter L. M. Patterson G. W. Sori M. M.	<u><i>Radar Response of Lunar Cryptomaria and Pyroclastic Deposits in Mini-RF Data</i></u> [#2673] We characterize explosive (pyroclastics) and buried effusive (cryptomare) volcanism on the Moon in the monostatic and bistatic Mini-RF data from LRO.
9:15 a.m.	Jozwiak L. M. * Head J. W.	<u><i>Reassessing the Formation Process of Lunar Floor-Fractured Craters</i></u> [#2413] Using detailed mapping, we determine that FFC sill/laccolith formation occur as part of a continuum, and are not discrete end-members as previously suggested.
9:30 a.m.	Kerber L. * Jozwiak L. M. Whitten J. Wagner R. V. Denevi B. W. et al.	<u><i>The Geologic Context of Major Lunar Mare Pits</i></u> [#3134] We analyze several major mare pits to determine their geologic contexts, what lava layers they expose, and assess their potential for exploration.
9:45 a.m.	Aleinov I. * Way M. J. Harman C. Tsigaridis K. Wolf E. T. et al.	<u><i>The Properties of the Moon's Ancient Maria-Outgassed Atmosphere</i></u> [#2947] Ancient Moon could have a short-lived thin atmosphere due to outgassing from maria. We study it with ROCKE-3D general circulation model and present the results.
10:00 a.m.	Needham D. H. * Siegler M. Li S. Kring D. A.	<u><i>Calculated Thicknesses of Volcanically Derived Water Ice Deposits at the Lunar Poles</i></u> [#1087] Volcanism represents a viable source for lunar polar H deposits. We investigate thicknesses of initial deposits formed from H ₂ O released during these eruptions.
10:15 a.m.	Zhang Y. *	<u><i>H₂O and Other Volatiles in the Moon, 50 Years and On</i></u> [#1319] This report will discuss the paradigm shift from a completely dry Moon to a relatively wet Moon, and new debate about H ₂ O in the Moon.
10:30 a.m.	Tartese R. * Anand M.	<u><i>In the Earth's Shadow: Have We Known the Bulk D/H of Indigenous Lunar Water Since Apollo Days?</i></u> [#1500] A fresh look at data obtained on Apollo 17 mare basalts in the 1970's suggest we may have known the H isotope composition of lunar indigenous water since then.
10:45 a.m.	McIntosh E. C. * Day J. M. D. McCubbin F. M. Porrachia M.	<u><i>Moderately Volatile Element Ratios in Lunar Pyroclastic Glasses 74220 and 15426</i></u> [#1911] Pyroclastic glasses 74220 and 15426 have been measured using LA-ICP-MS and show moderately volatile element enrichment compared to mare basalts.
11:00 a.m.	Greenwood J. P. * Itoh S. Kawasaki N. Sakamoto N. Yurimoto H.	<u><i>Hydrogen Isotopes, Volatiles, and Refractory Trace Element Compositions of Melt Inclusions and Apatite in a Consanguineous Suite of Apollo 12 Olivine Basalts</i></u> [#2371] Hydrogen isotopes show exchange of originally high-D lavas with a low-D component upon emplacement at the lunar surface. F and Cl appear unmobilized and high.
11:15 a.m.	Burney D. * Neal C. R. Day J. M. D.	<u><i>Moderately Volatile Elements in Lunar and Martian Meteorites; What Differences Do They Reveal Between Lunar and Martian Volatile Element Inventories?</i></u> [#2895] Lunar volatiles/ Are distinct from those on Mars/ As seen in bolides.

FRI ORAL

11:30 a.m.	Brounce M. * Boyce J. McCubbin F. M. Eiler J. Stolper E.	<u><i>The Oxidation State of Sulfur in Lunar, Martian, and Terrestrial Apatite</i> [#2601]</u> Lunar apatites contain 100s–1000s ppm sulfur as S ²⁻ . Terrestrial apatites contain sulfur as S ⁶⁺ . Martian apatites contain 100s of ppm sulfur as both S ⁶⁺ and S ²⁻ .
------------	--	--

Friday, March 22, 2019

[F702]

MARTIAN POLAR PROCESSES AND CRYOSPHERE

8:30 a.m. Waterway Ballroom 4

Chairs: Peter Buhler and Candice Hansen

Times	Authors (*Denotes Presenter)	Abstract Title and Summary
8:30 a.m.	Bills B. G. * Keane J. T.	<u><i>Mars Obliquity Variations are Both Non-Chaotic and Probably Fully Damped</i> [#3276]</u> Obliquity variations of Mars are not chaotic. In fact, energy dissipation has driven the spin pole into a configuration similar to that of a Cassini state.
8:45 a.m.	Buhler P. B. * Piqueux S. Ingersoll A. P. Ehlmann B. L. Hayne P. O.	<u><i>The Origin, Age, and Stratigraphy of Mars' Massive South Polar CO₂ Deposit and Its Control of Mars' Atmospheric Pressure</i> [#1031]</u> Mars' large south polar CO ₂ deposit exchanges mass with its CO ₂ atmosphere as its orbit evolves. We model Mars' pressure history and the deposit's stratigraphy.
9:00 a.m.	Becerra P. * Sori M. M. Thomas N. Tulyakov S. Sutton S. S. et al.	<u><i>Climate Record Signals in the South Polar Cap of Mars from HiRISE and CaSSIS Stereo Imaging</i> [#1283]</u> HiRISE and CaSSIS DTMs show previously undetected signals of a climate record in the south polar cap of Mars, providing limits on the timescale of accumulation.
9:15 a.m.	Orosei R. * Lauro S. E. Pettinelli E. Cicchetti A. Coradini M. et al.	<u><i>Radar Evidence of Subglacial Liquid Water on Mars</i> [#2363]</u> Strong radar echoes from the bottom of the martian southern polar deposits are interpreted as being due to the presence of liquid water under 1.5 km of ice.
9:30 a.m.	Sori M. M. * Bramson A. M.	<u><i>A Story of Water, Ice, and Fire on Mars: Conditions for Generating Liquid Water Under the South Polar Layered Deposits</i> [#1073]</u> High geothermal heat (>72 mW/m ²) is needed to melt ice and create liquid water on Mars today, even if salt is present. Recent magmatism could provide the heat.
9:45 a.m.	Morgan G. A. * Putzig N. E. Perry M. R. Bramson A. M. Petersen E. I. et al.	<u><i>The Mars Subsurface Water Ice Mapping (SWIM) Project</i> [#2918]</u> Looking for Mars ice / How will the SWIM team find it? / Data synthesis..
10:00 a.m.	Cross A. J. * Hager T. F. Smith I. B. Goldsby D. L.	<u><i>Rheological Behavior of CO₂ Ice with Application to Glacial Flow on Mars</i> [#2587]</u> Mars' south polar ice cap may contain solid CO ₂ deposits up to 1 km thick. We perform experiments to determine the flow properties of CO ₂ ice.
10:15 a.m.	Calvin W. M. * Seelos K. D. James P. B.	<u><i>At the Margins of the Martian Southern Seasonal Cryptic Terrain, Evolution at CTX Scales</i> [#2913]</u> CTX and CRISM observe the margins of the southern cryptic terrain over regions identified in MARCI as having unique seasonal patterns.
10:30 a.m.	Portyankina G. * Aye K.-M. Hansen C. J. Schwamb M. E.	<u><i>Mars Spring Seasonal Ice Cleaning as Detected by Planet Four Project</i> [#1695]</u> We report on a statistical evidence for surface brightening event of seasonal ice cap in the southern martian polar region derived by Planet Four project.
10:45 a.m.	Sinha P. * Horgan B. Seelos F.	<u><i>Dateable Volcanic and Impact Sediments within the North Polar Layered Deposits on Mars</i> [#2027]</u> Sediments within north polar layered deposits on Mars have the potential for horizontal correlation of relative stratigraphy and quantitative geochronology.

11:00 a.m.	Nerozzi S. * Holt J. W. Forget F. Spiga A. Millour E.	<u>Combining Radar Sounding and General Circulation Models to Reveal the Initial Accumulation of the Martian North Polar Layered Deposits</u> [#2854] Mars' north polar cap / Swing planet — grow ice on sand? / Ask the GCM!
11:15 a.m.	Ojha L. * Nerozzi S. Lewis K. W.	<u>Constraints on the Density of the Martian North Polar Cap from Gravity and Topography</u> [#2712] We utilize the martian gravity and topography data to constrain the bulk density of the north polar layered deposit and the basal unit.
11:30 a.m.	Wilcoski A. X. * Hayne P. O.	<u>Mass Balance and Surface Texture of the Martian North Polar Residual Cap</u> [#2210] Polar cap texture / Modeling the mass balance / Surfaces evolve.

Friday, March 22, 2019

[F703]

IMPACTS: FRONTIERS IN SHOCK METAMORPHISM

8:30 a.m. Waterway Ballroom 5

Chairs: Gavin Kenny and Kathryn Harriss

Times	Authors (*Denotes Presenter)	Abstract Title and Summary
8:30 a.m.	Harriss K. H. * Burchell M. J.	<u>An Experimental Study of Shock Alteration in Individual Minerals and Mineral Pairs Up to 140 Gpa</u> [#1589] An investigation into the shock alteration of individual and paired minerals enstatite, diopside, and peridot.
8:45 a.m.	McCanta M. C. * Dyar M. D.	<u>Effects of Oxidation and Shock on Pyroxene Spectral Features</u> [#1383] Pyroxene spectra / Show signs of oxidation / Shock too — How to read?
9:00 a.m.	Sims M. * Rucks M. Lobanov S. Young J. Daly J. A. et al.	<u>Strain-Rate and Temperature Effects on Kinetics of Phase Transitions in Albite</u> [#3021] We completed laser-heated fast decompression experiments using diamond anvil cells on albite samples in order to simulate decompression during natural impacts.
9:15 a.m.	Cox M. A. * Cavosie A. J. Bland P. A. Miljković K. Wingate M. T. D.	<u>Shocked Zircon from the Woodleigh-1 Core: The Largest Known Section of Coherent Reidite-Bearing Bedrock?</u> [#1505] An example of Reidite, the ~30 GPa high-pressure ZrSiO ₄ polymorph, throughout a 60 m core of coherent shocked granitoid.
9:30 a.m.	Stangarone C. * Angel R. J. Prencipe M. Mihailova B. Alvaro M. et al.	<u>New Insights into the Zircon-Reidite Phase Transition as an Indicator of Impact Structures</u> [#1817] Calculations of zircon under hydrostatic pressure led to a new polymorph that may trigger reidite (high pressure ZrSiO ₄ polymorph), an impact indicator mineral.
9:45 a.m.	Garde A. A. * Johansson L. Lindgren P.	<u>Zircon Microtextures from the Maniitsoq Impact Structure, West Greenland</u> [#1379] Planar zircon microstructures spaced ~1 μm in ~3 directions and surficial ribbons resembling quenched, extruded zircon melt, reported from two Maniitsoq sites.
10:00 a.m.	Kenny G. G. * Karlsson A. Schmieder M. Whitehouse M. J. Nemchin A. A. et al.	<u>A Review of Shock-Metamorphic Features in Apatite from Terrestrial Impact Structures and Possible Implications for Extra-Terrestrial Phosphates</u> [#1357] Including the first unequivocal evidence for shock recrystallisation in terrestrial apatite — found in grains from the Paasselkä impact structure, Finland.
10:15 a.m.	Erickson T. M. * Timms N. E. Pearce M. A. Cayron C. Keller L. P. et al.	<u>Lath Structured Monazite from Haughton Dome, Canada Reveals Shock-Induced Tetragonal High Pressure Polymorph of REEPO₄</u> [#1704] Monazite shocked / Tetragonal plates form / Reversion twinning.
10:30 a.m.	Schmieder M. * Erickson T. M. Kring D. A. IODP— ICDP Expedition 364 Science Party	<u>Microstructural Characterization of TiO₂-II in the Chicxulub Peak Ring</u> [#1658] Chicxulub's peak ring / Has a high-P polymorph / TiO ₂ -II!
10:45 a.m.	Kurosawa K. * Moriwaki R. Komatsu G. Okamoto T. Yabuta H. et al.	<u>Shock Devolatilization/Vaporization of Evaporites in an Open System</u> [#2442] Shock vaporization/devolatilization from evaporitic minerals, halite and gypsum, was investigated in an open system.

11:00 a.m.	Acquadro J. J. * MacPherson G. J. Corrigan C. M. Lunning N. G.	<u>Evidence for Impact-Induced Shock Melting in Carbonaceous Chondrites</u> [#2529] Impact melt has been identified surrounding CAIs in two CV chondrites, Leoville and Efremovka.
11:15 a.m.	Hopkins R. H. * Spray J. G.	<u>Shock Veins in Paired Lunar Meteorites Northwest Africa 3163 and 4881</u> [#2429] This study examines shock features within lunar meteorites Northwest Africa 3163 and 4881 in an attempt to better constrain their conditions during formation.
11:30 a.m.	Liu Y. *	<u>Internal Workings of Shock Melting: Views from the First X-Ray Computed Tomography (XCT) of the Tissint Meteorite</u> [#1767] Report the first X-ray CT study of impact-melt-pockets in Tissint. Results provide insights on shock melting and origin of volatile-rich melt pockets.

Friday, March 22, 2019

[F704]

DIFFERENTIATED METEORITE PARENT ASTEROIDS AND THEIR PROVENANCE

8:30 a.m. Waterway Ballroom 6

Chairs: Steven Desch and Hilary Downes

Times	Authors (*Denotes Presenter)	Abstract Title and Summary
8:30 a.m.	Desch S. J. * O'Rourke J. G. Schaefer L. K. Sharp T. G. Schrader D. L.	<u>Diamonds in Ureilites from Mars</u> [#1646] Ureilites, including their 100 um diamonds, are explained as mixtures of a Vesta-like parent body and a fragment from the pre-overturn upper mantle of Mars.
8:45 a.m.	Collinet M. * Grove T. L.	<u>Experimental Constraints on the Major-Element Composition of the Ureilite Parent Body</u> [#3229] Olivine-pigeonite residues identical to ureilites are produced by the incremental melting of materials resembling the Sun's photosphere and CI chondrites.
9:00 a.m.	Rai N. * Downes H. Smith C. L.	<u>A New Model for Planetesimal Formation: Case Study of the Ureilite Parent Body</u> [#3265] We have presented a model of the accretion, thermochemical evolution, collisional destruction, and reaccretion of the ureilite parent body (UPB).
9:15 a.m.	Goodrich C. A. * Zolensky M. Kohl I. Young E. D. Yin Q.-Z. et al.	<u>Carbonaceous Chondrite-Like Xenoliths in Polymict Ureilites: A Large Variety of Unique Outer Solar System Materials</u> [#1312] Mineralogy and oxygen and Cr isotopes of CC-like clasts in polymict ureilites, including Almahata Sitta, show unique materials not found as whole meteorites.
9:30 a.m.	Kleine T. * Nanne J. A. M. Nimmo F. Cuzzi J.	<u>Origin of the Non-Carbonaceous-Carbonaceous Meteorite Dichotomy</u> [#3076] NC-CC dichotomy established during infall from the Sun's protostellar envelope; CAIs record isotopic composition of early, NC of later infalling material.
9:45 a.m.	Homma Y. * Iizuka T. Ishikawa A.	<u>Hf-W Dating of Main-Group Pallasites</u> [#2254] We decided model Hf-W ages of four Main-Group pallasites, and all of them are within 2 Myrs after the CAI formation.
10:00 a.m.	Tornabene H. A. * Hilton C. D. Ash R. D. Walker R. J.	<u>New Insights to the Genetics, Age, and Crystallization of Group IIC Iron Meteorites</u> [#1236] The anomalous Mo and Ru isotopic compositions of the IIC iron meteorite group are investigated, as well as a crystallization model to trace their evolution.
10:15 a.m.	Dey S. * Yin Q.-Z. Sanborn M. E. Ziegler K. McCoy T. J.	<u>Planetary Genealogy of Iron Meteorites and Pallasites Using $\epsilon^{54}\text{Cr}-\Delta^{17}\text{O}$ Isotope Systematics</u> [#2977] Planetesimals formed and broke with a roar / Nucleosynthetic isotopes in meteorites; find the crust, mantle, and core.
10:30 a.m.	Spitzer F. * Burkhardt C. Budde G. Kruijer T. S. Kleine T.	<u>Genetic Heritage and Chronology of Ungrouped Iron Meteorites</u> [#2592] Ungrouped irons confirm fundamental dichotomy between NC and CC meteorites. Formation of planetesimals in both reservoirs occurred under variable conditions.

FRI ORAL

10:45 a.m.	Sanborn M. E. * Yin Q.-Z.	<u>Magmatism in the Outer Solar System: What We Know Now from Isotope Forensics of Carbonaceous Achondrites</u> [#1498] We discuss the rapidly evolving understanding of the diversity and timing of magmatic activity in the early, outer solar system using new Cr-Ti-O data.
11:00 a.m.	Huyskens M. H. * Sanborn M. E. Yin Q.-Z. Amelin Y. Koefoed P.	<u>Chronology of Carbonaceous Achondrites from the Outer Solar System</u> [#2736] Achondrites from the outer solar system formed in a brief time interval of ~1 Myr.
11:15 a.m.	Crossley S. D. * Ash R. D. Sunshine J. M. Corrigan C. M. McCoy T. J.	<u>R Chondrites to Brachinites: Insights from Discrete Platinum Group Phases and Sulfides</u> [#2018] Whoever heard of / Niggliite or platarsite? / Brachinites... weird stuff.
11:30 a.m.	Yasutake M. * Yamguchi A. Greenwood R. C. Hibiya Y. Iizuka T. et al.	<u>Unique Differentiated Meteorite Northwest Africa 7312</u> [#1796] We investigated unique differentiated meteorite NWA 7312. It has O isotope compositions within the range of CR-chondrites and well-developed petrofabric.

Friday, March 22, 2019

[F705]

PROTOPLANETARY DISK EVOLUTION AND CHRONOLOGY

8:30 a.m. **Montgomery Ballroom**

Chairs: **Glenn MacPherson and Andrea Isella**

Times	Authors (*Denotes Presenter)	Abstract Title and Summary
8:30 a.m.	Isella A. * Andrews S. M. Dullemond C. P. Pérez L. Huang J. et al.	<u>The Disk Substructures at High Angular Resolution Project: What Observations of Protoplanetary Disks Tell Us About Planet Formation</u> [#2821] Presentation of the first results of the Atacama Large Millimeter Array Disk Substructure at High Angular Resolution project.
8:45 a.m.	Umurhan O. M. * Kavelaars J. J. Cuzzi J. N. McKinnon W. B. Lyra W. et al.	<u>Ultima Thule: Possible Gravitational Collapse Scenarios for its Origin</u> [#2809] What are the possible gravitational collapse scenarios to explain the origin of Ultima Thule? The answer hinges on the protoplanetary disk's turbulent state.
9:00 a.m.	Dwarkadas V. V. * Dauphas N. Meyer B.	<u>Can a Model of the Formation of the Solar System by Triggered Star Formation Within the Dense Shell of a Wolf-Rayet Bubble Explain the Initial Abundance of all Short-Lived Radionuclides in the Early Solar System?</u> [#1304] Formation of the solar system by triggered star formation in the shell of a Wolf-Rayet bubble can account for the abundances of most short-lived radionuclides.
9:15 a.m.	Hibiya Y. * Iizuka T. Enomoto H.	<u>The Initial Abundance of Niobium-92 in the Outer Solar System</u> [#1781] We've found that the initial abundance of niobium-92 in the outer solar system was distinctly higher than the value in the inner solar system.
9:30 a.m.	Blichert-Toft J. Göpel C. Chaussidon M. Albarede F. *	<u>A Th/U Perspective on the Age of the Solar System</u> [#1335] We present Pb isotopic abundances and Th/U ratios for single and multiple Allende chondrules, and assess the implications for the Pb-Pb age of the solar system.
9:45 a.m.	Fukai R. * Yokoyama T.	<u>Nucleosynthetic Sr-Nd Isotope Correlation in Chondrites: Evidence for Nebular Thermal Processing and Dust Transportation in the Early Solar System</u> [#1171] We propose a new disk evolutionary model that accounts for the planetary-scale nucleosynthetic Sr and Nd isotope heterogeneities in the early solar system.
10:00 a.m.	Yokoyama T. * Nagai Y. Fukai R. Hirata T.	<u>Molybdenum Isotopic Evidence for Nebular Thermal Processing and Material Transportation in the Inner Solar System</u> [#1329] Mo isotopic variation in the inner solar system is reflected in the formation location of the Earth and parent bodies of enstatite, ordinary, and R chondrites.

FRI ORAL

10:15 a.m.	Liu M.-C. * Chaussidon M.	<u><i>The Lithium and Boron Isotopic Compositions of Chondrules</i></u> [#1979] Extra boron-11 in the solar system / Low energy spallation or neutrino process / Chondrules may know.
10:30 a.m.	Dunham E. T. * Wadhwa M. Liu M.-C. Hertwig A. T. Kita N. et al.	<u><i>Pristine CR2 CAIs Preserve Initial Abundances of Short-Lived Radionuclides ^{10}Be and ^{26}Al</i></u> [#1928] CR CAIs / Received same particle dose / In hot disk midplane.
10:45 a.m.	Kita N. T. * Hertwig A. T. Sobol P. E. Spicuzza M. J.	<u><i>Reassessment of $^{26}\text{Al}/^{27}\text{Al}$ Ratios Among Chondrules in Y-81020 (CO3.05)</i></u> [#2213] Re-analyses of FeO-rich chondrules with improved SIMS methods show well-behaved Al-Mg isochron diagrams with ages younger than FeO-poor chondrules by ~ 0.5 Ma.
11:00 a.m.	Gregory T. * Luu T.-H. Coath C. D. Russell S. S. Elliott T.	<u><i>$(^{26}\text{Al}/^{27}\text{Al})_0$ Homogeneity Reinstated, and an Early Onset of Silicate Formation in the Nascent Solar System</i></u> [#1173] By constraining the initial Mg isotopic composition of the solar system, we have found evidence of initial $(^{26}\text{Al}/^{27}\text{Al})$ homogeneity in the nascent solar system.
11:15 a.m.	Zhu K. * Liu J. Qin L. P. Alexander C. M.O'D. He Y. S. et al.	<u><i>Chromium Isotopic Evidence for an Early Formation of Chondrules from the Ornans CO Chondrite</i></u> [#2405] CO chondrules formed at 4567.6 ± 1.3 Ma dated by Mn-Cr bulk isochron, and their varied $\epsilon^{54}\text{Cr}$ suggests a transportation process in the early solar system.
11:30 a.m.	Schneider J. M. * Burkhardt C. Brennecka G. A. Kleine T.	<u><i>Insights into Early Solar System Mixing Dynamics from Chromium and Titanium Isotope Anomalies in Individual Chondrules</i></u> [#2303] We show that ^{50}Ti and ^{54}Cr variations in individual chondrules are decoupled. This has important implications for the origin of the meteorite dichotomy.

TUESDAY POSTER SESSIONS

Tuesday Evening, March 19, 6:00 p.m.

Session	Session Title	Page
T301	OSIRIS-REx at Asteroid Bennu	65
T302	Special Session: Hayabusa2 Unveiling Asteroid Ryugu	67
T303	Chondrites: Whole Rocks	69
T304	Chondrites: Alteration Processes	71
T305	Special Session: New Horizons at KBO 2014 MU ₆₉ (Ultima Thule)	72
T306	Kuiper Belt Objects: From Eris to Ultima Thule	74
T307	Going Inside with InSight: Global Geophysics	74
T308	Going Inside with InSight: Seismology	75
T309	Going Inside with InSight: Landing Site	77
T310	Planetary Interior Dynamics: Gravity, Density and Seismicity	79
T311	Habitability: To Explore Strange New Worlds	80
T312	Extrasolar Planets (Those Other Worlds — Promising Untold Opportunities — Beckon)	80
T313	Atmospheres of the Solar System	82
T314	50 Years of Apollo Legacy: From Origin to Exploration	84
T315	Lunar Remote Sensing I: New Exploration	85
T316	Lunar Basins, Impacts, and Ejecta	86
T317	Lunar Impacts and Regolith Processes	88
T318	Lunar Volatiles: From Surface to Exosphere	90
T319	Mercury: Magnetism, Magma, and More	92
T320	Impacts: Target Earth II	94
T321	Impacts: Candidate Structures and Deposits	96
T322	The Horcrux Rings of Saturn	97
T323	Ministry of Icy Moon Compositions	98
T324	Icy Tastic Beasts and Where to Find Them	99
T325	The Cursed Ice	99
T326	The Goblet of Titan	100
T327	Planetary Tectonics and Structural Geology	101
T328	Martian Sample Studies: Mostly Meteorites	102
T329	Mars Exploration Rover: Perseverance in Endeavour	104
T330	MSL: Results Across Gale	105
T331	Martian Orbital Spectral Processing: Improving Results from CRISM and TES	107
T332	Icy Mars Geomorphology	108
T333	Thing Fall Down Go Boom: Mars Downslope Motion	110
T334	Planetary Aeolian Processes	111
T335	Education and Public Engagement: Models, Opportunities, and Products for Engaging Audiences	112
T336	CAESAR and Dragonfly: New Frontiers Phase A Studies	114
T337	Mission and Instrument Concepts: Venus	114
T338	Mission Concepts: Moon	115
T339	Instrument Concepts: Moon	117
T340	Advanced Curation	118

T341	Mission and Instrument Concepts: Mars	119
T342	Mission and Instrument Concepts: Asteroids and Small Bodies	120
T343	Mission and Instrument Concepts: Europa	122
T344	Mission and Instrument Concepts: Outer Solar System	123
T345	Mission and Instrument Concepts: Organics	124
T346	Mission and Instrument Concepts: Surface and Subsurface Exploration	125
T347	Mission and Instrument Concepts: Human Exploration	127
T348	Mission and Instrument Concepts: IgLuna	129

Tuesday, March 19, 2019

[T301]

POSTER SESSION I: OSIRIS-REX AT ASTEROID BENNU

6:00 p.m. Town Center Exhibit Area

Authors (*Denotes Presenter)	Abstract Title and Summary	Poster Location
Enos H. L. Laurretta D. S.	<u><i>OSIRIS-REx Project Planning and Control Process for Communication and Collaboration in Mission Development and Operations</i></u> [#1410] The distinctive requirements of a sample return mission require an inclusive approach of cost estimating methods to ensure confidence and team ownership.	Poster Location #1
Regberg A. B. Castro C. L. Connolly H. C. Jr. Davis R. E. Dworkin J. P. et al.	<u><i>Microbial Ecology of the OSIRIS-REx Assembly Test and Launch Environment</i></u> [#1113] Government shutdown / prompts placeholder abstract / Lorem ipsum dolor.	Poster Location #2
Farnocchia D. Takahashi Y. Chesley S. R. Park R. S. Mastrodemos N. et al.	<u><i>The Ephemeris of Asteroid (101955) Bennu from OSIRIS-REx Approach Data</i></u> [#1512] We report on the improved knowledge on the trajectory of asteroid (101955) Bennu based on the data acquired during the OSIRIS-REx approach phase.	Poster Location #3
Palmer E. E. Weirich J. R. Barnouin O. S. Gaskell R. W. Antreasian P. et al.	<u><i>Stereophotoclinometry Models in Support of the OSIRIS-REx Mission</i></u> [#2588] Quality of the different shape models used for the initial part of the OSIRIS-REx mission and how they were used during operations.	Poster Location #4
Chojnacki M. Sutton S. DellaGiustina D. N. Becker K. Bennett C. N. et al.	<u><i>High-Resolution Digital Terrain Models of Asteroid (101955) Bennu Through Stereo-Photogrammetry of OSIRIS-REx OCAMS Images</i></u> [#2973] To characterize the surface of asteroid Bennu, we will use stereo-photogrammetry to derive high-resolution topography from OCAMS stereo images.	Poster Location #5
Daly M. G. Barnouin O. S. Seabrook J. Johnson C. L. Al Asad M. et al.	<u><i>The OSIRIS-REx Laser Altimeter at >7km from Asteroid 101955 Bennu</i></u> [#1550] The first operational use of OLA in the OSIRIS-REx mission is presented.	Poster Location #6
Roberts J. H. Barnouin O. S. Johnson C. L. Daly M. G. Perry M. E. et al.	<u><i>Deviation of the Shape of Bennu from Rotational Figures of Stability</i></u> [#1756] Rubble, boulders, slopes / Swiftly spinning asteroid / Must have some shear strength.	Poster Location #7
Nolan M. C. Al Asad M. M. Barnouin O. S. Benner L. A. M. Daly M. G. et al.	<u><i>Comparing the RADAR Shape Model of (101955) Bennu with Ground Truth from OSIRIS-REx</i></u> [#2162] We compare the ground-based RADAR/lightcurve shape and rotation state of Bennu to the OSIRIS-REx image-based images and model.	Poster Location #8
Daly R. T. Bierhaus E. B. Barnouin O. S. Susorney H. C. M. Johnson C. L. et al.	<u><i>The Crater Morphometry of (101955) Bennu from the OSIRIS-REx Mission</i></u> [#1631] We present preliminary depth-diameter measurements of impact crater candidates on Bennu.	Poster Location #9
Perry M. E. Barnouin O. S. Jawin E. R. Walsh K. J. Pajola M. et al.	<u><i>Topographic Lineaments on Bennu</i></u> [#2951] The surface of Bennu has a range of linear features including scarps, shallow groves, and large N/S ridges, some of which reach from pole to equator.	Poster Location #10
McMahon J. W. French A. S. Scheeres D. J. Brack D. N. Chesley S. R. et al.	<u><i>Mass and Gravity Field Estimation of (101955) Bennu from Osiris-Rex Observations</i></u> [#1605] The estimate of Bennu's mass obtained by the Radio Science team using radiometric and optical measurements from the OSIRIS-REx spacecraft are presented.	Poster Location #11
Michel P. Barnouin O. S. Ballouz R.-L. Walsh K. J. Richardson D. C. et al.	<u><i>Disruption and Reaccumulation as the Possible Origin of Ryugu and Bennu Top Shapes</i></u> [#1659] We investigate by numerical simulations the disruption and reaccumulation process and its role in the formation of top shapes, in particular Bennu and Ryugu.	Poster Location #12

TUES POSTERS

Pajola M. Burke K. DellaGiustina D. Laurretta D. Rizk B. et al.	<u><i>Global and Select Regional Size-Frequency Distribution of Boulders on Asteroid (101955) Benu</i> [#1575]</u> We present the global as well as the localized boulders size-frequency distribution on the surface of Asteroid (101955) Benu.	Poster Location #13
Schwartz S. R. Ballouz R.-L. Asphaug E. I. Barnouin O. S. Bennett C. et al.	<u><i>What Can the Orientations of Benu's Boulders Tell Us About Its Evolution?</i> [#2595]</u> Here we examine boulder orientations on Benu as signatures of small-scale energy events and seismic efficiency. The latter may relate to subsurface structure.	Poster Location #14
Ryan A. J. Pino-Munoz D. Bernacki M. Delbo M. Emery J. P. et al.	<u><i>Full-Field Modeling of Heat Transfer in Asteroid Regolith: Thermal Conductivity Results for Mono- and Polydisperse Particulates</i> [#2512]</u> A new thermal model for asteroid regolith, including results for particle size mixtures, which will aid in our interpretation of Benu thermal inertia.	Poster Location #15
Golish D. R. Clark B. E. Li J.-Y. Zou X.-D. DellaGiustina D. N. et al.	<u><i>Early Resolved Photometry of Asteroid Benu</i> [#2556]</u> We present an initial analysis of resolved photometry of asteroid Benu from the OSIRIS-REx Camera Suite.	Poster Location #16
Zou X.-D. Li J.-Y. Clark B. E. Golish D. R. Reuter D. C. et al.	<u><i>Preliminary Analysis of the Photometric Properties of Asteroid (101955) Benu from OVIRS Observations</i> [#2650]</u> A global average photometric analysis of Benu is performed based on disk-resolved reflectance spectra obtained with the OVIRS instrument.	Poster Location #17
Simon A. A. Reuter D. C. Emery J. Cosentino R. G. Gorius N. et al.	<u><i>The OSIRIS-REx Earth Flyby: OVIRS Views of the Earth and Moon</i> [#1242]</u> OSIRIS Earth pass / Calibrate all those spectra! / O-H on the Moon?	Poster Location #18
Le Corre L. DellaGiustina D. Becker K. J. Golish D. Bennett C. et al.	<u><i>Investigating Surface Color Variegation on Near-Earth Asteroid Benu Using OSIRIS-REx Mapcam Data</i> [#2794]</u> Our goal is to analyze trends in color parameters, and map the distribution of potential absorption features on the surface of Benu using MapCam color images.	Poster Location #19
Clark B. E. Zou X. D. Kaplan H. H. Ferrone S. Howell E. S. et al.	<u><i>Search for Iron Oxide and Iron Sulfide on Asteroid (101955) Benu from Osiris-Rex Visible and Infra-Red Spectrometer Preliminary Survey Data</i> [#3278]</u> Evidence for an absorber near 0.55 microns (iron oxide?) in the Benu imaging data has sparked a search for supporting evidence in the spectrometer data.	Poster Location #20
McCoy T. J. Connolly H. C. Jr. Corrigan C. M. Jawin E. R. Sandford S. et al.	<u><i>Scales of Brecciation in Hydrated Carbonaceous Chondrites: Thin Sections to Asteroidal Boulders</i> [#1686]</u> Breccias are ubiquitous in mm-cm scale hydrated carbonaceous chondrites, but rare at larger. This may be due to fragmentation, mixing, and/or reconsolidation.	Poster Location #21
Haberle C. W. Christensen P. R. Garvie L. A. J. Hamilton V. E. Hanna R. D. et al.	<u><i>The Mineralogy of Recently Fallen Carbonaceous Meteorites, Mukundpura and Sutter's Mill, in the Context of Asteroid (101955) Benu</i> [#2144]</u> The mineralogy of two recent observed carbonaceous meteorites falls will be discussed in detail. The spectra of these meteorites will be compared to Benu.	Poster Location #22
Breitenfeld L. B. Kling A. Kim G. Rogers A. D. Glotch T. D. et al.	<u><i>VNIR and TIR Spectra of Fine-Grained Minerals Under Ambient and Simulated Asteroid Environment Conditions with Applications to OSIRIS-REx</i> [#1866]</u> We use 13 minerals to develop fine-grained, albedo-constrained VNIR and TIR libraries applicable to PLS analysis of the OVIRS and OTES data from OSIRIS-REx.	Poster Location #23
Lim L. F. Barucci A. Campins H. Christensen P. Clark B. E. et al.	<u><i>The Global Thermal Infrared Spectrum of (101955) Benu in the Context of Spitzer IRS Asteroid Spectra</i> [#1124]</u> OTES thermal infrared spectra of (101955) Benu are closer to laboratory meteorite analogues than spectra of other B-types in the Spitzer archive.	Poster Location #24

Tuesday, March 19, 2019

[T302]

POSTER SESSION I: SPECIAL SESSION: HAYABUSA2 UNVEILING ASTEROID RYUGU

6:00 p.m. Town Center Exhibit Area

Authors (*Denotes Presenter)	Abstract Title and Summary	Poster Location
Tsuda Y. Yoshikawa M. Watanabe S. Nakazawa S. Terui F. et al.	<u><i>Hayabusa2 Mission Up to Now</i></u> [#2318] We present what Hayabusa2 has done up to now after arriving at Asteroid Ryugu on June 27, 2018 and what it will do from now on.	Poster Location #25
Yabuta H. Watanabe S. Nakamura T. Hirata N. Sugita S. et al.	<u><i>Landing Site Selection for Hayabusa2: Scientific Evaluation of the Candidate Sites on Asteroid (162173) Ryugu</i></u> [#2304] We carried out the landing site selection for the first touch-down of Hayabusa2. The site that met both operation safety and scientific interest was selected.	Poster Location #26
Hirata N. Demura H. Tsuchiya T. Yamaguchi Y. Endo T. et al.	<u><i>New Features of AiGIS: A 3D-GIS for Visualization of Map and Shape of Irregular-Shaped Small Bodies</i></u> [#2347] New features of AiGIS, GIS-oriented visualization tool for irregular-shaped small bodies, are introduced.	Poster Location #27
Nasu S. Kitazato K. Hirata N.	<u><i>Study on Resolution Enhancement of Multi-Overlapping Scan Images: Application to Hayabusa2 NIRS3 Data</i></u> [#2316] Albedo maps derived from data obtained from observation methods used for NIRS3 have not good resolution. We attempted to improve resolution of the albedo map.	Poster Location #28
Sugiyama T. Hirata N. Watanabe S. Noguchi R. Shimaki Y. et al.	<u><i>Shape Reconstruction of the Asteroid Ryugu by Structure-from-Motion Technique in Hayabusa2 Mission</i></u> [#2384] The shape of asteroid Ryugu is reconstructed by Structure from Motion technique from Hayabusa2 imaging data.	Poster Location #29
Tachibana S. Sawada H. Okamoto C. Yano H. Okazaki R. et al.	<u><i>Hayabusa2 Touch-and-Go Sampling at Ryugu</i></u> [#1939] We review the Hayabusa2 sample acquisition and storage system. We also expect to report preliminary results of touch-and-go sampling operation at Ryugu.	Poster Location #30
Yamada R. Araki H. Yamamoto K. Senshu H. Namiki N. et al.	<u><i>Albedo Observation of C-Type Asteroid Ryugu Using the Hayabusa2 LIDAR</i></u> [#1733] We have derived normal albedo of C-type asteroid Ryugu at 1064 nm using the Hayabusa2 LIDAR. The average is 0.042 around the equator in Lommel-Seeliger model.	Poster Location #31
Domingue D. L. Tatsumi E. Yokota Y. Sugita S. Honda R. et al.	<u><i>Hayabusa2's Multiband Disk-Integrated Photometry of 162173 Ryugu</i></u> [#1943] Far is Ryugu / Brightness changing discreetly / A dark mystery.	Poster Location #32
Tatsumi E. Sugita S. Kameda S. Honda R. Kouyama T. et al.	<u><i>Visible Color Variation of Boulders on 162173 Ryugu</i></u> [#1753] The largest boulder shows different spectra from face to face, indicating space weathering. The ultraviolet variation was also observed among small boulders.	Poster Location #33
Tatsumi E. Kameda S. Moroi K. Ishida M. Kouyama T. et al.	<u><i>Updated Flat-Fields of ONC-T/Hayabusa2 Based on Close Encounter with Ryugu</i></u> [#1745] Flat-fields for ONC/Hayabusa2 are updated. Uniformity by applying new flat-fields is better than 1%. No clear detection of 0.7-micron band absorption.	Poster Location #34
Matsumoto K. Noda H. Ishihara Y. Senshu H. Yamamoto K. et al.	<u><i>Improved Trajectory of Hayabusa2 by Combining LIDAR Data and a Shape Model</i></u> [#1270] A way of improving Hayabusa2 spacecraft trajectory is proposed. This method minimizes discrepancies between LIDAR footprints and a shape model.	Poster Location #35
Vincent J.-B. Jaumann R. Schmitz N. Schröder S.	<u><i>Comparison of Morphological Parameters of Boulders Larger Than 1m on Ryugu and 67P</i></u> [#1531] Boulders everywhere / On comets, asteroids / Are they similar?	Poster Location #36
Kikuchi H. Hemmi R. Komatsu G. Miyamoto H. Hirata N. et al.	<u><i>3D Mapping of Structural Features on Ryugu</i></u> [#2409] We map structural features on the shape model of asteroid Ryugu.	Poster Location #37

TUES POSTERS

Miyamoto H. Hemmi R. Kikuchi H. Komatsu G. Honda C. et al.	<u><i>Geomorphological Characteristics of Asteroid Ryugu and its Preliminary Geologic Map</i> [#2398]</u> Geological characteristics of Ryugu are different from Itokawa, another rubble-pile asteroid closely studied by spacecraft.	Poster Location #38
Hirabayashi M. Tatsumi E. Miyamoto H. Komatsu G. Sugita S. et al.	<u><i>The Longitudinal Dichotomy of 162173 Ryugu as a Result of Recent Deformation</i> [#1397]</u> Longitudinal dichotomy seen on Ryugu. The sharp ridge of the western bulge. Likely rotationally induced deformation feature.	Poster Location #39
Ernst C. M. Cho Y. Morota T. Kanamaru M. Barnouin O. S. et al.	<u><i>The Distribution of Crater Morphologies Across Ryugu</i> [#2683]</u> We use Optical Navigation Camera images and the Hayabusa2 stereophotoclinometry shape model to investigate the morphologies of crater candidates on Ryugu.	Poster Location #40
Varatharajan I. Maturilli A. Sivaraman B. Helbert J. Meka J. K. et al.	<u><i>UV to FIR Reflectance Spectroscopy of Fresh Carbonaceous Chondrite, Mukundpura Meteorite: A Potential Analogue to JAXA Hayabusa 2's Target Ryugu</i> [#2247]</u> The study presents phase-angle dependent UV to FIR spectroscopy of fresh fall carbonaceous chondrite Mukundpura meteorite, a potential analog of Ryugu.	Poster Location #41
Hamm M. Grott M. Knollenberg J. Miyamoto H. Biele J. et al.	<u><i>Thermal Conductivity and Porosity of Ryugu's Boulders from In-Situ Measurements of MARA — the MASCOT Radiometer</i> [#1373]</u> MARA observed a boulder on Ryugu with low thermal conductivity and high porosity that we compare to lab measurements of a Tagish Lake analogue material.	Poster Location #42
Senshu H. Sakatani N. Shimaki Y. Yokota Y. Morota T.	<u><i>Direct Simulation of Thermal Moment on an Asteroid with Rough Surface</i> [#2153]</u> The surface of Ryugu is very rough, resulting in the shift of the total thermal moment. We conduct numerical simulation to estimate the moment.	Poster Location #43
Shimaki Y. Senshu H. Sakatani N. Fukuhara T. Tanaka S. et al.	<u><i>Surface Roughness and Thermal Inertia of Asteroid Ryugu Inferred from TIR on Hayabusa2</i> [#1724]</u> We report a thermal calculation on rough surface, a one-rotational thermal imaging of asteroid Ryugu, and an investigation on its roughness and thermal inertia.	Poster Location #44
Suko K. Kobayashi T. Demura H. Ogawa Y. Arai T. et al.	<u><i>TIR Data Processing by HEAT During Rendezvous of Hayabusa2 with the Asteroid (162173) Ryugu</i> [#2275]</u> We have provided TIR data of brightness temperature and radiance by a tool called HEAT (Hayabusa2 Exploration Assistant for TIR). We show its current status.	Poster Location #45
Kurokawa H. Shibuya T. Sekine Y. Ehlmann B. L.	<u><i>A Forward Modeling of Infrared Reflectance Spectra of Asteroids: The Implications for Ryugu's Parent Body</i> [#1815]</u> We show the model reflectance spectra of mineral assemblages obtained by chemical equilibrium calculations. We discuss the implications for Ryugu's parent body.	Poster Location #46
Matsuoka M. Nakamura T. Hiroi T. Kitazato K. Iwata T. et al.	<u><i>Infrared Spectra of Asteroid Ryugu: Comparison to Laboratory-Measured Carbonaceous Chondrites</i> [#1534]</u> We compared Ryugu infrared spectra with laboratory chondrite spectra mainly from RELAB database.	Poster Location #47
Neumann W. O. Grott M. Hamm M. Biele J. Jaumann R. et al.	<u><i>Thermal Evolution Modeling of (162173) Ryugu and Its Precursors</i> [#1810]</u> We calculate the interior evolution of a potential parent body for Ryugu, estimate its key properties, and trace, in particular, the evolution of porosity.	Poster Location #48
Shibuya T. Sekine Y. Kikuchi S. Fukushi K. Nakamura T. et al.	<u><i>Thermodynamic Modeling of Water-Rock Reactions in the Parent Body of Ryugu</i> [#2386]</u> Water-chondrite reactions were thermodynamically analyzed for constraining the conditions of aqueous alteration in the parent body of Ryugu.	Poster Location #49

Hiroi T. Milliken R. E. Robertson K. M. Kaiden H. Misawa K. et al.	<u><i>Gaussian Deconvolution of the 2.7-Micron Band of Hayabusa2/NIRS3 Spectrum of Asteroid Ryugu — Possibly a Heavily Space-Weathered CM Chondrite Body</i> [#1129]</u> Gaussian deconvolution of NIRS3 spectrum in comparison with carbonaceous chondrites indicates that asteroid Ryugu is a heavily space-weathered CM chondrite.	Poster Location #50
Ito M. Tomioka N. Uesugi M. Uesugi K. Ohigashi T. et al.	<u><i>Phase 2 Curation “Team Kochi” for Hayabusa2 Returned Sample: In-Depth Analysis of a Single Grain Utilizing Linkage Microanalytical Instruments</i> [#1394]</u> We report Phase2 Curation “Team Kochi” for Hayabusa2 sample analysis, the universal sample holders for microanalysis, and a transport vessel among institutes.	Poster Location #51
Yada T. Abe M. Nakato A. Yogata K. Sakamoto K. et al.	<u><i>Preparation for Curation of Samples Returned from the C-Type Asteroid Ryugu by Hayabusa2</i> [#1795]</u> Installation of clean chamber system in the new, dedicated clean room has been accomplished for curation of Hayabusa2-returned samples in the last October.	Poster Location #52

Tuesday, March 19, 2019

[T303]

POSTER SESSION I: CHONDRITES: WHOLE ROCKS

6:00 p.m. Town Center Exhibit Area

Authors (*Denotes Presenter)	Abstract Title and Summary	Poster Location
Verchovsky A. B. Fisenko A. V. Semjonova L. F. Shiryayev A. A.	<u><i>The Acid Residue from Saratov (L4) with High Q Concentration</i> [#2669]</u> Isotopically light N and bi-modal noble gas release associated with Q are observed in the residue from Saratov meteorite.	Poster Location #53
Hashiguchi M. Naraoka H.	<u><i>Abundant Magnesium-Containing Organic Compounds in the Tagish Lake Meteorite</i> [#1499]</u> We identified abundant Mg-containing organic compounds in Tagish Lake meteorite. The characteristics of SOM of Tagish Lake are quite different from Murchison.	Poster Location #54
Qin L. Xu L. Zhang J. Hao J. Lin Y. et al.	<u><i>NanoSIMS Analysis of Siderophile Elements in Metallic Phases of Chondrites</i> [#2696]</u> The Nanoscale SIMS is used to analyze Ru, Rh, Pd, Os, Ir, Pt, Au, Ni, and Ge of metal targets, two iron meteorites and metallic phases of a L3 chondrite.	Poster Location #55
Csámer Á. Nagy D. Posta J. Soós Á. Nyeste E. et al.	<u><i>New Study of the Elemental Composition of Kaba Meteorite</i> [#2998]</u> A small chip taken from Kaba meteorite bulk was gradually dissolved and analyzed using ICP-OES and ICP-MS techniques for main, trace, and ultra-trace elements.	Poster Location #56
Ebihara M. Sekimoto S.	<u><i>Halogen Contents in Meteorites (1) Carbonaceous Chondrites</i> [#2338]</u> We analyzed 19 carbonaceous chondrites for determining three halogen (Cl, Br, I) contents and discussed their cosmochemical behaviors in the early solar system.	Poster Location #57
Ku Y. Jacobsen S. B.	<u><i>Potassium Isotope Variations in Chondrites</i> [#1675]</u> We present our initial results of K isotopic studies of chondrites. Variations between Ordinary, CV, and CI chondrites are found except three outliers.	Poster Location #58
Zhao C. Bloom H. Chen H. Tian Z. Koefoed P. et al.	<u><i>Potassium Isotopic Compositions of Enstatite Chondrites and Aubrites</i> [#2689]</u> We report high-precision K isotopic compositions of enstatite chondrites and aubrites, and compare results to those of the Earth and other types of meteorites.	Poster Location #59
Dobrica E. Engrand C. Ogliore R. C. Brearley A. J.	<u><i>Alteration Versus Morphology of Antarctic Micrometeorites: A Simple Procedure for Sample Characterization</i> [#1014]</u> We are exploring the possibility that the surface morphology of AMMs may be a useful and simple criterion for distinguishing between different types of AMM.	Poster Location #60

Forman L. V. Timms N. E. Bland P. A. Daly L. Benedix G. K. et al.	<u><i>A Morphologic and Crystallographic Comparison of CV Chondrite Matrices</i> [#1350]</u> The morphology and crystallography of the matrices of 3 CV chondrites are explored. A process for defining the 'average' forsteritic matrix grain is proposed.	Poster Location #61
Dall'Asén A. G. Paul R. Stokke A. R. Kayastha R. Bromley B. C. et al.	<u><i>Comparing Carbonaceous Chondritic Meteorites Using Micro-Raman Spectroscopy and SEM/EDS</i> [#2897]</u> Topography, and mineralogical and elemental composition, of several carbonaceous chondritic meteorites using Raman spectroscopy and SEM/EDS.	Poster Location #62
Irving A. J. Kuehner S. M. Garvie L. A. J. Ziegler K. Sanborn M. E. et al.	<u><i>Evidence for a Unique Carbonaceous Chondrite Parent Body ('CX') and Another One with a Dunitic Mantle</i> [#2542]</u> We document a new class of carbonaceous chondrites, as well as achondrites related to other differentiated, CC-veneered parent bodies.	Poster Location #63
King A. J. Russell S. S.	<u><i>Revisiting the CY (Yamato) Carbonaceous Chondrite Group</i> [#1386]</u> We show that several hydrated and heated carbonaceous meteorites are related, supporting a previous proposal that they form a distinct CY chondrite group.	Poster Location #64
Yin Q.-Z. Sanborn M. E.	<u><i>An Update on Disconnecting CV and CK Chondrites Parent Bodies and More</i> [#3023]</u> CV and CK chondrites are distinct in Cr isotopic composition. Hart is still a CK, but NWA 6047 is a new type of carbonaceous chondrite (neither CV nor CK).	Poster Location #65
Bigolski J. N. Weisberg M. K. Ebel D. S.	<u><i>The Primitive Chondrite Watonga (LL3.1): Unusual Clasts and the Accretion of Ordinary Chondrites</i> [#2668]</u> We analyze unusual clasts and inclusions within Watonga in order to better understand the transport and mixing of materials in early solar nebula.	Poster Location #66
Greer J. Heck P. R. Boesenberg J. S. Bouvier A. Caffee M. W. et al.	<u><i>Hamburg: A Pristine H4 Chondrite Fall</i> [#1638]</u> Here we present the initial results from a consortium study that was formed to thoroughly characterize the meteorite Hamburg, an H4 OC that fell in January 2018.	Poster Location #67
Jansen C. A. Brenjer F. E. Krot A. N. Zipfel J. Pack A. et al.	<u><i>Mineralogy, Petrology, and Oxygen Isotopic Composition of Northwest Africa (NWA) 12379, a New Metal-Rich Chondrite with Affinity to Ordinary Chondrites</i> [#2741]</u> Mineralogy, petrology, and O-isotope composition of NWA 12379, a new metal-rich chondrite (~70 vol% Fe,Ni) with affinity to mildly metamorphosed (type 3) OC's.	Poster Location #68
Agee C. B. Vaci Z. Ziegler K. Spilde M. N.	<u><i>Northwest Africa 12273: Unique Ungrouped Metal-Rich Chondrite</i> [#1176]</u> We report here the discovery of a unique ungrouped chondrite, which consists primarily of Fe-Ni metal (~64%) and small porphyritic type II chondrules (~30%).	Poster Location #69
Kling A. M. Ebel D. S.	<u><i>Modal Abundance of EH3 Chondrites Using Image Analysis of X-Ray Maps</i> [#1698]</u> The goal of this work is to determine the modal abundance of EH3 chondrites using image analysis of X-ray maps as a replacement for optical point counting.	Poster Location #70
Brand H. E. A. Langendam A. D. Whitworth A. J. Alkemade S. L. Mitchell J. T. et al.	<u><i>Meteorites on the Nullarbor Plain, Insights from Synchrotron Powder Diffraction</i> [#1361]</u> We have studied a range of Australian meteorites of various classes using SXRD to determine the phases present, with particular sensitivity to minor phases.	Poster Location #71
Herd R. K.	<u><i>Comparing Chondrites and Conglomerates</i> [#3093]</u> Textural and structural similarities between terrestrial conglomerates and extraterrestrial chondrites are inescapable. Similarities and differences are explored here.	Poster Location #72

Alexander C. M. O'D.	<u><i>Modeling the Elemental and Isotopic Fractionations in the Carbonaceous Chondrites</i> [#2796]</u> Almost all elemental and isotopic properties of the carbonaceous chondrite classes can be reproduced by mixing of just four components.	Poster Location #73
Alexander C. M. O'D.	<u><i>Modeling the Elemental and Isotopic Fractionations in the Non-Carbonaceous Chondrites</i> [#2810]</u> Almost all features of the non-CC compositions can be explained by mixing of six components that are distinct from the components that influenced the CCs.	Poster Location #74
Zeng H. Z. Dauphas N. D. Rozsa V. R. Galli G. G.	<u><i>Ab Initio Approach to Equilibrium Fractionation of K and Rb</i> [#2237]</u> We presented a theoretical study of equilibrium fractionation properties for K and Rb.	Poster Location #75
Righter K. Pando K. M. Butterworth A. L. Jilly-Rehak C. E. Gainsforth Z. et al.	<u><i>Vanadium Valence as a Sensor of Oxygen Fugacity in Buffered Experiments at High Pressure</i> [#2231]</u> A new experimental approach for synthesizing equilibrated melts uses metal-oxide buffer pairs to specify fO_2 across a wide range of values relevant to natural astromaterials.	Poster Location #76

Tuesday, March 19, 2019

[T304]

POSTER SESSION I: CHONDRITES: ALTERATION PROCESSES

6:00 p.m. Town Center Exhibit Area

Authors (*Denotes Presenter)	Abstract Title and Summary	Poster Location
Hutson M. L. Ruzicka A. M. Tutorow S.	<u><i>Abundant Water in Ordinary Chondrites: Evidence from a Clast with Unique Alteration Assemblage in the Northwest Africa (NWA) 12380 (L3) Chondrite</i> [#1764]</u> A cm sized clast in NWA 12380 contains hydrous minerals that appear to have formed by extensive aqueous alteration of an ordinary chondrite.	Poster Location #77
El-Shenawy M. I. Niles P. B. Socki R. Ming D.	<u><i>Oxygen and Carbon Isotope Composition of the Magnesium Carbonates in Lewis Cliff 85320: Revisited</i> [#2196]</u> Oxygen and carbon isotope compositions of nesquehonite from LEW 85320 were measured to reconstruct the environmental conditions under which it is formed.	Poster Location #78
Lucas M. P. Dygert N. Patchen A. D. Miller N. R. McSween H. Y.	<u><i>An Application of REE-in-Two-Pyroxene Thermometry to H Chondrites: Evidence for Early Fragmentation — Reassembly of the H Chondrite Parent Body</i> [#2495]</u> REE-in-two-px thermometry applied to six H chondrites indicates early fragmentation-reassembly, rather than onion-shell cooling, for the H chondrite parent body.	Poster Location #79
Lee M. R. Cohen B. E. King A. J. Greenwood R. C. Gibson J.	<u><i>Moonmilk in the Carbonaceous Chondrites</i> [#1367]</u> Is moonmilk calcite a previously unrecognized product of parent body aqueous alteration?	Poster Location #80
Fujiya W. Aoki Y. Ushikubo T. Hashizume K.	<u><i>Evolution of Fluid Composition Inferred from Calcite in the Yamato 791198 CM Chondrite</i> [#1725]</u> We measured C isotope ratios along the crystal growth of carbonate grains in Y 791198. The variations in the $d^{13}C$ values within individual grains are small.	Poster Location #81
Ogliore R. C. Liu N. Dobrica E. Donohue P. H. Jilly-Rehak C. E. et al.	<u><i>^{53}Mn-^{53}Cr Radiometric Dating of Secondary Carbonates in a Hydrated Antarctic Micrometeorite</i> [#2778]</u> We developed small particle analytical techniques for ^{53}Mn - ^{53}Cr by NanoSIMS and measured this system in a hydrated, fine-grained Antarctic micrometeorite.	Poster Location #82
Lee M. R. Cohen B. E. Boyce A.	<u><i>Quantifying the Intensity of Post-Hydration Heating of CM Carbonaceous Chondrites Using Carbonates</i> [#1540]</u> Calcite/oldamite in CM chondrites is a sensitive indicator of heating temperature.	Poster Location #83

Velbel M. A. Zolensky M. E.	<u><i>Dehydroxylation and Peak Temperature of C1 and C2 Carbonaceous Chondrite Matrix</i> [#2679]</u> High temperatures dehydrate carbonaceous chondrite matrices.	Poster Location #84
Haenecour P. Howe J. Y. Zega T. J. Sunaoshi T. Thompson M. S. et al.	<u><i>Thermal Alteration of Organics and Volatiles in Carbonaceous Chondrites: Insights from In-Situ Heating Experiments</i> [#1469]</u> We report initial results from the in situ heating of Murchison and Tagish Lake fine-grained material in the transmission electron microscope.	Poster Location #85
Simon S. B. Sutton S. R. Brearley A. J. Krot A. N. Nagashima K.	<u><i>The Effects of Thermal Metamorphism as Recorded in CO3.0 Through CO3.2 Chondrites</i> [#1444]</u> Observations of multiple features of CO3.0–3.2 chondrites document changes that give an improved picture of the effects of the initial stages of metamorphism.	Poster Location #86
Johnson J. M. Brearley A. J.	<u><i>Complex Behavior of Fluid-Mobile Elements in a Lithic Inclusion from the Northwest Africa NWA 2364 CV3OxA Chondrite: Evidence for Extensive Fluid-Rock Interaction and Metasomatism on the CV3 Chondrite Parent Body</i> [#1926]</u> Large CV LI / Depleted in S, Na, K / Indicates wet past.	Poster Location #87
Komatsu M. Fagan T. J. Kimura M. Yamaguchi A. Yasutake M. et al.	<u><i>Examination of Silica Polymorphs in the CR Chondrites</i> [#1750]</u> We examined the chondrule rims and the occurrence of silica in CR chondrites to understand the primary formation and secondary processing of CR parent body.	Poster Location #88

Tuesday, March 19, 2019

[T305]

POSTER SESSION I: SPECIAL SESSION: NEW HORIZONS AT KBO 2014 MU₆₉ (ULTIMA THULE)

6:00 p.m. Town Center Exhibit Area

Authors (*Denotes Presenter)	Abstract Title and Summary	Poster Location
Beddingfield C. B. Beyer R. Schenk P. Moore J. Weaver H. A. et al.	<u><i>Deriving an Ultima Thule Digital Shape Kernel</i> [#1901]</u> We present a technique to create a digital shape kernel (DSK) for 2014 MU ₆₉ , nicknamed Ultima Thule, using LORRI and MVIC stereo-pairs.	Poster Location #90
Bierson C. J. Umurhan O. M. Robbins S. J. Lisse C. Nimmo F. et al.	<u><i>Limb Topography of 2014 MU₆₉: First Results from the New Horizons Flyby</i> [#1944]</u> The tallest mountains / The shape of worlds collided / Seen along the limb.	Poster Location #91
Kinczyk M. J. Runyon K. Robbins S. J. Keane J. T. Grundy W. M. et al.	<u><i>Generating a 3D Shape Model of 2014 MU₆₉ for Scientific Visualization and Public Outreach</i> [#2456]</u> Bi-lobate form is / Hard to visualize but / When in doubt, use clay.	Poster Location #92
Cheng A. F. Weaver H. A. Stern S. A. McKinnon W. B. Moore J. M. et al.	<u><i>Shape of 2014 MU₆₉: Contact Binary from Low Speed Merger?</i> [#3273]</u> The shape of 2014 MU ₆₉ suggests a contact binary formed in a low speed merger, and the merger speed may be ~1 m/s.	Poster Location #93
Bray V. J. White O. L. Singer K. N. Schenk P. M. Robbins S. J. et al.	<u><i>Crater Morphology on 2014 MU₆₉ — Predictions for New Horizons High Resolution Imaging</i> [#2550]</u> No craters seen yet / High-resolution cometh! / What will they look like?	Poster Location #94
Cook J. C. Dalle Ore C. M. Scipioni F. Cruikshank D. P. Grundy W. M. et al.	<u><i>Comparison of Near Infrared Spectra Between Pluto-System Objects and 486958 2014 MU₆₉: Analysis of New Horizons Spectral Images</i> [#2818]</u> We compare New Horizons LEISA spectra of 2014 MU ₆₉ to sites and objects in the Pluto system, specifically we compare to Nix and Cthulhu Regio, on Pluto.	Poster Location #95
Cruikshank D. P. Grundy W. M. Britt D. T. Quirico E. Schmitt B. et al.	<u><i>The Colors of 486958 2014 MU₆₉ ("Ultima Thule"): The Role of Synthetic Organic Solids (Tholins)</i> [#2051]</u> The red-orange color of 2014 MU ₆₉ is strongly suggestive of the presence of refractory organic complexes synthesized in the laboratory (tholins).	Poster Location #96
Dalle Ore C. M. Cruikshank D. P. Scipioni F. Cartwright R. J. Binzel R. P. et al.	<u><i>Color and Albedo of Ultima Thule: A Comparison to TNOs and Centaurs</i> [#2770]</u> We compare photometric data for 486958 2014 MU ₆₉ with respect to similar objects to investigate the dynamical and chemical evolution of the outer solar system.	Poster Location #97

Dhingra R. D. White O. L. Umurhan O. Banks M. E. Moore J. M. et al.	<u><i>Kuiper Belt Object 2014 MU₆₉: Correlation Between Albedo and Landforms</i> [#2697]</u> Distribution of bright albedo material and its probable connection to landforms on Kuiper Belt Object — MU ₆₉ .	Poster Location #98
Gladstone G. R. Young L. A. Steffl A. J. Parker J. Wm. Summers M. E. et al.	<u><i>Searching for a Coma During the New Horizons Flyby of 2014 MU₆₉ (Ultima Thule)</i> [#2866]</u> New Horizons data reveal no evidence of airglow emission or continuum absorption associated with MU ₆₉ . Stringent limits on a coma around MU ₆₉ will be provided.	Poster Location #99
Hofgartner J. D. Buratti B. J. Weaver H. A. Cheng A. F. Lisse C. M. et al.	<u><i>Photometry of Kuiper Belt Object Ultima Thule and Comparisons with Cognate Solar System Objects</i> [#2257]</u> Ultima Thule's lobes have the same I/F. But slightly different distributions. The I/F is similar to Pluto's Cthulhu Regio. The neck is the brightest region.	Poster Location #100
Keane J. T. Verbiscer A. J. Parker J. W. Olkin C. B. Weaver H. A. et al.	<u><i>The Illustrated Guide to the New Horizons Flyby of 2014 MU₆₉</i> [#3180]</u> A pinpoint of light / Transforms into a full world / I sketch the journey.	Poster Location #101
Binzel R. P. Earle A. M. Grundy W. M. Moore J. M. Stern S. A. et al.	<u><i>Highly Localized Seasonal Cold-Trapping in the Neck of 2014 MU₆₉ 'Ultima Thule'</i> [#2933]</u> Cold trapping in the 'crevasse' of the neck, seasonally shadowed by the lobes of Ultima Thule, could be responsible for the sharply delineated bright "collar."	Poster Location #102
Parker A. H. Weaver H. A. Porter S. B. Verbiscer A. J. Spencer J. R. et al.	<u><i>The Search for Rings and Binary Companions of Kuiper Belt Objects by New Horizons</i> [#3130]</u> New Horizons observed a number of KBOs at 0.1–1 AU range, delivering strong forward-scattering ring limits and better-than-HST limits on binary companions.	Poster Location #103
Quirico E. Schmitt B. Gabasova L. Grundy W. M. Cook J. C. et al.	<u><i>Spectral Properties of 486958 2014MU₆₉ (Ultima Thule) Versus 67P/Churyumov-Gerasimenko</i> [#2487]</u> Here we compare LEISA and MVIC/RALPH spectrophotometric data of MU ₆₉ with VIRTIS-M data collected for comet 67P/CG.	Poster Location #104
Runyon K. D. Banks M. E. Britt D. El-Maarry M. R. Weaver H. et al.	<u><i>Theoretical Underpinnings on Aeolian Transport on 2014 MU₆₉ "Ultima Thule"</i> [#1670]</u> Ultima Thule / Does the wind blow and snow go? / Waiting for downlink.	Poster Location #105
Scipioni F. Dalle Ore C. M. Grundy W. M. Cruikshank D. P. Cook J. C. et al.	<u><i>Ultima Thule, TNOs, and the Irregular Satellites of the Outer Planets: Spectroscopic and Color Comparison</i> [#2843]</u> We present a comparison of the colors and the spectrum of 2014 MU ₆₉ with those known TNOs, and of the irregular satellites of Saturn, Uranus, and Neptune.	Poster Location #106
Linscott I. R. Bird M. K. Stern S. A. Vincent M. A. Deboy C. C. et al.	<u><i>REX Radiometry at 4.2 cm During the New Horizons Encounter of Ultima Thule</i> [#1996]</u> Preliminary results from the Ultima Thule encounter where the REX instrument New Horizons measured thermal emission and performed a bistatic radar experiment.	Poster Location #107
Elliott H. A. McComas D. J. McNutt R. L. Jr. Horanyi M. Gladstone G. R. et al.	<u><i>The Solar Wind, Pickup Ion, Energetic Particle, Cosmic Ray, and Dust Space Environment at 2014 MU₆₉ (Ultima Thule)</i> [#2282]</u> We discuss the solar wind, pickup ion, energetic particle, and dust conditions local to MU ₆₉ . Initial results indicate NH remained in the solar wind.	Poster Location #108

Tuesday, March 19, 2019

[T306]

POSTER SESSION I: KUIPER BELT OBJECTS: FROM ERIS TO ULTIMA THULE

6:00 p.m. Town Center Exhibit Area

Authors (*Denotes Presenter)	Abstract Title and Summary	Poster Location
Ahrens C. J. Chevrier V. F.	<u><i>Spectral and Surface Characteristics of Carbon Monoxide on Pluto</i></u> [#1552] Experimental / Carbon monoxide mixtures / Phases of landforms?	Poster Location #109
Ahrens C. J. Earle A. M. Chevrier V. F.	<u><i>Lobate Debris Aprons Observed on Pluto from New Horizons</i></u> [#1555] Pluto icy blocks / Slide lobate debris aprons / Local climate zones!	Poster Location #110
Izenberg N. R. Byrne P. K. Calef F. J. III Rothery D. A. Pegg D. et al.	<u><i>Collisional Terminology For Cold Classical KBOs</i></u> [#1248] MU ₆₉ / Did the lobes grow by blorping / Then join by a flomp?	Poster Location #111
Skjetne H. L. Singer K. N. Hynek B. M. Knight K. I. Olkin C. B. et al.	<u><i>Chaos Terrains on Pluto, Europa, and Mars — Morphological Comparison of Blocks</i></u> [#2146] The size and height distribution of chaotic terrain blocks could provide information about the formation of chaos, and the lithologic structure of the crust.	Poster Location #112
Byers G. Evans R. Byers S. Nguyen J.	<u><i>Analysis of Pluto's Al-Idrisi Montes and the Adjacent Deep Trench Feature</i></u> [#1483] Study of the elevations of the trench and mountains seeking a correlation with the movement of Sputnik Planitia, by solid state convection or another mechanism.	Poster Location #113
Wagner N. L. Kay J. P. Schenk P. M.	<u><i>The Orientation of the Bladed Terrain Feature in Tartarus Dorsa, Pluto and Possible Reorientation of Pluto</i></u> [#1931] We are looking for evidence of the reorientation of Pluto through polar wander. Specifically, we're looking at the orientation of the bladed terrain feature.	Poster Location #114
Mills A. C. Montési L. G. J.	<u><i>Elastic Flexure Around Sputnik Planitia, Pluto, and Evidence for a Very High Heat Flux</i></u> [#1995] We test if the current topography of Sputnik Planitia and its surroundings contain evidence for a flexural bulge that formed by a large load of nitrogen ice.	Poster Location #115

Tuesday, March 19, 2019

[T307]

POSTER SESSION I: GOING INSIDE WITH INSIGHT: GLOBAL GEOPHYSICS

6:00 p.m. Town Center Exhibit Area

Authors (*Denotes Presenter)	Abstract Title and Summary	Poster Location
Russell C. T. Joy S. P. Yu Y. Rowe K. M. Johnson C. et al.	<u><i>The InSight Magnetic Field Measurements: Preliminary Results</i></u> [#1729] We present initial results on the InSight magnetometer.	Poster Location #116
Johnson C. L. Mittelholz A. Langlais B. Lognonne P. Pike W. T. et al.	<u><i>First Results from the InSight Fluxgate Magnetometer: Constraints on Mars' Crustal Magnetic Field at the InSight Landing Site</i></u> [#1487] We summarize initial results from the InSight FluxGate magnetometer, including the first surface-based estimates of Mars' crustal magnetic field.	Poster Location #117
Chi P. J. Russell C. T. Joy S. Banfield D. Johnson C. L. et al.	<u><i>Magnetic Pulsations on Martian Surface: Initial Results from InSight Fluxgate Magnetometer</i></u> [#1752] InSight makes the first magnetic field measurement on the surface of Mars. We present initial results concerning the magnetic pulsations observed by InSight.	Poster Location #118
McLennan S. M. Ojha L. Plesa A.-C. Smrekar S. E. Wieczorek M. A. et al.	<u><i>Geochemistry of the Martian Crust and Mantle: Constraints from the InSight Lander Mission</i></u> [#2844] Seismic and heat flow data returned by the InSight Lander mission will provide important constraints on the geochemistry of the martian crust and mantle.	Poster Location #119

Ojha L. Karimi S. Lewis K. W. Smrekar S. Siegler M.	<u><i>Depletion of Heat Producing Elements in the Martian Mantle</i> [#2391]</u> We model the deflection of the lithosphere by the weight of the polar caps and show that the present-day mantle heat flow cannot exceed 7 mW m ⁻² on either pole of Mars.	Poster Location #120
Bagheri A. Khan A. Efroimsky M. Giardini D.	<u><i>Orbital Evolution of the Mars-Phobos Tidal System</i> [#3183]</u> We study the orbital evolution of Mars and its satellites based on the results of inverting geodetic data for the interior structure and dissipation properties.	Poster Location #121

Tuesday, March 19, 2019

[T308]

POSTER SESSION I: GOING INSIDE WITH INSIGHT: SEISMOLOGY

6:00 p.m. Town Center Exhibit Area

Authors (*Denotes Presenter)	Abstract Title and Summary	Poster Location
McClellan J. B. Pike W. T. Charalambous C. Stott A. E. Warren T. et al.	<u><i>Operation of the InSight Short Period (SP) Seismometers During Cruise</i> [#2777]</u> Results include the SP seismometer noise floor, observations of attitude control thrusters firing, spacecraft resonances, and a micrometeoroid impact search.	Poster Location #122
de Raucourt S. Lognonne P. Robert O. Gabsi T. Nebut T. et al.	<u><i>The Very Broad Band Sensor of SEIS/InSight: Validation from Cruise to Mars Ground</i> [#2256]</u> VBB sensors performances are validated by trending their key parameters through Earth tests, cruise health check, and commissioning on Mars surface.	Poster Location #123
Panning M. P. Pike W. T. Lognonné P. Banerdt W. B. Banfield D. et al.	<u><i>InSight Lessons on Science Potential from On-Deck Operation of a Broadband Seismometer</i> [#2053]</u> Sitting on the deck / Planet shakes lander and me / Science can be done.	Poster Location #124
Mimoun D. Lognonné Ph. Banerdt W. B. Pike W. T. Giardini D. et al.	<u><i>Preliminary Assessment of the InSight Landing Site Seismic Noise and Comparison to Models</i> [#1879]</u> This abstract discusses the first characterization of the SEIS landing site seismic noise and compares it to models before landing.	Poster Location #125
Pou L. Nimmo F. Lognonné P. Mimoun D. Garcia R. F.	<u><i>Taking the Pulse of Mars with the InSight VBB Seismometer</i> [#2329]</u> Using the InSight VBB seismometer to measure the Phobos tides on Mars, it should be possible to constrain the state and size core of Mars better than 120 km.	Poster Location #126
Barkaoui S. Lognonné P. Drilleau M. Kawamura T. Kenda B. et al.	<u><i>Sensibility Analysis of the InSight Seismic Data to the Martian Structure: Application to the MSS Blind Test Data</i> [#2354]</u> Sensibility analysis of the InSight seismic data to the martian structure: Application to the MSS blind test data using Machine Learning and Pattern Search.	Poster Location #127
Saadé M. Lognonné P. Clévéde E. Drilleau M. Fernando B. et al.	<u><i>Benchmark Between HOPT/AxiSEM3D/SpecFM3D with 3D Structure of Mars: Focused on Ellipticity and Dichotomy</i> [#1826]</u> We compute normal modes of Mars and investigate their coupling due to rotation, ellipticity, and dichotomy of the planet.	Poster Location #128
Clinton J. F. Ceylan S. Stähler S. C. Giardini D. Böse M. et al.	<u><i>Marsquake Service for InSight: Preliminary Observations and Operations in Practice</i> [#2915]</u> The Marsquake Service (MQS) has been setup to create and curate a seismicity catalogue for Mars during the lifetime of the InSight mission.	Poster Location #129
Stähler S. C. van Driel M. Clinton J. F. Giardini D. Khan A. et al.	<u><i>Marsquake Service for InSight: Methods to Locate Events in a 3D Planet</i> [#2928]</u> Locating marsquakes is made difficult by the strong crustal thickness variations of the planet. We present methods to mitigate this effect using gravimetry.	Poster Location #130
Khan A. Drilleau M. Beucler E. Panning M. Lognonne P. et al.	<u><i>Mars Structure Service: Single-Station and Single-Event Marsquake Inversion for Structure Using Synthetic Martian Waveforms</i> [#1788]</u> We test our single-station and single-event inversion methods for determining interior structure using synthetic martian waveforms.	Poster Location #131

TUES POSTERS

Karakostas F. Lognonné P. Larmat C. Schmerr N.	<u><i>A Martian Impact Full Rayleigh Waveform Inversion Technique for 1D Identification of Crustal Structure</i></u> [#1530] This is a full waveform inversion technique, applied to Rayleigh waves generated by meteoroid impacts, for identification of the martian crustal structure.	Poster Location #132
Stähler S. C. Brinkman N. Böse M. Khan A. van Driel M. et al.	<u><i>Probabilistic Source Inversion Using Body Wave Coda from a Single Seismic Station</i></u> [#3247] We present methods to infer the source mechanism of marsquakes from the seismic record of InSight. This allows to infer the tectonic context of the quake.	Poster Location #133
Murdoch N. Lorenz R. Spiga A. Garcia R. F. Mimoun D. et al.	<u><i>Predicting the Meteorological and Seismic Signals of Martian Dust-Devil Vortices as Observed on the Insight Lander</i></u> [#2108] Modelling of dust-devil vortices as observed by the meteorological (pressure and wind) and seismic instruments on the InSight lander deck.	Poster Location #134
Warren T. Pike W. T. Stott A. McClellan J. M. Charalambous C. et al.	<u><i>InSight Short Period Seismometers Detection of Dust Devils on Mars</i></u> [#2091] We will present initial results on detecting martian dust devil vortices from short period seismometer from the InSight lander.	Poster Location #135
Teanby N. A. Myhill R. Horleston A. Wookey J. Pike W. T. et al.	<u><i>Seismic Noise Polarization as a Measure of Wind Direction and Speed by Correlating InSight SEIS/APSS Observations on Mars</i></u> [#1567] We attempt to use seismic measurements to infer the wind direction and speed at the InSight landing site on Mars.	Poster Location #136
Teanby N. A. Daubar I. J. Lognonne P. Kawamura T. Wookey J. et al.	<u><i>Impact Detection with InSight: Updated Estimates Using Measured Seismic Noise on Mars</i></u> [#1565] Updated seismic impact detection rate estimates using Mars actual noise level. Consider how we might identify impacts from tectonic/other events in seismograms.	Poster Location #137
Wójcicka N. Collins G. S. Bastow I. Miljkovic K. Teanby N. A. et al.	<u><i>Investigating the Relationship Between Seismic Efficiency and Seismic Moment and Impactor Properties on Mars</i></u> [#2633] A numerical study of m-scale impacts on Mars to quantify the effect of impactor properties on the seismic efficiency and seismic moment.	Poster Location #138
King S. D. Caddick M. J. Myhill R. Panning M. P. Khan A. et al.	<u><i>Density and Seismic Structure of Mars from Mineral Physics Constraints: What InSight Do We Need?</i></u> [#1840] Mars structure models / Need a well-balanced crust / Just like all great breads.	Poster Location #139
Tauzin B. Pan L. Michaut C. Quantin C. Schmerr N. et al.	<u><i>Investigating the Seismic and Geological Structure of the Martian Crust at the Dichotomy Boundary</i></u> [#2105] We use orbital analyses of rock exposures in craters and scarps to build a geological model and predict the seismic response recorded at the SEIS instruments.	Poster Location #140
Beghein C. Xu H. Irving J. Drilleau M. Kenda B. et al.	<u><i>Constraining Mars Crust and Mantle Structure from Waveform Inversion of Fundamental and Higher Mode Surface Waves</i></u> [#2073] We present a waveform modeling method that we will use to constrain Mars crustal and mantle structure, and its application to a blind dataset.	Poster Location #141
Zhou W-Y. Zhang J. S. Shearer C. K. Agee C. B. Townsend J. P.	<u><i>Geophysical Properties of Martian Basalt at High Pressure-Temperature Condition</i></u> [#1727] PerpleX computation and multi-anvil experiments on Yamato 980459 to study its mineral composition and geophysical properties along a typical martian areotherm.	Poster Location #142
Jacob A. Drilleau M. Kawamura T. Lognonné P. Perrin C. et al.	<u><i>Building Martian Seismograms from California and Nevada Seismic Events: Inversion of the Californian Crust Using InSight Mars Structure Service Routines</i></u> [#1822] California and Nevada seismic dataset are transformed into martian seismograms, then inverted to retrieve the internal model of California using InSight tools.	Poster Location #143
Lucas A. Kenda B. Mangeney A. Kawamura T. Daubar I. et al.	<u><i>Seismic Detection of Mass Wasting on Mars with SEIS/InSight: A Loony Attempt?</i></u> [#2441] We investigate our capabilities of detecting and characterising mass wasting (e.g., slope streaks) with the seismometer SEIS/InSight in Elysium Planitia.	Poster Location #144

Fayon L. Knapmeyer-Endrun B. Lognonné P. Delage P. Llorca-Cejudo R. et al.	<u><i>LVL Transfer Function and Ground/Duricrust Mechanical Properties Predicted from InSight SEIS Data on the Ground</i></u> [#2566] The SEIS LVL structure model, its preliminary results and the new ones by knowing the configuration and resonances on Mars, are described.	Poster Location #145
Dell'Agnello S. Delle Monache G. O. Porcelli L. Tibuzzi M. Salvatori L. et al.	<u><i>Laser Retroreflectors for InSight and an International Mars Geophysical Network (MGN)</i></u> [#1492] Since 2015 we delivered to ESA and JPL miniaturized laser retroreflector payloads for InSight and an international Mars Geophysical Network (ExoMars, Mars 2020, etc.).	Poster Location #146

Tuesday, March 19, 2019

[T309]

POSTER SESSION I: GOING INSIDE WITH INSIGHT: LANDING SITE

6:00 p.m. Town Center Exhibit Area

Authors (*Denotes Presenter)	Abstract Title and Summary	Poster Location
Kedar S. Banerdt W. B. Brinkman N. Delage P. Fayon L. et al.	<u><i>Characterization of the InSight Near Surface Seismic Properties Using the Heat Flow and Physical Properties Probe (HP3) Mole as a Seismic Source</i></u> [#1837] We will report on data analysis methods and algorithms used for near surface seismic properties characterization using the InSight HP3 mole as a seismic source.	Poster Location #147
Kawamura T. Garcia R. F. Kenda B. Lognonné P. Pike T. W. et al.	<u><i>Decorrelation of Pressure Signals on SEIS Records and Ground Compliance Estimation</i></u> [#2314] We discuss the pressure noise expected for InSight SEIS instrument and its decorrelation. We also discuss the subsurface property estimated from decorrelation.	Poster Location #148
Grott M. Knollenberg J. Wippermann T. Spohn T. Scharringhausen M. et al.	<u><i>The Influence of Regolith Compaction on InSight-HP3 Thermal Conductivity Measurements</i></u> [#1269] Soil compaction by HP3 hammering can cause a moderate increase of thermal conductivity for loosely compacted soils.	Poster Location #149
Morgan P. Smrekar S. E. Grott M. Spohn T. Nahihara S.	<u><i>Estimation of Mars Regolith Temperatures Undisturbed by the InSight HP3 Probe Penetration by Extrapolation of Cooling Curves Recorded During Scheduled Stops in Probe Penetration</i></u> [#2725] Before LPSC, the first subsurface temperature measurements will be made in the Mars regolith. This poster will present data reduction and present results.	Poster Location #150
Mueller N. T. Grott M. Piqueux S. Kopp E. Spohn T. et al.	<u><i>HP³ Radiometer Measurements from the Mars Mission InSight</i></u> [#2436] We will present first results of the HP ³ radiometer observing two spots in the vicinity of the InSight lander.	Poster Location #151
Warner N. H. Golombek M. P. Grant J. Wilson S. Hauber E. et al.	<u><i>Geomorphology and Origin of Homestead Hollow, the Landing Location of the InSight Lander on Mars</i></u> [#1184] InSight landed in a small depression dubbed "Homestead hollow" that may be a degraded crater. This analysis describes the hollow and local surface processes.	Poster Location #152
Wilson S. A. Warner N. H. Grant J. A. Golombek M. P. DeMott A. et al.	<u><i>Crater Retention Ages at the InSight Landing Site: Implications for the Degradation History of the Homestead Hollow</i></u> [#2161] We estimate the age of the ~25 m depression where InSight landed, known as "Homestead hollow," based on the retention age of 20 to 30 meter-diameter craters.	Poster Location #153
Ansan V. Hauber E. Golombek M. Warner N. Grant J. et al.	<u><i>InSight Landing Site: Stratigraphy of the Regolith Beneath the Lander and in Its Surroundings, and Implications for Formation Processes</i></u> [#1310] Stratigraphy of the regolith beneath the lander and in its surroundings (InSight landing site: Homestead hollow), and implications for its formation processes.	Poster Location #154

TUES POSTERS

Grant J. A. Weitz C. M. Wilson S. A.	Warner N. H. Golombek M. P. et al.	<u><i>Modification of Homestead Hollow at the InSight Landing Site Based on the Distribution and Properties of Local Deposits</i></u> [#1199] Homestead hollow is a degraded impact crater modified by early mass wasting and eolian activity followed by slow infilling and weathering that removed the rim.	Poster Location #155
Charalambous C. Golombek M. P. Warner N. H. et al.	Pike W. T. Weitz C. M. et al.	<u><i>Rock Distributions at the InSight Landing Site and Implications from Fragmentation Theory</i></u> [#2812] We present a quantitative analysis of the rock distributions at distinct areas nearby the InSight lander and implications from fragmentation theory.	Poster Location #156
Newland E. L. McMullan S. Teanby N. A.	Collins G. S. Daubar I. J. et al.	<u><i>Meteoroid Fragmentation in the Martian Atmosphere and the Formation of Crater Clusters</i></u> [#2569] Small crater clusters / Complicate seismic signals / Models give InSight.	Poster Location #157
Devlin K. R. Golombek M. P. Huertas A.	Williams N. R. Daubar I. J. et al.	<u><i>Size-Frequency Distributions of Rocks Around Impact Craters in the InSight Landing Ellipse in Elysium Planitia, Mars</i></u> [#2950] Investigation of spatial distributions of rocky ejecta surrounding impact craters at the InSight landing ellipse.	Poster Location #158
Weitz C. M. Warner N. H. Wilson S. A.	Grant J. A. Golombek M. P. et al.	<u><i>Clast Sizes and Shapes at the InSight Landing Site</i></u> [#1392] We used the highest resolution InSight camera images to measure the sizes and shapes of clasts in the work volume where the instruments could be deployed.	Poster Location #159
Warner N. H. Williams N. DeMott A.	Golombek M. P. Hausmann R. et al.	<u><i>Probing the Regolith at the InSight Landing Site Using Rocky Ejecta Craters</i></u> [#1185] We evaluate the local stratigraphy of InSight's specific landing location using nearby Rocky Ejecta Craters to revise regolith thickness estimates.	Poster Location #160
Perrin C. Jacob A. et al.	Rodriguez S. Lucas A. Kenda B. et al.	<u><i>Searching for Geological Surface Changes Around the InSight Landing Site (Mars) from HiRISE Satellite Images</i></u> [#2390] Following the landing of InSight, we explore how the formation of new dust devil tracks can be evidenced in sets of successive HiRISE images.	Poster Location #161
Williams N. R. Warner N. H. Hausmann R. B.	Golombek M. P. Daubar I. J. et al.	<u><i>Surface Alteration from Landing InSight on Mars and Its Implications for Shallow Regolith Structure</i></u> [#2781] InSight lands on Mars / Exposing the regolith / With dust blown away.	Poster Location #162
Parker T. J. Calef F. J. LeMaistre S.	Golombek M. P. Williams N. R. et al.	<u><i>Localization of the InSight Lander</i></u> [#1948] InSight landed on Mars at 4.502384°N, 135.623447°E, Northing 266877.460m, Easting 8039038.792m at -2613.426m elevation with respect to the MOLA geoid.	Poster Location #163
Golombek M. Warner N. Piqueux S.	Williams N. Daubar I. et al.	<u><i>Initial Assessment of InSight Landing Site Predictions</i></u> [#1696] Images from the InSight lander show a moderately dusty, smooth cratered plain with low rock abundance, as predicted from orbital remote sensing data.	Poster Location #164
Maki J. N. Banerdt W. B. Bailey P.	Trebi-Ollenu A. Sorice C. et al.	<u><i>Imaging from the InSight Lander</i></u> [#2176] A view from the Mars InSight lander, as seen from the Instrument Deployment Camera (IDC) and Instrument Context Camera (ICC).	Poster Location #165
Deen R. G. Abarca H. E. Maki J. N.	Ayoub F. Ruoff N. A. et al.	<u><i>Production of the InSight Workspace Mosaics</i></u> [#2151] Discusses how the InSight workspace mosaics were created. These mosaics were used to determine where to deploy the InSight instruments.	Poster Location #166

Tuesday, March 19, 2019

[T310]

POSTER SESSION I: PLANETARY INTERIOR DYNAMICS: GRAVITY, DENSITY AND SEISMICITY

6:00 p.m. Town Center Exhibit Area

Authors (*Denotes Presenter)	Abstract Title and Summary	Poster Location
Izquierdo K. Lekic V. Montesi L.	<u><i>Constraining Density Anomalies in the Interior of Planetary Bodies from Gravity Data Using Bayesian Inference and Voronoi Cells</i></u> [#2157] Synthetic lunar gravity is used as input in a MCMC algorithm. Using a Bayesian approach, it finds a group of density models with good fit to the gravity data.	Poster Location #168
Bierson C. J. Nimmo F.	<u><i>Explaining the Galilean Satellites' Density Gradient by Hydrodynamic Escape</i></u> [#1935] The Galilean satellites smoothly transition from the rocky Io to the icy Callisto. Why? The energy of accretion can form surface oceans that lose mass to space.	Poster Location #169
Cline C. J. II Jackson I. Faul U. H.	<u><i>The Effect of Redox Conditions on Seismic Waves in Iron-Bearing Olivine: Implications for Understanding Planetary Interiors Through Seismology</i></u> [#1178] Attenuation / Seismic waves elucidate / Interior view.	Poster Location #170
Plesa A.-C. Bozdog E. Padovan S. Tosi N. Peter D. et al.	<u><i>Combining Large-Scale Numerical Simulations of Thermal Evolution and Seismic Wave Propagation to Model the Interior of Mars</i></u> [#2926] Combined calculations of 3D thermal evolution and seismic wave propagation will help to select interior models of Mars compatible with the InSight measurements.	Poster Location #171
Manga M. Wang C.-Y. Zhai G.	<u><i>Squeezing Marsquakes Out of Groundwater</i></u> [#1226] Cold water freezes / Aquifers get squeezed and stressed / Marsquakes will happen.	Poster Location #172
Tharimena S. Panning M. P. Vance S. D. Staehler S. C. Boehm C. et al.	<u><i>Insights into the Seismic Structure of Icy Moons from Full Waveform Modeling</i></u> [#1606] Full waveform modeling of the 3D seismic wavefield of Enceladus using a suite of thermodynamically self-consistent interior models.	Poster Location #173
DellaGiustina D. N. Bailey S. H. Bray V. J. Dahl P. Schmerr N. C. et al.	<u><i>On-Lander Seismology at an Ocean Worlds Analog Site in Northwest Greenland</i></u> [#2764] We present a seismic experiment at an Ocean Worlds analog site in Northwest Greenland and demonstrate the viability of on-lander seismology for planetary exploration.	Poster Location #174
Marusiak A. G. Schmerr N. C. Bailey S. H. DellaGiustina D. N. Bray V. J. et al.	<u><i>Location of Seismicity with a Small Aperture Array: Implications for Seismology with an Ocean World Lander</i></u> [#1546] Analogues on ice / Will ocean world lander find / Ice seismicity?	Poster Location #175
Mills M. Pappalardo R. T. Panning M. P.	<u><i>Moonquake Triggered Mass Wasting on Icy Worlds</i></u> [#2013] Distant icy worlds / Faults and fractures crosscutting / Moonquakes jar the ground.	Poster Location #176
Maguire R. Schmerr N. C. Lekic V. Hurford T. Dai L. et al.	<u><i>Constraining the Thickness of Europa's Ice Shell with Observations of Fundamental Mode Rayleigh Wave Dispersion</i></u> [#2819] We use simulations of seismic wave propagation on Europa to explore the potential of using surface wave dispersion to constrain ice shell thickness.	Poster Location #177
Zhang J. S. Hao M. Chen B.	<u><i>The Extreme Acoustic Anisotropy and Fast Sound Velocities of Cubic High-Pressure Ice Polymorphs at Mbar Pressure</i></u> [#1264] We presented the first experimentally determined single-crystal elasticity model of ice up to 103(3) GPa.	Poster Location #178

TUES POSTERS

Tuesday, March 19, 2019

[T311]

POSTER SESSION I: HABITABILITY: TO EXPLORE STRANGE NEW WORLDS

6:00 p.m. Town Center Exhibit Area

Authors (*Denotes Presenter)	Abstract Title and Summary	Poster Location
Godin P. J. Stone H. Bahrami R. Schuerger A. C. Moore J. E.	<u>Habitability of Bodies of Water on Ancient Mars: Attenuation of UV Radiation from Aqueous Solutions of Minerals Found on Mars</u> [#2525] The absorption of UV light by brines believed to have existed on the surface of ancient Mars was investigated. Brines that block UV have the potential for life.	Poster Location #179
Posnov N. Osinski G. R. Flemming R. L. Pontefract A. Crósta A.	<u>Hydrothermal Alteration of Vista Alegre Basalts: Implication for the Search for Life on Mars</u> [#2856] Is there life on Mars? / Hydrothermal impact bugs / Below the surface.	Poster Location #180
Muñoz-Iglesias V. Prieto-Ballesteros O.	<u>Heat Storage of Cryogenic Fluids of Ocean Worlds</u> [#2301] Specific heat measurements and Raman spectroscopy analyses of aqueous solutions with salts, ammonia, and methanol to apply the data to planetary processes.	Poster Location #181
Hermis N. H. Chin K. C. Barge L. M. B. LeBlanc G. L.	<u>Simulation of Prebiotic Early Earth Hydrothermal Chimney System in a Thermal Gradient Environment</u> [#3270] We successfully simulated the growth of hydrothermal chimneys in a thermal gradient environment.	Poster Location #182
Higgins P. M. Cockell C. S.	<u>A Power Driven Model for Predicting Microbial Growth in Poorly Characterised Environments</u> [#1687] A new model for habitability is presented, and we explore the Enceladean ocean in a case study of how it could be energetically limiting for microbial growth.	Poster Location #183
Clement T. V. M. de Winter B. Foing B. H. Heemskerck M. V. VUSE Igluna Team	<u>Characterization of Mars and Moon Microbial Life Through Terrestrial Analogue Field Research</u> [#2445] VUSE team of IGLUNA is designing experiments to look for microbial life on Moon and Mars. For this, spectrometry, microscopy, and sequencing will be used.	Poster Location #184
Pantha P. P. Wang G. W. Tran K. T. Oh D. O. Dassanayake M. D.	<u>Growing Plants on Mars: The Development of Sustainable Crops for Future Human Habitats</u> [#3257] Plants that thrive in extreme environments offer underexplored genetic blueprints to develop crops needed to support life in low resource growth systems.	Poster Location #185

Tuesday, March 19, 2019

[T312]

POSTER SESSION I: EXTRASOLAR PLANETS (THOSE OTHER WORLDS —

PROMISING UNTOLD OPPORTUNITIES — BECKON)

6:00 p.m. Town Center Exhibit Area

Authors (*Denotes Presenter)	Abstract Title and Summary	Poster Location
Ortiz-Ceballos K. N. Méndez A. Zuluaga J. Heller R. Alexander D. et al.	<u>Arecibo REDS: The Stellar Activity of Stars with Potentially Habitable Planets</u> [#3161] Radio observation of M dwarfs with potentially habitable planets, characterizing stellar activity to study its impact on planetary atmospheres and habitability.	Poster Location #186
Doyle A. E. Young E. D. Zuckerman B. Klein B. Schlichting H. E.	<u>Oxygen Fugacities of Rocky Exoplanets from Polluted White Dwarf Stars</u> [#1743] We calculate exoplanetary oxygen fugacities using spectroscopic analyses from white dwarf stars accreting rocky debris from previously orbiting bodies.	Poster Location #187
Stickle A. M. Izenberg N. Lisse C. M. Mandt K. E. Linden J. J. et al.	<u>Optimized Broadband Colors for Discriminating Earth-Like Exoplanets</u> [#2871] Using three wavelengths / Optimized exoplanet / Search for other earths.	Poster Location #188

TUES POSTERS

Marcum S. Kohler E.	<u><i>Temperature Dependent Laboratory Spectroscopy for Exoplanetary Atmospheric Condensates</i> [#2860]</u> An experimental apparatus was constructed to take IR spectral measurements of potential exoplanet atmosphere condensates at varying temperatures.	Poster Location #189
Barnett M. N. Kite E. S.	<u><i>The Transition from Primary to Secondary Atmospheres on Rocky Exoplanets</i> [#1855]</u> This work shows results from magma ocean outgassing and hydrodynamic escape processes on the mass and longevity of secondary atmospheres on rocky exoplanets.	Poster Location #190
Kite E. S. Fegley B. Jr. Ford E. B.	<u><i>The Fate of H on Mini-Neptunes and Super-Earths</i> [#1919]</u> Most H on mini-Neptunes can be held in the magma as "H ₂ O," even when H is derived from the nebula. Outgassing cannot explain mini-Neptune radii.	Poster Location #191
Kegerreis J. A. Eke V. R. Teodoro L. F. Massey R. J. Schaller M.	<u><i>Giant Impacts at High Resolution: Uranus, Atmospheric Erosion, and Observability of Exoplanet Collisions</i> [#2655]</u> Giant impact simulations with 1000x improved resolution reveal the detailed consequences for Uranus' atmosphere and internal structure, and exoplanet evolution.	Poster Location #192
Futó P.	<u><i>Modeling the Bulk Composition for the Large Terrestrial Planet: Kepler-328b</i> [#1306]</u> Kepler-328 b is thought to be a massive terrestrial planet with a relatively large core mass fraction.	Poster Location #193
Futó P.	<u><i>Possible Formation Scenarios and Mineralogical Types of Carbon-Rich Solid Planets</i> [#1307]</u> Numerous C-rich rocky exoplanets may exist in our galaxy and are thought to have a great diversity in their mineralogical composition.	Poster Location #194
Boujibar A. Driscoll P. Fei Y.	<u><i>Internal Structure, Thermal History, and Magnetic Field Generation in Super-Earths</i> [#2881]</u> Inside Super-Earths / Big ones have more dynamos? / Deep mantle melts too?	Poster Location #195
Byrne P. K. Heap M. J. Mikhail S.	<u><i>Toffee Planets: Influence of Surface Gravity on Exoplanetary Lithospheres</i> [#1315]</u> The ground is soft on / Rock worlds around other suns / If they're big enough.	Poster Location #196
Way M. J. Del Genio A. D.	<u><i>The Long-Term Evolutionary History of Venus' Climate and Applications to Exovenus Worlds</i> [#1808]</u> We examine a possible climate history of Venus from 4.2 billion years ago to today. These studies may help inform those of similar exoplanetary worlds.	Poster Location #197
Kane S. R. Arney G. Crisp D. Domagal-Goldman S. Glaze L. S. et al.	<u><i>Venus as a Laboratory for Exoplanetary Science</i> [#1969]</u> This talk will discuss Venus in the context of exoplanet discoveries and describe how Venus analogs are an essential part of studying planetary habitability.	Poster Location #198
Ostberg C. Kane S.	<u><i>Identifying Potential Venus Analogs from Exoplanet Discoveries</i> [#2123]</u> Venus analogs discovered in the coming years will be crucial to constraining the parameters that we use to define the habitable zone and Venus zone.	Poster Location #199
Ramirez R. M.	<u><i>Improving the Habitable Zone Using More Dynamic Definitions of Habitability</i> [#1812]</u> I review planetary and stellar processes and discuss how recent advances greatly improve how the habitable zone is used to search for life on other planets.	Poster Location #200
Broad K. E. Brock L. S. Melosh H. J.	<u><i>Viability of Lithopanspermia Between Planets of Gleise 581</i> [#1634]</u> By studying impact exchange within the Gleise 581 multiplanet system, we find that lithopanspermia is possible but different from that in our own solar system.	Poster Location #201
Jusino M. Mendez A.	<u><i>The Occurrence of Planets in the Abiogenesis Zone</i> [#3137]</u> Not a single Earth-sized planet has been discovered to be in both the Habitable Zone and the Abiogenesis Zone.	Poster Location #202

Tuesday, March 19, 2019

[T313]

POSTER SESSION I: ATMOSPHERES OF THE SOLAR SYSTEM

6:00 p.m. Town Center Exhibit Area

TUES POSTERS

Authors (*Denotes Presenter)	Abstract Title and Summary	Poster Location
Bills B. G. Navarro T. Schubert G. Ermakov A. Gorski K. M.	<u><i>Gravitational Signatures of Atmospheric Thermal Tides on Venus</i></u> [#1917] Atmospheric mass transport from thermal tides on Venus is sufficient to produce measurable gravitational signatures, which are diagnostic of deep structure.	Poster Location #203
Lyons J. R.	<u><i>Analytic Formulation of Isotope Fractionation Due to Self-Shielding</i></u> [#3140] Analytic expressions are derived to explain self-shielding isotope fractionation in symmetric and non-symmetric molecules of relevance to Archean sulfur MIF.	Poster Location #204
Wilson L. Head J. W. Deutsch A. N.	<u><i>Volcanically-Induced Transient Atmospheres on the Moon: Assessment of Duration and Significance</i></u> [#1343] We use lunar volcanic eruption rates and erupted magma volumes to predict amounts and rates of gas release and the range of possible transient atmospheres.	Poster Location #205
Palumbo A. M. Head J. W. Wordsworth R. D.	<u><i>Volcanism on Early Mars: Exploring the Influence of the SO₂ Plume on Localized and Short-Term Climate Change</i></u> [#2169] Following a volcanic eruption, localized and short-term heating can increase temperatures above 273 K for a few days near the eruption site.	Poster Location #206
Head J. W. III	<u><i>Toward an Understanding of Early Mars Climate History: New Themes, Directions, and Tests</i></u> [#2488] Twelve perspectives need to be considered to move forward with an understanding of early Mars warm and wet and cold and icy climate history end members.	Poster Location #207
Tarnas J. D. Mustard J. F. Sherwood Lollar B. Cannon K. M. Palumbo A. M. et al.	<u><i>An Insufficient Methane Budget for Warming Noachian and Hesperian Mars</i></u> [#2029] Abiotic CH ₄ production generates insufficient quantities of CH ₄ for a transient reducing greenhouse atmosphere capable of warming ancient Mars above 273 K.	Poster Location #208
Steakley K. E. Kahre M. A. Murphy J. R.	<u><i>Differences in Short Term Simulated Climate Response to Early Mars Impacts at Different Seasons</i></u> [#3012] Southern highlands receive the most precipitation following impacts at the autumnal equinox. We explore causes and potential influence beyond the short term.	Poster Location #209
Godin P. J. Campbell C. Nguyen T. G. Wizenberg T. Strong K. et al.	<u><i>A Possible Solution of the Early Mars Problem: Experimentally Verified Collision-Induced Absorption Cross-Sections of CO₂-H₂ and CO₂-CH₄ Complexes</i></u> [#2535] CIA between CO ₂ and H ₂ or CH ₄ has been proposed to provide additional greenhouse effect on Mars. The theoretical cross-sections are experimentally measured.	Poster Location #210
Hoffman M. E. Newsom H. E. Adair B. Williams J. M. Williams J. P. et al.	<u><i>The Recent Atmospheric History of Mars from Small Craters Observed by MSL</i></u> [#3147] Our 0.33 m cutoff of crater diameters indicates a much denser atmosphere during the ~ 20 Myr Crater accumulation time as suggested by obliquity calculations.	Poster Location #211
Smith C. L. Moores J. E. Gough R. Martinez G. Meslin P.-Y. et al.	<u><i>The Seasonal Cycle of Methane at Gale Crater, Mars, Replicated with Methane Adsorption and Diffusion Through the Regolith</i></u> [#1289] The observed methane mixing ratio cycle at Gale Crater can be reproduced with a diffusive-adsorptive model if methane seepage through the regolith is allowed.	Poster Location #212

Pla-Garcia J. Webster C. R. Karatekin O.	Rafkin S. C. R. Mahaffy P. R. et al.	<u><i>Seasonal Variations of the Hadley Cell and Differential Hemispheric Methane Release Could Drive the Seasonal Methane Cycle on Mars</i></u> [#2298] A meteorological model applied to Mars is used to explain the seasonal cycle of atmospheric methane detected by TLS-SAM instrument onboard the Curiosity rover.	Poster Location #213	
Newman C. E. Lemmon M.	Richardson M. I. Kahanpää H.	<u><i>Convective Vortex and Dust Devil Predictions in Gale Crater, Mars Using a Thermodynamic Theory and Comparison With Observations.</i></u> [#2312] Spatiotemporal variations in vortex activity predicted by the MarsWRF model are compared with MSL observations, showing the importance of sensible heat flux.	Poster Location #214	
Livengood T. A. Kostiuk T.	Kolasinski J. R. Hewagama T.	<u><i>Estimating the Pressure Ceiling of the June 2018 Mars Global Dust Storm</i></u> [#1700] Mars HIPWAC spectra / Super-high resolution / Reveal height of dust. Global dust obscures the ground / Hides the CO ₂ features.	Poster Location #215	
VanBommel S. J. Clark B. C. Schröder C.	Gellert R. Ming D. W. et al.	<u><i>Low-Latitude Near-Antipode Measurements of Atmospheric Argon with the Mars Exploration Rover and Mars Science Laboratory Alpha Particle X-Ray Spectrometers</i></u> [#1867] High-frequency atmospheric measurements with the Curiosity and Opportunity APXS instruments using argon as a tracer for condensation flow.	Poster Location #216	
Cassata W. S. Mark D. F. Smith C. L.	Cohen B. E. Lee M. R. et al.	<u><i>New Constraints on the Argon Isotopic Composition of the Martian Atmosphere Over the Past Three Million Years</i></u> [#2586] New Shergottite Ar isotope data precisely constrain the modern martian atmosphere. The implications for outgassing and atmospheric evolution will be discussed.	Poster Location #217	
Lillis R. J. Fox J. L.	Lo D. Yelle R.	Deighan J. et al.	<u><i>Photochemical Escape of Carbon from Mars: Greater Than Previously Thought?</i></u> [#3103] Martian carbon flees / Photochemistry drives it / Climate mystery clues?	Poster Location #218
Krishnaprasad C. Bhardwaj A.	Thampi S. V.	<u><i>Martian Ionospheric Response to the Passage of a Corotating Interaction Region: Observations from MAVEN</i></u> [#1757] The response of martian ionosphere to the passage of a CIR of June 2015 is studied using observations from several instruments onboard MAVEN.	Poster Location #219	
Franco A. M. S. Echer E.	Fränz M. Bolzan M.J. A.	<u><i>A Statistical Study of ULF Wave Scales Around Mars Using MEX and MAVEN Observations</i></u> [#2523] In order to study the scale of wave trains in the vicinity of Mars, correlation lengths around the planet were computed using MEX and MAVEN data.	Poster Location #220	
Fries M. Conrad P.	ten Kate I. L.	<u><i>The Mars Methane Plume of 2003 was Caused by a Meteor Storm from Comet C/2007 H₂ Skiff</i></u> [#1050] Methane and comet / Share time, place, and chemistry / Not an accident.	Poster Location #221	
Edgington S. G. Wilson E. H. West R. A.	Atreya S. K. Baines K. H. et al.	<u><i>Photochemistry in Saturn's Atmosphere: Ring Shadow and Ring Reflection</i></u> [#3053] This work studies the generation and variation of haze in Saturn's atmosphere and the chemistry and solar-seasonal insolation that modulates it.	Poster Location #222	
Horst S. M. Howett C. A.	Parker A. H. Ryan E. L.	<u><i>Monitoring Titan's Atmospheric Activity with Kepler/K2</i></u> [#3152] We used Kepler/K2 to look for variability in Titan's atmosphere. Titan did not vary in brightness by more than 1% from Dec 3 to Dec 7 2016.	Poster Location #223	

Tuesday, March 19, 2019

[T314]

POSTER SESSION I: 50 YEARS OF APOLLO LEGACY: FROM ORIGIN TO EXPLORATION

6:00 p.m. Town Center Exhibit Area

TUES POSTERS

Authors (*Denotes Presenter)	Abstract Title and Summary	Poster Location
Cambioni S. Asphaug E. Emsenhuber A. Gabriel T. S. J. Furfaro R. et al.	<u><i>Beyond Perfect Merging: Machine Learning Applied to Simulations of Giant Impacts</i></u> [#1518] Machine-learned impact models allow introducing realistic collision outcomes in N-body dynamical studies, going beyond the usual assumption of perfect merging.	Poster Location #225
Güldemeister N. Manske L. Burger C. Wünnemann K.	<u><i>The Thermal State of Earth After the Moon-Forming Impact Event Using Numerical Simulations</i></u> [#2430] Numerical simulations of giant impacts in 2D and 3D are carried out. We quantify the impact-induced melt that is produced after the Moon-forming impact event.	Poster Location #226
Korycansky D. G.	<u><i>Toward Self-Consistent-Field Models of the Moon after the Formation Impact</i></u> [#1190] I describe steps toward creation of Self-Consistent Field method models of the Moon after the formation impact.	Poster Location #227
Onodera K. Kawamura T. Ishihara Y. Maeda T. Tanaka S.	<u><i>Constraint on Impact-Seismic Efficiency from the Apollo Lunar Seismic Data Analysis and Numerical Simulation</i></u> [#1484] We estimated the lunar impact-seismic efficiency in order-scale through both numerical simulations and the analyses of the Apollo lunar seismic data.	Poster Location #228
Steenstra E. S. Berndt J. Rohrbach A. Klemme S. van Westrenen W.	<u><i>The Fate of Sulfur and Chalcophile Elements During Crystallization of the Lunar Magma Ocean</i></u> [#1137] The solubility of S in lunar magmas was experimentally studied. Results were applied to assess the fate of S and sulfides during magma ocean crystallization.	Poster Location #229
Schwinger S. Breuer D.	<u><i>Evolution of Lunar Mantle Mineralogy During Magma Ocean Crystallization and Mantle Overturn</i></u> [#2665] We investigate the mineralogical compositions of lunar magma ocean cumulates and their changes during mantle overturn by applying different petrological models.	Poster Location #230
Perera V. Schwinger S. Asimow P. D. Jackson A. P. Neal C. R.	<u><i>Developing an Integrated Thermochemical Code for Modeling Lunar Magma Ocean Evolution</i></u> [#2846] We are developing an open source code that can thermally evolve the early Moon by concurrently considering the geochemical evolution of the Lunar Magma Ocean.	Poster Location #231
Wood C. A.	<u><i>360 Years of Lunar Science: From Galileo to Apollo 10</i></u> [#3046] What were the enduring questions of lunar research in the 3.6 centuries before Apollo? Who were the lunar heroes who helped answer them?	Poster Location #232
Feist B. F. Petro N. E.	<u><i>Landing Humans on the Moon and Returning Them Safely to the Earth: Lessons from a New Time-Centered Apollo 11 Media Archive that Uncovers New Insight into How They Achieved the Greatest Technological Feat in Human History and Provides a New Context for Apollo 11 Lunar Samples</i></u> [#3164] Here we report on an archive of Apollo 11 data, its importance to interpreting Apollo 11's science, and lessons for future exploration.	Poster Location #233
Foing B. H. Racca G. Marini A. Camino O. Koschny D. et al.	<u><i>SMART-1 Highlights and Tribute to Apollo Legacy</i></u> [#3036] Celebrating APOLLO legacy after 50 years, we present SMART-1 highlights relevant for lunar science, exploration, and inspiration towards Moon Village.	Poster Location #234
Hahn T. M. Jr. Watkins R. N. Robinson M. S. Jolliff B. L.	<u><i>Assessing Formation Mechanisms for the South Massif Light Mantle Deposit</i></u> [#1963] We present photometric analyses of Tycho impact melt deposits at Apollo 17 and discuss the potential for Tycho secondaries to trigger debris flows in the TLV.	Poster Location #235

Chi P. J.	<u><i>Recent Findings from Apollo Magnetic Field Records</i> [#1920]</u> The study reviews the key characteristics and new findings of the lunar magnetic field environment based on the restored Apollo magnetic field records.	Poster Location #236
Borisov D. Hiesinger H. Iqbal W. van der Bogert C. H.	<u><i>Revised Crater Size-Frequency Distribution Measurements at the Apollo 14 Landing Site</i> [#2323]</u> We constrained the A14 calibration point on the Lunar Cratering Chronology with a new geological map and subsequent CSFDs.	Poster Location #237
Gebbing T. Hiesinger H. Iqbal W. van der Bogert C. H.	<u><i>New Crater Size-Frequency Distribution Measurements of the Apollo 16 Landing Site</i> [#2337]</u> New lunar data sets allow updating and improving the CSFD analyses in the Apollo 16 region on which the lunar cratering chronology is based.	Poster Location #238
van der Bogert C. H. Hiesinger H. Iqbal W. Clark J. D. Robinson M. S. et al.	<u><i>Timing of Recent Events near the Apollo 17 Landing Site</i> [#1527]</u> What are the temporal relationships between the Lee Lincoln scarp, light mantle deposit, and secondary craters from Tycho in Taurus Littrow Valley?	Poster Location #239
Mercer C. M. Hodges K. V. Jolliff B. L. van Soest M. C. McDonald C. S.	<u><i>Reviewing the Geochronologic Constraints from Samples of Boulders at Apollo 17 Stations 2, 6, and 7: Implications for Understanding the Stratigraphy of the North and South Massifs in the Valley of Taurus-Littrow</i> [#3049]</u> We review geochronologic data for the boulders at Apollo 17 and discuss potential implications for multiple basin inputs to the stratigraphy of the massifs.	Poster Location #240
Ding X. Z. Sr. Xu K. J. Jr.	<u><i>A New Lunar Geological Time Scale and the Geological Evolution of the Moon</i> [#1741]</u> Based on the new geological time scale, we discussed the evolutionary history of the lunar regional geology.	Poster Location #241
Rojas C. Mahanti P. Robinson M. S.	<u><i>Morphological Classification of Complex Eratosthenian Craters</i> [#2499]</u> Overview of factors to determine the age of rayless complex lunar craters (predominantly Eratosthenian) in absence of relative absolute model ages.	Poster Location #242

Tuesday, March 19, 2019

[T315]

POSTER SESSION I: LUNAR REMOTE SENSING I: NEW EXPLORATION

6:00 p.m. Town Center Exhibit Area

Authors (*Denotes Presenter)	Abstract Title and Summary	Poster Location
Meyer H. M. Hayne P. O. Ghent R. R. Denevi B. W. Cahill J. T. S. et al.	<u><i>Targeted Regolith and Impact Studies in the Next LRO Extended Mission</i> [#2615]</u> The next LRO extended mission will address key questions about impact processes, regolith development, space weathering, and the lunar chronology.	Poster Location #243
Wimmer-Schweingruber R. F. Zhang S. Yu J. Hellweg C. E. Guo J. et al.	<u><i>The Lunar Lander Neutron and Dosimetry (LND) Experiment on Chang'E4</i> [#2348]</u> Chang'E4 was launched on December 8, 2018 and landed on January 3, 2019. We present first data from the Lunar Lander Neutron and Dosimetry (LND) Experiment.	Poster Location #244
Guo D. Fa W. Zeng X. Cai Y. Du J. et al.	<u><i>Geological Investigation of the Chang'e-4 Landing Site and the Expected Scientific Return from the Lunar Penetrating Radar</i> [#1844]</u> The Chang'E-4 landing site is investigated with emphasis on the geological units, geochemical characteristics and radar exploration.	Poster Location #245
Binet R. Grizonnet M. Torres A. Malapert J-C. Jocteur-Moronzier F.	<u><i>Lunar Landing Site Localization, Trajectory Inversion, and DTM Update from CHANG'E-3 Descent Images</i> [#2433]</u> A SFM pipeline based only on lander descent images has been tested on CE3 images to determine the landing site localization and update the local DTM.	Poster Location #246

Li B. Zhang J. Yao P. W.	<u><i>Potential Landing Areas Selection for China's Chang'E-4 Probe</i></u> [#1363] NAC mosaic image was divided into undulating and flat areas using Otsu method. According to the FAP (flat area percentage) map, five safe landing areas were selected.	Poster Location #247
Fu X. H. Zhang J. Jia L. C. Ling Z. C. Jia Y. Z. et al.	<u><i>Geochemical Characteristics and Subsurface Structure of Chang'e-4 Landing Site</i></u> [#1848] We studied geochemical characteristics of Chang'E-4 landing site and its subsurface structure to provide geological background for further data interpretation.	Poster Location #248
Neumann G. A. Head J. W.	<u><i>Geophysical Characteristics of Von Kármán Crater: Chang'E 4 Landing Site Region</i></u> [#1962] We provide high-resolution crustal structure at the Chang'e-4 landing site revealing two basin-like circular regions of uplifted mantle and thinned crust.	Poster Location #249
Ravat D. Purucker M. E. Olsen N.	<u><i>New High Resolution Magnetic Field Models at the Surface of the Moon from Lunar Prospector Along-Track Vector Gradients</i></u> [#1906] Gradients from Lunar Prospector lead to high resolution crustal magnetic field models of the Moon in the region of Von Kármán Crater, Chang'E-4 landing site.	Poster Location #250
Nuno R. Hayne P. O. Rubanenko L. Paige D. A.	<u><i>Diviner Measured Brightness Temperatures and Rock Abundance of the Chang'E 4 Landing Site</i></u> [#2887] Chang'e has landed / In Aitken Basin. How warm? / Let's ask Diviner.	Poster Location #251
Michael G. G. Yue Z. Gou S. Di K.	<u><i>Dating Individual Several-km Lunar Impact Craters from the Rim Annulus in Region of Planned Chang'E-5 Landing</i></u> [#2837] We extend the Poisson statistics approach to analyse buffered crater counts on the rims of individual craters.	Poster Location #252

Tuesday, March 19, 2019

[T316]

POSTER SESSION I: LUNAR BASINS, IMPACTS, AND EJECTA

6:00 p.m. Town Center Exhibit Area

Authors (*Denotes Presenter)	Abstract Title and Summary	Poster Location
Bretzfelder J. M. Klima R. L. Greenhagen B. T. Buczowski D. L. Cartwright S. F. A. et al.	<u><i>Comparative Spectral Analysis of Three Distinct Lunar Basins</i></u> [#1933] Three lunar basins / Diverse mineralogy / Searching for mantle.	Poster Location #254
Jones M. J. Evans A. J.	<u><i>Thermal and Chemical Consequences of Large Impacts on the Lunar Interior</i></u> [#2180] Influence of large impacts on evolution of the lunar interior and exterior is investigated through shock heating and thermochemical evolution modeling.	Poster Location #255
Meyer H. M. Stopar J. D. Bhiravarasu S. S. Denevi B. W. Robinson M. S.	<u><i>Morphology and Physical Properties of Orientale Light Plains and Associated Flow Features</i></u> [#2581] We assess the morphology and physical properties of Orientale light plains exhibiting flow features to distinguish between proposed formation mechanisms.	Poster Location #256
Kendall J. D. Petro N. E.	<u><i>Lunar Ejecta Model of Crisium Basin-Forming Impact: Analyzing Ejecta Distribution and Provenance</i></u> [#2355] We utilize impact hydrocode modeling to determine the ejecta distribution of the Crisium basin-forming impact.	Poster Location #257
Hood L. L. Oliveira J. S.	<u><i>New Mapping and Modeling of Magnetic Anomalies in Lunar Impact Basins: First Mapping Results</i></u> [#1348] A new regional mapping approach is applied to map the interiors of large basins as needed for more accurate modeling and paleomagnetic pole position estimation.	Poster Location #258
Maxwell R. E. Garrick-Bethell I.	<u><i>Testing the Antipodal Ejecta Magnetization Hypothesis: Clustered Magnetization Directions of the Lunar Gerasimovich Magnetic Anomalies</i></u> [#2102] Gerasimovich / A magnetic fam of five / Why are you like this?	Poster Location #259

Kelley M. R. Garrick-Bethell I.	<u><i>Testing the Antipodal Ejecta Magnetization Hypothesis: A Closer Look at the Geologic Setting of the Lunar Gerasimovich Magnetic Anomalies</i></u> [#2071] Lunar magnetic anomalies / Have caused so many hypotheses / One way to decode / They're an antipode / Of an impact with high velocities.	Poster Location #260
Adler J. B. Asphaug E. Robinson M. S. Winhold A. Davison T. M. et al.	<u><i>Tycho Ejecta Deposits Near the Ballistic Antipode: New Modeling Methods</i></u> [#2201] We present a novel workflow for simulating high-velocity ejecta from Tycho Crater, using a 3D impact hydrocode and precise orbital propagation software.	Poster Location #261
Huang Y.-H. Minton D. A. Elliott J. R. Andronicus C. Nguyen P. Q. et al.	<u><i>A Short-Lived Lunar Impact Spike Induced by Copernicus Crater-Forming Sesquinaries Versus a Long-Duration Global Impact Resurfacing ~800 Ma Ago from a Modeling Perspective</i></u> [#3010] We investigated the relationship between the excess of ages of ~700–900 Ma of lunar "exotic" glasses and the formation age of Copernicus Crater on the Moon.	Poster Location #262
Halim S. H. Crawford I. A. Collins G. S. Joy K.	<u><i>Survival of Terrestrial Material Impacting the Lunar Surface</i></u> [#1816] Could there be a record of early terrestrial material on the Moon's surface? We investigate whether material would survive impacts using shock physics models.	Poster Location #263
McIntosh E. C. Day J. M. D. Liu Y.	<u><i>Impactor Populations Striking the Moon Determined from Melt Coat and Regolith Meteorite Compositions</i></u> [#2589] There is significant heterogeneity within impact melt coats. These segregations lead to significant HSE fractionation that occur at small scales.	Poster Location #264
Yamada R. Kawamura T. Yanagisawa M. Abe S. Fukuhara T. et al.	<u><i>The international observation of lunar impact flashes and application of the results to future lunar seismic experiments</i></u> [#1770] We have conducted first international observation of the lunar impact flashes in same days and applied the results to study about lunar seismic experiments.	Poster Location #265
Taylor S. E. Powell T. M. Williams J.-P. Paige D. A.	<u><i>The Longitudinal Distribution of Lunar Craters</i></u> [#2700] Analysis of the longitudinal distribution of lunar craters may provide insight on the differential fading of crater rays and cold spots.	Poster Location #266
Thomson B. J. Bhiravarasu S. S. Nypaver C. Neish C. D. Patterson G. W. et al.	<u><i>Latitudinal Trends of Anomalous Craters Observed with LRO Mini-RR Radar Data</i></u> [#2855] We re-examine lunar impact craters that are radar anomalous. Comparing the poles to non-polar regions, we find that one of these things is not like the other.	Poster Location #267
Karthi A.	<u><i>Mineralogical Study of Lunar Das Impact Crater Using Chandrayaan-1-Moon Mineralogical Mapper</i></u> [#2273] The Das Crater using CH-1 and LROC data through elemental mapping, topographical, and spectral characterization.	Poster Location #268
Chandnani M. Herrick R. R. Kramer G. Y.	<u><i>Geologic Study of Unusually Deep Simple Craters in the Lunar Simple-to-Complex Transition</i></u> [#2119] We conducted detailed geologic analyses of unusually deep lunar simple craters in the 15–20 km size range to constrain possible mechanisms for their formation.	Poster Location #269
Prieur N. C. Werner S. C.	<u><i>Constraining Impact Numerical Model Parameters with the Help of Fresh Simple Craters on the Moon</i></u> [#1391] Lunar fresh impact craters and geomorphological parameters derived from them are used to constrain more accurately impact numerical model parameters.	Poster Location #270
Wang J. T. Kreslavsky M. A. Liu J. Z. Head J. W. Kolenkina M. M.	<u><i>Quantitative Characterization of Impact Crater Materials on the Moon: Implications for the Role of Target Material</i></u> [#1263] Topographic roughness and thermophysical properties of subunits of impact craters give insight into regional variations of crater formation and degradation.	Poster Location #271

Ivanov B. A. Head J. W.	<u><i>Impacts into Magmatic Foam and the Age of Irregular Mare Patches: Experimental Data, Interpretations, and Outstanding Questions</i></u> [#1243] A review of the experimental data for impacts into porous targets to discuss theories for the formation of IMPs and the crater retention age determination.	Poster Location #272
Plescia J. B. Barnouin O. Anderson J. L. B. Cintala M. J.	<u><i>Morphometry and Morphology of Lunar Crates on Slopes</i></u> [#2984] Asymmetric lunar craters form even on shallow slopes. Ratios of the lateral dimensions appear independent of slope angle.	Poster Location #273
Neish C. D. Blewett D. T. Morse Z. Zheng Y.-C.	<u><i>Unusual Rocky Deposits Around Large Imbrian Lunar Impact Craters</i></u> [#1542] Old lunar basins / Preserve youthful appearance / Botox for the Moon?	Poster Location #274
Matiella Novak M. A. Patterson G. W. Greenhagen B. T. Neish C. Smith R.	<u><i>Characterizing Lunar Impact-Related Features, Emplacement, and Degradation Processes — Impact Melts at Copernicus Crater</i></u> [#3203] We compare LROC NAC, Mini-RF, and Diviner data to characterize regolith properties associated with Copernicus Crater impact melt flows and ponds.	Poster Location #275
Stickle A. M. Patterson G. W. Cahill J. T. S. Prem P. Mini-RF Team	<u><i>Observing the Radar Scattering (Phase) Function of Copernican Crater Ejecta with Mini-RF</i></u> [#2937] How does light scatter / On that serene cratered land? / RADAR reveals all.	Poster Location #276
Pajola M. Pozzobon R. Lucchetti A. Rossato S. Baratti E. et al.	<u><i>Size-Frequency Distribution of the Ejected Boulders Surrounding the Linné Crater (Moon)</i></u> [#1377] We present the size-frequency distribution of the ejected boulders surrounding one of the youngest craters located on the surface of the Moon: the Linné crater.	Poster Location #277
Atwood-Stone C. McElwaine J. Richardson J. Bray V. J. McEwen A. S.	<u><i>Crater Concentric Ridges: Kelvin-Helmholtz Instabilities in Lunar Ejecta</i></u> [#2164] Over regolith / Below flowing ejecta / Kelvin-Helmholtz waves.	Poster Location #278

Tuesday, March 19, 2019

[T317]

POSTER SESSION I: LUNAR IMPACTS AND REGOLITH PROCESSES

6:00 p.m. Town Center Exhibit Area

Authors (*Denotes Presenter)	Abstract Title and Summary	Poster Location
Wang Y. Xiao Z.	<u><i>The Minimum Confidential Diameter for Crater Counts</i></u> [#1506] The minimum confidential diameter for crater counts is 10 pixels of the image, and incomplete recognition and overestimate of crater sizes are the major cause.	Poster Location #279
Kirchoff M. R. Marchi S.	<u><i>The Effect of Terrain Properties on Crater Model Age Determination</i></u> [#2705] To understand influence of terrain properties on crater model ages, we fit expanded crater distributions of Apollo terrains with the Model Production Function.	Poster Location #280
Riedel C. Minton D. A. Michael G. G. van der Bogert C. H. Hiesinger H.	<u><i>Modeling the Formation of Densely Cratered Lunar Surfaces Under the Influence of Diffusive Crater Degradation</i></u> [#2694] We simulate densely cratered surfaces to investigate the influence of diffusive crater degradation on the formation of the lunar highlands.	Poster Location #281
Banks M. E. Grier J. A. Watkins R. N. Clark J. D. van der Bogert C. H. et al.	<u><i>A Preliminary Look at Lunar Lobate Scarps Through Comparisons of Crater Counts, Photometry, and Optical Maturity</i></u> [#2577] Lunar lobate scarps / Thrusting, disturb regolith / Future exploration sites?	Poster Location #282
Head J. W. III Wilson L.	<u><i>Rethinking Lunar Mare Basalt Regolith Formation: New Concepts of Lava Flow Protolith and Evolution of Regolith Thickness and Internal Structure</i></u> [#2532] Lunar mare regolith formation models assume a coherent basaltic bedrock protolith: We show that lava flow protoliths can be highly variable in space and time.	Poster Location #283

Mahanti P. Robinson M. S. Thompson T. J. van der Bogert C. H.	<u><i>Small Crater Lifetime and In-fill Rates at the Apollo Landing Sites</i> [#2001]</u> Compare small crater population lifetimes at the Apollo landing sites.	Poster Location #284
Powell T. M. Greenhagen B. T. Taylor S. Paige D. A. Williams J. -P. et al.	<u><i>The Thermophysical Properties of Lunar Cold Spots: Determining Age and Formation Mechanism</i> [#2238]</u> The thermophysical properties of lunar cold spots can be used to determine crater age and inform our understanding of impact processes.	Poster Location #285
Elder C. M. Douglass B. Hayne P. O. Ghent R. R. Williams J.-P. et al.	<u><i>Mapping Regolith Thickness on the Moon Using a New Class of Young Craters</i> [#2485]</u> Regolith thickness / Mapped using cold spot crater / Rocky ejecta.	Poster Location #286
Ruesch O. Sefton-Nash E. Vago J. L. Kueppers M. Krohn K. et al.	<u><i>Fragmentation of Blocks: Possible Relationship with Exposure Time Based on LROC NAC</i> [#2340]</u> The study of clustered blocks can inform on the fragmentation and erosion processes on the Moon.	Poster Location #287
Rubanenko L. Powell T. M. Paige D. A.	<u><i>Immigrant and Native Rocks in Simple Craters: A New Method for Dating Airless Surfaces</i> [#3098]</u> We derive a new metric to determine the age of airless surfaces and individual craters from their radiometrically sensed rock abundance.	Poster Location #288
Domingue D. L. Weirich J. Palmer E. E. Gaskell R.	<u><i>Photometric Characterization of On- and Off-Swirl Regions of the Lunar Surface: Textural Similarities and Differences</i> [#1936]</u> Intricate patterns / Swirling, dancing on the Moon / Textures to explore.	Poster Location #289
Choi T. X. Blewett D. T. Zheng Y. C. Cloutis E. A.	<u><i>Analysis of Chang'E-3 Rover Color Images</i> [#1453]</u> We are exploring the usefulness of Chang'E-3 rover color (red-green-blue) images of the surface for studies of rocks and soils at the landing site.	Poster Location #290
Ahmad A. Nair A. M.	<u><i>Lithological Discrimination of Reiner Gamma Using Remote Sensing Techniques</i> [#1957]</u> The lithological mapping of Reiner Gamma swirl obtained for olivine and pyroxene. The high albedo have the stronger mafic absorptions, especially due to olivine.	Poster Location #291
Rhodes D. J. Farrell W. M.	<u><i>Lunar Polar Crater Exploration: Electrical Grounding in an Electron Cloud</i> [#2449]</u> We examine the plasma environment inside a lunar polar crater, and its effect on electrical grounding of equipment on future exploration missions.	Poster Location #292
Wang X. Hood N. Carroll A. Mike R. Hsu H.-W. et al.	<u><i>Laboratory Measurements of Initial Conditions of Electrostatically Lofted Regolith Dust</i> [#1261]</u> Here we report the current laboratory measurements of initial conditions of electrostatically lofted dust, which are critical for dust dynamics studies.	Poster Location #293
Prem P. Greenhagen B. T. Yasanayake C. N. Donaldson Hanna K. L.	<u><i>Modeling Near-Surface Temperature Gradients and Thermal Emission from the Lunar Regolith</i> [#2425]</u> On airless bodies, infrared emission often originates from a thin, non-isothermal layer of the subsurface; we investigate the thermal structure of this layer.	Poster Location #294
Rubanenko L. Schorghofer N. Paige D. A.	<u><i>Analytic Model for the Equilibrium Temperature Distribution of a Sunlit Gaussian Airless Surface</i> [#3014]</u> We derive an analytic model for the temperature distribution of rough airless planetary bodies and apply it to the lunar surface.	Poster Location #295
Russell P. S. Paige D. A. Greenhagen B.	<u><i>Thermophysical Behavior of the Uppermost Lunar Surface from Diviner High Time-Resolution, Post-Sunset Observations</i> [#3003]</u> The thermal response of the upper ~1cm surface due to cessation of solar heating at dusk, via a multiyear observation campaign of a range of geologic features.	Poster Location #296
Siegler M. A. Feng J. Lucey P. Hayne P. O. Blewett D. et al.	<u><i>Deriving the Lunar Loss Tangent and Subsurface Temperatures from the Chang'E-2 MRM and LRO Diviner</i> [#3151]</u> Microwave thermal / It's all the same, you just need / The right loss tangent.	Poster Location #297

Feng J. Siegler M. A. Hayne P. O. Blewett D. T.	<u><i>Lunar Regolith Properties Constrained by LRO Diviner and Chang'e-2 Microwave Radiometer Data</i></u> [#3176] We use CE-2 MRM to extend our understanding of Diviner surface measurements and use Diviner to correct some calibration errors within the MRM dataset.	Poster Location #298
Byron B. D. Retherford K. D. Mand K. E. Greathouse T. K. Gladstone G. R.	<u><i>Porosity Maps of the Lunar Surface Derived from LRO-LAMP Albedo Data</i></u> [#3115] We have derived regolith porosity maps for the lunar surface from LRO-LAMP far-UV albedo data. PSRs are seen to have higher porosity than illuminated regions.	Poster Location #299
Wilson J. K. Spence H. E. Schwadron N. A. Looper M. D. Case A. W. et al.	<u><i>A Serendipitous New View of the Moon</i></u> [#2039] Search for SEPs / Results in a new Moon map / Serendipity!	Poster Location #300
Meshik A. Pravdivtseva O. Burnett D.	<u><i>Isotopic Composition of Solar Wind Xenon Captured by Genesis: Verification and Possible Implication for Indigenous Lunar Xenon</i></u> [#2004] The difference between Solar Wind xenon captured by Genesis and measured in lunar regolith brought by Apollo mission points to indigenous lunar xenon.	Poster Location #301
Terada K. T. Yokota S. Y. Kawai Y. K.	<u><i>Consideration on Oxygen Isotopic Composition Recorded on the Lunar Surface Based on the KAGUYA Observation of Terrestrial Oxygen</i></u> [#2177] We report observations from the Japanese spacecraft Kaguya of significant terrestrial O ⁺ ions only when the Moon was in the Earth's plasma sheets.	Poster Location #302
Morland Z. S. Joy K. H. Gholinia A. Degli-Alessandrini G.	<u><i>Metal in Lunar Meteorite North West Africa 10989: Insight into Survivability of Impactor Material Delivered to the Moon</i></u> [#1275] Metal found in lunar meteorite, thought to be exogenous because of its composition, texture, and internal micro-structure. Implications for ISRU of the Moon.	Poster Location #303
Martinez M. R. Barker D. C. Meen J. K.	<u><i>Lunar Soil Sample 74221,2 — A Study of Unusual Fines</i></u> [#1117] Careful X-ray mapping of the fine-grained fraction of lunar regolith, 74221,2, reveals the presence of micron scale grains of CaS, (Na,K)Cl, S, Sb, TiO ₂ , and CaO.	Poster Location #304

Tuesday, March 19, 2019

[T318]

POSTER SESSION I: LUNAR VOLATILES: FROM SURFACE TO EXOSPHERE

6:00 p.m. Town Center Exhibit Area

Authors (*Denotes Presenter)	Abstract Title and Summary	Poster Location
Tucker O. J. Farrell W. M.	<u><i>Monte Carlo Simulations of the Effect of Shielding on H Retention in the Moon's Surface and the H₂ Exosphere</i></u> [#3184] We used a 3D Monte Carlo model to examine the effect of shielding on the lunar OH surface concentration and H ₂ exosphere for comparisons to M ³ observations.	Poster Location #305
Baumgardner J. Schmidt C. Moore L. Mendillo M. Mayyasi M.	<u><i>20 Years of Observations of the Lunar Sodium Tail</i></u> [#1940] 20 years of observations of the lunar sodium tail have led to new insights to the source rates of the sodium liberated from the surface of the Moon.	Poster Location #306
Potter A. E. Killen R. M. Morgan T. H.	<u><i>Coronagraphic Observations of the Lunar Sodium Exosphere</i></u> [#1921] The lunar sodium was measured to one-half degree around the Moon. Column abundances are asymmetric north/south and are flatter than a cosine with latitude.	Poster Location #307
Bu C. Dukes C. A.	<u><i>Exospheric Potassium: Laboratory Measurements of Temperature-Dependent Depletion Cross-Sections for Potassium Absorbed on Ilmenite</i></u> [#3274] Laboratory measurements of ion-induced depletion cross-sections of potassium with applications for Mercury exosphere.	Poster Location #308

Zhang Z. Nie X. Mendybaev R. A. Dauphas N.	<u><i>Experimental Study of Potassium and Rubidium Evaporation Under Vacuum Conditions</i> [#2834]</u> Our experiments on potassium and rubidium evaporation have shown that K and Rb have similar evaporative behaviors under vacuum conditions.	Poster Location #309
Grava C. Hurley D. M. Retherford K. D. Gladstone G. R. Greathouse T. K. et al.	<u><i>LRO-LAMP Observations of Lunar Exospheric Helium</i> [#1882]</u> We present observations of the tenuous lunar helium exosphere obtained by the ultraviolet spectrograph LAMP onboard the Lunar Reconnaissance Orbiter.	Poster Location #310
Mandt K. E. Petro N. Keller J. Patterson G. W. Hendrix A. et al.	<u><i>Multi-Instrument Studies of Lunar Volatiles in the LRO Extended Mission: Global-Scale Objectives</i> [#2676]</u> During LRO's 4th extended mission, we will conduct a multi-instrument investigation of global processes to evaluate how transport influences distribution.	Poster Location #311
Sanin A. B. Mitrofanov I. G. Bakhtin B. N. Litvak M. L.	<u><i>Accounting of the Lunar Gravity Field at the Water Equivalent Hydrogen Estimation Based on the LEND/LRO Data</i> [#2554]</u> Results of LEND data processing and WEH estimation based on a procedure that takes into account the lunar gravity and finite neutron lifetime will be presented.	Poster Location #312
Aye K.-M.	<u><i>LRO Diviner Re-Calibration and Its Effect on Volatile Research</i> [#3259]</u> We describe the ongoing efforts to improve the calibration of the LRO Diviner instrument and its effect on volatile research.	Poster Location #313
Patrick E. Blase R. Libardoni M.	<u><i>The Moon is a Harsh Chromatogram: The Most Strategic Knowledge Gap (SKG) at the Lunar Surface</i> [#2766]</u> We present mission and laboratory evidence supporting our claim that the lunar surface is a giant 3D chromatogram sorting volatiles according to their mobility.	Poster Location #314
Orlando T. M. Clendenen A. R. Schieber G. L. Jones B. M. Loutzenhiser P. D. et al.	<u><i>Formation, Transport, and Release of Molecular Water On and Within Lunar Materials</i> [#2267]</u> Temperature program desorption measurements of H ₂ O from lunar samples provide activation energies, binding energies, adsorption lifetimes, and formation rates.	Poster Location #315
Deutsch A. N. Head J. W. Neumann G. A.	<u><i>Distribution of Surface Water Ice on the Moon: An Analysis of Host Crater Ages Provides Insights into the Ages and Sources of Ice at the Lunar South Pole</i> [#1150]</u> We estimate ages of craters that host surface water ice at the south pole of the Moon to provide insight into possible sources and ages of lunar ice.	Poster Location #316
Heggy E. Palmer E. M. Thompson T. W. Thomson B. J. Patterson G. W.	<u><i>Dielectric Constraints on Ice Detectability in Permanently Shadowed Lunar Crater Fills as Assessed from LRO/Mini-RF and Chandrayaan-1/Mini-SAR Radar Observations</i> [#3022]</u> The detectability of porous water-ice in permanently shadowed craters by S- and X-band radar is most likely achievable within craters ≥ 5 km in diameter.	Poster Location #317
Virkki A. K. Bhiravarasu S. S.	<u><i>Inferring Radar Scattering from Lunar Surface</i> [#2200]</u> The shiny craters / We see through Mini-RF / Water ice or not?	Poster Location #318
Parkinson A. E. Cloutis E. A. Applin D. M. Mann P. J.	<u><i>Mapping the Presence of Water Ice in Permanently Shadowed Lunar Regions Using a Two-Band Lidar</i> [#2099]</u> Testing for possible water ice presence at permanently shadowed lunar poles through the use of a lunar meteorite and ice mixtures.	Poster Location #319
Brown H. M. Robinson M. S. Boyd A. K.	<u><i>Identifying Resource-Rich Lunar Permanently Shadowed Regions: Table and Maps</i> [#1054]</u> We compare the lunar polar volatile datasets to identify sites that are most likely to host volatiles, and rank a selection of PSRs by their resource potential.	Poster Location #320
Thompson T. J. Mahanti P. Robinson M. S.	<u><i>Secondary Illumination Conditions at Cabeus Crater</i> [#3100]</u> Secondary illumination wattage is modeled for Cabeus Crater and compared to long exposure NAC images. Shadowing and slope is most important.	Poster Location #321

Patterson G. W. Jozwiak L. M. Kirk R. Becker T. L. Perkins R. et al.	<u><i>Mini-RF Radar Observations of Polar Craters: Are They Rough, Smooth, or Icy?</i> [#2861]</u> We present monostatic and bistatic radar data for polar crater floors of the Moon to address driving questions related to the form/abundance of water ice.	Poster Location #322
Behrens J. W. Zacny K. Prettyman T. H. Landis M. E. Atkinson J. et al.	<u><i>Laboratory Study of Mechanical and Thermodynamic Properties of Analog Lunar Polar Crater Ice-Regolith Mixtures</i> [#2604]</u> Icy lunar soils / Extraction brings pressure, heat / How will it react?	Poster Location #323
Roux V. G. Roth M. C. Roux E. L. McCafferty N. S.	<u><i>The Unique Physical Characteristics of Simulated Lunar Ice</i> [#2141]</u> Unknown for so long / Sublime priceless potential / Silently waiting.	Poster Location #324
Kloos J. L. Godin P. Moores J. E. Seguin A.	<u><i>The Anui Investigation: Lunar Frost Detection Using Reflected Lyman Alpha Starlight</i> [#2460]</u> We simulate an ice-covered lunar surface within a vacuum chamber and perform image studies using UV and visible multispectral imaging.	Poster Location #325
Jordan A. P. Wilson J. K. Looper M. D. de Wet W. C. Spence H. E. et al.	<u><i>Refining the Latitude Trend of Albedo Protons to Characterize Hydrogen in Shallow Regolith on the Moon</i> [#1942]</u> We use new techniques to revisit an earlier study that uses albedo protons to measure the hydrogen abundance in shallow lunar regolith (~1–10 cm).	Poster Location #326
Honniball C. I. Lucey P. G. Li S. Hibbitts K.	<u><i>Estimates of Molecular Water Abundance Using the 6 Micron H-O-H Bend</i> [#2199]</u> Spectroscopic observations at 6 μm offers a powerful unambiguous view of H ₂ O on the lunar surface enabling testing of the hypothesis that H ₂ O may be mobile.	Poster Location #327
Honniball C. I. Lucey P. G. Kaluna H. M. Li S. Takir D. et al.	<u><i>Diurnal Variations of Lunar Surface Water from Groundbased Telescopic Observations</i> [#2076]</u> Groundbased observations of three micron lunar surface water show latitude and diurnal variations.	Poster Location #328
Ferrari-Wong C. M. Honniball C. I. Lucey P. G. Gabieli A. Li S. et al.	<u><i>A Search for Organic Spectral Features on the Lunar Surface</i> [#3154]</u> A telescopic search for lunar surface organic spectral features in the 3.4–3.5 micron range, with an upper limit of 1% on the strength of such features.	Poster Location #329

Tuesday, March 19, 2019

[T319]

POSTER SESSION I: MERCURY: MAGNETISM, MAGMA, AND MORE

6:00 p.m. Town Center Exhibit Area

Authors (*Denotes Presenter)	Abstract Title and Summary	Poster Location
Nittler L. R. Cartier C. Charlier B. Crapster-Pregont E. Frank E. A. et al.	<u><i>The Surface Abundance of Titanium on Mercury</i> [#3156]</u> Mercury X-rays / Tell how much titanium / Iron sulfide layer?	Poster Location #331
Goossens S. Henning W. G. Renaud J. P. Genova A.	<u><i>Constraints on Models of the Interior Structure of Mercury from Measurements of Its Moment of Inertia and Tidal Response</i> [#2203]</u> We present an estimation of likely interior structure models for Mercury using measurements of its moments of inertia, bulk density, and tidal response.	Poster Location #332
Cournede C. Feinberg J. M. Johnson C. L. James R. D.	<u><i>Structure and Magnetic Properties of Fe_xNi_{100-x} (25<x<100) and FeCo Alloys: Implications for Planetary Crustal Mineralogy</i> [#2041]</u> We describe magnetic properties for a wide range of metallic alloys (mainly Fe-Ni). Their magnetic behavior will tentatively be linked with the observed microstructures.	Poster Location #333
Kelderman E. Steenstra E. S. Berndt J. Klemme S. Rohrbach A. et al.	<u><i>Sulfide-Silicate Partitioning Systematics of Th, U and Li, Rb, Cs: Implications for Differentiation of Mercury and Other Planets</i> [#1057]</u> Sulfide-silicate partitioning systematics were derived for Li-Rb-Cs-Th-U and used to study the role of sulfides in differentiation of Mercury and other bodies.	Poster Location #334

<p>Trautner V. Steenstra E. S. Berndt J. Klemme S. van Westrenen W.</p>	<p><u><i>Sulfide-Silicate and Metal-Silicate Partitioning Systematics at Highly Reduced Conditions: Implications for Distribution of Volatile Elements in Mercury and the Aubrite Parent Body</i></u> [#1059] Sulfide- and metal-silicate partitioning systematics of trace elements at highly reduced conditions were determined and applied to study Mercury and the AuPB.</p>	<p>Poster Location #335</p>
<p>Weber I. Morlok A. Heeger M. Adolphs T. Reitze M. P. et al.</p>	<p><u><i>Simulating Space Weathering on Mercury: Excimer Laser Experiments on Mineral Mixtures</i></u> [#2326] We study the effects of space weathering on infrared spectroscopy. The laser experiments were done with an 193 nm ArF UV excimer laser.</p>	<p>Poster Location #336</p>
<p>McGlaun M. L. Thompson M. S. Vander Kaaden K. E. Loeffler M. J. McCubbin F. M. et al.</p>	<p><u><i>Understanding the Space Weathering of Mercury via Simulation of Micrometeorite Impacts</i></u> [#2019] Reflectance spectroscopy and transmission electron microscopy of olivine and graphite mixtures exposed to pulsed laser irradiation.</p>	<p>Poster Location #337</p>
<p>Jones B. M. Orlando T. M.</p>	<p><u><i>In Situ Water Formation on Mercury</i></u> [#2477] A solar-wind initiated reaction cycle has been adapted to examine the possible source term for molecular water on Mercury.</p>	<p>Poster Location #338</p>
<p>Orgel C. Fassett C. I. Michael G. G. van der Bogert C. H. Manske L. et al.</p>	<p><u><i>Re-Examination of the Population, Stratigraphy, and Sequence of Mercurian Basins: Implications for Mercury's Early Impact History and Comparison with the Moon</i></u> [#2059] In this study, we re-investigate the number of the Mercurian impact basin (≥ 300 km) and their superposed crater populations.</p>	<p>Poster Location #339</p>
<p>Andre S. L.</p>	<p><u><i>Topographic Analysis of the Beethoven Basin of Mercury Using MESSENGER Stereo Imaging Data</i></u> [#3084] The topography of Beethoven basin, Mercury, is analyzed in an effort to characterize the interior structure of the basin.</p>	<p>Poster Location #340</p>
<p>Golder K. B. Burr D. M.</p>	<p><u><i>Constraining Source(s) of Circum-Caloris Smooth Plains Material Through Mapping, Mercury</i></u> [#1419] We investigated smooth plains material northwest of the Caloris Basin to determine their emplacement history, whether as lava(s) or impact melt.</p>	<p>Poster Location #341</p>
<p>Maturilli A. Helbert J. Varatharajan I.</p>	<p><u><i>Graphite as Potential Darkening Agent for Mercury: Spectral Measurements Under Simulated Mercury Conditions</i></u> [#1841] At the Planetary Spectroscopy Laboratory we measured emissivity and reflectance for granite, komatiite, and their mixtures under simulated Mercury conditions.</p>	<p>Poster Location #342</p>
<p>Stangarone C. Maturilli A. Helbert J.</p>	<p><u><i>Experimental and Modelled Mid-Infrared Spectra of Olivine: Simulations of Extreme Temperature Conditions on Mercury Surface</i></u> [#1553] Eleven olivine samples have been studied measuring their thermal emissivity up to 900 K and IR reflectance at RT to simulate Mercury surface conditions.</p>	<p>Poster Location #343</p>
<p>Morlok A. Charlier B. Renggli C. Klemme S. Namur O. et al.</p>	<p><u><i>Infrared Spectroscopy of Experimental and Synthetic Planetary Analogs for the BepiColombo Mission to Mercury</i></u> [#2411] We present mid-infrared spectra of synthetic and experimental analog materials for the surface of Mercury for the ongoing BepiColombo Mission.</p>	<p>Poster Location #344</p>
<p>Xiao H. Annibali S. Stark A. Hussmann H. Oberst J.</p>	<p><u><i>Impact of Pointing Aberration in Geolocation of Mercury Laser Altimeter (MLA) Time of Flight Measurements</i></u> [#2502] We demonstrate that the pointing aberration effect leads to an displacement of up to 100 m laterally and 25 m radially for MLA orbital profiles.</p>	<p>Poster Location #345</p>
<p>Morlok A. Hamann C. Martin D. J. P. Joy K. H. Wogelius R. et al.</p>	<p><u><i>Mid-Infrared Investigations of Laser Produced Impact Melt Analogs of Basalt</i></u> [#2417] We present mid-infrared spectra of melt glass from laser experiments on basalts for remote sensing of the hermean and other planetary surfaces.</p>	<p>Poster Location #346</p>
<p>Bauch K. E. Hiesinger H. Morlok A. Reitze M. P. Weber I. et al.</p>	<p><u><i>Deconvolution of Laboratory IR Spectral Reflectance Data for MERTIS Onboard the ESA/JAXA BepiColombo Mission</i></u> [#2521] MERTIS is part of ESA/JAXA's recently launched BepiColombo mission. Here we present results of a deconvolution model to quantify abundances of mineral mixtures.</p>	<p>Poster Location #347</p>

D'Amore M. Helbert J. Maturilli A. Varatharajan I. Ulmer B. et al.	<u><i>The Mercury Radiometer and Thermal Infrared Imaging Spectrometer (MERTIS) Onboard Bepi Colombo: First Inflight Calibration Results</i> [#1809]</u> MERTIS will study mineralogy and temperature of Mercury's surface. Near Earth Commissioning measurements are comparable with ground measurements.	Poster Location #348
Reitze M. P. Weber I. Kroll H. Morlok A. Hiesinger H.	<u><i>Mid-Infrared Spectroscopy of Well-Defined Alkali Feldspar Samples in Preparation of MERTIS Observations</i> [#2306]</u> Mid-infrared spectra of alkali feldspar show not only changes due to different chemical compositions but also due to different Al,Si order.	Poster Location #349

Tuesday, March 19, 2019

[T320]

POSTER SESSION I: IMPACTS: TARGET EARTH II

6:00 p.m. Town Center Exhibit Area

Authors (*Denotes Presenter)	Abstract Title and Summary	Poster Location
Faltys J. P. Wielicki M. M. Wielicki M. D. Stowell H. H.	<u><i>Analysis of $^{87}\text{Rb}/^{87}\text{Sr}$ and $^{143}\text{Nd}/^{144}\text{Nd}$ in Terrestrial Impact Melts: A Mechanism for Producing Early Felsic Crust in the Absence of Plate Tectonics</i> [#1691]</u> Isotopic analysis of terrestrial impacts to determine how impact melting can produce abundant early felsic crust in the absence of plate tectonics.	Poster Location #350
Osinski G. R. Grieve R. A. F. Hill P. Newman J. Patel P. et al.	<u><i>Impact Earth — New Insights into the Terrestrial Impact Record and Cratering Processes</i> [#2472]</u> The new Impact Earth database provides an unparalleled understanding of the impact record on Earth. 195 structures are confirmed.	Poster Location #351
Alpert S. P. Jaret S. J. Ebel D. S.	<u><i>Impactite Collection at The American Museum of Natural History</i> [#2621]</u> A brief description of the impactite collection at the AMNH and its importance as one of few well-documented, broad collections available for research.	Poster Location #352
Schmieder M. Ross D. K. Robinson K. L. Kring D. A.	<u><i>Titanium-in-Quartz Geothermometry of Impactites and Peak-Ring Lithologies from the Chicxulub Impact Crater</i> [#1665]</u> Ti-in-quartz temperatures for impact lithologies from Chicxulub place new constraints on the formation of the target rock and post-impact hydrothermal activity.	Poster Location #353
Burney D. Neal C. R.	<u><i>PGE Content of Impact Melt and Sulfides at the Chicxulub Basin; Evidence for PGE Mobilization/Fractionation?</i> [#1895]</u> PGEs did move / After Chicxulub impact / In and out of melt.	Poster Location #354
Garroni N. D. Osinski G. R. Simpson S. L.	<u><i>Exploring the Origin of Carbonates from Well M0077A, Chicxulub Crater, Mexico</i> [#2190]</u> Very large impact / Dinosaurs were vaporized / Carbonates melted?	Poster Location #355
Slivicki S. J. Schmieder M. Kring D. A. IODP– ICDP Expedition 364 Science Party	<u><i>Petrologic Analysis of Green-Black Impact Melt Rock with a History of Hydrothermal Alteration at Chicxulub</i> [#1718]</u> Crater peak-ring core. Reveals two melts past sagaOf alteration.	Poster Location #356
Simpson S. L. Osinski G. R. Longstaffe F. J.	<u><i>Clay Mineral Diversity Through the Chicxulub Peak-Ring: A Comparison of Microtextural, X-Ray Diffraction and Spectral Datasets</i> [#1682]</u> Hydrothermal clays / Change through the peak ring. Let's have / Fun with geochem.	Poster Location #357
Svensson M. J. O. Osinski G. R. Longstaffe F. J. Goudge T. A.	<u><i>Formation of Secondary Clay Minerals in Post-Impact Lacustrine Rocks at the Ries Impact Structure, Germany</i> [#2494]</u> Impact crater lakes / Amassed altered clay-rich rocks / Ries could reveal how.	Poster Location #358
Arp G. Jung D. Head J. W. III	<u><i>Sedimentary Crater Fill of the Ries Impact Structure: Hydrological and Chemical Evolution, Sediment Body Geometry, and Implications for Martian Craters</i> [#1365]</u> New data for the Ries impact crater lake permit reconstruction of crater fill lithostratigraphic units, providing an analog for Gale and Jezero craters on Mars.	Poster Location #359

Heap M. J. Byrne P. K. Gilg H. A. Reuschlé T.	<u><i>The Mechanical Behaviour and Failure Modes of Suevite</i> [#1375]</u> We provide physical (porosity, permeability) and mechanical (strength, failure mode) properties of suevite collected from the Ries Crater in Germany.	Poster Location #360
O'Brien H. C. McDonald A. M. Burney D. A. Cronberger K. A. Torcivia M. A. et al.	<u><i>Applying an Automated Crystal Size Distribution Method to Compare Lunar and Terrestrial Impact Melts.</i> [#2166]</u> Auto CSDs / Lunar and terrestrial / Method and compare.	Poster Location #361
Pickersgill A. E. Lee M. R.	<u><i>Micro-"tubules" in Glass from the Boltysch Impact Structure, Ukraine</i> [#2675]</u> Tubules at Boltysch / Probably small pyroxene / Really really small.	Poster Location #362
Newman J. D. Osinski G. R.	<u><i>Impact-Generated Dykes from the Haughton Impact Structure, Canada</i> [#1558]</u> An in-depth investigation of dykes reveals wide diversity within the sample suite including melt rocks, shock effects, glass, and an unusual dyke composition.	Poster Location #363
Crósta A. P. Reimold W. U. Vasconcelos M. A. R.	<u><i>Cerro do Jarau and São Miquel do Tapuio: Two Newly Confirmed, Large Impact Structures in Brazil</i> [#3042]</u> We present the evidence of the impact origin of two new, large impact structures, based on the occurrence of shock deformation.	Poster Location #364
Vasconcelos M. A. R. Rocha F. F. Crósta A. P. Wünnemann K. Güldemeister N.	<u><i>Numerical Modeling of the Vista Alegre Impact Crater, a Basaltic Crater in Southern Brazil</i> [#2082]</u> We present the first results of numerical modeling performed with the iSALE code on the Vista Alegre structure, Brazil, an impact crater formed on basalts.	Poster Location #365
Posnov N. Osinski G. R. Flemming R. L. McCausland P. J. A. Pontefract A. et al.	<u><i>Classification of Shocked Basalt from Vargeão Dome and Vista Alegre: Implication for the Search of Life on Mars</i> [#2863]</u> Impacts shock basalts / Shocked basalts have pores for life / Home for life on Mars.	Poster Location #366
Gurov E. P. Permiakov V. Koeberl C.	<u><i>Chromferide Found in Impact Melt Rocks of the El'gygytgyn Crater, Chukotka, Russia</i> [#1347]</u> The rare mineral chromferide was discovered in impact melt rocks at the El'gygytgyn Crater, Chukotka, the first time this mineral was found in impactites.	Poster Location #367
Kavkova R. Kletetschka G.	<u><i>Magnetic Structure and Paleointensity from the Rock that Experienced Impact During the Santa Fe Crater Formation</i> [#1761]</u> New method that does not involve heating and capture the amount of magnetic information described. Amount of lost intensity due to impact investigated.	Poster Location #368
Wulf G. Hergarten S. Kenkmann T.	<u><i>Remote Sensing Analysis and Landscape Evolution Modeling of the Bosumtwi Impact Structure, Ghana: Indications for Ejecta Ramparts</i> [#1624]</u> The morphological characteristics of Bosumtwi Crater possess striking similarities to those of martian rampart craters, especially to DLE craters.	Poster Location #369
King D. T. Jr. Petruny L. W. Ormo J. Chinchalkar N. S. Heider E. S.	<u><i>Crater-Filling Units of Wetumpka Impact Structure, Alabama</i> [#2662]</u> At Wetumpka, there are three main crater filling units, which in age order are impactite sands, a transcrater slide unit, and a boulder-bearing diamictite.	Poster Location #370
De Marchi L. Agrawal V. King D. T. Jr.	<u><i>Hydrocode Simulations of Wetumpka Impact Crater</i> [#2644]</u> The formation of Wetumpka is simulated by iSALE, limiting the scope to short-time scales and to axisymmetric approximation of the original impact problem.	Poster Location #371
Bray V. J. Hagerty J. J. Collins G. S. King D. T. Jaret S. J.	<u><i>Hydrocode Simulation of the Flynn Creek Impact, Tennessee</i> [#3038]</u> Flynn Creek, Tennessee. Drilled by David J. Roddy, and modeled by me.	Poster Location #372
Rohleder N. J. Dulin S. A.	<u><i>Paleomagnetic Analysis of the Flynn Creek and Wells Creek Impact Structures, North Central Tennessee, USA</i> [#3221]</u> Paleomagnetic analysis of North Central Tennessee impact structures in order to validate and potentially confine age ranges.	Poster Location #373

Kring D. A. Angotti L. Bouchard M. Byron B. Chinchalkar N. et al.	<u><i>Traces of Fallback Breccia on the Rim of Barringer Meteorite Crater (a.k.a. Meteor Crater), Arizona</i> [#1835]</u> Despite geological deflation of the crater rim, traces of fallback breccia suitable for instruction and study can still be found on the crater rim.	Poster Location #374
Mitchell C. D. James P. B.	<u><i>Digitization, Georeferencing, and Modelling of Regan and Hinze's Barringer Crater Study</i> [#1951]</u> The recreation of the data set from Regan and Hinze's 1975 Barringer Crater study, with additional georeferencing and modelling performed with a modern DEM.	Poster Location #375
Dutta A. Raychaudhuri D. Pachpor S. V. Bhattacharya A. Bhattacharya A.	<u><i>Morphometric and Petrochemical Characterization of Impact Melt Spherules from Lonar Crater, Maharashtra, India</i> [#1038]</u> Morphology, petrography, and petrochemical characterization of impact melt spherules and glasses from Lonar Crater, India to decipher their genesis.	Poster Location #376
Angotti L. E. Harvey R. P.	<u><i>Geochemistry of Glassy Cosmic Spherules and Microtektites from the Transantarctic Mountains, Antarctica</i> [#1635]</u> Formed when an impact hit the crust / Microtektites look like dust / They're across Antarctica / How exotica! / Come to hear their colors discussed.	Poster Location #377

Tuesday, March 19, 2019

[T321]

POSTER SESSION I: IMPACTS: CANDIDATE STRUCTURES AND DEPOSITS

6:00 p.m. Town Center Exhibit Area

Authors (*Denotes Presenter)	Abstract Title and Summary	Poster Location
Kletetschka G. Klokočník J. Kostelecký J. Bezděk A. Čížek V.	<u><i>An Independent Discovery of Subglacial Impact Crater in Northwest Greenland by Gravity Aspects from Earth Gravity Model EIGEN 6C4 and Magnetic Anomaly Data</i> [#1318]</u> We independently support the recent discovery of a large impact crater beneath Hiawatha Glacier in northwest Greenland with the gravity and magnetic data.	Poster Location #378
Garde A. A. Funder S. Guvad C. Kjær K. H. Larsen N. K. et al.	<u><i>Organic Carbon from the Hiawatha Impact Crater, Northwest Greenland</i> [#1381]</u> Organic carbon in impact glass, coating microcrysts, in microbreccia and as charcoal, in glaciofluvial sand draining the crater and derived from subfossil wood.	Poster Location #379
Xie Z. Zuo S. Yuan Y.	<u><i>The Progress of the Origin Hypothesis of Taihu Lake Basin Relating to Airburst</i> [#3222]</u> One specific Holocene mud layer containing Fe-rich spherules in Taihu lake area were confirmed by grain size analysis; is key to solving origin of lake basin.	Poster Location #380
Schedl A. Mundy L. Buchner M.	<u><i>Evidence for an Impact Origin of Jephtha Knob Using Calcite Twin Analysis and Meteorite Impact as a Cause of Dolomitization</i> [#1132]</u> Using Jamison and Spang's [3] paleostress-piezometer for calcite and Groshong's [4] calcite-strain-gauge, Jephtha Knob is shown to be a meteorite impact crater.	Poster Location #381
Ernstson K. Molnár M. Hiltl M. Ventura K.	<u><i>Disputed, Forgotten, Revitalized: Alemnite — an Enigmatic Impact Breccia Probably Linked to the Ries Crater (Germany) Impact Event</i> [#1370]</u> A practically forgotten hypothesis about mysterious rocks in connection with the Ries Crater impact event is revived by new findings in the Czech Republic.	Poster Location #382
Poßekel J. Ernstson K.	<u><i>Anatomy of Young Meteorite Craters in a Soft Target (Chiemgau Impact Strewed Field, SE Germany) from Ground Penetrating Radar (GPR) Measurements</i> [#1204]</u> We report on geophysical ground penetrating radar measurements (GPR) on five meteorite impact craters in a soft target with diameters between 11 m and 1300 m.	Poster Location #383

Bauer F. Hiltl M. Rappenglück M. A. Ernstson K.	<u><i>Trigonal and Cubic Fe₂Si Polymorphs (Hapkeite) in the Eight Kilograms Find of Natural Iron Silicide from Grabenstätt (Chiemgau, Southeast Germany) [#1520]</i></u> EBSD analyses reveal trigonal and cubic Fe ₂ Si polymorphs (hapkeite) in an 8 kg iron silicide boulder from the Chiemgau meteorite impact strewn field.	Poster Location #384
Rappenglück B. Hiltl M. Ernstson K.	<u><i>Metallic Artifact Remnants in a Shock-Metamorphosed Impact Breccia: An Extended View of the Archeological Excavation at Stöttham (Chiemgau, SE-Germany) [#1334]</i></u> We report on artifact remnants in a suevitic breccia from a catastrophe impact layer, a hitherto unique observation within an archeological stratigraphy.	Poster Location #385
Ure A. Westaway R. Bridgland D. R. Claudin F. Ernstson K.	<u><i>Kaş (Turkey/Greece) and Rubielos de la Cérida (Spain) Meteorite Impact Structures: Comparative Insights into Prominent Sedimentary Carbonate Targets [#1196]</i></u> We report on two carbonate-dominant impact structures with amazing similarity of structural conditions, rock types, and deformations right down to micro range.	Poster Location #386
Connelly D. P. Sikder A. M. Hill T. R. Brum J. Xin-Chen L.	<u><i>Elemental Analysis of Musgrave Province Pseudotachylite [#2240]</i></u> This is an elemental analysis of pseudotachylite breccia from central Australia thought to be associated with a large impact known as MAPCIS.	Poster Location #387
Koerberl C. Crósta A. P. Schulz T.	<u><i>Geochemical Investigation of the Atacamaites, a New Impact Glass Occurrence in South America [#1255]</i></u> We present the results of a geochemical investigation of the atacamaites with the purpose of investigating their nature.	Poster Location #388
Harris R. S. Schultz P. H.	<u><i>Are Ti-Rich Particles in Late Pleistocene Sediments from Patagonia Distal Ejecta from an Atacama Airburst? [#2526]</i></u> Microanalysis of particles from an alleged late Pleistocene impact horizon in southern Chile suggests they represent distal ejecta from the Pica airburst.	Poster Location #389
Harris R. S. Schultz P. H.	<u><i>When Rubble Piles Attack: The Menagerie of Microscopic Meteorite Debris in Pica Impact Glass [#3253]</i></u> Impact glass formed during a late Pleistocene airburst over the Atacama contain extraterrestrial debris indicative of a volatile-rich, fragmental bolide.	Poster Location #390
Roberts S. E. Sheffer A. A. McCanta M. C. Dyar M. D. Sklute E. C.	<u><i>Investigating Redox Change During Impacts [#1285]</i></u> Investigating the changes that occur in Fe ³⁺ during impacts using Mössbauer spectroscopy and X-ray absorption spectroscopy (XAS) in fulgurites and Trinitite.	Poster Location #391

Tuesday, March 19, 2019

[T322]

POSTER SESSION I: THE HORCRUX RINGS OF SATURN

6:00 p.m. Town Center Exhibit Area

Authors (*Denotes Presenter)	Abstract Title and Summary	Poster Location
Morrison S. J. Zaidi S. G.	<u><i>Why So Muted? The Sources and Dynamical Mechanisms Responsible for Differing Regolith Cover on Satellites Embedded in Saturn's E Ring [#2790]</i></u> More surface cover? / By co-orbit sweep not trap / Of E-ring ice grains.	Poster Location #393
Zaidi S. G. Morrison S. J.	<u><i>Modeling the Dynamical Evolution of Saturn's E ring Following a Cryovolcanic Eruption on Enceladus [#2788]</i></u> Outward drifting grains / Show plasma drag dominates / More than big moons' grav.	Poster Location #394
Combe J.-Ph. McCord T. B. Johnson T. V. Rodriguez S.	<u><i>Search for Carbon Dioxide in Saturn's Rings Using the Cassini Mission Visual and Infrared Mapping Spectrometer (VIMS) [#1465]</i></u> The Cassini mission revealed that CO ₂ releases from Enceladus may build-up in Saturn's rings. As a test, we are searching for CO ₂ absorption in VIMS spectra.	Poster Location #395

Estrada P. R. Durisen R. H. Charnoz S.	<u><i>Inward Radial Drift of Material from Angular Momentum Loss Due to Ballistic Transport in Saturn's Rings: Implications for Observed Mass Loss Rates and Remaining Ring Lifetime</i></u> [#3236] Using an accretion disk analog, we demonstrate that ballistic transport can account for the measured mass inflow rates measured by Cassini in the Grand Finale.	Poster Location #396
Jerousek R. G. Colwell J. E. Hedman M. M. French R. G. Marouf E. A. et al.	<u><i>Particle Sizes and Sorting in Saturn's C Ring and Cassini Division from Cassini UVIS, VIMS, and RSS Observations</i></u> [#2707] Cassini UVIS, VIMS, and RSS observations constrain the four parameters of the power-law particle size distribution throughout the C ring and Cassini Division.	Poster Location #397

Tuesday, March 19, 2019

[T323]

POSTER SESSION I: MINISTRY OF ICY MOON COMPOSITIONS

6:00 p.m. Town Center Exhibit Area

Authors (*Denotes Presenter)	Abstract Title and Summary	Poster Location
Royer E. M. Esposito L. W. Elliott J. P.	<u><i>Mapping of the 185nm Absorption Feature on the Icy Satellites of Saturn</i></u> [#1824] We are presenting a map of the 185nm absorption feature observed on the icy satellites of Saturn.	Poster Location #398
Hendrix A. R. Hansen C. J. Royer E. M.	<u><i>Far-UV Spectral Variations on the Icy Saturnian Moons</i></u> [#2997] Cassini UVIS data of the icy moons of Saturn are presented as albedo maps and disk-resolved spectra to compare with data from other instruments and models.	Poster Location #399
Filacchione G. Adriani A. Mura A. Tosi F. Lunine J. I. et al.	<u><i>2–5 μm Observations of Europa by Juno-JIRAM</i></u> [#1801] We report about the analysis of 2–5 μm spectroscopic observations of Europa by JIRAM onboard Juno mission.	Poster Location #400
Ligier N. Paranicas C. Carter J. Poulet F. Calvin W. M. et al.	<u><i>Properties and Composition of Ganymede's Surface: Updates from Near-Infrared Ground-Based Observations with SINFONI/VLT/ESO</i></u> [#1214] High resolution ground-based near-IR data (ESO/VLT) are modeled to get the composition of Ganymede's surface. Salts and sulfuric acid are needed for modeling.	Poster Location #401
Nagihara S. Ngo P. Zacny K.	<u><i>Thermal Diffusivity-Conductivity Measurements on Ice Samples of Magnesium Sulfate and Sodium Sulfate Solutions: Implications for Europa's Ice Shell</i></u> [#1562] We present results of thermal properties measurements on ice samples of MgSO_4 and Na_2SO_4 solutions, likely analogues of Europa's ice shell.	Poster Location #402
Berdis J. R. Chanover N. J. Gudipati M. S. Murphy J. R.	<u><i>Discrepancies Between the Modeled and Observed Water Ice Crystallinity of Europa's Leading Hemisphere</i></u> [#2043] Europa's surface / Less crystalline than should be / Plumes? Or hone model?	Poster Location #403
Baron G. Wood I. G. Vocadlo L. Fortes A. D.	<u><i>Icy Worlds: How the High-Pressure Ice Phases Can Shape Their Geology</i></u> [#1896] The thermal expansion of ices II, III, V, VI has been measured at ambient pressure and low temperature using neutron powder diffraction methods.	Poster Location #404
Jost B. Hodyss R. Galli A. Johnson P. V.	<u><i>Dehydration Kinetics of Hydrohalite Under Photolytic and Radiolytic Environments</i></u> [#1966] Frozen NaCl brines are prepared in different ways and their dehydration kinetics are studied by IR-spectroscopy, Raman-spectroscopy and hyperspectral imaging.	Poster Location #405

Tuesday, March 19, 2019

[T324]

POSTER SESSION I: ICY TASTIC BEASTS AND WHERE TO FIND THEM

6:00 p.m. Town Center Exhibit Area

Authors (*Denotes Presenter)	Abstract Title and Summary	Poster Location
Patthoff D. A. Quick L. C. Rhoden A. R. Spitale J.	<u>Searching for European Plumes: Past, Present, and in the Future</u> [#2965] We've looked in the past / We are searching the present / Where will we look next?	Poster Location #406
Nunez K. A. Quick L. C. Glaze L. S. Fagents S. A. Beyer R. A. et al.	<u>Developing a Database for Candidate Cryovolcanic Domes on Europa</u> [#3264] New database of 38 domes made with new methods to calculate the true height values.	Poster Location #407
Zamora C. A. Noviello J. L. Rhoden A. R.	<u>Identification of Microfeatures on Europa's Surface in High Resolution Images: Assessing the Completeness of Available Datasets</u> [#2096] Here we present work on identification and classification of microfeatures smaller than 10 sq. km. in area by analyzing images with resolutions ≤ 100 m/pix.	Poster Location #408
Williams J. J. Goldstein D. B. Trafton L. M. Varghese P. L.	<u>The Hunt for European Penitentes: Light Scattering and Absorption Over a Rarified Bladed Surface</u> [#3033] To determine the potential for penitentes on Europa, the scattering and absorption of light on a triangular surface is simulated using photon Monte Carlo.	Poster Location #409

Tuesday, March 19, 2019

[T325]

POSTER SESSION I: THE CURSED ICE

6:00 p.m. Town Center Exhibit Area

Authors (*Denotes Presenter)	Abstract Title and Summary	Poster Location
Carballido A.	<u>Dynamics of Two-Phase Flows Inside Geyser Conduits on Enceladus</u> [#2815] A two-phase formalism originally developed for volcanic eruptions is applied to the flow inside geyser conduits on Enceladus.	Poster Location #410
Mahieux A. Goldstein D. B. Varghese P. V. Trafton L. M.	<u>Bayesian Constraints on the Outgassing Parameters of Enceladus Plumes Using DSMC Simulations</u> [#1138] The work focuses on the Enceladus plumes characterization based on DSMC simulations: We present a Monte Carlo sensitivity analysis and Bayesian constraints.	Poster Location #411
Valdez C. S. J. Kay J. P. Patthoff D. A. Schenk P.	<u>Assessment of Topography of Paleo Tiger Stripes</u> [#2968] Paleo Tiger Stripes underwent relaxation? Topography suggests not.	Poster Location #412
Czechowski L.	<u>Proto-Enceladus and Role of Its Activity for the Satellite and Solar System</u> [#2387] We discuss the role of endogenic activity of Enceladus for its evolution and for solar system.	Poster Location #413
Schoenfeld A. M. Yin A.	<u>Tectonic-Stress Map Across Enceladus' SPT and Possible Mechanical Causes</u> [#3104] Just a little moon / Such stress for Enceladus / Let us find out why.	Poster Location #414
MaArthur H. S. Stevenson D. J.	<u>Non-Steady State Model for Enceladus's Ice Shell</u> [#2233] The non-steady model of the Enceladus ice shell yields more realistic shell thicknesses than the steady-state case, but is more difficult to justify mechanically.	Poster Location #415
Nathan E. Berton M. Girona T. Karani H. Huber C. et al.	<u>Icy Moon Evolution: Experiments with Freezing Water Spheres and the Effects of Curvature and Dissolved Gas on Surface Features</u> [#1572] Experimental investigation of freezing water spheres to understand the evolution and surface features of icy moons as controlled by diameter and gas content.	Poster Location #416

TUES POSTERS

Hay H. C. F. C. Matsuyama I.	<u><i>Nonlinear Tidal Dissipation in Enceladus' Subsurface Ocean and Beyond</i> [#2504]</u> Tides slosh water / But ice crust floats on top / The two interact.	Poster Location #417
Montesi L. G. J. Howell S. M. Pappalardo R. T.	<u><i>Latitude-Dependent Ice Thickness of Europa: Effects of Convection and Rifting</i> [#2730]</u> Closer to the pole, ice should be thicker than at the equator. Convection may stop close to the pole. Active bands have low elevation and rise when inactive.	Poster Location #418
Howell S. M. Pappalardo R. T.	<u><i>The Physics of Subsumption: Implications for Detecting Active Convergent Margins in Ocean World Ice Shells</i> [#2112]</u> Creeping through the shell / My tail is manx, not lion / I pass by unseen.	Poster Location #419
Hopkins R. J. Soderlund K. M.	<u><i>The Potential for Double-Diffusive Convection in Europa's Ocean</i> [#1657]</u> From analysis of the Rayleigh number, density stability ratio, and double-diffusive layer height, we find that a double-diffusive system cannot exist on Europa.	Poster Location #420
Zimmerman W. K. Kattenhorn S. A.	<u><i>Bands on Europa: A New Geometry-Based Classification to Explain Why Bands Form</i> [#1953]</u> Dilational bands create new surface area on Europa. Our geometry based classification of these bands accounts for the reasons why bands initially develop.	Poster Location #421
Stark A. Hussmann H. Steinbrügge G. Oberst J. Roatsch T.	<u><i>Resonant Rotation States of the Jovian and Saturnian Satellites</i> [#2490]</u> We derive the resonant rotation states from the ephemerides of Jovian and Saturnian satellites.	Poster Location #422
Downey B. G. Nimmo F.	<u><i>Inclination Damping on Titan and Callisto</i> [#2195]</u> Titan and Callisto have relatively large inclinations. Either they have stiffer outer shells than expected, or a recent <0.5 Ga event excited their inclinations.	Poster Location #423
Tian Z. Nimmo F.	<u><i>Implications of Second Order Resonance for the Thermal and Orbital Evolution of Mimas</i> [#2857]</u> The 6:4 mixed term eccentricity type mean motion resonance between Mimas and Enceladus works to explain the high eccentricity of Mimas without severe heating.	Poster Location #424
O'Hara S. Dombard A. J.	<u><i>Simulating Formation of Triton's Cantaloupe Terrain by Compositional Diapirs</i> [#2089]</u> Dense ice on surface / Does not form a diapir / When heat is involved.	Poster Location #425

Tuesday, March 19, 2019

[T326]

POSTER SESSION I: THE GOBLET OF TITAN

6:00 p.m. Town Center Exhibit Area

Authors (*Denotes Presenter)	Abstract Title and Summary	Poster Location
Korycansky D. G. Umurhan O. M.	<u><i>Convection in Titan Lakes: Flux-Driven with Time-Dependent Upper Boundary Condition</i> [#1688]</u> We model convection in simple models of Titan lakes, with time-dependent surface boundary conditions.	Poster Location #426
Farnsworth K. Soderblom J. M. Rodriguez S. Czapinski E. Chevrier V.	<u><i>Constraining Ethane Concentration in Titan's Lakes and Seas</i> [#1488]</u> This study investigates the ethane detection limits of the Cassini VIMS instrument by incorporating laboratory experiments and observations.	Poster Location #427
Dzurilla K. Chevrier V. Nna Mvondo D. Mege D. Farnsworth K.	<u><i>Detection and Reactivity of Titan Tholins in Liquid Hydrocarbons</i> [#3234]</u> This study investigates the solubility of Titan tholins, as well as structurally similar compounds, in acrylonitrile, acetonitrile, and hexane mixtures.	Poster Location #428
Engle A. Hanley J. Grundy W. M. Dustrud S. Lindberg G. E. et al.	<u><i>Identifying the Solid Phases of Ethane Using Raman Spectroscopy at Conditions Relevant to Titan's Surface</i> [#2509]</u> Investigating pure ethane at temperatures relevant to Titan's surface to understand how the solid phases may impact the environment.	Poster Location #429

Maue A. D. Carnes L. K. Burr D. M.	<u><i>Grain Properties from Synthetic Aperture Radar: Terrestrial Radar Analogs for Titan's Alluvial Sediment</i> [#2734]</u> A pilot study analyzing sediment size, shape, and sorting in the field relative to C-band radar brightness with application to Titan's radar-bright features.	Poster Location #430
Nowak A. R. Hayes A. G. Birch S. P. D.	<u><i>Backscatter Curves for Specific Morphological Units on Titan</i> [#3067]</u> Early findings for using models for backscatter vs. incidence angle curves to parameterize Titan's surface and derive surface materials and roughness.	Poster Location #431
Daudon C. Lucas A. Rodriguez S. Jacquemoud S. Grieger B. et al.	<u><i>New Investigation on the Local Topography at the Huygens Landing Site: Implications for Landscape Formation on Titan</i> [#2439]</u> New investigation on the local topography at the Huygens landing site using an automatic and reproducible photogrammetric method.	Poster Location #432
Wood C. A.	<u><i>Titan Transmogrified</i> [#3032]</u> Recorded history began 500 m.y. ago on Titan when its crust thickened from 10 to 500 km. How did that transmogrifying event affect Titan's surface/atmosphere?	Poster Location #433
Mastrogiuseppe M. Poggiali V. Raguso M. C. Wall S. Elachi C.	<u><i>Inversion of Cassini Radar Data: The Liquid Contrast Method</i> [#3268]</u> Description of the liquid contrast method for the retrieval of dielectric properties of the surface of Titan.	Poster Location #434

Tuesday, March 19, 2019

[T327]

POSTER SESSION I: PLANETARY TECTONICS AND STRUCTURAL GEOLOGY

6:00 p.m. Town Center Exhibit Area

Authors (*Denotes Presenter)	Abstract Title and Summary	Poster Location
Lu T. Chen S. Zhu K. Sun M.	<u><i>Global Identification and Spatial Distribution of Lunar Faults</i> [#1482]</u> Lunar faults were globally mapped, and spatial distribution characteristics were analyzed. Formation mechanism of lunar faults was discussed.	Poster Location #449
Collins M. S. Byrne P. K. Klimczak C. Mazarico E.	<u><i>Spatial Relations Between Shortening Structures and Mascons in Lunar Mare Basins</i> [#1641]</u> Shortening structures delineate the highest gravity values in lunar mare basins. The mascons are marked / by a series of ridges. / Do thrusts control them?	Poster Location #450
Balcerski J. A. Byrne P. K.	<u><i>Fault Analysis of Venus Ridge Belts Near Aphrodite Terra</i> [#3168]</u> Buried Venus faults / Highways of crust displacement / Form ridge belts in plains.	Poster Location #451
Jacob A. Perrin C. Lucas A. Batov A. Gudkova T. et al.	<u><i>Geometry and Segmentation of the Cerberus Fossae Fault System: Implications on Marsquake Properties in Elysium Planitia, Mars</i> [#1825]</u> Cerberus Fossae fault system could generate marsquakes in the context of the InSight mission. We study its morphology related to tectonic stresses.	Poster Location #452
Studer-Ellis G. L. Williams D. A.	<u><i>Structural Mapping of the Thaumasia Graben, Implications for Formation</i> [#3078]</u> Large graben on Mars / Tectonics will reveal you / Structure key to past.	Poster Location #453
Mège D. Gurgurewicz J. Douté S. Schmidt F. Schultz R. A.	<u><i>Brittle-Plastic Shear Zones on Valles Marineris Floor: Identification and Implications</i> [#2064]</u> We present new mapping of brittle-ductile deformation in Valles Marineris, and explore geological and geomorphological implications.	Poster Location #454
Atkins R. M. Byrne P. K. Wegmann K. W.	<u><i>Morphometry and Timing of Major Crustal Shortening Structures on Mars</i> [#1734]</u> Tedious mapping / Got data for large thrust faults / Mars contracted lots.	Poster Location #455
Kling C. L. Byrne P. K. Wyrick D. Y. Wegmann K. W.	<u><i>Field-Based Assessment of Pit Crater Chains</i> [#1627]</u> Pit craters are ubiquitous structures found across the solar system. Pit craters are holes, and represent a collapse, but why do they form?	Poster Location #456
Naor R. Mushkin A. Halevy I.	<u><i>The "Jubot" Depressions as Terrestrial Analogs for Planetary Pits</i> [#3187]</u> A series of depressions, locally named "jubot," are situated on a basaltic plateau on the northwest margins of the Levantine volcanic field of Harrat Ash-Shaam.	Poster Location #457

Martin E. S. Whitten J. L.	<u><i>Analyzing Pit Chains in Iceland to Constrain Regolith Thickness on Enceladus</i> [#1997]</u> Looking at cold moons / Thick snow on Enceladus? / Iceland pits will help.	Poster Location #458
Gallagher A. T. Kattenhorn S. A.	<u><i>Pinwheel Rifts Emanating from the South Polar Terrain of Enceladus</i> [#2061]</u> Three rift systems grew radial to the south polar terrain on Enceladus for hundreds of kilometers and may have been driven by dikes intruding away from the SPT.	Poster Location #459
Leonard E. J. Yin A. Pappalardo R. T.	<u><i>Ridged Plains Reveal Europa's Compressive Past</i> [#2703]</u> Europa's ridged plains / Reveal hidden compression / From thickening ice.	Poster Location #460

Tuesday, March 19, 2019

[T328]

POSTER SESSION I: MARTIAN SAMPLE STUDIES: MOSTLY METEORITES

6:00 p.m. Town Center Exhibit Area

Authors (*Denotes Presenter)	Abstract Title and Summary	Poster Location
Bridges J. C. Cousin A. Sautter V. Rapin W. Schwenzer S. P. et al.	<u><i>Askival: A Silicified Feldspathic Cumulate Sample in Gale Crater</i> [#2345]</u> Gale Crater has plagioclase cumulate samples including Askival with a unique mafic component and silicification, hydration overprint.	Poster Location #461
Gellert R. Berger J. A. O'Connell-Cooper C. Thompson L. M. VanBommel S. J. et al.	<u><i>Igneous/Unaltered Rocks at Gale, Gusev, and Meridiani Planum</i> [#2243]</u> The APXS documented a diverse set of igneous rocks at all four rover landing sites on Mars. Similarities and indicators for alteration trends will be discussed.	Poster Location #462
Clegg S. M. Anderson R. B. Rapin W. Ehlmann B. L. Anderson D. E. et al.	<u><i>ChemCam Sulfur Quantitative Analysis of the Askival Altered Feldspathic Cumulate Target, Gale Crater, Mars</i> [#2768]</u> The variable SO ₃ compositions from the chemically heterogeneous Askival target are examined with ChemCam (ccam03015, sol2015).	Poster Location #463
Griffin S. Daly L. Lee M. R. Piazzolo S. Trimby P. W. et al.	<u><i>Nakhlite Meteorite Petrofabrics Revealed by Electron Backscatter Diffraction</i> [#1842]</u> Large area mapping using Electron Backscatter Diffraction (EBSD) has been applied to ten different nakhlites in order to assess their petrofabrics in 3D.	Poster Location #464
Hallis L. J. Barnes J. J. Franchi I. A.	<u><i>D/H Ratios of Early Crystallized and Late Stage Hydrous Minerals in Martian Meteorite MIL 090136: Tracing the Source of Nakhlite Cl-Rich Fluid</i> [#1838]</u> We studied the D/H ratio of apatite and amphibole within MIL 090136 olivine-hosted melt inclusions, and compared these values to late-stage mesostasis apatite.	Poster Location #465
Daly L. Lee M. R. Bagot P. A. J. Halpin J. Smith W. et al.	<u><i>Insights into Martian Fluid-Rock Reactions by Atom Probe Tomography of the Interface Between Nakhlite Olivine and Iddingsite</i> [#1521]</u> Mars water, rocks turn clay / Boundary of dry and wet / Hmm, still a bit damp.	Poster Location #466
Ostwald A. O. Udry A. Gross J.	<u><i>Parental Melt of Nakhlites as Determined from Melt Inclusions</i> [#1431]</u> Reconstruction of the nakhlite parental melt from melt inclusions in Miller Range 090030 and 090032, Northwest Africa 10645, and Governador Valadares.	Poster Location #467
Che S. Brearley A. J. Shearer C. K.	<u><i>Possible Formation Mechanisms of Chromite and Melt Inclusion Trails in Yamato 980459 Shergottite Olivine: Implications for Its Thermal History</i> [#1947]</u> We reported chromite and melt inclusion trails in Y-98 martian meteorite, and discussed their possible formation mechanisms.	Poster Location #468
Ferdous J. Brandon A. D. Humayun M. Peslier A. H.	<u><i>Trace Element Abundances of Olivine-Hosted Melt Inclusions in Shergottites Northwest Africa 7397 and Robert Massif 04262</i> [#1281]</u> Determining whether the olivine-hosted melt inclusions are derived from the host parent magma or instead reflect crustal contamination.	Poster Location #469

Dudley J. M. Hervig R. L.	Peslier A. H.	<u><i>Hydrogen Isotope Fractionation During Impact Degassing of Pyroxene and Maskelynite in Shergottite Larkman Nunatak 06319</i></u> [#2971] Degassing in pyroxene and maskelynite in martian meteorite LAR 06319 evidenced by SIMS hydrogen measurements.	Poster Location #470
Niihara T.	Misawa K.	<u><i>Petrogenesis and Shock Effects on Larkman Nunatak 12011</i></u> [#2242] We present petrology of LAR 12011 comparison with other evolved shergottites.	Poster Location #471
Povinec P. P. Jull A. J. T. Ferrière L.	Koerberl C. Sýkora I. et al.	<u><i>Radionuclides in the Tissint Meteorite: Implications for its Martian Origin</i></u> [#1905] Cosmogenic radionuclide studies of Tissint suggest that the depleted permafic olivine-phyric shergottites was likely ejected from Mars at around 1.05 ± 0.10 Myr.	Poster Location #472
Suarez S. E. Righter M. Irving A. J.	Lapen T. J. Beard B. L.	<u><i>Assessing the Heterogeneity of the Tissint Shergottite Strewnfield Using Rb-Sr, Sm-Nd, and Lu-Hf Isotope Systematics</i></u> [#3028] This study examined seven pieces of Tissint for Rb-Sr to confirm whether or not materials of different isotopic compositions and ages comprise the Tissint Strewnfield.	Poster Location #473
Righter M. Irving A. J.	Lapen T. J.	<u><i>Sm-Nd and Lu-Hf Isotopic Systematics of Shock-Melted Intermediate Olivine Gabbroic Shergottite Northwest Africa 11509</i></u> [#2940] NWA 11509 is a unique shergottite with isotope signature, falls in between intermediate and enriched shergottites. We present Lu-Hf and Sm-Nd isotopic results.	Poster Location #474
Lapen T. J. Righter M. Righter K.	Suarez S. E. Irving A. J.	<u><i>Trace Element and Pb Isotope Geochemistry of Tissint Impact Melt Glass and Sulfide Reveal No Contamination by Martian Soil</i></u> [#2921] Trace element (REE and HSE) concentrations and Pb isotopes of an impact glass and sulfide-rich fragment of Tissint were analyzed to assess crustal contamination.	Poster Location #475
Wilson B. J. Spray J. G.	McFarlane C. R. M.	<u><i>Mineralogy and U/Pb Phosphate Dating of the Los Angeles Martian Diabase</i></u> [#2952] We analyze phosphates in the Los Angeles martian meteorite. The phosphates are ferromerrillite and Cl- and F-apatites. They yield a U-Pb age of 170 ± 16 Ma.	Poster Location #476
Love A. B. Huang S.	Singletary S. J.	<u><i>Petrology and Geochemistry of Northwest Africa 11044, a New, Enriched low-Al Shergottite</i></u> [#1384] This study presents preliminary results of a petrologic and geochemical study of the enriched, low-Al shergottite NWA11044.	Poster Location #477
Kuehl E. C. Jones J. H.	Castle N. Treiman A. H.	<u><i>Petrology and Geochemistry of Xenolithic Fragments in Elephant Moraine 79001</i></u> [#2876] The compositional range of included xenolithic fragments in EET 79001 Lithology A suggests the fragments are not monolithic and are likely crustal-derived.	Poster Location #478
Niles P. B. Sun T. et al.	ElShenawy M. Berger E. L. Nyguen A.	<u><i>A Diversity of Ca-Rich Carbonates in EETA 79001</i></u> [#1108] A diversity of Ca-rich carbonates have been analyzed using TEM and NanoSIMS in martian meteorite EETA 79001, including aragonite and Mg-calcite.	Poster Location #479
Lapen T. J. Irving A. J. Carpenter P. K.	Righter M. Kuehner S. M. et al.	<u><i>Martian Meteorite Rain: Petrology, Elemental, and Isotopic Composition of Ten Recently Recovered Shergottites</i></u> [#2605] The petrologic and chemical diversity among shergottites (currently numbering 111) continues to grow as more specimens are recovered and analyzed.	Poster Location #480
Izawa M. R. M.	Hall B. J.	<u><i>Automated Mineral Segmentation Using EDS X-Ray Images: Application to Shergottites</i></u> [#2646] An automated method for segmenting and identifying minerals from a thin section EDS dataset from NWA 7257 is demonstrated.	Poster Location #481
Kizovski T. V. Tait K. T. Moser D. E.	White L. F. Darling J. et al.	<u><i>Identifying the Effects of Shock on the Composition of Martian Phosphate Minerals Using Correlative Structural and Chemical Techniques</i></u> [#2731] Examination of the structural effects of shock on the composition of martian phosphate minerals over a range of shock conditions using EBSD and EPMA.	Poster Location #482

Hamilton J. S. Walton E. L.	Herd C. D. K. Tornabene L. L.	<u><i>Geologic Mapping of Candidate Source Craters for Martian Meteorites</i> [#2985]</u> We present preliminary mapping of candidate source craters for martian meteorites to describe the craters and their relationships to the sampled geologic units.	Poster Location #483
Sillitoe-Kukas S. Hewins R. H. Moser D. E.	Humayun M. Zanda B. et al.	<u><i>Spherules in the Martian Polymict Breccias. I: Origin and Internal Chemical Zoning</i> [#1354]</u> Large (mm-sized) melt spherules in the martian polymict breccias are chemically zoned with feldspathic rims and magnesian cores, and volatile depleted.	Poster Location #484
Humayun M. Hewins R. H. Moser D. E.	Sillitoe-Kukas S. Zanda B. et al.	<u><i>Spherules in the Martian Polymict Breccias. II. Chemical Sedimentary Processes on Mars</i> [#2154]</u> Vitrophyric spherules in the paired martian polymict breccias are chemically shown to be melts of sedimentary protoliths rich in clays and sulfates.	Poster Location #485
Sillitoe-Kukas S. Moser D. E. Irving A. J.	Humayun M. Arcuri G.	<u><i>Hydrothermal Infilling of a Unique, Layered Spherule Within the Martian Polymict Breccia Northwest Africa 7475</i> [#2917]</u> We report the composition of hydrothermal material that filled former vesicles in a layered spherule from NWA 7475 prior to its incorporation in the breccia.	Poster Location #486
Smith A. Nagashima K.	Hallis L. J. Huss G. R.	<u><i>Hydrogen Isotope Analyses of Apatite in Martian Polymict Breccia Northwest Africa 11522 (Paired with NWA 7034)</i> [#1850]</u> Reported are the volatile budget and hydrogen isotope values from apatite within NWA 11522, a paired stone of martian polymict breccia NWA 7034.	Poster Location #487
Davidson J. Hervig R. L.	Wadhwa M. Stephant A.	<u><i>Water on Mars: Insights from Apatite in Regolith Breccia Northwest Africa 7034</i> [#1596]</u> Water contents and H-isotopic compositions of apatite in martian breccia NWA 7034 may reflect a complex history of magmatic processes and/or crustal exchange.	Poster Location #488
Suga H. Takeichi Y.	Miyahara M. Yabuta H. et al.	<u><i>Search for the Martian Carbonaceous Materials in the Northwest Africa 7034</i> [#2000]</u> We searched the martian organics in the matrix phase of NWA 7034. The $\delta^{13}\text{C}$ and δD of organics were $9.58 \pm 8.13\text{‰}$ and $373 \pm 68\text{‰}$ (partly near 1000‰), respectively.	Poster Location #489
Loiselle L. Ávila J. N. Bridges J. C.	Holden P. Lanc P. et al.	<u><i>The O Isotope Composition of Martian Meteorites Using SHRIMP SI: Evidence of Multiple Reservoirs in Silicate Minerals of the Regolith Breccia Northwest Africa 8114</i> [#2648]</u> We conduct high-resolution in situ $\Delta^{17}\text{O}$ isotopic measurements of martian meteorites and observe multiple, distinct reservoirs in the regolith breccia NWA 8114.	Poster Location #490

Tuesday, March 19, 2019

[T329]

POSTER SESSION I: MARS EXPLORATION ROVER: PERSEVERANCE IN ENDEAVOUR

6:00 p.m. Town Center Exhibit Area

Authors (*Denotes Presenter)	Abstract Title and Summary	Poster Location
Ashley J. W. Christensen P. R. Hill J. R.	<u><i>Evidence for Martian Atmospheric Dust Penetration into Closed Surface Assets — Implications for Particle Size and Behavior in the Martian Environment</i> [#2545]</u> Martian atmospheric and surface dust poses risks to surface assets. Evidence that dust can enter closed systems is found in the use history of MER Mini-TES.	Poster Location #491
Sullivan R. Crumpler L. Hughes M.	<u><i>MER Opportunity at Perseverance Valley: Evaluation of Multiple Working Hypotheses for Valley Formation</i> [#3244]</u> The MER Opportunity exploration of Perseverance Valley has revealed the influences of faulting/fracture, aeolian abrasion, and other erosional processes.	Poster Location #492

Farrand W. H. Johnson J. R. Bell J. F. III Mittlefehldt D. W. Schröder C. et al.	<u><i>Spectral Variability Among Rocks and Soils in Perseverance Valley, Mars as Observed by the Opportunity Pancam</i></u> [#2403] Multispectral observations made by the Opportunity rover's Pancam in Perseverance Valley of diverse rocks and soils are described.	Poster Location #493
Tait A. W. Schröder C. Farrand W. H. Ashley J. W. Cohen B. A. et al.	<u><i>Exploring Origins of Pitted/Vesicular Rocks in Perseverance Valley, Endeavour Crater</i></u> [#2327] Inside Perseverance Valley is an unusual unit of altered pitted/vesicular rocks. We explore formation origin for the protolith and later alteration history.	Poster Location #494
Bouchard M. C. Jolliff B. L. Farrand W. H.	<u><i>Lithochemical Rock Suites of Perseverance Valley, Endeavour Crater, Mars</i></u> [#2715] This valley has the highest density of rock suites (4) observed since Cape York, and indicates aqueous alteration, wind/mass wasting, and possibly a graben.	Poster Location #495
Crumpler L. S. Arvidson R. E. Mittlefehldt D. W. Grant J. E. Farrand W. H.	<u><i>In Situ Mapping of the Structural and Stratigraphic Complexities of Endeavour Crater's Rim</i></u> [#1179] Opportunity's study of the Endeavour Crater provides our first look at bedrock structure and stratigraphy of a topographically-preserved complex impact crater.	Poster Location #496

Tuesday, March 19, 2019

[T330]

POSTER SESSION I: MSL: RESULTS ACROSS GALE

6:00 p.m. Town Center Exhibit Area

Authors (*Denotes Presenter)	Abstract Title and Summary	Poster Location
Bristow T. F. McAdam A. C. Fox V. K. Bennett K. A. Rampe E. B. et al.	<u><i>Clay Minerals of the Clay-Bearing Unit, Mount Sharp, Gale Crater, Mars</i></u> [#2647] This presentation will discuss the latest mineralogical findings from the Mars Science Laboratory rover's investigation of the clay-bearing unit, Gale Crater.	Poster Location #498
Smith R. J. Horgan B. McLennan S. M. Achilles C.	<u><i>Bulk Compositions of X-Ray Amorphous Materials in Soils and Sediments on Earth Compared to X-Ray Amorphous Materials in Gale Crater, Mars</i></u> [#2617] Bulk compositions of terrestrial amorphous weathering products vary with environment. Some are similar to amorphous component compositions in Gale Crater, Mars.	Poster Location #499
Castle N. Treiman A. H.	<u><i>Systematic Error and the Identification of Minor Phases Using the CheMin X-Ray Diffractometer</i></u> [#2600] Statistical error constraints provide framework for determining if minor phases are detectable using CheMin X-ray diffractometer.	Poster Location #500
Wilhelm B. J. Gellert R. Flood V. A. VanBommel S. J. Hanania J. U.	<u><i>Comparison of the Iron-Manganese Ratio Dispersion in Martian Soils with the Mars Science Laboratory APXS and ChemCam</i></u> [#2597] A simplified method was developed to derive Mn peak areas from ChemCam spectra. The promising results are compared with Fe:Mn trends determined by APXS.	Poster Location #501
Flood V. A. Gellert R. Wilhelm B. J. Vanbommel S. J.	<u><i>Sulfur Observations and Analysis by APXS and ChemCam in Gale Crater, Mars</i></u> [#2643] We discuss the detection and quantification of S on Mars by the APXS and ChemCam on the MSL Rover, comparing sample size, principle limitations, and problems.	Poster Location #502
VanBommel S. J. Gellert R. Berger J. A. Boyd N. I. Flood V. A. et al.	<u><i>Enhanced Characterization of the Mars Science Laboratory Alpha Particle X-Ray Spectrometer Through Analyses of Software-Simulated Spectra</i></u> [#1872] Enhancing the capabilities and science return of the Mars Science Laboratory APXS through analyses of predictive simulated spectra.	Poster Location #503

Czarnecki S. Hardgrove C. Gasda P. Rapin W. Frydenvang J. et al.	<u><i>Identification of a High-Silica Layer in Gale Crater, Mars Using In Situ Active Neutron Spectroscopy</i></u> [#2060] We have mapped the extent and hydration of a silicic volcanic layer in Gale Crater, Mars using the Dynamic Albedo of Neutrons instrument on the Curiosity rover.	Poster Location #504
Martinez Sierra L. M. Jun I. Ehresmann B. Hassler D. Litvak M. L. et al.	<u><i>Galactic Cosmic Ray Induced Neutron Environment at the Surface of Mars as Seen by MSL DAN Instrument</i></u> [#2923] By using DAN, RAD, and REMS instruments onboard MSL, we expect to infer the galactic cosmic-ray environment at the surface of Mars and remove soil dependences.	Poster Location #505
Kerner H. R. Hardgrove C. Czarnecki S.	<u><i>Analysis of Intrinsic Variability and Outliers in Pulsed Neutron Data Using the Mars Science Laboratory Dynamic Albedo of Neutrons Instrument</i></u> [#1988] We present initial results from our analysis of intrinsic variability and outliers in pulsed neutron data from the Dynamic Albedo of Neutrons instrument on MSL.	Poster Location #506
Tate C. G. Moersch J. E. Mitrofanov I. Litvak M. Bellutta P. et al.	<u><i>Mars Science Laboratory Dynamic Albedo of Neutrons Passive Mode Data and Results from Sols 753 to 1292: Pahrump Hills to Naukluft Plateau</i></u> [#2163] Mars Science Laboratory Dynamic Albedo of Neutrons passive mode data from Pahrump Hills to Naukluft Plateau of Gale Crater are analyzed and presented.	Poster Location #507
Martin A. C. Moersch J. E. Tate C. G. Hardgrove C. Jun I. et al.	<u><i>Simulated DAN Active Measurements Using Geant4</i></u> [#2667] To model neutrons / Of DAN active measurements / We use Geant4.	Poster Location #508
Sullivan D. L. Hardgrove C. Gabriel T. S. J. Czarnecki S.	<u><i>Examining the Effect of Sand Cover on the Mars Science Laboratory Dynamic Albedo of Neutrons Instrument Data in Gale Crater, Mars</i></u> [#2241] In this abstract we examine the effect of sand cover on DAN active data in the Early Murray formation.	Poster Location #509
Stein T. C. Arvidson R. E. Van Bommel S. J. Wagstaff K. L. Zhou F.	<u><i>MSL Analyst's Notebook: Curiosity APXS Concentration Data Integration and Mars Target Encyclopedia and Interface Updates</i></u> [#1820] The MSL Analyst's Notebook now includes Alpha Particle X-ray Spectrometer concentration data; literature references and target search are updated.	Poster Location #510
Yawar Z. Schieber J. Bish D. Minitti M.	<u><i>Using Mahli Images for Detection of Gypsum in the Murray Formation at Gale Crater, Mars</i></u> [#2007] Parallel striations in Ca-sulfate vein fills are likely gypsum cleavage planes. They are a visual indicator for the presence of gypsum in the Murray Formation.	Poster Location #511
Gabriel T. S. J. Hardgrove C. Czarnecki S.	<u><i>From Bedrock to Dunes: Clues on Silica Diagenesis on Mars from Water Content and Amorphous Phase Analysis</i></u> [#2122] We discuss insights on silica diagenesis on Mars using in-situ geochemical/mineralogic assay and a new Markov-chain Monte Carlo routine for active neutron data.	Poster Location #512
Minitti M. E. House C. H. Sun V. Z.	<u><i>Tracking Variations of Depositional and Diagenetic Features with Elevation in the Murray Formation (Gale Crater, Mars) Using MARDI Images</i></u> [#2427] MARDI systematically records depositional and diagenetic features, and their variation with elevation, across the Murray formation. Science ensues.	Poster Location #513
Niles P. B.	<u><i>Geochemistry of Diagenetic Fluids and Sedimentary Protolith of Gale Crater</i></u> [#1111] The geochemical composition of the sediments of Gale Crater can be modeled using two component mixing between a weathered basalt and a sulfate-rich endmember.	Poster Location #514
Siebach K. L. Fedo C. M. Edgar L. E. Edgett K. Grotzinger J. P. et al.	<u><i>Overview of Gale Crater Stratigraphy and Sedimentology from 6 Years of Roving with Mars Science Laboratory</i></u> [#1479] Gale Crater had a / Long history with water / From surface to deep. Well recorded in / The sedimentary rocks / MSL observed.	Poster Location #515

Bedford C. C. Schwenzer S. P. Bridges J. C. Banham S. Wiens R. C. et al.	<u><i>Using ChemCam-Derived Geochemistry to Identify the Paleonet Sediment Transport Direction and Source Region Characteristics of the Stimson Formation in Gale Crater, Mars</i></u> [#1978] We have identified the geochemical signature of mineral sorting in Gale's ancient dune deposits and used this to estimate the net sediment transport direction.	Poster Location #516
Rudolph A. Horgan B. Bennett K. Rice M.	<u><i>Sources of Sand in Mt. Sharp: Possible Volcanic Layers in Gale Crater, Mars</i></u> [#1914] The composition of the marker beds and other sediments within Mt. Sharp are analyzed using a mafic mineralogy map made with VNIR hyperspectral CRISM images.	Poster Location #517
Hughes M. N. Arvidson R. E. Bryk A. B. Dietrich W. E. Lamb M. P. et al.	<u><i>Debris Deposits Within the Upper Gediz Vallis and Grand Canyon of Gale Crater</i></u> [#3196] Evidence of slope failure and downhill transport are present in both Grand Canyon and Gediz Vallis, with the Grand Canyon having better preserved deposits.	Poster Location #518
Sheppard R. Y. Milliken R. E. Itoh Y. Parente M.	<u><i>Lateral Continuity of Mineralogical and Morphological Contacts in Mt. Sharp: Linking Upcoming Rover Observations and Orbital Data</i></u> [#2124] Newly processed CRISM data allow for direct analysis of mineralogical changes associated with features around Mt. Sharp; we identify some through-going contacts.	Poster Location #519
Seeger C. H. Rice M. S. Starr M. Hughes C. M.	<u><i>Mascam Spectral Characterization of Stratigraphic Units Along Curiosity's Traverse in Gale Crater, Mars</i></u> [#2235] Gale stratigraphy / Enhanced by spectral data / Bless the database.	Poster Location #520
Bryk A. B. Dietrich W. E. Lamb M. P. Grotzinger J. P. Vasavada A. R. et al.	<u><i>In Curiosity's Path: The Geomorphology and Stratigraphy of the Greenheugh Pediment and Gediz Vallis Ridge in Gale Crater</i></u> [#2263] Curiosity is approaching strata that may record major environmental changes in martian history. We present observations and review hypotheses the rover can test.	Poster Location #521

Tuesday, March 19, 2019

[T331]

POSTER SESSION I: MARTIAN ORBITAL SPECTRAL PROCESSING: IMPROVING RESULTS FROM CRISM AND TES
6:00 p.m. Town Center Exhibit Area

Authors (*Denotes Presenter)	Abstract Title and Summary	Poster Location
Kamps O. M. Hewson R. D. van Ruitenbeek F. J. A. van der Meer F. D.	<u><i>Global Mapping of Mars with CRISM Summary Products</i></u> [#2548] Multivariate data analysis approach to describe surface types using CRISM summary products.	Poster Location #522
Seelos K. D. Viviano C. E. Ackiss S. E. Kremer C. H. Murchie S. L.	<u><i>The MICA Files: A Compilation and Reference Document for Minerals Identified Through CRISM Analysis</i></u> [#2745] The MICA Files is a guidebook and collection of two-page descriptions of 31 minerals or phases identified on Mars using CRISM data.	Poster Location #523
Seelos F. P. Cartwright S. F. A. Romeo G. Murchie S. L.	<u><i>CRISM Next Generation Mars Global Multispectral Map — Hydrated Mineralogy Spectral Parameter Mapping</i></u> [#2635] CRISM next generation Multispectral Reduced Data Records (MRDRs) and their applicability to hydrated mineralogy spectral parameter mapping.	Poster Location #524
Thomas N. H. Fraeman A. A. Amador E. S. Ehlmann B. L. Bandfield J. L. et al.	<u><i>Searching for Sedimentary Iron Formations Using CRISM Factor Analysis and Target Transformation</i></u> [#2065] Were iron formations emplaced on early Mars? We survey the iron mineralogy of candidate sedimentary outcrops and closed-basin lakes with semi-automated tools.	Poster Location #525
Mustard J. F. Tarnas J. D. Parente M.	<u><i>Laboratory Testing of the Factor Analysis-Target Transformation Method for Mineral Detection at Low Abundance from Visible-Infrared Hyperspectral Data</i></u> [#3008] What is present and how much? The first results of laboratory experiments designed to assess advanced mineral detection techniques with hyperspectral data.	Poster Location #526

Caggiano J. A. Sessa A. M. Wray J. J. Paty C. S.	<u><i>Application of Machine Learning to Identify Surface Minerals in CRISM Imagery</i> [#2564]</u> Deep neural network / Identifies martian rocks / Better than humans.	Poster Location #527
Saranathan A. M. Parente M.	<u><i>Adversarial Feature Learning for Improved Mineral Mapping in CRISM Images</i> [#2698]</u> We introduce a novel feature extraction technique for improved mineral mapping in CRISM images.	Poster Location #528
Itoh Y. Parente M.	<u><i>A new simultaneous atmospheric correction and de-noising of CRISM data</i> [#2025]</u> We have developed a new algorithm for atmospheric correction and de-noising of the CRISM images that can be applicable to variety of scenes and noise levels.	Poster Location #529
Brown A. J.	<u><i>Constrained Band Estimation for Absorption band Modeling and Simulation (C-BEAMS)</i> [#2817]</u> We developed an enhancement of the MGM that moves the fit into optical constants space. We thereby extend the admissible range to grain sizes > 250 microns.	Poster Location #530
Ye C. Sklute E. C. Glotch T. D.	<u><i>Mind the Gap: Methods for Combining Optical Constants from Visible to Infrared in the Kramers-Kronig Analysis Associated with Hapke Modeling</i> [#2211]</u> Different methods of combining optical constants from visible to infrared.	Poster Location #531
Arnaut M. Wohlfarth K. Grumpe A. Wöhler C.	<u><i>Mineralogical Maps of Mars from Hapke Modeling and Spectral Unmixing</i> [#2661]</u> We constructed a Hapke-based framework to perform spectral unmixing in order to infer mineralogical maps of selected areas on Mars using CRISM data.	Poster Location #532
He L. Arvidson R. E. Politte D. V. Conduis T. O'Sullivan J. A.	<u><i>Retrieving Temperatures and Single Scattering Albedos from Martian Spectral Data Using Neural Networks</i> [#2094]</u> We present a neural network approach to retrieve both surface single scattering albedos and kinetic temperatures using CRISM hyperspectral data as an example.	Poster Location #533
Conduis T. Arvidson R. E. He L. O'Sullivan J. A. Wolff M. J. et al.	<u><i>A Neural Network Approach to Retrieve Single Scattering Albedos and Temperatures from THEMIS and TES Infrared Data Over Gale Crater</i> [#3069]</u> Inferred mineralogy from retrieved surface spectra and temperatures from thermal infrared orbital data over Gale are consistent with Curiosity ground truths.	Poster Location #534
Alemanno G. Helbert J. Maturilli A. D'Amore M. Varatharajan I. et al.	<u><i>Analysis of Thermal Infrared Spectral Orbital and Laboratory Data for Planetary Surfaces Components Retrieval</i> [#1787]</u> An extreme flexible methodology for surface component retrievals of planetary bodies from TIR spectra is developed and applied to Mars and Mercury orbital data.	Poster Location #535

Tuesday, March 19, 2019

[T332]

POSTER SESSION I: ICY MARS GEOMORPHOLOGY

6:00 p.m. Town Center Exhibit Area

Authors (*Denotes Presenter)	Abstract Title and Summary	Poster Location
Grau Galofre A. Whipple K. X. Christensen P. R.	<u><i>The Effects of the Lower Martian Gravity on Shaping the Glacial Landscapes of Mars</i> [#2684]</u> Why are there no signs of extensive glaciation on Mars? Glaciers and ice sheets may behave and erode differently under the lower gravity. Water is the key.	Poster Location #537
Nguyen T. G. Smith C. L. Innanen A. Moores J. E.	<u><i>Simulating the Formation of Martian Penitentes</i> [#1600]</u> Penitente formation is modeled under martian conditions to determine favourable growth conditions of penitentes and their physical properties.	Poster Location #538

Soare R. J. Conway S. J. Mc Keown L. E. Godin E. Hawkswell J.	<u><i>Possible Ice-Wedge Polygons in Utopia Planitia, Mars, and Their Poleward Latitudinal-Gradient</i></u> [#2121] We present statistical data consistent with the possible latitudinal gradient of low and high-centred (ice-wedge) polygons in Utopia Planitia, Mars.	Poster Location #539
Nathan E. Head J.	<u><i>Concentric Crater Fill Ridge Spacing as a Martian Paleoclimate Archive</i></u> [#2410] The spacing between concentric crater fill ridges is correlated with crater latitude and may reflect local paleoclimate conditions.	Poster Location #540
Scanlon K. E. Head J. W. Fastook J. L. Wordsworth R. D.	<u><i>The Dorsa Argentea Formation and the Noachian-Hesperian Climate of Mars</i></u> [#1409] We used climate and glacial flow modeling to constrain Mars climates allowing ice distribution and basal melting consistent with the Dorsa Argentea Formation.	Poster Location #541
Hao J. Michael G. Adeli S. Jauman R.	<u><i>Survey of Sublimation Landforms at the South Pole of Mars — A Case Study of Angustus Labyrinthus</i></u> [#1401] A new spider formation model, detailing the mechanism of growth of central pits and radiating troughs, was proposed.	Poster Location #542
Fastook J. L. Head J. W.	<u><i>Lava Loads Superimposed on Martian Glaciers: An Assessment of Ice-Flow Velocity Enhancements</i></u> [#1345] The affect of a lava layer on a glacier is modeled and brief accelerations are observed, 1) from the added overburden, and 2) as the thermal wave reaches the bed.	Poster Location #543
Levy J. S. Fassett C. I. Tebolt M.	<u><i>Do Boulder Halos Reflect Shallow Bedrock Strength or Climate Processes?: Substrate Impacts on Boulder Formation and Preservation</i></u> [#2052] “Boulder halos” on Mars are thought to reflect shallow ice-substrate interactions, but new results suggest they may probe bedrock properties as well.	Poster Location #544
Levy J. S. Fassett C. I. Tebolt M.	<u><i>Do Boulder Distributions on Lobate Debris Aprons Indicate Regional-to-Global Synchronicity in Glacial Flow Rates?: Sediment Cover Patterns Resulting from Martian Glaciation</i></u> [#2055] Debris fall onto martian glaciers may record a “ticker tape” of glacial flow. Mapping suggests similarity in boulder density across widely spaced LDA.	Poster Location #545
Johnsson A. Raack J. Hauber E.	<u><i>Possible Recessional Moraines in the Nilosyrtis Mensae Region, Mars</i></u> [#3085] We report on unusual small-scale ridges associated with possible past glaciated valley systems. These ridges may represent recessional moraines on Mars.	Poster Location #546
Butcher F. E. G. Balme M. R. Gallagher C. Storrar R. D. Conway S. J. et al.	<u><i>3D Morphometries of Eskers on Mars, and Comparisons to Eskers in Finland</i></u> [#1874] A new database of esker morphometries on Mars and the Earth.	Poster Location #547
Butcher F. E. G. Balme M. R. Gallagher C. Storrar R. D. Conway S. J. et al.	<u><i>Multi-Phase Sediment-Discharge Dynamics of Subglacial Drainage Recorded by a Glacier-Linked Esker in NW Tempe Terra, Mars</i></u> [#1868] Multiple phases of meltwater flow formed a ‘stacked’ esker on Mars.	Poster Location #548
Kissick L. E. Carbonneau P. E.	<u><i>Order Out of Chaos Terrain: The Case Against Vast Glaciation in Valles Marineris, Mars</i></u> [#1037] Were the Valles Marineris of Mars, the largest system of inter-connected canyons in the solar system, ever widely glaciated? We use high-res images to say no.	Poster Location #549
Cook C. W. Bramson A. M. Christoffersen M. S. Byrne S. Holt J. W. et al.	<u><i>Radar Constraints on the Thickness of Subsurface Ice Near Hellas Planitia, Mars</i></u> [#2245] We mapped subsurface radar reflectors, but many are likely unresolved clutter. We constrained the depth of the reflectors near features associated with ice.	Poster Location #550
Watters T. R. Leuschen C. J. Campbell B. A. Cicchetti A. Orosei R. et al.	<u><i>MARSIS Subsurface Radar Sounding of Medusae Fossae Formation Deposits on Mars: Ice Rich or Ice Poor, That is the Question</i></u> [#2666] Newly acquired MARSIS radar sounder data shows evidence of layering in all major units of the MFF deposits, establishing another key similarity to PLD.	Poster Location #551

Collins-May J. L. Carr J. R. Balme M. R. Brough S. Gallagher C. et al.	<u><i>The Origin and Distribution of Icy Material in the Nereidum Montes, Mars</i></u> [#1802] The aim of this work is to investigate whether local and regional topography influences ice distribution in the Nereidum Montes mountain range on Mars.	Poster Location #552
--	---	----------------------

Tuesday, March 19, 2019

[T333]

POSTER SESSION I: THING FALL DOWN GO BOOM: MARS DOWNSLOPE MOTION

6:00 p.m. Town Center Exhibit Area

Authors (*Denotes Presenter)	Abstract Title and Summary	Poster Location
Lark L. Huber C. Head J. W.	<u><i>Anomalous Recurring Slope Lineae on Mars</i></u> [#1716] Three types of anomalous RSL are presented. These can be used to evaluate possible RSL formation and fading mechanisms.	Poster Location #553
Anderson R. B. Dundas C. M. Gasnault O. Le Mouelic S. Wiens R. C. et al.	<u><i>Results from Long Distance Remote Micro Imager Monitoring of Lineae-Forming Slopes on Aeolis Mons</i></u> [#1119] We report on the results of a two-Earth-year campaign to use ChemCam's Remote Micro Imager (RMI) to monitor locations where lineae were observed from orbit.	Poster Location #554
Nakamura M. Sekine Y. Fukushi K. Hasebe N. Davaadorj D. et al.	<u><i>Dark Streak Features in Mongolia as Terrestrial Analogues of Recurrent Slope Lineae on Mars</i></u> [#2269] We discover terrestrial RSL analogs in cold steppes, Mongolia, where streaks may form via removal of surface white sands by ice melting and surface runoff.	Poster Location #555
Czaplinski E. C. Ahrens C. J. Chevrier V. F.	<u><i>Comparative Morphologies Between Dune Slope Streaks and Recurring Slope Lineae on Mars</i></u> [#1160] Slope streaks, RSL / We measured their lengths to find / Similarities.	Poster Location #556
Raack J. Conway S. J. Balme M. R. Sylvest M. E. Hiesinger H. et al.	<u><i>New Insights into the Sediment Transport Mechanism Under Low Pressures and Implications for Mass Movements on Mars</i></u> [#1235] New results of our last experimental campaign of water-induced mass movements in a Mars-like environment, with a focus on different slope angles and flow rates.	Poster Location #557
Khuller A. R. Christensen P. R. Harrison T. N. Diniega S.	<u><i>Investigating the Distribution of Frosts in Relation to Present-Day Gully Activity on Mars</i></u> [#3045] We use thermal data to explore the global spatial, temporal variation of temperatures conducive to CO ₂ , H ₂ O frost formation on Mars in relation to gullies.	Poster Location #558
Berman D. C. Crown D. A. Conway S. J.	<u><i>Gullies Emanating from the Margins of Lobate Flow Features in Nereidum Montes, Mars</i></u> [#2607] We document evidence for well-developed gullies on the margins of lobate flow features, consistent with the formation of gullies due to melting of water ice.	Poster Location #559
Langenkamp T. R. Gulick V. C. Glines N. H.	<u><i>Geomorphic Analysis of Martian Gullies in Western Asimov Crater</i></u> [#3224] This study focuses on gullies in Asimov Crater, which is located in the southern hemisphere of Mars. Six gullies were analyzed and six recurrent slope lineae.	Poster Location #560
McCardle B. C. Kraal E. R.	<u><i>Geomorphic Mapping of Landslides in Aram Valley, Mars</i></u> [#2511] Sudden wall collapse / Petals of debris lay down / Valley feels deformed?.	Poster Location #561
Roback K. P. Ehlmann B. L.	<u><i>Topography and Other Factors Influencing the Spatial Distribution of Landsliding on Mars</i></u> [#1873] We investigate controls on the spatial distribution of martian landsliding, including topography and the possible impact of tectonic seismicity.	Poster Location #562
Tesson P-A. Conway S. J. Mangold N. Ciazela J. Lewis S. et al.	<u><i>Evidence for Thermal Fatigue on Mars from Rockfall Patterns on Impact Crater Slopes</i></u> [#2352] Study of recent rockfalls in martian impact craters between ±40° latitude shows that thermal stress is playing a key-role in rock breakdown on modern Mars.	Poster Location #563

Grindrod P. M. Davis J. M. Conway S. J. de Haas T.	<u>Significant Boulder Movement on Crater Slopes in Terra Sirenum, Mars</u> [#1405] Boulders bounce and roll / From seasons, 'quakes, impacts, wind? / In lonely crater.	Poster Location #564
---	---	----------------------

Tuesday, March 19, 2019

[T334]

POSTER SESSION I: PLANETARY AEOLIAN PROCESSES

6:00 p.m. Town Center Exhibit Area

Authors (*Denotes Presenter)	Abstract Title and Summary	Poster Location
Radebaugh J. Barnes J. Le Gall A. Yu X. Turtle E. P. et al.	<u>Properties of the Dune Sands of Titan: Knowns and Unknowns</u> [#2279] Titan sand is hard / Small, loose and jumps when wind blows / But organic too.	Poster Location #566
Yawar Z. Schieber J. Sullivan R. Minitti M. Edgett K.	<u>On the Eolian Transport Durability of Sand-Size Mudstone Clasts — The Potential for Martian Sand Dunes that are Composed of Fine Grained Aggregates and Implications for Interpreting Mudstone Strata at Gale Crater, Mars</u> [#1999] Observation of eolian transport and degradation of mudstone aggregates as a potential analog to eolian processes active at Gale Crater during Murray deposition.	Poster Location #567
Kling C. L. Craddock R. A. Morgan A.	<u>Linear Dune Formation in the Simpson Desert, Australia as a Planetary Analogue</u> [#2920] The Simpson Desert in Australia is host to hundreds of linear dunes. Linear dunes are long, Their formation remains strange, Maybe drone will help.	Poster Location #568
Preston S. Chojnacki M.	<u>Aeolian Ripple Rate Variability in Response to Different Boundary Conditions</u> [#2142] We aim to gain a better understanding of ripple migration trends at various locations across Mars where local topography and wind regime may be different.	Poster Location #569
Boazman S. J. Grindrod P. M. Balme M. R. Vermeesch P. Davis J. M. et al.	<u>Do Large Dunes on Mars Migrate? Ripple and Dune Movement in Coprates Chasma, Valles Marineris</u> [#1533] Large moving sand dunes / At Valles Marineris / Windy, large sand flux.	Poster Location #570
Davis J. M. Grindrod P. M. Boazman S. Vermeesch P. Baird T.	<u>Ten (Earth) Years of CTX Observations of Dune Movement at Nili Patera, Mars: A Comparison with HiRISE</u> [#1516] Nili dunes move fast / Little guys speeding along / Now in CTX.	Poster Location #571
Fenton L. K. Gullikson A. L. Hayward R. K. Charles H. Titus T. N.	<u>The Mars Global Digital Dune Database (MGD³): Composition and Stability</u> [#1115] In Mars dune fields, could / Glass denote activity / Or maturity? What other secretshide in our update to the Mars Dune Database?	Poster Location #572
Nguyen T. G. Radebaugh J. Innanen A. Moores J. E.	<u>Investigation of Small-Scale (<50 m) Wind-Driven Surface Features on Mars' Northern Polar Cap Using Data from HiRISE</u> [#1614] Dunes and ripples on the martian north polar cap are observed using HiRISE, where orientation and spacing tendencies are measured and mapped.	Poster Location #573
Emran A. Marzen L. J. King D. T. Jr.	<u>Automated Object-Based Identification of Dunes at Hargraves Crater, Mars</u> [#1157] We employed an automated object-based image analysis (OBIA) technique to extract the dunes at Hargraves Crater, Mars.	Poster Location #574
Hughes E. B. Zimbelman J. R.	<u>Preliminary Observations of Transverse Aeolian Ridges on Mars in Digital Terrain Models</u> [#2533] We surveyed 528 Digital Terrain Models of the martian surface for Transverse Aeolian Ridges, identifying unique morphologies and geographic locales.	Poster Location #575
Zimbelman J. R. Scheidt S. P. Foroutan M. Baker M. M.	<u>Investigating the Transition from Sand Ripples to Megaripples on Earth and Mars</u> [#1186] Sand ripples and megaripples have distinct bedform scales and surface particle sizes. We look for transitional forms between the two classes.	Poster Location #576

TUES POSTERS

Zimbelman J. R. Spagnuolo M. G.	de Silva S. L. Runyon K. D.	<u><i>First 2018 Results from Wind Profiles for Megaripples in the Puna of Argentina</i> [#1207]</u> New wind profiling measurements indicate the roughness length of both gravel-covered megaripples and a nearby gravel plain in the Puna of Argentina.	Poster Location #577
Hausmann R. Chojnacki M. Golombek M.	Daubar I. Ojha L. et al.	<u><i>The Distribution and Lifetimes of Dust Devil Tracks in HiRISE Images</i> [#2964]</u> We mapped dust devil tracks on Mars and measured the rate of fading at 12 sites. Lifetimes range between 58 and 279 Earth days and increase with elevation.	Poster Location #578
Dorn T. C.	Day M. D.	<u><i>Temporal Variations in Wind Patterns Within Jezero Crater</i> [#2081]</u> We assess the orientation and seasonal variability of wind streaks within Jezero Crater on Mars to understand the modern wind regime.	Poster Location #579
Detelich C. E. Seelos K. D.	Runyon K. D.	<u><i>Characterizing Anomalous Wind Eroded Terrain on Mars: The Olympus Maculae</i> [#1861]</u> Anomalous, low albedo, wind-eroded terrain with minimal surface dust act as windows into the enigmatic Medusa Fossae Formation; reveal complex aeolian processes.	Poster Location #580
Rabinovitch J. Radebaugh J. McDougall D.	Kerber L. Sevy J. M.	<u><i>Wind Flow Around Yardangs: Identifying Major Wind Directions from Flow Indicators in the Campo De Las Piedras Pomez, Argentina</i> [#2250]</u> Field-work from the Campo de las Piedras Pomez (CPP) yardang fleet is presented in this work.	Poster Location #581
McDougall D. S. Kerber L. Sevy J. M.	Radebaugh J. Christiansen E. H. et al.	<u><i>Lithologic Controls on Yardang Morphology from Field Observations of the Cerro Blanco Ignimbrites of Argentina</i> [#3202]</u> Don't try to see every yardang / The truth is, they never let you / Through all the wild winds / And Medusae Fossae / Just measure distance.	Poster Location #582
Wang J. Hiesiger H.	Xiao L. Huang J. Reiss D. et al.	<u><i>Geologic Characteristics of Yardangs on Mars and Their Implications for Paleo-Environments: Constraints from Comparison Between the Qaidam Basin/China and the Aeolis-Zephyria Region</i> [#2197]</u> In this study, we have investigated the types, distribution, geometry parameters, and formation of yardangs both in the Qaidam and the AZP region.	Poster Location #583

Tuesday, March 19, 2019

[T335]

POSTER SESSION I: EDUCATION AND PUBLIC ENGAGEMENT: MODELS, OPPORTUNITIES, AND PRODUCTS FOR ENGAGING AUDIENCES

6:00 p.m. Town Center Exhibit Area

Authors (*Denotes Presenter)	Abstract Title and Summary	Poster Location	
Patel P. P. DeCoito I.	<u><i>The Space Explorers Program at the Centre for Planetary Science and Exploration</i> [#2557]</u> The Space Explorers Program offers space science and technology-themed programming for students of ages 9–14 in London and Richmond Hill, Ontario, Canada.	Poster Location #585	
Barcenilla Garcia R.	<u><i>The Smell of Space: A Creative Approach to Planetary Science Outreach and Public Engagement</i> [#2771]</u> 'AromAtom: The Smell of Space' is a student-led science outreach project that uses the sense of smell to engage the public with planetary science.	Poster Location #586	
Cabrero-Gomez J. F. Rodriguez F.	<u><i>From Madrid-Apollo Station to Europe's Only Lunar Museum for Safeguarding Both Tangible and Intangible Heritage</i> [#1278]</u> "Museo Lunar" was inaugurated in order to show the Madrid station of NASA MSFN. The safeguarding of Apollo stations' legacy and heritage is proposed.	Poster Location #587	
Ságodi I. Szabó M.	Bérczi Sz. Hegyí S. Vizi P. G.	<u><i>2018 December — 2019 December: An Apollo Memorial Year for the Planetary Science Education</i> [#1813]</u> We propose a memorial program in teaching planetary science on 50 years anniversary of historical lunar flights of the Apollo program from the missions 8 to 12.	Poster Location #588

Hegyí S. Szabó M. Bérczi Sz. Vizi P. G. Ságodi I.	<u><i>The Role of Makerspace in Space Science Education: How Learning and Space Technology Forms an Attractive Curriculum for Creation in Digital Community</i></u> [#1899] Makerspace in the school can help in forming creative ideas, plans, design, a route toward finally the student's product.	Poster Location #589
Wasser M. L. Shaner A. Buxner S. Jones A. J. P. Tiedeken S. et al.	<u><i>Expanding an Established Public Science Event: Lessons from International Observe the Moon Night 2018</i></u> [#3091] People love the Moon / But always room to expand / So we did new things.	Poster Location #590
Tiedeken S. L. Fooshee J. Jones A. Myers D. Wasser M.	<u><i>Engaging the Public with Planetary Science at Comic Book Conventions</i></u> [#1260] Public engagement with science is becoming increasingly popular at comic book conventions, where the opportunity to reach diverse audiences is great.	Poster Location #591
Graff P. V. Foxworth S. Luckey M. K. Runco S. Willis K. et al.	<u><i>Generating Excitement and Increasing Awareness of NASA Planetary Science and Astromaterials Assets</i></u> [#2769] Sharing astromaterials at public outreach events, conferences, and through collaborations with others generates excitement and knowledge about NASA science.	Poster Location #592
Klug Boonstra S. Heward A.	<u><i>Opportunities to Engage and Partner with the Public in a Historic Science Endeavor: Mars Sample Return</i></u> [#2711] Mars Sample Return offers an unprecedented opportunity to engage the citizenry of this planet in one of the enduring questions of humanity, "Are we alone?".	Poster Location #593
Shaner A. Hackler A. Filiberto J. Shupla C. Evans M. E. et al.	<u><i>Sharing Planetary Science in a Planetarium</i></u> [#1692] Scientists inform / In a Planetarium / The public in awe.	Poster Location #594
Shupla C. Aponte Hernandez B. Valentín E. G. Buxner S. Rivera-Valentín E. G. et al.	<u><i>Professional Development for Planetary Scientists</i></u> [#1847] LPI staff hold / Seminars for scientists / Come hear, share, and grow.	Poster Location #595
Grier J. A. Schneider N. M. Buxner S. A.	<u><i>Understanding the Needs of Space Scientists in Education, Public Engagement, and Communications: Implications for Practice</i></u> [#2925] We asked scientists / "Outreach needs?" Community / Support spells success.	Poster Location #596
Gemma M. E. Trakinski V. Abbott B. Emmart C. Smith R. L. et al.	<u><i>Data Exploration Using OpenSpace</i></u> [#3178] Progress on OpenSpace, an open source interactive tool to visualize the known universe and dynamic data from observations, simulations, and space mission operations.	Poster Location #597
Shusterman M. L. Robinson M. S. Wing B. R.	<u><i>Optimizing Color Palettes for Color Vision Deficiency</i></u> [#2670] Selecting color palettes that are interpretable to those with color vision deficiency can be accomplished with the use of a dynamic palette-generation program.	Poster Location #598
Armstrong E. S.	<u><i>'For All Mankind': A Comparison Between Permanent Display and Temporary Events on Apollo 11 in the UK in the Lead Up to the 50th Anniversary of the Moon Landing</i></u> [#1904] Imaginary of science since Apollo in contemporary talks shapes access to STEM by public.	Poster Location #599
Terazono J. Yoshikawa M. Watanabe J. Sakamoto S. Wakabayashi N. et al.	<u><i>Twenty Years of The Moon Station: Toward the Next 20 Years</i></u> [#2168] This presentation summarizes our 20 years' activity of web-based outreach called "The Moon Station" and addresses future prospects and challenges.	Poster Location #600
Zaklynsky A. Glukhova E. Sitnikova A. Foing B.	<u><i>Growth of an Aesthetic Organism in the Moon Gallery After One Year</i></u> [#2563] An international collaborative artwork and a gallery of ideas to be sent to the Moon in 2022 within a compact format of 10 x 10 cm petri dish-like structure.	Poster Location #601
Hill J. R. Christensen P. R.	<u><i>Mars on the Mall: Walking on Mars in the Nation's Capital</i></u> [#2219] THEMIS' Walk on Mars map has been very successful with over 4,000 participants so far, and has partnered with AGU to bring the map to Washington, D.C. in 2019.	Poster Location #602

Robbins S. J. Keane J. T. Kinczyk M. Runyon K. Beddingfield C. B. et al.	<u>Using Computer-Generated Imagery (CGI) for Science and Outreach on Missions: New Horizons' Encounter with the Pluto-Charon System and (486958) 2014 MU₆₉ [#3057]</u> CGI is an / Important tool for our use / Stand with fed. workers.	Poster Location #603
Gabasova L. R. Olkin C. B. Spencer J. R. Parker J. Wm. Verbiscer A. J. et al.	<u>Sketching the New Horizons 2014 MU₆₉ Flyby Event [#3241]</u> Follow the mission / As it evolves day to day / Science is people!	Poster Location #604
Hargitai H. I. Dorsánszki A.	<u>Ultima Thule Cartography: New Approches, New Challenges [#3166]</u> This paper discusses the ongoing work of creating a map of Ultima Thule for children.	Poster Location #605
Urquhart M. L.	<u>Use of Creative Assessments in Space Science Courses Designed for Teachers [#2884]</u> Made to show learning / Assessments take many forms / Inspiration soars.	Poster Location #606

Tuesday, March 19, 2019

[T336]

POSTER SESSION I: CAESAR AND DRAGONFLY: NEW FRONTIERS PHASE A STUDIES

6:00 p.m. Town Center Exhibit Area

Authors (*Denotes Presenter)	Abstract Title and Summary	Poster Location
Turtle E. P. Trainer M. G. Barnes J. W. Lorenz R. D. Hibbard K. E. et al.	<u>Dragonfly: In Situ Exploration of Titan's Organic Chemistry and Habitability [#2888]</u> Dragonfly explores / Life's chemical origins / Titan holds the clues.	Poster Location #609
MacKenzie S. M. Nunez J. I. Turtle E. P. Lorenz R. D. Horst S. M. et al.	<u>Titan's Surface from Dragonfly: Bridging the Gap Between Composition and Environment [#2885]</u> Molecules present / Won't be all Dragonfly learns / On Titan's surface.	Poster Location #610
Lorenz R. D. Panning M. Stahler S. Shiraishi H. Yamada R. et al.	<u>Titan Seismology with Dragonfly: Probing the Internal Structure of the Most Accessible Ocean World [#2173]</u> Dragonfly will feel / Creaks and groans of Titan's ice / Revealing ocean!	Poster Location #611
Lauretta D. S. Squyres S. W. Bermúdez L. Blake G. Canham J. S. et al.	<u>The CAESAR New Frontiers Mission: 1. Expected Nature of the Returned Comet Sample [#2642]</u> We review the Sample Analysis and Curation Plans developed during the Phase A concept study for the CAESAR Comet Samples Return Mission.	Poster Location #612
Hayes A. G. Soderblom J. M. Getzandanner K. M. Ravine M. Kirk R. et al.	<u>The CAESAR New Frontiers Mission: 3. TAG Site Selection and Camera Suite [#2722]</u> CAESAR will acquire and return to Earth >80g of material from comet 67P/CG. We describe how the CAESAR Camera Suite will be used to select the sample site.	Poster Location #613
Glavin D. P. Squyres S. W. Chu P. C. Gerakines P. A. Yamada K. et al.	<u>The CAESAR New Frontiers Mission: 3. Sample Acquisition and Preservation [#2541]</u> CAESAR will return at least 80 g of sample from comet 67P, protecting volatile and non-volatile sample components from contamination or alteration.	Poster Location #614

Tuesday, March 19, 2019

[T337]

POSTER SESSION I: MISSION AND INSTRUMENT CONCEPTS: VENUS

6:00 p.m. Town Center Exhibit Area

Authors (*Denotes Presenter)	Abstract Title and Summary	Poster Location
Sands C. Huang A. Wilson E. Chan Y.	<u>DAS-Cubes-Independent Emitter/Receiver Cubesat Configuration for Planetary Atmospheric Measurements [#2599]</u> Cubesat system concept utilizing separate spacecraft with emitter and receiver to achieve planetary measurements of interest, such as atmospheres or plumes.	Poster Location #615

Knically J. J. Herrick R. R.	<u><i>Atmospheric Windows to Image the Surface from Beneath the Cloud Deck on the Night Side of Venus</i> [#1934]</u> Systems beneath the cloud deck of Venus will have an improved variety of wavelengths for viewing the surface and significantly improved spatial resolution.	Poster Location #616
Gregg T. Zasova L. Economou T. Eismont N. Gerasimov M. et al.	<u><i>Venera-D: A Potential Long-Lived Mission to Explore Venus' Surface, Atmosphere, and Plasma Environment</i> [#1738]</u> Venera-D would / Orbit and land on Venus / Lasting months to years.	Poster Location #617
Bugga R. V. Jones J.-P. Pauken M. T. Billings K. J. Ahn C. et al.	<u><i>New Power Technologies for Venus Low-Altitude and Surface Missions</i> [#1043]</u> The paper describes a novel power technology for 'Venus Interior Probe using in-situ Power and Propulsion' and the development of new primary batteries for Venus landers.	Poster Location #618
Blake D. F. Sarrazin P. Bristow T. S. Walroth R. Downs R. et al.	<u><i>CheMin-V: A Definitive Mineralogy Instrument for the Venera-D Mission</i> [#1468]</u> CheMin-V is an XRD/XRF instrument intended for quantitative mineralogical analysis of the surface of Venus. It will be proposed for the Venera-D mission.	Poster Location #619
Helbert J. Dyar D. Walter I. Rosas-Ortiz Y. Widemann T. et al.	<u><i>The Venus Emissivity Mapper — Obtaining Global Mineralogy of Venus from Orbit on the ESA EnVision and NASA VERITAS Missions to Venus</i> [#2046]</u> The Venus Emissivity Mapper is the first flight instrument designed to focus on mapping the surface of Venus using several atmospheric windows around 1 µm.	Poster Location #620
Krishnamoorthy S. Martire L. Bowman D. C. Komjathy A. Cutts J. A. et al.	<u><i>Advances Towards Balloon-Based Seismology on Venus</i> [#1662]</u> The surface of Venus is extremely inhospitable for instruments. We discuss our progress in the last year towards performing seismology from balloons on Venus.	Poster Location #621

Tuesday, March 19, 2019

[T338]

POSTER SESSION I: MISSION CONCEPTS: MOON

6:00 p.m. Town Center Exhibit Area

Authors (*Denotes Presenter)	Abstract Title and Summary	
Feng L. Deng C.	<u><i>DEM Generation and Rover Landing at the South Pole of the Moon and Mars</i> [#1886]</u> DTMs generation and fusion via photogrammetry and radargrammetry, automatic TRN algorithm for precise rover landing at the south pole of the Moon and Mars.	Poster Location #622
Basilevsky A. T. Krasilnikov S. S. Ivanov M. A. Malenkov M. I. Michael G. G. et al.	<u><i>Potential South Polar Lunar Base (Mons Malapert): Topographic, Geologic, and Trafficability Consideration</i> [#1140]</u> LROC NAC, LOLA data, and the Lunokhod-1/Apollo Lunar Roving Vehicle experience are used to assess Mons Malapert at the south pole as a lunar base location.	Poster Location #623
Neal C. R. Banerdt W. B. Beghein C. Chi P. Currie D. et al.	<u><i>The Lunar Geophysical Network Mission</i> [#2455]</u> Understanding the detailed structure, heat budget, and composition of the lunar interior will tell us about initial terrestrial planetary body differentiation.	Poster Location #624
Kerber L. Denevi B. Nesnas I. Keszthelyi L. Head J. W. et al.	<u><i>Moon Diver: A Discovery Mission Concept for Understanding Secondary Crust Formation Through the Exploration of a Lunar Mare Pit Cross-Section</i> [#1163]</u> After 50 years, Moon Diver aims to return to Mare Tranquillitatis, building on the legacy of Apollo to explore a >50 m exposure of the Moon's secondary crust.	Poster Location #625
Draper D. S. Klima R. L. Lawrence S. J. Denevi B. W.	<u><i>The Inner Solar System CHRONology (ISOCHRON) Discovery Mission: Returning Samples of the Youngest Lunar Mare Basalts</i> [#1110]</u> ISOCHRON will fix / Crater count models with age / Dates of young basalts.	Poster Location #626

Crites S. T. Ozaki N. Ballouz R. -L. Baresi N. Arahata S. et al.	<u><i>MARAUDERS: A Small-Sat Mission to Probe the Physical Properties of Volatiles in Lunar Permanently Shadowed Regions</i></u> [#2281] MARAUDERS is a smallsat concept that aims to characterize the surface and volatile properties of regolith in permanently shadowed regions at the Moon's poles.	Poster Location #627
Garrick-Bethell I. Paige D. A. Burton M. E.	<u><i>NanoSWARM: A Proposed Discovery Mission to Study Space Weathering, Lunar Water, Lunar Magnetism, and Small-Scale Magnetospheres</i></u> [#2786] NanoSWARM addresses a number of important problems in planetary science by visiting some of the most complex and least explored geologic features on the Moon.	Poster Location #628
Blewett D. T. Halekas J. Greenhagen B. T. Anderson B. J. Denevi B. W. et al.	<u><i>Magnetic Anomaly as Natural Laboratory: The Lunar Compass Mission Concept</i></u> [#1450] A rover traversing a lunar magnetic anomaly/swirl offers cross-cutting science spanning geophysics, geology, volatiles, space physics, and space weathering.	Poster Location #629
Tokle L. Palumbo A. Deutsch A. Anzures B. Boatwright B. et al.	<u><i>Scientific Exploration of Mare Imbrium with OrbitBeyond, Inc.: Characterizing the Regional Volcanic History of the Moon</i></u> [#2484] Mare Imbrium / New wave of exploration / With OrbitBeyond.	Poster Location #630
Aharonson O. Garrick-Bethell I. Grosz A. Head J. W. Russell C. T. et al.	<u><i>The Science Mission of the SpaceIL Lunar Lander</i></u> [#2290] The science mission of SpaceIL consists of detailed characterization of the landing site, measuring the crustal magnetic anomalies, and ranging to the lander.	Poster Location #631
Malespin C. A. Benna M. Raaen E. Sarantos M. Schmerr N. C. et al.	<u><i>LEMS: Lunar Environment Monitoring Station</i></u> [#2369] LEMS is an autonomous and self-sustaining instrument that enables the long-term, in-situ monitoring of the exosphere and the seismic activities of the Moon.	Poster Location #632
Inoue H. Yamamoto M. Ohtake M. Otake H. Hoshino T.	<u><i>Landing Site Analysis and Path Planning for JAXA's Future Lunar Polar Exploration Mission</i></u> [#2155] We present the result of landing site analysis and path planning for a surface exploration mission in the lunar polar region.	Poster Location #633
Xu L. Zou Y. L. Qin L.	<u><i>Overview of China's Lunar Exploration Program and Scientific Vision for Future Missions</i></u> [#2440] The CLEP has carried out four missions. On this basis, China has proposed a vision to preliminarily build a lunar research station at the lunar south pole.	Poster Location #634
Foing B. H. EuroMoonMars 2018– 2019 Team N.	<u><i>EuroMoonMars Instruments, Research, Field Campaigns, and Activities 2017–2019</i></u> [#3090] “EuroMoonMars” is an evolving pilot research programme with instruments, investigations, facilities, field campaigns for MoonMars science and workforce.	Poster Location #635
Ignatiev A. Curreri P. Sadoway D. Carol E.	<u><i>The Use of Lunar Resources for the Construction and Operation of a Lunar Radio Observatory on the Moon</i></u> [#1027] An in-situ radio observatory located on the Moon can be founded on the fabrication of thin film growth technology in the vacuum environment of the Moon.	Poster Location #636
Byers G.	<u><i>Analyzing an Increase in Micrometeorites Located in Low Earth Orbit in Comparison to Explorer 1</i></u> [#3280] Using a CubeSat and methods similar to Explorer 1, we propose to show evidence of Earth-sourced micrometeorites in low earth orbit.	Poster Location #637

Tuesday, March 19, 2019

[T339]

POSTER SESSION I: INSTRUMENT CONCEPTS: MOON

6:00 p.m. Town Center Exhibit Area

Authors (*Denotes Presenter)	Abstract Title and Summary	Poster Location
Benna M. Malespin C. A. Hurley D. H. Livengood T. A. Farrell W. M. et al.	<u>SEAL: Surface and Exosphere Alterations by Landers</u> [#2364] SEAL aims to investigate the interaction of lunar surface with volatiles from the lander's rocket exhaust, constraining the adsorptive properties of the regolith.	Poster Location #638
Farrell K. W. Jr. Bomse D. S. Milliken R. E. Mustard J. F. Head J. W. III	<u>Lunar Laser Surface Solar Occultation (LLSSO), a Payload Concept for Lunar Landers</u> [#2080] LLSSO is a heterodyne radiometer that uses interband cascade laser technology to detect the presence of water resources that are cycled from the lunar surface.	Poster Location #639
Nagihara S. Ngo P. Sanasarian L. Sanigepalli V. Zacny K.	<u>Heat Flow Probe for Short-Duration Lunar Missions on Small Landers</u> [#1557] We describe a new heat flow instrument suited for short-duration missions on small landers planned for NASA's Commercial Lunar Surface Payloads program.	Poster Location #640
Blake D. F. Bristow T. F. Chen J. Dera P. Downs R. et al.	<u>XTRA: An eXtraTerrestrial Regolith Analyzer for Lunar Soil</u> [#1144] The eXtraTerrestrial Regolith Analyzer (XTRA) is an in-situ X-ray diffraction/X-ray fluorescence instrument for characterizing as-received lunar soil.	Poster Location #641
Sobron P. Fahey M. Krainak M. Misra A. Rehmark F. et al.	<u>Redeployable Sensor Probe for In-situ Lunar Resource Mapping from Small Landers</u> [#2749] New technology that gives mobility and high spatial remote sensing ability to a lander, thus effectively removing the need for rover and sampling devices.	Poster Location #642
Furutani K. Haruyama J.	<u>Investigation of Machining Methods of Rock Samples in Lunar Vertical Holes and Lava Tube for UZUME Project</u> [#1170] Troublesome phenomenon during rock machining in vacuum are discussed. Machining devices for lunar vertical hole explorations by UZUME project are introduced.	Poster Location #643
Nakauchi Y. Saiki K. Ohtake M. Shiraishi H. Honda C. et al.	<u>Multi-Band Camera on SLIM to Investigate Mg# of Lunar Mantle Materials</u> [#1522] SLIM project is planning to observe olivine and to estimate Mg# of it using Multi-Band Camera (MBC). We talk about SLIM and MBC concepts.	Poster Location #644
Nunn C. Pike W. T. Panning M. P. Kedar S.	<u>Scoping MEMS Seismometers for Deployment on the Moon</u> [#2223] We consider the advantages of including MEMS-type (Micro-Electro-Mechanical Systems) seismometers on one or more landed missions to the Moon.	Poster Location #645
Erwin A. Stone K. J. Kedar S. Shelton D. Paik H. J. et al.	<u>A Planetary Broadband Seismometer (PBBS) for the Lunar Geophysical Network and Ocean Worlds: Experiment and Theory on the Thermal Drift Due to EFR</u> [#1052] We are developing a planetary broadband seismometer (PBBS) to meet the sensitivity requirements for the Lunar Geophysical Network.	Poster Location #646
Shin J. Jin H. Lee H. Lee S. Lee S. et al.	<u>KMAG: The Magnetometer of the Korea Pathfinder Lunar Orbiter (KPLO) Mission</u> [#2276] KMAG is a scientific magnetometer payload of the Korea Pathfinder Lunar Orbiter (KPLO) that is the first lunar exploration mission of the Korean space program.	Poster Location #647
Russell C. T. Rowe K. M. Joy S. P. Aharonson O. Amrusi S. et al.	<u>SILMAG: A Fluxgate Magnetometer on Board the SPACEIL Lunar Lander</u> [#1728] The SPACEIL organization is launching a mission to the Moon. It carries two scientific investigations: A magnetic fields investigation and a retroreflector.	Poster Location #648

TUES POSTERS

Warren T. J. King O. Bowles N. E. Sefton-Nash E. Fisackerly R. et al.	<u><i>The Oxford 3D Thermophysical Model with Application to the Lunar PROSPECT Mission</i> [#2040]</u> The PROSPECT mission's aim is to study lunar near-surface volatiles. We present 3D thermal model results for sites around the lunar south pole for the mission.	Poster Location #649
Bickel V. T. Honniball C. I. Martinez S. N. Rogaski A. Sargeant H. M. et al.	<u><i>Analysis of Lunar Boulder Tracks: Implications for Rover Mobility on Pyroclastic Deposits</i> [#1587]</u> Trafficability and bearing capacity of lunar pyroclastic deposits, maria, and highlands are estimated based on measurements of boulder tracks in Narrow Angle Camera imagery.	Poster Location #650
Retherford K. D. Moore T. Z. Raut U. Phillips-Lander C. M. Molyneux P. M. et al.	<u><i>Lunar Integrating Cavity Raman Ultraviolet Spectrograph (Lunar ICARUS) Concept</i> [#3141]</u> Development of an Integrating Cavity Enhanced Raman Spectroscopy technique for flight holds great promise for numerous studies requiring trace composition data.	Poster Location #651
Livengood T. A. Anderson C. M. Bonds Q. Bradley D. C. Bulcha B. T. et al.	<u><i>Submillimeter Solar Observation Lunar Volatiles Experiment (SSOLVE)</i> [#1640]</u> Submillimeter / Is the clear choice, to measure / Moon's water vapor. Rising from the ground / Maybe / How much? / And what happens next?	Poster Location #652
Zhu X. Y. Zhang G. L. Zhou Q. Zhang X. X. Xiong Y. Y.	<u><i>LFRS Onboard the Chang'e-4 Mission and Its Method to Suppress RFI</i> [#1821]</u> LFRS (Low Frequency Radio Spectrometer) is a scientific payload onboard the Chang'e-4 lunar lander, which was successfully launched to the lunar farside in 2018.	Poster Location #653
Patrick E. Necsoiu M. Hooper D.	<u><i>Lunar Advanced Vacuum Apparatus (LAVA)</i> [#2779]</u> We present early results for volatile diffusion through a 50-cm simulated regolith column in the 66-liter chamber of our Lunar Advanced Vacuum Apparatus (LAVA).	Poster Location #654
Clark P. E. Bugby D. Hofmann D.	<u><i>Wide Range of Low Cost Day and Night Operational Lunar Surface Payloads Enabled by High Performance Thermal Components Based Packaging</i> [#1123]</u> We have demonstrated the capability of a reverse thermal switch with a 2500:1 switching ratio that would enable a wide range of low-cost instrument packages.	Poster Location #655

Tuesday, March 19, 2019

[T340]

POSTER SESSION I: ADVANCED CURATION

6:00 p.m. Town Center Exhibit Area

Authors (*Denotes Presenter)	Abstract Title and Summary	Poster Location
Calaway M. J. Allton J. H. McCubbin F. M. Zeigler R. A.	<u><i>The Rise of Astromaterials Curation: NASA's 50 Years of Preserving Pristine Samples from the Solar System</i> [#1690]</u> A brief history and tribute to NASA's 50 years of curating extraterrestrial samples from the solar system and inherent legacy of Apollo program.	Poster Location #657
Russell S. S. Vaccaro E. King A. J. Almeida N. V. Salge T.	<u><i>Minimally Destructive Sample Characterisation: Implications for Sample Return Missions</i> [#2350]</u> We are developing protocols for minimally-destructive analysis of carbonaceous chondrites in preparation for sample return missions.	Poster Location #658
Li D. Wu Q. Fu Z. Li J.	<u><i>Design and Accomplishing of the Ground Facility for Lunar Sample's Transfer in a Non-Contamination Environment</i> [#1378]</u> In this paper, a design of a facility that guarantees lunar samples transfer in a non-contamination environment is described.	Poster Location #659
Calaway M. J. Burton A. S. Dworkin J. P. Righter K. Nakamura-Messenger K. et al.	<u><i>Selecting Cleanroom Construction Materials for the OSIRIS-REx and Hayabusa2 Curation Facility at NASA Johnson Space Center</i> [#1448]</u> Brief overview of construction materials chosen for the OSIRIS-REx and Hayabusa2 ISO Class 5 cleanroom curation laboratory facilities.	Poster Location #660

Hutzler A. Calaway M. J. Burton A. Zeigler R. A.	<u>Contamination Control and Knowledge During Construction of New Curation Facilities at NASA Johnson Space Center</u> [#2900] New place for samples / Out of an old dusty space / Next spring at NASA.	Poster Location #661
Davis R. E. Castro C. L. Castro-Wallace S. L. McCubbin F. M. Regberg A. B.	<u>Isolation and Monitoring of Cleanroom-Associated Microbial Contaminates from Geological Collections</u> [#2880] We assess microbial contamination of cleanrooms containing astromaterial collections. Contamination is low and cultured isolates were primarily human-associated.	Poster Location #662
Fries M. Rodriguez M. McBride K. Bastien R. Zeigler R. et al.	<u>NASA Cosmic Dust Current Status and Future Directions</u> [#1049] Cosmic dust is good / But it can always improve / Dusty winds of change.	Poster Location #663
Snead c. J. McCubbin F. M. Fries M. D.	<u>Development of Methods for the Curation of Interplanetary Dust Particles Collected on Polyurethane Foam Substrates</u> [#3235] We describe the development of methods to extract interplanetary dust particles from polyurethane foam collectors.	Poster Location #664
Holt J. M. C. Bridges J. C. Vrublevskis J. Gaubert F.	<u>Double Walled Isolator Technology for Mars Sample Return Facilities</u> [#2408] We are developing Double Walled Isolators that allow science and planetary protection for MSR.	Poster Location #665
Lewis E. K.	<u>Building a Planetary Chamber Instrument for Astrochemical Research</u> [#3066] A new 'Planetary Chamber' instrument is in progress that can either simulate the martian surface or the lunar exosphere environments.	Poster Location #666
Martin D. J. P. Duvet L.	<u>ESA's Sample Analogue Curation Facility (SACF), and Expanding ESA's Exploration Sample Analogue Collection (ESA2C)</u> [#2663] ESA's SACF is expanding its collection of simulants to meet demand, and investigating properties of Apollo regolith for the benefit of designing new simulants.	Poster Location #667

Tuesday, March 19, 2019

[T341]

POSTER SESSION I: MISSION AND INSTRUMENT CONCEPTS: MARS

6:00 p.m. Town Center Exhibit Area

Authors (*Denotes Presenter)	Abstract Title and Summary	Poster Location
Sarrazin P. C. Bristow T. F. Blake D. F. Gailhanou M. Chen J. et al.	<u>CheMinX: A Next Generation XRD/XRF for Mars Exploration</u> [#2236] CheMinX is a next generation planetary XRD/XRF instrument for future martian missions, operating on similar principles as the MSL CheMin instrument.	Poster Location #668
Usui T. Fujiya W. Koike M. Miura Y. N. Tachibana S. et al.	<u>Martian Moons Exploration: The Importance of Phobos Sample Return for Understanding the Mars-Moon System</u> [#2388] This paper summarizes the expected characteristics of the returned samples from Phobos and the prospective scientific outcomes from their laboratory analyses.	Poster Location #669
Kameda S. Kato H. Osada N. Ozaki M. Enya K. et al.	<u>Telescopic Camera (TENGOO) and Wide-Angle Multiband Camera (OROCHI) Onboard Martian Moons Exploration (MMX) Spacecraft</u> [#2292] In MMX, the angular resolution of telescopic camera (TENGOO) is ~1 arcsec/pix, and OROCHI is composed of seven independent narrowband cameras.	Poster Location #670
Royer C. R. Bibring J.-P. Hamm V. H. Pilorget C. P. Riu L. R. et al.	<u>The MacrOmega Instrument On-Board MMX, an Ultra-Compact NIR Hyperspectral Imager Based on AOTF Technology: Preliminary Tests on a Breadboard</u> [#2501] Presentation of preliminary results from the R&D campaign performed, in the frame of planetary exploration, on a representative breadboard of the instrument.	Poster Location #671

Koerberl C. Paar G. Barnes R. Gupta S. Traxler C. et al.	<u><i>Planetary Analog Study at the Danakil Depression, Ethiopia, to Test the Visualization Software PRO₃D for Mastcam-Z Instrument on Mars 2020</i></u> [#2226] This report is an update of visualization tests at a terrestrial planetary analog site in northern Ethiopia during field work in January 2019.	Poster Location #672
Chide B. Maurice S. Bousquet B. Jacob X. Mimoun D. et al.	<u><i>The Mars 2020 SuperCam Microphone to Constrain Rock Hardness and LIBS Crater Volume</i></u> [#1411] Acoustic signal associated with the plasma formation during LIBS under Mars atmosphere is studied with regard to the evolution of the laser induced pit volume.	Poster Location #673
Graff T. G. Bhartia R. Beegle L. W. Tran V. D. Weiner R. H. et al.	<u><i>The Calibration Target for the Mars 2020 SHERLOC Instrument</i></u> [#2717] Report on the design, target materials, and status of the calibration target for the SHERLOC instrument on the Mars 2020 rover mission.	Poster Location #674
Dibb S. D. Hardgrove C. J. Gabriel T. S. J. Czarnecki S. M.	<u><i>Influence of Nearby Topography on Passive Neutron Count Rates from the Dynamic Albedo of Neutrons Instrument on the Mars Science Laboratory Rover</i></u> [#2908] Nearby topography has a significant contribution to passive count rates from DAN on MSL and may enhance DAN's ability to measure local H ₂ O in passive mode.	Poster Location #675
Holme E. A. Yoshinaga Y. Chen A. Hurowitz J. A.	<u><i>Data Visualization of Mixed-Phase Iron Samples with the Planetary Instrument for X-Ray Lithochemistry (PIXL)</i></u> [#1222] New algorithm / Optimizes data from / Mixed-phase samples. Yay!	Poster Location #676
Liu Y. Allwood A. Hurowitz J. A. Heirwegh C. M. Elam W. T.	<u><i>Strategy of Investigating Igneous Rocks with the Planetary Instrument for X-Ray Lithochemistry (PIXL) in the Mars 2020 Mission</i></u> [#1768] Present strategies of using the Mars 2020 PIXL to investigate and select igneous samples.	Poster Location #677
Cattani F. Gillot P.-Y. Quidelleur X. Hildenbrand A. Cohen B. A.	<u><i>In-Situ K-Ar Dating on Mars Based on UV-Laser Ablation Coupled with a LIBS-QMS System: Development, Calibration, and Application of the KArMars Instrument</i></u> [#1311] In order to advance the LIBS-QMS approach to dating planetary body, we have selected a set of minerals and developed a new technique for estimating sample mass.	Poster Location #678
Putzig N. E. Diniega S. Byrne S. Calvin W. M. Dundas C. M. et al.	<u><i>Results from the Ice and Climate Evolution Science Analysis Group (ICE-SAG)</i></u> [#2035] Mars ice and climate / How they evolve over time / And why we should care.	Poster Location #679
Meyer M. A. Sefton-Nash E. Beaty D. W. Grady M. M. Haltigin T. et al.	<u><i>Strategies for Optimizing the Scientific Interactions with Returned Martian Samples for the International Scientific Community: Science in Containment</i></u> [#2560] A report from the workshop "Science in Containment" given by the Mars Sample Return (MSR) Science Planning Group.	Poster Location #680
Beaty D. W. Grady M. M. McSween H. Y. Sefton-Nash E. Carrier B. L. et al.	<u><i>The Proposed Scientific Objectives of Mars Sample Return</i></u> [#2573] The scientific objectives for Mars Sample Return as proposed by the International MSR Samples and Objectives Team (iMOST).	Poster Location #681

Tuesday, March 19, 2019

[T342]

POSTER SESSION I: MISSION AND INSTRUMENT CONCEPTS: ASTEROIDS AND SMALL BODIES

6:00 p.m. Town Center Exhibit Area

Authors (*Denotes Presenter)	Abstract Title and Summary	Poster Location
Zhang X. Huang J. Wang T. Huo Z.	<u><i>ZhengHe — A Mission to a Near-Earth Asteroid and a Main Belt Comet</i></u> [#1045] ZhengHe is a two-phase mission targeting a near-Earth asteroid 2016HO ₃ and a main belt comet 133P/Elst-Pizarro.	Poster Location #682

Ishibashi K. Kagitani M. Yamada M.	Kameda S. Hong P. et al.	<u><i>Cameras to Be Installed on the Destiny+ Spacecraft: Telescopic Camera for Phaethon (TCAP) and Multiband Camera for Phaethon (MCAP) [#1758]</i></u> We will report the progress of conceptual studies of the telescopic camera and the multiband camera for the asteroid 3200 Phaethon flyby mission DESTINY+.	Poster Location #683
O'Rourke J. G. Elkins-Tanton L. T. Harrison T. N.	Castillo-Rogez J. Fu R. R. et al.	<u><i>Athena: The First-Ever Encounter of (2) Pallas with a SmallSat [#2225]</i></u> Athena is a proposed SmallSat mission that would perform the first-ever encounter with (2) Pallas, the largest unexplored protoplanet in the main asteroid belt.	Poster Location #684
Fisher K. R.	Graham L. D.	<u><i>Ceres: A Prime Target for Robotic Sample Return and Future Human Exploration [#3062]</i></u> I am Ceres-ious / Let's go get some samples now / Then send some humans.	Poster Location #685
Weert A. M. P. Verheij R. S.	Mulder S. J. Mineur M. T.	<u><i>OCCATOR-Mission [#1637]</i></u> Design for a mission to Ceres.	Poster Location #686
Albers B. Foing B. H.	de Winter B. Molag K.	<u><i>WATER-II Mission Concept: Water Extraction Mission Based on WATER-I and OSIRIS-Rex [#3205]</i></u> Inspired by OSIRIS-REX and Hayabusa2, a group of students from VU Amsterdam propose a water extraction asteroid mission, WATER-II as follow-up to OSIRIS-REX.	Poster Location #687
Kohout T. APEX Team	Wahlund J.-E.	<u><i>Asteroid Prospection Explorer (APEX) CubeSat for Hera Mission [#2680]</i></u> Asteroid Prospection Explorer (APEX) is a 6U CubeSat for Hera spacecraft (ESA) with a set of instruments for a global characterization of the Didymos asteroid.	Poster Location #688
Kueppers M. Carnelli I. Abell P. A.	Michel P. Ulamec S.	<u><i>Hera — The European Contribution to the First Asteroid Deflection Demonstration [#2567]</i></u> Hera is ESA's contribution to the international Asteroid Impact Deflection Assessment (AIDA) cooperation, demonstrating the deflection of a hazardous asteroid.	Poster Location #689
Yokley Z. W. Goldsten J. O. Jun I.	Peplowski P. N. Lawrence D. J. et al.	<u><i>Neutron Spectroscopy on a Metal World: Tailoring the Psyche Neutron Spectrometer [#1295]</i></u> Unique metal world / Emitting many neutrons / Detect the right ones?	Poster Location #690
Lawrence D. J. Cully M. Goldsten J. O.	Burks M. T. Elkins-Tanton L. T. et al.	<u><i>The Psyche Gamma-Ray and Neutron Spectrometer: Update on Instrument Design and Measurement Capabilities [#1554]</i></u> The Psyche gamma-ray and neutron spectrometer (GRNS) will measure the elemental composition of (16) Psyche. The current design of the GRNS is presented.	Poster Location #691
Peplowski P. N. Liebel M. Burks M. T.	McCoy T. J. Beck A. W. et al.	<u><i>Gamma Ray Spectroscopy of Metal-Rich Meteorites: Preparations for the Psyche Gamma Ray Spectroscopy Investigation [#1731]</i></u> Laboratory analysis of gamma ray emissions from metal-rich meteorites guide preparations for the Psyche Gamma Ray and Neutron Spectrometer investigation.	Poster Location #692
Burks M. T. Kim G. B. Lawrence D. J.	Mozin V. V. Heffern L. E. et al.	<u><i>Exploring New Signatures for Determining the Ni/Fe Ratio on (16) Psyche [#1958]</i></u> This work explores gamma ray signatures for determining the Ni/Fe ratio in a metallic body, in preparation for the upcoming mission to the asteroid (16) Psyche.	Poster Location #693
Smith D. E. Mazarico E.	Sun X. Zuber M. T.	<u><i>Asteroid Lidar for Topography, Mapping, and Landing [#1421]</i></u> Investigations of asteroids can provide insight about their properties, their origin, the evolution of our solar system, and potential encounters with Earth.	Poster Location #694
Parker A. H. Durda D. D. Project ESPRESSO Team	Walsh K. J. Nowicki K.	<u><i>Magnetic Grapples for Low-g Anchoring and Multi-Point Asteroid Sample Return [#3111]</i></u> We outline a magnetic anchoring and sample collection system for asteroid surfaces and regoliths, and demonstrate it in relevant gravity and vacuum conditions.	Poster Location #695

Yant M. H. Lewis K. W. Parker A. H. Hörst S. M. McAdam A. C. et al.	<u><i>Project ESPRESSO: Exploration Roles of Handheld LIBS at the Potrillo Volcanic Field</i> [#2645]</u> The use of handheld LIBS is used to evaluate the ability of these field portable instruments to resolve meaningful geochemical trends.	Poster Location #696
Cheng A. F. Rivkin A. S. Chabot N. L.	<u><i>The Double Asteroid Redirection Test (DART): New Developments</i> [#2424]</u> NASA's DART mission will be the first demonstration of asteroid deflection by a kinetic impactor and the first hypervelocity impact experiment on an asteroid.	Poster Location #697
Evans M. E. Westphal A. J. Zolensky M. E. Trevino R. C. Ogilvie R.	<u><i>A Prototype Gateway Interstellar Dust Collector (GIDC)</i> [#1048]</u> Dust from other stars / Collected by the Gateway / Exciting data.	Poster Location #698

Tuesday, March 19, 2019

[T343]

POSTER SESSION I: MISSION AND INSTRUMENT CONCEPTS: EUROPA

6:00 p.m. Town Center Exhibit Area

Authors (*Denotes Presenter)	Abstract Title and Summary	Poster Location
Belgacem I. Schmidt F. Jonniaux G.	<u><i>A New Look at Europa's Photometry in Preparation of the JUICE Mission</i> [#1416]</u> Is equatorial ice penitentes compatible with the surface microtexture as seen by photometry? A new look at Europa's photometry on different regions of interest.	Poster Location #699
Turtle E. P. McEwen A. S. Collins G. C. Daubar I. J. Ernst C. M. et al.	<u><i>The Europa Imaging System (EIS): High-Resolution, 3-D Insight into Europa's Geology, Ice Shell, and Potential for Current Activity</i> [#3065]</u> Cameras to observe / Europa's fractured landscapes / Ice shell mysteries.	Poster Location #700
Zacny K. Sotin C. Howell S. Nagihara S. Tipton M. et al.	<u><i>Reaching Europa's Ocean with Nuclear Powered Thermo-Mechanical Drill</i> [#2048]</u> We present a thermal mechanical drill for penetrating Europa ice and reaching its ocean.	Poster Location #701
Blaney D. L. Hibbitts C. Green R. O. Clark R. N. Dalton J. B. et al.	<u><i>The Europa Clipper Mapping Imaging Spectrometer for Europa (MISE): Using Compositional Mapping to Understand Europa</i> [#2218]</u> The Mapping Imaging Spectrometer for Europa (MISE) on the Europa Clipper Mission is being designed as a high-optical through-put pushbroom imaging spectrometer.	Poster Location #702
Wagstaff K. L. Blaney D. L. Chakraborty S. Chien S. A. Davies A. G. et al.	<u><i>Spectral Anomaly Detection for the Mapping Imaging Spectrometer for Europa (MISE)</i> [#1604]</u> Europa Clipper / To find the unexpected / Analyze onboard.	Poster Location #703
Phillips-Lander C. M. Moore T. Z. Raut U. Molyneaux P. M. Miller M. A. et al.	<u><i>Europa Integrating Cavity Enhanced Raman Spectrometer for Exploration of Icy Worlds (ERSO) Concept</i> [#2992]</u> Our TRL4 Europa integrating cavity Raman spectrometer provides 10 ² –10 ⁶ x enhancement over traditional Raman spectroscopy for organic detection.	Poster Location #704
Phillips C. B. Hand K. P. Cable M. L. Hofmann A. E. Craft K. L. et al.	<u><i>Update on the Europa Lander Mission Concept</i> [#2685]</u> Europa lander / Would search for life's evidence / On an icy moon.	Poster Location #705
Hibbitts C. A. Turtle E. P. Blaney D. L. Paranicas C. P. McEwen A. S. et al.	<u><i>Inferring Salt Composition on Europa by Characterizing Vis-NIR Signatures of Color Centers with Europa Clipper EIS and MISE Instruments</i> [#2804]</u> By combining observations from the Europa Clipper EIS and MISE instruments, salts on the surface of Europa can potentially be robustly identified and mapped.	Poster Location #706

Tuesday, March 19, 2019

[T344]

POSTER SESSION I: MISSION AND INSTRUMENT CONCEPTS: OUTER SOLAR SYSTEM

6:00 p.m. Town Center Exhibit Area

Authors (*Denotes Presenter)	Abstract Title and Summary	Poster Location
Okada T. Iwata T. Matsumoto J. Chujo T. Kebukawa Y. et al.	<u><i>OKEANOS — A Solar Power Sail Mission to a Jupiter Trojan Asteroid and Its Updated Science Mission Proposal</i></u> [#1305] The OKEANOS is a proposed engineering and science mission to rendezvous with and land on a D/P type Jupiter Trojan asteroid using a large area solar power sail.	Poster Location #708
Walker C. C. Kimura J. Gardner A. S.	<u><i>Clues from Above: Topographic Signatures of Icy Surface Dynamics Using Laser Altimetry and Implications for the Ganymede Laser Altimeter (GALA)</i></u> [#3193] We prepare for science returns from the Ganymede Laser Altimeter (GALA) using a combination of modeling and altimetry measurements over floating ice on Earth.	Poster Location #709
McEwen A. S. Turtle E. Kestay L. Khurana K. Westlake J. et al.	<u><i>The IO Volcano Observer (IVO): Follow the Heat</i></u> [#1316] The IVO mission proposal has been re-focused in 2019 towards understanding tidal heating as a fundamental planetary process.	Poster Location #710
Davies A. G. Keszthelyi L. P. McEwen A. S.	<u><i>Determining Lava Eruption Temperature on Io Using Remote Sensing: Techniques, Requirements, and Targets for a New Io Mission</i></u> [#1440] We identify volcanic eruption styles suitable for determining lava eruption temperature remotely. A new Io mission can therefore constrain lava composition.	Poster Location #711
Park R. S. de Kleer K. McEwen A. Bierson C. J. Davies A. G. et al.	<u><i>Tidal Heating: Lessons from Io and the Jovian System (Report from the KISS Workshop)</i></u> [#1925] Summary of the Keck Institute for Space Studies workshop entitled “Tidal Heating: Lessons from Io and the Jovian System,” held on October 15–19, 2018.	Poster Location #712
Vance S. D. Behoukova M. Bills B. G. Cadek O. Castillo-Rogez J. et al.	<u><i>Enceladus Distributed Geophysical Exploration</i></u> [#1749] At Enceladus / Geophysics give context / When searching for life.	Poster Location #713
Tallarida N. R. Edwards P. H. Lanbert J., Hutchinson I. McHugh M. et al.	<u><i>Proton Irradiation Tests of Lasers for Instrumentation on Icy Moon Missions</i></u> [#2178] To prepare for high radiation missions to Europa, two lasers were irradiated with photons. These were characterized, finding little reduction in capabilities.	Poster Location #714
Tallarida N. Schubert W. Lambert J.	<u><i>Isolation, Concentration, and Characterization of Icy Worlds Samples via Flow Cytometry</i></u> [#1471] A sorting flow cytometer can quickly isolate dilute biotic particles from large volumes of mineral-containing sample, improving science output of a mission.	Poster Location #715
Jarmak S. Leonard E. Schurmeier L. Akins A. Cofield S. et al.	<u><i>QUEST: A New Frontiers Uranus Orbiter Concept Study</i></u> [#1621] QUEST is a mission / To study an ice giant / That’s tipped on its side.	Poster Location #716
Mitchell K. L. Prockter L. M. Frazier W. E. Smythe W. D. Sutin B. M. et al.	<u><i>Implementation of Trident: A Discovery-Class Mission to Triton</i></u> [#3200] Triton ‘38 / Discovery enabled / Jupiter assist.	Poster Location #717
Prockter L. M. Mitchell K. L. Howett C. J. A. Smythe W. D. Sutin B. M. et al.	<u><i>Exploring Triton with Trident: A Discovery Class Mission</i></u> [#3188] Neptune’s captured world / Revealed in winter’s cold light / We return next spring?	Poster Location #718
Hartwig J. W. Sagmiller D. C. Colozza A. J. Landis G. A. Oleson S. R.	<u><i>Thermal Design Concerns for the Phase 2 Triton Hopper</i></u> [#1002] NASA is developing a hopper for exploring icy outer planetary bodies of the solar system.	Poster Location #719
Bering E. A. III Giambusso M. Carter M. Squire J. P. Chang-Diaz F. R.	<u><i>Solar Electric Propulsion Missions to Saturn, Neptune, and Beyond</i></u> [#1159] We explore the use of a solar-electric VASIMR® to send a 4000+ kg spacecraft to Saturn or beyond. The VASIMR® dives close to the Sun to access high solar flux.	Poster Location #720

TUES POSTERS

Hedman M. M.	<u><i>Constraining the Surface Ages of Icy Objects in the Outer Solar System with Cosmogenic Lithium, Beryllium, and Boron</i> [#1398]</u> We examine whether a lander on an icy moon could constrain the ages of surface deposits by measuring concentrations of cosmogenic elements.	Poster Location #721
Mesick K. E. Coupland D. D. S. Bartlett K. D. Beckman D. T. West S. T. et al.	<u><i>Elpasolite Planetary Ice and Composition Spectrometer (EPICS): A Low-Resource Combined Gamma Ray and Neutron Spectrometer for Planetary Science</i> [#2875]</u> EPICS is a low-resource combined neutron and gamma ray spectrometer for planetary science enabled by new scintillator and photodetector technologies.	Poster Location #722
Zhang H. Li B. C. Yin J. J. Wang W. G. Huang J. C. et al.	<u><i>Scientific Objectives and Design Concept of the Spectrometers for Proposed Flyby Mission to Main Belt Comet 133p/Elst-Pizarro</i> [#2462]</u> We present the design concept of the visible, near-infrared and thermal infrared spectrometers for a proposed flyby mission to main belt comet 133P/Elst-Pizarro.	Poster Location #723
Mandt K. E. Runyon K. Rymer A. McNutt R. Brandt P. et al.	<u><i>Planetary Science with an Interstellar Probe</i> [#2709]</u> An Interstellar Probe intended to explore the heliosphere can conduct important planetary science investigations enroute to interstellar space.	Poster Location #724
Lisse C. M. McNutt R. L. Brandt P. C. Zemcov M. Poppe A. R. et al.	<u><i>The Potential for Unique and Transformative Observations of the Solar System's Debris Disks from the Interstellar Probe Explorer</i> [#3171]</u> With an Interstellar Probe Explorer Mission flying out to 1000AU in the next 50 years, we will conduct transformative solar system circumsolar dust measurements.	Poster Location #725

Tuesday, March 19, 2019

[T345]

POSTER SESSION I: MISSION AND INSTRUMENT CONCEPTS: ORGANICS

6:00 p.m. Town Center Exhibit Area

Authors (*Denotes Presenter)	Abstract Title and Summary	Poster Location
Cook C. W. Viola D. Byrne S. Drouet d'Aubigny C.	<u><i>Detection Limits for Chiral Amino Acids Using a Polarization Camera</i> [#1774]</u> We assess the potential of the Cold Lightweight Imagers for Europa (C-LIFE) polarimetric imager to quantify amino acid enantiomeric excesses.	Poster Location #726
Acosta-Maeda T. E. Misra A. K. Porter J. Sandford M. Egan M. J. et al.	<u><i>Standoff Compact Color Biofinder Imager for Fast, Non-Contact Detection of Organics and Biological Materials</i> [#1713]</u> The color Biofinder provides photographs and color fluorescence images that can be used to quickly detect biogenics and PAHs, even embedded in water ice.	Poster Location #727
Craft K. L. Van Volkenburg T. Ohiri K. Irons K. Skerritt J. et al.	<u><i>On Chip Desalination of Proteinogenic Amino Acids for In Situ Extraterrestrial Analyses</i> [#2740]</u> Micro-chip design / Desalts amino acids / Next, find life out there?	Poster Location #728
Egan M. J. Misra A. K. Sharma S. K. Acosta-Maeda T. E. Porter J. N. et al.	<u><i>Fluorescence Detection Limits of Organic and Biological Targets Using a Compact Spectrometer from 5 m Distance</i> [#3177]</u> Quantify the limit of detection of biosignatures using a fluorescence spectrometer in order to bound the conditions in which a future mission might find life.	Poster Location #729
Sandford M. W. Misra A. K. Acosta-Maeda T. E. Sharma S. K. Porter J. et al.	<u><i>Detection Limits for Various Molecules of Astrobiological Significance Using a Compact Standoff Raman Spectrometer</i> [#3086]</u> This compact Raman system detected 2.5 μ l of H ₂ O and 2.14 mm ³ of KClO ₃ at 5 meters, and will present the LOD of various samples of astrobiological significance.	Poster Location #730
Walroth R. C. Blake D. F. Sarrazin P. Marchis F. Thompson K.	<u><i>MapX: An In-Situ Mapping X-Ray Fluorescence Instrument for Detection of Biosignatures and Habitable Planetary Environments</i> [#1616]</u> MapX is a full field XRF imager capable of returning element composition information on the 100 μ m scale, revealing evidence of habitability or biosignatures.	Poster Location #731

Wiens R. C. Misra A. K. Sharma S. K.	Gasda P. J. Acosta-Maeda T. E. et al.	<u><i>OrganiCam: A Lightweight Time-Resolved Fluorescence Imager and Raman Spectrometer for Icy World Organic Detection and Characterization</i> [#1629]</u> An instrument for bio-organic detection on icy worlds.	Poster Location #732
Soares C. E. Hoey W. A. Fugett D. A.	Anderson J. R. Ferraro N. W.	<u><i>Spacecraft Induced Molecular Return Flux Considerations fro Icy Moon Missions Targeting Detection of Organics with Mass Spectrometers</i> [#1209]</u> During icy moon flybys, molecular emissions from spacecraft interact with the local exosphere producing molecular return flux to science instruments.	Poster Location #733

Tuesday, March 19, 2019

[T346]

POSTER SESSION I: MISSION AND INSTRUMENT CONCEPTS: SURFACE AND SUBSURFACE EXPLORATION

6:00 p.m. Town Center Exhibit Area

Authors (*Denotes Presenter)	Abstract Title and Summary	Poster Location
Park R. S. Riedel J. E.	<u><i>Advanced Pointing Imaging Camera (APIC) Concept</i> [#1916]</u> APIC is a high-resolution imaging system that simultaneously takes images of targets and star fields with two-axis control capability.	Poster Location #735
Homor F. Gucsik A.	<u><i>The CPT (Charge, Parity, Time) Symmetry Breaking-Based Quantum Optical Telecommunicational Invention and Its Application to the Space and Planetary Sciences</i> [#3211]</u> The CPT (Charge-Parity-Time) symmetry breaking-based telecommunication would be a very useful invention as a telecommunicational tool for the satellites.	Poster Location #736
Maturilli A. Helbert J.	<u><i>What's New at the Planetary Spectroscopy Laboratory (PSL)</i> [#1846]</u> PSL provides reflection, transmission, and emission spectra from UV to FIR (0.2–200 μm) of samples under simulated planetary conditions (T sample 70–1000K).	Poster Location #737
Helbert J. De Vera J. P.	<u><i>Planetary Sample Analysis Laboratory (SAL) at DLR</i> [#1834]</u> DLR will establish over the next four years capabilities for detailed mineralogical and geochemical characterization of material return by sample return missions.	Poster Location #738
Joshua M. Tinetti G. Savini G.	<u><i>Twinkle — a Low-Earth Orbit Visible and Infrared Exoplanet Spectroscopy Observatory</i> [#1388]</u> Twinkle is a small, dedicated satellite for providing high-quality data of exoplanet atmospheres and solar system objects using infrared spectroscopy.	Poster Location #739
Edwards B. Savini G. Lindsay S.	<u><i>Small Bodies Science with the Twinkle Space Telescope</i> [#1578]</u> Twinkle, a space-based telescope, offers the capability to obtain visible and near-infrared spectra of thousands of small bodies (asteroids and comets).	Poster Location #740
Motaghian S. Allender E. J. Cousins C. R.	<u><i>The ExoMars-Like Field Trials (ExoFIT): PanCam Emulator Multispectral Observations</i> [#1539]</u> The ExoFIT trials / Emulates martian missions / Informs ExoMars.	Poster Location #741
Ehlmann B. L. Chen X. Kenyon M.	<u><i>A 2U SWIR-MIR Point Spectrometer for Smallsat and Landed Missions: Enabling Characterization of Solar System Volatiles</i> [#2806]</u> We have prototyped a new 2U SWIR and MIR point spectrometer for small satellite and landed missions requiring capable, low-mass, low-power instruments.	Poster Location #742
Schindhelm R. N. Veto M.	<u><i>A Compact, Low-Power Planetary Imager for Radiometric LWIR and Remote Thermal Imaging</i> [#2825]</u> Ball Aerospace has developed a low size, weight and power instrument for radiometrically calibrated imaging in multiple Long Wave Infrared bands.	Poster Location #743

TUES POSTERS

Núñez J. I. Klima R. L. Murchie S. L. Warriner H. E. Boldt J. D. et al.	<u><i>The Advanced Multispectral Infrared Microimager (AMIM) for Planetary Surface Exploration</i> [#3004]</u> AMIM is a compact instrument for future landed missions that provides spatially-correlated mineralogy and microtexture of rocks and soils at the microscale.	Poster Location #744
Hong J. Romaine S. Kashyap V. Sethares L. Ramsey B. et al.	<u><i>Characterizing Miniature Lightweight X-Ray Optics (MiXO) for Solar System Exploration</i> [#3139]</u> We report the recent progress in the development of Miniature Wolter-I X-ray Optics (MiXO) for solar system exploration.	Poster Location #745
Chide B. Maurice S. Bousquet B. Jacob X. Mimoun D. et al.	<u><i>Focusing a Laser-Induced Breakdown Spectroscopy (LIBS) Telescope with a Microphone</i> [#2296]</u> We demonstrate that it is possible to focalise a LIBS setup by listening to laser sparks.	Poster Location #746
Misra A. K. Acosta-Maeda T. E. Porter J. Sandford M. Sharma S. K. et al.	<u><i>Long Range Remote Raman and LIBS Spectroscopy Using a Compact System with Low Laser Pulse Energy</i> [#1674]</u> We describe a simple two component approach to obtain remote Raman and LIBS spectra of targets from 246 m with 3 mJ/pulse, 532 nm, 1 s detection in daylight.	Poster Location #747
Such P. Lalla E. Gilmour C. Daly M. G.	<u><i>LIBS Shock Wave Deformation Area: Material Redistribution and Mineral Recrystallization</i> [#1650]</u> Terrestrial samples with compositions similar to those of Mars and ureilite meteorites were analyzed in this study.	Poster Location #748
Breitenfeld L. B. Dyar M. D. Tremblay C.	<u><i>Quantification of Mineral Abundances in Binary Mixtures Using Raman Spectroscopy and Multivariate Analysis</i> [#1754]</u> We report a sample library and spectral database of fine-grained mixtures using 38 pure minerals and predict phase abundances using multivariate analysis.	Poster Location #749
Cabrero-Gomez J. F. Fernández M. Colombo M. Escribano D. Gallego P. et al.	<u><i>Raman Laser Spectrometer, a Very Demanding Instrument for Planetary Exploration</i> [#1519]</u> The ESA's ExoMars Raman Laser Spectrometer is a very demanding instrument for next future planetary in-situ exploration missions.	Poster Location #750
Kubitza S. Schröder S. Rammelkamp K. Hagelschuer T. Böttger U. et al.	<u><i>Evaluation of Close-Up Remote cw-Raman Spectroscopy for In-situ Planetary Exploration</i> [#2421]</u> Raman spectroscopy is usually done in a contact geometry or over several meters. This study explores the limits for short distances <20 cm with ambient light.	Poster Location #751
Sobron P. Barge L. Davila A. Fahey M. Krainak M. et al.	<u><i>Programmable Raman Sensing for In-Situ Planetary Exploration</i> [#2760]</u> New compact Raman Spectrometer architecture that enables on-chip, sub-ppb quantitation of molecular compounds.	Poster Location #752
Prettyman T. H. Burger A. Yamashita N. Pearson N. Landis M. E.	<u><i>Progress on the Development and Testing of New Scintillators for Planetary Gamma Ray Spectroscopy</i> [#2143]</u> Scintillators flash / Nonproportional, bright / Elements delight.	Poster Location #753
Sava P. Asphaug E.	<u><i>Orbital Seismology by Laser Doppler Vibrometry</i> [#1709]</u> Seismology on small bodies can be conducted remotely using orbital Laser Doppler Vibrometers, which are cheap, robust, and mobile to provide dense global coverage.	Poster Location #754
Courville S. W. Sava P.	<u><i>Speckle Noise in Orbital Laser Doppler Vibrometry</i> [#1720]</u> For slow orbits around small planetary bodies, we show that a laser Doppler vibrometer can record seismic ground motion on the order of 1 micron per second.	Poster Location #755
Hoza K. M. Rice M. S.	<u><i>An Automated Goniometer System for Reflectance Spectroscopy</i> [#2958]</u> A new automated goniometer enables efficient collection of reflectance spectra for hand samples, slabs, and powders across a wide range of viewing geometries.	Poster Location #756
Carter L. M. Rincon R. F. Lu D. Baker D. M. H. Du Toit C. F. et al.	<u><i>Space Exploration SAR: A Digital Beamforming Synthetic Aperture Radar for Planetary Science</i> [#1706]</u> SESAR is a digital beamforming radar that operates at P-band (435 MHz) with full polarimetry. It will enable exploration of the upper meters of the surface.	Poster Location #757

Amos C. C. Putzig N. E. Perry M. R. Paulsson B. N. P. Thornburg J. et al.	<u><i>Fiber Optic Geophones for Use in Planetary Subsurface Exploration</i></u> [#2623] We propose a fiber optic geophone based on the Fiber Optic Seismic Vector Sensor developed by Paulsson, Inc. for use in planetary active source seismic surveys.	Poster Location #758
Lorenzo J. M. Patterson D. A. Karunatillake S. Weber R. Haviland H. et al.	<u><i>Seismic Characteristics of the Shallow (0–1 m) Soils on the Moon and Mars: Ice in Soils</i></u> [#3246] Piezoelectric sensors and sources may be integrated into lander legs and rover wheels in order to characterize Moon and Mars soils.	Poster Location #759

Tuesday, March 19, 2019

[T347]

POSTER SESSION I: MISSION AND INSTRUMENT CONCEPTS: HUMAN EXPLORATION

6:00 p.m. Town Center Exhibit Area

Authors (*Denotes Presenter)	Abstract Title and Summary	Poster Location
Frank E. A.	<u><i>Questioning the Status Quo in Pursuit of Lowering Planetary Mission Costs</i></u> [#2723] To maximize mission science return, the planetary science community must first change our culture and assumptions regarding how we explore our solar system.	Poster Location #760
Young K. E. Miller M. Graff T. G. Delgado F. Noyes M. et al.	<u><i>Scientific Hybrid Reality Environments (SHyRE)</i></u> [#1109] The Scientific Hybrid Reality Environment project is developing a high-fidelity test environment for advancing human exploration hardware and procedures.	Poster Location #761
Miller M. J. Pittman C. P. Graff T. G. Abercromby A. Norcross J. et al.	<u><i>Scientific Physical and Operations Characterization (SPOC) — Capturing Terrestrial Fieldwork in Context</i></u> [#2120] The SPOC project aims to examine terrestrial scientific field campaigns to inform future human planetary surface extravehicular activity.	Poster Location #762
Leland J. R. Booth S. Crowell J. M. Deran A. Estes N. M. et al.	<u><i>Tycho — A Modern Astronaut Training Vehicle</i></u> [#2133] We are building an astronaut training vehicle; a more technically advanced version of the original Grover used to train Apollo Astronauts.	Poster Location #763
Hadler K. Martin D. J. P. Carpenter J. Cilliers J. J.	<u><i>A Universal Flowsheet and Terminology for In Situ Resource Utilization (ISRU)</i></u> [#2609] ISRU is the future / A framework is required / This is defined here.	Poster Location #764
Sargeant H. M. Abernethy F. Anand M. Barber S. J. Sheridan S. et al.	<u><i>Experimental Development and Testing of the Ilmenite Reduction Reaction for a Lunar ISRU Demonstration with ProSPA</i></u> [#1797] A breadboard model of ProSPA has been built, and ilmenite reduction has successfully been performed in the static system to produce water.	Poster Location #765
Meen J. K. Barker D. C. Martinez M. R. Luna D. Mueller K.	<u><i>In Situ Resource Utilization of Lunar Regolith by Thermal Reduction — A New Look</i></u> [#1652] In oxygen-poor environment, heating a multi-element material can result in step-wise reduction of oxides with complete separation of metals for utilization.	Poster Location #766
Chevrel S. D. Pinet P. C.	<u><i>Apollo Lunar Surface Operations as a Basis for Challenges in Future Human and Robotic Geological Exploration of the Moon</i></u> [#2393] Future exploration of the Moon will benefit from Apollo missions, with improvements, as the in situ study of impact craters represents a big technical challenge.	Poster Location #767
Heemskerk M. V. Daeter M. I. Foing B. H. Gasser M. Feucht C. M.	<u><i>Concept for a Semi-Permanent Moon-Analogue Habitat Inside a Lava Tube</i></u> [#1693] Concept for a moon-analogue lava tube habitat in Iceland, capable of hosting short to midterm duration analogue missions.	Poster Location #768
Hubbard K. M. Elkins-Tanton L. T. Hadfield C.	<u><i>Streamlining a Critical Path to Lunar Settlement</i></u> [#1481] Eight major technology categories for lunar settlement were identified. For each category, a system/tech actor list is being constructed. We welcome your input.	Poster Location #769

TUES POSTERS

Mehta J. Kothandhapani A. Vatsal V. Head J. Shah U.	<u><i>A Sequence for Future Lunar Landings to Enhance Scientific Returns</i> [#1843]</u> Engineering considerations to target high scientific value lunar landing sites in a sequence of technological progression that maximizes scientific returns.	Poster Location #770
Harrington A. D. McCubbin F. M. Kaur J. Vander Kaaden K. E. Smirnov A. et al.	<u><i>Cardiopulmonary Inflammatory Responses to Subacute Meteorite Dust Exposures — Implications for Human Space Exploration</i> [#2891]</u> Strong correlations exist between geochemical features of an array of meteorite dust samples and cardiopulmonary inflammation upon exposure in a rodent model.	Poster Location #771
Battler M. Faragalli M. Reid E. Raimalwala K. Smal E. et al.	<u><i>“Mission Control Software:” Cloud-Based Robotic Control and Communications Software for Distributed Operations of Commercial Lunar Missions and Payloads</i> [#3266]</u> MCS is a cloud-based mission operations tool that will facilitate operation of commercial lunar space-craft (including payloads and rovers).	Poster Location #772
Spedding C. P.	<u><i>Technology Assessment of Lunar Radiation Shield Construction Methods</i> [#1231]</u> Hard systems analysis of prevailing construction methods for lunar habitat radiation and meteorite shield, including thermal and chemical processing techniques.	Poster Location #773
Wani S. C. Shah U. B. Kothandhapani A. Garg P. Sahai M. et al.	<u><i>Requirement Analysis for Night Survival Concept for Lunar Landing Mission Using Fuel Cell</i> [#2389]</u> Duration of solar-powered lunar landing missions are limited. This paper presents a fuel cell based concept to extend mission life by surviving lunar night.	Poster Location #774
Hiesinger H. Landgraf M. Carey W. Karouji Y. Haltigin T. et al.	<u><i>HERACLES: An ESA-JAXA-CSA Joint Study on Returning to the Moon</i> [#1327]</u> HERACLES (Human Enhanced Robotic Architecture Capability for Lunar Exploartion and Science) prepares lunar human missions and science using the lunar Gateway.	Poster Location #775
Osinski G. R. Bourassa M. Cross M. Hill P. King D. et al.	<u><i>A Canadian Science Maturation Study for the Precursor to Human and Scientific Rover (PHASR) as Part of the HERACLES Mission Concept</i> [#2418]</u> We present an overview of the goals, payload, and operations concept for the Precursor to Human and Scientific Rover as part of the HERACLES mission concept.	Poster Location #776
Morse Z. R. Osinski G. R. Bourassa M. Tornabene L. L. Pilles E. et al.	<u><i>Traverse Planning Within Schrodinger Basin in Support of a Canadian Contribution to the Proposed HERACLES Mission</i> [#2886]</u> 'Cross the basin floor / A future rover wanders / Along this planned path.	Poster Location #777
Bourassa M. Osinski G. R. Cross M. Hill P. King D. et al.	<u><i>Development of an Integrated Vision System for the Precursor to Human and Scientific Rover (PHASR) as a Potential Canadian Contribution to the Proposed HERACLES Mission</i> [#2062]</u> Proposed development of an Integrated Vision System that combines a science camera, LiDAR, and imaging spectrometer for a lunar rover sample return mission.	Poster Location #778
Landgraf M. Picard M. Narita S. Whitley R. J.	<u><i>Scientific Opportunities in HERACLES enabled by the Gateway</i> [#1030]</u> The international HERACLES mission will provide significant opportunities in returned sample (15 kg) investigation and in-situ measurements (90kg).	Poster Location #779
Karouji Y. Hiesinger H. Landgraf M. Carrey W. Haltigin T. et al.	<u><i>Scientific Examination of the Lunar Sample Return Mission “Heracles”</i> [#1736]</u> The scientific examination of the Heracles mission is reported. The HERACLES mission is planning a sample return from the Moon.	Poster Location #780
Henson P G.	<u><i>Fox Hunt and Telescope EVAs at the Inflatable Lunar Martian Habitat</i> [#3263]</u> Space suit research is conducted at the Inflatable Lunar Martian Analog Habitat in Grand Forks, ND. These were two EVAs conducted for Mission VI last fall.	Poster Location #781

Gallegos Z. E. Newsom H. E. Scuderi L. A. Edge E.	<u><i>Protonilus Mensae: Continued Analysis of an Exploration Zone on the Northern Planetary Dichotomy of Mars. Prospects for Future Robotic and Human Missions</i> [#3249]</u> The Protonilus Mensae exploration zone is a prime candidate for future mid-latitude missions, including in-situ resource exploration and preparation for humans.	Poster Location #782
Rubinstein H. Sorek-Abramovich R. Shikar A. Zagai M. Nevenzal H. et al.	<u><i>Mars Analogs at Ramon Crater Region: D-MARS</i> [#2813]</u> The Desert Mars Analog Ramon Station: A platform for testing mission concepts, instrumentation, and scientific methods, in a unique geological environment.	Poster Location #783
Visaya B. Day B. Lee P.	<u><i>Noctis Landing, Mars: Concept Vehicular Traverse Paths from a Proposed Human Landing Site and Exploration Zone in West Valles Marineris</i> [#3272]</u> Noctis Landing, a proposed landing site/exploration zone for humans on Mars, would allow access, via vehicular traverses, to many important science targets.	Poster Location #784
Buckner D. K. De Leon P. Anamika F. N. U. Henson P. G.	<u><i>Martian Meteorology: Weather Forecasting EVA from an Analog Martian Habitat</i> [#3149]</u> This poster discusses an autonomous weather monitoring system for martian crews to forecast dust storms with miniature sensors on high altitude balloons.	Poster Location #785
Yano H. Yamamoto K. Minakami E. Eitel M. Sasaki S. et al.	<u><i>Extraterrestrial Material Accretion Rate to the Earth Measured by the Tanpopo Capture Panels Onboard the ISS in 2015–2017</i> [#3155]</u> Tanpopo aerogel and aluminum targets witnessed hypervelocity impacts by meteoroids on ISS in 2015–17 and revised the dust flux to the Earth.	Poster Location #786
John K. K. Saucedo V. L. Fisher K. R. Curiel P. H. Chavalithumrong A. L. et al.	<u><i>Hermes — A New ISS Research Facility for Multiple Regolith Experiments</i> [#3081]</u> Hermes I-S-S / Regolith experiment / Build, launch, and repeat.	Poster Location #787
Own C. S. Martinez J. DeRego T. Own L. S. Weppelman G. et al.	<u><i>Mochii Portable Spectroscopic Electron Microscope on ISS: Progress Toward Flight</i> [#3238]</u> Mochii S is a novel portable SEM with X-ray spectroscopy (EDS) we are preparing for use on ISS. We report on our progress toward mission science and flight.	Poster Location #788

Tuesday, March 19, 2019

[T348]

POSTER SESSION I: MISSION AND INSTRUMENT CONCEPTS: IGLUNA

6:00 p.m. Town Center Exhibit Area

Authors (*Denotes Presenter)	Abstract Title and Summary	Poster Location
Heemskerk M. V. Benavides T. Foing B. H. De Winter B. Daeter M. I. et al.	<u><i>IGLUNA — Habitat in Ice: An ESA Lab Project Hosted by the Swiss Space Center</i> [#2416]</u> IGLUNA is the first ESA_Lab interuniversity demonstrator project, and is hosted by the SSC with the vision to create an analogue habitat inside lunar ice caps.	Poster Location #789
Korthouwer R. B. de Winter B. Heemskerk M. Daeter M. Foing B. H.	<u><i>EuroMoonMars 2018–2019 and VUSE IqLuna: External Exploration of the Moon Village</i> [#2475]</u> The external exploration components of an external lander and drones of the EuroMoonMars 2018/2019 VUSE IGLUNA.	Poster Location #790
de Winter B. Heemskerk M. Clement T. Foing B. Benavides T. et al.	<u><i>VUSE, VU Science Experiments at Igluna, a Science Showcase for a Moon Ice Habitat</i> [#1588]</u> VU Science Experiments (VUSE) is part of IGLUNA, a Moon-ice simulation habitat. VUSE researches the history of the glacier with ice core analysis and field data.	Poster Location #791
van Bloois S, J. de Winter B. Foing B. Heemskerk M. VU Amsterdam Igluna Team	<u><i>VUSE Life Science Experiments: Growing Plants in a Moon-Ice Habitat</i> [#2415]</u> VUSE (VU Science Experiments) to test growing plants under dry and cold conditions for testing the survival of plants inside a glacier.	Poster Location #792

Daeter M. I. Heemskerk M. V. De Winter B. Foing B. H. VU Amsterdam Igluna Team	<u><i>Geology and Astrobiology Instruments Suite for IGLUNA's VU Science Experiments (VUSE) [#2530]</i></u> Application, testing, and instrument definition for the VU Science Experiments (VUSE) IGLUNA team.	Poster Location #793
Beentjes D. de Winter B. Heemskerk M. V. Foing B.	<u><i>Geology and Astrobiology Research and Data Analysis for Igluna [#2614]</i></u> VUSE project is focused on research in/on a glacier: To construct the history of the glacier and to conduct experiments, simulating a moon habitat, with IGLUNA.	Poster Location #794
Vaessen G. C. de Winter B. Heemskerk M. V. Foing B. H.	<u><i>Chemical Sample Analysis for the IGLUNA Project [#2664]</i></u> Description of experiments that can aid the chemical analysis of geological samples for the IGLUNA project.	Poster Location #795
Berg M. J. R. de Winter B. Foing B. H. Heemskerk M. V.	<u><i>Subprojects HCAM, RCAM, FDB, and GHIS from the Igluna Project [#2687]</i></u> The subprojects HCAM, RCAM, FDB, and GHIS are part of the IGLUNA project. This project simulates a habitat on the south pole of the Moon. Collaboration with ESA.	Poster Location #796
Kruijver A. Dingemans A. Foing B. de Winter B. Heemskerk M.	<u><i>Instruments and Power Supply for Igluna, VU Science Experiments [#2869]</i></u> A report on the technical necessities for the scientific instruments and tools used for IGLUNA in Zermatt, Switzerland (June 2019); VUSE Division.	Poster Location #797
Sitnikova A. Sanden G. v.d. Foing B. Benavides T. Grosjean M. et al.	<u><i>Smart Ice Lab, ILEWG — Igluna Project [#2066]</i></u> ILEWG role to facilitate scientific experiments during IGLUNA lunar mission. IGLUNA is the first ESA_Lab interuniversity demonstrator project.	Poster Location #798
Albers B. de Winter B. Heemskerk M. Foing B. IGLUNA Team	<u><i>Igluna Project: Glaciology Research Goals [#1336]</i></u> The IGLUNA project is developing a simulation habitat in ice. In this habitat, scientific research will take place, for example, glaciology.	Poster Location #799

THURSDAY POSTER SESSIONS

Thursday Evening, March 21, 6:00 p.m.

Session	Session Title	Page
R601	Venus, or How I Stopped Worrying and Learned to Love the Second Planet	133
R602	50 Years of Apollo Legacy: Interior to Surface in All Its Glory	134
R603	Lunar Remote Sensing II: Techniques and Advances	136
R604	Lunar Crust: From Micro to Macro Scale	137
R605	Lunar Basalts: From Micro to Macro Scale	139
R606	Advancements in Analytical and Experimental Methods	141
R607	Presolar, Interplanetary, and Cometary Dust	143
R608	Genesis	144
R609	Protoplanetary Disk Evolution and Chronology	145
R610	Chondrites: Refractory Components	146
R611	Space Weathering: From Samples to Spectra and Everything in Between	148
R612	Small Bodies: Physical Characterization and Dynamics	149
R613	Small Bodies: Spectral Characterization and Laboratory Experiments	151
R614	Small Bodies: Missions and Comets	152
R615	Ceres and Vesta	154
R616	Differentiated Meteorites: Howardites, Eucrites, Diogenites	155
R617	Differentiated Meteorites: Ureilites, Aubrites, Angrites, Brachinites, Unique, and Unknown	156
R618	Differentiation of Planets and Asteroids: From Cores to Late Veneers	157
R619	Impacts: From Planetary Formation to Modern Experiments	158
R620	Impacts: Shock Metamorphism and Geochronology	160
R621	Impacts: Mars and Beyond	162
R622	Mars from Orbit: Spectroscopy and Landing Sites	164
R623	Mars from Orbit: Non-Spectral Instruments and Methods	166
R624	MSL: Vera Rubin Ridge Results	167
R625	MSL: Rover Methods	169
R626	Martian Laboratory Results: Formation, Alteration, and Detection of Minerals	170
R627	Mars Geomorphology	171
R628	Planetary Polar Processes and Cryospheres	173
R629	Mars Mud Volcanos: Mud, Mud, Glorious Mud	175
R630	Mars Volcanology	176
R631	Planetary Volcanism: A Song of Fire and Ice	177
R632	Mars Analogs: Volcanic and Hydrothermal Processes	179
R633	Mars Analogs: Sedimentary Processes	180
R634	Mars Analogs: Visible/Near-Infrared Spectroscopy	181
R635	Analogs for the Moon and Other Airless Bodies	183
R636	Planetary Simulants	184
R637	Geologic Mapping Through the Solar System	184
R638	Visualizing Worlds: Planetary Spatial Data and Infrastructure	186
R639	Visualizing Worlds: Moon and Asteroids Spatial Data	187
R640	Visualizing Worlds: Mars Spatial Data and Infrastructure	188

R641	Visualizing Worlds: Outer Planets and Satellites Spatial Data and Infrastructure	190
R642	Biosignatures: To Seek Out New Life	191
R643	Astrobiology Missions and Instrumentation: Boldly Going Where No Spectrometer has Gone Before!	192
R644	Searching for Meteorites in Weird Places	193
R645	Workforce Development, Diversity, and Inclusion	194

THURSDAY POSTER SESSIONS

Thursday, March 21, 2019

[R601]

POSTER SESSION II: VENUS, OR HOW I STOPPED WORRYING AND LEARNED TO LOVE THE SECOND PLANET

6:00 p.m. Town Center Exhibit Area

Authors (*Denotes Presenter)	Abstract Title and Summary	Poster Location
Cheng H. C. J. Webb A. A. G. Michalski J. R. Moore W. B.	<u>Testing Crustal Plateau Formation Models for Venus Using Geological Mapping of Ishtar Terra Marginal Areas</u> [#1332] We perform detailed geological mapping along northern Ishtar Terra margin to test the crustal plateau formation models for Venus.	Poster Location #1
Rader L. X. Thomson B. J. McCanta M. C.	<u>A Review of Surface-Atmosphere Interactions on Venus via Observable Aeolian Features</u> [#2979] A review of Magellan SAR data to quantify aeolian field characteristics on Venus, and to better understand both erosional and depositional surface processes.	Poster Location #2
Bondarenko N. V. Kreslavsky M. A.	<u>Aeolian Deposits on Venus: View from the Analysis of Magellan Radar Altimeter Backscattering Data</u> [#1187] Aeolian deposits signatures derived from Magellan altimeter backscattering data indicate the diversity of plains in age and/or in original lava surface textures.	Poster Location #3
Toner K. Gilmore M. S. Brossier J. F.	<u>Complex Radar Emissivity Variations at Some Large Venusian Volcanoes</u> [#3153] The radar emissivity at large volcanoes varies wildly, indicating different types and volumes of high dielectric minerals in these flows.	Poster Location #4
Jodhpurkar M. J. Whitten J. L. Bailey C. M.	<u>Relationship Between Radar-Bright Areas and Geologic Landforms in Venusian Tesserae</u> [#2570] Tesserae show signs / Other landforms can be dark / Not just ejecta.	Poster Location #5
Wroblewski F. W. Treiman A. H. Bhiravarasu S. S.	<u>Anomalous Radar Properties of Maxwell Montes: Results from Stereo Altimetry</u> [#1702] Maxwell Montes shows a snowline of radar properties appearing at ~5km. With stereo DEMs, either flank of Maxwell shows new radar structure with elevation plots.	Poster Location #6
Wroblewski F. W. Treiman A. H. Bhiravarasu S. S. Gregg T. K. P.	<u>Ovda Fluctus, the Festoon Lava Flow on Ovda Regio, Venus: Most Likely Basalt</u> [#1699] Evaluating several properties affecting the rheology of Ovda Fluctus, the available data suggest it is a basaltic flow and not a silica-rich flow.	Poster Location #7
Lee J. Ernst R. E. Samson C. Cousens B.	<u>Emplacement of the Henwen Flow Field, Venus</u> [#2224] Insights into the emplacement of the Henwen Flow Field, Venus, using detailed geological mapping of lava flows and associated fracture systems.	Poster Location #8
Perkins R. P. Gilmore M. S.	<u>Volumes and Potential Origins of Crater Dark Floor Deposits on Venus</u> [#2032] Plains embayment of / Venus' craters, or melt from / Impacts? You decide!	Poster Location #9
Filiberto J. Trang D. Treiman A. H. Gilmore M. S.	<u>Weathering on Venus: The Effect of Oxidation on the VNIR Spectra of Olivine</u> [#1062] Surface of Venus / Obscured from view by clouds / And oxide coatings.	Poster Location #10
Teffeteller H. McCanta M. Cherniak D. Treiman A. Filiberto J. et al.	<u>Experimental Study of the Alteration of Basalt on the Surface of Venus</u> [#1858] Preliminary results from laboratory experiments on alteration of basalts under P, T, and atmospheric compositions similar to those at the Venus surface.	Poster Location #11
Santos A. R. Lewis J. A. McCubbin F. M. Nakley L. M. Phillips K. et al.	<u>Experimental Investigation of Granite and Basalt Weathering on Venus</u> [#2579] Secondary iron sulfides were observed to form from iron-bearing minerals within basalt and granite when exposed to Venus surface-like conditions in experiments.	Poster Location #12

THURS POSTERS

Port S. T. Briscoe A. C. Chevrier V.	<u><i>The Stability of Pyrrhotite at Venusian Conditions</i> [#2549]</u> The stability of pyrrhotite (Fe ₇ S ₈) was tested for 24 to 96 hours in a simulation chamber at Venus temperatures and pressures in CO ₂ .	Poster Location #13
Lessis M. Izenberg N. R. Osiander R.	<u><i>Simulating Venus with AVEC: The APL Venus Environment Chamber</i> [#1084]</u> Laboratory / Study Venus with AVEC? / Oui, we show you how.	Poster Location #14
Karimi S. Ojha L. Perera V. Lewis K.	<u><i>A New Assessment of Venusian Impact Crater Shapes</i> [#3219]</u> In this study we simulate impacts of various sizes and determine the initial shape of Venusian craters.	Poster Location #15
Dudek M. J. McGary R. S.	<u><i>Constraining the Age of Crustal Resurfacing on Venus Using a Theoretical Crater Size-Frequency Distribution</i> [#3150]</u> We extrapolated a range of likely impactors from a lunar CSFD, and migrated them to Venus to get a theoretical CSFD and compare it to the present-day surface.	Poster Location #16
Fang J. Tian W. Wang L. Fa W. Liu X.	<u><i>Modeling of Steep-sided Dome Formation on Venus</i> [#1528]</u> Modeling based on Bingham fluid dynamics shows Venusian steep-sided domes are formed mainly by acidic lava at effusion rates much higher than terrestrial ones.	Poster Location #17
McGovern P. J. Buz J.	<u><i>Self-Consistent, Lithospheric Stress-Modulated Growth of Large Volcanic Edifices on Venus: Scenarios for Creation of Conical and Domical Edifices, and Several Different Topographic Groups of Coronae</i> [#2805]</u> Second world's ringed hills / Not just shoved up from below / Also grown on top.	Poster Location #18
Russell M. B. Johnson C. L.	<u><i>Lithospheric Flexure Modeling at Narina Tholi: Evidence for a Locally Thinned Lithosphere</i> [#2896]</u> A surface so thinned / With Narina dome perched, sags / How thin? She reveals.	Poster Location #19
Jessup K.-L. Marcq E. Bertaux J.-L. Mills F. P. Limaye S. et al.	<u><i>Impact of Topography on Venus' Cloud Top Properties as Observed by HST</i> [#2728]</u> The 2010/2011 HST Venus cloud top spectra reveal the impact of local solar time and topography on large- and small-scale transport processes and the albedo.	Poster Location #20
Green J. A. M. Way M. J. Barnes R.	<u><i>Ocean Tides and Rotation Rates: Applications to Venus and Exoplanet Worlds</i> [#2315]</u> Tidal simulations of an ancient Venusian ocean show tides comparable to Earth's tides today, with the potential to alter the rotational period by five days/Myr.	Poster Location #21
Ma Y. J. Toth G. Nagy A. F. Russell C. T.	<u><i>The Formation and Evolution of Large Scale Magnetic Fields in Venus Ionosphere</i> [#2903]</u> In this study, we use a multi-species MHD model to understand the formation and evolution of large scale magnetic fields in Venus ionosphere.	Poster Location #22
Izenberg N. R. Dyar M. D.	<u><i>VEXAG Venus Exploration Documents 2019 Update</i> [#1083]</u> #BacktoVenus with / Revised goals, roadmap, tech plan / Your input needed.	Poster Location #23

Thursday, March 21, 2019

[R602]

POSTER SESSION II: 50 YEARS OF APOLLO LEGACY: INTERIOR TO SURFACE IN ALL ITS GLORY

6:00 p.m. Town Center Exhibit Area

Authors (*Denotes Presenter)	Abstract Title and Summary	Poster Location
Williams D. R. Hills H. K. Taylor P. T. Nagihara S. Nakamura Y. et al.	<u><i>The Apollo Surface Experiment Packages: 50 Years of Science and Counting</i> [#1122]</u> The Apollo 11 EASEP station was the forerunner of a set of six long-lived Apollo surface stations. Data from these stations are still being restored and used.	Poster Location #25
Phillips D. Weber R. C.	<u><i>Thermal Moonquake Location Algorithm and Analysis</i> [#1747]</u> Plenty of moonquakes / Produced by thermal changes / Location unknown.	Poster Location #26

Yamamoto Y. Yamada R. Ishihara Y. Nakamura Y. Ishikawa H.	<u><i>Apollo Seismic Data Analysis in Python: ObsPy Module and Response Function</i> [#2492]</u> The decoding Apollo seismic data is a heavy task. We extended an analysis tool: ObsPy to support Apollo seismic data.	Poster Location #27
White M. Siegler M. A.	<u><i>Apollo Lunar Heat Flow Experiment: An Evaluation of Potential Causes of Subsurface Temperature Drift</i> [#2634]</u> We model lunar subsurface temperatures to understand observed temperature drift in newly restored Apollo 15 and 17 data sets.	Poster Location #28
Dhingra D. Patidar S. Ghosal D.	<u><i>Near Surface Expression of Linear Gravity Anomalies (LGAs): Potential Clues and Implications for Emplacement</i> [#3204]</u> Clues to the magma below / Playing peek-a-boo / Hey! / Floor-fractured craters are there / See that through!	Poster Location #29
Lau H. C. P. Carroll K. A.	<u><i>Tidal Tomography to Probe the Moon's Mantle Structure Using Lunar Surface Gravimetry</i> [#3117]</u> Lunar surface gravity measurements can detect the Moon's elastic response to tidal forcing, probing the Moon's deep interior structure.	Poster Location #30
Qiao L. Head J. W. Ling Z. Wilson L.	<u><i>Exploring a Sub-Classification Scheme for Irregular Mare Patches (IMPs)</i> [#2358]</u> We get an updated catalog of 81 IMP occurrences and present a preliminary classification scheme for the geologic settings and characteristics of all IMPs.	Poster Location #31
Stopar J. Watters T. Petro N. Morgan G. Lawrence S. et al.	<u><i>New Discoveries and Objectives of the Lunar Reconnaissance Orbiter's Extended Mission: Volcanism and Interior</i> [#1927]</u> As LRO approaches its 10th year of discovery, key questions about volcanic, tectonic, and interior processes are addressed via multi-instrument investigations.	Poster Location #32
McBride M. J. Bennett K. A. Gaddis L. R. Horgan B. H. N. Glaspie L. M.	<u><i>Volcanic Glass Distribution and Potential Source Vents for the Taurus-Littrow Pyroclastic Deposit at the Apollo 17 Landing Site Region</i> [#3039]</u> The Taurus-Littrow / Volcano: Rima Carmen / Is NOT the source vent.	Poster Location #33
Thesniya P. M. Rajesh V. J. Juda Benhur I. S.	<u><i>Evidences for Late Stage Volcanic Activity from the Ohm Crater on the Farside of the Moon</i> [#2624]</u> The present study investigates distinct morphological features in the Ohm Crater on the farside of the Moon.	Poster Location #34
Chen Y. Head J. W. Li C. L. Kreslavsky M. Wilson L. et al.	<u><i>The Role of Pre-Existing Topography in Modulating Lunar Lava Flow Widths, Depths, and Channel Structure: An Example of an Eratosthenian Lava Flow in Mare Imbrium (Part 1-Observations)</i> [#2182]</u> A well-preserved young lava flow in Mare Imbrium was chosen to document the effects of pre-existing topography on constructing lava flow geometry and structure.	Poster Location #35
Chen Y. Head J. W. Li C. L. Liu J. J. Ren X.	<u><i>Source Regions of Young Lava Flows in Southwest Mare Imbrium: Characterization of the Euler and Lambert Regions</i> [#2942]</u> We characterize volcanic features around crater Lambert to speculate their volcanic processes and assess the implications for the nature of source regions.	Poster Location #36
Stooke P. J.	<u><i>Lunar Wreaths — Unusual, Apparently Young, Mare Landforms</i> [#1009]</u> Wreaths are roughly circular mare features 1 to 3 km across, with wrinkled surfaces, flat to slightly raised rims, and depressed floors and low crater densities.	Poster Location #37
Ravi S. Robinson M. S.	<u><i>Lunar Floor-Fractured Craters: A Case for Viscous Relaxation</i> [#2677]</u> We present evidence for viscous relaxation caused by thermal anomalies as a formation mechanism for a subset of lunar floor-fractured craters.	Poster Location #38
Pathak S. Bhattacharya S. Chauhan M. Gupta S. Panigrahi M. K.	<u><i>Compositional and Morphological Study of Class-5 Lunar Floor-Fractured Crater Arzachel</i> [#1193]</u> In this study, an attempt has been made to infer the compositional variability in the spatial context within the Arzachel Crater.	Poster Location #39
Pathak S. Bhattacharya S. Chauhan M. Gupta S. Panigrahi M. K.	<u><i>Geological Investigation of Class-3 Lunar Floor-Fractured Crater Thebit</i> [#1192]</u> In this study, we have conducted spectral vis-à-vis morphological analyses of a class-3 lunar floor-fractured crater, Crater Thebit.	Poster Location #40

Giguere T. A. Lemelin M.	Gillis-Davis J. J.	<u><i>Cryptomare Mineralogy and Lava Lake Processes within the Gassendi Crater</i></u> [#2325] Lunar lava lakes / Once graced Gassendi crater / Terraces preserved.	Poster Location #41
Robertson K. M. Pieters C. M.	Milliken R. E. Isaacson P.	<u><i>Textural and Compositional Considerations for Mapping Ilmenite on the Lunar Surface Using VIS-NIR Reflectance Spectroscopy</i></u> [#2513] Here we demonstrate how ilmenite textural and composition affect the spectral properties of Apollo 17 high-Ti lunar basalts at VIS-NIR wavelengths.	Poster Location #42
Pinet P. C. Daydou Y. H.	Chevrel S. D.	<u><i>Reassessing the Relationship Between Olivine Composition and Reflectance Spectroscopy from Advanced MGM Deconvolution</i></u> [#1806] The behavior of the olivine absorptions near 1 micron is revisited with an advanced MGM analysis to determine olivine composition from reflectance spectroscopy.	Poster Location #43
Zhao Y. Guttenberg N. van Westrenen W.	Laneuville M.	<u><i>Inferring Global Patterns of Lunar Surface Mineralogy from Elemental Abundance Data Using Artificial Neural Networks</i></u> [#3144] We use artificial neural networks to infer global patterns of lunar surface mineralogy using elemental abundance data.	Poster Location #44
Sun L. Zhang J.	Lucey P. G. Chen J. Ling Z.	<u><i>Deriving Abundances and Chemistries of Minerals with Radiative Transfer Modeling</i></u> [#2905] We built a new model with radiative transfer theory to derive abundances and chemistry of lunar minerals, then validate this model with LSCC lunar soil data.	Poster Location #45
Boivin A. L. Tsai C. Daly M. G.	Hickson D. C. Ghent R. R.	<u><i>Systematic Broadband Complex Permittivity Measurements of Ilmenite-Bearing Lunar Analog Materials</i></u> [#2104] In order to constrain the effects of ilmenite content on radar and microwave signals on the Moon, we measure the permittivity of ilmenite-bytownite mixtures.	Poster Location #46
Deutsch A. N. Head J. W.	Neumann G. A. Lucey Paul G.	<u><i>Investigating Diurnal Changes in the Normal Albedo of the Lunar Surface at 1064 nm: A New Analysis with the Lunar Orbiter Laser Altimeter</i></u> [#1151] We study how the surface reflectance of the Moon changes as measured from orbit by LOLA during extreme temperature fluctuations experienced during a lunar day.	Poster Location #47

Thursday, March 21, 2019

[R603]

POSTER SESSION II: LUNAR REMOTE SENSING II: TECHNIQUES AND ADVANCES

6:00 p.m. Town Center Exhibit Area

Authors (*Denotes Presenter)	Abstract Title and Summary	Poster Location	
Boyd A. K. Robinson M. S.	<u><i>LROC NAC Global Photometry: Terrain Types and Phase Curves</i></u> [#1992] A new photometric function is used to investigate surface properties for a range of maturity and compositionally diverse regions.	Poster Location #49	
Martin A. C. Speyerer E. J. Boyd A. K. Robinson M. S.	<u><i>Examining Surface Properties with Robust Photometric Sequences</i></u> [#2752] Photometric image sequences derived from a series of LROC NAC observations provide unique information for understanding surface properties on the Moon.	Poster Location #50	
Barker M. K. Smith D. E. Zuber M. T.	Mazarico E. Sun X. et al.	<u><i>Photometric Properties of the Moon with the Lunar Orbiter Laser Altimeter (LOLA)</i></u> [#2598] LOLA passive radiometry continues to provide a unique global view of the spatially resolved near-infrared phase function behavior of the Moon.	Poster Location #51
Barker M. K. Smith D. E. Zuber M. T.	Mazarico E. Sun X. et al.	<u><i>Measuring Photometric Surface Roughness with the Lunar Orbiter Laser Altimeter (LOLA)</i></u> [#2572] The Lunar Orbiter Laser Altimeter (LOLA) Laser Ranging (LR) system can make unique measurements of photometric surface roughness at phase angles > 120 deg.	Poster Location #52

Raut U. Karnes P. L. Retherford K. D. Poston M. Davis M. W. et al.	<u><i>Far-Ultraviolet Photometric Response of Mare and Highland Apollo Soils: Laboratory Investigations in Support of LRO-LAMP Observations</i></u> [#3132] We present results on FUV photometric response of mare and highland Apollo soils. The soils are strong absorbers, but presents different scattering anistropy.	Poster Location #53
Sim C. K. Kim S. S. Hong S. A. Jeong M.	<u><i>Estimating Maximum Polarization of Lunar Surface from Observations with Limited Phase-Angle Coverage</i></u> [#1721] Polarization phase curve of the lunar surface can be fitted with a simpler formula even when the observational data were obtained at limited phase-angles.	Poster Location #54
Nagori R. Dagar A. K.	<u><i>BRDF Computation Over Lunar Surface Using Multi-View TMC/Chandrayaan-1 Images</i></u> [#1191] Bi-directional Reflectance Distribution Function (BRDF) has been calculated on per pixel basis over a selected lunar site using TMC/Chandrayaan-1 images.	Poster Location #55
Lemelin M. Daly M. Deliège A.	<u><i>Investigating Lunar 2-Dimensional Topographic Properties at Different Spatial Scales Using Lunar Orbiter Laser Altimeter Data and the Wavelet Leaders Method</i></u> [#2457] We identify three topographic scaling regimes on the Moon using LOLA topographic data and the Wavelet Leaders Method.	Poster Location #56
Kornienko Yu. V. Dulova I. A. Bondarenko N. V.	<u><i>Optimal Surface Relief Retrieval from the Set of Photometric and Altimeter Data</i></u> [#1125] The statistical approach allows calculation of the most probable surface relief consistent with source images and altimeter data.	Poster Location #57
Wagner R. V. Robinson M. S.	<u><i>3D Modeling of Lunar Pit Walls from Stereo Images</i></u> [#2138] We created 3D models of the interiors of four lunar mare pits, and used them to calculate overhangs and mare flow unit thicknesses.	Poster Location #58
Modiriasari A. Boener A. Theinat A. K. Bobet A. Melosh H. J. et al.	<u><i>Effect of Induced Seismicity of Indirect Meteorite Impacts on the Stability of Lunar Lava Tubes</i></u> [#2862] Induced seismicity from indirect meteorite impacts is modeled and will be used to analyze stability of lava tubes under effects of the induced seismicity.	Poster Location #59
Bickel V. T. Lanaras C. Manconi A. Loew S. Mall U.	<u><i>Lunar Rockfall Detection and Mapping Using Deep Neural Networks</i></u> [#1595] A Deep Neural Network is implemented to automatically detect and map lunar rockfalls in Narrow Angle Camera imagery, allowing to produce a global rockfall distribution map.	Poster Location #60
Kim J. Sim C. K. Kim S. S. Jin H.	<u><i>Evaluation of lucky imaging algorithm for lunar observations</i></u> [#2814] This presentation describes the results of the lucky imaging algorithm evaluation for the processing of lunar polarized observation image.	Poster Location #61
Shukla S. Kumar S. Tolpekin V. A.	<u><i>Advancing to Lunar Lava Tube Sensing: A New Radar Perspective of Philolaus Skylight Candidates</i></u> [#2283] Behavior of Philolaus lava tube skylights towards the interaction of EM wave, thereby characterizing potential water-ice deposits near prospective candidates.	Poster Location #62
Bhiravarasu S. S. Rivera-Valentín E. G. Taylor P. A. Patterson G. W. Neish C. D. et al.	<u><i>Radar Circular Polarization Ratio Characteristics of Lunar Terrain as a Function of Viewing Geometry</i></u> [#2742] We examine the variations in radar scattering properties of some lunar terrains as a function of viewing geometry of the radar observations.	Poster Location #63

Thursday, March 21, 2019

[R604]

POSTER SESSION II: LUNAR CRUST: FROM MICRO TO MACRO SCALE

6:00 p.m. Town Center Exhibit Area

Authors (*Denotes Presenter)	Abstract Title and Summary	Poster Location
Robinson K. L. Lemelin M. Crites S. T.	<u><i>The Search for Rock: Hunting Rare Lithologies with High-Resolution Global Lunar Mineral Maps</i></u> [#2956] Kaguya finds / Meteorite source / Apollo too.	Poster Location #64

Zhou Q. Zhang G. L. Zhu X. Y. Zhang X. X. Xiong Y. Y. et al.	<u><i>Petrography and Mineralogy of Northwest Africa 8687</i> [#2372]</u> NWA 8687 is a troctolitic lunar meteorite collected from the Northwest African desert in 2014. Here, we presented the petrological and mineralogical studies of NWA 8687.	Poster Location #65
Cernok A. Anand M. White L. Darling J. Whitehouse M. et al.	<u><i>A Young Impact Event Recorded by Phosphates in 78235 and 78236 Norites</i> [#2228]</u> A young ~500 Ma impact event is recorded by Pb-Pb ages of phosphates in 78235 and 78236 norites. Nm-scale investigation indicate Pb-loss along subgrain boundaries.	Poster Location #66
Nelson W. S. Hammer J. Shea T. Hellebrand E. Taylor G. J.	<u><i>Diffusion Chronometry Applied to Plagioclase in Troctolite 76535 to Resolve Magmatic Cooling History</i> [#2227]</u> Diffusion chronometry is applied to plagioclase in lunar troctolite 76535. This permits for constraints on the early cooling history of this important sample.	Poster Location #67
Lunning N. G. Gross J.	<u><i>Lunar Feldspathic Regolith Breccia with Magnesium-Rich Components: Northwest Africa 11303</i> [#2407]</u> Many lithic clasts with Mg-rich olivine and pyroxene plus some curiously textured clasts, in a low KREEP lunar meteorite.	Poster Location #68
Pernet-Fisher J. F. Clay P. L. Burgess R. Joy K. H.	<u><i>Halogen (Cl, Br, I) Systematics of Lunar Ferroan Anorthosites: Evidence for Sub-Chondritic Lunar Volatiles</i> [#1402]</u> Halogen systematics of lunar anorthosites display evidence that the lunar magma ocean had a sub-chondritic halogen composition.	Poster Location #69
Torcivia M. A. Neal C. R.	<u><i>Analysis of Plagioclase-Pyroxene Partition Coefficients in Ferroan Anorthosites: Determining Co-genetic Relationships</i> [#1883]</u> Plag and pyroxene / Relationships are unclear? / Compare D-values.	Poster Location #70
Torcivia M. A. Neal C. R.	<u><i>Are Ferroan Anorthosites Derived from the Lunar Magma Ocean? Exploring the Petrology of the Youngest FAN 62236</i> [#2536]</u> 62236 / LMO product or not? / The Moon's youngest FAN.	Poster Location #71
Park J. Nagao K. Nyquist L. E. Herzog G. F. Choi J. et al.	<u><i>Noble Gas Studies of Lunar and Enstatite Meteorites</i> [#2272]</u> We report noble gas studies of lunar meteorites, MIL 090034, 090036, 090070, together with enstatite meteorites. PCA is promising for Xe isotope investigation.	Poster Location #72
Tremblay M. M. Mark D. F. Carter J. N. Cohen B. E. Robinson A. et al.	<u><i>Thermal Evolution of Lunar Feldspathic Breccias Constrained by ⁴⁰Ar/³⁹Ar Thermochronology</i> [#1828]</u> Lunar rocks get hot / But when are they hot, or not? / Argon will tell all.	Poster Location #73
Brum J. McLeod C. Gawronska A. Shaulis B. Duley M. et al.	<u><i>Early Lunar Chronology: Insights from Allan Hills (ALHA) 81005 Meteorite</i> [#2012]</u> Examining clasts within ALHA 81005 to understand crystallization and impact history of the Moon using U-bearing minerals to perform in-situ U-Pb techniques.	Poster Location #74
Hidaka Y. Yamaguchi A. Ebihara M.	<u><i>Geochemical Study of Feldspathic Lunar Meteorites Dho 307, 309, 908, and Dho 733</i> [#2394]</u> Chemical compositions of Dho 307, 309, 908, and Dho 733 are determined and are compared with literature data to evaluate the representativeness of our data.	Poster Location #75
Gu X. Chen J. Cao H. Ling Z. Fu X.	<u><i>Petrography and Mineralogy of Lunar Fragmental Breccia Dhofar 910</i> [#2367]</u> In this work, we report preliminary characterization of petrography and mineral compositions of Dhofar 910.	Poster Location #76
Cao H. J. Ling Z. C. Chen J. Fu X. H.	<u><i>Mineralogy and Petrography of Lunar Feldspathic Breccia Northwest Africa 11460</i> [#2359]</u> We present preliminary results on the mineralogy and petrography of NWA 11460, focusing on the shock metamorphism and potential source of individual lithic clasts.	Poster Location #77
Huidobro J. Aramendia J. Ruiz-Galende P. Torre-Fdez I. Madariaga J. M.	<u><i>Raman Spectroscopy on the New Northwest Africa 11273 Lunar Meteorite to Understand the Initial Impact and the Final Terrestrial Weathering</i> [#2476]</u> Raman spectra of zircon allow us to estimate the impact pressure that created the NWA 11273 meteorites as 20 GPa. Calcite and hematite are Earth weathering compounds.	Poster Location #78

Schonwald A. R. Hahn T. M. Jr. Watkins R. M. Jolliff B. L.	<u><i>Correlating NIR Spectra and LROC NAC Photometric Data at Sites of Direct Plagioclase Detection</i> [#1239]</u> We use NIR spectra and LROC NAC photometric data to investigate the extent and purity of anorthosite and rock type variation at five sites on the lunar far side.	Poster Location #79
Philpotts J. A.	<u><i>Evolution of the Moon in Light of Europium Anomalies and Abundances of Lanthanide and Other Lithophile Trace Elements in Apollo Returned Lunar Samples</i> [#1198]</u> Continuing research on lunar evolution in terms of Apollo sample REE abundances and Eu anomalies, and lithophile trace element composition of the Moon.	Poster Location #80
Togashi S. Kita N. T. Tomiya A. Morishita Y.	<u><i>Magmatic Evolution Estimated from Trace Elements in Plagioclase from Procellarum KREEP Terrane Breccias</i> [#1390]</u> The high-Ba and -Ti host magma from plagioclase in the PKT can evolve from cBSM (crustal-component-enriched BSM), and may represent a composition of urKREEP.	Poster Location #81
O'Brien H. C. Robinson K. L. Kring D. A.	<u><i>Petrologic Context of Phosphate Minerals in Apollo 14 Samples</i> [#2159]</u> We studied the petrologic context of phosphate and zircon minerals in three Apollo 14 breccias: 14303,209; 14314,10; and 14306,60.	Poster Location #82

Thursday, March 21, 2019

[R605]

POSTER SESSION II: LUNAR BASALTS: FROM MICRO TO MACRO SCALE

6:00 p.m. Town Center Exhibit Area

Authors (*Denotes Presenter)	Abstract Title and Summary	Poster Location
Beaulieu K. R. Blumenfeld E. H. Thomas A. B. Liddle D. A. Oshel E. R. et al.	<u><i>Visualization of Fused Structure from Motion and Micro X-Ray Computed Tomography Data Sets for Novel 3D Virtual Astromaterials Samples Collection of NASA's Apollo Lunar and Meteorite Samples</i> [#2877]</u> This abstract documents new processes developed to fuse and visualize photography-based and X-ray CT data of Lunar Sample 79115,0.	Poster Location #83
Gawronska A. J. McLeod C. L. Blumenfeld E. H. Hanna R. Zeigler R. A.	<u><i>Preliminary Analyses of Apollo 15 Sample 15085 via X-Ray Computed Tomography</i> [#1660]</u> We examine the utility of X-ray computed tomography to non-destructively analyze the internal components of Apollo samples in 3D.	Poster Location #84
Gawronska A. J. McLeod C. L.	<u><i>Basalts: Insights into Planetary Magmatic Processes from the Moon and Earth</i> [#3271]</u> Basaltic magmatism on the Earth and Moon is considered.	Poster Location #85
Xue Z. Q. Cronberger K. A. Xiao L. Neal C. R.	<u><i>Quantitative Textural Analysis of Ilmenite in Apollo 11 High-Ti Basalts</i> [#2466]</u> Crystal size distribution (CSD) analysis of ilmenite in different Apollo 11 and 17 high-Ti lunar basalt types.	Poster Location #86
Stu Webb Neal C. R. Gawronska A. Day J. M. D.	<u><i>Crystal Size Distribution Patterns for Lunar Meteorites Northwest Africa 12008, 4898, 8632, 3136 and Four LaPaz Icefield Lunar Meteorites</i> [#2686]</u> Crystal size distributions of plagioclase and olivine in several lunar meteorites.	Poster Location #87
Cronberger K. Neal C. R.	<u><i>KREEP Basalt Petrogenesis</i> [#2453]</u> The KREEPy rocks form / They melt 1 mix 2 make 3 / Pure and-or impact.	Poster Location #88
Cronberger K. Neal C. R.	<u><i>KREEP Basalt 15382: Not as Pristine as Originally Thought</i> [#2444]</u> This pristine Moon rock / Hidden remelting confirmed / New KREEP on the edge.	Poster Location #89
Kuhn de Chizelle J. Ross D. K. Boyce J. W.	<u><i>Electron Beam Damage in Apatite: Limitations for SKa Measurements of S⁶⁺/ΣS</i> [#1298]</u> This research aims to test the viability of the electron probe for sulfur speciation measurements in apatites.	Poster Location #90

THURS POSTERS

Chen J. Jolliff B. L. Korotev R. L. Wang K. Wang A. et al.	<u><i>Northwest Africa 10985: A New Lunar Gabbro?</i></u> [#2463] We studied compositional and mineralogical characteristics of NWA 10985, to address whether this new gabbro-rich sample is another member of the NWA 773 clan.	Poster Location #91
Gargano A. M. Sharp Z. D. Shearer C. K.	<u><i>Halogen Isotope Geochemistry of Lunar Materials</i></u> [#1891] We measure the halogen contents and chlorine isotope compositions of lunar materials to better understand the mechanisms of volatile loss from the Moon.	Poster Location #92
Cohen M. E. Kuehner S. M. Tepper J. H. Burney D. C. Neal C. R. et al.	<u><i>Mineralogy and Bulk Composition of Lunar Mare Basalt Northwest Africa 12008</i></u> [#2508] This low-Ti mare basalt meteorite has compositional similarities to the NNL clan meteorites, but differs from returned lunar samples.	Poster Location #93
Carpenter P. K. Jolliff B. L. Korotev R. L. Tepper J. H. Irving A. J. et al.	<u><i>Quantitative EPMA Compositional Mapping of Lunar Mare Basalt Breccia Northwest Africa 12384</i></u> [#2148] Quantitative EPMA compositional mapping of a basalt clast in lunar mare basalt breccia Northwest Africa 12384. Methods will be discussed.	Poster Location #94
Carpenter P. K. Jolliff B. L. Korotev R. L. Tepper J. H. Irving A. J. et al.	<u><i>Petrology and Bulk Composition of Lunar Mare Basalt Breccia Northwest Africa 12384</i></u> [#2125] We present an overview, clast locator map, and bulk and mineral chemistry for recently found meteorite Northwest Africa 12384, a lunar mare basalt breccia.	Poster Location #95
Shearer C. K. Petro N. Papike J. Goossens S. Kendall J. et al.	<u><i>Revisiting the Luna Mission Basalts Within the Context of Recent Orbital Observations</i></u> [#2515] We place the basalts collected by the Luna missions within the context of remotely sensed mineral, chemical, and geophysical data and basin-forming modeling.	Poster Location #96
Nyquist L. E. Shih C.-Y. Park J. Herzog G. F.	<u><i>Implications for Lunar History from Ancient Basalts of the Secondary Crust</i></u> [#1086] Ancient ages => 4.3 Ga for some basaltic lunar meteorites show that these basalts carry important information about derivation of the secondary lunar crust.	Poster Location #97
Tian Z. Chen H. Korotev R. L. Koefoed P. Wang K.	<u><i>Potassium Isotope Constraints on Near-Surface Fractionation Effects of Bulk Lunar Soils</i></u> [#1586] Potassium isotope system enhances our understanding of the complex history of lunar soils and the interaction between the solid Moon and the space environment.	Poster Location #98
Ma C. Liu Y.	<u><i>Nanomineralogy of Lunar Orange Beads: Discovery of a Zinc-Rich Mineral (Probably Gordaite), Derived from Volcanic Vapor Condensates on the Moon</i></u> [#1463] This is the first observation of a host mineral for Zn, S, Cl, and Na on the pristine surface of orange beads from Apollo 17 soil 74220.	Poster Location #99
Tang H. Li Y. Trail D. McKeegan K. D.	<u><i>Lithium Stable Isotope Records of Irradiation in Apollo Lunar Zircon</i></u> [#1945] We revisited exposure ages of Apollo zircons through the cosmic ray effects on lithium isotope compositions to improve our understanding of lunar regolith.	Poster Location #100
Crow C. A. Moser D. E. McKeegan K. D.	<u><i>Compositional Variations in Lunar Zircon Impact Melt Inclusions</i></u> [#2023] We present the results of an extensive compositional survey of impact melt inclusions in Apollo 14 zircons.	Poster Location #101
Chen S. Ni P. Zhang Y. Gagnon J.	<u><i>Element Partitioning Between Olivine and Melt Inclusions in Lunar Samples</i></u> [#3025] Partition coefficients of 23 elements were precisely determined between olivine and melt inclusions for lunar samples.	Poster Location #102
Cottrell R. D. Lawrence K. Bono R. K. Johnson C. L. Tarduno J. A.	<u><i>Evidence for a Late Lunar Dynamo Revisited</i></u> [#1211] Magnetization of two million-year-old Apollo glass (64455) questions the existence of a late lunar dynamo.	Poster Location #103
Hess K. A. Fu R. R. Zellner N. E. Tikoo S. M.	<u><i>Paleomagnetic Field Intensity and Magnetic Field Recording Characteristics of Apollo 15 Glasses</i></u> [#3190] A quantitative look at lunar glasses being a potential recorder of lunar magnetic fields.	Poster Location #104

Authors (*Denotes Presenter)	Abstract Title and Summary	Poster Location
Marquez R. T. C. Tissot F. L. H.	<u><i>Optimal Double Spike for High-Precision Measurements of Stable Isotopes in Early Solar System Materials</i></u> [#3159] The study implements multiple computational tools to prescribe optimal double spike combinations specific to cosmochemistry and meteoritics.	Poster Location #106
Tucker E. S. Crow C. A.	<u><i>Multi-Diffusion Domain Modeling of Meteorite ⁴⁰Ar-³⁹Ar Data</i></u> [#2931] We have developed new software to model ⁴⁰ Ar- ³⁹ Ar data from samples with multiple diffusion domains. We present the software design and preliminary results.	Poster Location #107
Donohue P. H. Huss G. R. Nagashima K.	<u><i>New Synthetic Carbonates for Investigation of Manganese-Chromium Chronology by Secondary Ion Mass Spectrometry</i></u> [#1959] Our new synthetic calcite produced reliable matrix-matched correction factors for Mn-Cr isotope measurements by SIMS. Additional carbonates are in development.	Poster Location #108
Trappitsch R. Savina M. R. Rolison J. M. Harrison L. N. Dauphas N.	<u><i>Towards the 1000 Atom Detection Limit for Pu-244</i></u> [#2978] Using resonance ionization mass spectrometry we show a Pu244 detection limit of 1100 atoms. This method will allow us to determine the origin of the r-process.	Poster Location #109
Chen X. C. Dauphas N. McKeegan K. D. Barboni M. Schoene B. et al.	<u><i>Progress Report on Lu-Hf Measurements of Single Zircon Grains at The University of Chicago</i></u> [#3251] We report our progress to implement the Lu-Hf technique at the University of Chicago for measurements of single zircon grains.	Poster Location #110
Anderson F. S. Whitaker T. J. Levine J.	<u><i>Effects of Femtosecond Ablation and Sample Preparation on Neutral Isotope Production for In-situ Dating</i></u> [#3277] Using femtosecond laser ablation, we explore the effects of pulse duration and sample preparation on measurement uncertainty for Rb and Sr isotopes.	Poster Location #111
Lanzirotti A. Lee L. Head E. Sutton S. R. Newville M. et al.	<u><i>Direct Measurements of Copper Speciation in Basaltic Glasses Using X-Ray Absorption Spectroscopy: Understanding the Role of Sulfur in Copper Complexation in Melts</i></u> [#1099] Direct measurement of Cu speciation in basaltic glasses by synchrotron X-ray absorption spectroscopy and the control of S on Cu complexation in silicate melts.	Poster Location #112
Berndt J. Steenstra E. S. Klemme S. van Westrenen W.	<u><i>Quantification of Matrix Effects During LA-ICP-MS Analyses of Trace Element Abundances in Iron-Rich Alloys: Implications for Metal/Silicate and Sulfide/Silicate Partition Coefficients</i></u> [#1056] Matrix effects during LA-ICP-MS analyses of Fe-rich alloys vary systematically with volatility. We present a predictive model to correct for these effects.	Poster Location #113
Chernozhkin S. M. McKibbin S. J. Goderis S. Van Malderen S. J. M. Claeys Ph. et al.	<u><i>LA-ICP-MS 2D Mapping and Trace Element Analysis of Oscillatory Zoned Olivines in Imilac PMG</i></u> [#2469] 2D LA-ICP-MS element mapping is used to discover Al, Cr oscillatory zoning in olivine of Imilac PMG. Olivine REE patterns of eight PMGs are presented and discussed.	Poster Location #114
Bell S. K. Hartley M. E. Joy K. H. Pernet-Fisher J. F.	<u><i>Crystal Size Distribution Analysis of Apollo 15 Mare Basalts: New Methods and Some Recommendations</i></u> [#1789] Apollo 15 mare basalt samples are utilized to investigate the feasibility of using QEMSCAN for semi-automated crystal size distribution analysis.	Poster Location #115
Verchovsky A. B. Anand M. Barber S. J.	<u><i>A Quantitative Evolved Gas Analysis for Meteorite and Lunar Samples</i></u> [#2641] We developed a quantitative evolve gas analyses and apply it to the Murchison meteorite.	Poster Location #116

Elsila J. E. Aponte J. C. Dworkin J. P. Glavin D. P. Graham H. V. et al.	<u><i>Developing an Efficient Coordinated Organic Analysis for Returned Samples</i> [#1051]</u> Our work aims to understand and optimize the effects of sample preparation methods for the analysis of soluble organic compounds in extraterrestrial samples.	Poster Location #117
Stroud R. M. Lagos M. Batson P. E.	<u><i>Infrared Spectroscopy of Individual Sub-Micron Presolar and Early Solar System Dust Grains in the Electron Microscope</i> [#2259]</u> Dust absorption / Infrared spectroscopy / Now in TEM.	Poster Location #118
Visser R. John T. Senges G.	<u><i>Raman Spectroscopy of Heated Synthetic, Terrestrial, and Extraterrestrial Carbon — Implications for the Method?</i> [#1524]</u> In this study, we evaluate the reliability of Raman thermometers by investigating the effects of controlled heating on different kinds of extracted carbon.	Poster Location #119
Gilmour C. M. Such P. Freemantle J. Daly M. G.	<u><i>Physical Property Measurement System and Atomic Force Microscope Thermal Conductivity Measurements of Carbonaceous Chondrites</i> [#2206]</u> Want more C chondrite / Thermal conductivities? / We're working on it!	Poster Location #120
Harrington R. S. Righter K.	<u><i>Polished Sample Preparation Without Epoxy</i> [#1075]</u> Preparation of extraterrestrial sample sections without the use of epoxy as a mounting or encapsulating agent is discussed. Polishing methods are also introduced.	Poster Location #121
Manga V. R. Zega T. J. Muralidharan K.	<u><i>Thermodynamics of Twin Complexions in Spinel: Deducing the Loci of Temperature and Pressure of Deformation Processes Within the Solar Protoplanetary Disk</i> [#2845]</u> Faults such as twins and their complexions in refractory mineral phases such as spinel provide unique clues to the nebular processes that have caused them.	Poster Location #122
Koch T. E. Spahr D. Merges D. Beck A. A. Christ O. et al.	<u><i>Chondrule Formation Experiment Aboard the ISS — First Results</i> [#1560]</u> We present the latest results of our chondrule formation experiment onboard the International Space Station (ISS) that launched in November 2018.	Poster Location #123
Rietmeijer F. J. M. Brearley A. J. Dobrica E. Nuth J. A..	<u><i>Avoiding Turbulence in Metastable Eutectic Condensation of Refractory Fe-Mg-Al-O Ternary Vapor Systems in Microgravity</i> [#1607]</u> Testing metastable eutectic condensation of refractory dust in circumstellar outflows.	Poster Location #124
Whizin A. D. Durda D. D. Tsang C. S. Love S. G.	<u><i>Aggregate Accretion from Dust Particles in Free-Float Microgravity Experiments</i> [#2953]</u> We conducted microgravity experiments with dust samples representing early nebular and small bodies surface compositions to determine aggregation dependencies.	Poster Location #125
Schmidt J. Carballido A. Matthews L. S. Laufer R. Herdrich G. et al.	<u><i>Concept for an Experimental Study of Dust Rim Formation on Chondrules</i> [#1910]</u> An experiment in the IPG6-B plasma facility is proposed to study the growth of fine-grained dust rims chondrules by electrically neutral and charged dust.	Poster Location #126
Hooper D. Ximenes S. Palat A. Battaglia R. Mauro M. et al.	<u><i>Developing a QCM for Measuring Dust in the Lunar Environment</i> [#2671]</u> We are developing a Quartz Crystal Microbalance (QCM) as a tool to measure real-time lunar dust accumulation rates and deposition.	Poster Location #127
Dominguez G. D. Tafla L. T. Lucas J. L. Salem M. S. Liu M- C. L. et al.	<u><i>Electron Irradiation of Water Ice on Dust Results in Anomalous Oxygen Isotope Exchange</i> [#2872]</u> How dust affected your measurements: Heterogeneous chemistry on dust can explain the anomalous distribution of oxygen isotopes in the solar system.	Poster Location #128
Zhang Mingming. Zhang Chi. Lin Yangting	<u><i>A Novel Method for Synthesizing Melilite Crystals Standards</i> [#2194]</u> We synthesized a series of melilite crystals with homogeneous chemical and oxygen isotopic compositions, which could be used as SIMS standards.	Poster Location #129
Adcock C. T. Hausrath E. M. Ren M.	<u><i>Synthesis of Iron- and Sodium-Bearing Whitlockite for Interpretation of Extraterrestrial Phosphate Minerals</i> [#1676]</u> The synthesis of whitlockite for use in producing merrillite with cation chemistry relevant to lunar, martian, and other meteoritic materials.	Poster Location #130

POSTER SESSION II: PRESOLAR, INTERPLANETARY, AND COMETARY DUST

6:00 p.m. Town Center Exhibit Area

Authors (*Denotes Presenter)	Abstract Title and Summary	Poster Location
Bose M. Starrfield S.	<u><i>Presolar SiC Grains in Meteorites from Carbon-Oxygen Nova Outbursts</i></u> [#1152] New evolutionary simulations of thermonuclear runaways in CO white dwarfs show that nova dust is a component of the presolar grain inventory in meteorites.	Poster Location #132
Garg A. Goyal V. Marhas K. K.	<u><i>Sputtering of Presolar Grains via Galactic Cosmic Rays in Interstellar Medium</i></u> [#2708] Model calculations have been carried out for sputtering yield, the total sputtering, and the percentage destruction of mantle in Presolar grains due to the GCR in ISM.	Poster Location #133
De Gregorio B. T. Stroud R. M. Alexander C. M. O'D.	<u><i>Nanodiamonds in Carbonaceous Chondrites: Contextual Clues of Formation</i></u> [#1643] We reveal a non-homogenous nanodiamond distribution in chondritic carbonaceous matter by STEM-EELS, and may also be associated with N-rich organic matter.	Poster Location #134
Nevill N. D. Clemett S. J. Messenger S. Thomas- Keptra K. L. Bland P. A. et al.	<u><i>In Situ Coordinated Analysis of Carbonaceous Chondrite Organic Matter</i></u> [#2307] Measured chemical, isotopic, and contextual trends of organic assemblages across a suite of carbonaceous chondrites, focusing nanoglobule origins and evolution.	Poster Location #135
Seifert L. B. Haenecour P. Zega T. J.	<u><i>Elemental Composition and Microstructure of a Supernova Polycrystalline Olivine Aggregate in the CO Chondrite Dominion Range 08006</i></u> [#2585] This study details the analysis of a supernova polycrystalline olivine aggregate using TEM to explore the thermodynamic conditions in supernovae ejecta.	Poster Location #136
Jadhav M. Haenecour P. Amari S. Davidson J. Zega T. J.	<u><i>A Preliminary Search for Presolar Grains in a New Acid Residue of the Tagish Lake Meteorite</i></u> [#3121] We report on a search for presolar grains in a new acid residue of Tagish Lake. EDS and EELS data are presented for the IOM and candidate presolar grains.	Poster Location #137
Verdier-Paoletti M. J. Nittler L. R. Wang J.	<u><i>First Detection of Presolar Grains in Paris, the Most Preserved CM Chondrite</i></u> [#2948] We reported the first in situ detections of presolar grains in the least altered CM chondrite known so far: Paris.	Poster Location #138
Liu N. Ogliore R. C.	<u><i>Circumstellar and Interstellar Material in Volatile-Rich Clasts from Achondritic Kapoeta Meteorite</i></u> [#1880] We discuss the abundances and isotopic ratios of circumstellar and interstellar material in volatile-rich clasts from Kapoeta based on NanoSIMS isotope data.	Poster Location #139
Piquette M. Poppe A. R. Bernardoni E. Szalay J. R. James D. et al.	<u><i>Student Dust Counter: Status Report at 42 AU</i></u> [#2637] The Student Dust Counter has been recording dust hits from 1 to 42 AU. We present the interplanetary dust density distribution compared with current models.	Poster Location #140
Burgess K. D. Bour D. Stroud R. M. Bardyn A. Alexander C. M. O'D. et al.	<u><i>Mineralogy of Dust Collected by the Cosmic Dust Sucker in Antarctica</i></u> [#1878] Wind blows across snow / Full of dust and dirt and ice / Is this dust from space?	Poster Location #141
Maupin R. Djouadi Z. Brunetto R.	<u><i>Vis-NIR Reflectance Micro-Spectroscopy of Interplanetary Dust Particles</i></u> [#1775] We present and discuss Visible near infrared (Vis-NIR) reflectance spectra of 3 IDPs obtained with one-side illumination set-up we developed in our laboratory.	Poster Location #142

Flynn G. J. Wirick S. Northrup P.	<u><i>P Speciation in Large, Cluster Interplanetary Dust Particles</i> [#1403]</u> Phosphorous in nine cluster IDPs occurs mainly as phosphate, but two distinctly different X-ray absorption near-edge structure spectra are observed in 17 hot-spots.	Poster Location #143
Jilly-Rehak C. E. Gainsforth Z. Butterworth A. L. Hsiao S. Naito K. et al.	<u><i>Coordinated TEM and NanoSIMS Oxygen Isotope Analysis of Interplanetary Dust Particles Prepared by Focused Ion Beam</i> [#2649]</u> We measured O-isotopes of IDP components from FIB sections after petrographic analysis with TEM, employing new sample preparation and data reduction techniques.	Poster Location #144
Ishii H. A. Ohtaki K. K. Bradley J. P. Joswiak D. J. Brownlee D. E. et al.	<u><i>Pristine GEMS, Altered GEMS, and GEMS-Like Material</i> [#2058]</u> To better enable identification of interstellar silicates in primitive chondrite matrices, we distinguish properties of pristine, altered, and “faux” GEMS.	Poster Location #145
Joswiak D. J. Brownlee D. E. Westphal A. J.	<u><i>Fe-Mg-Mn Systematics of Kool Grains from Comets: Unique Solar System Materials</i> [#2130]</u> Fe/Mg vs. Fe/Mn plots of Kool grains, which have only been found in comet samples, demonstrate that Kool grains are unique solar system materials.	Poster Location #146

Thursday, March 21, 2019

[R608]

POSTER SESSION II: GENESIS

6:00 p.m. Town Center Exhibit Area

Authors (*Denotes Presenter)	Abstract Title and Summary	Poster Location
Yurimoto H. Sakamoto N. Bajo K. Jurewicz A. J. G. Burnet D. S.	<u><i>Hydrogen Depth Profile in Genesis DOS Collectors</i> [#2221]</u> We found that the Genesis returned solar wind hydrogen from coronal mass ejection of the Halloween solar storms of 2003 in addition to low and high speed flows.	Poster Location #147
Rieck K. D. Ogiore R. C. Jurewicz A. J. G. Burnett D. S. Guan Y. et al.	<u><i>Measuring Solar Wind C and O Abundances in Genesis Regime Collectors Using SIMS Ion Imaging Depth Profiling</i> [#2944]</u> We report preliminary bulk, low- and high-speed solar wind ¹² C fluences measured in Genesis silicon collectors using SIMS ion imaging back-side depth profiling.	Poster Location #148
Jurewicz A. J. G. Olinger C. Burnett D. S. Rieck K. D. Woolum D. S.	<u><i>SW Mg from Genesis; New Method of Data Reduction and Implications</i> [#2353]</u> Solar wind (SW) Mg analyses from Genesis DoS collectors are compared with Si collectors. Radiation-induced segregation in Si has not changed the total fluence.	Poster Location #149
Westphal A. J. Koeman-Shields E. Huss G. R. Welten K. Westphal L. K. T.	<u><i>Abundance of Manganese in the Solar Wind Using Dual-Implant Calibration</i> [#2016]</u> We report preliminary measurements of the Mn/Mg ratio and the fluence of Mn in the solar wind, using SIMS and a novel, dual high-contrast calibration.	Poster Location #150
Hofmann A. E. Paque J. M. Burnett D. S. Guan Y. Jurewicz A. J. G. et al.	<u><i>Genesis Solar Wind Aluminum Abundance: Creating an Aluminum Standard for SIMS Analyses</i> [#1337]</u> Electron microprobe analyses of Al in olivine calibrate an Al implant standard that will enable an accurate measurement of the solar wind Al fluence.	Poster Location #151
Veryovkin I. V. Tripa C. E. Wickramasinghe R. C. Gross J. M. Hanley L. et al.	<u><i>Towards RIMS Measurements of Ultra-Low Elemental Abundances in Genesis Solar Wind Collectors</i> [#2432]</u> Progress in development of improved RIMS instrumentation capable of measurements of solar wind fluences of Rb, Sr, Y, Zr, and Se in Genesis samples is described.	Poster Location #152
Vogel N. Heber V. S. Bochsler P. Burnett D. S. Maden C. et al.	<u><i>Elemental Abundances of Noble Gases in Solar Wind Regimes Collected by Genesis</i> [#1232]</u> Noble gas elemental abundances in Genesis regime targets are presented and discussed in terms of theories on elemental fractionation in the solar wind.	Poster Location #153

Schmeling M.	<u><i>Quantification of Surface Contamination on Genesis Solar Wind Samples</i> [#1955]</u> Quantification of surface contaminants on Genesis solar wind samples was performed using total reflection X-ray fluorescence analysis and external calibration.	Poster Location #154
Welten K. C. Bixler A. J. Nishiizumi K. Caffee M. W. Burnett D. S.	<u><i>Updated Status of the Genesis Mo-Pt Foils for Solar Wind Radionuclide Analysis</i> [#2718]</u> We have stretched the Mo-Pt foils and developed methods to remove surface contamination. We will apply these methods to analyze SW radionuclides in the foils.	Poster Location #155
Welten K. C. Bixler A. J. Nishiizumi K. Caffee M. W. Jurewicz A. J. G. et al.	<u><i>Cleaning of Genesis Sapphire Target 61530 for Solar Wind Chlorine, Cobalt, and Iridium Measurements</i> [#2626]</u> We describe aggressive cleaning procedures of a Genesis sapphire target to remove Si and stainless steel contamination, paving the way for solar wind analysis.	Poster Location #156
Allton J. H. Keller L. P. Rahman Z. Gonzalez C. P. Allums K. K. et al.	<u><i>Solar Wind Effects on Genesis Silicon Collector Substrate Structure: Observation of Layers in TEM Cross-Section</i> [#1118]</u> A TEM cross-section of a Genesis bulk solar wind silicon collector was prepared to assist in developing ellipsometry models of the solar wind surface.	Poster Location #157
Goreva Y. S. Woolum D. S. Paque J. M. Burnett D. S.	<u><i>Understanding Features from the Genesis Capsule Earth Impact</i> [#2399]</u> 3D confocal imaging permits quantitative mapping of deposits in collector materials from the Genesis capsule crash, including possibly meteoritic impact pits.	Poster Location #158

Thursday, March 21, 2019

[R609]

POSTER SESSION II: PROTOPLANETARY DISK EVOLUTION AND CHRONOLOGY

6:00 p.m. Town Center Exhibit Area

Authors (*Denotes Presenter)	Abstract Title and Summary	Poster Location
Meyer B. S.	<u><i>Simple Model of Chromium Isotopic Abundance Evolution in Interstellar Dust</i> [#3226]</u> I present a simple model for the evolution of chromium isotopic evolution in interstellar dust in order to understand chromium isotopic carriers and anomalies.	Poster Location #159
Amelin Y. Rydeblad E. Krestianinov E. Huyskens M. H. Yin Q.-Z.	<u><i>Pb-Isotopic and Initial Sr Ages of the Achondrite NWA 4587</i> [#2261]</u> Pb-isotopic age of NWA 4587 is 4563 ± 0.23 Ma. Initial $^{87}\text{Sr}/^{86}\text{Sr}$ suggests accretion of the parent body 3.7 Ma after CAI formation.	Poster Location #160
Crowther S. A. Gilmour J. D. Ruzicka A. M.	<u><i>Iodine-Xenon Systematics of Large Igneous Inclusions in Ordinary Chondrite Meteorites</i> [#2629]</u> Inclusion of various chemical types show evidence for both early and late formation. Some may date chondrule formation; others formed 10s of Ma after CAIs.	Poster Location #161
Smith L. R. Lewis R. D. Gudipati M. S. Smith R. L.	<u><i>Fractionation Through Photodesorption of ^{12}CO-^{13}CO Interstellar Ice Analogues</i> [#2935]</u> Experiments investigating fractionation from photodesorption of ^{12}CO - ^{13}CO interstellar ice analogues reveal preferential fractionation of ^{12}CO compared to ^{13}CO .	Poster Location #162
Barnett M. N. Ciesla F. J.	<u><i>Formation of Layered vs. Mixed Ices in Proto-Planetary Environments</i> [#1697]</u> Presentation of research on environments in proto-planetary disks that produce layered or mixed ices, and the resulting chemical and evolutionary implications.	Poster Location #163
Leitner J. Vollmer C. King A. J. Schofield P. F. Mosselmans J. F. W. et al.	<u><i>Probing the Early Solar Nebula with Meteoritic Silicon Nitride</i> [#2961]</u> We find evidence for structurally bound sulfur in Si_3N_4 from ECs and present N-isotopic data for Mezö-Madaras- Si_3N_4 , indicating relationship with EC nitrides.	Poster Location #164

THURS POSTERS

Hartlep T. Cuzzi J. N. Umurhan O. M.	<u><i>Planetesimal Formation in the Outer Nebula in the Presence of Turbulence</i> [#3044]</u> We discuss refinements of our planetesimal formation scenario in which turbulence-driven overdensities lead to gravitational sedimentation into large objects.	Poster Location #165
Lyons J. R.	<u><i>Simultaneous CO and N₂ Self-Shielding in a Vertically Mixed Solar Nebula</i> [#3107]</u> Self-shielding of CO and N ₂ is modeled in the outer solar nebula. O isotope results are consistent with the Sun, but N isotope results are not.	Poster Location #166
Pignatale F. C. Chaussidon M. Jacquet E. Charnoz S.	<u><i>Fingerprints of the Protosolar Cloud Collapse in the Solar System: Refractory Inclusions Distribution and Aluminum-26</i> [#1422]</u> Modeling protoplanetary disk formation shows that the abundances of ²⁶ Al observed in CAIs and bulk chondrites imply its homogeneous distribution in the disk.	Poster Location #167
Lee Y.-N. Charnoz S. Hennebelle P. Pignatale F. Commerçon B.	<u><i>Protoplanetary Disk Assemblage and Evolution Revisited with Effects of Non-Ideal Magneto-Hydrodynamics</i> [#2377]</u> We present numerical simulations with non-ideal magneto-hydrodynamic effects to study the protoplanetary disk formation from a collapsing prestellar core.	Poster Location #168
Fu R. R. Kehayias P. Weiss B. P. Schrader D. L. Walsworth R. L.	<u><i>Outer Solar System Magnetic Fields Recorded in CR Chondrites</i> [#2447]</u> Chondrules extracted from CR chondrites record a weak nebular magnetic field, possibly from the outer solar system.	Poster Location #169
Bryson J. F. J. Weiss B. P. Biersteker J. B. King A. J. Russell S. S.	<u><i>Constraints on the Timescales and Distances of Solid Migration in the Solar Nebula from Meteorite Palaeomagnetism</i> [#1338]</u> We constrain asteroid, chondrule, CAI, and ice migration using the formation distances of meteorite parent bodies recovered from meteorite paleomagnetism.	Poster Location #170
Borlina C. S. Weiss B. P. Bryson J. F. J. Fu R. R. Lima E. A.	<u><i>Constraining Nebular Magnetic Fields in the Outer Solar System from CO Chondrites</i> [#2720]</u> In this study, we constrain the solar nebula magnetic fields in the chondrule-forming region through paleomagnetism of CO chondrites.	Poster Location #171

Thursday, March 21, 2019

[R610]

POSTER SESSION II: CHONDRITES: REFRACTORY COMPONENTS

6:00 p.m. Town Center Exhibit Area

Authors (*Denotes Presenter)	Abstract Title and Summary	Poster Location
Ross D. K. Simon J. I. Simon S. B.	<u><i>Remarkable Diversity of Refractory Inclusions in the Miller Range 090019 CO3.1 Chondrite</i> [#1581]</u> One section of the MIL090019 chondrite contains the whole compositional range of CAI types. Bulk chemistry and mineralogy of 140 inclusions will be presented.	Poster Location #173
Gyollai I. Kereszturi A. Szabo M. Kereszty Zs.	<u><i>New inputs on CAI formation based on a new CV3 meteorite Northwest Africa 10261.</i> [#1203]</u> The aim of this work is the correlated optical microscopy and SEM-BSE, SEM-EDX analyses of a recently found new meteorite NWA10261, which shows AOAs and CAIs.	Poster Location #174
DeFelice J. D. Friedrich J. M. Ebel D. S. Flores K. E. Weisberg M. K.	<u><i>Analysis of the Shapes of CAIs in CV Chondrites Using 2D and 3D Petrography</i> [#2919]</u> Calcium-Aluminum rich inclusions (CAIs) in CV chondrites exhibit a range of plastic and brittle deformation that can be analyzed using 2D and 3D petrography.	Poster Location #175
Ivanova M. A. Shornikov S. I. Ryazantsev K. M. Mendybaev R. A. MacPherson G. J.	<u><i>Model Calculations of Evaporation of CAI-Like Melts Enriched in TiO₂</i> [#2357]</u> We report results of theoretical modeling of evaporation process of TiO ₂ -rich CAIs melts to investigate titanium behavior during evaporation.	Poster Location #176

Gupta A. Sahijpal S.	<u><i>Thermodynamic Equilibrium Condensation for Dust Enriched Solar Gas</i> [#1326]</u> A novel numerical code has been developed in Python that indicates a thermodynamic proof of existence of inosilicate and Ti-rich oxides in nebular condensation.	Poster Location #177
Ramprasad T. Haenecour P. Zega T. J.	<u><i>Microstructural Analysis of a Compact Type-A Calcium-Aluminum Rich Inclusion in the Northwest Africa (NWA) 5028 CR2 Chondrite</i> [#2129]</u> We probe the structure and chemistry of high temperature phases from a compact type-A CAI using electron microscopy, to understand their origin and histories.	Poster Location #178
Che S. Brearley A. J.	<u><i>A Complex Evolution Sequence Revealed by the Textures of Fine-Grained, Spinel-Rich Inclusions from the Leoville CV3 Chondrites: A Genetic Link Between Fluffy Type-A CAIs, Spinel-Rich Inclusions, and Amoeboid Olivine Aggregates</i> [#1486]</u> We studied fine-grained, Sp-rich inclusions from the Leoville CV3 chondrite, and proposed that they record a complex evolution sequence.	Poster Location #179
Sanders I. S. Scott E. R. D.	<u><i>Whence CAIs? From Beyond Jupiter, from the Young Sun, or from a Sibling Star?</i> [#2980]</u> CAIs are probably not from beyond Jupiter, but the idea that they formed around a sibling star to the young Sun should be explored.	Poster Location #180
Umstätter Ph. M. J. Gunkelmann N. Dullemond C. P. Urbassek H. M.	<u><i>Granular Mechanics Simulations of Collisions of Dust-Covered Chondrules</i> [#1395]</u> We present Granular Mechanics simulations of collisions of dust-covered chondrules and results about bouncing behaviour, energy dissipation, and ejection yield.	Poster Location #181
Bercovici H. L. Franco G. S. Dolinski J. Garani J. Loescher G. et al.	<u><i>Northwest Africa 12281: The Story of an Unequilibrated LL3 Chondrite Through the Lens of Sawtooth Pyroxene</i> [#1763]</u> We examine the appearance of a pyroxene sawtooth pattern around olivine phenocrysts in ordinary Type-LL chondrite NWA12281.	Poster Location #182
Greenwood J. P. Herbst W.	<u><i>Experimental and Theoretical Progress on the Flyby Model for Chondrule and Chondrite Formation</i> [#2366]</u> The Flyby Model for Chondrule and Chondrite Formation appears to be able to satisfy all current constraints on chondrule formation. We report on progress.	Poster Location #183
Xiang C. Matthews L. S. Carballido A. Hyde T. W.	<u><i>Modeling the Growth of Chondrule Dust Rims Under Various Plasma Conditions</i> [#2591]</u> A molecular dynamics code is used to model the growth of fine-grained chondrule rims through the collection of micron-sized dust grains in protoplanetary disks.	Poster Location #184
Carballido A. Hanna R. Xiang C. Matthews L. S. Hyde T. W.	<u><i>Experimental and Numerical Study of the Accretion of Chondrule Rims</i> [#2765]</u> Numerical models of chondrule rim accretion and laboratory measurements of chondrule rim fabric are used to determine conditions of nebular rim formation.	Poster Location #185
Tissot F. L. H. Burkhardt C. Budde G. Kleine T.	<u><i>Multi-Elemental and Isotopic Characterization of Coarse-Grained Allende CAIs</i> [#3136]</u> We report REE patterns, Ti, Mo, and W nucleosynthetic anomalies, as well as the first mass-dependent W isotope data for nine Allende coarse-grained CAIs.	Poster Location #186
Render J. Ebert S. Burkhardt C. Kleine T. Brennecka G. A.	<u><i>Titanium Isotopes in Refractory Inclusions from CO and CM Chondrites</i> [#1526]</u> We explore the genetic relationships of refractory inclusions from various groups of carbonaceous chondrites employing high-precision Ti isotope analyses.	Poster Location #187

Nagashima K. Libourel G. Krot A. N.	<u><i>Oxygen Isotope Systematics in a Compound Amoeboid Olivine Aggregate — Chondrule Object from Acfer 094 Meteorite: Implications to O-Isotope Exchange Between Melt and Gas During Chondrule Formation</i></u> [#2167] Oxygen isotopic compositions in a compound AOA/chondrule object suggest efficient O-isotope exchange between melt and ¹⁶ O-poor gas during chondrule formation.	Poster Location #188
Ohtaki K. K. Nagashima N. Bradley J. P. Krot A. N. Ishii H. A.	<u><i>Correlated Scanning/Transmission Electron Microscopy and Oxygen Isotope Imaging Study of Isotopically Heterogeneous Anorthite</i></u> [#2158] The cause of heterogeneous O-isotope distribution in a Type B CAI, whether partial melting or hydrothermal alteration, is explored by correlated TEM analyses.	Poster Location #189
Daly L. Bland P. A. Saxey D. W. Reddy S. M. Tessalina S. et al.	<u><i>Re-Os Model Ages for Refractory Metal Nuggets</i></u> [#1514] RMN are small / Atom probe tomography / Now dating for all!	Poster Location #190
Parman S. W. Jacobsen S. B. Petaev M. I. Akey A. J.	<u><i>Atom Probe Tomography of Opaque Assemblage in Allende CAI</i></u> [#2890] Nanometer-scale chemical heterogeneity in a CAI from the Allende meteorite is revealed by laser-assisted atom probe tomography (APT).	Poster Location #191

Thursday, March 21, 2019

[R611]

POSTER SESSION II: SPACE WEATHERING: FROM SAMPLES TO SPECTRA AND EVERYTHING IN BETWEEN
6:00 p.m. Town Center Exhibit Area

Authors (*Denotes Presenter)	Abstract Title and Summary	Poster Location
Hicks L. J. Bridges J. C. Noguchi T. Ireland T. Miyake A. et al.	<u><i>Nanoprobe XANES Analysis of Space Weathered Itokawa Grains</i></u> [#1805] Nanoprobe Fe-K XANES mapping experiment suggests oxidation in the space weathered rims of Itokawa olivine grains, analogous to lunar space weathering.	Poster Location #192
Thompson M. S. Haenecour P. Howe J. Y. Laczniak D. L. Zega T. J. et al.	<u><i>Simulating Space Weathering in the Transmission Electron Microscope via Dynamic In Situ Heating and Helium Irradiation of Olivine</i></u> [#1425] New experiments / Blowing bubbles and growing / Nanoparticles!	Poster Location #193
Kaiden H. Hiroi T. Misawa K. Tanaka H. Sasaki S. et al.	<u><i>Space Weathering of Olivine and the Murchison CM2 Carbonaceous Chondrite Simulated by Ultraviolet Irradiation</i></u> [#2630] Ultraviolet irradiation experiments on olivine and Murchison were performed to investigate possible mechanisms of space weathering on asteroid surfaces.	Poster Location #194
Trang D. Keller L. P. Connolly H. C. Clark B. E. Hamilton V. E. et al.	<u><i>A Preliminary Look at Space Weathering on 101955 Bennu: A Radiative Transfer Modeling Perspective</i></u> [#2172] We examine the spectral characteristics of nanophase and microphase troilite and magnetite using the radiative transfer model.	Poster Location #195
van der Sanden G. A. Foing B. H.	<u><i>Conservative Radiation Countermeasures in Response to Space Radiation Effects on the Lunar South Pole</i></u> [#2346] We present a quantitative estimation of the ionizing radiation environment and countermeasures for a manned operation to the lunar South Pole-Aitken Basin.	Poster Location #196
Trang D. Lemelin M. Crites S. T. Lucey P. G.	<u><i>Space Weathering Maps of the Lunar Poles Using Kaguya Spectral Profiler Data</i></u> [#2293] We investigate the nanophase and microphase iron abundances across the lunar poles.	Poster Location #197
Sato H. Denevi B. W. Hapke B. Robinson M. S. Otake H.	<u><i>Polar Reflectance Analyses of the Moon by LROC WAC</i></u> [#1525] We found and analyzed a systematic trend of reflectance changes on the slopes in the north polar region (>60°N) from new LROC WAC polar color mosaic.	Poster Location #198
Jhoti E. Liu Y. Powell T. M. Retherford K. D. Greathouse T. K. et al.	<u><i>LRO LAMP Far Ultraviolet Investigation of Cold Spots on the Moon and Implications for Space Weathering Rates on Airless Bodies</i></u> [#2858] LRO LAMP far ultraviolet study of cold spots around fresh craters on the Moon using crater ages and regolith maturity to constrain space weathering rates.	Poster Location #199

Chrbolková K. Ďurech J. Kohout T.	<u><i>Statistical Analysis of Lunar Swirls' Spectral Parameters Relevant to Space Weathering</i> [#1034]</u> We will present results of Principal Component Analysis and histograms of seven lunar swirls' spectral parameters.	Poster Location #200
Wu Y. Z. Wang Z. C. Xu T. Y.	<u><i>Space Weathering of the Real Lunar Surface: From the In Situ Rover Detection</i> [#1541]</u> The space weathering of real lunar surface derived from Chang'e-3 rover data is shown, which was not represented by lunar samples.	Poster Location #201
Sun L. Lucey P. G. Honniball C. I. Sandford M. Costello E. S. et al.	<u><i>Understanding Space Weathering of Lunar Soils with a Polarized Perspective</i> [#2017]</u> We derived real refractive index n from polarized spectra of lunar soils, and the spectra of n get redder and higher in value after space weathering.	Poster Location #202
Penttilä A. Väisänen T. Markkanen J. Martikainen J. Escobar-Cerezo J. et al.	<u><i>Space-Weathering Spectra Explained with Light Scattering Simulations</i> [#2287]</u> We give conceptual scattering explanations on the spectral effects caused by space weathering on the regolith, and verify these with extensive simulations.	Poster Location #203
Legett C. IV Glotch T. D. Lucey P. G.	<u><i>Limitations of Effective Medium Approximations for Spectral Modeling of Space Weathered Particles</i> [#2859]</u> Key assumptions wrong / With effective media / For space weathered grains.	Poster Location #204
Jiang T. Zhang H. Yang Y. Ma P. Hu X. et al.	<u><i>Bi-Directional Reflectance Measurement of Pulse-Laser Irradiated Airless Body Analog Materials</i> [#2719]</u> Simulated space weathering by using pulse laser irradiations has made the bi-directional reflectance of airless body analog materials more backscattering.	Poster Location #205
Saxena P. Killen R. M. Airapetian V. Petro N. E. Curran N. et al.	<u><i>The Sun was likely a Slow Rotator: Lunar Geochemical Constraints</i> [#3050]</u> Joint constraints of sodium and potassium abundance in lunar samples and evolution of activity of solar analogues over time suggest the Sun was a slow rotator.	Poster Location #206

Thursday, March 21, 2019

[R612]

POSTER SESSION II: SMALL BODIES: PHYSICAL CHARACTERIZATION AND DYNAMICS

6:00 p.m. Town Center Exhibit Area

Authors (*Denotes Presenter)	Abstract Title and Summary	Poster Location
Ostrowski D. R. Dotson J. Wooden D. Bryson K.	<u><i>Physical Properties of Near Earth Asteroids and Meteorites: Introducing a Publicly Available Database</i> [#2829]</u> Physical properties of asteroids and meteorites are determined and are provided to the general public in online database.	Poster Location #208
Roberts J. H. Buczkowski D. L. Ernst C. M. Barnouin O. S. Gaskell R. W. et al.	<u><i>Updated Geologic Database for 433 Eros</i> [#1494]</u> Update the pointing? / Need to update locations / Of all mapped structures.	Poster Location #209
Mazarico E. Potter S. F. Barker M. K.	<u><i>Illumination and Thermal Conditions at Small Bodies</i> [#2478]</u> Revisiting the illumination and thermal conditions at various small bodies using recent shape models and modeling software.	Poster Location #210
Cambioni S. Delbo M. Ryan A. J. Furfaro R. Asphaug E.	<u><i>Constraining the Thermal Properties of Airless Bodies Using Machine Learning</i> [#1284]</u> We present a new method for the determination of surface properties of airless bodies, including rock abundance, from observed infrared fluxes.	Poster Location #211
Dina D. F.	<u><i>Rotational Period of Near-Earth Asteroid (410088) 2007 EJ</i> [#1599]</u> The final period of (410088) 2007 EJ was obtained from a fourth-order Fourier fit using MPO Canopus program $P = 2.721 \pm 0.002$ h with an amplitude $A = 0.27$ mag.	Poster Location #212
Taylor P. A. Rivera-Valentin E. G. Virkki A. K. Warner B. D. Oey J. et al.	<u><i>Radar and Optical Observations of Equal-Mass Binary Near-Earth Asteroids (190166) 2005 UP156 and 2017 YE5</i> [#2945]</u> Double NEAs / Twins in mutual orbit / Yet no two alike.	Poster Location #213

Hickson D. C. Boivin A. L. Tsai C. Daly M. G. Ghent R. R.	<u>Quantifying Asteroid Regolith Porosity from Radar Data [#2480]</u> Radar data of asteroids allows estimation of the near-surface permittivity, which is inverted for porosity using models validated by laboratory experiments.	Poster Location #214
Nelson R. M. Boryta M. D. Vides C. Palmer M. Guitierrez J.	<u>Understanding the Physical Properties of Planetary Regolith: Theory and Experiment [#2957]</u> We compare laboratory reflectance and polarization measurements of analog regolith materials with predictions based on theoretical models.	Poster Location #215
Lorenz C. A.	<u>The Properties of the Upper Regolith Layer on the Phobos [#1628]</u> Bearing strength of the upper regolith on the Phobos had been estimated using a trace of impactor, rolled out of its crater downward to the groove bottom.	Poster Location #216
Sánchez P. Azéma E. Scheeres D. J.	<u>Scaling in Cohesive Self-Gravitating Aggregates [#2262]</u> We define a modified inertial number that incorporates interparticle cohesion and gravity to describe the behaviour of simulated granular asteroids.	Poster Location #217
Nimmo F. Matsuyama I.	<u>Tidal Dissipation in Rubble-Pile Asteroids and Icy Bodies [#1476]</u> Frictional dissipation in a ~30m thick regolith can explain the inferred tidal dissipation in small asteroids. Applications to Ultima Thule and Bennu are given.	Poster Location #218
Golubov O. Scheeres D. J.	<u>Evolution of Asteroids Under Non-Gravitational Torques [#2284]</u> We give a review of the non-gravitational torques acting on asteroids, with the main focus on new results about evolution of asteroids and YORP equilibria.	Poster Location #219
Scott E. R. D. Sanders I. S. Krot A. N.	<u>Planet Formation: Insights from Asteroids, Comets, and Meteorites [#1510]</u> We outline an accretion scenario for the early solar system that attempts to satisfy constraints from cosmochemical, astronomical, and theoretical studies.	Poster Location #220
Ipatov S. I.	<u>Probabilities of Collisions of Bodies from the Feeding Zone of the Terrestrial Planets with the Planets, the Moon, and Their Embryos [#2289]</u> The amount of bodies from different parts of the zone beyond 0.7 AU, which collided with almost formed Earth and Venus, differed by no more than two times.	Poster Location #221
Ipatov S. I.	<u>Migration of Planetesimals to the Earth and the Moon from Different Distances from the Sun [#2594]</u> Probabilities of collisions of planetesimals from different initial distances from the Sun between 2.5 and 40 AU with the Earth and the Moon are studied.	Poster Location #222
Hyodo R. H. Genda H. G.	<u>Distribution of Martian Materials in the Inner Solar System by a Giant Impact on Mars [#1777]</u> Our impact simulation showed that a giant impact on Mars can distribute impact-generated debris including martian mantle material within the inner solar system.	Poster Location #223
Wren P. F. Fevig R. A.	<u>Comparing Small Main Belt Binary Asteroids of the Inner and Intermediate Zones Using Doublet Craters on Vesta and Ceres [#3095]</u> Doublet craters on Vesta and Ceres are used to characterize and compare small binary asteroid systems in both the inner and intermediate zones of the Main Belt.	Poster Location #224
Feoktistova E. A. Ipatov S. I. Svetsov V. V.	<u>Triples of Lunar Craters Formed by Encounters of Satellite System of Near Earth Object with the Moon [#1946]</u> We found eight sequences consisted of three craters of close ages located in one line in the area which is 19% of the surface of the Moon.	Poster Location #225
Steckloff J. K. Sarid G.	<u>On the Survival of Amorphous Water Ice Within Icy Bodies During Collisional Events in the Early Solar System [#2470]</u> Comets hit comets / A shockingly cold affair / That keeps ice glassy.	Poster Location #226

Sztakovics J. Forgács-Dajka E. Sándor Zs. Vanyó J. Gucsik A.	<u><i>Statistical Study of Mean Motion Resonances and Physical Properties of Hungaria Asteroids Using FAIR</i></u> [#2674] We apply the method FAIR (Fast Identification of mean motion Resonances) to the Hungaria family objects to identify dynamically relevant mean motion resonances.	Poster Location #227
--	--	----------------------

Thursday, March 21, 2019

[R613]

POSTER SESSION II: SMALL BODIES: SPECTRAL CHARACTERIZATION AND LABORATORY EXPERIMENTS

6:00 p.m. Town Center Exhibit Area

Authors (*Denotes Presenter)	Abstract Title and Summary	Poster Location
Gaffey M. J. Fieber-Beyer S. K.	<u><i>Is the (20) Massalia Family the Source of the L-Chondrites?</i></u> [#1441] The (20) Massalia asteroid family is a strong candidate as the source of the L-chondrites, the most common meteorite type currently falling to Earth.	Poster Location #229
Jozwiak L. M. Blewett D. T.	<u><i>New Investigations of Color Variation on Eros</i></u> [#3037] Improved photometric normalization of NEAR images with high-res. Eros shape model permits re-evaluation of color variations among ponds and other features.	Poster Location #230
Gartrelle G. M. Hardersen P. S. Izawa M. R. M. Nowinski M. C.	<u><i>D-Type Asteroids: Primordial Organic Reservoirs, Compositional Cousins, or Ordinary Black Rocks?</i></u> [#1811] Our project attempts to spectrally constrain D-type asteroids from different solar system regions and find plausible links to analogous meteorite samples.	Poster Location #231
Harison B. A. Thomas C. A. Moskovitz N. A. Trilling D. E. Lim L. F.	<u><i>Spectral Analysis of Agnia Family Members</i></u> [#2067] We calculated spectral band parameters for eight members of the Agnia family. The spectra are consistent with PAC meteorites and partial differentiation.	Poster Location #232
Takir D. Neumann W. Emery J. P. Raymond S. N.	<u><i>3-μm Reflectance Spectroscopy of Outer Main Belt Asteroids: Context and Implications</i></u> [#2906] New 3- μ m spectral analyses of primitive outer main-belt asteroids are placed in the context of the current thermal and dynamical theories.	Poster Location #233
Sultana R. Beck P. Poch O. Potin S. Quirico E. et al.	<u><i>Visible Near-Infrared Reflectance Spectroscopy of Sub-μm Silicate Grains</i></u> [#2299] This study is exploring the effect of sub-wavelength grains size on visible and near-infrared spectra of cometary analogues.	Poster Location #234
Hendrix A. R. Vilas F. Li J. Y. Bodewits D. Feaga L.	<u><i>The UV Asteroid and Small Bodies Archive</i></u> [#3001] We describe our progress on creation of the UV Asteroid and Small Bodies Archive.	Poster Location #235
Michalik T. Maturilli A. Otto K. Schmitt B. Poch O. et al.	<u><i>The Dependence of Spectral Features on Ice Content and Temperature for Vesta and Ryugu</i></u> [#1984] We present spectral measurements of various ice/rock mixtures at different temperatures as analogues for the regoliths on Vesta and Ryugu.	Poster Location #236
Jones S. M. Heinz N.	<u><i>Effects of hypervelocity capture in aerogel on the compositions of iron-nickel-sulfide and feldspar minerals</i></u> [#2092] Hypervelocity impact tests were conducted with iron-nickel-sulfide and feldspar projectiles to determine if they are altered during capture in aerogel.	Poster Location #237
Teodoro L. Roush T. Blewett D. Cahill J.	<u><i>The Modeling of the Magnetite Reflectance Spectra Revisited: A Generalized Hapke's Formalism</i></u> [#3172] We have introduced a generalized Hapke theory to model the magnetite reflectance spectra.	Poster Location #238
Potin S. Beck P. Schmitt B.	<u><i>"It's Only a Matter of Perspective": Bidirectional Reflectance Spectroscopy of Small Bodies and Meteorites</i></u> [#1782] We present the variations on reflectance spectra of small bodies with the geometry of observation. Laboratory measurements are conducted on several meteorites.	Poster Location #239

THURS POSTERS

Lanzirotti A. Newville M. Sutton S. R. Koker M. Brearley A. J. et al.	<u><i>Development of Synchrotron 2D and 3D Micro-XRD Techniques Applicable to the Analysis of Picogram Materials Returned by Sample-Return Missions</i></u> [#1098] Development of synchrotron 2D and 3D micro-XRD analytical capabilities for analysis of picogram returned extraterrestrial samples in an imaging modality.	Poster Location #240
Sutton S. R. Lanzirotti A. Newville M. Brearley A. J. Dobrica E. et al.	<u><i>Effect of Focused Ion Beam (FIB) Sectioning on Cr and Ti Valences in Semarkona Olivine</i></u> [#1288] FIB sample preparation has essentially no effect on Cr and Ti valence determinations by microXANES for ~10 pg quantities of Semarkona olivine.	Poster Location #241
Schrader D. L. Zega T. J.	<u><i>Comparison of the Sulfide-Bearing Hayabusa Particles RB-CV-0234 and RB-QD04-0039 to LL Chondrite Sulfides</i></u> [#2009] We further constrain the formation and alteration conditions of asteroid Itokawa via comparison of sulfide-bearing Hayabusa particles to LL chondrite sulfides.	Poster Location #242
Potin S. Beck P. Vernazza P. Schmitt B.	<u><i>Irreversible Metamorphism of Warm C-Type Near-Earth Asteroids Investigated with Carbonaceous Chondrites</i></u> [#1780] We analyzed the thermal alteration of NEAs using reflectance spectroscopy of meteorites. Irreversible alteration and hysteresis effects are observed.	Poster Location #243
Pohl L. Britt D. T.	<u><i>The Dehydration and Alteration of Cronstedtite</i></u> [#2527] Thermal alteration of Cronstedtite is observed and dehydration temperature, the temperatures of phase changes, the change in mineralogy and spectra are reported.	Poster Location #244
Rivkin A. S. Stickle A. M.	<u><i>Are There Large, Never-Lithified Asteroids?</i></u> [#3015] Graupel-, gravel-born / A megameter in size / Transmuted for sure?	Poster Location #245
Burbine T. H. Wallace S. M. Dyar M. D.	<u><i>Applying the Bus-DeMeo Asteroid Taxonomy to Meteorite Spectra</i></u> [#1655] This study shows the successes and limitations of the Bus-DeMeo taxonomy in mineralogically classifying reflectance spectra.	Poster Location #246

Thursday, March 21, 2019

[R614]

POSTER SESSION II: SMALL BODIES: MISSIONS AND COMETS

6:00 p.m. Town Center Exhibit Area

Authors (*Denotes Presenter)	Abstract Title and Summary	Poster Location
Dibb S. D. Bell J. F. III Williams D. A. Elkins-Tanton L. T. Psyche Mission Team	<u><i>Reflectance Spectra of Metal-Rich Meteorites and Implications for the Psyche Discovery-Class Mission's Multispectral Imager</i></u> [#1602] Reflectance spectra of several classes of metal-rich meteorites are presented and convolved to Psyche Multispectral Imager bandpasses.	Poster Location #248
Denk T. Mottola S.	<u><i>Cassini Observations of Saturn's Irregular Moons</i></u> [#2654] Twenty-five irregular moons of Saturn have been investigated with the Cassini ISS camera to determine basic physical properties like rotation periods.	Poster Location #249
Hemmi R. Miyamoto H.	<u><i>HiRISE Digital Elevation Model of Phobos: Implications for Morphological Analysis of Grooves</i></u> [#1759] We studied raised rims of grooves on Phobos by creating a high-resolution digital elevation model.	Poster Location #250
D'Amore M. Maturilli A. Miyamoto H. Niihara T. Grott M. et al.	<u><i>Phobos Regolith Simulant for MMX Mission: Spectral Measurement for Remote Target Identification and Deconvolution System Training</i></u> [#2383] Phobos regolith simulant for MMX Mission. Spectral measurement for remote target identification and deconvolution system training via Neural Network.	Poster Location #251
Eubanks T. M.	<u><i>Efficient Searches for Galactic Stream Interstellar Asteroids</i></u> [#3262] Interstellar asteroids passing through the solar system likely come from galactic dynamical streams, which can be used to help find such bodies.	Poster Location #252

Grav T. Mainzer A. Spahr T. Masiero J. Bauer J. M. et al.	<u>NEOCam Survey Cadence and Simulation</u> [#3175] The NEOCam Survey Simulator is a tool to investigate mission architecture trades as well as to determine a cadence suitable for PHA discovery and tracking.	Poster Location #253
Barnouin O. S. Daly R. T. Ernst C. M. Palmer E. E. Daly M.	<u>Shape Modeling Validation for the Double Asteroid Redirection Test (DART)</u> [#2448] We assess how accurately we will be able to model the shape of Didymos B during the proximity operations undertaken by the DART spacecraft.	Poster Location #254
Raducan S. D. Davison T. M. Collins G. S.	<u>Numerical Modelling of the DART Impact and the Importance of the Hera Mission</u> [#1799] DART slams Didymos / Hera crater pics needed / To show models true.	Poster Location #255
Arai T. DESTINY+ Team	<u>DESTINY+ Target Asteroid (3200) Phaethon: Recent Understandings from 2017 Observation Campaign and the Mission Science Overview</u> [#3223] We present the recent understanding of DESTINY+ mission target asteroid (3200) Phaethon from 2017 observation campaign and the mission science overview.	Poster Location #256
Kim M.-J. Lee H.-J. Kim D.-H. Yoshida F. Lee S.-M. et al.	<u>Rotational and Surface Properties of NEA 3200 Phaethon</u> [#1497] This research is investigation into the rotational and surface properties of NEA 3200 Phaethon based on photometric and spectroscopic observations.	Poster Location #257
Nuth J. A. III Johnson N. M. Abreu N.	<u>Are B-Type Asteroids Dormant Comets?</u> [#3059] We examine the properties of B-type asteroids as a bridge to active comets and as the potential end point in the physical evolution of cometary material.	Poster Location #258
Xing Z. X. Li Z. Y. Su M.	<u>Prediction of Cometary Solar Wind Charge Exchange Spectra in Extreme-Ultraviolet Waveband for Satellite Design</u> [#2702] Predicted extreme ultraviolet spectra of comets by fitting their X-ray emission data observed by Chandra to suggest design parameters of a planned satellite.	Poster Location #259
Clark B. C. Mason L. W.	<u>Compositional Heterogeneity Within Cometary Bodies</u> [#1302] The cometary nucleus emits aggregates that have differing compositional biases, as seen in mixed, silicate, and CHON particles and their subclasses.	Poster Location #260
Kramer E. A. Mainzer A. K. Wright E. L. Bauer J. Cutri R. M. et al.	<u>Modeling the Photometric Behavior of the Near-Earth Comet Population</u> [#3243] Near-Earth comets have / Variable behavior / That we model here.	Poster Location #261
Ernst C. M. Gaskell R. W. Daly R. T. Barnouin O. S. Thomas P. C.	<u>A Stereophotoclinometry Model of Comet Tempel 1</u> [#2640] Our new Tempel 1 shape model is a 20x improvement over existing models, and for the first time resolves flow margins, scarps, and impact crater candidates.	Poster Location #262
Soler C. Q. Westphal A. J.	<u>Measuring Al:Fe Atom Ratio of Fine-Grained Material from Comet Wild 2</u> [#3128] This describes our ongoing work on Stardust samples. We anticipate finding a value for the Al:Fe ratio in Wild 2 material by the time of the presentation.	Poster Location #263
Statella T. Geiger B.	<u>Radiometric Cross-Calibration of the Rosetta Navigation Camera</u> [#1136] In this work, we perform the radiometric cross-calibration of the NavCam based on images acquired by the OSIRIS instrument.	Poster Location #264
Heather D. J. Fraga D. O'Rourke L. Taylor M.	<u>The Rosetta Science Archive: Enhancing the Science Archive Content</u> [#1881] In this presentation, we will show the status and plans for enhancing the science content of the Rosetta archive.	Poster Location #265
Clark C. S. Clark P. E.	<u>Progress 2019: Constant-Scale Natural Boundary Mapping to Depict Material Transport on Comet 67P/C-G</u> [#2936] We fine-tune our 2018 maps of 67P/C-G, preparatory to adding photomosaics.	Poster Location #266

THURS POSTERS

Czechowski L. Kossacki K. J.	<u><i>Dynamics of Landslides on Comet 67P/Churyumov-Gerasimenko: Ejecta from Imhotep Region and the Places of Their Depositions</i></u> [#2134] Slow ejecta from large lobe of comet 67P/CG was considered. The places of their deposition was indicated. It could be important for future mission to that comet.	Poster Location #267
------------------------------	--	----------------------

Thursday, March 21, 2019

[R615]

POSTER SESSION II: CERES AND VESTA

6:00 p.m. Town Center Exhibit Area

Authors (*Denotes Presenter)	Abstract Title and Summary	Poster Location
Bland M. T. Buczkowski D. L. Sizemore H. G. Ermakov A. I. King S. D. et al.	<u><i>A Salt-Tectonics Analogy for Understanding Ceres' Surface Morphology</i></u> [#1114] Ceres' large domes form by a mechanism directly analogous to terrestrial salt tectonics, negating the need for cryovolcanism. Other features may form similarly.	Poster Location #269
Wyrick D. Y. Buczkowski D. L. Sizemore H. G.	<u><i>Testing Domal Formation Mechanisms on Ceres</i></u> [#3239] Laboratory experiments on various subsurface mass migration mechanisms shed light on resultant fracture patterns.	Poster Location #270
Schenk P. Buczkowski D. Scully J. Nathues A. Neesemann A. et al.	<u><i>Occator Crater, Ceres: High Resolution Dawn Stereo and Topography of a Large Tycho-Class Crater on an Ice-Rich Dwarf Planet</i></u> [#2828] Big rock fall from sky; go boom! Leave impact melt; similar to lunar yet different; carbonate deposits have complex topographic relations, we sort them out!	Poster Location #271
Pasckert J. H. Scully J. E. C. Williams D. A. Buczkowski D. L. Hiesinger H. et al.	<u><i>Geologic Mapping (1:10,000) of Cerealia Facula Based on Dawn's High Resolution XM2 Data</i></u> [#2308] We derived a detailed geologic map (1:10,000) of Cerealia Facula based on Dawn's final high resolution XM2 data.	Poster Location #272
Landis M. E. Prettyman T. H. Byrne S. Yamashita N. Scully J. E. C. et al.	<u><i>Survival of Water Ice and Hydrated Salts at Occator Crater, Ceres</i></u> [#1653] Occator could have/water ice or hydrated/salts. What are the odds?	Poster Location #273
Schmedemann N. Nathues A. Thangjam G.	<u><i>Size-Distance-Velocity Analysis of Occator Secondary Craters</i></u> [#2431] We investigate relationships between the sizes of secondary craters, their distances from the primary and impact velocities of respective secondary projectiles.	Poster Location #274
Jia Y.-D. Castillo-Rogez J. C. Raymond C. A. Villarreal M. N. Russell C. T.	<u><i>Time-Variable Magnetic Field Responses at Ceres with Different Conductance</i></u> [#2738] We present our simulation of the interaction between the time-varying solar wind and Ceres.	Poster Location #275
Parks M. Nixon C. Cordiner M. Charnley S. Thelen A. et al.	<u><i>Using ALMA Spectra to Investigate a Potential Transient Exosphere of Ceres</i></u> [#2974] This research uses archival spectra from ALMA to investigate the possibility of a transient exosphere and detect its composition.	Poster Location #276
Li J.-Y. Moullet A. Titus T. N. Sykes M. V. Hsieh H. H.	<u><i>Thermal Rotational Lightcurve of (1) Ceres at 1.2 mm Wavelength and Search for HCN with ALMA</i></u> [#2939] The thermal lightcurve of Ceres has a small amplitude of 3.5% that may be caused by variations in thermal properties. No HCN is detected on Ceres.	Poster Location #277
Sachse M. Kappel D. Haack D. Otto K.	<u><i>Discrete Element Simulations of Test Scenarios for Studying Landslides on Asteroids</i></u> [#2497] We use DEM simulations to study landslides on asteroids after constraining the numerical parameters of the model and the mechanical properties of the material.	Poster Location #278
Schroeder S. E. Carsenty U. Schulzeck F. Hauber E. Jaumann R. et al.	<u><i>The Boulder Population of Vesta</i></u> [#1833] We present an overview of the boulder population of asteroid Vesta as observed by the Dawn camera, with emphasis on the boulder size-frequency distribution.	Poster Location #279

Thursday, March 21, 2019

[R616]

POSTER SESSION II: DIFFERENTIATED METEORITES: HOWARDITES, EUCRITES, DIOGENITES

6:00 p.m. Town Center Exhibit Area

Authors (*Denotes Presenter)	Abstract Title and Summary	Poster Location
Peng Z. X. Mittlefehldt D. W. Ross D. K.	<u><i>Elemental Variation and Petrogenesis of Pyroxenes in HED Meteorites by Multivariable Discriminant Analysis Method</i></u> [#1016] Using multivariable discriminant analysis to study geochemical changes of HED would help us better understand their petrologic processes and classification.	Poster Location #280
Fagan A. L. Turner L. Waters-Tormey C. Casale G.	<u><i>Observations of Deformation in Orthopyroxene-Rich Subsample of Diogenite Northwest Africa 1877</i></u> [#2822] We examine the chemistry and structural orientation of orthopyroxene in NWA 1877 as a proxy for internal processes (e.g., deformation) within the parent body.	Poster Location #281
Anderkin C. J. Sheikh D.	<u><i>Petrography and Geochemistry of Northwest Africa 11997, a Newly-Classified Howardite</i></u> [#1013] We report preliminary petrographic and geochemical data from a new howardite, Northwest Africa 11997.	Poster Location #282
Kagami S. Haba M. K. Nagao K. Yokoyama T. Yamaguchi A.	<u><i>Noble Gas Isotopic Compositions of Four Stannern-Group Euclrites</i></u> [#2185] We measured noble gases in four Stannern-group euclrites and discussed the distribution and thermal evolution process of this group on the euclrite parent body.	Poster Location #283
McQuaig D. R. Simon J. I. Mittlefehldt D. W. Armytage R. M. G.	<u><i>Petrographical and Geochemical Investigations of Stannern Group Euclrites</i></u> [#3000] Basaltic euclrites / With potassium feldspar / Even in main group.	Poster Location #284
Kanemaru R. Imae N. Yamaguchi A. Hirotsugu H.	<u><i>XRD Analyses of Basaltic and Cumulate Euclrites: Implication for Shock Metamorphism</i></u> [#2321] X-ray diffraction (XRD) analyses using the in-place rotation of polished thin sections (PTSs) for euclrites provide the information for the shock degrees.	Poster Location #285
Nicolau-Kuklińska A. Łosiak A.	<u><i>Investigation of the Source of Vesicles in the Euclitic Fusion Crust</i></u> [#2145] If variable contents of troilite in euclitic meteorites are the source of the variable number of vesicles in the fusion crust?	Poster Location #286
Marquardt M. Sharp T. G. Irving A. J.	<u><i>Preservation of High-Pressure Minerals in the Euclite Northwest Africa 8677</i></u> [#2184] Northwest Africa (NWA) 8677 was analyzed petrographically to document shock events in the genomict euclite.	Poster Location #287
Barrett T. J. Cernok A. Degli-Alessandrini G. Anand M. Franchi I. A. et al.	<u><i>Apatite Microstructures and Its Volatile Composition in Euclrites</i></u> [#1689] Exploring the relationship between apatite microstructures and volatile composition in euclrites.	Poster Location #288
Dunlap D. R. Wadhwa M. Krestianinov E. Koefoed P. K. Amelin Y. et al.	<u><i>Chronology of the Euclite Northwest Africa 8661: A Record of Ancient Volcanism on Vesta</i></u> [#2832] Chronology of the remarkably pristine euclite NWA 8661 is reported using three high-resolution chronometers and discussed with the implications for Vesta.	Poster Location #289
Warren P. H. Sawchuk K.	<u><i>Igneous-minicumulate derivation of enigmatic intergrowths of quartz and augite, without feldspar, in euclite Northwest Africa 10553</i></u> [#3133] Quartz-augite intergrowths in euclite NWA 10553, near-devoid of plagioclase, formed as end-stage products of differentiation of a small-scale igneous cumulate.	Poster Location #290
Ono H. Mikouchi T. Yamaguchi A.	<u><i>Silica Minerals in the Yamato-790266 Polymict Brecciated Euclite</i></u> [#2336] We studied silica minerals in Yamato-790266 euclite. We propose that cristobalite is present in weakly metamorphosed euclrites (types 1–3).	Poster Location #291
Lewis J. A. McCubbin F. M. Burkemper L. K. Agee C. B.	<u><i>Characterization of the Berthoud Euclite Fall</i></u> [#1876] A fall from the sky / The Berthoud euclite reveals / K-peppered feldspar.	Poster Location #292

THURS POSTERS

Forman L. V. Daly L. Barrett T. J.	<u><i>Comparing the Crystallographic Structures of the Howardite, Eucrite, and Diogenite (HED) Meteorites</i> [#1374]</u> Evidence of activated slip systems are demonstrated and compared to allude to conditions at the time of deformation for three HED meteorites.	Poster Location #293
Karageozian M. E. Dillon S. M. Fitch R. T. Sedler M. A. Teichert Z. G. et al.	<u><i>Crescent Shaped Feature in Eucrite NWA 12282: Implications for the Impact History of Vesta</i> [#3212]</u> An examination of a unique crescent shaped class in eucrite NWA 12282 as a potential window into Vesta's impact and shock history.	Poster Location #294
Fudge C. Sharp T. G. Irving A. J.	<u><i>Shock Effects and Mineralogy in Eucrites: Expanding our Knowledge of the Impact History of Vestoids</i> [#2077]</u> We discuss mineral assemblages and thermal signatures preserved in NWA 7643, 8120, and 8677 to explore early impacts on Vesta and V-type asteroids.	Poster Location #295

Thursday, March 21, 2019

[R617]

POSTER SESSION II: DIFFERENTIATED METEORITES: UREILITES, AUBRITES, ANGRITES, BRACHINITES, UNIQUE, AND UNKNOWN

6:00 p.m. Town Center Exhibit Area

Authors (*Denotes Presenter)	Abstract Title and Summary	Poster Location
Vaci Z. Agee C. B. Ziegler K.	<u><i>Unique Dunite Breccia Northwest Africa 12217: Mineralogy, Petrology, and Oxygen Isotopes</i> [#1175]</u> Monomict brecciated dunite with O isotopes similar to brachinites, with more forsteritic olivine and alkali feldspar, likely from a unique differentiated body.	Poster Location #295
Guo Z. Bouvier A. Webb E. Alexandre A. Longstaffe F. J. et al.	<u><i>A New Not So Eucrite-Like Ungrouped Achondrite: Northwest Africa 12338</i> [#1583]</u> NWA 12338 is a new ungrouped achondrite. It has close geochemical characteristics to basaltic achondrites, but is petrologically and isotopically distinct.	Poster Location #296
Barnes J. J. Goodrich C. A. McCubbin F. M. Bischoff A. Decker S. et al.	<u><i>Non-Chondritic Volatile Signatures in a Ureilite Trachyandesite</i> [#1875]</u> Ureilites were born / Not from a magma ocean / But chlorine heavy.	Poster Location #297
Boleaga Y. Goodrich C. A.	<u><i>Xenolithic Fe,Ni Metal in Polymict Ureilite Meteorites</i> [#1622]</u> Polymict ureilites are breccias that represent regolith on a ureilitic asteroid. We studied the distribution of Fe,Ni-rich grains in two polymict ureilites.	Poster Location #298
Goodrich C. A. Kita N. T. Zolensky M. Shaddad M. H.	<u><i>Oxygen Isotope Compositions of Magnetite in CC-Like Clasts from Almahata Sitta and Other Polymict Ureilites</i> [#1551]</u> Oxygen isotopes of magnetite in CC lithologies in polymict ureilites show that they represent volatile-rich SS materials not sampled as whole meteorites.	Poster Location #299
Worsham E. A. Kleine T.	<u><i>Genetic Tracing of Impactors on the HED Parent Body Using Mo and Ru Isotopes</i> [#2602]</u> Mo and Ru isotopes from a eucrite impact melt reveal that the impactor formed in the inner solar system. Possible sources of the impactor will be discussed.	Poster Location #300
Loftus C. L. May B. A. Molesky M. J. Straitf M. M. Flynn G. J. et al.	<u><i>Comparison of Compression Strength of Hydrated Meteorites</i> [#3138]</u> Compression strength was measured for meteorites and their hydrated analogs to examine trends with other physical properties.	Poster Location #301
Hoffmann V. H. Wimmer K. Hochleitner R. Kaliwoda M. Funaki M. et al.	<u><i>Almahata Sitta Magnetic Susceptibility Database — Update of the Enstatite Chondritic Lithologies</i> [#2839]</u> We have developed a database of the magnetic susceptibility of all Almahata Sitta samples investigated by us so far. Here we report an update for the E-chondrites.	Poster Location #302
Wilbur Z. E. Udry A. Zeigler R. A. McCubbin F. M. Vander Kaaden K. E. et al.	<u><i>The Geochemistry of Aubrites: Investigating Reduced Parent Bodies</i> [#1648]</u> We investigate aubrite meteorites using various geochemical techniques to better understand their conditions of formation.	Poster Location #303

Irving A. J. Kuehner S. M. Righter M. Lapen T. J. Ziegler K. et al.	<u><i>Petrologic, Elemental, Isotopic, and Magnetic Characterization of Vesicular Hypabyssal Angrites Northwest Africa 12004 and Northwest Africa 12320</i></u> [#2758] We describe two new angrites that are similar to Sahara 99555 and D'Orbigny, and that bring the current total number of unpaired specimens to 20.	Poster Location #304
Bernard R. E. Day J. M. D. Chin E. J.	<u><i>Strong Olivine Lattice Preferred Orientation in Brachinite-Like Achondrites</i></u> [#1432] Electron backscattered diffraction (EBSD) reveals that brachinite-like achondrites MIL 090206 and 090405 contain strong olivine lattice preferred orientation.	Poster Location #305

Thursday, March 21, 2019

[R618]

POSTER SESSION II: DIFFERENTIATION OF PLANETS AND ASTEROIDS: FROM CORES TO LATE VENEERS

6:00 p.m. Town Center Exhibit Area

Authors (*Denotes Presenter)	Abstract Title and Summary	Poster Location
Zube N. G. Nimmo F. Fischer R. A. Jacobson S. A.	<u><i>Hf/W Isotopic Evolution for Post Last-Giant-Impact Earths and Moons in Grand Tack Accretion Simulations</i></u> [#2260] We examine the evolution of ¹⁸² W for canonical Moon-forming impacts in Grand Tack accretion scenarios, determining the likelihood of an Earth-Moon W similarity.	Poster Location #307
Luo H. Karki B. B. Ghosh D. B. Cao X. Bao H.	<u><i>Temperature and Pressure Effects on Diffusional Mg Isotopes in MgSiO₃ Liquid</i></u> [#3208] We used first-principles molecular dynamic simulations to explore diffusional isotope effect of Mg in MgSiO ₃ melt under a series of pressures and temperatures.	Poster Location #308
Frossard P. Boyet M. Bouvier A. Hammouda T. Monteux J.	<u><i>Magma Ocean-Derived Anorthositic Crust on Early (< 5 Ma) Planetesimal</i></u> [#1772] NWA 8486 (paired with NWA 7325) composition suggests that it is the first occurrence of an anorthositic crust on a planetesimal formed within 5 Ma after CAI.	Poster Location #309
Hopp T. Budde G. Kleine T.	<u><i>The Molybdenum-Ruthenium Cosmic Correlation Revisited: New Constraints on Earth's Late Accretionary History</i></u> [#1200] We present combined Ru-Mo isotopic data for a large set of meteorites to assess whether or not the bulk silicate Earth (BSE) plots on the Mo-Ru correlation defined by non-carbonaceous (NC) meteorites.	Poster Location #310
Dasgupta R. Grewal D. S. Sun C. Tsuno K. Costin G.	<u><i>The Origin of Earth's Major Volatiles via Accretion of a Large Planetary Embryo</i></u> [#2610] Through lab experiments and inverse Monte-Carlo simulations, we show that the abundance of C, N, and S in the Earth can be explained by the Moon-forming impact.	Poster Location #311
Zhu K. Sossi P. Julien S. Moynier F.	<u><i>Chromium Stable Isotopic Insights into the Origin of the Volatile Element Depletion of Vesta</i></u> [#1523] Isotopically light Cr was observed in Vesta, which suggests a low-temperature volatile process (i.e., magma ocean).	Poster Location #312
van Westrenen W. Steenstra E. S. Berndt J. Klemme S. Rohrbach A.	<u><i>Did Euclites and Angrites Experience Sulfide Saturation?</i></u> [#1148] S solubility limits were experimentally determined for euclites and angrites and used to study the nature of siderophile element depletions in Vesta and the APB.	Poster Location #313
van Haaster F. Steenstra E. S. van Mulligen R. Berndt J. Klemme S. et al.	<u><i>Experimental Quantification of the Sulfide-Silicate Partitioning Behavior of Halogens and Implications for Halogen Depletions in Planetary Mantles</i></u> [#1058] Sulfide-silicate partitioning systematics of halogens were experimentally studied and applied to study the nature of halogen depletions in planetary mantles.	Poster Location #314

THURS POSTERS

Bercovici H. L. Elkins-Tanton L. T. Schaefer L.	<u><i>The Effect of Bulk Composition on the Behavior of Sulfur During Core Formation</i> [#1366]</u> We model how oxygen fugacity and the bulk composition of a parent body, based on carbonaceous and ordinary chondrites, affects the amount of sulfur in a core.	Poster Location #315
Seiler S. Roth A. Hunt A. C. Maden C. Wieler R. et al.	<u><i>Noble Gases from In Situ and Whole Rock Analyses of Main-Group Pallasite Sericho</i> [#2894]</u> We investigated the noble gas isotopic composition of the MG pallasite Sericho by in situ and whole rock analyses and estimated a cosmic-ray exposure age.	Poster Location #316
Caves L. R. Mayne R. G. McCoy T. J. McDonough W. F. Ash R. D.	<u><i>Understanding Metal-Silicate Mixing in Mesosiderites</i> [#1735]</u> Mesosiderites / More than redox going on / During mixing phase.	Poster Location #317
Pittarello L. McKibbin S. J. Yamaguchi A. Gang J. Schryvers D. et al.	<u><i>The Tale of Pyroxene in Mesosiderite Asuka 09545, Inferred from Two Generations of Exsolution Lamellae</i> [#2328]</u> In mesosiderite Asuka 09545, pyroxene exhibits two generations of exsolution lamellae. The thermal history of the pyroxene shed light on that of mesosiderites.	Poster Location #318
Delaney J. S. Boesenberg J. S. Herzog G. F. Turrin B. D. Swisher C. S. III	<u><i>Metamorphism in Mesosiderites Revisited: (I) Mount Padbury Enclaves and the Thermochronological Implications of Tridymite</i> [#1340]</u> Mafic clasts in mesosiderite Mount Padbury are metamorphosed. They contain plag and tridymite. Both are datable ⁴⁰ Ar hosts that may elucidate cooling history.	Poster Location #319
Boesenberg J. S. Humayun M.	<u><i>Northwest Africa 1911: The Second Pallasite from the Zinder-IIIIF Iron Parent Body</i> [#1438]</u> Pyx pallasite NWA 1911 may be paired with Zinder. Both have metal that matches IIIIFs. Mo and O isotopes may suggest different parents for NWA and Zinder vs. IIIIFs.	Poster Location #320
Sharma S. Humayun M. Hewins R. Zanda B. Gattacceca J. et al.	<u><i>Elemental Abundances in the Metal of Los Vientos 263 — An Anomalous Pallasite Formed in a Reduced Environment</i> [#1442]</u> The origin of Los Vientos 263 (LoV 263), a new orthopyroxene-olivine-kamacite pallasite, is investigated using metal chemistry and oxygen isotopes.	Poster Location #321
Lyons R. J. Ciesla F. J. Dauphas N.	<u><i>Widmanstätten Pattern Growth in Impacted, Mantle-Stripped Iron Meteorites</i> [#2464]</u> In mantle-stripped bodies, cooling rates vary greatly for a single sample. We report the effects these variations will have on Widmanstätten pattern growth.	Poster Location #322
Hilton C. D. Walker R. J.	<u><i>Chemical and Isotopic Compositions of the IIG Iron Meteorites</i> [#1240]</u> The chemical and isotopic compositions of the IIG iron meteorites are examined to evaluate the potential relationship between the IIG and IIAB iron meteorites.	Poster Location #323
Corrigan C. M. McCoy T. J. Wasson J. T. Sirbescu M. Gilchrist A. M.	<u><i>Edmore, Michigan: A New IIIAB Iron Meteorite</i> [#2970]</u> Used as a doorstop / Recognized as space rock / A new IIIAB.	Poster Location #324
Mayne R. G. Corrigan C. M. McCoy T. J. Day J. M. D. Rose T.	<u><i>From a Camel to the Smithsonian: Tracing the Origin of Qarabawi's Charm</i> [#2404]</u> Charming, who are you? / Science gives fairytale end / Probably Wabar.	Poster Location #325

Thursday, March 21, 2019

[R619]

POSTER SESSION II: IMPACTS: FROM PLANETARY FORMATION TO MODERN EXPERIMENTS

6:00 p.m. Town Center Exhibit Area

Authors (*Denotes Presenter)	Abstract Title and Summary	Poster Location
Pepper A. C. Lock S. J. Davies E. J. Stewart S. T.	<u><i>Giant Impacts Between Rotating Bodies in an Eulerian Code</i> [#3228]</u> Rotating planets / In giant impacts begin / With layers to mesh.	Poster Location #327

Gabriel T. S. J. Asphaug E. Jackson A. P.	<u><i>Giant Impact Outcomes are Dependent on Scale and Density Stratification</i></u> [#3245] We report new potential dependencies of the outcomes of giant impacts on the internal structure and size of the colliding bodies.	Poster Location #328
Duncan M. S. Davies E. J. Root S. Bliss D. E. Spaulding D. K. et al.	<u><i>Building Planets One High Velocity Impact at a Time: Silicate Vapor Curve Experiments</i></u> [#2116] High speed impacts make / Vaporized rocks that are used / When building planets.	Poster Location #329
Rufu R. Canup R. M.	<u><i>Evection Resonance in the Earth-Moon System</i></u> [#2010] Early and late resonance-escapes are possible in different parameter regimes. In both cases, angular momentum is removed, although through different mechanisms.	Poster Location #330
Carter P. J. Davies E. J. Lock S. J. Stewart S. T.	<u><i>High Collision Velocities Between Planetesimals During Planet Growth and Migration</i></u> [#1246] Big planets excite / Planetesimals hit fast / Vapor plumes ensue.	Poster Location #331
Carter P. J. Davies E. J. Lock S. J. Stewart S. T.	<u><i>Collapsing Impact Vapor Plumes: A New Planetesimal Formation Environment</i></u> [#1247] Vapor plumes collapse / Inward flow collects debris / New bodies accrete.	Poster Location #332
Stewart S. T. Carter P. J. Davies E. J. Lock S. J. Kraus R. G. et al.	<u><i>Collapsing Impact Vapor Plume Model for Chondrule and Chondrite Formation</i></u> [#1251] Impact disturbance / In nebula makes warm cloud / Of chondrules and dust.	Poster Location #333
Lock S. J. Stewart S. T. Carter P. J. Davies E. J. Petaev M. I. et al.	<u><i>Size Distribution of Chondrules Set by Droplet Breakup and Coupling During Vaporizing Collisions in the Nebula</i></u> [#1783] Droplets are broken / Down to millimeter size / Large chunks left behind.	Poster Location #334
Davies E. J. Root S. Carter P. J. Duncan M. S. Spaulding D. K. et al.	<u><i>Impact Vaporization Criteria During Planet Formation</i></u> [#1257] When planets collide / When do ice, rock and iron / Vaporize? Look here.	Poster Location #335
Davies E. J. Carter P. J. Duncan M. S. Root S. Spaulding D. K. et al.	<u><i>Impact Generated Vapor Plumes After Dispersal of the Solar Nebula</i></u> [#1256] Impacts generate / Vapor plumes: liquids, vapor / Expand together.	Poster Location #336
Allibert L. Charnoz S. Siebert J. Raymond S. N.	<u><i>Crustal Stripping and Chemical Evolution of the Proto-Earth During Accretion</i></u> [#1415] Quantification of the influence of collisional erosion during accretion on the budget of lithophile and refractory elements such as Sm and Nd.	Poster Location #337
Rougier E. Lei Z. Euser B. Kedar S. Knight E. E. et al.	<u><i>The Numerical Road to Determination of Fracture Role on Impacts as Seismic Sources: Finite-Discrete Modeling of Impacts</i></u> [#3075] We present a newly developed Discrete-Finite Element Method (HOSS) applied to impacts in geologic materials. We benchmark it to other numerical methods.	Poster Location #338
Schultz P. H. Daly R. T.	<u><i>Projectile Effects on Crater Diameter and Depth Scaling in Metal Targets</i></u> [#2909] Laboratory experiments reveal that projectile fate affects the energy and momentum scaling relations for oblique impacts into metal targets.	Poster Location #339
Reagan J. R. Congram S. N. May B. A. Molesky M. J. Strait M. M. et al.	<u><i>Asteroid Impact Studies: Mass and Speed Observation Nexus</i></u> [#3215] We are designing a variable speed detector to examine the disruption patterns of meteorites in catastrophic disruptions.	Poster Location #340
Takac M. T. Kavkova R. K. Kletetschka G. K. Petrucha V. P.	<u><i>Magnetic Anomalies of Crater Fields Detected by Drone</i></u> [#3070] Airless planetary surfaces are covered by multiple impact craters. In this work, we focus on impact craters that were created by an iron impactor.	Poster Location #341
Alesbrook L. S. Marques M. J. New J. Harriss K. Podoleanu A.	<u><i>Analysis of Impact Craters Using Optical Coherence Tomography</i></u> [#1830] We present our work on the use of OCT to analyse impact samples.	Poster Location #342
Hodges K. V. Brunner A. E. Cartwright J. A. McDonald C. S. Mercer C. M. et al.	<u><i>Recent Successes and Future Promise of Laser Ablation Microprobe Noble Gas Geochronology of Planetary Materials</i></u> [#2214] Ultraviolet laser microprobe ⁴⁰ Ar/ ³⁹ Ar geochronology provides new insights about the ages and thermal evolution of lunar and vestan impact melt breccias.	Poster Location #343

Ebel J. M. Dechant L. E. Anderson J. L. B. Cintala M. J. Plescia J. B.	<u><i>Easing Toward Reality: Experimental Impacts into Slopes and Layers</i></u> [#2911] We present results from two suites of impact crater experiments using sloped and layered targets, and compare them to those observed on planetary surfaces.	Poster Location #344
Nishizawa M. Matsui Y. Suda K. Saito T. Shibuya T. et al.	<u><i>Hypervelocity Impact Experiments to Study Meteorite Fragmentation in the Ocean and Impact-Derived Products</i></u> [#2248] Impact experiments at ca. 5km/s showed an extensive fragmentation and dispersion of a variety of projectiles within water column.	Poster Location #345
Harriss K. H. Dugdale A. Adentunji S.	<u><i>Initial Investigations of Hypervelocity Impact Experiments on Volatile Bearing Materials</i></u> [#1590] Initial method investigations about impacting volatile bearing materials such as clathrates and zeolites to investigate the gas released.	Poster Location #346
Marchi S. Durda D. D. Polanskey C. A. Asphaug E. Bottke W. F. et al.	<u><i>Impact Experiments in Fe-Ni Ingot and Iron Meteorites: Implications for the NASA Psyche Mission</i></u> [#1563] Heavy metal / Hard rock / Psyche metal rock.	Poster Location #347
Flynn G. J. Durda D. D.	<u><i>Strengths of Meteorites and Fragmenting Meteors: Implications for Strength Scaling for the Asteroids</i></u> [#1400] Data provides no compelling evidence for significant variation of asteroid strength with mass over the size range of meteorites and fragmenting meteors.	Poster Location #348
Langlois V. J. Quantin-Nataf C.	<u><i>Dynamics of Ejecta During the Formation of an Impact Crater: Discrete Numerical Simulations</i></u> [#2606] A novel model for impact cratering based on a discrete element method allows us to compute explicitly the fragmentation and trajectories of ejecta.	Poster Location #349
Artemieva N. Morgan J. V.	<u><i>Interaction of Crater Ejecta with Atmosphere</i></u> [#2518] Non-ballistic transport of ejecta is able to modify ejecta from large craters if the atmosphere is thick enough.	Poster Location #350
Plesko C. S. Becker S. A. Biwer C. M. Boslough M. E. Harwell M. L. et al.	<u><i>Hypothetical Deflection Scenarios for a 100-m-Diameter Didymos-B-Like Asteroid and a 200-m-Diameter Low-Density Contact Binary Asteroid</i></u> [#3233] Kinetic impacts / Modeled for two asteroids / Betas more than 2.	Poster Location #351
Baroo S. Ramesh K. T.	<u><i>A Computational Approach to Modelling the DART Impact</i></u> [#3217] Simulation of the DART impact based on the Tonge-Ramesh material model implemented with the Uintah material point method computational framework.	Poster Location #352

Thursday, March 21, 2019

[R620]

POSTER SESSION II: IMPACTS: SHOCK METAMORPHISM AND GEOCHRONOLOGY

6:00 p.m. Town Center Exhibit Area

Authors (*Denotes Presenter)	Abstract Title and Summary	Poster Location
Jenkins L. E. Flemming R. L. Burchell M. Harriss K. Peslier A. H. et al.	<u><i>Creating Calibration Curves to Determine Shock Pressure in Clinopyroxene</i></u> [#1974] X-ray diffraction is used to measure lattice strain and strain-related mosaicism to create calibration curves to evaluate shock metamorphism in clinopyroxene.	Poster Location #353
Tielke J. Peslier A. H. Christoffersen R. Cintala M. Morris R. et al.	<u><i>Water Storage and Transport Processes During Impact Experiments on Nominally Anhydrous Minerals</i></u> [#2613] Preliminary results from impact experiments on olivine and pyroxene indicate water contents are modified during impact, but more data are needed.	Poster Location #354
Simpson E. N. Milam K. A.	<u><i>An Analysis of the Effects of Sample Processing on X-Ray Powder Diffraction Peaks and the Implications for Studies of Shock Metamorphosed Carbonates</i></u> [#2882] X-ray powder diffraction (XRD) is commonly used to assess shock metamorphism in carbonates. This study analyzes multiple methods of sample processing for XRD.	Poster Location #355

Ebert M. Poelchau M. H. Kenkmann T. Sah R.	<u><i>Feather Features in Shocked Quartz as a Tool to Constrain Deformation in Impact Craters: A Case Study of Chicxulub's Peak Ring</i></u> [#2465] Based on feather feature orientations we determined local σ_1 orientations in order to identify the deformation path and stress history of Chicxulub's peak ring.	Poster Location #356
Yin F. Chen M.	<u><i>Microtextures of Coesites with Different Occurrences from the Xiuyan Crater</i></u> [#2659] The microtextures of crystallized coesites from the Xiuyan Crater was studied through TEM.	Poster Location #357
Shirley K. A. Jaret S. J. Thompson L. Glotch T. D.	<u><i>Mid-Infrared Emissivity of Impact Materials Under Simulated Lunar Environment Conditions</i></u> [#2493] Can we distinguish / Impact materials by / Their spectral features?	Poster Location #358
Rucks M. J. Glotch T. D. Whitaker M. L. Sharp T. G. Fudge C. et al.	<u><i>The Behavior of Calcium-Rich Plagioclase Under Impact Relevant Conditions and Implications for Impact Studies</i></u> [#2691] Mars is red / Neptune is blue / Tissintite is cool / I can't write a haiku.	Poster Location #359
Szumila I. Miller M. Trail D. Simon J. Cintala M. et al.	<u><i>Impact Shocking of a Zircon-Sanidine Mixture and Investigations of Pb Mobility</i></u> [#2015] Results of an artificial impact shock experiment targeting a zircon and sanidine mixture. Analysis of Pb isotopes of starting and resultant shocked material.	Poster Location #360
Martell J. Alwmark C. Lindgren P. Johansson L.	<u><i>Former Reidite in Granular Neoblastic Zircon Grains (FRIGN zircon) from the Mien Impact Structure, Sweden</i></u> [#2422] Here we report the first documentation of so-called "FRIGN zircon" (Former Reidite in Granular Neoblastic zircon) in a Swedish impact structure.	Poster Location #361
Wielicki M. M. Wielicki M. D. Mulcahey J. Fiechtner C.	<u><i>Shocked Minerals: Evidence of the Chicxulub Impact Event Within the K-Pg Boundary in Alabama</i></u> [#1673] Evidence of the Chicxulub impact event, shocked zircon minerals, identified within the K-Pg boundary layer in Marengo County, Alabama.	Poster Location #362
Cavosie A. J. Koeberl C.	<u><i>Evidence of Former Reidite in Granular Zircon from Libyan Desert Glass</i></u> [#1233] Granular zircon grains in Libyan desert glass (LDG) preserve evidence that they were formerly reidite. High-pressure shock deformation is thus required to form LDG.	Poster Location #363
Rasmussen C. Stockli D. F.	<u><i>Spatial U-Pb Age Preservation in Shocked Zircon — A Brief Case Study from the Rochechouart Impact Crater</i></u> [#2820] U-Pb depth profiling of shocked zircon from the Rochechouart Crater reveals the spatial age distribution (including the impact age) within individual crystals.	Poster Location #364
McGregor M. McFarlane C. R. M. Spray J. G.	<u><i>The Viability of Apatite as an Impact Chronometer: The Manicouagan Impact Structure as a Chronologic Standard</i></u> [#2434] We demonstrate the viability of apatite as a U-Pb impact chronometer by using the Manicouagan impact structure as a chronologic standard.	Poster Location #365
Takenouchi A. Sumino H. Hayashi H. Mikouchi T. Bizzarro M.	<u><i>Noble Gas Analysis of Uniquely Shocked Angrite Northwest Africa 7203</i></u> [#1719] We measured noble gas contents and Ar-Ar/I-Xe ages of NWA 7203 shocked angrite. Ar-Ar age is highly disturbed and may represent the shock age at 2300 ± 140 Ma.	Poster Location #366
Farrant B. E. Holland G. Jones R. H. Clay P. L.	<u><i>Behaviour of Chlorine and Argon During Impact Melting of Ordinary Chondrites</i></u> [#2966] Differences in the Cl and Ar budget of the host and impact melted fractions of Chelyabinsk and Chico are reported with comment as to reasons for the disparity.	Poster Location #367
Leili M. H. Chennaoui Aoudjehane H. Devouard B. Folco L. Gemelli M.	<u><i>Sinoite (Si₂N₂O) and Silica Inclusions (Cristobalite and Tridymite) Inside Graphite Grains in Al Haggounia 001 Enstatite Chondrite</i></u> [#2361] The Al Haggounia 001 meteorite is an enstatite chondrite. We did report sinoite within a millimetric graphite with silica polymorphs (tridymite, cristobalite).	Poster Location #368

Xie Z. Si J. Zuo S. Li Y. Guo Z.	<u><i>Understanding Shock Metamorphism Based on High-Pressure Silicate Phases in Shocked-Induced Melt Veins of Chondrite GRV 022115</i></u> [#2618] We present striking silicate phase transformation features in shock-induced melt vein of GRV 022115 chondrite, to understand vein formation and P-T-t profile.	Poster Location #369
Lorenz C. A. Kononkova N. N. Franchi I. A.	<u><i>NWA 6485: Partially Fractionated LL Chondrite Melt Rock</i></u> [#1632] NWA 6485 is LL-related poikilytic rock. Probably, it is a partially fractionated chondrite melt that was re-heated due to an impact event and slowly cooled.	Poster Location #370
Dunn T. L. Lunning N. G. Robak K. N. Gross J.	<u><i>Initial Description of an Impact Melt Clast in LL3 Chondrite Northwest Africa 10598</i></u> [#1570] New impact melt clast / In an LL3 chondrite / Where did it come from?	Poster Location #371
Moreau J. Schwinger S.	<u><i>2-D Heat Diffusion in Numerically Shocked Ordinary Chondrites</i></u> [#1025] Diffusing heat from numerically shocked ordinary chondrites in iSALE is important to understand the true extent of heating and melting of individual phases.	Poster Location #372
Moreau J. Kohout T. Wünnemann K.	<u><i>Shock-Darkening in Ordinary Chondrites: Mesoscale Modeling of the Shock Process and Comparison with Shock-Recovery Experiments</i></u> [#1024] We studied shock-darkening in ordinary chondrites using iSALE and investigated its probable occurrence in shock-recovery experiments and asteroid collisions.	Poster Location #373
Kohout T. Petrova E. V. Yakovlev G. A. Grokhovsky V. I. Penttilä A. et al.	<u><i>Spherical Shock Experiments with Chelyabinsk Meteorite: Reflectance Spectra Changes with Increasing Shock</i></u> [#2704] Spherical shock experiments reproduced shock darkening and impact melting. New lithology was observed at intermediate pressures with suppressed shock darkening.	Poster Location #374
Sanchez J. A. Reddy V. Le Corre L. Campbell T. Chabra O.	<u><i>Spectral Characteristics of Ordinary Chondrite Impact Melts</i></u> [#1594] We studied NIR spectra of ordinary chondrites that contain impact melt material in order to understand its effect on taxonomic classification of asteroids.	Poster Location #375
Hu J. Asimow P. D. Ma C.	<u><i>First Shock Synthesis of Khatyrkite, Stolperite, and a Newly-Found Natural Quasicrystal: Implications for the Impact Origin of Quasicrystals from the Khatyrka Meteorite</i></u> [#3126] New shock experiment produced the exact Al-Cu-Fe quasicrystal plus alloy assemblage as in the Khatyrka meteorite, which supports its special impact history.	Poster Location #376
Ma C. Tschauner O. Beckett J. R.	<u><i>Discovery of a New High-Pressure Silicate Phase, (Fe,Mg,Cr,Ti,Ca,□)₂(Si,Al)O₄ with a Tetragonal Spinelloid Structure, in a Shock Melt Pocket from the Tissint Martian Meteorite</i></u> [#1460] We report a high P, Fe-rich, Cr-,Ti-bearing, vacancy-stabilized silicate spinel, crystallized from a shock-induced melt during the Tissint impact event on Mars.	Poster Location #377
Guo Z. Li Y. Chen H. Y. Li S. J. Li X. Y. et al.	<u><i>Pure Metallic Iron and Hercynite in Eucrite Imply a Thermal Condition After Impactation</i></u> [#1739] Pure metallic iron and hercynite particles were found in the melt pocket of Northwest Africa 11592, implying a thermal condition after impactation on Vesta.	Poster Location #378

Thursday, March 21, 2019

[R621]

POSTER SESSION II: IMPACTS: MARS AND BEYOND

6:00 p.m. Town Center Exhibit Area

Authors (*Denotes Presenter)	Abstract Title and Summary	Poster Location
Woo J. M. Y. Genda H. Brassler R. Mojzsis S. J.	<u><i>Mars in the Aftermath of Colossal Impact</i></u> [#1067] Using SPH simulations and analytical analysis, we show that a short live H ₂ atmosphere would have been generated after a giant impact on the early Mars.	Poster Location #379

Ruedas T. Breuer D.	<u><i>Electrical Conductivity and Seismic Velocity of the Martian Mantle: Signatures of Large Meteorite Impacts</i></u> [#2335] Seismic velocity, electrical conductivity derived from mantle convection models: Can impact signatures in the interior be detected?	Poster Location #380
Trowbridge A. J. Boener A. Horgan B. Elliott J. Weiss B. P. et al.	<u><i>Excavation of Martian Lower Crust and Mantle by the Isidis Impact and Implications for the Mars 2020 Mission</i></u> [#2710] Hydrocode modeling of the Isidis impact event to identify if lower crust and mantle materials form the basement unit outside of Jezero Crater.	Poster Location #381
Cartwright S. F. A. Seelos K. D.	<u><i>New Ring Structure Estimates of Ladon Basin, Mars, from Mafic Mineral Mapping with CRISM</i></u> [#2755] Mafic minerals / Around Ladon basin, Mars / Indicate six rings.	Poster Location #382
Spray J. G.	<u><i>Structural and Morphometric Controls on the Original Form of the Gale Impact Structure: Terrestrial Constraints from Vredefort, Chicxulub, and Sudbury</i></u> [#2498] The largely buried 155 km-diameter Gale impact structure, Mars, was originally probably a protobasin, but could have been a peak-ring or central peak structure.	Poster Location #383
Sneed J. W. Day M. D. Edgett K. S.	<u><i>Fresh Impact Crater Detection from Difference Mapping of CTX Images</i></u> [#1224] Fresh craters hidden / Photographed but yet unseen / Use the difference maps!	Poster Location #384
Herrick R. R.	<u><i>Initial Survey of Well-Preserved Martian Craters in the Southern Hemisphere in the Simple-to-Complex Transition</i></u> [#2954] Survey of craters with $7 < D < 9$ km in the southern hemisphere of Mars. Vertical and lateral heterogeneity of near-surface controls their shapes.	Poster Location #385
Boatwright B. D. Head J. W.	<u><i>Early Mars Crater Degradation Processes: Testing the Effectiveness of Small Impact Bombardment with Numerical Simulations</i></u> [#2612] We find that topographic diffusion through small impact bombardment is capable of lowering wall slopes of Noachian craters on Mars in an atmosphere up to 1 bar.	Poster Location #386
Nuno R. G. Paige D. A.	<u><i>Martian Microcraters as Evidence for Obliquity-Driven Pressure Variations</i></u> [#3096] The pressure changes / So should the production rates / Of microcraters.	Poster Location #387
Bart G. D. Daubar I. J. Ivanov B. A. Dundas C. M. McEwen A. S.	<u><i>Dark Impact Halos on Mars</i></u> [#2020] Dark impact halos on Mars are examined to determine the relationship between halo diameter and crater diameter and the implications for halo formation.	Poster Location #388
Boyce J. M. Mougini-Mark P.	<u><i>Evidence of Late Stage Flow of Ejecta Across the Boundary Between Ejecta Layers of Martian Double Layered Ejecta Craters</i></u> [#1063] Evidence is presented for flow of ejecta across the boundary between ejecta layers on martian double layer craters. This ejecta is superposed on both layers.	Poster Location #389
Cawley J. C. Irwin R. P. III Craddock R. A.	<u><i>Geomorphology of Large Basin Impact Ejecta, Moon and Mars</i></u> [#2467] Large basin impact ejecta provides significant landscape and subsequent geomorphic structure on both the Moon and on Mars.	Poster Location #390
Mohr D. Ahrens C.	<u><i>Ejecta Mobility and Lobateness of Martian Impact Craters On and Off Volcanic Lava Field Boundaries</i></u> [#1294] Ejecta morphologies of martian impact craters on lava fields can show information regarding ejecta formation and volatile concentrations.	Poster Location #391
Sacks L. E. Tornabene L. L. Osinski G. R. Sopoco R. McEwen A. S.	<u><i>Hargraves-Type Ejecta on Mars: Implications for Impact Ejecta Processes</i></u> [#2904] Impact ejecta / Windows through melt-bearing rock / Beautiful breccia.	Poster Location #392
Piatek J. L. Tornabene L. L. Glanovsky T. Murphy I. Barlow N. G. et al.	<u><i>Preservation of Thermophysical Ejecta Facies in Martian Craters Near the Transition Diameter</i></u> [#2993] Ejecta ages, lose / Fine ejecta first. Yes, but / Can we quantify?	Poster Location #393
Raducan S. D. Davison T. M. Collins G. S.	<u><i>Numerical Modelling of Impacts into Asteroid (16) Psyche Analogues</i></u> [#1798] How was Psyche born? / Can impacts erode mantle / To expose its core?	Poster Location #394

Zeilhofer M. F. Barlow N. G.	<u><i>The Characteristics and Distribution of Polygonal Craters on Ceres</i> [#1259]</u> Polygonal craters are observed on both rocky and icy bodies, including Ceres. Ceres displays a large number of polygonal craters indicating a weakened target.	Poster Location #395
Wagner R. J. Schmedemann N. Werner S. C. Head J. W. Stephan K. et al.	<u><i>Ray Craters on Ganymede as Time-Stratigraphic Markers</i> [#1849]</u> In this study we constrain the time-stratigraphic position and age of several bright ray craters on Ganymede, such as Osiris and Achelous.	Poster Location #396
Lucchetti A. Pajola M. Dalle Ore C. Galluzzi V. Stephan K. et al.	<u><i>Geological and Compositional Analysis of Ganymede's Melkart Impact Crater</i> [#2324]</u> We performed a geological and compositional analysis of the Melkart impact crater located on the surface of Ganymede.	Poster Location #397
Costello E. S. Ghent R. R. Lucey P. G.	<u><i>Impact Gardening on Europa: The Depth to Organic Molecules</i> [#1998]</u> Europa gardened / By multitudes of impacts / Digging organics.	Poster Location #398
Kay J. P. Rhoden A. R. Stickle A. M.	<u><i>Investigating the Effects of Shallow Liquid Water on Crater Formation</i> [#1888]</u> Craters into ice / May reveal hidden layers / Model all the things.	Poster Location #399
New J. S. Butterworth A. L. Mathies R. A. Price M. C. Spathis V. et al.	<u><i>Feasibility of Capturing Organic Ice Particles in Hypervelocity Transits of Enceladus Plumes</i> [#2500]</u> Hypervelocity impact experiments indicate that soft metals can be used as an Enceladus plume capture medium that preserves organic content.	Poster Location #400
Crósta A. P. Silber E. A. Lopes R. M. C. Johnson B. C. Malaska M. J.	<u><i>Modeling the Formation of Menrva Impact Crater in Titan: Implications for a Potentially Habitable Hydrocarbon World</i> [#3018]</u> We have modeled the formation of large impact craters on Titan using the case of Menrva.	Poster Location #401
Aponte-Hernandez B. Rivera-Valentín E. G. Schenk P. M. Kirchoff M. R.	<u><i>Crater Formation and Modification on Rhea from Topography</i> [#3052]</u> Craters on Rhea / Modified later they are / But what makes it work?	Poster Location #402
Ferguson S. N. Rhoden A. R.	<u><i>Dimpled Dione: A Look at the Cratering Distributions and History on Saturn's Moon Dione and Implications for Crater Source Populations</i> [#1478]</u> Craters near and far / Pepper Dione's surface / Where did they come from?	Poster Location #403
López-Oquendo A. J. Rivera-Valentín E. G. Dalle-Ore C. M. Kirchoff M. R. Nichols-Fleming F. et al.	<u><i>Constraints on Crater Formation Ages on Dione from Cassini VIMS and ISS</i> [#2435]</u> Young or older moons? / Dione's ice may foretell / Cassini lives on!	Poster Location #404

Thursday, March 21, 2019

[R622]

POSTER SESSION II: MARS FROM ORBIT: SPECTROSCOPY AND LANDING SITES

6:00 p.m. Town Center Exhibit Area

Authors (*Denotes Presenter)	Abstract Title and Summary	Poster Location
Riu L. Carter J. Poulet F.	<u><i>Global Distribution of Abundances of Hydrated Minerals on Mars and Derived Water Content</i> [#1177]</u> We present here global distributions of hydrated minerals at Mars derived from the OMEGA instrument. The water content is also derived at the global scale.	Poster Location #407
Salvatore M. R. Goudge T. A. Liu Y. Bramble M. S.	<u><i>The Composition of NASA's Mars 2020 Rover Landing Site at Jezero Crater: A Summary of Remote Spectral Analyses</i> [#1454]</u> A summary of the primary and alteration mineralogy within Jezero Crater in preparation for the Mars 2020 rover mission. Ongoing analyses are also highlighted.	Poster Location #408
Christian J. R. Arvidson R. E.	<u><i>Use of MRO/CRISM Hyperspectral Imaging Data for Mapping the Mineralogy of Jezero Crater</i> [#3061]</u> Improvements to CRISM hyperspectral image processing to better detect subtle mineral signatures in Jezero Crater.	Poster Location #409

Frizzell K. R. Seelos F. P. Rice M. S.	<u><i>Mars Hyperspectral Data Processing in the Jezero Crater and NE Syrtis Region: Implications for Mineralogical Analysis</i></u> [#2204] Mars spectroscopy / ENVI crashes easily / So many pixels.	Poster Location #410
Brown A. J. Goudge T. A. Viviano C. E. Seelos F. P.	<u><i>Jezero Watershed Mapping of Olivine-Carbonate Lithology</i></u> [#2085] We mapped the olivine 1 micron band in the Jezero watershed and compare to previous geomorphic mapping. We place limits on the grain size and lower olivine Fo#.	Poster Location #411
Noe Dobrea E. Z. Clark R.	<u><i>Detection of Serpentine at Jezero Crater</i></u> [#1249] We used tetracorder to find multiple primary igneous and alteration minerals. We report the detection of serpentine on the rim and delta of Jezero Crater.	Poster Location #412
Douté S. Conway S. Massé M.	<u><i>Small Scale Topographical Characterization of Jezero Crater Region, Mars</i></u> [#2528] We perform the topographical characterization of the Jezero region of Mars down to the metric horizontal scale by generating improved high-resolution DEMs.	Poster Location #413
Miklusicak N. B. Hudson M. D. Kronyak R. E. Kah L. C.	<u><i>Fractures Within the Dark Toned Floor Unit of Jezero Crater as Potential Targets of Astrobiological Interest</i></u> [#1253] Fractures in lavas / Contraction or expansion / Targets for fluids.	Poster Location #414
Kremer C. H. Bramble M. S. Mustard J. F.	<u><i>A Hemispherically Integrated Sedimentary Geological System at Nili Fossae, Mars</i></u> [#1656] Nili Fossae, Mars / Sediment sources and sinks / A two for one deal!	Poster Location #415
Tirsch D. Bishop J. L. Viviano C. Loizeau D. Tornabene L. L. et al.	<u><i>The Effects of Aqueous Processes and Impacts on Mineral Alteration and Weathering in Libya Montes and Tyrrhena Terra, Mars</i></u> [#1532] We introduce our recently started project on the mineralogy of Tyrrhena Terra, and present our geologic mapping and a mineral map of the entire study region.	Poster Location #416
Kumar C. Chatterjee S. Oommen T. Farrand W. H.	<u><i>Detecting Hydrated Minerals in Libya Montes, Mars Using MRO CRISM Hyperspectral Data</i></u> [#2716] Detecting the Mg/Fe-OH bearing minerals using CRISM hyperspectral to understand the mineralogy of the Libya Montes.	Poster Location #417
Seelos K. D. Buczkowski D. L. Fraeman A. A. Thomson B. J. Crumpler L. S.	<u><i>Spatial Distribution of Hematite Around the Base of Aeolis Mons, Gale Crater, Mars</i></u> [#2785] CRISM data are used to provide an expanded view of the distribution of hematite around Mt. Sharp and give context for MSL Curiosity observations.	Poster Location #418
Phillips B. P. Glotch T. D. Rogers A. D. Osterloo M. M.	<u><i>A Comprehensive View of the Stratigraphy and Mineralogy of Chloride-Bearing and Hydrated Units in Noachis Terra, Mars</i></u> [#3209] Embayed chloride salts / Phyllosilicates present / What more can we learn?	Poster Location #419
Singh P. Sarkar R. Porwal A.	<u><i>Signatures of Hydrated Minerals from Lampland Crater in the Thaumasia Region of Mars</i></u> [#2949] We report upon hydrated minerals, including sulfates and phyllosilicates, in Lampland Crater, which is located in the Thaumasia region of Mars.	Poster Location #420
Buczkowski D. L. Seelos K. D. Viviano C. E. Murchie S. L. Seelos F. P. et al.	<u><i>Anomalous Phyllosilicate-Bearing Outcrops South of Coprates Chasma: A Study of Possible Emplacement Mechanisms</i></u> [#1299] A second Fe/Mg-smectite layer is observed above Al-phyllosilicates near Coprates Chasma, suggesting that not just a single pedogenic episode must be occurring.	Poster Location #421
Beck A. W. Murchie S. L. Viviano C. E.	<u><i>CRISM Multispectral Mapping of Noachian Crust at Equatorial Latitudes on Mars — Update</i></u> [#2693] Here we present results from mapping primary and secondary minerals in mid-latitude Noachian material on Mars using the CRISM instrument.	Poster Location #422
Parkes Bowen A. Bridges J. C. Page J. El-Maarry M. R. Thomas N. et al.	<u><i>Fracture Mapping and CaSSIS Imaging of the ExoMars 2020 Landing Site Oxia Planum: Characterising Clay-Rich Sediments</i></u> [#1952] Characterising Oxia Planum via analysing fracturing visible in HiRISE images along with using band ratio CaSSIS imagery to distinguish ferric/ferrous minerals.	Poster Location #423

Ruesch O. Sefton-Nash E. Vago J. L.	<u><i>Abundance of Blocks and Small Scale Topographic Reliefs at the ExoMars Landing Sites</i> [#2593]</u> Automatic detection and abundance estimates of blocks and small scale topographic reliefs at the two final landing sites of the ExoMars mission.	Poster Location #424
Gross C. Bishop J. L. Carter J. Horgan B. Loizeau D. et al.	<u><i>Investigating Fractured Phyllosilicate-Rich Deposits at Mawrth-Vallis, Mars</i> [#1517]</u> We examine the hypothesis if a part of the clay stratigraphy could have been formed under low temperature hydrothermal conditions.	Poster Location #425
Danielsen J. M. Bishop J. L. Usabal G. S. Miura J. K. Sessa A. M. et al.	<u><i>Characterization of Outcrops Containing "Doublet" Spectra at Mawrth Vallis, Mars</i> [#3017]</u> Laboratory minerals standards and mixtures were compared to CRISM image spectra to identify components in "doublet"-type spectra found at Mawrth Vallis, Mars.	Poster Location #426
Usabal G. S. Bishop J. L. Danielsen J. M. Itoh Y. Parente M. et al.	<u><i>Characterization of Jarosite-Bearing Outcrops Northwest of Mawrth Vallis</i> [#2234]</u> Multiple small outcrops of jarosite occurring in mixtures with phyllosilicates have been observed across the region to the west of the Mawrth Vallis channel.	Poster Location #427
Miura J. K. Bishop J. L. Danielsen J. M. Sessa A. M. Itoh Y. et al.	<u><i>Spectral Properties of Alunite-Kaolinite Mixtures and Detection of These Minerals at Mawrth Vallis</i> [#2576]</u> Laboratory mixtures of alunite and kaolinite were prepared and VNIR spectra measured and compared to CRISM images at Mawrth Vallis.	Poster Location #428
Putnam E. T. Palucis M. C.	<u><i>Mineralogy of Martian Craters with Alluvial Fans Versus Those Without: Insights into the Controls on Martian Alluvial Fan Distribution</i> [#2505]</u> Crater minerals / To form fans or not to form / That is the question.	Poster Location #429
Bates A. R. Karunatillake S.	<u><i>Placing Putative Arabia Paterae Eruptions in Context with Regional Martian Geologic Events</i> [#2774]</u> Eruptions from Paterae within Arabia Terra may have occurred due to geochemical evidence and overall chain of martian geologic events.	Poster Location #430

Thursday, March 21, 2019

[R623]

POSTER SESSION II: MARS FROM ORBIT: NON-SPECTRAL INSTRUMENTS AND METHODS

6:00 p.m. Town Center Exhibit Area

Authors (*Denotes Presenter)	Abstract Title and Summary	Poster Location
Tornabene L. L. Thomas N. Cremonese G. Almeida M. Douté S. et al.	<u><i>Colour and Stereo Surface Imaging System (CaSSIS) on the ExoMars Trace Gas Orbiter (TGO): Potential Colour Data Products and Their Use for Scientific Investigations</i> [#2678]</u> We present a summary and a few examples of suggested CaSSIS colour data products, useful for scientific investigations of Mars geomorphology and geologic history.	Poster Location #431
Thomas N. Cremonese G. Almeida M. Banaszkiwicz M. Bapst J. N. et al.	<u><i>CaSSIS: Overview of Imaging in the First 9 Months of the Prime Mission</i> [#1585]</u> A review of data acquired by CaSSIS onboard the Trace Gas Orbiter is provided. We emphasize the contribution CaSSIS can make to Mars surface geomorphology.	Poster Location #432
Thomas N. Cremonese G. Almeida M. Backer J. Becerra P. et al.	<u><i>CaSSIS on the ExoMars Trace Gas Orbiter: Operational Approach</i> [#1582]</u> We discuss the approach used to operate the CaSSIS instrument onboard ESA's ExoMars Trace Gas Orbiter. We also discuss preparation of data for public release.	Poster Location #433
Robbins S. J. Hoover R. H. Kirchoff M. R.	<u><i>Fully Controlled 6 Meters/Pixel Mosaic of Mars' South Pole and Equator from Mars Reconnaissance Orbiter Context Camera</i> [#1678]</u> CTX camera's / Images: Controlling them / All... and mosaics!	Poster Location #434
Persaud D. M. Campbell J. D. Tao Y. Muller J.-P.	<u><i>Visualisation of 3D Multi-Resolution Orbital Images for Fluvial Geomorphology in Gale Crater, Mars</i> [#3072]</u> Rivers cut through Gale / Curious in their nature / Let's see them up close.	Poster Location #435

Ettahri M. A. Hargitai H.	<u><i>Relevance of Mapping Meter-Scale Background Terrains on Mars Using HiRISE Images. [#1121]</i></u> Investigate and map featureless background terrain on Mars using Grid mapping approach in order to create a database of surface types for landing site selection.	Poster Location #436
Hess M. Wohlfarth K. Grumpe A. Wöhler C. Ruesch O. et al.	<u><i>Overcoming Troublesome Stereo Artifacts: Towards the Perfect Digital Terrain Model of Mars [#2565]</i></u> We show how Shape-from-Shading (2D-Photoclinometry) based on physical reflectance and atmospheric modeling can improve Stereo DTMs of HiRISE resolution.	Poster Location #437
Hood D. R. Karunatillake S. Fassett C. I. Sholes S. F.	<u><i>Verification of Automatically Measured Boulder Populations in HiRISE Images [#1893]</i></u> Boulders all around / Computers measure for us / Can we find them all?	Poster Location #438
Musiol S. Balthasar H. Dumke A. Gross C. Michael G. et al.	<u><i>15 Years High Resolution Stereo Camera Observations with ESA's Mars Express Mission [#1537]</i></u> Within the last 15 years, HRSC has delivered a large quantity of images that build the basis for mosaic generation.	Poster Location #439
Schreiner B. P. Neu D. Musiol S. Balthasar H. Dumke A. et al.	<u><i>HRSC on Mars Express — Image Mosaicking for Public Outreach: Korolev Crater [#2735]</i></u> Public outreach image mosaic of Korolev Crater and volume estimation of ice filling.	Poster Location #440
Petersen E. I. Holt J. W.	<u><i>Surface Roughness Prevents SHARAD Penetration of Some Martian Debris-Covered Glaciers: A Fractal Analysis of HiRISE DTMs [#2079]</i></u> Radar is scattered / By a rough fractal surface / This ice we can't see.	Poster Location #441
Grima C. Steinbrügge G. B. Scanlan K. M. Young D. A. Putzig N. E. et al.	<u><i>Deciphering the Martian Surface and Near-Surface with Radar Statistics [#1280]</i></u> The echo strength of SHARAD surface return contains precious information about the crust's roughness, its composition, and the structure of the upper decameter.	Poster Location #442
Ahern A. A. Rogers A. D.	<u><i>Apparent Thermal Inertia Trends from Mars Odyssey THEMIS and Implications for Selected Regions of Mars [#1610]</i></u> Surface properties / Of Mars shown by apparent / Thermal inertia.	Poster Location #443
Serla J. K. Christensen P. R.	<u><i>Modeling Diurnal Temperature Variation on Mars Using Themis Infrared Data and KRC Numerical Model: A Study of Three Sites [#3227]</i></u> Temporally variable THEMIS IR data can be used to derive diurnal temperature variations on Mars using KRC Numerical Model to study the surface thermophysics.	Poster Location #444

Thursday, March 21, 2019

[R624]

POSTER SESSION II: MSL: VERA RUBIN RIDGE RESULTS

6:00 p.m. Town Center Exhibit Area

Authors (*Denotes Presenter)	Abstract Title and Summary	Poster Location
McAdam A. C. Sutter B. Archer P. D. Franz H. B. Eigenbrode J. L. et al.	<u><i>Constraints on the Mineralogy of Mudstones from the Vera Rubin Ridge, Gale Crater, Mars, from Evolved Gas Analyses [#1130]</i></u> We discuss trends in the major volatiles observed in SAM evolved gas analyses of Vera Rubin Ridge samples and their implications.	Poster Location #449
Newsom H. E. Cong C.	<u><i>Regional Gamma Ray Spectrometer (GRS) Data for Mars and Comparison to Gale Crater Mars Science Laboratory Analytical Data [#2803]</i></u> Igneous rocks in Gale Crater have a geochemical affinity with the highlands crustal regions south of the dichotomy boundary compared to regional GRS data.	Poster Location #450
Noda N. Sekine Y. Tan S. Shibuya T. Genda H.	<u><i>Groundwater Upwelling into a Gale Crater Lake on Early Mars: A Source of Silica and Ferrous Iron [#1791]</i></u> Modeling and experiments suggest that silica deposits in Murray mudstone may be derived from deep groundwater upwelled into Gale lake supported by arid climate.	Poster Location #451

Berger J. A. King P. L. Gellert R. Clark B. C. O'Connell-Cooper C. D. et al.	<u><i>Manganese Enrichment Pathways Relevant to Gale Crater, Mars: Evaporative Concentration and Chlorine-Induced Precipitation</i></u> [#2847] Localized manganese enrichments in Gale Crater may have formed via evaporative concentration and oxidation by chlorate in a brine; free O ₂ is not required.	Poster Location #452
Gasda P. J. Lanza N. Meslin P.-Y. Forni O. L'Haridon J. et al.	<u><i>High-Mn Sandstone as Evidence for Oxidized Conditions in Gale Crater Lake</i></u> [#1620] High manganese rocks: A story of water oxidation in Gale Crater, Mars.	Poster Location #453
Goetz W. Payré V. Wiens R. C. Clegg S. M. Gasnault O. et al.	<u><i>Detection of Copper in Gale Crater, Mars by the Chemcam Instrument Onboard the Curiosity Rover</i></u> [#2848] We estimate the distribution of Cu in Gale crater. This is part of an extended project to estimate Cu abundance in the martian crust and constrain Cu minerals.	Poster Location #454
Rice M. S. Starr M. S. Hughes C. M. Seeger C. H. Fraeman A. A. et al.	<u><i>Science Results from a Comprehensive Mastcam Spectral Database for Curiosity's Traverse</i></u> [#3030] A new database / Of Mastcam data from Gale / Spectral trends abound.	Poster Location #455
Jackson R. S. Ollila A. M. Nellessen M. A. Baker A. M. Wiens R. C. et al.	<u><i>Strontium in Ca-Sulfate Veins and Cements at Gale Crater, Mars</i></u> [#1909] Characterizing the Sr/Ca ratio in Ca-sulfates throughout the Gale Crater stratigraphy in order to constrain paleo-environmental conditions, like salinity.	Poster Location #456
David G. Cousin A. Forni O. Meslin P.-Y. Johnson J. R. et al.	<u><i>Iron Oxide Mineral Grains Observed by ChemCam on the Vera Rubin Ridge at Gale Crater, Mars</i></u> [#1228] We analyzed dark-toned feature analogs observed on Mars with a ChemCam like setup, to confirm iron oxide composition and better constrain their mineralogy.	Poster Location #457
Das D. Gasda P. J. Wiens R. C. Leveille R. J. Berlo K.	<u><i>Measurement of Boron in Gale Crater Near Vera Rubin Ridge</i></u> [#2437] This abstract summarizes the observation for boron measured after sol 1537 in calcium sulfate veins present in sedimentary rocks of Gale Crater.	Poster Location #458
O'Connell-Cooper C. D. Thompson L. M. Spray J. G. Gellert R. Berger J. A. et al.	<u><i>Compositional Trends Within the Murray formation, from the Base of Pahrump Hills to the End of the VRR Campaign, as Determined by APXS</i></u> [#3237] APXS analyses of the Murray formation indicate increasing Si-Al-Na-K (with elevation); decreasing Ti-Fe-Mg-P-Zn and highly variable K-Mn-Cl-Br-Zn.	Poster Location #459
Jacob S. R. Wellington D. F. Bell J. F. III Peters G. H. Fraeman A. A. et al.	<u><i>Rock Hard Science: Multispectral and Mineralogical Investigations to Understand Bedrock Spectral Properties and Strength at Vera Rubin Ridge, Gale Crater, Mars</i></u> [#1671] It was thought that hematite caused the strong 860 nm CRISM absorption across the Vera Rubin Ridge, but maybe that's not the whole story.	Poster Location #460
Rivera-Hernandez F. Sumner D. Y. Mangold N. Stack K. M. Edgett K. S. et al.	<u><i>Vera Rubin Ridge (Gale Crater, Mars) Grain Size Observations from ChemCam LIBS Data, and Interpretations</i></u> [#3029] Inferred grain sizes and possible depositional environments for Murray formation rocks in the Vera Rubin Ridge, Gale Crater from ChemCam LIBS data.	Poster Location #461
Lewis K. W. Turner M. L.	<u><i>Geologic Structure of the Vera Rubin Ridge, Gale Crater, Mars</i></u> [#2216] Stereo image data from the Curiosity rover are used to measure layer orientations at the Vera Rubin Ridge, showing good agreement with orbital observations.	Poster Location #462
Johnson J. R. Bell J. F. III Lemmon M. Pinet P.	<u><i>Mastcam Visible/Near-Infrared Spectrophotometric Observations of the Red Hills Region of Vera Rubin Ridge</i></u> [#1313] Hematite VNIR absorption bands weaken with increasing phase angle, as shown by MSL Mastcam photometry data and lab studies of hematite calibration targets.	Poster Location #463

Thursday, March 21, 2019

[R625]

POSTER SESSION II: MSL: ROVER METHODS

6:00 p.m. Town Center Exhibit Area

Authors (*Denotes Presenter)	Abstract Title and Summary	Poster Location
Schröder S. Vogt D. S. Rammelkamp K. Hansen P.B. Kubitza S. et al.	<u><i>Time-Resolved LIBS Plasma Imaging for an Improved Understanding of Martian LIBS Data</i></u> [#2793] We study the particular characteristics of martian LIBS plasmas, their dynamics, and typical spatial + temporal evolution with time-resolved LIBS plasma imaging.	Poster Location #465
Le Mouélic S. Gasnault O. Herkenhoff K. E. Newsom H. E. Gallegos Z. et al.	<u><i>Correction of Stray Light in CHEMCAM Remote Micro-Imager Long Distance Images</i></u> [#1399] We discuss the radiometric correction of a bright halo that is observed in some long distance images taken by the ChemCam/RMI camera onboard Curiosity.	Poster Location #466
Lepore K. Ytsma C. Dyar M. D.	<u><i>Comparisons Among Laser-Induced Breakdown Spectra from ChemCam, ChemLIBS, and SuperLIBS</i></u> [#1103] Measurable parameters in LIBS spectra, including ionization ratios and peak widths, were compared to assess plasma reproducibility among instruments.	Poster Location #467
Lepore K. Dyar M. D.	<u><i>Temporal Changes in LIBS Spectra Observed Using Time-Series Collection Protocols</i></u> [#1096] Time-series collection protocols are used to observe changes in LIBS spectra throughout the plasma lifetime.	Poster Location #468
Ytsma C. R. Dyar M. D.	<u><i>Updated Hydrogen, Lithium, Boron, Carbon, and Sulfur Prediction Accuracies with LIBS Under Vacuum, Earth, and Martian Atmospheres</i></u> [#1081] Investigation of LIBS' univariate and multivariate prediction accuracies for H, Li, B, C, and S using doped standards in Earth, martian, and vacuum atmospheres.	Poster Location #469
Ytsma C. R. Hurowitz J. Dyar M. D.	<u><i>LIBS and PIXL Prediction Accuracies for Ni, Mn, S, and Major Elements: A Comparative Study Using the Same Standards</i></u> [#1080] First direct comparison of PIXL and LIBS quantitative multivariate model accuracies for Ni, Mn, S, and major elements using identical doped and USGS standards.	Poster Location #470
Forni O. Gasnault O. Cousin A. Anderson R. B. Dehouck E. et al.	<u><i>Machine Learning Applied to MSL/Chemcam Data</i></u> [#1404] We want to test and evaluate the performances in terms of classification and prediction of machine learning techniques applied to the ChemCam data.	Poster Location #471
Hanania J. U. Gellert R. Wilhelm B. J. VanBommel S. J.	<u><i>Quantification of Invisible Elements and Layering Effects with the Mars Science Laboratory Alpha Particle X-Ray Spectrometer</i></u> [#2175] Discussion of methods used in the quantification of light elements and compositional layering effects by the MSL APXS using backscattered Pu X-rays.	Poster Location #472
Yingst R. A. Bray S. Edgett K. S. Fey D. Herkenhoff K. et al.	<u><i>Accumulation and Removal of Dust on Curiosity's Mars Hand Lens Imager (MAHLI) Calibration Target Associated with the Planet-Encircling Dust Event of 2018</i></u> [#1180] Results from imaging the MAHLI calibration target indicate you can't avoid dust accumulation by being mounted vertically, or hiding under the rover chassis.	Poster Location #473
Caravaca G. Le Mouélic S. Mangold N. L'Haridon J. Le Deit L. et al.	<u><i>3D Digital Reconstruction of the Kimberley Outcrop (Gale Crater, Mars) from Photogrammetry Using Multi-Scale Imagery from Mars Science Laboratory</i></u> [#1382] 3D digital outcrop modeling of the Kimberley Area (Gale Crater, Mars) and its integration within a virtual reality environment for geological analysis.	Poster Location #474

THURS POSTERS

Alemanno G. Garcia-Caurel E. Carter J. Brunetto R. Poulet F. et al.	<u>Experimental Determination of Optical Constants from Martian Analog Materials Using a Spectro-Polarimetric Approach</u> [#1794] We present our experimental approach to derive the optical constants of some martian analogue materials based on the infrared ellipsometry technique.	Poster Location #475
Starr M. S. Rice M. S. Hughes C. M. Seeger C. H. Bell J. F. III et al.	<u>Methodology for the Creation and Analysis of a Comprehensive Mastcam Multispectral Database of Curiosity's Traverse</u> [#3087] All Mastcam spectra / Placed into a database / Quick science return.	Poster Location #476

Thursday, March 21, 2019

[R626]

POSTER SESSION II: MARTIAN LABORATORY RESULTS: FORMATION, ALTERATION, AND DETECTION OF MINERALS

6:00 p.m. Town Center Exhibit Area

Authors (*Denotes Presenter)	Abstract Title and Summary	Poster Location
Tu S. Parise J. B. Lars E. Rogers A. D.	<u>Combined Differential Scanning Calorimetric-Raman Spectral Study of Ion Pairing in Aqueous Calcium Perchlorate Solution Under Mars-Relevant Temperature</u> [#1317] We measured the formation of ion pair in aqueous Ca-perchlorate solution at different martian temperatures with the help of a DSC-Raman microscope set-up.	Poster Location #477
Grady M. M. Batty C. Farsang S. Rowden P.	<u>Laboratory-Based UV Reflectance Spectroscopy in Support of Mars 2020 Returned Sample Science</u> [#3220] We have measured the UV spectra of Nakhla and Zagami for comparison with organic and inorganic species.	Poster Location #478
Gregerson J. C. Rogers A. D. Zaman M. Sklute E. C. Ehm L. et al.	<u>Raman Spectroscopy and X-Ray Diffraction Characterization of Amorphous Ferric Sulfate-Bearing Salts: Application to MSL, Mars 2020, and ExoMars Data</u> [#1924] The first step in using Raman spectroscopy and X-ray diffraction data to distinguish amorphous ferric sulfate salts from other disordered phases on Mars.	Poster Location #479
Wang Alian. Yan Y. C. Jolliff B. L. Wang K.	<u>Iron Phase Transformations Induced by Plasma Chemistry During Martian Dust Events</u> [#2036] We report the effect of plasma chemistry induced by martian dust storm and dust devils on Fe-bearing minerals, i.e., sulfides, sulfates, and chlorides.	Poster Location #480
Torre-Fdez I. Ruiz-Galende P. Aramendia J. Gomez-Nubla L. Castro K. et al.	<u>New Quantitative Model to Determine Fayalite-Forsterite Content in Olivine Minerals by Raman Spectroscopy</u> [#2486] The upcoming correct characterization of Mars surface requires quantitative calibration models for key minerals, such as olivines, for which we propose one.	Poster Location #481
Xin Y. Q. Ling Z. C. Qu H. K. Shi E. B. Liu C. Q.	<u>Laboratory Synthesis and Raman Spectroscopic Studies of Ferric Oxides</u> [#2331] We have performed laboratory synthesis and Raman measurements of hematite produced from ferric sulfate and ferric hydroxide.	Poster Location #482
Gregerson J. C. Rogers A. D. Ehm L. Parise J. B.	<u>Changes in Atomic Structure of Amorphous Iron(III) Sulfate as a Function of Hydration: Implications for Martian Soils and Sample Return</u> [#1930] The atomic structure of a potential Fe- and S-bearing amorphous component in martian soils is examined to study the effects of hydration of such materials.	Poster Location #483
Wang X. Zhou D.. Zhao Y.- Y. S. Li D. Li X. et al.	<u>Evaporation of Fe(II)- and Fe(III)- Sulfate Brines Under CO₂ and Ultraviolet Light: Implications for Fe Redox and Fe Mineral Assemblages on Mars</u> [#3275] Fe assemblages produced by evaporating Fe ²⁺ /Fe ³⁺ -sulfate with or without UV irradiation under CO ₂ .	Poster Location #484

Laserna J. J. Cabalin L. M. Delgado T. Garcia L.	<u><i>Exploring the Formation of Emitting Species in Laser-Induced Plasmas from Organic and C-Containing In-Organic Compounds Under Simulated Martian Atmosphere</i></u> [#2590] In the context of Mars 2020 mission, how the CO ₂ molecules from martian atmosphere may alter the LIBS signal of plasmas of C-containing compounds is evaluated.	Poster Location #485
Luu N. C. Hausrath E. M. Sanchez A. M. Gainey S. Rampe E. et al.	<u><i>Saponite Dissolution Experiments and Implications for Mars</i></u> [#1981] Syntheses of ferrous and magnesian saponites and dissolution experiments of natural saponite under ambient conditions.	Poster Location #486
Tu V. M. Rampe E. B. Morris R. V. Perry S. E.	<u><i>Partially Chloritized Smectites: Analogues of Smectites at Gale Crater, Mars</i></u> [#2960] Partial chloritization could be responsible for inhibiting the collapse of the Cumberland smectite down to 10Å at Gale Crater, Mars.	Poster Location #487
Wang Xiyu. Lacznia Dara. Zhao Yu-yan Sara. Karunatilake Suniti.	<u><i>Laboratory and in situ characterization of halogen volatility in martian soil.</i></u> [#3002] Laboratory and in situ characterization of halogen volatility in martian soil.	Poster Location #488
Li D. Zhao Y.-Y. S. Wu Z. Wang X.	<u><i>Thermodynamic Constraints on Limited-Water Induced Fractionation of Magnesium -Perchlorate and -Chloride: Implications for High ClO₄⁻/Cl⁻ Ratios in Martian Polar Regions</i></u> [#2188] Solubility in the Mg(ClO ₄) ₂ +MgCl ₂ +H ₂ O system was measured at subzero temperatures and its implication for ClO ₄ ⁻ /Cl ⁻ fractionation on Mars surface was discussed.	Poster Location #489
Heard A. W. Dauphas N.	<u><i>Redetermining the Kinetics of Ferrous Iron Photo-Oxidation Under UV Fluxes Relevant to Early Mars and Earth</i></u> [#1467] We are working to improve constraints on the kinetics of UV photo-oxidation, a potentially important abiotic pathway to producing ferric iron on Mars.	Poster Location #490
Mansell C. Downes H.	<u><i>Experimental Weathering of Meteorites Under Terrestrial and Martian Conditions in Environmental Chambers</i></u> [#1035] Artificial weathering of stony and iron meteorites under experimental martian and terrestrial conditions show why iron meteorites are abundant on Mars' surface.	Poster Location #491

Thursday, March 21, 2019

[R627]

POSTER SESSION II: MARS GEOMORPHOLOGY

6:00 p.m. Town Center Exhibit Area

Authors (*Denotes Presenter)	Abstract Title and Summary	Poster Location
Chesnutt J. M. Wegmann K. W. Szymanski E. D. Byrne P. K. Kling C. L.	<u><i>Landscape Evolution Comparison Between Valles Marineris, Mars, and the Rio Chama Canyon, New Mexico, USA</i></u> [#2811] Earth–Mars analog landscape evolution study of Valles Marineris and Rio Chama Canyon, NM that focuses on escarpment-flank mass wasting and valley formation.	Poster Location #493
Smith B. Horgan B.	<u><i>Estimating Flow Rates in Outflow Channels on Mars from Sediment Grain Size</i></u> [#1293] Using THEMIS-derived thermal inertia to determine deposited sediment grain sizes and fluid velocity in outflow channels on the martian surface.	Poster Location #494
Anbazhagan S. Chinnamuthu M.	<u><i>Geomorphic Processes and Origin of Cusus Valles on Mars</i></u> [#1023] Abstract reveals the origin of valley networks in Cusus Valles. Precipitation, runoff, erosion, and infiltration are the reasons for formation of channels.	Poster Location #495
Scheidt S. P. Crown D. A. Berman D. C.	<u><i>Distribution and Morphology of Valley Networks on the Flanks of Alba Mons, Mars</i></u> [#2014] We are presenting geomorphological mapping and hydrological modeling results of valley networks on Alba Mons, Mars.	Poster Location #496
Davis J. M. Balme M. Gupta S. Grindrod P. M. Fawdon P. et al.	<u><i>Diversity and Downslope Transitions of Exhumed Fluvial Systems in Arabia Terra, Mars</i></u> [#1513] Ridges and valleys / Dynamic Noachian / Their interplay shows.	Poster Location #497

THURS POSTERS

Boatwright B. D. Head J. W.	<u><i>Fluvial Geology of the Northwest Hellas Region, Mars: Evidence for Localized Drainage and Terrain Inversion</i></u> [#2688] We describe inverted fluvial channels in degraded crater floors that may be locally derived from top-down melting of a highlands ice sheet.	Poster Location #498
Matherne C. M. Skok J. R. Mustard J. F. Karunatillake S.	<u><i>Fluvial Activity in Northeast Syrtis Major and Its Relationship to Glacial Processes in the Hesperian</i></u> [#1922] Basin and channel / Hesperian-aged glaciers / Look! Morphology!	Poster Location #499
Dickeson Z. I. Grindrod P. M. Crawford I. Balme M. R. Gupta S. et al.	<u><i>Hydrological History of a Complex Lake and Valley System in Western Arabia Terra, Mars</i></u> [#1559] Lonely Mars valleys / Topographic lows reveal / Connected lake chains.	Poster Location #500
Roseborough V. A. Palucis M. C.	<u><i>Relative Role of Groundwater Versus Surface Water in the Gale Crater Region</i></u> [#3051] Valley networks end / Suggesting paleolakes / How did water flow?	Poster Location #501
Goudge T. A. Fassett C. I. Osinski G. R.	<u><i>How Do Crater Lakes on Mars Develop Inlet Valleys?</i></u> [#1223] Crater lakes on Mars / Inlets cross uplifted rim / How did that happen??	Poster Location #502
Holo S. J. Kite E. S.	<u><i>Dynamics of Mars Lake-Overflow Valley Incision</i></u> [#2481] We present a reduced complexity model of lake-overflow valley incision on Mars.	Poster Location #503
Kanine M. K. Putnam E. T. Rivera-Hernandez F. Palucis M. C.	<u><i>Quantitative Geomorphic and Hydrologic Analysis of Paleo-Lake Basins in the Gale Crater Region, Mars</i></u> [#2491] Paleobasins / What was the source of water? / What was the climate?	Poster Location #504
Peel S. E. Burr D. M.	<u><i>Identification of Paleo-Lakes in Floor-Type Central Pits, Mars: An Update</i></u> [#1003] We test the hypothesis that individual central pits in complex craters once hosted lakes. Our results support paleo-lake activity in seven of the 96 tested craters.	Poster Location #505
Newsom H. E. Scuderi L. A. Gallegos Z. E. Nagle-Mcnaughton T.	<u><i>Upper Drainage and Watershed of the Multi-Stage Peace Vallis Alluvial Fan System, Gale Crater, Mars</i></u> [#2568] Gale Crater's northern rim shows integration of large channel networks, stream capture of watersheds, and late very small late channels only a few meters wide.	Poster Location #506
Gallegos Z. E. Newsom H. E. Scuderi L. A. Wiens R. C. Grant J. A. et al.	<u><i>Formation and Architecture of the Multi-Stage Peace Vallis Alluvial Fan System, Gale Crater, Mars</i></u> [#2841] MSL ChemCam RMI rover imagery and HiRISE orbital data are utilized to interpret the formation processes and the sedimentary architecture of the Peace Vallis fan.	Poster Location #507
Morgan A. M. Wilson S. A.	<u><i>Utilizing a Global Database to Explore Morphologic Trends of Martian Alluvial Fans</i></u> [#3256] We created a global inventory of alluvial fans using CTX data and explore morphologic trends and characteristics of the fans.	Poster Location #508
Mondro C. A. Fedo C. M. Moersch J. E.	<u><i>Identification and Morphologic Characterization of Small and Medium Alluvial Fans on Mars Using the CTX Global Mosaic</i></u> [#2739] This study presents morphologic analysis of new small and medium alluvial fans on Mars that have been identified from the CTX global mosaic.	Poster Location #509
Grindrod P. M. Davis J. M. Gupta S. Banham S.	<u><i>Repeat Syn-Tectonic Sedimentation in Coprates Chasma, Mars</i></u> [#1407] Repeat features tale / Of faults, fans, faults, fans, faults, fans / Sediments downthrown.	Poster Location #510
Salese F. Pondrelli M. Neeseman A. Schmidt G. Ori G. G.	<u><i>A Geological Model for Martian Groundwater Based on Water-Formed Features Within Deep Basins</i></u> [#3240] Geological evidence supporting martian planet-wide groundwater upwelling and putative relations with the ocean shorelines around - 4000m below the Mars DATUM.	Poster Location #511
Sarkar R. Edgett K. Singh P. Porwal A.	<u><i>Origin of the Light-Toned Sedimentary Rocks in Juventae Chasma, Mars</i></u> [#2835] In this abstract, we report on the formation of Juventae Chasma and the origin of the light-toned layered rocks that are exposed within it.	Poster Location #512

Cowart J. C. Bunce L. E. Rogers A. D.	<u><i>Isolated Chaos and Colles in the Martian Highlands: Potential Insights into Basin-Fill and Modification Processes</i> [#1579]</u> Mounds in basin plains / Hold clues to the martian past / In their sites and forms.	Poster Location #513
Mouginis-Mark P. J. Garbeil H.	<u><i>CTX Digital Elevation Models Facilitate Geomorphic Analysis of Mars</i> [#1069]</u> We describe our production of digital elevation models from CTX images of Mars, and give examples of what is available using the University of Hawaii RPIF website.	Poster Location #514
Scheller E. L. Ehlmann B. L.	<u><i>Stratigraphy and Geological History of the Noachian Basement on the Western Rim of Isidis Basin</i> [#1515]</u> We investigate the complex stratigraphy, including several compositional subunits of the Noachian basement on the western rim of Isidis basin.	Poster Location #515
Annex A. M. Koepfel A. H. D. Pan C. Edwards C. E. Lewis K. W.	<u><i>Scarp Associated with Martian Layered Deposits in Arabia Terra</i> [#1973]</u> We studied a scarp-like structure overlaying layered deposits in Arabia Terra on Mars. It may record a climatic shift ending deposition in the region.	Poster Location #516
Voelker M. Orgel C. Ramsdale J. D. Séjourné A. Cardesín-Moinelo A. et al.	<u><i>Quantifying the Latitudinal Distribution of Landforms on Mars' Southern Hemisphere, Noachis Terra — Preliminary Results</i> [#1776]</u> By applying the grid-mapping method, we were able to quantify the latitudinal distribution of landforms in Noachis Terra from the equator to the south pole.	Poster Location #517
Cunje A. B. Dombard A. J. Noe Dobrea E. Z.	<u><i>Relaxation of Small Icy Craters at Mid-Northern Latitudes on Mars in the Absence of Flow by Grain Boundary Sliding</i> [#3131]</u> Dusty ice craters / Relax with no GBS / In the north of Mars.	Poster Location #518
Noguchi R. N. Ishiyama K. I. Kumamoto A. K. Usui T. U. Uemura C. U.	<u><i>First Detection of Subsurface Reflectors in Coprates Chasma, Mars</i> [#2333]</u> This study investigated radargrams and assigned prominent subsurface reflectors to the layers exposed on the wall of Coprates Chasma.	Poster Location #519

Thursday, March 21, 2019

[R628]

POSTER SESSION II: PLANETARY POLAR PROCESSES AND CRYOSPHERES

6:00 p.m. Town Center Exhibit Area

Authors (*Denotes Presenter)	Abstract Title and Summary	Poster Location
Bramson A. M. Petersen E. I. Bain Z. M. Putzig N. E. Morgan G. A. et al.	<u><i>Mars Subsurface Water Ice Mapping (SWIM): Radar Subsurface Reflectors</i> [#2069]</u> Looking for Mars ice / How will the SWIM team find it? / With radar data.	Poster Location #520
Putzig N. E. Hollibaugh Baker D. M. Morgan G. A. Bain Z. M. Bramson A. M. et al.	<u><i>Mars Subsurface Water Ice Mapping (SWIM): Geomorphic Mapping</i> [#2087]</u> Looking for Mars ice / How will the SWIM team find it? / With morphology.	Poster Location #521
Bain Z. B. Morgan G. A. Putzig N. E. Campbell B. A. Bramson A. M. et al.	<u><i>Mars Subsurface Water Ice Mapping (SWIM): Radar Surface Reflectivity</i> [#2726]</u> Looking for Mars ice / How will the SWIM team find it? / With surface power.	Poster Location #522
Perry M. R. Bain Z. M. Putzig N. E. Morgan G. A. Bramson A. M. et al.	<u><i>Mars Subsurface Water Ice Mapping (SWIM): The SWIM Equation and Project Infrastructure</i> [#3083]</u> Looking for Mars ice / How will the SWIM team find it? / The SWIM equation!	Poster Location #523
Hoover R. H. Sizemore H. G. Bain Z. Putzig N. E. Morgan G. A. et al.	<u><i>Mars Subsurface Water Ice Mapping (SWIM): Thermal Analysis</i> [#1679]</u> Looking for Mars ice / How will the SWIM team find it? / With thermal data.	Poster Location #524
Stamenkovic V. Plesa A.-C. Breuer D. Mischna M.	<u><i>Mars Subsurface Hydrology in 4D</i> [#2795]</u> The depth of potential groundwater follows a distribution that reflects the combined effects of crustal thickness and surface temperature variations.	Poster Location #525

Buz J. Edwards C. S. Piqueux S.	<u><i>New Technique for Calculating Ice Depths on Mars at THEMIS Resolution</i> [#3082]</u> Utilizing the season on Mars when the depth to an ice is independent of the surface thermal inertia allows for independent calculation of the two parameters.	Poster Location #526
Alwarda R. Smith I. B.	<u><i>Mapping and Characterization of the Bounding Layers of the CO₂ Deposit in Planum Australe, Mars</i> [#3026]</u> Carbon dioxide / Layers within the south ice / We find thicknesses.	Poster Location #527
Scanlan K. M. Young D. A. Grima C. Steinbrugge G. Kempf S. D. et al.	<u><i>Englacial Radar Attenuation Rates in the Promethei Lingula Area of the Martian South Polar Layered Deposits</i> [#1994]</u> Internal layers revealed in SHARAD datasets are used to constrain englacial radar attenuation within the Promethei Lingula region of the martian SPLD.	Poster Location #528
Steinbrügge G. Scanlan K. M. Young D. A. Grima C. Kempf S. D. et al.	<u><i>SHARAD Radar Altimetry and Geodesy</i> [#1993]</u> We present SHARAD altimetry results and compare them to HRSC DTM data. Combining with MOLA data allows for an increased temporal and horizontal resolution.	Poster Location #529
Pascuzzo A. C. Conduis T. Mustard J. F. Arvidson R. E.	<u><i>VNIR Characterization of the Martian North Polar Ice Cap 1): The Importance of Rigorous Corrections of Atmospheric Aerosols and Surface Scattering</i> [#1913]</u> Unaccounted for, dust aerosols and surface scattering result in erroneous spectral interpretations of icy surfaces.	Poster Location #530
Pascuzzo A. C. Tarnas J. D. Mustard J. F. Lin H.	<u><i>VNIR Characterization of the Martian North Polar Ice Cap 2): Constraining the Surface Composition</i> [#3063]</u> Evaluating the presence of sulfates along the trough walls of the north polar ice cap.	Poster Location #531
Litvak M. L. Mitrofanov I. G. Malakhov A. V. Sanin A. B. Boynton W. V.	<u><i>Joint Observations of Martian Seasonal Cycle from HEND/Odyssey and FREND/TGO</i> [#2443]</u> The main goal is to compare simultaneous HEND/Odyssey and FREND/TGO observations to perform joint analysis of growth and sublimation of martian seasonal caps.	Poster Location #532
Auerbach V. L. Calvin W. M. James P. B. Cantor B. A.	<u><i>Annual and Long-Term Mars Northern Seasonal Cap Recession Observed with MARCI</i> [#2987]</u> Observations of the Mars northern seasonal cap retreat using MARCI images and comparison of new and previous data collected through different techniques.	Poster Location #533
Widmer J. M. Diniega S.	<u><i>Constraining the Spatial Extent and Timing of Local-Scale Seasonal Frost in the Northern Mid Latitude Region of Mars</i> [#1990]</u> Mars instruments ask / Seasonal frost, where art thou? / Tricky frost responds.	Poster Location #534
Diniega S. Widmer J. M. Gary-Bicas C. Fraeman A. A. Hayne P. O. et al.	<u><i>Correlating Present-Day Surface and Subsurface Frost Conditions with Geomorphologic Activity on Mars</i> [#2165]</u> Alcoves erode dunes / Prompted by frost of some sort / Must find the driver.	Poster Location #535
Angell P. Christensen P. R.	<u><i>Seasonal Temperature Variations, Albedo Variations, and CO₂ Sublimation Activity Near the Martian South Pole</i> [#3199]</u> The south pole of Mars is a dynamic region where every spring and summer the seasonal CO ₂ ice layer sublimates, forming dark spots and streaks on the surface.	Poster Location #536
Hansen C. J. Aye K.-M. Portyankina G. Schwamb M.	<u><i>Interannual Variability of Seasonal Activity in Mars' South Polar Region Dubbed "Manhattan"</i> [#3110]</u> The level of activity associated with sublimation of the CO ₂ polar cap, as evidenced by numbers of fans on the seasonal cap, may be correlated to dust storms.	Poster Location #537
Sori M. M. Bapst J. Becerra P. Byrne S.	<u><i>The Paleoclimate Record of Outlier Ice Deposits Near the Martian Poles</i> [#1181]</u> Ice deposits located within craters at high latitudes on Mars contain decipherable climate records that can be compared to those in the larger NPLD and SPLD.	Poster Location #538

Mesick K. E. Mullin E. R. West S. T. Feldman W. C.	<u><i>Characterization of Mars' Polar Caps Over 8 Martian Years: New and Extended Analysis of Mars Odyssey Neutron Spectrometer Data</i></u> [#2750] Using the Mars Odyssey Neutron Spectrometer to study inter-annual variability in the martian seasonal polar caps.	Poster Location #539
Russell P. S. Parra S. A. Milkovich S. M. Becerra P. Byrne S.	<u><i>Visible and Topographic Texture of the North Polar Residual Cap of Mars</i></u> [#3048] We map the characteristic wavelength and orientation of the NPRC surface texture, using 2D FFT of brightness of visible images and relief of DTMs.	Poster Location #540
Hibbard S. M. Osinski G. R.	<u><i>Brain Terrain on Earth? A Potential Periglacial Analogue in the Canadian High Arctic</i></u> [#2126] Brain terrain on Earth? / What could that mean for Mars' past? / Regardless, it's cool.	Poster Location #541
Andres C. N. Godin E. Osinski G. R. Zanetti M. Kukko A.	<u><i>A Quantitative Analysis of Sorted Patterned Ground Within the Haughton Impact Structure, Devon Island, with Implications to Mars</i></u> [#2103] Semi-automated analysis of the form and spatial distribution of LIDAR-derived sorted patterned ground with implications to periglacial landform evolution.	Poster Location #542
Meng T. M. Petersen E. I. Holt J. W. Levy J. S. Larsen C. F.	<u><i>Local Variability in Debris-Covered Glacier Evolution on Earth and Mars</i></u> [#3197] Trends are observed between martian and terrestrial debris-covered glacier evolution; they have some correlation with the orientation of their basal slopes.	Poster Location #543
Miller J. L. Hibbitts C. A. Mellon M. T. Sizemore H. G.	<u><i>Salt and Water Migration in Mars-Like Permafrost Soils</i></u> [#3077] Duricrusts form in cold, dry martian regolith. We investigate a possible mechanism of salt and water migration via thin films through a series of experiments.	Poster Location #544
Sizemore H. G. Demchenko V. Zent A. P. Rempel A. W. Stillman D. E.	<u><i>Water Activity of Premelted Films in High Latitude Martian Ground Ice</i></u> [#2907] Thin films of liquid / Too cold for bugs. Salt may help. / So will axis tilt.	Poster Location #545

Thursday, March 21, 2019

[R629]

POSTER SESSION II: MARS MUD VOLCANOS: MUD, MUD, GLORIOUS MUD

6:00 p.m. Town Center Exhibit Area

Authors (*Denotes Presenter)	Abstract Title and Summary	Poster Location
Dapremont A. M. Wray J. J.	<u><i>A Global Assessment of Mars Mud Volcanism Products: Preliminary Results Provided by CRISM</i></u> [#2916] A global examination of the visible and near-infrared (VNIR) spectroscopy characteristics of Mars mud volcanism products.	Poster Location #547
Rodriguez J. A. P. Kargel J. S. Oehler D. Z. Crown D. A. Baker V. R. et al.	<u><i>Potential Cryospheric Mud Volcanism in the Northern Plains of Mars: Geologic and Astrobiological Implications</i></u> [#2580] Cryospheric mud volcanoes might populate northern plains zones affected by major denudation, likely reflecting a heterogeneous subsurface methane production.	Poster Location #548
Brož P. Krýza O. Conway S. J. Raack J. Patel M. R. et al.	<u><i>Experimental Simulation Reveals that Mud Behaves Like Lava Under Martian Conditions</i></u> [#1511] Mud experiments performed inside a low pressure chamber revealed that mud on the cold martian surface could behave in some aspects similar to the pahoehoe lava.	Poster Location #549
Brož P. Krýza O. Conway S. J. Raack J. Patel M. R. et al.	<u><i>Violent Mud Propagation on Mars: Evidence from Laboratory Simulations</i></u> [#1769] Experiments show that a warm and unconsolidated surface has a profound effect on the behavior of mud in a low (7mbar) pressure environment, because of boiling.	Poster Location #550

THURS POSTERS

Hemmi R. Miyamoto H.	<u>High-resolution Topographic Analysis of Pitted Mounds in Southern Acidalia Planitia, Mars: Updates on Morphometric Parameters of Candidate Mud Volcanoes</u> [#2479] We accurately measured morphometry of pitted mounds on Mars and discussed about mud volcano origin.	Poster Location #551
Komatsu G. Ishimaru R. Kawai K. Miyake N. Kobayashi M. et al.	<u>Sedimentary Records of Ancient Mud Volcanism: How Do We Identify Mud Volcanoes in the Stratigraphy of Mars?</u> [#1149] We present terrestrial examples of mud volcanoes identifiable in stratigraphy, which could be useful in interpretation of similar features in martian outcrops.	Poster Location #552

Thursday, March 21, 2019

[R630]

POSTER SESSION II: MARS VOLCANOLOGY

6:00 p.m. Town Center Exhibit Area

Authors (*Denotes Presenter)	Abstract Title and Summary	Poster Location
Berman D. C. Crown D. A.	<u>Chronology of Volcanism in Southern Tharsis, Mars: Constraints from Lava Flows in Daedalia Planum</u> [#1418] Age constraints from crater size-frequency distributions in southern Tharsis show two distinct pulses of volcanic activity in the Amazonian Period.	Poster Location #554
Mouginis-Mark P. J. Wilson L.	<u>Late-Stage Intrusive Activity at Olympus and Ascræus Montes, Mars</u> [#1068] Lava flows that appear to flow uphill are identified at the summits of Olympus and Ascræus Montes, Mars, and imply summit inflation after flow emplacement.	Poster Location #555
Ciazela J. Mège D. Pieterek B. Ciazela M. Gurgurewicz J. et al.	<u>Largest Tharsis Volcanoes Keep Growing and Mark >4-Ga-Lasting Martian Hot Spots</u> [#1364] Dating and morphology of large Tharsis volcanoes suggest Olympus Mons and Tharsis Montes are dormant, with a current long-term eruptive flux of 80–150 km ³ /m.y.	Poster Location #556
Fawdon P. Balme M. R. Vye-Brown C. Jordan C. J. Rothery D. A.	<u>The Age of Syrtis Major Planum and Implications for the Circum-Isidis Region</u> [#2362] Syrtis Major Planum is a good stratigraphic marker and is useful differentiating when regional processes occurred.	Poster Location #557
Ackiss S. Horgan B. Suda M. Minton D. Campbell A.	<u>Geomorphologic Mapping of a Possible Hesperian Subglacial Volcanic Environment in the Sisyphi Montes, Mars</u> [#1491] Here, we map units within the Sisyphi Montes region to elucidate the origin of edifices within the region.	Poster Location #558
Stacey K. Kerber L. Hamilton C. W.	<u>Interactions Between Athabasca Valles Flood Lavas and the Medusae Fossae Formation: Implications for Lava Emplacement Mechanisms and the Triggering of Steam Explosions</u> [#3160] Rootless cones in Cerberus Palus, atop the Athabasca Valles Flood Lava, display morphologies that indicate different triggering mechanisms of steam eruptions.	Poster Location #559
Neruzzi S. Tober B. S. Holt J. W.	<u>Investigating Magma-Cryosphere Interactions and Outflow Channel Activity in Hebrus Valles and Hephaestus Fossae, Mars</u> [#3040] Magma and rivers / Precious scars on Mars' surface / Fund my proposal.	Poster Location #560
Graettinger A. H. Hughes C. G.	<u>Criteria for Candidate Maars on Mars</u> [#1254] Maar recognition on Mars based on a list of morphologic criteria, with one remaining limitation of secondary craters.	Poster Location #561
Simurda C. M. Ramsey M. S. Crown D. A.	<u>Quantifying the Areal Percentages of Dust, Sand, and Lava Outcrops in Daedalia Planum, Mars</u> [#1475] This thermophysical modeling reveals that lava flows in Daedalia Planum are not completely dust mantled and some surfaces contain ~40% observable outcrops.	Poster Location #562

Thursday, March 21, 2019

[R631]

POSTER SESSION II: PLANETARY VOLCANISM: A SONG OF FIRE AND ICE

6:00 p.m. Town Center Exhibit Area

Authors (*Denotes Presenter)	Abstract Title and Summary	Poster Location
Morrison A. A. Whittington A. G. Zhong F. Mitchell K. L. Carey E. M.	<u><i>Rheological Investigation of Cryovolcanic Slurries: Viscosity of Chloride Brines</i></u> [#1923] Experimental data for rheology of cryovolcanic material lacks compositional diversity. Rheological data will be produced for chloride brines relevant to Ceres.	Poster Location #563
Flynn I. T. W. Ramsey M. S.	<u><i>Thermorheological Modeling of Channelized Lava Flows on Earth and Mars</i></u> [#1452] Test and refine the PyFLOWGO flow model to quantify the properties of martian flows including eruption rate, viscosity, crystal content, and flow velocity.	Poster Location #564
Grewal D. S. Dasgupta R. Farnell A. Hough T. Costin G. et al.	<u><i>The Speciation of Nitrogen and Carbon in Magma Oceans and the Resulting Compositions of Early Atmospheres</i></u> [#2192] Spectrographic analysis of high pressure-temperature experiments is used to predict the dissolution behavior of carbon and nitrogen in magma oceans.	Poster Location #565
Huang R. I. Radebaugh J. Christiansen E. H.	<u><i>Quantitative Analysis of Caldera Shape</i></u> [#2783] Terrestrial caldera shape comparison to martian shield calderas using discriminant analysis.	Poster Location #566
Reeder A. Rader E. Doloughan A. Ackiss S. Sisson T. et al.	<u><i>The Identification of Lava/Water Interaction Through VNIR Analysis: A Trial Study at Jordan Craters, Oregon</i></u> [#1630] Identifying the potential VNIR signatures formed during the lava/water interactions of basalt at Jordan Craters, Oregon.	Poster Location #567
Leight C. J. McCanta M. C. Thomson B. J.	<u><i>Spectral Characterization of Explosive Volcanic Products</i></u> [#2747] We present VSWIR and MIR data on a suite of terrestrial tephra samples to study the spectral effects of glass compositions and phase assemblages.	Poster Location #568
James D. H. Anderson S. W.	<u><i>Using Structure from Motion and High-Resolution Digital Elevation Models to Investigate the Relationships Between Emplacement History and Lava Surface Roughness: Mauna Ulu (Hi), Amboy (Ca), and Tharsis</i></u> [#2114] Goal: Use roughness to / Describe the emplacement style / Of martian lava.	Poster Location #569
Carr B. B. Bennett K. A. Lev E. Edwards C. S.	<u><i>Utilization of an sUAS-Based Thermal Camera to Determine Relative Thermal Inertia of Volcanic Deposits</i></u> [#3129] We investigate the thermophysical properties of volcanic deposits using repeat surveys by a small unmanned aerial system carrying a thermal infrared camera.	Poster Location #570
Cataldo V. Williams D. A. Schmeeckle M. W.	<u><i>Estimating the Extent of Thermal Versus Mechanical Erosion at a Rille-Like Lava Channel at Raqlan, Northern Québec, Canada</i></u> [#3124] We use the first 3-D model of thermal erosion by turbulently flowing lava to derive an estimate of the extent of thermal vs. mechanical erosion at Raqlan, Canada.	Poster Location #571
Kaku T. Haruyama J. Miyake W. Kumamoto A. Ishikawa K. et al.	<u><i>Global Distribution of Possible Lava Tubes from Near-Surface to a Hundred Meter Depth on the Moon</i></u> [#2205] Global distribution of possible lava tubes from near-surface to a hundred-meter depth on the Moon, suggested from SELENE Lunar Radar Sounder (LRS) data.	Poster Location #572
Morgan G. A. Campbell B. A. Patterson G. W. Mini-RF Team	<u><i>Multi-Wavelength Bistatic View of the Lunar Mare Using Mini-RF</i></u> [#2969] Here we present our ongoing targeting campaign to investigate the composition and structure of the lunar mare.	Poster Location #573

THURS POSTERS

Basilevsky A. T. Zhang F. Wöhler C. Bugiolacchi R. Head J. W. et al.	<u><i>Lunar Ring-Moat Dome Structures and Their Relationships with Small Impact Craters</i> [#1507]</u> The RMDS-crater age relationships and crater morphology are analyzed to further test models of the ages and physical properties of lunar RMDSs.	Poster Location #574
Morgan C. R. Wilson L. Head J. W.	<u><i>Factors Controlling the Size Distributions of Lunar Pyroclasts</i> [#1341]</u> We review the factors controlling the release of volatiles from lunar magmas and the ways in which they determine the size distribution of pyroclastic droplets.	Poster Location #575
Brown M. A. Hood D. R. Karunatillake S.	<u><i>Chemical Investigations of Friable Deposits in Northeast Arabia Terra, Mars</i> [#1217]</u> Chemical analysis using Gamma Ray Spectrometer (GRS) and thermal inertia data derived from THEMIS mosaics were applied to friable deposits in NE Arabia Terra to examine their origin.	Poster Location #576
Moitra P. Horvath D. G. Andrews-Hanna J. C.	<u><i>Explosive Magma-Water Interaction on Mars: Insight from a Young Pyroclastic Deposit in Elysium Planitia</i> [#2721]</u> A young volcanic deposit in the Elysium Planitia region on Mars is interpreted to be a consequence of explosive interaction between magma and ground water/ice.	Poster Location #577
Fuqua Haviland H. Karunatillake S. Susko D. Ojha L. Baratoux D. et al.	<u><i>Characterizing Elysium's Magmatic Evolution and Chemistry Initial Study</i> [#3206]</u> We discuss initial results from a modeling (melts, equations of state, gravity) and observations analysis to investigate the spatiotemporal evolution of Elysium.	Poster Location #578
Voigt J. R. C. Hamilton C. W.	<u><i>Constraining Effusive Eruption Styles Throughout Elysium Planitia, Mars</i> [#2620]</u> Young lava flows in Elysium Planitia are evaluated according to their volume and effusion rate to constrain eruption styles reflecting magmatic storage regions.	Poster Location #579
Leverington D. W.	<u><i>Formation of Ares Vallis by Effusions of Low-Viscosity Lava at Iani, Aram, Margaritifer, and Hydaspis Chaos</i> [#2128]</u> Though Ares Vallis is widely interpreted as a product of catastrophic outbursts from aquifers, its attributes are instead aligned with dry volcanic origins.	Poster Location #580
Lo M. Wilson L. Chevrel M. O.	<u><i>The Rheology and Eruption Conditions of Fissure-Fed Lavas Near Jovis Tholus, Mars</i> [#1101]</u> We analyze the emplacement of lava flows and fissure ramparts from an eruption in Tharsis using rheological properties relevant to martian basalt chemistry.	Poster Location #581
Shoemaker E. S. Carter L. M. Garry W. B.	<u><i>Radar Sounding of Lava Flows in the Tharsis Province, Mars</i> [#2611]</u> The SHARAD and MARSIS radar sounders detect new subsurface interfaces beneath lava flows surrounding the Tharsis Montes on Mars.	Poster Location #582
Pieterek B. Ciazela J. Mège D. Tesson P.-A. Ciazela M. et al.	<u><i>Parasitic cones in the Tharsis volcanic province on Mars: Implications for its recent magmatic plumbing system</i> [#1369]</u> Based on the distribution of small cones, orientations of their summit craters, and ages we conclude they represent parasitic cones of the large Tharsis volcanoes.	Poster Location #583
Patel R. R. Nair A. M. Nagori R. Arya A. S.	<u><i>Identification of Altered Silicate Minerals on Arsia, Pavonis, and Ascraeus Mons of Tharsis Volcanic Provinces of Mars</i> [#1851]</u> CRISM-based mineralogy confirms presence of mafic mineral pyroxene with alterations on tharsis volcanic province suggesting active weathering.	Poster Location #584
McKeeby B. E. Ramsey M. S. Simurda C. M.	<u><i>THEMIS ROTO Images: A Unique Off-Axis Dataset for Determining Surface Roughness Characteristics</i> [#2603]</u> THEMIS ROTO-derived radiance values and spectral shape variation are used to study surface roughness and local slope changes of landforms in Daedalia Planum.	Poster Location #585
Mura A. Adriani A. Tosi F. Lopes R. Sindoni G. et al.	<u><i>Observations of Jupiter's Moon Io by Juno/JIRAM</i> [#2801]</u> Juno/JIRAM spectrometer observed Io on December 2017. A possible new hot spot/volcano is found close to the south pole.	Poster Location #586

Rathbun J. A. Spencer J. R.	<u><i>Io's Loki Volcano: An Explanation of Its Tricky Behavior and Prediction for the Next Eruption</i> [#2402]</u> Loki Volcano / What you get when feature named / After a trickster.	Poster Location #587
Naegeli K. M. Lehto H. L. Carrell K. W.	<u><i>The Gravitational Effects on the Volcanism of Io</i> [#2800]</u> This study will be analyzing the eruption by date in order to see if there are any correlation to eruption and placement in its orbit on the satellite Io.	Poster Location #588
Schools J. Montesi L. G. J.	<u><i>The Lifespan of Heat Pipes on Io, Modeled with Melt Migration</i> [#3182]</u> We model heat pipe evolution on Io using numerical models with melt migration.	Poster Location #589

Thursday, March 21, 2019

[R632]

POSTER SESSION II: MARS ANALOGS: VOLCANIC AND HYDROTHERMAL PROCESSES

6:00 p.m. Town Center Exhibit Area

Authors (*Denotes Presenter)	Abstract Title and Summary	Poster Location
Cao X. Bao H. Gao C. Liu Y. Huang F. et al.	<u><i>Triple Oxygen Isotope Constrains on Interactions Between Planetary Interior and Surface</i> [#2454]</u> Triple oxygen isotope compositions in olivine provide a unique tool to reveal the interactions between planetary interior and surface.	Poster Location #591
DiFrancesco N. J. Rogers A. D. Yant M. Nekvasil H. King P. L.	<u><i>Chemical and Spectral Properties of Sulfates Produced by Magmatic Gas/Mineral Surface Reactions on Mars</i> [#3127]</u> Sulfates are produced by interaction of S- and Cl-rich magmatic gas with martian surface rock, producing coatings that are identifiable in VNIR and TIR.	Poster Location #592
Carson G. L. McHenry L. J. Hynek B. M. Cameron B. I. Glenister C. T.	<u><i>Leaching, Precipitation, and Oxidation in an Icelandic Hydrothermal System: Comparison to Columbia Hills, Mars</i> [#2209]</u> Sulfate-rich precipitates and silica-rich leached deposits near Icelandic fumaroles and mud pots compare favorably to likely hydrothermal deposits at Home Plate.	Poster Location #593
Achilles C. N. McAdam A. C. Knudson C. A. Young K. E. Bleacher J. et al.	<u><i>Acidic Alteration in a Young Basaltic Lava Field: Sulfur-Bearing Products and Implications for Mars</i> [#3043]</u> To explore conditions related to basaltic alteration and sulfate formation, we discuss the mineralogy of fumarole-associated rocks and cave-like mineral deposits.	Poster Location #594
Perrin S. L. Bishop J. L. Gruendler L.	<u><i>Investigation of Altered Volcanic Material from the Polihua Trail Site on Lana'i as an Analogue for Mars</i> [#3158]</u> Lana'i volcanics / Are isolated, arid / Martian analogues.	Poster Location #595
Weert A. M. P. Foing B. H. Rogers H. Musilova M. Gonzalez Y.	<u><i>Hydrous Alteration of Lava Flows on Mauna Loa (Hawaii) Compared to Mars Volcanic Soils</i> [#1633]</u> Samples from Hawaii will be compared to martian rocks, to provide more insight in the effects of hydrous alteration of volcanic rocks on Mars.	Poster Location #596
Barbato A. B. Karunatillake S. K. Hood D. H. Vithanage M. V.	<u><i>Variations in Serpentine Along the HC-VC Suture Zone of Sri Lanka: An Analogue for Studying Martian Serpentes</i> [#3143]</u> Serpentes from Sri Lanka may provide insight for serpentine deposits on Mars, making the island a useful analogue for future Mars field work.	Poster Location #597
Glotch T. D. Ye C. Young J. M. Lindsley D. H. Nekvasil H. et al.	<u><i>Spectroscopy of Synthetic Pigeonite Standards</i> [#2420]</u> My friends are furloughed / Here's a pigeonite abstract / Hope they can read it.	Poster Location #598
Scudder N. A. Horgan B. Rampe E. B. Smith R. J. Rutledge A. M.	<u><i>Spectral Interpretation of Magmatic Evolution, Oxidation, and Crystallinity in a Volcanic Planetary Analogue System</i> [#1987]</u> Combined VNIR and TIR spectroscopy can estimate rock type, mineral composition, oxidation, and crystallinity of a diverse volcanic analog sample suite.	Poster Location #599
Seidel R. G. W. Bridges J. C. Kirnbauer T. Sherlock S. C. Schwenzer S. P.	<u><i>The Frankenstein Gabbro (Odenwald, Germany): A New Analogue for Martian Hydrothermal Systems</i> [#1666]</u> Mars analogue study for basalt-hosted hydrothermal systems. Small-scale variability of fluid properties needs to be considered in predicting habitability.	Poster Location #600

THURS POSTERS

Mallozzi S. Samson C. Monteiro Santos F. A. Cunningham M. Holladay S. et al.	<u>Surface Magnetic and Interior Electromagnetic Surveying of the Juniper Lava Tube at Lava Beds National Monument, California</u> [#1219] Geophysical detection and characterization of terrestrial lava tubes as guidelines for future Mars missions.	Poster Location #601
Lo Presti D. Gallo G. Bonanno D. L. Bonanno G. Bongiovanni D. G. et al.	<u>The MEV (Muography of Etna Volcano) Project and Its Future Applications to the Earth and Mars</u> [#1884] The talk proposes the use of muography to study the morphology of volcanoes on Mars. A muon tracker telescope was built and deployed on the top of Etna volcano.	Poster Location #602

Thursday, March 21, 2019

[R633]

POSTER SESSION II: MARS ANALOGS: SEDIMENTARY PROCESSES

6:00 p.m. Town Center Exhibit Area

Authors (*Denotes Presenter)	Abstract Title and Summary	Poster Location
Skinner L. A. Edgar L. A. Gaither T. A. Gullikson A. L. Kestay L. P. et al.	<u>Assessing Community Needs and Developing Resources for Terrestrial Analog Studies</u> [#2990] Results from a web-based survey to evaluate community needs for terrestrial analog work, and progress update on resources that are under development.	Poster Location #603
Cloutis E. Stromberg J. Applin D. Connell S. Kubanek K. et al.	<u>A Simulated Rover Exploration of a Mars Analogue Site: Gypsumville/Lake St. Martin, Manitoba, Canada</u> [#1426] A Mars rover-like analogue mission was conducted at a Mars analogue site in Manitoba, Canada. Lessons learned are many.	Poster Location #604
Feldman A. D. Hausrath E. M. Tschauner O. Lanzirotti A. Rampe E. B. et al.	<u>X-Ray Amorphous and Poorly Crystalline Fe-Containing Phases in Terrestrial Field Environments and Implications for Materials Detected on Mars</u> [#2111] Preliminary analyses of soils forming on ultramafic material in subarctic, desert, and mediterranean climates and a forsterite and fayalite burial experiment.	Poster Location #605
Martin P. E. Ehlmann B. L. Thomas N. H. Wiens R. C. Razzell-Hollis J. J. et al.	<u>Mars-2020-Like Studies of a Lacustrine-Volcanic Mars Analog Field Site</u> [#2892] A Mars analog was analyzed to determine the inter-instrument synergies and limitations for the Mars-2020 mission.	Poster Location #606
Thorpe M. T. Hurowitz J. A. Siebach K. L.	<u>Constraining the Climate of Ancient Mars Using Terrestrial Analogs</u> [#1266] Basaltic watersheds on Earth provide a reference frame for the environmental conditions present during the fluvially active history of Gale Crater, Mars.	Poster Location #607
Kaufman S. V. Mustard J. F. Head J. W. III	<u>A Song of Ice and Fire: Weathering of Antarctic Ash and Implications for Alteration on a Cold and Icy Early Mars</u> [#2198] Antarctic products / Include phyllosilicates / From altering ash.	Poster Location #608
Liu X. Wang Q. Peng Y. Bao H.	<u>A Neogene Weathering Origin of a Jarosite Ore from a Caroniferous Pyrite-Clay Deposit in North China Craton</u> [#2596] A new-type highly enriched jarosite ore deposit provide formation mechanism and model of the martian jarosites.	Poster Location #609
Bao H. M. Cao X. B. Peng Y. B.	<u>Sulfate's Triple-Oxygen Isotope Hydrogeochemistry</u> [#2503] Sulfate oxygen record large-magnitude secular changes in a planetary surface system as well as fine-scale variations in source partition at a site.	Poster Location #610
Buer S. F. Hiesinger H. Reiss D. Hauber E. Johnsson A. et al.	<u>Sorted Stone Circles on Svalbard — An Analog Study for Mars</u> [#2313] Our results of analyzed sorted stone circles on Svalbard — nn analog to martian sorted stone circles — do not support a convection-like movement.	Poster Location #611
Dame R. H. Radebaugh J. Lorenz R. D. Hudson S. M.	<u>Roughness of Surfaces in the Ethiopian Danakil from Remote Handheld Image Surveys</u> [#2772] The comparison between roughness calculations from field work and RADAR will facilitate the interpretation of RADAR smooth regions present on other planets.	Poster Location #612

THURS POSTERS

Dang Y. N. Xiao L. Xu Y. Zhang F.	<u><i>Stages of Development and Growth of Salt Polygonal Surface Structures in Qaidam Basin, Western China, and Their Counterparts on Mars</i></u> [#1504] Different stages of salt polygon development are observed on Earth and Mars, which suggests a similar playa environment and climate evolution history on Mars.	Poster Location #613
Buz J. Wood K. M.	<u><i>Paired Analysis of Dry Lakes on Earth and Mars</i></u> [#3092] Closed basins are common on Earth and Mars and utilizing similar remote sensing spectroscopic instruments on each planet allows for direct comparison.	Poster Location #614
Knightly J. P. Clarke J. D. A. Rupert S. Chevrier V. F.	<u><i>Thermal Properties of Wet Patterned Ground in Haughton Crater and Implications for Mars</i></u> [#2181] Discussion of the thermal and geomorphological properties of terrestrial intra-crater patterned ground in relation to intra-crater patterned ground on Mars.	Poster Location #615
De Hon R. A.	<u><i>Breached Craters on Mars: Terrestrial Analog of Downstream Erosion</i></u> [#1116] The gorge carved by the 2002 Canyon Lake(Tx) discharge through the emergence spillway provide a terrestrial analog of discharge from martian breached craters.	Poster Location #616
Velbel M. A. Rapp J. R. Brugman B. L. Wade B. D. Swiat A. K. et al.	<u><i>Grain Shapes and Surface Textures of Some Micro-Landform, Material, and Mineral Mars-Regolith Analogs: Implications for Interpreting Sand and Silt Imaged by the Phoenix Optical Microscope at the Phoenix Mars Lander Landing Site</i></u> [#2938] Old basaltic and / Periglacial and new sand / Regolith analogs.	Poster Location #617
McMahon W. J. Davies N. S.	<u><i>Mars on Earth? Pre-Vegetation Alluvium as an Analogue for Extra-Terrestrial Sedimentary Strata</i></u> [#1773] In this presentation we discuss the merits and limitations of an analogy between the pre-vegetation Earth and martian stratigraphic records.	Poster Location #618
Rivera-Hernandez F. Palucis M. C.	<u><i>Alluvial Fans in the Aklavik Range, Northwest Territories: Analogs for Fans in a Cold and Icy Mars Scenario</i></u> [#2976] Periglacial alluvial fans in the Canadian Arctic may serve as good analogs for martian fans that formed in a cold and icy climate scenario.	Poster Location #619

Thursday, March 21, 2019

[R634]

POSTER SESSION II: MARS ANALOGS: VISIBLE/NEAR-INFRARED SPECTROSCOPY

6:00 p.m. Town Center Exhibit Area

Authors (*Denotes Presenter)	Abstract Title and Summary	Poster Location
Lasue J. Dehouck E. Johnson J. R. Beck P. Freissinet C. et al.	<u><i>Cumberland and Rocknest Analog Near-Infrared Reflectance Measurements</i></u> [#2265] Martian analogs / Observed in infrared / Are dissimilar.	Poster Location #621
Lantz C. Poulet F. Loizeau D. Veneranda M. Dypvik H. et al.	<u><i>Near-Infrared Spectral Characterization of H₂O₂/PTAL Mineral Samples</i></u> [#1566] We present NIR spectral characterization of terrestrial mineral samples (project PTAL) used as martian analogues to prepare ExoMars and Mars2020 observations.	Poster Location #622
Turenne N. N. Cloutis E. A. Applin D. M.	<u><i>Reflectance Spectroscopy of Mars Astrobiology- and Habitability-Relevant Minerals Exposed to Mars-Like Surface Conditions</i></u> [#2097] Hydrated minerals exposed to long duration Mars-like surface conditions show various spectral changes.	Poster Location #623
Connell S. A. Cloutis E. A. Poitras J. T. Applin D. M. Dixon D. A.	<u><i>Reflectance Spectral Properties of Relevant Minerals Exposed to Mars-Like Surface Conditions</i></u> [#2583] Hydrous minerals showing spectral changes after being exposed to Mars-like surface conditions.	Poster Location #624
Bhattacharya S. Sarkar S. Dagar A. Ray D. Shukla A. D. et al.	<u><i>Visible/Near Infrared (VNIR) Spectral Characterization of Borates from Puga Hot Spring Deposit, Ladakh, India and Its Implications for Mars</i></u> [#1194] VNIR spectral characterization of Borax and Tincalconite (Sodium Borates) from Puga hot spring deposit and its planetary implications.	Poster Location #625

Roush T. L.	<u><i>Estimated Refractive Indices of Calcite, Dolomite, and Magnesite: ~0.3–500 μm [#2088]</i></u> The ~0.3–500 micrometer complex refractive indices of calcite, dolomite, and magnesite are estimated using reflectance spectra and infrared literature values.	Poster Location #626
Jia L. C. Fu X. H. Wang A. L. Cao H. J. Ling Z. C.	<u><i>Temperature and Humidity Effects on Spectral Features of Akaganeite and Implications for Its Stability on Mars [#1786]</i></u> To constrain the stability of akaganeite $\beta\text{-FeOOH}$ on Mars, its structural and spectral modifications introduced by heating and dehydration were investigated.	Poster Location #627
Shi E. B. Ling Z. C. Wang A.	<u><i>MIR, NIR, and Raman Spectra of Magnesium Chlorides with Six Hydration Degrees — Implication for Mars and Europa [#2546]</i></u> We report the MIR, VNIR, and Raman spectra of magnesium chlorides with all six hydration degrees, to support future detection of them on planetary bodies.	Poster Location #628
Carmack R. Hanley J. Horgan B.	<u><i>Strategies for Detecting Chlorine Salts in Visible/Near-Infrared Spectra at Mars [#1701]</i></u> We developed two new parameters and a rubric for identification of oxychlorine salts in visible/near-infrared spectra at Mars.	Poster Location #629
Ye C. Glotch T. D.	<u><i>Spectral Properties of Chloride Salt-Bearing Assemblages: Implications for Detection Limits of Minor Phases in Chloride-Bearing Deposits on Mars [#1609]</i></u> VNIR reflectance and MIR emissivity spectral properties of chloride salt-bearing mixtures and detection limits of minor phases in salt/silicate mixtures.	Poster Location #630
Burton Z. F. M. Bishop J. L. Englert P. Koeberl C. Gibson E. K.	<u><i>Salts and Clays Beneath Surface Sediments in Antarctica Provide Clues to Weathering and Geochemistry on Mars [#1766]</i></u> Subsurface salts and clays from a brine pond site in Antarctica provide an excellent analogue for weathering and geochemical processes on Mars.	Poster Location #631
Englert P. Bishop J. L. Burton Z. F. M. Gibson E. K. Koeberl C. et al.	<u><i>Near Surface Geochemistry and Mineralogy at the McMurdo Dry Valleys, Antarctica, Serves as an Analog for Some Near Surface Sites on Mars [#2252]</i></u> A large collection of Antarctic sediments is studied for trends in geochemistry and mineralogy with depth, supporting understanding of Mars surface processes.	Poster Location #632
Perrin S. L. Bishop J. L. Sessa A. M.	<u><i>Analysis of Unique Martian Sulfate Outcrops Based on Samples from the Painted Desert Sulfate Hill Analog Site and Lab Mixtures [#1903]</i></u> A Painted Desert / Shows “doublet type” signatures / So do lab mixtures. CRISM instrument / Paints Mawrth and Noctis spectra / In similar hues.	Poster Location #633
Liu C. Q. Ling Z. C.	<u><i>Laboratory Spectroscopic Studies of K-H₃O-Na Jarosite Solid Solutions Relevant to Mars [#2295]</i></u> We have synthesized 25 jarosite with different K-Na-H ₃ O contents, and derived equations to assess percentages of K, Na, and H ₃ O contents in jarosite by VNIR.	Poster Location #634
Bishop J. L. Hinman N. W. Danielsen J. M. Baker L. L. Jeute T. J. et al.	<u><i>Spectral Properties of Hydrated Poorly Crystalline Materials for Spectral Analysis of the Moon and Mars [#2288]</i></u> VNIR spectra of amorphous and poorly crystalline materials: opal, allophane, imogolite, iron hydroxides/oxyhydroxides, synthetic Si/Al/Fe phases.	Poster Location #635
Fox V. K. Kupper R. J. Ehlmann B. L. Catalano J. G. Nickerson R. D. et al.	<u><i>Characterization of Synthetic Fe(III)-Fe(II)-Al-Mg Smectites [#2850]</i></u> Spectroscopic characterization of synthetic, intermediate composition smectites with both ferric and ferrous iron to improve planetary remote sensing libraries.	Poster Location #636

Thursday, March 21, 2019

[R635]

POSTER SESSION II: ANALOGS FOR THE MOON AND OTHER AIRLESS BODIES

6:00 p.m. Town Center Exhibit Area

Authors (*Denotes Presenter)	Abstract Title and Summary	Poster Location
Lee P. Kommedal E. Horchler A. Amoroso E. Snyder K. et al.	<u><i>Lofthellir Lava Tube Ice Cave, Iceland: Subsurface Micro-Glaciers, Rockfalls, Drone Lidar 3D-Mapping, and Implications for the Exploration of Potential Ice-Rich Lava Tubes on the Moon and Mars</i></u> [#3118] The Lofthellir lava tube, Iceland, contains micro-glaciers. We mapped the cave by drone-borne lidar. Implications for Moon and Mars cave exploration are examined.	Poster Location #637
Theinat A. K. Modiriasari A. Bobet A. Melosh H. J. Dyke S. J. et al.	<u><i>Geology Explorations of Lava Tubes in the National Beds Lava Monuments</i></u> [#3232] This paper presents the results of the geology explorations for the lava tubes in the National Beds Lava Monuments.	Poster Location #638
Kim K. J. Sun C. Heldmann J. Lim D. Yi E. et al.	<u><i>Comparitive Geochemical Analysis of King's Bowl, Idaho and Ulleung Island Volcanic Roks, Korea</i></u> [#2401] Comparative geochemical analysis of the King's Bowl, Idaho and Ulleung Island volcanic rocks, Korea.	Poster Location #639
Bell E. Schmerr N. Bleacher J. Porter R. Young K. et al.	<u><i>Geophysical Characterization of a Volcanic Cinder Cone Field, an Analog to Lunar Exploration</i></u> [#2868] Near-surface seismic and magnetic examination of magma propagation along local fault planes within a volcanic field as an analog to lunar geophysical exploration.	Poster Location #640
Lane M. D. Maturilli A. Helbert J. Hendrix A. R. TREX SSERVI Team	<u><i>Enabling the Interpretation of Dusty Asteroids, the Moon, and Other Airless Bodies with Mid-Infrared Spectra of Fine-Particulate Minerals Acquired Under Vacuum and High-temperature Conditions</i></u> [#3210] For airless bodies / Use spectra of hot, fine-grained / Powders in vacuum.	Poster Location #641
Pearson N. C. Clark R. N. Hendrix A. R.	<u><i>TREX Measurements of Mineralogical Samples in the PSI Lab from the Vacuum-UV to the Thermal Infrared Wavelengths</i></u> [#2842] We present the PSI Laboratory's support of the TREX SSERVI project and the instrumentation used for this.	Poster Location #642
Holsclaw G. M. Osterloo M. M. Munsat T. Hendrix A. R.	<u><i>TREX UV-VIS Lab Measurements of Minerals and Mineral-Ice Mixtures</i></u> [#3088] We present a new UV-VIS spectral reflectance facility, supporting the SSERVI-TREX project, to study fine-grained geologic materials and ice-mineral mixtures.	Poster Location #643
Mateo-Velez J.-C. Oudayer P. Monnin L. Roggero A. Roussel J.-F. et al.	<u><i>Simulation and Experimental Investigation of Lunar Dust Charging and Adhesion</i></u> [#3122] Dust charging and adhesion during exploration missions is assessed by experimental and numerical simulations using lunar dust analogs.	Poster Location #644
Oudayer P. Matéo-Vélez J.-C. Roussel J.-F. Peillon S. Gensdarmes F. et al.	<u><i>Experimental Determination of Adhesion Force of Lunar Dust Simulants Using Centrifugal Force</i></u> [#2446] Samples made of lunar dust simulants are spun. Comparison of before/after images helps determining adhesion force knowing the used centrifugal force.	Poster Location #645
Saturnino T. J. D. C. Freemantle J. Daly M.	<u><i>Direct Current (DC) Resistance Properties of Asteroid Analogue Minerals at Low Temperatures</i></u> [#2983] Samples chemically analogue to asteroids were selected for laboratory measurements of DC resistance properties at cryogenic temperatures up to room temperature.	Poster Location #646

THURS POSTERS

Thursday, March 21, 2019
POSTER SESSION II: PLANETARY SIMULANTS
6:00 p.m. Town Center Exhibit Area

[R636]

Authors (*Denotes Presenter)	Abstract Title and Summary	Poster Location
Nuth J. A. III Johnson N. M. Ferguson F. T.	<u><i>Making Amorphous Silicate and Carbonaceous Dust Analogs Available to the Cosmochemistry Community</i></u> [#1141] The poster describes analog silicate dust grains and carbonaceous solids that are available to the cosmochemical community at no charge.	Poster Location #647
Hamp R. E. Ramkisson N. K. Olsson-Francis K. Schwenzer S. P. Pearson V. K.	<u><i>A New Simulant to Represent the Silicate Interior of Enceladus</i></u> [#1091] The design of a new simulant to chemically represent the interior of Enceladus, which can be used in simulating and modeling the internal environment.	Poster Location #648
Morland Z. S. Pearson V. K. Patel M. R. Green S. F.	<u><i>Chemical and Textural Characterisation of Two Phobos Regolith Simulants</i></u> [#1274] Without direct samples from Phobos, regolith simulants are vital for engineering and scientific testing. Here we characterise two — chemical and physical.	Poster Location #649
Hogancamp J. V. Archer P. D. Gruener J. Ming D. W. Tu V.	<u><i>JSC-Rocknest: A Large-Scale Mojave Mars Simulant (MMS) Based Soil Simulant for In-Situ Resource Utilization Water-Extraction Studies</i></u> [#1218] The Johnson Space Center Rocknest (JSC-RN) simulant was developed to be used in component and system testing for water extraction from Mars regolith.	Poster Location #650
Knudson C. A. Freissinet C. Graham H. McAdam A. C. Millan M. et al.	<u><i>The Characterization and Development of a Mineralogical Analog of the MSL Cumberland Drill Sample for Organic Molecule Identification in SAM-Like Experiments</i></u> [#2489] The Cumberland analog was created to better understand the organic decomposition of precursor molecules that lead to the first detection of martian organics.	Poster Location #651
Leone G. Barbieri M. Soto M. Riveros K. Rodriguez N. et al.	<u><i>Comparison of Lunar and Martian Simulants to Volcanic Rocks of the Atacama Desert and (Pre-)Cordillera Regions of Chile</i></u> [#1389] The current simulants used by the space agencies are not adequate for multiuse purposes. The scope of this study is to find a simulant for various experiments.	Poster Location #652
Zhang X. Osinski G. R. Newson T. Ahmed A. Touqan M. et al.	<u><i>A Comparative Study of Lunar Regolith Simulants in Relation to Terrestrial Tests of Lunar Exploration Missions</i></u> [#3071] This study compares some fundamental physical and chemical properties of a selected set of lunar regolith simulants produced in China, Germany, Japan, and USA.	Poster Location #653

Thursday, March 21, 2019
POSTER SESSION II: GEOLOGIC MAPPING THROUGH THE SOLAR SYSTEM
6:00 p.m. Town Center Exhibit Area

[R637]

Authors (*Denotes Presenter)	Abstract Title and Summary	Poster Location
Varatharajan I. D'Amore M. Domingue D. Helbert J. Maturilli A.	<u><i>Global Spectral Parameter Map of Mercury: Derived from MASCS Spectrometer Onboard NASA MESSENGER Mission</i></u> [#2300] Global Spectral Parameter Map of Mercury is derived from Mercury Surface and Atmospheric Composition Spectrometer (MASCS) onboard NASA MESSENGER mission.	Poster Location #655
Hareyama M. Ishihara Y. Honda C. Ohtake M.	<u><i>Global Map of Spectral Classification for the Mercury and Its Chemical Composition</i></u> [#1714] This report shows the global map of Mercury's spectral classification by auto classification method and compares with elemental content maps.	Poster Location #656

Wright J. Rothery D. A. Balme M. R. Conway S. J.	<u><i>The First Geological Map of the Hokusai Quadrangle (H05) of Mercury</i> [#1372]</u> Complete quadrangle geological map with both 3 and 5 crater degradation classes. Contains smooth and intercrater plains, and a third, distinct plains type.	Poster Location #657
Malliband C. C. Rothery D. A. Balme M. R. Conway S. J.	<u><i>1:3M Geological Mapping of the Derain (H-10) Quadrangle of Mercury</i> [#1807]</u> We are producing a 1:3 million geologic map of the Derain quadrangle of Mercury in preparation for BepiColombo.	Poster Location #658
Pegg D. L. Rothery D. A. Balme M. R. Conway S. J.	<u><i>Geological Mapping of the Debussy Quadrangle (H-14) of Mercury, Preliminary Results</i> [#1271]</u> We present the current status of the geological map of Debussy Quadrangle, Mercury.	Poster Location #659
Aubele J. C.	<u><i>Geologic Mapping of V11-Shimti Tessera and V-12 Vellamo Planitia, Venus</i> [#2578]</u> Venus geologic maps results: Shield plains are comparable to Snake River Plains shields with widespread melt sources over a restricted, specific geologic time.	Poster Location #660
McGowan E. M. Buczowski D. L. McGill G. E.	<u><i>The Lachesis Tessera Quadrangle (V-18), Venus</i> [#1303]</u> We present the draft geologic map of the Lachesis Tessera (V-18) quadrangle completed by George McGill before his death.	Poster Location #661
Suter P. F. Gregg T. K. P. Yingst R. A.	<u><i>Lunar Geologic Mapping: Preliminary Map of the Southwest Quadrant of Lunar LQ-10 ("Marius") Quadrangle</i> [#2571]</u> Mapping the Moon with / LROC, Clementine, LOLA / Reveals new contacts.	Poster Location #662
Farrant B. E. Bell S. K. Czaplinski E. C. Harrington E. M. Tolometti G. D. et al.	<u><i>Geologic Map and Potential Rover Traverses for Human-Assisted Sample Return Missions to the Schrödinger Basin, Lunar Farside</i> [#1790]</u> Geologic mapping of the Schrödinger basin peak ring shows faulted and magmatic lithologic contacts. Robotic traverses are planned to investigate these features.	Poster Location #663
Gonzales N. R. Henriksen M. R. Wagner R. V. Robinson M. S.	<u><i>Apollo 11: Where They Were When — A New Spatiotemporal EVA Map</i> [#3089]</u> Retrace history / Each "small step" upon the Moon / Walk with Neil and Buzz.	Poster Location #664
McCardle B. Garry W. B.	<u><i>Renovating and Digitizing the 1:25k Geologic Map of the Apollo 11 Landing Site</i> [#3282]</u> This project was to renovate the original Apollo 11 Landing Site Map, to join the other Apollo mission maps in the USGS online archive.	Poster Location #665
Iqbal W. Hiesinger H. van der Bogert C. H.	<u><i>Geology of the Apollo 11 and Apollo 12 Landing Sites- New Maps and Insights</i> [#1070]</u> We reanalyzed the geology of the Apollo 11 and Apollo 12 landing sites using modern data including LROC, Clementine, and M ³ data.	Poster Location #666
Iqbal W. van der Bogert C. H. Hiesinger H.	<u><i>New Geological maps and Crater Size-Frequency Distribution Measurements of the Apollo 17 Landing Site</i> [#1005]</u> The Apollo 17 landing site was mapped with the recent lunar data to measure CSFDs for the calibration of the lunar cratering chronology.	Poster Location #667
Crown D. A. Berman D. C. Scheidt S. P. Hauber E.	<u><i>Geology of Alba Mons, Mars: Results from 1:1M-Scale Geologic Mapping</i> [#2160]</u> Geologic mapping of the summit and western flank of Alba Mons has provided new constraints on volcanic, tectonic, and erosional processes.	Poster Location #668
Yingst R. A. Berman D. C. Mest S. C. Williams D. A. Gregg T. K. P.	<u><i>Geologic Mapping Methods for Small, Rocky Bodies: The Vesta Example</i> [#1451]</u> First, single maps. Then / A confluence of data / Bring Vesta to life.	Poster Location #669
Williams D. A. Buczowski D. L. Crown D. A. Frigeri A. Hughson K. et al.	<u><i>Final Dawn LAMO-Based Global Geologic Map of Ceres</i> [#1252]</u> This poster presents our final global geologic map of Ceres, combined from 15 quadrangle maps made using Dawn LAMO images (35m/px). Cover of Icarus, December 2018.	Poster Location #670

THURS POSTERS

Senske D. A. Leonard E. J. Patthoff D. A.	<u><i>Geologic Mapping of Europa at Global and Regional Scales: Providing Comprehensive Insight into Crustal History and Evolution</i> [#1615]</u> Based on our 1:15M scale global geologic map of Europa, mapping of 10% of this icy world at the ~160-m scale provides greater insight into unit characteristics.	Poster Location #671
Seignovert B. Le Mouélic S. Brown R. H. Karkoschka E. Pasek V. et al.	<u><i>Titan's Global Map Combining VIMS and ISS Mosaics</i> [#1423]</u> This study combines Cassini VIMS and ISS global mosaic of Titan to provide a combined color map revealing the diversity of its geological structures.	Poster Location #672
Poehler C. M. Iqbal W. van der Bogert C. H. Hiesinger H. Lewang A. M. et al.	<u><i>Geological Mapping of Large Basins on the Terrestrial Planets in the Scope of PLANMAP</i> [#2910]</u> Within the EU PLANetary MAPping project network, we are producing standardized geological maps of three large basins: South Pole-Aitken, Beethoven, and Argyre.	Poster Location #673
Bernhardt H. Williams D. A. Clark J. D.	<u><i>Preliminary Photogeologic Map of Malea Planum, Mars</i> [#1434]</u> 1:2,000,000 mapping product of oldest of Mars' large volcanic provinces. Based on all state-of-the-art datasets on current USGS-technique standards.	Poster Location #674
Bernhardt H. Williams D. A. Clark J. D.	<u><i>Malea Planum: Timing and Scale of Deposition and Erosion on the Oldest of Mars' Large Volcanic Provinces</i> [#1435]</u> 0.5 million km ³ of material removed from Malea Planum during several distinct episodes over 100s of Ma. Based on map presented in companion abstract #1434.	Poster Location #675

Thursday, March 21, 2019

[R638]

POSTER SESSION II: VISUALIZING WORLDS: PLANETARY SPATIAL DATA AND INFRASTRUCTURE

6:00 p.m. Town Center Exhibit Area

Authors (*Denotes Presenter)	Abstract Title and Summary	Poster Location
Radebaugh J. Thomson B. J. Archinal B. Beyer R. DellaGuistina D. et al.	<u><i>A Roadmap for Planetary Spatial Data Infrastructure</i> [#1667]</u> Planetary spatial data should be accessible, in properly registered form, to all science users now and into the future.	Poster Location #677
Acton C. Bachman N. Liukis M. Semenov B. Thomson F. et al.	<u><i>Observation Geometry for Planetary Science</i> [#1028]</u> Poster provides an overview of NASA's de facto standard, named "SPICE," for computing observation geometry. Includes information on newer methods to use SPICE.	Poster Location #678
Conrad A. Archinal B. A. WG Cartographic Coord. and Rotational Elements I. A. U.	<u><i>Update for 2019 from the IAU Working Group on Cartographic Coordinates and Rotational Elements</i> [#2110]</u> Summary of report from the IAU WG on Cartographic Coordinates and Rotational Elements, with recommendations on planetary coordinate systems and body shapes.	Poster Location #679
Naß A. Asch K. van Gasselt S. Laura J. Hare T. et al.	<u><i>Earth Data Infrastructures as a Basis for a Map and Information Library in the Domain of Planetary Sciences</i> [#2559]</u> Present requirements for a Dynamic Spatio-Temporal Map and Information Library for Planetary Science, and highlight Earth-based efforts and their benefit for planetary science.	Poster Location #680
Nelson D. M. Williams D. A.	<u><i>Digitization of the Photographic Image Archive of Earth Analog Site, Amboy Crater, for the Planetary Data System</i> [#2047]</u> Description of the digitization of historic photographs of field research of Amboy Crater, CA, for the Planetary Data System archive.	Poster Location #681
Slavney S. Guinness E. A. Stein T. C. Wang J. Arvidson L. E. et al.	<u><i>PDS Geosciences Node Data and Services</i> [#1685]</u> The PDS Geosciences Node works with missions, individual providers, and users to create and distribute high quality well-documented science data archives.	Poster Location #682
Wang J. Scholes D. Arvidson R. E. Slavney S. Guinness E. A. et al.	<u><i>PDS Geosciences Node's Orbital Data Explorer and the Latest Update for PDS4</i> [#1918]</u> Overview of key features and PDS4 updates of NASA PDS Geosciences Node's web-based search tool, ODE, to access orbital data from planetary missions and instruments.	Poster Location #683

Lehnert K. A. Markey K. Ji P. Evans C. Zeigler R.	<u><i>The Astromaterials Data System: Transforming Access to Planetary Sample Data</i> [#2799]</u> We will present the Astromaterials Data System (AstroMat), a comprehensive data system for analytical data of all astromaterial collections curated by the JSC.	Poster Location #684
Hunter M. A. Skinner J. A. Fortezzo C. M. Okubo C.	<u><i>Planetary Geoscience Ontology Testbed: Using Semantic Technology to Enhance the Discovery of Geologic Maps</i> [#1107]</u> Summary of an ongoing testbed project to integrate web semantic technologies with open geospatial data services to enhance geologic map discovery.	Poster Location #685
Henneken E. A. ADS Team	<u><i>Discovering and Accessing Planetary Sciences Literature with the New Astrophysics Data System (ADS)</i> [#1568]</u> The NASA Astrophysics Data System (ADS) helps astronomers and planetary scientists navigate, without charge, the complex environment of scholarly publications.	Poster Location #686
Henneken E. A. Muench G. Holm Nielsen L. Blanco-Cuaresma S. Accomazzi A.	<u><i>Capturing Software Citations in Astronomy and Planetary Sciences</i> [#1569]</u> This poster discusses the importance of capturing software citations and how this has been implemented in the Asclepias project of the AAS, ADS, and Zenodo.	Poster Location #687
Tai Udovicic C. J. Boivin A. L.	<u><i>Plutopy: An Open-Source Community for Learning Reproducible Planetary Science</i> [#3218]</u> Scientists gather / To learn to reproduce work / In community.	Poster Location #688
Hargitai H. I.	<u><i>Building a Cartographic Planetary Feature Database: The Significance of Feature Maps</i> [#3157]</u> This paper discusses the significance of GIS-ready feature databases.	Poster Location #689
Mahmood Q. Brooks A. J.-W. Fink W.	<u><i>Instant and Intuitive Visual Exploration of Planetary Spatial Data</i> [#3216]</u> Tool to visualize instantaneously and interactively the results of an anomaly detection system by preserving the spatiality of analyzed regions.	Poster Location #690

Thursday, March 21, 2019

[R639]

POSTER SESSION II: VISUALIZING WORLDS: MOON AND ASTEROIDS SPATIAL DATA

6:00 p.m. Town Center Exhibit Area

Authors (*Denotes Presenter)	Abstract Title and Summary	Poster Location
Estes N. M. Bowley K. S. Barnett J.	<u><i>LROC PDS Toolchain Redevelopment and Faster Release Schedule</i> [#1626]</u> The LROC PDS toolchain has been completely redeveloped, resulting in more reliable volume production as well as more frequent releases.	Poster Location #691
Malaret E. Battisti A. Gaddis L.	<u><i>2019 Status of Geometric Restoration of Moon Mineralogy Mapper Data</i> [#2816]</u> 2019 Status of Geometric Restoration of Moon Mineralogy Mapper Data.	Poster Location #692
Nypaver C. Thomson B. J. Patterson G. W. Bhiravarasu S. S. Neish C. D. et al.	<u><i>Improved Geospatial Control of Mini-RF Bistatic Observations</i> [#2524]</u> Bistatic data / Fixed geospatial offsets / Upgraded control.	Poster Location #693
Yamashita N. Prettyman T. H.	<u><i>Update on Archiving High-Resolution Lunar Gamma-Ray Spectra</i> [#1623]</u> High-res gamma rays / Lunar elements await / PDS archive.	Poster Location #694
Roy H. Chaudhury S. Yamasaki T. DeLatta D. M. Ohtake M. et al.	<u><i>Lunar Surface Image Restoration Using U-Net Based Deep Neural Networks</i> [#2656]</u> In this work, we show that U-net based deep neural networks can successfully restore the missing pixels on the lunar surface image with impressive quality.	Poster Location #695
Wang Y. Wu B.	<u><i>A New Global Catalog of Lunar Impact Craters (≥ 1 km) with 3D Morphological Information</i> [#1019]</u> We present a new global catalog of lunar craters (≥ 1 km) with 3D morphological information. It is more complete than any previously published efforts.	Poster Location #696

Daket Y. Yamamoto M. Takita J. Tanaka S.	<u>Surface Temperature Map of The Moon: Visualiazation Tool for Mapping DIVINER Data and Simulation Program. [#2286]</u> We aim to simluate surface temperature on the Moon. This study reports a tool for creating brightness temperature map and a surface temperature simluation.	Poster Location #697
Blumenfeld E. H. Beaulieu K. R. Thomas A. B. Evans C. A. Zeigler R. A. et al.	<u>3D Virtual Astromaterials Samples Collection of NASA's Apollo Lunar and Antarctic Meteorite Samples to Be an Online Database to Serve Researchers and the Public [#3056]</u> NASA's 3D Virtual Astromaterials Samples Collection will provide information-rich visualization of research-grade 3D models for researchers and the public.	Poster Location #698
Gibson E. K. Kindle A. G. Schwenzer S. P. Kelley S. . Anand M. et al.	<u>Apollo Virtual Microscope Collection: Lunar Mineralogy and Petrology of Apollo Rocks [#1076]</u> The Apollo Virtual Microscope process has been used to produce 575 images of the Apollo and Luna 16 lunar samples. Images can be viewed from any computer.	Poster Location #699
Lehnert K. A. Markey K. Ji P. Cai Y. Hodges K. et al.	<u>MoonDB: 50 Years of Lunar Sample Data Ready for the Data Revolution [#2996]</u> This presentation provides an update on the ongoing development of the MoonDB database for lunar sample geochemical and geochronological data.	Poster Location #700
Weirich J. R. Palmer E. E. Domingue D. L.	<u>Digital Terrain Models of Mathilde and the Moon [#2681]</u> Four models for you / Asteroid, crater, and swirls / Upgrade your science.	Poster Location #701
Day B. H. Law E. S.	<u>Visualizing Dawn Mission Data with NASA's Ceres Trek and Vesta Trek Online Portals [#1964]</u> The Dawn Mission commissioned NASA's Solar System Treks Project to update the existing Vesta Trek portal and also release a new portal for Ceres.	Poster Location #702
Kingston C. Palmer E. Stone J. Drum M. Neese C. et al.	<u>Archiving Data in the PDS with OLAF [#3074]</u> Archive data with the PDS easily using OLAF, a web-based tool that eliminates the need to learn challenging and evolving PDS4 standards.	Poster Location #703

Thursday, March 21, 2019

[R640]

POSTER SESSION II: VISUALIZING WORLDS: MARS SPATIAL DATA AND INFRASTRUCTURE

6:00 p.m. Town Center Exhibit Area

Authors (*Denotes Presenter)	Abstract Title and Summary	Poster Location
Abercrombie S. P. Menzies A. Abarca H. E. Luo V. X. Samochina S. et al.	<u>Multi-Platform Immersive Visualization of Planetary, Asteroid, and Terrestrial Analog Terrain [#2268]</u> We present a set of tools for immersive and web-based 3D terrain visualization, with applications to Mars rover missions, asteroids, and terrestrial analogs.	Poster Location #705
Powell K. E. Bahremand A. Gonzalez A. LiKamWa R. Edwards C. S.	<u>An Integrated Environment for Visualizing In-Situ and Orbital Planetary Data [#1459]</u> A new environment for visualization of Curiosity rover data together with orbital data in augmented/virtual reality.	Poster Location #706
Schwenzer S. P. Woods M. Karachalios S. Phan N. Joudrier L.	<u>LabelMars: Creating an Extremely Large Martian Image Dataset Through Machine Learning [#1970]</u> 5000 annotated images taken by Mars rovers were used to investigate the suitability of state-of-the-art machine learning technology for classification on Mars.	Poster Location #707
Ono M. Rothrock B. Mattmann C. Islam T. Didier A. et al.	<u>Make Planetary Images Searchable: Content-Based Search for PDS and On-Board Datasets [#2552]</u> We use machine learning to make PDS images searchable and make a drive-only rover scientifically valuable by auto-finding features of interest in camera images.	Poster Location #708

Garcia A. H. Sutter B. Archer P. D. Niles P. B. Stein T. C. et al.	<u><i>The 2008 Mars Phoenix Lander Thermal and Evolved Gas Analyzer (TEGA) Dataset: Placing Easily Interpretable Evolved Gas Data on the Planetary Data System (PDS) [#1965]</i></u> Meaningful Thermal and Evolved Gas Analysis (TEGA) data set from the 2008 Mars Phoenix Lander to be placed on the Planetary Data System (PDS).	Poster Location #709
Walter S. H. G. Jaumann R.	<u><i>A Dynamic Spatial Data Infrastructure for Mars Based on Data from the High Resolution Stereo Camera [#1889]</i></u> We present our map-based data system and propose to integrate dynamic visualization capabilities into future Planetary Spatial Data Infrastructures.	Poster Location #710
Lim T. L. Docal R. Metcalf L. Besse S. Barbarisi I. et al.	<u><i>Plans for the EXOMARS 2020 Rover Data Archive Within the PSA [#2412]</i></u> This presentation will describe the plans for new Rover data views in the PSA to support the ExoMars 2020 mission.	Poster Location #711
Kodikara G. R. L. McHenry L. J.	<u><i>Application of Machine Learning Methods for Identification of Surface Composition Through the ExoMars PanCam Instrument [#1147]</i></u> Here we demonstrate the application of advanced Machine Learning algorithms for the identification of mineral assemblages using the ExoMars PanCam instrument.	Poster Location #712
Balme M. R. Barrett A. M. Woods M. Karachalios S. Joudrier L. et al.	<u><i>NOAH-H, a Deep-Learning, Terrain Analysis System: Preliminary Results for ExoMars Rover Candidate Landing Sites [#3011]</i></u> Deep-learning terrain analysis has been used to assess traversability of the ExoMars candidate landing sites.	Poster Location #713
De Cesare C. M. Deen R. G. Padams J. H. Grimes K. M. Algermissen S. S.	<u><i>But What About the Archive? Developing a PDS4 Archive for InSight Image Data [#3279]</i></u> This presentation will describe the challenges of archiving data products from planetary science missions, and will use InSight camera data as an example.	Poster Location #714
Calef F. J. III Soliman T. Abarca H. E. Deen R. G. Ruoff N. et al.	<u><i>Science Operations with the InSight WebGIS [#1977]</i></u> A web-based GIS tool was developed to allow science team members to evaluate surface instrument placements against a list of constraints and disirements.	Poster Location #715
Plesea L. Hare T. M.	<u><i>Uncontrolled Global HiRISE Mosaic [#1986]</i></u> The technologies and process to build an uncontrolled mosaic from all the HiRISE imagery and to make the result available as a GIS tile service is described.	Poster Location #716
Mayer D. P.	<u><i>Filling the Gap: Building a CTX-Based Digital Terrain Model Mosaic of the South Pole of Mars [#1128]</i></u> Sparse topography / C-T-X terrain models / Progress, fill the gap.	Poster Location #717
Parsons R. A. Miyamoto H.	<u><i>Change Detection in Repeat Imagery Using Principle Component Analysis [#2381]</i></u> Variations in pixel brightness in repeat imagery can be transformed into principle components in which geologic changes can be more readily identified.	Poster Location #718
Heyer T. Hiesinger H. Reiss D. Raack J. Jaumann R.	<u><i>The Multi-Temporal Database (MUTED): New Features to Study Dynamic Mars [#1001]</i></u> The Multi-Temporal Database of Planetary Image Data (MUTED) is a web-based tool to support the identification of surface changes and processes on Mars.	Poster Location #719
Makarewicz J. S. Makarewicz H. D.	<u><i>Predicting a Gypsum-Dolomite Mixture Spectrum with a Spectrum Mixture Model Based on Principle Component Analysis [#2400]</i></u> A PCA-based mineral mixture model was applied to a gypsum-dolomite mixture dataset and then used to generate a 90% Gypsum and 10% Dolomite mixture spectrum.	Poster Location #720
Politte D. V. Arvidson R. E. O'Sullivan J. A. He L.	<u><i>Pipeline for Retrieval of Surface Temperatures and Single Scattering Albedos [#2690]</i></u> End-to-end processing software for retrieval of CRISM and OMEGA single scattering albedos and temperatures.	Poster Location #721

Bapst J. Piqueux S. Edwards C. S. Ferguson R. L.	<u><i>When and Where? Prioritizing Temperature Measurements for Thermophysical Analysis</i></u> [#1902] We outline temperature measurement conditions, in both space and time, that yield reliable thermal property derivations. Mars and other bodies are explored.	Poster Location #722
---	---	----------------------

Thursday, March 21, 2019

[R641]

POSTER SESSION II: VISUALIZING WORLDS: OUTER PLANETS AND SATELLITES SPATIAL DATA AND INFRASTRUCTURE

6:00 p.m. Town Center Exhibit Area

Authors (*Denotes Presenter)	Abstract Title and Summary	Poster Location
Williams D. A. Nelson D. M. Noss D. Dickensied S. Milazzo M.	<u><i>Completing the Io GIS Database</i></u> [#1053] This presentation discusses our new project to complete the Io database, archiving all Galileo/post-Galileo Io data in ArcGIS and JMARS as one example of a PSDI.	Poster Location #723
Davies A. G. Veeder G. J.	<u><i>Towards Understanding Io's Heat Flow: The Incorporation of Multi-Wavelength IRTF Data into the PDS</i></u> [#1427] Multi-wavelength IRTF observations of thermal emission from Io obtained between 1983 and 1993 are now available from NASA's Planetary Data System.	Poster Location #724
Kay J. Schenk P. Prockter L.	<u><i>Triton, Europa, Enceladus, and Pluto, Oh my!: Topography of Active Icy Ocean Worlds</i></u> [#2975] Oceans run deep, some shallow / Those that are hidden betray themselves / Beware the surface of thine world for it is low.	Poster Location #725
Laura J. R. Bland M. T. Ferguson R. L. Hare T. M. Archinal B. A. et al.	<u><i>Framework for the Development of a Europa Planetary Spatial Data Infrastructure</i></u> [#2317] Herein, we describe the use of the SDI-framework, coupled with an implementation strategy to develop a Europa centric SDI-implementation.	Poster Location #726
Peters S. T. Schroeder D. M. Castelletti D. Haynes M. S. Romero-Wolf A.	<u><i>Correcting Europa's Ionospheric Distortion with Passive Radar Using Jovian Decametric Radiation</i></u> [#3260] We demonstrate the potential to use Jupiter's decametric radio emissions to passively correct for Europa's ionospheric effects and radio wave signal distortion.	Poster Location #727
Bland M. T. Weller L. A. Mayer D. P. Edmundson K. L. Archinal B. A. et al.	<u><i>A New Global Shape Model of Enceladus from a Dense Photogrammetric Control Network</i></u> [#1090] We have created a global shape model for Enceladus from a dense photogrammetric control network. The model provides a foundational dataset for an Enceladus PSDI.	Poster Location #728
Tyler R. H.	<u><i>Introducing the Tidal Response of Planetary Fluids (TROPF) Software Package</i></u> [#2883] This presentation announces the initial release of a package of highly-optimized solution algorithms and integrated software (TROPF).	Poster Location #729
Day B. H. Law E. S.	<u><i>Titan Trek: A New Online NASA Visualization and Analysis Portal for Saturn's Largest Moon</i></u> [#1971] NASA's Titan Trek is a new online portal commissioned by the Cassini mission for dissemination, visualization, and analysis of data gathered at Titan.	Poster Location #730
Edgington S. G. Tapella R. K. Beebe R. F. Buratti B. J. Burton M. E. et al.	<u><i>Cassini-Huygens Scientific Legacy: The Cassini Mission Archive at the Planetary Data System</i></u> [#2932] We present the Cassini Mission Archive web site, which is designed to consolidate years of scientific experience into a guide for future researchers.	Poster Location #731
Gabasova L. R. Schmitt B. Grundy W. Olkin C. B. Young L. A. et al.	<u><i>Intensity-Based Registration for Planetary Cartography: Application to New Horizons LEISA Approach Scans of Pluto</i></u> [#2638] With wisdom borrowed / From our medical colleagues / Pluto gets full maps.	Poster Location #732

Thursday, March 21, 2019

[R642]

POSTER SESSION II: BIOSIGNATURES: TO SEEK OUT NEW LIFE

6:00 p.m. Town Center Exhibit Area

Authors (*Denotes Presenter)	Abstract Title and Summary	Poster Location
Carrier B. L. Beaty D. W. Meyer M. A. Bakermans C. Boston P. et al.	<u><i>Searching for Extant Life on Mars: What's Next?</i></u> [#2539] A report on the recommended next steps for searching for extant life on Mars, which resulted from the recent conference "Mars Extant Life: What's Next?".	Poster Location #733
Huang T. Fernández-Remolar D. C.	<u><i>Long-Term Preservation of Organic Compounds Under the Extreme Acidic Conditions of Río Tinto Suggests that the Acidic Mars Deposits are a Hot Target for Mars Astrobiology</i></u> [#1740] We searched for organic compounds and their relation with the mineral matrix of 2.1-Ma old terrace from Río Tinto, an analog of paleo-environments of Mars.	Poster Location #734
Aaron L. M. Steele A. Shkolyar S. Seelos K. Viviano C. et al.	<u><i>Detecting Oxalate Minerals on Mars Using CRISM and In-Situ Spectroscopy</i></u> [#3125] Significant amounts of carbonate minerals should be observed on Mars, but only small exposures have been detected. Could oxalates be the answer?	Poster Location #735
Patel H. J. Ewing R. C. Tice M. M. Nachon M.	<u><i>Biosignature Screening in Modern Wet Aeolian Environments Using X-Ray Fluorescence and X-Ray Diffraction Technologies</i></u> [#2113] In this study, we examine the textural and geochemical characteristics of microbially-influenced wet aeolian deposits at Padre Island, Texas.	Poster Location #736
Ryan C. H. Daly M. G. Brady A. L. Slater G. F. Lee K. J.	<u><i>The Distribution of Organic Material Within Martian-Analogue Volcanic Rocks Measured Through Laser-Induced Fluorescence Spectroscopy</i></u> [#2782] Organic species / Create a constellation / In volcanic rocks.	Poster Location #737
Perl S. M. Celestian A. J. Baxter B. K. Tasoff P.	<u><i>Chemical Biomarker Robustness in Martian Planetary Analogue Evaporite Mineralogy</i></u> [#2930] The purpose is to discuss the biological feedback from microbial communities preserved from martian analogue mineralogy and geobiological interpretation.	Poster Location #738
Zalewska N. E. Kotlarz J. P. Kubiak K.	<u><i>Variability of Enceladus' Plumes Reflectance as a Function of the Potential Occurrence of Microbes</i></u> [#2759] Modelling the possibility of finding microorganisms originated from the bottom of the ocean in plumes and near rifts on the icy surface.	Poster Location #739
Perl S. M. Lindensmith C. A. Nadeau J. L. Cockell C. S. Bedrossian M. et al.	<u><i>Quantifying Extant Life and Microbial Community Preservation within Icy Brine and Evaporitic Environments</i></u> [#2899] The purpose of this paper is to discuss the astrobiological significance of motility as a biosignature for preserved extant life in planetary analogue brines.	Poster Location #740
Sandford S. A. Bera P. P. Nuevo M. Lee T. J. Materese C. K.	<u><i>Production and Potential Detection of Functionalized Hexamethylene-Tetramine Compounds in Space</i></u> [#1036] The exposure of astrophysical ice analogs to ionizing radiation results in the production of hexamethylenetetramine (HMT; C ₆ N ₄ H ₁₂) and functionalized variants.	Poster Location #741
Aponte J. C. Elsila J. E. Glavin D. P. Dworkin J. P.	<u><i>Why are Monocarboxylic Acids the Most Abundant Chondritic Aliphatic Organic Compounds?</i></u> [#1829] We aim to discuss recent new data regarding the abundance of MCAs in carbonaceous chondrites and its parallel to other species such as IOM and carbonates.	Poster Location #742
Trigo-Rodríguez J. M. Moyano-Camero C. E. Lee M. R. Tanbakouei S.	<u><i>Did Martian Organic Deposits form Through Catalytic Reactions in a Hydrothermal Environment that was Subjected to an Intense Meteorite Flux?</i></u> [#2507] Mars was under a rain of chondritic materials at a time in which significant hydrothermal activity was at work. Catalytic reactions increased organic complexity.	Poster Location #743

THURS POSTERS

Thursday, March 21, 2019

[R643]

POSTER SESSION II: ASTROBIOLOGY MISSIONS AND INSTRUMENTATION: BOLDLY GOING WHERE NO SPECTROMETER HAS GONE BEFORE!

6:00 p.m. Town Center Exhibit Area

Authors (*Denotes Presenter)	Abstract Title and Summary	Poster Location
Williams A. J. Eigenbrode J. L. Johnson S. S. Craft K. L. Wilhelm M. B. et al.	<u>Preparation for the SAM TMAH Wet Chemistry Experiment Onboard Curiosity: Detection in Mars-Analog Rocks and Candidate Locations for the In Situ Experiment on Mars [#1258]</u> Organic biosignature preservation in Mars-analog environments, and potential for detection by the Curiosity rover SAM instrument in the Mt. Sharp Clay Unit.	Poster Location #744
Millan M. Malespin C. A. Freissinet C. Glavin D. P. Mahaffy P. R. et al.	<u>Lessons Learned from the First Full Cup Wet Chemistry Experiment Performed on Mars with the Sample Analysis at Mars Instrument [#2873]</u> First full cup derivatization on Mars: Why? How? Results and laboratory experiments to optimize future wet chemistry runs and improve the detection of organics.	Poster Location #745
Manrique-Martinez J. A. Lopez-Reyes G. Bozic T. Alvarez-Perez A. Veneranda M. et al.	<u>Data Fusion of Raman and LIBS Applied to Planetary Exploration Relevant Compounds [#2995]</u> In the present work we evaluate the advantages of Raman-LIBS combination in binary and ternary mixtures, as well as data fusion approaches for both techniques.	Poster Location #746
Nachon M. Ewing R. C. Tice M. M. Cheffer K. Coker M.	<u>Protocol for Biosignature Identification in Wet Aeolian Deposits, Using Micro-XRF Analyses that Simulate the PIXL Instrument Onboard the Mars 2020 Rover [#1485]</u> Research includes field work on aeolian and microbial deposits, XRF analyses, and participative "survey" for biosignatures identification.	Poster Location #747
Razzell Hollis J. Sapers H. Fries M. Bhartia R. Beegle L.	<u>Quantified DUV Raman Analysis for Detecting Organic Biosignatures [#2748]</u> Quantitative analysis of potential biosignatures using DUV Raman spectroscopy can be achieved by careful measurement of molecular standards and Earth analogues.	Poster Location #748
Kuik J. C. Cloutis E. A. Latendresse V. Kruzelecky R. V.	<u>Laser-Induced Breakdown Spectroscopy (LIBS) Analysis of Organic-Bearing Mars Analogue Samples [#2701]</u> LIBS analysis on organic-bearing Mars analogue samples, focusing on organic detection, with the LiRS instrument developed by MPB Communications.	Poster Location #749
Loizeau D. Balme M. R. Bibring J.-P. Bridges J. C. Fairén A. G. et al.	<u>ExoMars 2020 Surface Mission: Choosing a Landing Site [#2378]</u> The landing site selection process for ExoMars 2020 evaluated the two exciting final candidate sites Mawrth Vallis and Oxia Planum, and recommended Oxia Planum.	Poster Location #750
Stoker C. R. Noe Dobrea E. Z. Alkemade S. L.	<u>Rapid Infilling of Small Craters on High N. Latitude Mars: Implications for Missions to Search for Evidence of Life [#1472]</u> We counted and characterized craters in the icy N. plains of Mars to determine how much recent erosion has overprinted the record of past habitable conditions.	Poster Location #751
Kehl F. Kovarik N. A. Creamer J. S. Willis P. A.	<u>Automated Subcritical Water Extraction and Analysis Platform for Martian Regolith: Remote Operation on Rover in the Atacama Desert [#2174]</u> We present an automated extractor unit that could be used to support landed robotic missions seeking chemical signatures of habitability and life on Mars.	Poster Location #752
Kurosawa K. Genda H. Hyodo R. Yamagishi A. Fujita K.	<u>Planetary Protection Issues: A Phobos Case Study [#2660]</u> We investigate the transportation of potential microbes from Mars to Phobos. The contamination probability of collected samples was derived at a selected depth.	Poster Location #753

THURS POSTERS

Thursday, March 21, 2019

[R644]

POSTER SESSION II: SEARCHING FOR METEORITES IN WEIRD PLACES

6:00 p.m. Town Center Exhibit Area

Authors (*Denotes Presenter)	Abstract Title and Summary	Poster Location
Patzek M. Bischoff A. Hoppe P. Pack A. Visser R. et al.	<u><i>Oxygen and Hydrogen Isotopic Evidence for the Existence of Several C1 Parent Bodies in the Early Solar System</i></u> [#1779] D/H ratios and oxygen isotope data of various CI- and CM-like clasts from differentiated and undifferentiated meteorite breccias will be presented.	Poster Location #754
Lasue J. Meslin P. Y. Sautter V. Maroger I. Krämer Ruggiu L. et al.	<u><i>Probable Chondritic Fragments Detected by ChemCam in Gale Crater</i></u> [#2274] ChemCam identified two fragments with elevated Ni (>1wt.%) and MgO (~20–30wt.%) and an Mg/Si ratio consistent with ordinary chondrites.	Poster Location #755
Ashley J. W. Curtis A. G. Oij S. J. Wellington D. F. Meslin P. -Y.	<u><i>Morphometric Comparison of Martian Iron Meteorite Finds with Curated Terrestrial Analog Samples Using 3D Visualization and Measurement Techniques</i></u> [#2773] Surface morphologies of iron meteorites found on Mars are assessed using 3D visualization and measurement techniques with terrestrial analog meteorite samples.	Poster Location #756
Tait A. W. Schröder C. Ashley J. W. Velbel M. A. Bland P. A.	<u><i>What Meteorites on Mars Tell Us About the Martian Environment and the Case for Returning One</i></u> [#1387] Meteorite chemistry is well known, allowing them to become witness plates for environmental change on Mars. Recording atmospheric and water-rock histories.	Poster Location #757
Wellington D. F. Meslin P.-Y. Van Beek J. Johnson J. R. Wiens R. C. et al.	<u><i>Iron Meteorite Finds Across Lower Mt. Sharp, Gale Crater, Mars: Clustering and Implications</i></u> [#3058] The MSL/Curiosity rover has encountered a surprising number of likely iron meteorites across lower Mt. Sharp, Gale Crater, Mars.	Poster Location #758
Meslin P.-Y. Wellington D. Wiens R. C. Johnson J. R. Van Beek J. et al.	<u><i>Diversity and Areal Density of Iron-Nickel Meteorites Analyzed by Chemcam in Gale Crater</i></u> [#3179] A dozen iron meteorites have been analyzed in Gale Crater, with distinct compositions. We estimate their areal density, discuss their fate and distribution.	Poster Location #759
Joy K. H. Evatt G. E. Smedley A. R. D. Abrahams I. D. Peyton A. et al.	<u><i>The Lost Meteorites of Antarctica Project: A New UK-Led Antarctic Meteorite Recovery Programme</i></u> [#1018] An overview of Lost Meteorites of Antarctica Project and our 2018 Antarctic field expedition outcomes will be presented.	Poster Location #760
Rojas J. Duprat J. Engrand C. Dartois E. Delauche L. et al.	<u><i>Micrometeorite Mass Flux Measurements at Dome C, Antarctica.</i></u> [#1968] A new estimation of the micrometeorite flux at Earth surface inferred from the Antarctic CONCORDIA collection. Implications for the Zodiacal Cloud sources.	Poster Location #761
Caplan C. E. Huss G. R. Nagashima K. Schmitz B.	<u><i>Classification of Remnant Extraterrestrial Chrome-Spinel Grains from Jurassic Sediments</i></u> [#2068] Meteorite abundances of the Jurassic were different than in other time periods; the story from O-isotopes and chemistry of remnant chrome-spinels.	Poster Location #762
Anderson S. L. Bland P. A. Towner M. C. Paxman J. P.	<u><i>Utilizing Drones and Machine Learning for Meteorite Searching and Recovery</i></u> [#2426] We train convolutional neural networks to detect fallen meteorites observed by the Desert Fireball Network, in drone-obtained images of the Australian outback.	Poster Location #763
Scholar P. W. Harvey R. P. Karner J. M. Schutt J. W.	<u><i>A Geospatial Comparison of Meteorites Recovered from the North and Middle Icefields of the Miller Range, Transantarctic Mountains, Antarctica</i></u> [#1613] They differ, MIL North and MIL Middle / Their climate's the same, so they pose quite a riddle? / Is it wind? / Is it age? / We're quite noncommittal.	Poster Location #764

THURS POSTERS

Hegedüs T. Jäger Z. Csizmadia Sz. Zekó Z. Gucsik A. et al.	<u><i>Strewn Field Simulations and Field Searches of a Few Latest Bolides Over Hungary — Connection with the Fragmentation Height</i> [#1474]</u> We reanalyzed most recently observed blowing bolides over Hungary: 08/04/2018, 04/06/2015, 08/24/2013. We simulated the strewnfields and present field searches.	Poster Location #765
Ostrowski D. R. Haskins J. B.	<u><i>High Temperature Emissivity of Meteorites and the Relationship to Ablation Rates</i> [#2761]</u> Meteorite emissivity profiles are examined in relationship to atmospheric entry temperatures. Profiles are used to determine time to melt meteor surface.	Poster Location #766
Alesbrook L. S. Wozniakiewicz P. J. Price M. C. Cole M. J. Avdellidou C. et al.	<u><i>Simulating the Atmospheric Entry of Micrometeorites Using a Two Stage Light Gas Gun</i> [#1827]</u> We report on the results of our attempts to replicate the effect of atmospheric entry on micrometeorite using a two-stage light gas gun.	Poster Location #767
Petrova E. V. Kopysov A. S. Kokorin A. F.	<u><i>Plasmatron Experiments: Modelling of the Fusion Crust</i> [#2924]</u> A model fusion crust formation was performed for terrestrial samples and stony meteorites in the plasmatron with the high-speed flow of air.	Poster Location #768

Thursday, March 21, 2019

[R645]

POSTER SESSION II: WORKFORCE DEVELOPMENT, DIVERSITY, AND INCLUSION

6:00 p.m. Town Center Exhibit Area

Authors (*Denotes Presenter)	Abstract Title and Summary	Poster Location
Graff T. G. Evans C. A. Bleacher J. E. Young K. E. Helper M. A. et al.	<u><i>Earth and Planetary Science Training for NASA's Newest Astronauts: 2018 Training and 2019 Planning</i> [#2139]</u> Earth and Planetary Science training was conducted in 2018 for NASA's newest astronaut class. Planning is currently underway for 2019 training activities.	Poster Location #769
Budney C. J. Lowes L. L. Mitchell K. L. Wessen A. S.	<u><i>Across the Solar System: A Survey of NASA Planetary Science Summer Seminar Mission Studies 1999–2018</i> [#3225]</u> Student-designed mission concepts in NASA's Planetary Science Summer Seminar address community priorities with point designs and instrument selection.	Poster Location #770
Tornabene L. L. Block K. Pilles E. Baugh N. McEwen A. S. et al.	<u><i>Mission Science/Operations Support and Training for Spacecraft Payloads: Building the Next Generation of Planetary Mission Professionals</i> [#2962]</u> A summary of the last four years of mission science/operations support and training with MRO/HIRISE provided to 17 HQP by a CPSX/WesternU-based HIRISE team member.	Poster Location #771
Klug Boonstra S. Kretke K. Levison H. Christensen P. R. Olkin C. et al.	<u><i>The Lucy Student Pipeline Accelerator and Competency Enabler (L'SPACE): A New Model for NASA Student Collaborations to Enhance STEM Workforce Development at Scale</i> [#3258]</u> The Lucy Student Pipeline Accelerator and Competency Enabler (L'SPACE) Program is the student collaboration portion of NASA's Lucy Mission.	Poster Location #772
Olgin J. G. O.	<u><i>Increasing Student Enrollment and Retention in STEAM Careers Centered in Planetary Science by Incorporating NASA's SOLVE Programs in College Level Service Learning and Internship Programs</i> [#2054]</u> Using NASA SOLVE program and service learning to enhance learning in planetary science through Earth analogs.	Poster Location #773
Patkos Cs. Mika J. Gucsik A. Juhasz T. Homoki E. et al.	<u><i>Planetology Related Aspects in University Education of Geography and Environment</i> [#3261]</u> Summary of the educational background of a Hungarian university.	Poster Location #774
Grier J. A. Buxner S. A. Rathbun J. A. Richardson M.	<u><i>Effective Approaches to Increasing the Accessibility of Postdoctoral Opportunities Through Remote Advising</i> [#2791]</u> Remote mentoring / Postdocs — invites and supports / Diverse scientists.	Poster Location #775

Richey C. R. Pappalardo R. T. Senske D. A. Korth H. Kilma R. et al.	<u><i>“One Team:” The Dynamics and Structure of the Europa Clipper Science Team</i></u> [#2022] The Europa Clipper Mission will explore Europa to investigate its habitability. The Europa Clipper Science Team operates as a single ‘one team’ entity.	Poster Location #776
Diniega S. Klima R. Phillips C. B. Richey C. Turtle E. et al.	<u><i>Learning Ways to Improve Collaboration and Communication Within a Distributed, Large Team — Via the Europa Clipper Mission Social Science Journal Club</i></u> [#2170] With a large, spread team / How to do better science? / Social science knows.	Poster Location #777
Molaro J. L. Walsh K. Jawin E. Ballouz R.-L. Pajola M. et al.	<u><i>Team Dynamics During a Four-Day Effort to Map Bennu’s Surface: A Collaborative Effort</i></u> [#1591] We share methodologies used by our OSIRIS-REx working group to collaborate effectively and cohesively as a team during our preliminary mapping campaign.	Poster Location #778
Zellner N. E. B. Rathbun J. A. Ziegelman E. A.	<u><i>LPSC @ 50: What Do 18 Years of Presentation Data Tell Us?</i></u> [#3024] Eighteen years worth of LPSC attendance and abstract data has been analyzed to determine whose science is visible as talks and/or poster presentations.	Poster Location #779
Lynch K. L. Diniega S. Quick L. C. Horst S. M. Rivera-Valentin E. G. et al.	<u><i>50 Years of Planetary Science Workforce: Hidden Figures and the Legacy of Apollo</i></u> [#3162] The Apollo program was a critical component of the civil rights movement, but the modern planetary science workforce still lags in diversity and inclusion.	Poster Location #780
Piatek J. L. Gosselin G.	<u><i>Promoting Accessibility in Geoscience Education: What Practices from Planetary Science Can We Apply?</i></u> [#3006] We bring Mars to you / Pluto, Venus... remotely / How to “share” Earth, too?	Poster Location #781
Schindhelm R. N. Rathbun J. A. Diniega S. Brooks S. M. Hörst S. M. et al.	<u><i>Making Planetary Science More Inclusive: An Introduction to the Work of the American Astronomical Society’s Division of Planetary Sciences Professional Culture and Climate Subcommittee (PCCS)</i></u> [#2849] The AAS DPS Professional Culture and Climate Subcommittee was formed in 2016 to explore the broad issues surrounding inclusion in planetary science.	Poster Location #782
O’Brien A. C. Damale A. R. Lappin L. J. Garner R. J. Dudley J. N.	<u><i>Diversity in Student Space Activities in the United Kingdom</i></u> [#2380] Why not as many / People as others looking / At why things happen?	Poster Location #783

THURS POSTERS

Program Author Index

- Aaron L. M. R642
 Aaronson A. T328
 Abarca H. E. T309, R640
 Abbott B. T335
 Abe M. T253, T302, T347, W401
 Abe S. T253, T302, T316
 Abedin M. N. T345, T346
 Abell P. A. T253, T342, T347
 Abercrombie S. P. R640
 Abercromby A. T347
 Abernethy F. T347
 Abidin Z. R634
 Abplanalp M. J. W405
 Abrahams I. D. R644
 Abrahams J. N. H. R554*
 Abramov O. M155*
 Abreu N. R614
 Abreu N. M. M104*
 Accomazzi A. R638
 Achilles C. N. T252, T330, R552, R624, R632
 Ackiss S. R630, R631
 Ackiss S. E. T331
 Acosta-Maeda T. E. T345, T346
 Acquadro J. J. F703*
 ACS Team M154
 Acton C. R638
 Acuna D. D. R503
 Adair B. T313
 Adam C. T301
 Adamkovics M. M154
 Adams D. S. T336
 Adams E. R. M154
 Adams M. C. T255
 Adcock C. R626
 Adcock C. T. R606, R633
 Adeli S. T202, T332
 Adentunji S. R619
 Adler J. B. T316
 Adolphs T. T319
 Adriani A. T323, R631
 ADS Team R638
 Afanasiev M. T308
 Agarwal A. R505
 Agee C. B. T303, T308, R503, R616, R617
 Agrawal V. T320
 Agresti D. G. W405
 Aharonson O. T308, T338, T339, T347
 Ahern A. A. R623
 Ahmad A. T317
 Ahmed A. R636
 Ahn C. T337
 Ahrens C. T306, T333, R621
 Aid M. T328
 Airapetian V. R611
 Akey A. J. R610
 Akins A. T344
 Al Asad M. M. T203*, T301
 Albarede F. F705*
 Albers B. T342, T348
 Alday-Parejo J. M154
 Aleinov I. F701*
 Aleksandrov A. B. T318
 Alemanno G. T331, R625
 Alèon-Toppani A. R625
 Alesbrook L. S. R619, R644
 Alexander C. M. O'D. M104, T303, W406, W451, R504, R607, F705
 Alexander D. T312
 Alexandre A. R617
 Alexashkin S. R643
 Algermissen S. S. R640
 Ali K. T309
 Alkemade S. L. T303, R643
 Allen C. C. M101*
 Allen V. R615
 Allender E. J. T346
 Allibert L. T251, R619
 Allton J. H. T340, R608
 Allums K. K. R608
 Allwood A. T341
 Almeida M. T314, R623
 Almeida N. V. T340
 Alpert S. P. T320
 Altheide T. S. M155
 Altieri F. T323
 Alvarez-Candal A. R555
 Alvarez-Perez A. R643
 Alvaro M. F703
 Alwarda R. R628
 Alwmark C. T255, R620
 Amador E. W451
 Amador E. S. T331, R502
 Amano K. T253, T302
 Amari S. W455, R504, R607
 Amelin Y. R609, R616, F704
 Amoroso E. R635
 Amos C. C. T346
 Amrusi S. T339
 Anamika F. N. U. T347
 Anand M. M101, M104, T347, R501, R551, R604, R606, R616, R639, F701
 Anbazhagan S. R627
 Anderkin C. J. R616
 Anderson B. J. T338, W453
 Anderson C. M. T339
 Anderson D. E. T328
 Anderson F. S. R606
 Anderson J. L. B. T316, R619
 Anderson J. R. T345
 Anderson K. L. T346
 Anderson R. T252
 Anderson R. B. T328, T333, R625
 Anderson R. C. T204*, T338
 Anderson S. L. R644
 Anderson S. W. R631
 Andre S. L. T319
 Andrejkovicova S. R624
 Andres C. N. R628
 Andres P. T309
 Andrews S. M. F705
 Andrews-Hanna J. C. M101, T204*, R554, R631
 Andronicus C. T316
 Andrys J. L. R551
 Angel R. J. F703
 Angell P. R628
 Angle G. R503
 Angotti L. E. T320
 Annex A. M. R627
 Annibali S. T319
 Ansan V. M152, T307, T308, T309, R502
 Antonangeli D. M152
 Antreasian P. T203, T301
 Anzures B. T338
 Anzures B. A. M104*, T205
 Aoki J. T344
 Aoki Y. T304
 Aoudjehane M. T255
 APEX Team T342
 Aponte J. C. W451, R606, R642
 Aponte Hernandez B. T335
 Aponte-Hernandez B. R612, R621
 Applin D. R633, R642
 Applin D. M. T318, R503, R634
 Arahata S. T338
 Arai K. T347
 Arai T. T253, T302, T342, R501, R555, R614
 Arakawa M. T253, T302
 Arakawa T. T339
 Araki H. T253, T302
 Araki T. W406
 Aramendia J. R604, R626
 Arana G. R626
 Archer P. D. W402, R624, R636, R640
 Archer P. D. Jr W402*
 Archinal B. A. R638, R641
 Arcoverde P. R555
 Arcuri G. T328
 Arevalo R. Jr. W451
 Arjdal M. T328

Codes correspond to session codes used in the program where the first letter indicates the day (M for Monday, T for Tuesday, etc.). The three-digit number indicates the session code and DOES NOT reference a poster location.

- Arlinghaus H. F. T319
 Armstrong E. S. T335
 Armytage R. M. G. R616
 Arnaut M. T331
 Arney G. T312
 Arnold G. T331, T337
 Arnold N. S. T332
 Arp G. T320
 Artemieva N. T316, R619
 Arvidson R. E. T329, T330, T331,
 W402, W453, R502, R552,
 R622, R628, R638, R640
 Arya A. S. R631
 Asari K. T253
 Asch K. R638
 Ash J. R639
 Ash R. D. R618, F704
 Ashley J. W. T329, T338, R644
 Asimow P. D. T314, R620
 Aslam S. T336
 Asmar S. M152
 Aspahaug E. M101, T201*, T314,
 T316, T346, R505, R612,
 R619
 Aspahaug E. I. T301
 Atkins R. M. T327
 Atkinson J. T318
 Atreya S. T313, W453
 Atwood-Stone C. T316
 Aubele J. C. R637
 Aubuchon P. T343
 Auerbach V. L. R628
 Augé B. W406
 Auro M. T251
 Auster H.-U. T344
 Avdellidou C. T316, R644
 Avenson B. T310
 Ávila J. N. T328
 Avouac J. P. T256
 Aye K.-M. M151, T318, R628, F702
 Ayoub F. T256, T309
 Azéma E. R612
 Aziz M. T347
 Aznar A. R612
 Azua B. R633
 Babad A. T347
 Bachman N. R638
 Backer J. R623
 Baek J. M. R604
 Bagenal F. T305, W453*
 Baggio L. M154
 Bagheri A. T307
 Baglioni P. T308
 Bagot P. A. J. T328
 Bahia R. W452*
 Bahrami R. T311
 Bahreman A. R640
 Bailey C. M. R601
 Bailey L. R503
 Bailey P. T309
 Bailey S. H. T310
 Bain Z. M. R628, F702
 Baines K. H. T313
 Baird T. T334
 Bajo K. R608
 Baker A. M. T252, R624
 Baker D. M. H. T346, R628, F702
 Baker L. L. R634
 Baker M. B. W454
 Baker M. M. M152, T334
 Baker V. R. W452, R629
 Bakerman M. T335
 Bakermans C. R642
 Bakhtin B. N. T318
 Balcerski J. A. T327
 Ball M. R. R553
 Ballouz R.-L. T203*, T301, T338,
 W401, R645
 Balme M. R. T205, T332, T333,
 T334, T346, R502, R554,
 R627, R629, R630, R637,
 R640, R643
 Balta J. B. M102*
 Balthasar H. R623
 Banaszkiwicz M. R623
 Bandfield J. L. T205*, T317, T331,
 R611
 Banerdt W. B. M152*, T307, T308,
 T309, T338
 Banerjee N. R. T255
 Banfield D. M152*, T307, T308,
 T309, W453
 Banham S. T330, R627
 Banks M. M152
 Banks M. E. T305, T309, T314, T317
 Bannert W. B. T308
 Bao H. R618, R632, R633
 Bao H. M. R633
 Bapst J. R628, R640
 Bapst J. N. R623
 Baratoux D. T255, R631
 Baratti E. T316
 Barbarisi I. R640
 Barbato A. B. R632
 Barber S. J. T347, R606
 Barbieri M. R632, R636
 Barboni M. R551*, R606
 Barcenilla Garcia R. T335
 Bardin N. W406
 Bardyn A. R504, R607
 Baresi N. T203, T338
 Barge L. T346
 Barge L. M. W451*
 Barge L. M. B. T311
 Barkaoui S. T308
 Barker D. C. T317, T347
 Barker I. T328
 Barker M. K. T315, R603, R612
 Barlow N. G. R621
 Barnerdt B. T308, T309
 Barnes J. T334
 Barnes J. J. T328, W403, R617
 Barnes J. W. M105, T305, T336
 Barnes R. T341, R601
 Barnett J. R639
 Barnett M. N. T312, R609
 Barnouin O. S. M103, T203*, T253,
 T301, T316, T302, W401,
 R505, R612, R614
 Baron G. T323
 Barr A. C. T254
 Barraud O. R554
 Barrett A. M. R640
 Barrett T. J. R616
 Barr Mlinar A. C. T343
 Bart G. D. R621
 Bartczak P. R614
 Bartlett K. D. T344
 Barucci M. A. T253, T301, T302,
 T314, W401*
 Basilevsky A. T. T338, R631
 Bass D. S. T341
 Bastide L. T346
 Bastien R. T340
 Bastow I. T308
 Bates A. R. R622
 Bates H. C. R503*
 Batov A. T327
 Batson P. E. R606
 Battaglia R. R606
 Battisti A. R639
 Battler M. T347
 Batty C. R503, R626
 Bauch K. T319
 Bauer F. T321
 Bauer J. M153, R614
 Bauer J. M. M153, R555*, R614
 Bauer P. W. R645
 Baugh N. R645
 Baum M. M. W451
 Baumgardner J. T318
 Baumgartner R. M102, T328
 Baxter B. K. R642
 Bay X. F705
 Bayle O. R643
 Bayon S. R643
 Beard B. L. T328, R504
 Bearden D. A. T344
 Beaton K. H. T347
 Beaty D. W. T341, R642
 Beaulieu K. R. R605, R639
 Beauvivre S. T314
 Becerra P. R623, R628, F702*
 Bechtel H. A. W405
 Beck A. A. R606
 Beck A. W. T342, R622
 Beck P. R613, R624, R634, R644
 Becker H. M101, W455, R501
 Becker K. J. T203, T301
 Becker S. A. R619
 Becker T. L. T318, R641
 Becker T. W. T204
 Beckett J. R. R620
 Beckman D. T. T344
 Beddingfield C. B. M103, M153,
 T203, T305, T335
 Bedford C. T328
 Bedford C. C. T330, R552
 Bedini P. T336

Bedrossian M. R642
 Beebe R. F. R641
 Beegle L. R643
 Beegle L. W. T341, R633
 Beentjes D. T348
 Beghein C. M152, T308, T338
 Behoukova M. T344
 Behrens J. W. T318
 Beichman C. A. T344
 Beirhaus B. T203
 Belcher C. T255
 Belenguer T. T346
 Belgacem I. T343
 Bell E. R635
 Bell J. R631
 Bell J. F. R634
 Bell J. F. III T329, R552, R614, R624,
 R625, R644
 Bell S. K. T206, T339, R606, R637
 Bellucci J. J. F703
 Bellutta P. T330
 Belyaev D. M154
 Benavides T. T348
 Bender H. T343
 Benecchi S. D. M103, M153
 Benedetto C. T308
 Benedix G. K. M102, T303, T328
 Benison K. C. R643
 Benisty M. F705
 Benna M. T313, T338, T339, W403
 Benner L. A. M. T301, R555, R612
 Bennett C. A. T203, T301
 Bennett K. A. T256, T330, W402,
 R502, R554, R602, R624,
 R631, F701
 Benson E. T347
 Bera P. P. R642
 Bercovici H. L. R610, R618
 Bérczi Sz. T335
 Berdis J. R. T323
 Berg M. J. R. T348
 Berger E. L. T328
 Berger J. A. T252, T313, T328, T330,
 R552, R624
 Berger L. M152, T256*, T309, R640
 Berger T. T315
 Bergin E. A. R553
 Bergman D. T343
 Bering E. A. III T344
 Berlin R. T319
 Berlo K. R624
 Berman D. C. T333, W452, R554,
 R627, R630, R637
 Birmingham K. R. R553*
 Bermúdez L. T336
 Bernacki M. T301
 Bernal J. J. R504
 Bernard R. E. R617
 Bernardoni E. T305, R607
 Berndt J. T314, T319, R553, R606,
 R618
 Bernhardt H. T202, R633, R637
 Berrocal A. T346

Berry K. E. T336
 Bertaux J.-L. R601
 Berton M. T325
 Bertrand T. T306
 Besse S. T314, R554*, R638, R640
 Bethell E. M. W404*
 Beucier E. M152, T308
 Beyer R. A. M103, M153*, T305,
 T324, T335, R638
 Bezděk A. T321
 Bhakta D. T337
 Bhandari S. R634
 Bhardwaj A. T302, T313
 Bhartia R. T341, R633, R643
 Bhattacharjee A. T205
 Bhattacharya A. T320
 Bhattacharya S. R602, R634
 Bhiravarasu S. S. T316, T318, R601,
 R603, R612, R639
 Bianco G. T308
 Bibring J.-P. T253, T302, T341,
 T344, R643
 Bickel V. T. T206, T339, R603, R637
 Biele J. T253, T302
 Bierhaus E. B. T203, T301, W401*
 Bierson C. J. M103, M153, T305,
 T310, T344, F705
 Biersteker J. B. R609
 Bierwirth M. M152, T308
 Bigolski J. N. T303
 Billings K. J. T337
 Bills B. G. T313, T344, F702*
 Bina A. R645
 Binet R. T315
 Binzel R. P. M103, T305, T335
 Birch S. M105
 Birch S. P. D. T326, T336, R555*
 Bird M. K. T305
 Birgisson A. F. R635
 Birnstiel T. F705
 Bischoff A. R617, R644
 Bish D. T330
 Bishop J. L. T252*, W402, R622,
 R632, R634
 Biwer C. M. R619
 Bixler A. J. R608
 Bizzarro M. T303, R620
 Bjønnes E. M101*
 Bjoraker G. L. T313
 Blacksberg J. T346
 Blake D. F. T252, T330, T337, T339,
 T341, T345, W402, R552
 Blake G. A. T336, R553
 Blanco N. T255
 Blanco-Cuaresma S. R638
 Bland M. T343
 Bland M. T. W454, R615, R641
 Bland P. A. T303, R505, R555, R607,
 R610, R644, F703
 Blaney D. T252, T328
 Blaney D. L. T343, R633
 Blankenship D. D. R623, R628
 Blase R. T318

Blase R. C. T339, T343
 Bleacher J. R632, R635
 Bleacher J. A. R554
 Bleacher J. E. T347, R645
 Blewett D. T. T205, T316, T317,
 T338, R612, R613
 Blichert-Toft J. F705
 Bliss D. E. R619
 Block K. R645
 Bloom H. T303
 Blumenfeld E. H. R605, R639
 Boatwright B. T338R621, R627
 Boazman S. T334
 Bobet A. R603, R635
 Bochsler P. R608
 Bodewits D. R555, R613
 Bodnar R. J. W451
 Boduch P. W406
 Boehm C. T310
 Boehnke P. R504, R606
 Boener A. R603, R621
 Boerner A. T337
 Boesenberg J. S. M104, T303, R618
 Bohnenstiehl D. R. T201, T204
 Boivin A. L. R602, R612, R638
 Bolden R. T338
 Boldt J. D. T346
 Boleaga Y. R617
 Bolton S. R631
 Bolton S. J. T201, T323
 Bolzan M. J. A. T313
 Bomse D. S. T339
 Bonanno D. L. R632
 Bonanno G. R632
 Bonato E. W406*
 Bondarenko N. V. R601, R603
 Bonds Q. T339
 Bongiovanni D. G. R632
 Bonifacie M. R551
 Bono R. K. R605
 Bonsall A. R555, R612
 Booth S. T347
 Borg L. E. R501
 Borisov D. T314
 Borlina C. S. R609, R617
 Borrini G. R623
 Borst A. T314
 Boryta M. D. R612
 Bose M. M104, T308, R504, R607
 Boslough M. E. R619
 Boston P. R642
 Böttcher S. I. T315
 Böttger U. T346
 Bottke W. F. T301, W453*, R503,
 R619
 Bouchard M. T320
 Bouchard M. C. T329, W402
 Boujibar A. T312
 Boukaré C.-E. T251
 Boukari C. R625
 Bouley S. T255
 Bour D. R607
 Bourassa M. T347, R645

- Bourke M. C. T202
 Bousquet B. T341, T346
 Bouvier A. T303, R617, R618
 Bower D. W451, R632
 Bowers M. T343
 Bowles N. M152, T346
 Bowles N. E. T339, R501, R503
 Bowley K. S. R639
 Bowman D. C. T337
 Boyce A. T304
 Boyce J. F701
 Boyce J. M. R621
 Boyce J. W. R605, R617
 Boyd A. M101, T318, R603
 Boyd N. T328
 Boyd N. I. T313, T330, R552, R624
 Boyet M. R617, R618
 Boynton W. V. T203, T301, T330, R628, R640
 Bozdag E. M152, T308, T310
 Bozic T. R643
 Brack A. T255
 Brack D. N. T203, T301
 Bradburne C. T345
 Bradley D. C. T339
 Bradley J. P. W405, R504, R607, R610
 Brady A. L. R642
 Bramble M. T338
 Bramble M. S. T256, T313, R502, R503*, R622
 Bramson A. M. T332, R628, F701*, F702
 Brand H. E. A. T303
 Brandon A. D. T328
 Brandt P. T344
 Braroo S. R619
 Brasser R. M155, R621
 Bray S. R625
 Bray V. J. M103, T305, T310, T316, T320
 Brearley A. J. M104*, T303, T304, T328, R504, R606, R610, R613
 Breitenfeld L. B. T203, T301, T346
 Brenker F. E. T303, R606
 Brennan M. C. T204*
 Brennan R. R611
 Brennecka G. A. R504, R610, F705
 Breton S. R505
 Bretzfelder J. M. T316
 Breuer D. M152, T204, T310, T314, T344, R621, R628
 Bridges J. C. T328, T330, T340, R502, R552, R611, R622, R623, R625, R632, R643, R644
 Bridgland D. R. T321
 Briggs J. M154
 Brinckerhoff W. B. T336, W451
 Brinkman N. T308, T309
 Briscoe A. C. W404, R601
 Bristow T. W402
 Bristow T. F. T330, T339, T341, R552, R624
 Bristow T. S. T337
 Britt D. T. M103, T305, W454, R613
 Broad K. E. T312
 Brock L. S. T312
 Brodsky H. F. T251*
 Bromley B. C. T303
 Brooks A. J.-W. R638
 Brooks S. T323, R631
 Brooks S. M. R641, R645
 Broquet A. T204*
 Brossier J. F. W404*, R601
 Brough S. T332
 Brounce M. F701*
 Brown A. J. T331, R622
 Brown H. M. T318
 Brown M. A. R631
 Brown R. H. M154, R637
 Brown S. M. T251, R501
 Brown Z. R503
 Brownlee D. E. R504, R607
 Brož P. R629
 Brozovic M. R555, R612
 Brucato J. R. T301, W401
 Bruce C. T343
 Brugman B. L. R633
 Brum J. T321, R604
 Bruneton A. T255
 Brunetto R. T253, T302, R607, R625
 Brunner A. E. R619
 Bryce B. T343
 Bryk A. B. T330
 Bryson J. F. J. R553, R609
 Bryson K. R612
 Bu C. T318
 Buch A. R643
 Buchenberger B. R505
 Buchner E. T255
 Buchner M. T321
 Buckner D. K. T347
 Buczkowski D. L. T316, W454*, R612, R615, R622, R637
 Budde G. T251*, R610, R618, F704
 Budney C. T344
 Budney C. J. R645
 Buer S. F. R633
 Buffo J. J. T254*
 Bugby D. T339
 Bugga R. V. T337
 Bugiolacchi R. R631
 Buhler P. B. F702*
 Buie M. W. M103*, M153, T305
 Bulcha B. T. T339
 Bullock E. W406
 Bunce L. E. R627
 Buratti B. J. M103, M153*, T305, R641
 Burbine T. H. M104, R613
 Burchell M. T314, R620
 Burchell M. J. R621, R644, F703
 Burgener J. A. M153*
 Burger A. T346
 Burger C. T314
 Burgess K. R504
 Burgess K. D. R607
 Burgess R. R604
 Burke K. N. T203, T301
 Burkemper L. K. R616
 Burkhard L. R611
 Burkhardt C. T251, R610, F704, F705
 Burkhonov O. R614
 Burks M. T. T336, T342
 Burmeister S. T315
 Burnet D. S. R608
 Burnett D. T317, R608
 Burney D. T320, F701*
 Burney D. C. R605
 Burr D. M. M105, T319, T326, W405, R627
 Burton A. S. T340, T341
 Burton M. E. T338, R641
 Burton Z. F. M. T252, R634
 Busan D. C. R555
 Busch M. W. R555
 Busemann H. R618
 Bustillo K. C. R607
 Butcher F. E. G. T332
 Butterworth A. L. T303, R504, R607, R621
 Buxner S. A. T335, R645
 Buz J. W404, R601, R628, R633
 Byers G. T306, T338
 Byers S. T306
 Byon A. J. R640
 Byrne P. K. T201, T204, T205, T306, T312, T320, T327, W453*, R627
 Byrne S. T332, T341, T345, W405, R615, R623, R628
 Byron B. T320
 Byron B. D. T317
 Cabalin L. M. R626
 Cable M. L. M105*, T336, T343, W451
 Cabrero-Gomez J. F. T335, T346
 Caddick M. J. T308
 Cadek O. T344
 Caffee M. W. T303, R501, R608
 Caggiano J. A. T331
 Cagle N. T330
 Cahill J. T317, R602, R613
 Cahill J. T. W405, R639
 Cahill J. T. S. T315, T316, T318, T338, R611
 Cai Y. T315, R639
 Cairney J. R610
 Calaway M. J. T203, T340, T341
 Calcutt S. T308
 Calcutt S. B. M152
 Calef F. T309, T330, R644
 Calef F. J. T309, T313
 Calef F. J. III T306, R505*, R640, R644
 Calentropio F. R643

Calvet R. T343
Calvin W. R633
Calvin W. M. T323, T341, R628,
F702*
Cambioni S. T314, R612
Cameron B. I. R632
Camino O. T314
Campbell A. R630
Campbell B. A. T332, W404, R623,
R628, R631, F702
Campbell C. T313
Campbell J. D. R623
Campbell T. R503, R620
Campins H. T301
Canchal R. T346
Cang X. W452*
Canham J. S. T336
Cannon K. M. T313, W454*, R634
Cano E. C. T251*
Canora C. P. T346
Cantillo D. C. R503*
Cantor B. A. R628
Cantrell T. W451
Canup R. M. W403*, R619
Cao H. J. T206, R604, R634
Cao X. R618, R632
Cao X. B. R633
Capelli L. S. R633
Capitan R. R645
Caplan C. E. R644
Caravaca G. R625
Carballido A. T325, R606, R610
Carbone D. R632
Carbonneau P. E. T332
Carcich B. T301
Cardenas B. T. W452*
Cardenas F. R620
Cardesín-Moinelo A. R627
Cardinale M. T256
Carey E. M. R631
Carey W. T347
Carillo-Sánchez J. D. R644
Carli C. T319
Carmack R. R634
Carnelli I. T342
Carnes L. K. T326
Carol E. T338
Carpenter J. T347
Carpenter J. M. F705
Carpenter P. K. T328, R605
Carr B. B. R631
Carr J. R. T332
Carrell K. W. R631
Carrey W. T347
Carrier B. L. T341, R642
Carroll A. T317
Carroll K. A. R602
Carsenty U. R615
Carson G. L. R632
Cartacci M. F702
Carter J. T323, R622, R625, R604,
R634
Carter J. N. R604

Carter L. M. T318, T346, R554,
R631, F701
Carter M. T344
Carter P. J. R505, R619
Cartier C. T319
Cartwright J. A. R619
Cartwright R. J. T305
Cartwright S. F. A. T316, T331, R621
Casale G. R616
Case A. W. T317
Casey G. T338
Cassata W. T303
Cassata W. S. T313, R501
Cassenti F. F702
CaSSIS Science and Operations
Teams R623
CaSSIS Team F702
Castelletti D. R641
Castillo J. R636
Castillo-Rogez J. T342, T344, R615
Castillo-Rogez J. C. W453, W454*,
R615
Castle N. M102, T328, T330, R552
Castro C. L. T301, T340
Castro K. R626
Castro-Wallace S. L. T340
Catalano J. G. T330, W402, R634
Catalano T. R620
Cataldo V. R554, R631
Cattani F. T341
Caudill C. R645
Caves L. R. R618
Cavosie A. J. R620, F703
Cawley J. W452
Cawley J. C. W452, R621
Cayron C. M101, F703
Celestian A. J. R642
Çelik O. T338
Cernok A. M101, T328, R501*,
R604, R616
Cerroni P. T314
Ceylan S. M152, T308
Chabot N. L. T205, T342, R553
Chabra O. R503, R620
Chaikin A. M103
Chakraborty S. T343
Chan Q. H.-S. W451, R551
Chan Y. T337
Chandnani M. T316
Chang-Diaz F. R. T344
Chanover N. J. M151, T323
Chappaz L. R631
Chappell S. P. T347
Charalambous C. M152, T308, T309
Charles H. T334
Charlier B. T319
Charnley S. R615
Charnoz S. T251*, T322, R609, R619
Chatterjee S. R622
Chaudhury S. R639
Chauhan M. R602
Chaussidon M. R609, F705
Chavalithumrong A. L. T347

Chavez C. L. M103
Che S. T328, R610
Cheffer K. R643
Chen A. T341
Chen B. T310
Chen H. T303, W455, R605
Chen H. Y. R620
Chen J. T339, T341, R602, R604,
R605
Chen L. C. T347
Chen M. R620
Chen S. T327, R605
Chen W. R611
Chen X. T346
Chen X. C. R606
Chen Y. T338, R602
Cheng A. F. M103, M153, T305,
T342
Cheng H. C. J. R601
Chennaoui Aoudjehane H. T255,
R620
Cherniak D. R601
Chernozhukhin S. M. R606
Chesley S. T203
Chesley S. R. T301
Chesnutt J. M. R627
Chevrel M. O. R631
Chevrel S. T314
Chevrel S. D. T347, R602
Chevrier V. M105, T326, R601
Chevrier V. F. M105, M155*, T202,
T252, T306, T333, W404,
R633
Chi H. T316
Chi P. M152, T338
Chi P. J. T307, T314, R602
Chide B. T341, T346, R624, R644
Chien S. A. T343
Chilton H. T. W454
Chin E. J. R617
Chin G. T339
Chin K. C. T311
Chinchalkar N. T320
Chinnamuthu M. R627
Chipera S. J. T330, R552
Chivers C. J. T204*
Cho Y. T253, T301, T302, W401*
Choblet G. T344
Chocron S. R555
Choi J. R604, R614, R635
Choi T. X. T317
Choi Y. R635
Chojnacki M. T202, T203, T256,
T301, T334, W452
Chopdekar R. V. R553
Chow P. T343
Chrbolková K. R611
Christ O. R606
Christensen P. R. T202, T203, T252,
T301, T329, T332, T333,
T335, R623, R628, R645
Christensen U. M152, T308
Christeson G. L. T255

- Christian J. R. R622
 Christiansen E. H. T334, R631
 Christoffersen M. S. T332
 Christoffersen R. W405, R551*, R611, R620
 Chu P. C. T336
 Chuang Y.-L. R615
 Chui T. C. P. T339
 Chujo T. T344
 Chung P. M102, T328, R604
 Ciarnello M. R613
 Ciarniello M. T323
 Ciazela J. T333, R630, R631
 Ciazela M. R630, R631
 Cicchetti A. T323, T332, F702
 Ciesla F. J. R553, R609, R618
 Cieszecki J. R633
 Cílek V. T321
 Cilliers J. J. T347
 Cintala M. R620
 Cintala M. J. T316, R505, R619
 Citron R. I. T204*
 Claeys P. T255
 Claeys Ph. R606, R618
 Clark B. T203, R624
 Clark B. C. T252, T313, W401, W402, W451*, R614, R624
 Clark B. E. T203, T301, W401, R611
 Clark C. S. R614
 Clark J. D. T204*, T314, T317, R637
 Clark N. T252
 Clark P. E. T339, R614
 Clark R. R622
 Clark R. N. T343, R635
 Clarke J. D. A. R633
 Claudin F. T321
 Clay P. L. R604, R620
 Clegg S. M. T252, T328, T345, W402, R624, R633
 Clement T. T348
 Clement T. V. M. T311
 Clemett S. T336
 Clemett S. J. W405, R607
 Clendenen A. R. T318
 Clévéde E. T308
 Cline C. R620
 Cline C. J. II T310
 Clinton J. M152, T308
 Clinton J. F. T308
 Cloutis E. W454, R552, R633, R642
 Cloutis E. A. T317, T318, R503, R624, R634, R643
 Coan D. T347
 Coath C. D. F705
 Cockell C. S. T311, R642
 Codd S. L. T252
 Cody G. D. W406*
 Cofield S. T344, R502
 Cohen B. R644
 Cohen B. A. T206, T329, T341, W403*
 Cohen B. E. M102, T304, T313, T328, R604
 Cohen M. E. R605
 Coia D. R640
 Coker M. R643
 Colaprete A. M151*
 Cole M. J. R644
 Collinet M. F704*
 Collins G. C. T204, T343
 Collins G. S. M152, T308, T309, T316, T320, R505, R614, R621
 Collins M. S. T327
 Collins-May J. L. T332
 Colombo M. T346
 Colozza A. J. T344
 Colwell J. E. T322
 Combe J.-Ph. T322
 Combs L. M. M102
 Comellas J. M. T313
 Commerçon B. R609
 Conduis T. T331, R628
 Cong C. R624
 Congram S. N. R619
 Connell A. M. R641
 Connell S. R633
 Connell S. A. R634
 Connelly D. P. T321
 Connelly H. C. R645
 Connolly H. C. T203, T301, W401, R611
 Conrad A. R555, R638
 Conrad P. T313
 Conway S. R622, R623
 Conway S. J. T202, T205, T332, T333, R554, R629, R637
 Cook C. W. T332, T345
 Cook J. C. M103, T305
 Cooper G. W. W451*
 Coradini M. F702
 Cordiner M. R615
 Corlies P. M154*
 Cornet T. R554
 Corrigan C. T303
 Corrigan C. M. M104, T301, R618, F703, F704
 Coscia D. R643
 Cosciotti B. F702
 Cosentino R. G. T301
 Costello E. T317
 Costello E. S. M101, M151*, W403, R611, R621
 Costin G. R553, R618, R631
 Cottrell R. D. R605
 Coupland D. D. S. T344
 Courne de C. T319
 Courtin Nomade A. T255
 Courville S. W. T346
 Cousens B. R601
 Cousin A. T252, T328, T341, T346, W402, R552, R624, R625, R644
 Cousins C. R. T346
 Covey-Crump S. W452
 Cowart J. C. R627
 Cox M. A. F703*
 Craddock R. A. T334, W452*, R621
 Craft K. R645
 Craft K. L. T254*, T343, T345, R643
 Craig P. I. M155*, T330, R552
 Cramer F. W404
 Crapster-Pregont E. T319
 Crawford D. A. R505
 Crawford I. R627
 Crawford I. A. T316
 Creamer J. S. R643
 Cremonese G. T316, R621, R622, R623, F702
 Cremons D. R. T344
 Crisp D. T312
 Crisp J. A. T330
 Crispin K. L. M104
 Cristallo S. R504
 Crites S. C. T341
 Crites S. T. T203, T338, R604, R611, R631
 Crocco R. R640
 Cronberger K. R605
 Cronberger K. A. T320, R605
 Cross A. J. F702*
 Cross M. T347
 Crossley S. D. F704*
 Crósta A. T311, T320
 Crósta A. P. T320, T321, R621
 Crow C. A. R605, R606
 Crowell J. M. T347
 Crown D. A. T333, R554*, R627, R629, R630, R637
 Crowther S. A. R609
 Cruikshank D. P. M103, T305, W453*
 Crumpler L. T329
 Crumpler L. S. T329, W402, R622
 Csámer Á. T303
 Cseres J. R. R551
 Cszimadia Sz. R644
 Cuk M. T201
 Cullen D. W451
 Cullen T. W451
 Cully M. T342
 Cunje A. B. R627
 Cunningham M. R632
 Cupak M. R555
 Cupples J. S. T347
 Curiel P. H. T347
 Curran N. R611
 Curreri P. T338
 Currie D. T338
 Curtis A. T338, T344
 Curtis A. G. R644
 Cutri R. M. R555, R614
 Cutts J. A. T337
 Cuzzi J. T201, F704
 Cuzzi J. N. R609, F705
 Czaplinski E. C. M105*, T206, T326, T333, T339, R637
 Czarnecki S. T330
 Czarnecki S. M. T341

Czechowski L. T325, R614
 da Deppo V. R623
 Daeter M. I. T347, T348
 Dagar A. R634
 Dagar A. K. R603
 Dahl E. T344
 Dahl P. T310
 Dahl-Møller J. T321
 Dai L. T310, T338
 Daket Y. R639
 Dall'Asén A. G. T303
 Dalle Ore C. M. M103, M153, T305, R621
 Dallmann N. A. T344
 Dalton J. B. T343
 Daly J. A. F703
 Daly L. M102, T303, T328, W451, R610, R616
 Daly M. T203, T301, W401, R603, R614, R635
 Daly M. G. T203, T301, T346, R602, R606, R612, R642
 Daly R. T. T203, T301, R505*, R614, R619
 Damale A. R. R645
 Dame R. H. R633
 D'Amore M. T319, T331, T337, R614, R637
 Danell R. M. W451
 Dang Y. N. R633
 Danielsen J. M. R622, R634
 Danielson L. R620
 Dantras E. R635
 Dapremont A. M. R629
 Darling J. T328, R501, R604, R616
 Darling J. R. M101
 Dartois E. W406, R644
 Das D. R624
 Dasgupta R. M102, R553, R618, R631
 Dassanayake M. D. T311
 Daubar I. J. M152, T308, T309, T334, T343, R621
 d'Aubigny C. D. T203, T301, W401
 Daudon C. T326
 Dauphas N. T251, T318, W455, R553*, R606, R618, R626, F705
 Dauphas N. D. T303
 Davaadorj D. T333
 David G. T341, T346, R552, R624, R625, R634
 Davidson J. T328, W455, R607, R644, F705
 Davidsson B. M103, R555
 Davies A. G. T343, T344, R641
 Davies E. J. R505, R619
 Davies N. S. R633
 Davila A. T346
 Davis A. M. T303, R504
 Davis D. T303
 Davis J. L. R627
 Davis J. M. T333, T334, R502, R627

Davis K. N. T341
 Davis M. W. T339, T343, R603
 Davis R. E. T301, T340
 Davison T. M. T316, R505*, R614, R621
 Day B. T347
 Day B. H. R639, R641
 Day J. M. D. M102, T316, R605, R617, R618, F701
 Day M. D. T334, R621
 Daydou Y. H. R602
 Debaille V. R618
 Debei S. R623
 Deboy C. C. T305
 Deca J. T338
 De Cesare C. M. R640
 Dechant L. E. R619
 Decker S. R617
 DeCoito I. T335
 Deen R. T309
 Deen R. G. T309, R640
 DeFelice C. R617
 DeFelice J. D. R610
 Degli-Alessandrini G. T317, R616
 De Graaff S. T320
 De Gregorio B. T. R607
 de Haas T. T333, R502
 Dehais T. T320
 Dehant V. M152
 De Hon R. A. R633
 Dehouck E. R624, R625, R634
 Deighan J. T313
 de Kleer K. T344
 Delage P. T308, T309
 Del'Agnello S. T338
 Delaney J. S. R618
 Delapp D. W402
 DeLatte D. M. R639
 Delauche L. R644
 Delbo M. T203, T253, T301, W401*, R612
 De León J. R555
 De Leon P. T347
 Delgado F. T347
 Delgado T. R626
 Del Genio A. D. T312
 Delière A. R603
 DellaGiustina D. T203, T301, T310, T344, W401, R638
 Dell'Agnello S. T308
 Delle Monache G. O. T308
 Delouie E. R501
 De Marchi L. T320
 Demchenko V. R628
 DeMott A. M152, T309
 Demura H. T253, T302
 Dence M. R. T255
 Denevi B. W. M101, M151, T206, T315, T316, T338, W403*, R611, F701
 Deng C. T338
 Denk T. R614
 Denton C. T338

Denton C. A. W452*
 de Oliveira Lobo A. T344
 De Prá M. N. R555
 Dera P. T339
 Deran A. T347
 de Raucourt S. M152, T308
 DeRego T. T347
 Desai M. T338
 De Sanctis M. C. W454
 Desch S. J. F704*
 Deshapriya J. D. P. W401
 de Silva S. L. T334
 Des Marais D. J. T330, R552
 Despan D. T314
 DESTINY+ Team R614
 Detelich C. E. T334
 Deutsch A. T338, F703
 Deutsch A. N. T313, T318, R602
 De Vera J. P. T346
 Devillepoix H. A. R. R555
 Devlin K. R. T309
 Devouard B. R620
 de Wet W. T317
 de Wet W. C. T318
 de Winter B. T311, T342, T348T348
 Dey S. F704*
 Dhingra D. R602
 Dhingra R. D. M103, M105*, T305, F705
 Di K. T315
 Dibb S. D. T341, R614
 DiBraccio G. A. T205
 Di Cecco V. E. T328
 Dickenshied S. R641
 Dickeson Z. I. R627
 Dickson J. L. W402
 Didier A. R640
 Dietrich W. E. T330
 DiFrancesco N. D. M102
 DiFrancesco N. J. R632
 Dillinger J. M. R639
 Dillon S. M. R616
 Dimova L. T348
 Dina D. F. R612
 Ding X. Z. Sr. T314
 Dingemans A. T348
 Diniega S. T333, T341, T343, R628, R645
 Di Paolo F. F702
 Dirks G. J. T339, T343
 Dixon D. A. R634
 Djouadi Z. R607
 Dobrica E. T303, T304, R606, R613
 Docasal R. R640
 Dodds K. H. T201
 Doerres D. R645
 Dogel S. T304
 Dohm J. M. T204
 Dolinschi J. R610
 Dolocan A. W451
 Doloughan A. R631
 Domagal-Goldman S. T312
 Dombard A. J. T201, T325, R627

- Domingue D. T253, T302, T317,
W401, R637, R639
- Dominguez G. D. R606
- Donaldson Hanna K. L. T317, R501,
R503, R554
- Donaldson-Hanna K. T338
- Dong C. T344
- Dong C. F. T205*
- Donohue P. H. M104*, T304, R606
- Doran G. T343
- Doressoundiram A. R554
- Dorn T. C. T334
- Dorsánszki A. T335
- Dotson J. R612
- Dotto E. T301
- Douglass B. T317
- Douté S. T327, R622, R623
- Dove A. R606
- Dove A. R. T347
- Downes H. R626, F704
- Downey B. G. T325
- Downs G. W. T330, T341, R552
- Downs R. T337, T339
- Downs R. T. T330, T341, R552
- Doyle A. E. T312
- Dragonfly Team T336
- Draine B. T. T344
- Draper D. S. T338
- Drilleau M. M152, T308, T309, T327
- Driscoll P. T312
- Driver G. R555
- Dromart G. T252, R502, R625
- Drouet d'Aubigny C. T203, T301
- Drouet d'Aubigny C. T345
- Drube L. T253
- Drum M. R639
- Du J. T205*, T315, R501
- Duarte K. D. W454*
- Duca Z. W451
- Duck A. L. R612
- Dudek M. J. R601
- Dudley J. M. T328
- Dudley J. N. R645
- Dudzinski G. R614
- Dugdale A. R619
- Duhamel Achin I. T255
- Dukes C. A. T318, W405
- Duley M. R604
- Dulin S. A. T320
- Dullemond C. P. R610, F705
- Dulova I. A. R603
- Dumke A. R623
- Duncan A. G. M155
- Duncan M. S. R619
- Dundar M. R502*
- Dundar M. M. T252
- Dundas C. M. T332, T333, T341,
R621
- Dunham E. T. T344, W455, R610,
R616, F705*
- Dunlap D. R. R616
- Dunlop J. M101, R501
- Dunn J. T347
- Dunn T. L. R620
- Duprat J. T304, W406*, R644
- Durda D. D. T342, R555, R606,
R617, R619
- Đurech J. R611
- Durisen R. H. T322
- Dustrud S. M105, T326
- Du Toit C. F. T346
- Dutrow B. T252
- Dutta A. T320
- Duvet L. T340
- Dwarkadas V. V. F705*
- Dworkin J. R643
- Dworkin J. P. T203, T301, T336,
T340, W451, R606, R642,
R645
- Dyar D. T337
- Dyar M. D. T318, T321, T346, R601,
R613, R625, R632, F703
- Dygart N. T205, T251*, T304
- Dyke S. J. R603, R635
- Dypvik H. R634
- Dzurilla K. T326
- Earle A. M. M103, T305, T306
- Ebel D. S. T255, T303, T320, T335,
W455*, R604, R610
- Ebel J. M. R619
- Eberhardt M. M152
- Ebert M. R620
- Ebert R. T338
- Ebert S. R610
- Ebihara M. T303, R551, R604
- Echer E. T313
- Echeverría C. R636
- Economou T. T337
- Edelmann R. R604
- Edgar L. A. W453, R502, R633, R645
- Edgar L. E. T330
- Edge E. T347
- Edgett K. T330, T334, R627
- Edgett K. S. W453, R621, R624,
R625
- Edgington S. G. T313, R641
- Edmundson K. L. R641
- Edwards B. T346
- Edwards C. E. R627
- Edwards C. S. T256, R502, R556,
R628, R631, R640
- Edwards H. R643
- Edwards P. H. T344
- Efroimsky M. T307
- Egan A. F. R611
- Egan M. T345, T346
- Ehgamberdiev S. A. R614
- Ehlmann B. L. T252, T302, T328,
T331, T333, T346, W402,
W454, R502, R505, R627,
R633, R634, F702
- Ehm L. R626, F703
- Ehrenfreund P. T314
- Ehresmann B. T330
- Eigenbrode J. L. W402, W451,
R624, R632, R643
- Eiler J. F701
- Eismont N. T337
- EIS Team T343
- Eitel M. T347
- Eke V. T201
- Eke V. R. T312
- Elachi C. T326
- Elam W. T. T341
- Elardo S. M. W403*
- Elder C. T301, T338
- Elder C. M. T201, T203, T317
- Elgner S. T253
- El Kerni H. T255*
- Elkins-Tanton L. T. M101, T342,
T347, R614, R618, R619
- Elliott H. A. M103, T305
- Elliott J. R621
- Elliott J. P. T323
- Elliott J. R. T316, R505*
- Elliott T. F705
- Ellison D. M154
- Ellouzi M. T314
- El Maarry R. R631
- El-Maarry M. R. M103, T305, R622,
R623, R555*
- Elphic R. C. M151
- Elrod M. K. T313
- ElShenawy M. T328
- El-Shenawy M. I. T304, R556*
- Elsila J. E. W451, R606, R642
- Elvis. M. T346
- Emery J. P. T203*, T301, R555,
R613
- Emmart C. T335
- Emran A. T334
- Emsenhuber A. T201, T314, R505*
- Encinas J. M. T346
- Endo T. T302
- Engle A. T326
- Engle A. E. M105
- Englert P. T252, R634
- Engrand C. T303, T304, W406, R644
- Ennico K. W453, R641
- Ennis M. E. M102
- Enomoto H. F705
- Enos H. L. T203, T301
- Enya K. T341
- Erard S. T314, R638
- Ergashev K. E. R614
- Erickson T. M. T320, F703*
- Ermakov A. T313
- Ermakov A. I. T344, W454*, R615
- Ernst C. M. M103, T203, T205,
T253, T301, T302, T316,
T336, T343, W401, R505,
R612, R614
- Ernst R. R632
- Ernst R. E. W404*, R601
- Ernstson K. T321
- Erwin A. T339
- Escarcega K. T313
- Escobar-Cerezo J. R611
- Escribano D. T346

Espinoza A. R645
 Espiritu J. T203
 Espiritu R. M. T203
 Esposito F. T256
 Esposito L. W. T322, T323
 Estes N. M. T347, R639
 Estrada P. T201
 Estrada P. R. T322, F705
 Ettahri M. A. R623
 Eubanks T. M. R614
 Euchner F. T308
 EuroMoonMars 2018–2019
 Team T338
 Europa Clipper Team R645
 Europa Project Engineering
 Team T343
 Europa Project Science Team T343
 Euser B. R619
 Evans A. J. T251*, T316, R553
 Evans C. A. R605, R638, R639, R645
 Evans M. E. T328, T335, T342
 Evans M. W. R641
 Evans R. T306
 Evatt G. E. R644
 Ewing R. C. R642, R643
 ExoFIT Team T346
 Fa W. T204, T205, T315, R501*,
 R601
 Fabre C. R625
 Faes Z. R505
 Fagan A. L. R616
 Fagan T. J. T304, R551*
 Fagents S. A. T324
 Fahey M. T339, T346
 Fairén A. G. W402, R624, R643,
 R644
 Faltys J. P. T320
 Fang J. R601
 Faragalli M. T347
 Farley K. R504
 Farley K. A. W402
 Farnell A. R631
 Farnocchia D. T203, T301
 Farnsworth K. M105*, T202, T326
 Farquhar J. R617
 Farrand W. H. T329, W402, R622
 Farrant B. E. T206, T339, R620,
 R637
 Farrell K. W. Jr. T339
 Farrell W. M. T317, T318, T339,
 W403, W405
 Farsang S. R503, R626
 Fassett C. T346, R638
 Fassett C. I. T319, T332, W405,
 R623, R627
 Fastook J. L. T332
 Fatemi S. T338
 Faul U. H. T310
 Fawdon P. R502*, R627, R630
 Fayon L. M152, T308, T309
 Feaga L. R613
 Fedo C. M. T330, W453, R502, R627
 Fedorova A. M154

Fedosi J. T343
 Fedosov F. T330
 Fegley B. Jr. T312
 Fei Y. T205*, T312, R553
 Feinberg J. M. T319
 Feist B. F. T314
 Feldman A. D. R633
 Feldman W. C. T344, R628
 Feng J. T317
 Feng L. T338
 Fennema A. R623
 Fenton L. K. T334, T341
 Feoktistova E. A. R612
 Ferdous J. T328
 Férellec L. T323
 Ferguson R. L. R640, R641
 Ferguson F. M154
 Ferguson F. T. R636
 Ferguson S. N. R621
 Ferlito C. R632
 Fernadez S. A. R640
 Fernandes R. R503
 Fernández M. T346
 Fernandez Y. R614
 Fernandez Y. R. M153, R555
 Fernández-Remolar D. C. R642
 Fernández-Valenzuela E. R555
 Fernando B. T308
 Ferrari S. T337
 Ferrari-Wong C. R611
 Ferrari-Wong C. M. T318, W405
 Ferraro N. W. T345
 Ferrière L. T328
 Ferrone S. T301, W401
 Feucht C. M. T347
 Fevig R. A. R612
 Fey D. R625
 Fieber-Beyer S. K. R503*, R613
 Fiechtner C. R620
 Filacchione G. T323, R631
 Filiberto J. M102, T335, R601
 Fillingim M. M152, T307
 Findlay R. M104
 Fink W. R638
 Finzi Y. T347
 First E. C. R551*
 Fisackerly R. T339
 Fischer R. A. T204, T251*, R618
 Fischer W. W. M155, T252, W402,
 R624
 Fisenko A. V. T303
 Fisher E. A. M151
 Fisher K. R. T342, T347
 Fitch R. T. R616
 Fitting A. B. W404
 Flahaut J. R643
 Flamini E. F702
 Flemming R. L. T311, T320, R620
 Fletcher L. T343
 Fletcher L. N. T313
 Floc'h J. P. T255
 Flom A. T318
 Flom A. J. T318, W405*

Flood V. A. T313, T330
 Florence M. M105
 Flores E. W451
 Flores K. E. R610
 Floss C. R504
 Flynn G. J. R504, R607, R617, R619
 Flynn I. T. W. R631
 Foing B. T335, T348
 Foing B. H. T311, T314, T338, T342,
 T347, T348, R611, R632
 Folco L. R620
 Folkner W. M152, T309
 Folsom M. T330
 Fooshee J. T335
 Ford E. B. T312
 Forgács-Dajka E. R612
 Forget F. M152, M154, T308, T309,
 R643, F702
 Forman L. V. M102, T303, T328,
 R607, R610, R616
 Fornasier S. T301
 Forni O. T252, T328, W402, R624,
 R625, R634, R644
 Foroutan M. T334
 Fortes A. D. T323
 Fortezzo C. M. R638
 Fortney J. W453
 Fougerouse D. R604, R610
 Foustoukos D. W406*, W451
 Fox A. C. W451*
 Fox J. L. T313
 Fox V. T252, R643
 Fox V. K. T330, W402*, R502, R634
 Foxworth S. T335
 Fraeman A. A. T330, T331, W402,
 W405, W453, R552*, R622,
 R624, R628
 Fraga D. R614
 Fralick C. T252
 Franchi I. R501, R604, F704
 Franchi I. A. M104, T328, R551,
 R616, R620
 Franco A. M. S. T313
 Franco G. S. R610
 Frank D. R. R504*
 Frank E. A. T319, T347
 Franz H. B. R624
 Franz H. F. W402
 Fränz M. T313
 Frazier W. E. T344
 Freed A. M. M101
 Freeman K. H. W451
 Freeman M. A. T339, T343
 Freemantle J. R606, R635
 Freissinet C. T336, W402, W451,
 R634, R636, R643
 French A. S. T203, T253, T301
 French B. M. T255
 French R. G. T322
 Frew D. T314
 Frick D. A. W455
 Friedrich J. M. R610
 Fries M. T303, T313, T340, R643

- Fries M. D. T340, T341, T347
 Frigeri A. R637, F702
 Frigge R. W405
 Fritz J. R620
 Frizzell K. R. R622
 Fronton J.-F. R624
 Frossard P. R618
 Fry E. S. T339, T343
 Frydenvang J. T252, T328, T330, W402, R552, R624
 Fu R. R. T342, W404, R605, R609
 Fu X. H. T206, T315, R604, R634
 Fu Z. T340
 Fuchs L. T204
 Fudge C. T255, R616, R620
 Fugett D. A. T345
 Fuji N. T308, T327
 Fujii Y. F. T253
 Fujimoto M. T253
 Fujita K. T302, R643
 Fujita S. R606
 Fujiya W. T304, T341
 Fujui A. T253
 Fukai R. F705*
 Fukuda K. W455, R504*, F705
 Fukuda S. T206, T339
 Fukuhara T. T253, T302, T316
 Fukushi K. T302, T333
 Fulchignoni M. W401
 Fuller J. T344
 Fultz B. T337
 Funaki M. R617
 Funase R. T338
 Funder S. T321
 Fuqua Haviland H. R631
 Furfaro R. T314, R503, R612
 Furi E. R501*
 Furukawa Y. T336
 Furutani K. T339
 Furuya S. T302
 Fusco M. S. T202
 Fuse R. T316
 Fuse T. T253
 Futó P. T312
 Gabasova L. M103, T305
 Gabasova L. R. T335, R641
 Gabriel T. R505, R644
 Gabriel T. S. J. T252, T314, T330, T341, R619
 Gabrieli A. T318
 Gabsi T. M152, T308
 Gaddis L. R638, R639
 Gaddis L. R. R554, R602, F701
 Gaffey M. J. R503, R613
 Gaffney A. M. R501*
 Gagnon J. R605
 Gailhanou M. T337, T339, T341
 Gainey S. R626
 Gainsforth Z. T303, R504*, R607
 Gaither T. A. R633
 Galdanes K. T347
 Galiano A. T253, T302
 Gallagher A. T. T327
 Gallagher C. T202, T332
 Gallant E. W404
 Gallego P. T346
 Gallegos Z. R625
 Gallegos Z. E. T347, W452, R627
 Galli A. T323
 Galli G. G. T303
 Gallino R. R504
 Gallo G. R632
 Galluzzi V. T316, R621
 Ganesh I. R554*
 Gang J. R618
 Ganguly K. T345
 Gao C. R632
 Garani J. R610
 Garbeil H. R627
 Garbino A. T347
 Garcia A. H. R640
 Garcia D. R645
 Garcia L. R626
 Garcia R. M152, T204, T308
 Garcia R. F. T308, T309, T337
 Garcia-Caurel E. R625
 Garcia-Martínez J. T346
 Garczynski B. J. W451*
 Garde A. A. T321, F703*
 Gardner A. S. T344
 Garg A. R607
 Garg M. T347
 Garg P. T347
 Gargano A. M. R605
 Garmire D. G. T345
 Garner R. J. R645
 Garozzo S. R632
 Garrick-Bethell I. M151, T316, T338, T339, W405
 Garrison D. H. T341
 Garroni N. D. T320
 Garry W. B. T347, R631, R637
 Gartrelle G. M. R613
 Garvie L. A. J. T301, T303, R619
 Garvin J. M152, T309
 Garvin J. B. M101*, T309
 Gary-Bicas C. R628
 Gasda P. T252, T328, T330
 Gasda P. J. T330, T345, W402, R624
 Gaskell B. T203, T301
 Gaskell R. T203, T253, T317, R555
 Gaskell R. W. T203, T301, T302, T336, R612, R614
 Gasnault O. T252, T328, T330, T333, W452, R552, R624, R625, R627, R634, R644
 Gasser M. T347
 Gattacceca J. T255, R618
 Gaubert F. T340, T341
 Gawronska A. R604, R605
 Gebbing T. T314
 Geeraert J. T203, T301
 Geiger B. R614
 Gellert R. T252, T313, T328, T329, T330, W402, R552, R624, R625
 Gemelli M. R620
 Gemma M. E. T335
 Genda H. T251, R503, R621, R624, R643
 Genda H. G. R612
 Gendreau K. T346
 Gengl H. T330
 Genova A. T205, T319
 Gensdarmes F. R635
 Gentry D. W451
 Genzel P.-T. R606
 Geppert W. W451
 Gerakines P. A. T336
 Gerasimov M. T337
 Germaschewski K. T205
 Germinario M. R633
 Gerrish L. R644
 Gerritzen C. W455
 Gessler N. T328
 Getty S. A. W451
 Getzandanner K. T203, T301, T336
 Ghail R. T337
 Ghail R. C. W404*, W453
 Ghent R. R. M151, T315, T317, W403, R602, R612, R621
 Ghigo F. D. R555, R612
 Gholinia A. T317
 Ghosal D. R602
 Ghosh D. B. R618
 Giambusso M. T344
 Giardini D. M152, T307, T308
 Gibson E. K. T252, R634, R639
 Gibson J. T304
 Gibson M. M104
 Gibson R. L. T255
 Giguere T. A. R602
 Gilchrist A. M. R618
 Gilg H. A. T320
 Gillis-Davis J. J. W405*, R602
 Gillmann C. W404
 Gillot P.-Y. T341
 Gills-Davis J. J. W405
 Gilmore M. S. W404*, W453, R601
 Gilmour C. T346
 Gilmour C. M. R606
 Gilmour J. D. R609
 Giorgini J. D. T301, R612
 Girona T. T325
 Giuppi S. F702
 Gladman B. M103
 Gladstone G. R. M103, T305, T317, T318, R603, R611
 Glanovsky T. R621
 Glaspie L. T320
 Glaspie L. M. R554*, R602
 Glassmeier K.-H. T302
 Glavin D. R643
 Glavin D. P. T336, W402, W451, R606, R642, R643
 Glaze L. S. T312, T324
 Glein C. W453
 Glein C. R. T201
 Gleißner P. M101*

Glenister C. T. R632
Glines N. H. T333
Gloesener E. T313
Glotch T. D. T301, T331, W403,
W406, R502, R611, R620,
R622, R632, R634, F703
Glukhova E. T335
Góbi S. W405
Godard M. W406
Godard V. R625
Goderis S. T255, R606
Godin E. T332, R628
Godin P. T318
Godin P. J. T311, T313
Goesmann F. W451
Goetz W. T328, W451*, R624, R644
Goldblatt C. T312
Golder K. B. T319
Goldsby D. L. F702
Goldstein D. W454
Goldstein D. B. T324, T325
Goldsten J. O. T342
Golish D. R. T203, T301
Golombek M. M152*, T256, T309,
T329, T334
Golovin D. T330
Golubov O. R612
Gomez D. R603, R635
Gomez-Elvira J. M152
Gomez-Nubla L. R626
Gonzales N. R. R637
Gonzalez A. R640
Gonzalez C. P. R608
Gonzalez Y. R632
Goodrich C. A. W406, R617, F704*
Goossens S. T205*, T319, R605
Göpel C. F705
Gordillo C. T346
Gordon T. T347
Goreva Y. S. R608
Gorevan S. T336
Gorin B. R606
Gorinov D. T337
Gorius N. T301, T336
Gorski K. M. T313
Gosselin G. R645
Gou S. T315
Goudge T. T202
Goudge T. A. T320, T332, R502,
R556, R622, R627
Gough R. T313
Gough R. V. T252
Goyal V. R607
Grady M. M. T341, R503*, R626
Graettinger A. H. R630
Graff P. V. T335
Graff T. G. T341, T347, R645
Graham H. R636
Graham H. V. R606, R634
Graham L. D. T342, T347
Grambling N. L. T205
Grand N. T344
Grande M. T314

Grant J. M152, T309, T329
Grant J. A. T309, T313, W402,
W452, R627
Grant J. E. T329
Grassi D. T323
Graul Galofre A. T332, W452*
Grav T. R555, R614
Grava C. T318, R611
Graves K. M101
Gray J. M104
Greathouse T. K. T317, T318, R603,
R611
Green J. A. M. R601
Green R. O. T343
Green S. F. R636
Green W. H. M101
Greenberg J. M. T346
Greenhagen B. M151, T317, R602
Greenhagen B. T. M151, T316,
T317, T338, W403, R501*
Greenstreet S. M103
Greenwood J. P. R610, F701*
Greenwood R. C. M104*, T304,
F704
Greer J. T303
Gregerson J. C. R626
Gregg T. T337
Gregg T. K. P. M105*, R554, R601,
R637
Gregory T. F705*
Grewal D. S. R553*, R618, R631
Grieger B. T314, T326
Grier J. T335
Grier J. A. T317, T335, R645
Grieve R. A. F. T255, T320
Griffin S. M102*, T328
Grigoriev A. M154
Grima C. R623, R628
Grimes K. R640
Grimes K. M. R640
Grimm R. T338
Grimm R. E. T202*, T252
Grinblat J. F. T308
Grindlay J. T346
Grindrod P. M. T333, T334, T346,
R623, R627
Grinspoon D. T312
Grisolia C. R635
Grizonnet M. T315
Grokhovsky V. I. R620
Gronoff G. F701
Grosch D. J. R555
Grosjean M. T348
Gross C. R622, R623
Gross J. M104, T328, W403*, R501,
R604, R620
Gross J. M. R608
Grosz A. T338
Grosz A. G. T339
Grott M. M152, T253*, T302, T307,
T309, T338, T344, R614
Grotzinger J. R552
Grotzinger J. P. T330, W453

Grove T. L. T251, R501, F704
Groven J. J. M105
Gruber M. R623
Grubisic A. W451
Gruel D. C. T308
Gruendler L. R632
Gruener J. R636
Grumpe A. T331, W405, R623
Grundy W. M. M103*, M105,
M153, T305, T306, T326,
T335, R641, F705
Grygorczuk J. M152
Gu X. R604
Guan Y. R608
Gucsik A. T303, T346, R612, R644,
R645
Gudipati M. S. T254, T323, R609
Gudkova T. T308, T327
Guenther M. E. R501*
Guerlet S. M154
Guerquin-Kern J.-L. W406
Guignan G. T337
Guimpier A. T202*
Guinness E. A. R602, R638
Guitierrez J. R612
Güldemeister N. T314, T320
Gulick S. P. S. T255*
Gulick V. C. T252, T333
Gullikson A. L. T334, R633
Gunkelmann N. R610
Gunn M. D. T346
Guo D. T315
Guo J. T315
Guo Z. R617, R620
Gupta A. R610
Gupta S. T330, T341, R502, R602,
R627, R634
Gurgurewicz J. T327, R630, R631
Gurov E. P. T320
Guttenberg N. R602
Guvad C. T321
Guzewich S. T252
Guzewich S. D. M154
Guzman D. R636
Guzman V. V. F705
Gyalay S. T201*
Gyllai I. R610
Haack D. R615
Haapala-Chalk A. T344
Haba M. K. R616
Haber J. T. W402*
Haberle C. W. T203, T301
Hackler A. T335
Hacuk S. A. II T205
Hadfield C. T347
Hadler K. T347
Haenecour P. T304, T319, R504*,
R607, R610, R611
Hagedon M. T345
Hagelschuer T. T346
Hager T. F. F702
Hagermann A. M152, T253, T302,
T332

- Hagerty J. R638
Hagerty J. J. T320
Hahn D. T343
Hahn T. H. Jr. T317
Hahn T. M. Jr. M101*, T314, R604, R605
Hakim A. T205
Halekas J. S. T307, T338
Halevy I. T327
Halim S. H. T316
Hall B. J. T328, R503
Hall J. T309
Hallis L. J. T328, W451
Halpin J. T328
Haltigin T. T341, T347
Hamann C. T319
Hamara D. R640
Hamilton C. T344, R632
Hamilton C. W. T338, R630, R631
Hamilton D. P. M103, M153
Hamilton J. S. T328
Hamilton V. E. T203*, T301, W401, R556, R611
Hamm M. T253, T302
Hamm V. H. T341
Hammer J. R604
Hammond N. P. T254*
Hammouda T. R618
Hamp R. E. R636
Han J. W455*
Hanania J. U. T313, T330, R625
Hand K. T336, T343
Hankey M. T303
Hanley J. M105*, T326, R634
Hanley L. R608
Hanna R. R605, R610
Hanna R. D. T203, T301, R605, R639
Hansen C. R645
Hansen C. J. T323, T343, R623, R628, F702
Hansen K. R645
Hansen P. B. T346, R625
Hansen U. T201
Hao J. T202*, T303, T332
Hao M. T310
Hapke B. R611
Hardersen P. S. R613
Hardgrove C. T252, T330, T341
Hardiman H. T346
Hare T. R638
Hare T. M. R640, R641
Hareyama M. R637
Hargitai H. I. T335, R623, R638
Harman C. F701
Harrington A. D. T341, T347
Harrington E. R645
Harrington E. M. T206, T339, R637
Harrington R. S. R606
Harris C. T344
Harris R. S. T255, T321
Harris W. M. R503
Harrison L. N. R606
Harrison T. N. T333, T342
- Harriss K. R619, R620
Harriss K. H. R619, F703*
Harshman K. T330
Hartig B. A. D. R555
Hartlep T. R609, F705
Hartley M. E. R606
Hartwig J. W. T344
Hartzell C. T203
Hartzell C. M. R503
Haruyama J. T338, T339, T347, R631
Harvey R. P. T320, R644
Harvey T. R644
Harvison B. A. R613
Harwell M. L. R619
Hasebe N. T333, T347, R551
Hasegawa H. T333
Hasegawa M. M. T336
Hasegawa S. T253, R555
Hash C. R622
Hashiguchi M. T303
Hashimoto H. T347
Hashimoto T. R639
Hashizume K. T304, T347
Haskins J. B. R644
Hasselmann P. H. W401
Hassler D. T330
Hattingh R. M102
Hauber E. M152, T202, T309, T332, R615, R623, R629, R633, R637, R643
Hauck, II S. A. T201
Hauri E. H. M104
Hauser N. T255
Hausmann R. T309, T334, R640
Hausrath E. M. W402*, R606, R626, R633
Haviland H. T338, T346
Hawkins S. E. T343
Hawkswell J. T332
Hay H. T344
Hay H. C. F. C. T204*, T325
Hayabusa2 LSSAA and LSS-IDS Teams T302
Hayabusa2 Team T301, W401
Hayakawa M. T253, T301, T302, W401
Hayashi H. R620
Hayashi R. H. T253
Hayes A. G. M105, M154, T326, T336, T343, W453, R555
Hayes J. T343
Hayne P. O. M101, M151*, M153, T315, T317, T338, T341, W403, R628, F702
Haynes M. S. R641
Hayward R. K. T334
Hazen R. M. T330, R552
He C. M105
He L. T331, R640
He R. T346
He Y. S. F705
Head E. R606
- Head J. T325, T332, T338, T347
Head J. W. M101, T312, T313, T315, T316, T318, T332, T333, T338, T339, W452, R554, R602, R603, R621, R627, R631, F701
Head J. W. III T205, T313, T317, T320, T339, R502, R633
Heap M. J. T312, T320
Heard A. W. R626
Heasman B. R633
Heather D. J. R614
Heber V. S. R608
Heck P. R. T303
Hedgepeth J. T320
Hedman M. T343, W453
Hedman M. H. M105
Hedman M. M. T322, T344
Hedrick G. R640
Heeger M. T319
Heemskerck M. T348
Heemskerck M. V. T311, T347, T348
Heffern L. E. T342
Hegedüs T. R644
Heggy E. T316, T318
Hegyi S. T335
Heider E. S. T320
Heine D. E. R633
Heinz N. R613
Heirwegh C. M. T341
Helbert J. T253, T302, T319, T331, T337, T344, T346, R613, R614, R635, R637, F703
Heldmann J. R631, R635
Heldmann J. L. T252
Helfenstein P. M153
Hellebrand E. R504, R604
Heller R. T312
Hellmann J. L. M104*
Hellweg C. E. T315
Helper M. A. R645
Hemingway D. W405
Hemingway D. J. T201, T254*
Hemmi R. T202, T253, T302, W401, R614, R629
Henderson B. L. T254
Hendrix A. T318
Hendrix A. R. T323, W403, R603, R611, R613, R635
Hennebelle P. R609
Henneken E. A. R638
Henning W. G. T319
Henriksen M. R. R637
Henson P. G. T347
HERACLES International Science Definition Team T347
Herbst W. R610
Herd C. D. K. M102*, T328, T336, W453
Herd R. K. T303
Herdrich G. R606
Hergarten S. T320
Hergenrother C. T203, T301, R555

Herique A. T344
 Herkenhoff K. T329, R625
 Hermis N. H. T311
 Hernandez B. A. T335
 Hery C. T333
 Herrick R. R. T316, T337, W404, R621
 Hertwig A. T. W455*, F705
 Hervig R. L. T328
 Herzog G. F. R604, R605, R618
 Heslar M. F. M105*
 Hess K. A. R605
 Hess M. R623
 Hess S. R635
 Hesse M. W454
 Hesse M. A. M155*
 Hewagama T. T313, T339, R632
 Heward A. T335
 Hewins R. R618
 Hewins R. H. M102, T328
 Hewson R. D. T331
 Hewson R. H. R502
 Heyd R. R623
 Heydari E. R624
 Heyer T. T202*, R640
 Hezel D. C. M104
 Hibbard K. E. T336
 Hibbard S. R645
 Hibbard S. M. R628
 Hibbits C. A. T318, T343, R503, R628
 Hibbits K. T318
 Hibert C. T308
 Hibiya Y. F704, F705*
 Hicks J. T347
 Hicks L. J. R611
 Hicks M. D. M153
 Hickson D. C. R602, R612
 Hidaka Y. R604
 Hiesiger H. T334
 Hiesinger H. M101, T202, T204, T206, T314, T317, T319, T333, T347, W403*, R615, R633, R637, R640
 Higashi K. M104*
 Higashide M. T347
 Higgins P. M. T311
 Higuchi A. T253
 Hikosaka K. R505
 Hildebrand A. W401
 Hildebrand A. R. T255*
 Hildenbrand A. T341
 Hill H. R636
 Hill J. R. T252*, T329, T335
 Hill M. E. T305
 Hill P. T320, T347
 Hill P. J. A. T255*, T347
 Hill T. R. T321
 Hills H. K. R602
 Hiltl M. T321
 Hilton C. D. R501, R618, F704
 Himeno Y. T338
 Hinman N. W. R634

Hirabayashi M. T203, T253, T301, T302, W401
 Hirai T. T344
 Hirata N. T203, T253, T302, W401
 Hirata T. F705
 HiRISE Team F702
 Hiroi T. T253, T302, W401, R611
 Hirose C. T253
 Hirotsugu H. R616
 Hirschmann M. M. R551, R553*
 Hirth G. T251
 Ho G. C. T338
 Ho T.-M. T253, T302
 Hochleitner R. R617
 Hodges K. R639
 Hodges K. V. T255, T314, R619
 Hodyss R. M105, T323
 Hoefnagels B. T303, T328, R605, R617
 Hoey W. A. T345
 Hoffman M. E. T313
 Hoffmann H. R621
 Hoffmann V. H. R617
 Hofgartner J. F705
 Hofgartner J. D. M103, M153*, T305
 Hofmann A. E. T343, R608
 Hofmann D. T339
 Hofstadter M. D. W453
 Hogan A. R611
 Hogancamp J. V. W402, R624, R636
 Holden P. T328
 Holladay S. R632
 Holland G. R620
 Hollibaugh Baker D. M. T341, R628
 Hollins G. T309
 Holme E. A. T341
 Holmes A. K. R553, R631
 Holm Nielsen L. R638
 Holo S. J. R505*, R627
 Holsclaw G. M. T205, R635
 Holt J. M. C. T340
 Holt J. W. T332, T341, R623, R628, R630, F702
 Homma Y. F704*
 Homoki E. R645
 Homor F. T346
 Honda C. T206, T253, T301, T302, T339, W401, R637
 Honda R. T253*, T301, T302, W401
 Hong J. T346
 Hong P. T342
 Hong S. A. R603
 Honniball C. I. T206, T318, T339, W405, R611, R637
 Hood D. R502
 Hood D. H. R632
 Hood D. R. T252*, R623, R631
 Hood L. L. T316, T338
 Hood N. T317
 Hooper D. T339, R606
 Hoover R. H. R623, R628, F702
 Hopkins R. R645

Hopkins R. H. F703*
 Hopkins R. J. T325
 Hopkins R. T. R505*
 Hopp T. R618
 Hoppe P. R504*, R609, R644
 Horanyi M. T305, T317, T344, R607
 Horányi M. M153
 Horchler A. R635
 Horgan B. T330, W402, W451, R502, R552*, R556, R621, R622, R624, R627, R630, R632, R634, F702
 Horgan B. H. N. R554, R602, F701
 Horleston A. M152, T308, T309
 Horst S. T334
 Horst S. M. T313, T336, R645
 Hörst S. M. M105, T336, T342, R645
 Horvath D. G. R554*, R631
 Horz F. T255, R620
 Hoshino T. T338
 Hosoda S. T253
 Hospodarsky G. W453
 Hough T. R631
 Houghton J. T256
 Houghton M. B. T336
 Hourani R. T343
 House C. W402, R552
 House C. H. T330
 Housen K. R. R555
 Hovik W. T343
 Howard K. T. M104
 Howarth G. H. M102
 Howe J. Y. T304, R504, R611
 Howell E. S. T203, T301, W401
 Howell K. C. R631
 Howell S. T254, T343
 Howell S. M. T325
 Howett C. J. A. M103*, M153, T305, T313, T339, T343, T344
 Howie R. M. R555
 Howington-Kraus E. T326
 Hoza K. M. T346
 HP3 Team M152
 Hrubiak R. F703
 Hsia C.-H. T344
 Hsiao S. R607
 Hsieh H. H. R615
 Hsu H.-W. T317
 Hsu W. M104
 Hu J. R611, R620
 Hu J. Y. W455*
 Hu X. R611
 Huang A. T337
 Huang F. R632
 Huang J. T206, T334, T342, F705
 Huang J. C. T344
 Huang R. I. R631
 Huang S. T328
 Huang T. R642
 Huang Y.-H. T316
 Hubbard K. M. T347
 Huber C. T254, T325, T333
 Huber M. S. T255*

- Hübbers H.-W. T346, R625
Hudson M. D. R622
Hudson R. W405
Hudson S. M. R633
Hudson T. M152, T309
Huertas A. T309
Hughes A. M. F705
Hughes C. G. R630
Hughes C. M. T330, R624, R625
Hughes E. B. T334
Hughes M. T320, T329
Hughes M. N. T330
Hughson K. R637
Hughson K. H. G. W454
Huidobro J. R604
Humayun M. M102, T255, T328, R618
Humm D. T343
Humm D. C. T343
Hunt A. C. R618
Hunter M. A. R638
Huo Z. T342
Hupe G. M. T303
Hurford T. T310, T344
Hurford T. A. T343
Hurley D. T318
Hurley D. H. T339
Hurley D. M. M151, T318, T338, W403*, R611
Hurowitz J. R624, R625
Hurowitz J. A. T341, R633
Hurst K. M152, T308, T309
Hurtado J. M. Jr. R645
Huss G. R. M104, T328, R504, R551, R606, R608, R644
Hussan A. M. R644
Hussmann H. T319, T325
Hutchinson I. T344, T346
Hutson M. L. T304
Hutzler A. T340
Huyskens M. H. R609, F704*
Hvidberg C. S. T341
Hviid S. R555
Hyde T. W. R606, R610
Hynek B. M. T306, W402, R632
Hyodo R. T251, R643
Hyodo R. H. R612
Ielpi A. W452
IGLUNA Team T348
Ignatiev A. T338
Ignatiev N. M154, T337
Iijima Y. T253
Iizuka T. F704, F705
Ikeda H. T253, T302
ILEWG Team T348
Imae N. T253, T302, R504, R616
Imai E. T347
Imamura S. T202*
Imamura T. T253
Imani J. T347
Immè J. R632
iMOST Team T341
Ingersoll A. P. F702
- Innanen A. T332, T334
Inoue H. T338
InSight Science Team M152, T307
InSight Team T308
IODP-ICDP Expedition 364 Science Party T320, F703
Ioppi I. T308
Ip W. H. R555
Ipatov S. I. R612
Iqbal W. T314, R637
Ireland T. R611
Ireland T. J. W455
Ireland T. R. T328
Irons K. T345
Irving A. J. T303, T328, R605, R616, R617
Irving J. M152, T308
Irving J. C. T204
Irwin R. P. III W452*, R621
Isaacson P. T338, R602
Isella A. F705*
Ishibashi K. T342
Ishida M. T302
Ishiguro M. T253, T302, R614
Ishihara Y. T206, T253, T302, T314, T316, T339, T347, R602, R637
Ishii H. A. W405, R607, R610
Ishikawa A. F704
Ishikawa H. R602
Ishikawa K. R631
Ishimaru R. R629
Ishimaru T. T342
Ishiyama K. I. R627
Islam T. R640
ISP Explorer Design Team T344
Ito M. T302, T328, T344, W406
Ito T. R614
Itoh S. F701
Itoh Y. T330, T331, W402, R502, R622
Ivanov A. R623
Ivanov B. A. T316, R621
Ivanov M. T337
Ivanov M. A. T338, R637
Ivanova M. A. R610
Iwamae A. T302
Iwamori H. M104
Iwata T. T253, T302, T342, T344, W401, R631
Iwata T. I. T341
Izawa M. R. M. T301, T328, R503*, R613
Izenberg N. R. T306, T312, R601
Izquierdo K. T310
Jabob A. T308
Jackson A. P. M101*, T314, R619
Jackson B. M154*
Jackson C. T338
Jackson I. T310
Jackson J. M. T337
Jackson R. S. T252, R624
Jacob A. T308, T309, T327
- Jacob S. R552
Jacob S. R. R552, R624
Jacob X. T341, T346
Jacobsen S. B. T251, T303, R505, R610, R619
Jacobsen S. D. M104
Jacobson R. T344
Jacobson S. A. R618
Jacquemoud S. T326
Jacquet E. R609
Jadhav M. R607
Jäger Z. R644
Jakosky B. M. T313
James D. R607
James D. H. R631
James P. B. T205*, T320, R628, F702
James R. D. T319
Jamison-Hooks T. L. T339
Jansen C. A. T303
Jansen-Sturgeon T. R555
Jao J. S. R555, R612
Jaret S. J. T255*, T320, R620
Jarmak S. T344
Jauman R. T332
Jaumann R. T202, T253, T302, T344, W401, R615, R621, R622, R623, R637, R638, R640
Jawin E. T203, T301, W401, R645
Jawin E. R. T203*, T301
Jellinek M. A. W452
Jenkins L. E. R620
Jennings D. E. M103
Jennings D. J. T305
Jenniskens P. T303
Jeong B. T339
Jeong M. R603
Jephcoat A. P. R503
Jerousek R. G. T322
Jessup K. T337
Jessup K. L. M154, R601
Jeute T. J. R634
Jhoti E. R611
Ji P. R638, R639
Jia L. C. T315, R634
Jia Y.-D. R615
Jia Y. Z. T315
Jiang T. R611
Jilly-Rehak C. E. T303, T304, R504, R607
Jin H. T339, R603
Jin Z. L. M104*
Jocteur-Moronzier F. T315
Jodhpurkar M. J. R601
Jöeleht A. T255
Johansson L. R620, F703
John K. K. T347
John T. R606, R644
Johnson B. C. M101, R553*, R621
Johnson C. M152, T307
Johnson C. L. T203, T205, T301, T307, T319, R601, R605

Johnson D. T343
Johnson J. T334
Johnson J. B. M151
Johnson J. M. T304
Johnson J. R. T329, T336, W402,
R552*, R624, R625, R634,
R644
Johnson N. R601
Johnson N. M. R614, R636
Johnson P. V. T323
Johnson S. W402
Johnson S. S. R624, R643
Johnson T. V. T322
Johnson W. T346
Johnsson A. T202, T332, R633
Johnstone S. E. R627
Jolliff B. T329, W405, R602
Jolliff B. L. M101, T206, T256, T314,
T329, W402, W403, R501*,
R551, R604, R605, R626
Jones A. T335
Jones B. M. T318, T319
Jones J. H. T328
Jones J.-P. T337
Jones J. S. M101
Jones M. W452
Jones M. J. T316
Jones R. H. R620
Jones S. M. R613
Jonniaux G. T343
Jorda L. R555
Jordan A. P. T317, T318
Jordan C. J. R630
Jordan J. T254
Jordan J. S. M155
Joseph E. T335
Joshi D. R636
Joshua M. T346
Josset J. L. T314
Jost B. T323
Joswiak D. J. R504, R607
Joudrier L. R640, R643
Jourdan F. T255
Journaux B. T344
Joy B. T328
Joy K. T316
Joy K. H. M101, T317, T319, R604,
R606, R644
Joy S. P. T307, T339
Jozwiak L. M. T206, T318, T338,
R612, R613, R639, F701*
Juda Benhur I. S. R602
Juhasz T. R645
Julien S. R618
Jull A. J. T. T328
Jun I. T330, T342
Jung D. T320
Jurewicz A. J. G. R608
Jusino M. T312
Jutzi M. T301
Ka H. T253
Kadlag Y. W455*
Kaevelars J. J. M153

Kagami S. R616
Kagitani M. T342
Kah L. T252
Kah L. C. W451, R622, R625
Kahanpää H. T313
Kahre M. A. T313, T341
Kaiden H. T302, R611
Kaiser R. I. W405
Kaku T. R631
Kaliwoda M. R617
Kaluna H. M. T318
Kameda S. T253, T301, T302, T341,
T342, W401
Kameda S. K. T253
Kamps O. M. T331, R502*
Kanamaru M. T253, T302, W401,
R555*
Kanda S. W401
Kane S. T312
Kanemaru R. R616
Kanine M. K. R627
Kanzaki T. T202
Kanzaki Y. T252
Kaplan H. H. T203, T301, W401*
Kappel D. T337, R615
Karachalios S. R640
Karageozian M. E. R616
Karakostas F. M152, T204, T308
Karani H. T325
Karatekin O. M152, T313
Kareta T. R555*
Kareta T. R. R503
Kargel J. S. W452, R629
Kargl G. M152
Karimi S. T307, R601
Karki B. B. R618
Karkoschka E. T326, T336, R637
Karlsson A. F703
Karner J. M. R644
Karnes P. L. T339, T343, R603
Karouji Y. T302, T347, R551
Karthi A. T316
Karunatillake S. T252, T346, R502,
R622, R623, R626, R627,
R631, R632
Kashyap V. T346
Kaskes P. T320
Kasper J. T317
Kato H. T341, T344
Kattenhorn S. A. T325, T327
Katz S. M. R634
Kaufman S. V. R502*, R633
Kaufmann D. E. M103, M153
Kaulich B. W406
Kaur J. T347
Kavelaars J. J. M103, M153, T305,
F705
Kavkova R. T320
Kavkova R. K. R619
Kawaguchi J. T344
Kawaguchi Y. T347
Kawai K. R629
Kawai Y. T344

Kawai Y. K. T317
Kawakatsu Y. T341
Kawamura T. M152, T204, T308,
T309, T314, T316
Kawasaki N. F701
Kay J. T335, R641
Kay J. P. T306, T325, R621
Kayama M. T347, R551
Kayastha R. T303
Kazemian M. W406
Keane J. T344
Keane J. T. M103, M153*, T305,
T335, F702, F705
Kebukawa Y. T344, T347, W406*,
W451
Kedar S. M152, T308, T309, T338,
T339, T344, R619
Keeney B. M103
Kegerreis J. T201
Kegerreis J. A. T312
Kehayias P. R609
Kehl F. R643
Kelderman E. T319
Kelland J. M154
Keller J. M151, T318, R602
Keller J. W. T315, W403, W405
Keller L. P. M104, W405, W455,
R504*, R608, R611, F703
Kellett B. T314
Kelley M. R. T316
Kelley S. T255
Kelley S. R639
Kelly M. S. R555
Kemper J. T308
Kempf S. D. R623, R628
Kenda B. M152, T308, T309
Kendall J. R605
Kendall J. D. M101, T316
Kenkmann T. T255, T320, R505,
R620
Kennedy B. M. T301
Kenny G. G. F703*
Kent J. J. R501
Kent R. M101
Kenyon M. T346
Kenyon S. J. T303
Kerber L. T334, T338, R630, F701*
Kereszturi A. R610
Kereszty Zs. R610, R644
Kerner H. R. T330
Kerscher J. R606
Kestay L. T344
Kestay L. P. R633
Keszthelyi L. T338, R554, R623
Keszthelyi L. P. T344
Ketcham R. A. R605, R639
Khan A. M102, T307, T308
Khan O. T309
Khatuntsev I. T337
Khawja S. W404*
Khuller A. R. T202*, T333
Khurana K. T344
Kiefer W. S. T201*, R602

- Kieft T. R642
 Kiely A. T309
 Kikuchi H. T253, T302, W401
 Kikuchi S. T253, T302
 Kilaru K. T346
 Kilcoyne A. L. D. W406
 Killen R. M. T318, R611
 Kilma R. R645
 Kim C.-H. R614
 Kim E. T339
 Kim G. T301
 Kim G. B. T342
 Kim H. T347
 Kim J. R603
 Kim K. T252
 Kim K.-H. T339
 Kim K. J. T347, R635
 Kim M.-J. R614
 Kim S. S. W405, R603
 Kim W. T309
 Kimura J. T253, T344
 Kimura M. T304, W455, R504
 Kimura Y. T336
 Kinczyk M. M103, T335
 Kinczyk M. J. M103, T204*, T305
 Kindle A. G. R639
 King A. J. M104, T303, T304, T340,
 W406, R503, R609
 King D. T347
 King D. T. T320
 King D. T. Jr. T255
 King D. T. Jr. T320, T334
 King O. T339
 King P. L. M102
 King P. L. R624, R632
 King S. M152
 King S. D. T308, R615
 Kingston C. R639
 Kinzler R. T335
 Kipp D. T309
 Kirby K. T344
 Kirchoff M. R. T317, R621, R623
 Kirk R. T318, T326, T336, R623
 Kirk R. L. T343
 Kirnbauer T. R632
 Kishiki K. T206
 Kissi-Ameyaw J. R645
 Kissick L. E. T332, R556*
 Kita N. T. W455, R504, R604, R617,
 F705*
 Kitazato K. T253, T302, W401
 Kite E. S. M154*, T312, R505, R627
 Kizovski T. V. T328
 Kjær K. H. T321
 Klar R. A. T339, T343
 Klein B. T312
 Kleine T. M104, T251, R610, R617,
 R618, F704*, F705
 Kleinhans M. G. R502
 Klemme S. T314, T319, R553, R606,
 R618
 Kletetschka G. T320, T321
 Kletetschka G. K. R619
 Klima R. T338, R645
 Klima R. L. T316, T338, T346
 Klimczak C. T201*, T327
 Kling A. T301
 Kling A. M. T303
 Kling C. L. T327, T334, R627
 Klingelhofer G. T344
 Klokočník J. T321
 Kloos J. L. M151*, T318
 Klug Boonstra S. T335, R645
 Klyne L. A. R640
 Kminek G. R643
 Knapmeyer M. M152, T253, T310
 Knapmeyer-Endrun B. M152, T308,
 T309
 Knappmann A. T315
 Kneissl T. R637
 Knicely J. J. T337
 Knierim V. T315
 Knight E. E. R619
 Knight K. I. T306
 Knightly J. P. T202*, R633
 Knoll A. H. W452
 Knollenberg J. M152, T253, T302,
 T309, R614
 Knudson C. A. T342, T347, R624,
 R632, R634, R636, R643
 Knuth A. A. R505
 Kobayashi K. T347, W406
 Kobayashi M. R629
 Kobayashi S. T253, T302
 Kobayashi T. T302
 Kobs S. T252
 Koch T. E. R606
 Kodikara G. R. L. R640
 Kodolányi J. R504
 Koeberl C. T252, T320, T321, T328,
 T341, R620, R634
 Koefoed P. T303, W455*, R605,
 F704
 Koefoed P. K. R616
 Koeman-Shields E. R608
 Koemle N. M152
 Koeppl A. H. D. R627
 Kohl I. F704
 Kohler E. M154*, T312
 Kohout T. T342, R611, R620
 Koike M. T341
 Kojima H. T253, T302
 Koker M. R613
 Kokorin A. F. R644
 Kolasinski J. R. T313
 Kolb V. M. W451
 Kolenkina M. M. M101, T316
 Kollman P. T305
 Komatsu G. T253, T302, T334,
 W452, R629, F703
 Komatsu M. T253, T302, T304
 Komjathy A. T337
 Kommedal E. R635
 Koncz A. T253
 Kono Y. T205
 Kononkova N. N. R620
 Konopkova Z. F703
 Kopp E. M152, T309
 Kopp M. M152, T309
 Kopysov A. S. R644
 Korablev O. M154, T337, R643
 Kornienko Yu. V. R603
 Korotev R. A. R617
 Korotev R. L. R501, R551, R605
 Korth H. R645
 Korthouwer R. B. T348
 Korycansky D. G. T314, T326
 Koschny D. T314
 Kossacki K. J. R614
 Kostelecký J. T321
 Kostiuk T. T313
 Kothandhapani A. T338, T347
 Kotlarz J. P. R642
 Kouyama T. T253, T301, T302,
 T341, W401
 Kouyama T. K. T253
 Kováčik A. T328
 Kovács B. T303
 Kovaleva E. T255
 Kovarik N. A. R643
 Kozyrev A. S. T330
 Kraal E. R. T333
 Kracher A. M104
 Krainak M. T339, T346
 Kral T. A. M155
 Kramer A. M152
 Kramer E. M153, R555, R614
 Kramer G. Y. T316
 Krämer Ruggiu L. R634, R644
 Krasilnikov S. S. T338
 Kraus R. G. R505, R619
 Krause C. M152, T253, T307, T309
 Krawczynski M. J. T251
 Kremer C. H. T256*, T331, R622
 Kremic T. T337
 Kreslavsky M. T202, R602
 Kreslavsky M. A. M101, T205*,
 T316, R601
 Krestianinov E. R609, R616
 Kretke K. R645
 Kreyche S. M154
 Kring D. A. T206, T255, T320, T339,
 R551, R604, R637, F701,
 F703
 Krishnamoorthy S. T337
 Krishnaprasad C. T313
 Kroemer O. M152
 Krohn K. T253, T317, R621, R637
 Kroll H. T319
 Kronyak R. E. R622
 Krot A. N. T303, T304, W455*,
 R610, R612
 Krugov M. R614
 Kruijjer T. S. M104, F704
 Kruijver A. T348
 Kruzelecky R. V. R643
 Krysher C. H. R501
 Krýza O. R629
 Ku Y. T303

Kuan Y.-J. R615
 Kubanek K. R633
 Kubiak K. R642
 Kubitza S. T346, R625
 Kuehl E. C. T328
 Kuehner S. M. T303, T328, R605, R617
 Kueppers M. T317, T342
 Kuhn O. R555
 Kuhn de Chizelle J. R605
 Kühne P. W455
 Kührt E. T253, T302
 Kuik J. R633
 Kuik J. C. R643
 Kuiper Y. D. W404
 Kukita A. T336
 Kukko A. R628
 Kulchitsky A. V. M151*
 Kum R. R633
 Kumagai K. T302
 Kumamoto A. T344, R631
 Kumamoto A. K. R627
 Kumar C. R622
 Kumar P. M155
 Kumar S. R603
 Kumler B. M102
 Kupper R. J. R634
 Kuramoto K. T341
 Kurihara S. T316
 Kurokawa H. T302
 Kurosawa K. R643, F703*
 Kurtovic N. T. F705
 Kushiki K. T339
 Kutsop N. T343
 Kutsop N. W. M154*
 Kuzmin R. R623, R643
 Labenne L. T303, R605
 Laczniak Dara R626
 Laczniak D. L. M102, W405*, R611
 La Fontaine A. R610
 Lafuente B. T341
 Lagain A. R630, R631
 Lagos M. R606
 Lai V. T337
 Lainey V. T344
 Lalich D. E. M105*
 Lalla E. T346
 Lamadrid H. W451
 Lamb M. T329, T330, W452
 Lambert J. T344
 Lambert P. T255*
 Lamm S. N. W402, R624
 Lanaras C. R603
 Lanbert J. T344
 Lanc P. T328
 Landgraf M. T347
 Landis G. A. T344
 Landis M. E. T318, T346, W454, R615
 Lane M. D. R622, R635
 Laneville M. R602
 Langelaan J. W. T336
 Langendam A. D. T303

Langenhorst F. T255
 Langenkamp T. R. T333
 Langevin Y. T343
 Langlais B. T307
 Langlois V. J. R619
 Lanjewar K. T347
 Lantz C. T253, R634
 Lanza N. T252, T345, R624, R644
 Lanza N. L. W402*
 Lanzirotti A. R606, R613, R626, R633
 Lapen T. J. T328, R553, R617
 Lapotre M. G. A. W452*
 Lappin L. J. R645
 Lark L. T333, T338
 Larmat C. T308
 Larmat C. S. R619
 La Rocca P. R632
 Lars E. R626
 Larsen C. F. R628
 Larsen N. K. T321
 Laserna J. J. R626
 Lasue J. T252, T341, T346, R624, R625, R634, R636, R644
 Latendresse V. R643
 Lau H. C. P. R602
 Lauer T. A. M103
 Lauer T. R. M103, M153, T305, T335
 Laufer R. R606
 Laura J. R638
 Laura J. R. R641
 Lauretta D. S. T203*, T301, T336, T340, W401, R555, R611, R645
 Lauro S. E. F702
 Law E. S. R639, R641
 Lawrence D. J. M151, T336, T342
 Lawrence K. R605
 Lawrence S. R554, R602, R638
 Lawrence S. J. T338, F701
 Lazio J. T344
 Lazzaro D. R555
 Leask E. R502
 Leask E. K. T252*
 LeBlanc G. L. T311
 Lebreton J. P. T255
 Lechowicz A. R633
 Le Corre L. T203, T301, T302, W454, R503, R620
 LeCorre L. L. T253
 LeDeit L. T252
 Le Deit L. R625
 Lee B.-C. R614
 Lee D. T339
 Lee H. T339
 Lee H.-J. R614
 Lee J. R601
 Lee J. I. R604
 Lee J.-K. T339
 Lee K. J. R642
 Lee L. R606
 Lee M. T339

Lee M. J. R604
 Lee M. R. M102, M104, T255, T304, T313, T320, T328, W406, W451, R642
 Lee P. T347, R635
 Lee S. T339
 Lee S.-M. R614
 Lee T. J. R642
 Lee Y. T313
 Lee Y.-N. R609
 Lee YN. T251
 Lee Y. S. R635
 Lefevre F. M154
 Leftwich K. R626
 Le Gall A. M105, T334, T336
 Legett C. IV R611
 Lehnert K. A. R638, R639
 Lehto H. L. R631
 Lehtonen S. J. T346
 Lei P. T252
 Lei Z. R619
 Leight C. J. R631
 Leili M. H. R620
 Leitner J. R504*, R609
 Lejoly C. R503
 Lekic V. T308, T310
 Leland J. R. T347
 LeMaistre S. T309
 Lemelin M. T317, R602, R603, R604, R611
 Lemmon M. M152, T313, R624, R625
 Le Mouélic S. T313, T333, M154, R624, R625, R634, R637, R644
 LeMoulic S. W452, R627
 Lenardic A. T312
 Leng K. T308
 Leonard E. T344
 Leonard E. J. T254*, T327, R637
 Leonard G. J. W452
 Leonard J. T203, T301
 Leonard M. J. T347
 Leone G. R554, R632, R636
 Lepore K. R625
 Lerman H. T344
 Lerner A. R606
 Lessis M. R601
 Lethcoe H. T309, R640
 Lethcoe-Wilson H. M152, T309
 Leuschen C. J. T332
 Lev E. R631
 Leveille R. R632, R642
 Leveille R. J. R624
 Lever J. H. R504, R607
 Leverington D. W. R631
 Levine J. R606
 Levison H. R645
 Levy J. T202
 Levy J. S. M105, T332, R628
 Lewang A. M. R637
 Lewin C. R503
 Lewin E. R644

- Lewis E. K. T340
 Lewis J. A. R601, R616
 Lewis J. M. T. W451*, R624, R643
 Lewis K. T334, R601
 Lewis K. W. M152, T307, T342, R624, R627, F702
 Lewis R. D. R609
 Lewis S. M152, T333
 Lewis S. R. M152, T332
 L'Haridon J. T252, R552*, R624, R625
 Li B. T206, T315
 Li B. C. T344
 Li C. L. R602, R604
 Li D. T340, R626
 Li D. R626
 Li J. T340, R553
 Li J.-Y. M103, T301, R615
 Li J. Y. T301, R613
 Li Q. L. T303
 Li S. T318, W405*, F701
 Li S. J. R620
 Li X. W451
 Li X.-H. T303
 Li X. R626
 Li X. Y. R620
 Li Y. M104*, R553, R605, R620, R631
 Li Z. Y. R614
 Liang Y. T251
 Libardoni M. T318
 Libourel G. R610
 Licandro J. T301
 Lichtenheldt R. M152
 Lidawer A. H. R640
 Liddle D. A. R605, R639
 Liebel M. T342
 Liebske C. M102*
 Liermann H. P. F703
 Light S. L. R505
 Ligier N. T323
 LiKamWa R. R640
 Liller S. T343
 Lillis R. J. T313, W404
 Lim D. R635
 Lim G. T309
 Lim L. F. T203, T301, R613
 Lim T. L. R640
 Lima E. A. R609
 Limaye S. T337, R601
 Lin H. R502, R628
 Lin Y. T303
 Lin Yangting R606
 Lin Z.-Y. R614
 Lindberg G. E. M105, T326
 Linden J. J. T312
 Lindensmith C. A. R642
 Linder T. R555
 Lindgren P. T255, R620, F703
 Lindner M. R606
 Lindsay S. T346
 Lindsay S. S. R555
 Lindsley D. R620
 Lindsley D. H. R632
 Ling Z. R602, R604, R605
 Ling Z. C. T206*, T315, R604, R626, R634
 Linscott I. E. M103
 Linscott I. R. M103, T305
 Lisov D. T330
 Lisse C. T305
 Lisse C. M. M103, M153*, T305, T312, T344, R555
 Litvak M. L. T318, T330, R628
 Liu C. Q. T206, R626, R634
 Liu J. F705
 Liu J. J. R602
 Liu J. Z. M101, T206, T316
 Liu M.-C. W455, F705*
 Liu M.-C. L. R606
 Liu N. T304, R504*, R607
 Liu S. R620
 Liu T. T206, T338, R501
 Liu X. R601, R633
 Liu Y. T303, T316, T341, W403, R502, R556*, R603, R605, R611, R622, R632, F703*
 Liukis M. R638
 Livengood T. A. T313, T339
 Llorca-Cejudo R. T308
 Lo D. T313
 Lo M. R631
 Lobanov S. F703
 Lock S. J. T251*, R505, R619
 Ladders K. T303
 Loeffler M. J. T319, W405
 Loesch G. R610
 Loew S. R603
 Löffler M. T348
 Lofi J. T255
 Loftus C. L. R617
 Lognonne O. T309
 Lognonné P. M152*, T204, T307, T308, T309, T327
 Lohf H. T315
 Loiselle L. T328
 Loizeau D. R622, R634, R643
 Lomakin I. T337
 Long C. J. R621
 Longhitano F. R632
 Longstaffe F. J. T255, T320, R617
 Looche M. R604
 Looper M. D. T317, T318
 Lopes R. R631
 Lopes R. M. C. M105, R621
 López-Oquendo A. J. R621
 Lopez-Reyes G. T346, R643
 Lo Presti D. R632
 Lora J. M154
 Lora J. M. M105, T336
 Lorand J.-P. T328
 Lorand J. P. T255
 Lorenston C. C. T336
 Lorenz C. A. R612, R620
 Lorenz R. M105, M152, T308, T309, T334
 Lorenz R. D. M105, T309, T336, W453*, R633
 Lorenzo J. M. T346
 Lorenzoni L. R643
 Losiak A. T255*
 Łosiak A. R616
 Loutzenhiser P. D. T318
 Love A. B. T328
 Love S. G. R606
 Love S. P. T345
 Lowell R. P. T254
 Lowes L. T344
 Lowes L. L. R645
 LRO Science Team M151
 LRO Team R602
 Lu D. T346
 Lu T. T327
 Luais B. T255
 Lucas A. M152, T308, T309, T326, T327
 Lucas J. L. R606
 Lucas M. P. T304
 Lucchetti A. T316, R621, R623
 Lucey P. T317, T339, W405
 Lucey P. G. M151, T318, T338, W403, W405, R602, R611, R621
 Luchetti A. R623
 Luchsinger K. M. M151*
 Luckey M. K. T335
 Luginin M. M154
 Luhmann J. G. T307
 Luna D. T347
 Lundeen S. T343
 Lunine J. M154, T334, W453
 Lunine J. I. T323, T336, T343
 Lunning L. G. W454
 Lunning N. G. M104*, R604, R620, F703
 Lunsford A. T301
 Lunsford A. W. M103, T305
 Luo H. R618
 Luo V. X. R640
 Luo W. W452
 Luongo O. T308
 Luu N. C. R626
 Luu T.-H. F705
 Lynch K. L. R645
 Lyons J. R. T313, R609
 Lyons R. J. R553, R618
 Lyra W. F705
 Ma C. W455, R605, R608, R620
 Ma P. R611
 Ma Y. T307
 Ma Y. J. R601
 MaArthur H. S. T325
 Maas B. J. T346
 MacArthur J. T320
 MacArthur J. L. T328
 Mac Clean J. T308
 Mackelprang R. R642
 MacKenzie S. T334
 MacKenzie S. M. M105*, T336

MacPherson G. J. W455*, R610,
F703
Madariaga J. M. R604, R626
Maden C. R608, R618
Maeda T. T206, T314, T339
Maekawa Y. T202
Maghareh A. R603, R635
Magri C. T301
Maguire R. T310
Mahaffy P. R636, R643
Mahaffy P. H. W402
Mahaffy P. R. T313, T330, R624,
R643
Mahanti P. T314, T317, T318, T347
Mahieux A. T325
Mahmood Q. R638
Mainsant G. M152
Mainzer A. R555*, R614
Mainzer A. K. R555, R614
Makarewicz H. D. R640
Makarewicz J. S. R640
Maki J. M152, T308, T309
Makowski J. M. T336
Malakhov A. T330
Malakhov A. V. R628
Malapert J-C. T315
Malaret E. R622, R639
Malaska M. T334
Malaska M. J. M105*, R621
Malenkov M. I. T338
Malespin C. R636, R643
Malespin C. A. T330, T338, T339,
R643
Mall U. T314, T347, R603
Malliband C. C. T205*, R637
Mallozzi S. R632
Mance D. M152, T308
Manconi A. R603
Mandell A. M. R611
Mandt K. T338, T343, W453
Mandt K. E. M151, T312, T317,
T318, T344, R611, R645
Manga M. T204, T254, T310
Manga V. R. R606
Mangeney A. T202, T308
Mangold N. T202, T252, T333,
R502, R552, R623, R624,
R625, R634, R644
Mann P. J. T318
Manrique-Martinez J. A. R643
Mansell C. R626
Manske L. T314, T319, R505*
Mao X. W454*
Mapel J. A. R641
Marchese K. R503
Marchi S. T317, T342, W454, R505,
R619
Marchis F. T345
Marcq E. M154, T337, R601
Marcum S. M154, T312
Marcus M. A. W406
Margerin L. M152, T204
Margolin L. G. R619

Margot J. L. T301, R612
Marhas K. K. R607
Marinangeli L. R623
Marini A. T314
Mark D. F. T255, T313, R604
Markey K. R638, R639
Markkanen J. R611
Marks N. E. R501
Marnocha C. L. M155
Maroger I. R644
Marouf E. A. T322
Marquardt M. R616
Marques M. J. R619
Marquez R. T. C. R606
Marriner C. R623
Marrocchi Y. M104
Marsaglia K. M. W452
Marschall R. R555
Marsh L. A. R644
Marshall J. T203
Marshall S. E. R555, R612
Martel L. T339
Martell J. R620
Martikainen J. R611
Martin A. C. M101, T330, R555*,
R603
Martin D. T341
Martin D. J. P. T319, T340, T347
Martin E. S. T204*, T327
Martin P. R627
Martin P. E. W402*, R633
Martinez G. T313
Martinez J. T347
Martinez M. R. T317, T347
Martinez S. N. T206, T339, R637
Martinez Sierra L. M. T330
Martín-Torres J. T330
Martire L. T337
Martufi R. F702
Marty B. T341
Martynov A. T337
Maru Y. T336
Marusiak A. G. T310
Marzarico E. T203
Marzen L. J. T334
Masai H. R611
Masaitis V. T255
Masdea A. F702
Masiero J. R555, R614
Mason J. D. T339, T343
Mason L. W. R614
Massé M. R622, R625
Massey R. T201, T312
Massironi M. R623, R637
Masters A. W453
Mastrodemos N. T301
Mastroguseppe M. M105, T326,
R628
Matéo-Vélez J.-C. R635
Materese C. K. R642
Matherne C. M. R627
Mathies R. A. R621
Matiella Novak M. A. T316

Matney M. J. T335
Matsika P. R633
Matsui T. R629, F703
Matsui Y. R619
Matsumoto J. T344
Matsumoto K. T253, T302
Matsumoto T. W405*
Matsunaga T. T253, T302
Matsuoka A. T344
Matsuoka M. T253, T301, T302,
W401
Matsuoka M. M. T253, T341
Matsushita M. T344
Matsuura S. T253, T302, T344
Matsuyama I. T204, T325, T344,
R612
Mattei E. F702
Matthews L. S. R606, R610
Mattingly R. L. T341
Mattmann C. R640
Matulka P. R. M105*
Maturilli A. T253, T302, T319, T331,
T337, T346, R613, R614,
R635, R637
Maturilli A. R620
Matusmoto K. T253
Matz K-D. T253
Matz K.-D. T253
Matz K. D. T253
Mauda S. T347
Maue A. D. M105, T326
Maupin R. R607
Maurel C. R553*
Maurice S. T252, T328, T341, T345,
T346, R552, R624, R625,
R634, R644
Mauro M. R606
Maxwell R. E. T316
May B. A. R617, R619
Mayer D. P. R640, R641
Maynard K. T343
Maynard-Casely H. E. M105
Mayne R. G. R618
Mayyasi M. T318
Mazarico E. T203, T205, T301,
T327, T336, T342, R603,
R612, R638
Mazzini A. R629
McAdam A. R552, R643
McAdam A. C. T252, T330, T342,
W402, W451, R624, R632,
R636, R643
McArthur G. R623
McBride K. T340
McBride M. J. R602, F701*
McCafferty N. S. T318
McCanta M. R601, R606
McCanta M. C. T321, R601, R631,
F703*
McCardle B. R637
McCardle B. C. T333
McCarthy C. M155, T344
McCausland P. J. A. T320

- McClanahan T. M151
 McClanahan T. P. W403, R603
 McClannahan T. T318
 McClean J. M152, T308
 McClean J. B. M152, T308
 McClean J. M. T308
 McCollom T. M. W402*
 McComas D. J. T305
 McCord T. B. T322, T343
 McCoy T. J. M104, T203, T301,
 T342, W401, W453, R617,
 R618, F704
 McCubbin F. T328, T340
 McCubbin F. M. T205, T301, T319,
 T340, T347, W403*, R501,
 R601, R616, R617, F701
 McDonald A. M. T320
 McDonald C. S. T314, R619
 McDonough W. F. R618
 McDougall D. T334
 McDougall D. S. T334
 McElwaine J. T316
 McElwaine J. N. T202
 McEwen A. S. T202*, T252, T316,
 T343, T344, R621, R623,
 R645
 McFadden J. A. W405*
 McFadzean S. T328
 McFarland E. L. T346
 McFarlane C. R. M. T255, T328,
 R620
 McGary R. S. R601
 McGill G. E. R637
 McGlasson R. R612
 McGlaun M. L. T319
 McGovern P. J. R554*, R601
 McGowan E. M. R637
 McGrath T. T347
 McGraw A. R503
 McGregor M. T255*, T320, R620
 McGuiggan P. M105
 McHenry L. J. R632, R640
 McHugh M. T344
 McIntosh E. C. T316, F701*
 McKay C. P. M155, T336, T345,
 W402
 McKeeby B. E. R631
 McKeegan K. D. W453*, R551,
 R605, R606
 McKeegan K. M. R606
 McKenzie W. T339
 McKeown L. E. T202*, T332
 McKibbin S. J. R606, R618
 McKinley I. M. T343
 McKinnon W. B. M103*, M153,
 T201, T305, T306, W454,
 F705
 McKinnon W. B. T335
 McLain H. L. W451, R606
 McLain J. L. W405*
 McLaughlin S. A. R602
 McLennan S. M152
 McLennan S. M. T307, T330, W453
- McLeod C. R604
 McLeod C. L. R605
 McMahan J. W. T203, T253, T301
 McMahan W. J. R633
 McMannamon P. T314
 McMullan S. T309
 McNutt R. T344
 McNutt R. L. Jr. T305
 McQuaig D. R. R616
 McSween H. Y. M102, T304, T341,
 W453, W454*
 Mederos Leber D. R606
 Medina-Garcia J. R643
 Meech K. J. R555
 Meen J. K. T317, T347
 Mège D. T326, T327, T333, R630,
 R631
 Mehoke D. S. M153
 Mehta J. T338, T347
 Meka J. K. T302
 Melchiorri R. M155
 Mellon M. T. R628
 Melosh H. J. M101, T312, R505,
 R603, R621, R631, R635
 Melwani Daswani M. T201, T344
 Méndez A. M155*, T312
 Mendillo M. T318
 Mendybaev R. A. M104, T318, R610
 Meng T. M. R628
 Mengel K. W454
 Ménina S. T308
 Menzies A. R640
 Mercer C. M. T314, R619, R639
 Merges D. R606
 Merlo A. R643
 Mertzman S. R633
 Meshel M. R503
 Meshik A. T317
 Mesick K. E. T344, R628
 Meslin P.-Y. T252, T346, T313,
 T341, W402, R552, R624,
 R625, R634, R644
 Messenger S. T301, T336, R607
 Messina A. R632
 Mest S. C. R637
 Metcalfe L. R640
 Metzler K. M104
 Meunier A. T255
 Meyer B. R609, F705
 Meyer C. R620
 Meyer H. A. T252
 Meyer H. M. T315, T316
 Meyer M. A. T341, R642
 Michael G. T206, T332, R623
 Michael G. G. T202, T315, T317,
 T319, T338, R623
 Michaelis H. T253
 Michaels T. T202
 Michalik T. R613
 Michalski J. R. R601
 Michaut C. M152, T308, R505
 Michel P. T203, T253, T301, T302,
 T342, W401
- Michikami T. T253, T302, W401,
 R631
 Mickol R. L. M155
 Miconi C. E. T347
 Mihailova B. F703
 Mihara T. T344
 Mika J. R645
 Mike R. T317
 Mikesell T. D. T346
 Mikhail S. T312
 Mikhaylov V. R643
 Miklusicak N. B. R622
 Mikouchi T. M104, T304, R501*,
 R616, R620
 Milam K. A. R620
 Milam S. T336
 Milazzo M. R641
 Milewski D. R555
 Miljković K. M152*, T308, T309,
 F703
 Milkovich S. M. R628
 Millan M. W451, R636, R643
 Miller D. M. W404
 Miller J. L. R628
 Miller K. E. T201*
 Miller M. T347, R620
 Miller M. A. T339, T343
 Miller M. J. T347
 Miller M. L. R501
 Miller N. R. T304
 Miller R. S. M151, T336
 Milliken R. T253, T302
 Milliken R. E. M104, T253, T302,
 T330, T339, W402, R503,
 R602, R611
 Millot C. T202
 Millour E. M152, T308, T309, F702
 Mills A. C. T306
 Mills F. P. M154*, R601
 Mills M. T310
 Mimasu Y. T253
 Mimoun D. M152, T308, T337,
 T341, T346
 Minakami E. T347
 Mineur M. T. T342
 Ming D. T304
 Ming D. W. T252, T313, T330,
 W402, W453, R552, R624,
 R636
 Mini-RF Team T316, T318, R631
 Minitti M. T330, T334
 Minton D. R630
 Minton D. A. T316, T317
 Misawa K. T302, T328, R611
 Mischna M. M155, T330, R628
 Mischna M. A. M154, T341
 MISE Team T343
 Misra A. K. T339, T345, T346
 Missbach H. W451
 Mita H. T253, T347
 Mitchell C. D. T320
 Mitchell J. M154
 Mitchell J. L. T336

Mitchell J. T. T303
Mitchell K. L. T344, R631, R645
Mitchell N. W452
Mitra K. W402*
Mitri G. F702
Mitrofanov I. G. T318, T330, R628
Mittelholz A. T307
Mittlefehldt D. W. T329, W402*,
R616
Miura A. T253, T302
Miura J. K. R622
Miura Y. N. T302, T341
Mivumbi O. R625
Miyahara M. T328
Miyake A. W405, R611
Miyake N. R629
Miyake W. R631
Miyamoto H. T202, T253, T301,
T302, T341, W401, R614,
R629, R640
Mizuno T. T253, T302
Mocquet A. M152
Modiriasari A. R603, R635
Moersch J. E. M102, T330, R627
Mogi K. T253
Mohr D. R621
Mohrig D. W452
Moitra P. R554, R631
Mojzsis S. J. M155, R621
Mokashi P. R603
Molag K. T342
Molaro J. L. T203*, T301, W401,
R645
Molesky M. J. R617, R619
Molina A. M152
Molnár M. T321
Molyneaux P. M. T343
Molyneux P. M. T339
Momary T. W. T313
MOMA Science Team W451
Mondaini C. T308
Mondro C. A. R627
Monnin L. R635
Monteiro Santos F. A. R632
Montes R. R620
Montesi L. T310
Montesi L. G. J. T306, T325, R631
Monteux J. R618
Montmessin F. M154*
Moody S. R610
Moon H.-K. R614
Moon Diver Team F701
Moon Station Operation
Team T335
Moore C. A. M155*
Moore C. B. T255
Moore E. M. R633
Moore J. T305
Moore J. M. M103*, M153, T305,
T306, T335, R555, F705
Moore L. T318
Moore L. B. T343
Moore T. Z. T339, T343

Moore W. B. R601
Moore J. E. M151, M154, M155,
T311, T313, T318, T332,
T334
Moral A. T346
Mora Sotamayor L. M152
Moreau J. R620
Moreau M. T203, T301
Morgan A. T334, W452
Morgan A. M. W452*, R627
Morgan C. R. R554, R631
Morgan G. R602
Morgan G. A. T341, R628, R631,
F702*
Morgan G. H. R639
Morgan J. T255
Morgan J. A. T347
Morgan J. V. R619
Morgan P. M152, T309
Morgan T. H. T318
Mori O. T253, T344
Moriarty D. T206, R605
Moriarty D. P. T316
Moriarty D. P. III M101*
Moriconi M. L. T323
Morida K. T333
Morishita Y. R604
Moritz D. T348
Moriwaki R. F703
Morland Z. S. T317, R636
Morlok A. T319
Moroi K. T302
Morota T. T253*, T301, T302,
W401
Morota T. M. T253
Morris R. R620
Morris R. V. M102, T252, T330,
T331, W402, W405, W453,
R552*, R624, R626, R636
Morrison A. A. R631
Morrison S. J. T322
Morrison S. M. T252, T330, R552
Morse A. T347
Morse Z. T316, T347, R645
Morse Z. R. T347
Mosenfelder J. L. R551*
Moser D. E. T328, R605
Mosie A. B. R501
Moskovitz N. A. R613
Mosselmans J. F. W. R609
Motaghian S. T346
Matora T. T253
Mottola S. T253, R614
Mouginis-Mark P. J. R621, R627,
R630
Moulet A. R615
Mouroulis P. T343
Mouser M. D. T205*, R551
Mousis C. T344
Moussi A. T253
MoussiSoffys A. T302
Moussi-Soffys A. T253
Moyano-Camero C. E. R642

Moynier F. T251, R618, F705
Mozin V. V. T342
MSL Science Team R624
Muccino M. T308
Mueller B. R639
Mueller K. T347
Mueller N. M152, T337
Mueller N. T. T309
Mueller T. T253
Muench G. R638
Mugnuolo R. T308
Muinonen K. T314, R611
Mulcahey J. R620
Mulder S. J. T342
Muller J.-P. R623
Müller N. T253, T302
Mullin E. R. R628
Mumma M. T336
Munch F. T308
Mundy L. T321
Munoz C. R554
Muñoz-Iglesias V. T311
Munsat T. R635
Mura A. T323, R631
Murakami D. T344
Muralidharan K. R606
Murchie S. T336
Murchie S. L. T331, T343, T346,
R622
Murdoch N. M152, T308, T309,
T341, T346
Murphy I. R621
Murphy J. R. T313, T323
Murukesan G. W451
Mushkin A. T327
Musilova M. R632
Musiol S. R623
Mustard J. F. T256, T313, T331,
T339, R502, R503, R622,
R627, R628, R633
Muszyński A. R631
Myers D. T335
Myhill R. M152, T308, T309
Nachon M. T252, R642, R643, R644
Nadeau J. L. R642
Naegeli K. M. R631
Nagai Y. F705
Nagao K. R604, R616
Nagaoka H. T347, R551*
Nagashima K. M104, T304, T328,
W455, R504, R551, R606,
R610, R644
Nagihara S. M152, T323, T338,
T339, T343, R602
Nagle-Mcnaughton T. R627
Nagori R. R603, R631
Nagy A. F. R601
Nagy D. T303
Nahihara S. T309
Naidu S. P. R555, R612
Nair A. M. T317, R631
Nair H. T203
Nair S. T347

- Naito K. R607
 Nakagawa H. N. T341
 Nakamura A. M. R503
 Nakamura M. T333
 Nakamura R. T344
 Nakamura T. T253*, T302, T336, T341, W401, R504
 Nakamura Y. R602
 Nakamura-Messenger K. T336, T340
 Nakanishi N. M104*
 Nakano Y. T302
 Nakao T. T336
 Nakashima D. R504
 Nakato A. T253, T302
 Nakauchi Y. T206, T253, T302, T339, R503
 Nakazawa S. T253, T302
 Nakley L. M. R601
 Nallapu R. T. R503
 Namiki N. T253*, T302, W401
 Namur O. T319
 Nanne J. A. M. F704
 Naor R. T327, T347
 Naraoka H. T303
 Narita S. T347
 Nass A. R637, R638
 Naß A. R638, R641
 Nasu S. T302
 Nathan E. T325, T332, T338
 Nathues A. T314, W454*, R615
 Navarro S. M152
 Navarro T. T313
 Navarro-Gonzalez R. W402, R624, R636, R643
 Navea L. R636
 Neal C. R. M102, T314, T320, T338, R551, R604, R605, F701
 Nebut T. M152, T308
 Necsoiu M. T339, R606
 Needham D. H. F701*
 Needham D. M. T338
 Neese C. R639
 Neeseman A. R627
 Neesemann A. R615
 Nehrke G. T321
 Neidhart T. M152
 Neish C. D. T316, T318, T334, T336, T346, R554, R603, R639
 Nekvasil H. M102*, R620, R632
 Nellessen M. A. T252*, R624
 Nelson A. T345
 Nelson D. M. R638, R641
 Nelson R. M. R612
 Nelson W. S. R604
 Nemchin A. A. T251, R551, F703
 Nenna C. F702
 NEOCam Team R614
 NEOWISE Team R555
 Nepal S. M155
 Nerozzi S. R630, F702*
 Nesnas I. T338
 Neu D. R623
 Neumann G. A. T203, T301, T315, T318, R602, R603
 Neumann W. T253, T302, R613
 Nevenzal H. T347
 Neveu M. W454
 Nevill N. D. R607, R610
 Neville T. T343
 New J. R619
 New J. S. R621
 Newell R. T345
 New Horizons Composition Team M153, T305, R641
 New Horizons Geology and Geophysics Team M103, M153, T305
 New Horizons GGI Team M103, M153, T305
 New Horizons LORRI Team M103, T305
 New Horizons Occultation Team M103
 New Horizons PATM Team T305
 New Horizons Ralph Team M103
 New Horizons Ralph Team and LORRI Team M103
 New Horizons Science Team M103, T305, T335
 New Horizons Team M103, M153, T305
 Newland E. L. T309
 Newman C. M152, T308, T309, T313
 Newman C. E. M152*, T256, T313, T336
 Newman J. T320, R645
 Newsom H. T328, T330, R505, R624, R644
 Newsom H. E. T252, T313, T347, W452, R624, R625, R627
 Newson T. R636
 Neville M. R606, R613
 Nez G. R645
 Ng W. T344
 Ngo P. T323, T339
 Nguyen A. T336
 Nguyen G. T347
 Nguyen J. T306
 Nguyen L. T203
 Nguyen P. Q. T316
 Nguyen T. G. M151, T313, T332, T334
 NH Geology, Geophysics, and Imaging Team M103, T305
 NH Geology, Geophysics, Imaging Science Theme Team T335
 Ni P. R553*, R605
 Niazi H. K. R503
 Nichols K. D. R503*
 Nichols-Fleming F. R621
 Nicholson P. D. M154, T322
 Nickerson R. D. R634
 Nicklin R. I. T328
 Nicolau-Kuklińska A. R616
 Nie N. X. T251*
 Nie X. T318
 Nielsen S. G. T251*
 Niesch C. D. W405
 Niihara T. T328, R614
 Nikiforov S. T330
 Niles P. B. T304, T328, T330, R556, R640
 Nimmo F. M103, M152, T201, T251, T305, T308, T310, T325, T343, T344, R554, R612, R618, F704
 Nishi M. T347
 Nishibori T. R631
 Nishiizumi K. R501*, R608
 Nishikawa N. T253
 Nishimura M. T302
 Nishizawa M. R619
 Nissen-Meyer T. T308
 Nittler L. T346
 Nittler L. R. T319, W453, R504, R607
 Nixon C. R615, R632
 Nna Mvondo D. T326
 Noble S. K. W403
 Nock K. T. T337
 Noda H. T253, T302
 Noda N. R624
 Noe Dobrea E. Z. R622, R627, R643
 Noguchi R. T302, W401
 Noguchi R. N. R627
 Noguchi T. T347, W401, R504*, R611
 Nolan M. T203, T301
 Nomura R. T344
 Noonan J. W. R503*
 Norcross J. T347
 Nordheim T. A. T323
 Northrup P. R607
 Noschese R. T323, F702
 Noss D. R641
 Novak A. M. R554
 Noviello J. R645
 Noviello J. L. T254*, T324
 Nowak A. R. T326
 Nowicki K. T339, T342, T343
 Nowicki S. T330
 Nowinski M. C. R613
 Noyes M. T347
 Nuding D. L. T252*
 Nuevo M. R642
 Núñez J. I. T336, T338, T346
 Nunez K. A. T324
 Nunn C. T339
 Nuno R. T315
 Nuno R. G. R621
 Nuth J. A. III R614, R636
 Nuth J. A. R606
 Nyeste E. T303
 Nyguen A. T328
 Nypaver C. T316, W405*, R639
 Nyquist L. E. T252, R604, R605

Oberg D. T336
 Oberg K. I. F705
 Oberst J. T319, T325
 Oberst O. T206
 O'Brien A. C. W451*, R645
 O'Brien H. C. T320, R604
 O'Brien P. W405*
 Ocampo A. M103, T337
 O'Connell-Cooper C. T313, T328,
 T330, R552, R624
 Oehler D. Z. T341, R629
 Oehlke M. W451
 Oey J. R612
 Ogawa K. T253, T302, W401, R614
 Ogawa N. T253, T302
 Ogawa Y. T253, T302, T347
 Oglione R. C. T303, T304, T342,
 W405, R607, R608
 Ogura T. T333
 Oh D. O. T311
 O'Hara S. T325
 Ohashi N. R504
 Ohigashi T. T302, W406
 Ohiri K. T345
 Ohja L. T309
 Ohkawa S. R551
 Ohno T. R631
 Ohtake M. T206*, T253, T302,
 T338, T339, T347, R637,
 R639
 Ohtaki K. K. W405*, R607, R610
 Ohtani E. T328
 Ohtsuka K. R614
 Oij S. J. R644
 Ojha L. T252, T307, T334, R601,
 R631, F702*
 Okabayashi S. M104
 Okada T. T253*, T302, T342, T344
 Okamoto C. T302
 Okamoto T. T342, F703
 Okazaki R. T302
 Okazaki S. T336
 Oklay N. R555
 Okubo C. R623, R638
 Okudaira K. T347
 Okudaira O. T342
 Oleson S. R. T344
 Olgin J. G. O. R645
 Olinger C. R608
 Oliveira J. S. T316
 Olkin C. B. M103, M153, T305,
 T306, T335, W453, R607,
 R641, R645, F705
 Ollila A. T252, T345, R624
 Ollila A. M. W402, R624
 Olmos H. R636
 Olsen K. M154
 Olsen N. T315
 Olson P. L. R553
 Olsson-Francis K. R556, R636
 Omura T. R503*
 Onaka T. R555
 Ono G. T253

Ono H. R616
 Ono M. R640
 Onodera K. T314, T316
 Onstott T. C. R642
 Oommen T. R622
 Ootsubo T. R555
 O'Reilly S. S. R643
 Orgel C. T319, R622, R627
 Ori G. G. R627, R643
 Orlando T. M. T318, T319
 Orleanski P. R623
 Ormó J. T255*, T320
 Orosei R. T332, F702*
 O'Rourke J. G. T342, W404*, F704
 O'Rourke L. R614
 Ortiz-Ceballos K. N. T312
 Ortner T. T341
 Osada N. T341
 Osawa T. T253, T302
 Oshel E. R. R605, R639
 Oshigami S. T253
 Osiander R. R601
 Osinski G. R. T255, T311, T320,
 T335, T347, W452, R505,
 R621, R627, R628, R636,
 R645
 OSIRIS-REx Science Team T301
 OSIRIS-REx Team T203, T301,
 W401, R611
 Ostberg C. T312
 Osterloo M. M. T205, R622, R635
 Osterman D. T346
 Ostrowski D. R. R612, R644
 Ostwald A. O. T328
 O'Sullivan J. A. T331, R640
 Otake H. T302, T338, T341, R611
 Otsubo T. T253, T302
 Otsuki M. T339
 Ott J. P. M102*
 Otto K. T253, T302, T317, R613,
 R615
 Otto K. A. W401
 Oudayer P. R635
 Owaga K. T253
 Own C. S. T347
 Own L. S. T347
 Oyama T. T345
 Ozaki M. T253, T341
 Ozaki N. T338
 Paar G. T341
 Pace L. F. T336, T340
 Pachpor S. V. T320
 Pacini A. T312
 Pack A. T303, R644
 Padams J. H. R640
 Padovan S. M152, T310
 Page B. T203, T301
 Page J. R622
 Pahmakova A. F703
 Paige D. A. M101, M151, T315,
 T316, T317, T338, R501,
 R621
 Paik H. J. T339

Pajola M. T203, T301, T316, W401,
 R621, R622, R623, R645,
 F702
 Pajtok-Tari I. R645
 Palacios J. T336
 Palat A. R606
 Palmer E. T203, T253, T301, R639
 Palmer E. E. T301, T302, T317,
 T336, R614, R639
 Palmer E. M. T318
 Palmer M. R612, R615
 Palmer T. W. T346
 Palomba E. T253, T302, T344
 Palucis M. C. R622, R627, R633
 Palumbo A. T338
 Palumbo A. M. T313, W452*
 Palumbo P. R621
 Pamer J. R. R640
 Pan C. T256*, R627
 Pan L. T308, T309, R505*
 PanCam Team T346
 Pando K. R553
 Pando K. M. T303
 Panigrahi M. K. R602, R634
 Panning M. M152, T308, T336,
 T338, T344
 Panning M. P. T308, T310, T336,
 T339, T344
 Pantha P. P. T311
 Papike J. R605
 Pappalardo R. T. T310, T325, T327,
 W453*, R645
 Paque J. M. R608
 Paquet M. M102*
 Paranicas C. T323, T338, T343, T344
 Pardo C. M152
 Parekh R. T253*
 Parente M. T330, T331, W402,
 R502*, R622
 Parise J. B. R626
 Parise M. T308
 Park C. R604
 Park J. R604, R605, R614
 Park R. S. T301, T342, T344, T346,
 W454
 Parker A. T338
 Parker A. H. M103, M153, T305,
 T313, T342
 Parker E. T. W451*, R606
 Parker J. M103, T305, T335, R607,
 F705
 Parker J. E. T336
 Parker J. Wm. M103, M153, T305,
 T335
 Parker T. M152, T309
 Parker Bowen A. R622, R623
 Parkinson A. R633
 Parkinson A. E. T318
 Parkinson C. D. M154
 Parkrer J. W. T305
 Parks M. R615
 Parman S. T205
 Parman S. W. M104, T251, R610

- Parmentier E. M. T251*, T254
Parness A. T338
Parra S. A. R628
Parson R. R633
Parsons A. M. T336
Parsons R. A. T202*, R640
Pasckert J. H. W454, R615, R637
Pascuzzo A. C. R628
Pasek V. R637
Pasquali F. T308
Patchen A. D. T304
Patel A. V. R503*
Patel H. J. R642
Patel M. R. T202, T333, R623, R629, R636
Patel P. T320
Patel P. P. T335
Patel R. R. R631
Patel S. A. R633
Pathak S. R602
Pathoff A. R638
Patidar S. R602
Patkos Cs. R645
Patrick E. T318, T339, R606
Patrick E. L. R603
Patterson D. A. T346
Patterson G. W. M151*, T204, T316, T318, T343, W405, R603, R631, R639, F701
Patterson W. R. III R503
Patthoff D. A. T324, T325, R637
Paty C. S. T331
Patzek M. R644
Pauken M. T. T337
Paul M. V. T344
Paul R. T303
Paulsen G. T346
Paulsson B. N. P. T346
Pavlov A. A. W451
Paxman J. P. R644
Payre V. M102, T328
Payré V. T252, R624
Peabody H. L. T336
Pearce M. A. F703
Pearson N. T346, R503
Pearson N. C. R635
Pearson V. K. R556, R636
Peel S. E. R627
Pegg D. T306
Pegg D. L. R554*, R637
Peillon S. R635
Pelivan I. T253
Pellin M. J. R504
Peng Y. R632, R633
Peng Z. X. R616
Penttilä A. R611, R620
Peplowski P. N. T205, T336, T342
Pepper A. C. R619
Perera V. M101, T314, R601
Peretyazhko T. W402, R626, R633
Peretyazhko T. S. R552
Pérez L. F705
Perkins R. T318
- Perkins R. P. W404*, R601
Perl S. M. W451, R642
Permiakov V. T320
Perna D. T253, T302, W401
Pernet-Fisher J. F. R604, R606
Peroud S. T255
Perrin C. M152, T308, T309, T327
Perrin S. L. R632, R634
Perrine M. T346
Perron T. T326
Perry J. T344, R623
Perry J. E. M154
Perry M. E. T203, T301
Perry M. R. T346, R623, R628, F702
Perry S. E. R626
Persaud D. M. R623
Persson K. B. T339, T343
Peruzzetto M. T202
Peslier A. H. M102, T328, R620
Petaev M. I. T251, R505, R610, R619
Peter D. T310
Peter G. T319
Peters G. H. R624
Peters S. T. R641
Petersen E. R628
Petersen E. I. R623, R628, F702
Petit. D. T255
Petrassi M. T308
Petro N. M151, T318, T338, R602, R605
Petro N. E. M101, T314, T315, T316, W403*, R611
Petrova E. V. R620, R644
Petrucha V. P. R619
Petruny L. W. T320
Pettinelli E. F702
Pettit D. R635
Pettit D. R. T347
Pettit E. C. T310
Peyton A. R644
Pezard P. T255
Phan N. R640
Phillippe M. T202
Phillips B. P. R622
Phillips C. B. T343, R645
Phillips D. R602
Phillips K. R601
Phillips M. S. M102*, R556
Phillips-Lander C. M. T339, T343
Philpotts J. A. R604
Piani L. M104
Piatek J. R645
Piatek J. L. R621, R645
Piazolo S. M102, T328
Picard M. T347
Piccioni G. T323
Pickersgill A. E. T255*, T320
Piercy J. D. R611
Pieterek B. R630, R631
Pieters C. T338, R615
Pieters C. M. W403*, W454, R501, R602
- Pignatale F. R609
Pignatari M. R504
Pike W. T. M152*, T307, T308, T309, T339
Pilles E. T347, R623, R645
Pilorget C. T253, T302, R634
Pilorget C. P. T341
Pimentel A. T338
Pinet P. T314, T328, R552, R624, R625, R644
Pinet P. C. T347, R602
Pinilla-Alonso N. R555
Pino-Munoz D. T301
Piquette M. T305, T344, R607
Piqueux S. M152, T309, R628, R640, F702
Piralla M. M104
Pitt D. R617
Pittarello L. R618
Pittman C. T347
Plado J. T255
Pla-Garcia J. M152, T308, T313
Plainaki C. T323
Plane J. M. C. R644
PLANMAP Team R637
Plattner A. M. T205*
Platz T. R637
Plaut J. J. T332
Plesa A. T308
Plesa A.-C. M152*, T307, T310, T313, R628
Plesa A. C. M152, T309
Plescia J. B. T316, T338, R619
Pleseal L. R640
Plesko C. S. R619
Poch O. R613
Podoleanu A. R619
Poehler C. M. M101*, R637
Poelchau M. T255
Poelchau M. H. R505*, R620
Poggiali G. T301, W401
Poggiali V. P. M105*, T326
Pohl J. T255
Pohl L. R613
Poitras J. T. R634
Polanskey C. A. T342, R619
Polgari M. R645
Politte D. V. T331, R638, R640
Pommerol A. T343, R623, F702
Pommier A. T344
Pondrelli M. R627
Pontefract A. T311, T320
Poppe A. R. M153*, T344, R607
Porat Y. T347
Porcelli L. T308
Porrachia M. F701
Port S. T. W404*, R601
Porter F. T347
Porter J. T345, T346
Porter R. R635
Porter S. B. M103*, M153, T305
Portyankina G. T202, T341, R628, F702*

Porwal A. R622, R627
Posnov N. T311, T320
Poßekel J. T321
Posta J. T303
Postberg F. W453
Poston M. R603
Poston M. J. T339
Potin S. R613, R624
Potter A. E. T318
Potter S. F. R612
Pou L. T308
Poulakis P. R643
Poulet F. T253, T302, T323, R622,
R625, R634
Povilaitis R. Z. M101
Povinec P. P. T328
Powell K. E. R502*, R640
Powell T. M. T316, T317, R611
Pozzobon R. T316, R623
Pradeepkumar Girija A. T344
Praet A. T301
Prasad Gokul H. T338
Pravdivtseva O. T317, W455*
Pravec P. R612
Prem P. T316, T317, W403
Prencipe M. F703
Presler-Marshall B. R612
Preston S. T334
Presuker F. T253
Prettyman T. H. T318, T342, T346,
W454*, R615, R639
Preusker F. T253
Price M. C. R621, R644
Prieto J. A. R. T346
Prieto-Ballesteros O. T311
Prieur N. C. T316
Primm K. M. T252*
Prissel K. B. T251*
Prissel T. T338
Prissel T. C. W403, R501*
Pritchard I. R645
Prockter L. T343, R641
Prockter L. M. T324, T344
Project ESPRESSO Team T342
Protopapa S. M103*, M153, T305,
R555
Psyche Mission Team T342, R614
Purucker M. E. T315
Putnam E. T. R622, R627
Putzig N. E. T341, T346, W452,
R623, R628, F702
Qian Y. Q. T206
Qiao L. T206, R602
Qin L. T303, T338
Qin L. P. F705
Qiu D. R640
Qu H. K. R626
Quadir Z. R604
Quantan-Nataf C. R502, R619
Quantin C. T308, W452, R505
Quesnel Y. T255
Quick L. C. T254, T324, T336, T343,
W454, R645

Quidelleur X. T341
Quillen A. C. T301
Quilligan G. T336
Quinn H. T345
Quinn R. T339, R642
Quintero N. R503
Quirico E. M103, T305, R613
Raack J. T202*, T332, T333, R629,
R640
Raaen E. T338, R643
Rabib R. R. M102
Rabinovitch J. T334
Racca G. T314
Racette P. E. T339
Radebaugh J. M105, T334, T336,
T344, R631, R633, R638
Rader E. W451*, R631
Rader L. X. R601
Radke A. M. R633
Raducan S. D. R505, R614, R621
Rafkin S. C. R. T313, T336
Raguso M. C. T326
Rahib R. R. M102
Rahman Z. T319, T328, T347,
W406, R608
Rai N. F704*
Rai V. K. W455, R553
Raimalwala K. T347
Rajesh V. J. R602
Rajsic A. M152
Ramboz C. T255
Ramesh K. T. R619
Ramirez J. R603, R635
Ramirez M. R633
Ramirez P. R640
Ramirez R. M. T312
Ramkissoon N. K. R556*, R636
Rammelkamp K. T346, R625
Rampe E. B. M102, T252, T330,
W402, W453*, R552, R624,
R626, R632, R633, R634
Ramprasad T. R610
Ramsdale J. D. R627
Ramsey B. T346
Ramsey M. S. R630, R631
Ramsley K. T338
Rannou P. M154
Rao M. N. T252*
Rapin W. T252*, T328, T330, W402,
R552, R625, R644
Raponi A. T323
Rapp J. R. R633
Rappenglück B. T321
Rasmussen C. R620
Rathbun J. T344, R631, R645
Raub E. T337
Raulin F. W451
Raut U. T339, T343, R603, R611
Ravat D. T315
Ravi S. R602
Ravine M. T336
Ray D. R634
Ray S. R553*, R619

Ray T. L. R641
Raychaudhuri D. T320
Rayman M. D. W454
Raymond C. A. T346, W453*,
W454, R615, R637
Raymond S. N. R613, R619
Razzell Hollis J. R633, R643
Re C. R623
Read A. R645
Read M. R623
Reagan J. R. R619
Reddy S. R604,
Reddy V. T301, W454, R503*, R555,
R620
Redick R. T343
Reeder A. W451, R631
Reershemius R. M152
Rees S. R635
Reeves H. T255
Regberg A. B. T301, T340, R645
Regensburger P. V. T201
Rehak J. S. R607
Rehnmark F. T339, T346
Reid E. T347
Reimold W. U. T255, T320
Reinhardt M. W451
Reiss D. T202, T334, R633, R640
Reito S. R632
Reitsema H. J. M103
Reitze M. P. T319
Reitze M. R. T319
Rempel A. W. T252, R628
Ren M. R606
Ren X. R602
Renaud J. P. T319
Render J. R610
Renggli C. T319
Rennie V. W451
Restano M. F702
Retherford K. M151, T318, T343
Retherford K. D. T317, T318, T339,
R603, R611
Reuschlé T. T320
Reuter D. C. M103, T203, T301,
T305
Reva I. R614
Reyes-Newell A. W402
Reynolds E. L. T343
Rhoden A. T310
Rhoden A. R. T254, T324, R621
Rhodes D. J. T317
Ricci L. F705
Rice J. T329
Rice M. S. T330, T346, R552, R622,
R624, R625
Richardson D. C. T203, T301
Richardson J. T316, T347, R554,
R632, R635
Richardson J. A. W404*
Richardson M. T313, R645
Richey C. R645
Rickard W. R604
Rickard W. D. A. R610

- Rider S. R642
 Riebe M. E. I. W406
 Rieck K. D. R608
 Riedel C. T317
 Riedel J. E. T346
 Rietmeijer F. J. M. R606
 Riggi S. R632
 Righter K. M102, T301, T303, T328, T340, R553*, R605, R606, R639
 Righter M. T328, R553, R617
 Rignot E. T344
 Rincon R. F. T346
 Ringer S. P. R610
 Rink K. T344
 Rios A. C. W451
 Risk B. T203
 Riu L. T253*, T302, T338, R622, R634
 Riu L. R. T341
 Rivera-Hernandez F. T252, W402, R624, R627, R633
 Rivera-Valentín E. G. M155, T252, T335, R555*, R603, R612, R621, R645
 Riveros K. R636
 Rivkin A. S. T342, R613
 Rivoldini A. M152
 Rizk B. T203*, T301, W401
 Roatsch T. T253, T325, R615, R621, R638
 Roback K. P. T256*, T333
 Robak K. N. R620
 Robbins S. J. M103, M153, T305, T335, R621, R623
 Robert O. M152, T308
 Roberts J. H. T203, T301, R612
 Roberts S. E. T321
 Robertson D. K. W452
 Robertson K. M. T302, R602, R611
 Robinson A. R604
 Robinson K. L. T320, R551*, R604
 Robinson M. S. M101, T204, T314, T316, T317, T318, T335, T347, W403, R602, R603, R611, R637
 Robrtsson J. T309
 Rocha F. F. T320
 Rochette P. T255
 Rocholl A. R501
 Rodionov D. R643
 Roderiguez-Manfredi J. A. T309
 Rodriguez J. T343
 Rodriguez J. A. P. W452*, R629
 Rodriguez M. T340
 Rodriguez N. R636
 Rodriguez S. M152, M154, T308, T309, T322, T326, T327, T334
 Rodriguez-Manfredi J.-A. M152
 Rodriguez-Manfredi J. A. M152
 Rodriguez Sanchez-Vahamonde C. R554*, R612
- Rogaski A. M102*, T206, T339, R637
 Rogers A. D. M102, T301, T341, W453, R556, R622, R623, R626, R627, R632
 Rogers H. R632
 Roggero A. R635
 Roh D.-G. R614
 Rohleder N. J. T320
 Rohrbach A. T314, T319, R618
 Rojas C. T314
 Rojas J. R644
 Rojo P. M154
 Rolf T. W404
 Rolison J. M. R606
 Romaine S. T346
 Roman A. R601
 Romeo G. T331, R632
 Romero V. W454
 Romero-Wolf A. R641
 Rondón E. R555
 Root S. R505, R619
 Rosas-Ortiz Y. T337
 Rose M. R644
 Rose T. W452, R618
 Roseborough V. A. R627
 Roskosz M. R613
 Ross A. J. T341
 Ross C. T320
 Ross D. K. T252, T303, T320, R551, R553, R605, R610, R616
 Ross N. T332
 Rossato S. T316
 Rossi A. P. R638
 Rossman G. R. R608
 Roth A. R618
 Roth L. T343
 Roth M. C. T318
 Rothard H. W406
 Rothery D. A. T205, T306, R554, R630, R637
 Rothrock B. R640
 Rougier E. R619
 Roush T. R613, R634
 Roussel J.-F. R635
 Roux E. L. T318
 Roux V. G. T318
 Rowden P. R503, R626
 Rowe K. M. T307, T339
 Rowland D. T303
 Rowland R. II R553
 Rowlands D. T203, T301, T336
 Roy H. R639
 Royer C. R. T341
 Royer E. M. T323
 Rozitis B. T203
 Rozsa V. R. T303
 Rubanenko L. T315, T317
 Rubin A. E. M104
 Rubinstein H. T347
 Rucks M. F703
 Rucks M. J. R620
 Rudolph A. T330
- Rudolph M. L. T254
 Rueckert C. R637
 Ruedas T. R621
 Ruesch O. T317, W454, R622, R623, R637
 Ruff S. W. T329, R556*
 Rufu R. R619
 Ruiz-Galende P. R604, R626
 Rull F. T346
 Rull-Perez F. R634, R643
 Rumpf M. E. R633
 Runco S. T335
 Runyon K. D. M103, T206*, T256, T305, T306, T334, T335, T344
 Ruoff N. T309, R640
 Rupert S. R633
 Rush B. P. T301
 Russell A. J. T332
 Russell C. T. M152, T307, T338, T339, W453, W454, R601, R615, R637
 Russell M. B. R601
 Russell P. S. T317, R628
 Russell S. S. T303, T340, W406, R503, R609, F705
 Russo G. R632
 Rutherford M. R551, R601
 Rutledge A. M. R632
 Ruzicka A. M. T304, R609
 Ryan A. T203
 Ryan A. J. T301, R612
 Ryan C. H. R642
 Ryan C. J. R553
 Ryan E. L. T313
 Ryan K. T343
 Ryazantsev K. M. R610
 Rydeblad E. R609
 Rymer A. T344
 Saadé M. T308
 Saal A. E. R501
 Sabatose A. C. M104
 Sachse M. R615
 Sacks L. E. R621
 Sadoway D. T338
 Sagar J. T304
 Sagmiller D. C. T344
 Ságodi I. T335
 Sah R. R620
 Sahai M. T347
 Sahijpal S. R610
 Saiki K. T206, T339
 Saiki S. T253
 Saiki T. T253, T302, T344
 Saito S. T344
 Saito T. R619
 Saiz J. R643
 Sakai S. T206, T339
 Sakamoto K. T302
 Sakamoto N. R608, F701
 Sakamoto S. T335
 Sakatani N. T253*, T301, T302, W401, R614

Sakatani N. S. T253
 Sakimoto S. E. H. M105, R554*
 Sakuma H. R629
 Salem M. S. R606
 Salese F. R502*, R627
 Salge T. T340
 Salinas H. R636
 Salvatore M. T330, W402, R552, R624
 Salvatore M. R. R552, R556, R622
 Salvatori L. T308
 Samochina S. R640
 Samson C. W404, R601, R632
 Sanasarian L. T339
 Sanborn M. E. T303, R617, F704*
 Sanchez A. M. R626
 Sanchez J. A. R503, R555, R620
 Sanchez P. T203
 Sánchez P. R612
 Sanden G. v.d. T348
 Sanders I. S. R610, R612
 Sandford M. T345, T346, R611
 Sandford S. T203, T301
 Sandford S. A. W401, R642
 Sandidge W. M154
 Sándor Zs. R612
 Sands C. T337
 Sanei H. T321
 Sangha J. M151
 Sanigepalli V. T339
 Sanin A. B. T318, T330, R628
 Sanmartin J. R636
 Sansom E. K. R555
 Santiago A. T346
 Santo A. T343
 Santos A. R. R601
 Sapers H. R643
 Sapers H. M. T255
 Sarafian A. R. M104
 Saranathan A. M. T331, R502
 Sarantos M. T338
 Sargeant H. M. T206*, T339, T347, R637
 Sarid G. R612
 Saripalli S. T347
 Sarkar R. R622, R627
 Sarkar S. R634
 Sarrazin P. T337, T339, T345
 Sarrazin P. C. T341
 Sasaki S. T253, T302, T347, W401*, R555, R611
 Sasaki T. T202
 Sato H. T206, T302, R611
 Sato S. T339, T342
 Sato Y. T253, T341
 Satoh Y. T336
 Saturnino T. J. D. C. R635
 Saucedo V. L. T347
 Saur J. T344
 Sautter V. T328, R644
 Sava P. T346
 Savin I. T308
 Savina M. R. R606

Savini G. T346
 Savoie D. M152
 Sawada H. T253, T301, T302, T341, W401
 Sawai S. T206, T339
 Sawchuk K. R616
 Saxena P. R611
 Saxey D. R604
 Saxey D. W. R610
 S. Calcutt S. M152
 Scanlan K. M. R623, R628
 Scanlon K. E. T332
 Schaefer B. F. R610
 Schaefer L. R618
 Schaefer L. K. F704
 Schafer E. T202
 Schaller C. R623
 Schaller M. T312
 Scharringhausen M. M152, T309
 Schatz L. R503
 Schedl A. T321
 Scheeres D. T203
 Scheeres D. J. T203*, T253, T301, T302, R503, R612
 Scheidt S. R623, R632
 Scheidt S. P. T334, T347, R554, R627, R637
 Scheller E. L. R505*, R627
 Schenk P. M103*, T305, T306, T325, T335, W454, R615, R621, R641
 Schenk P. S. M153
 Schieber G. L. T318
 Schieber J. T252, T330, T334
 Schiller M. T303
 Schimmel M. M152, T308, T309
 Schindhelm R. N. T342, T346, R645
 Schlacht I. T348
 Schlichting H. E. T312
 Schlotterer M. T253
 Schmedemann N. W454, R615, R621
 Schmeeckle M. W. R554, R631
 Schmeling M. R608
 Schmelzbach C. T309
 Schmerr N. M152, T204, T308, T309, T310, T338, R635
 Schmidt B. T343
 Schmidt B. E. T204, T254, T342, W454
 Schmidt C. T318
 Schmidt F. T327, T343
 Schmidt G. R627
 Schmidt J. R606
 Schmidt M. E. W453*, R625
 Schmieler M. T255, T320, F703*
 Schmitt B. M103, T305, R613, R641
 Schmitt H. H. W403
 Schmitt-Kopplin P. T303
 Schmitz B. R644
 Schmitz N. T253, T302, W401
 Schmitz S. T336
 Schneider J. M. F705*

Schneider N. M. T335
 Schoene B. R606
 Schoenfeld A. M105
 Schoenfeld A. M. T325
 Schofield P. F. W406, R609
 Scholar P. W. R644
 Scholes D. R638
 Scholl A. R553
 Schonwald A. R. M101, R604
 Schools J. R631
 Schoonen M. A. A. T347
 Schorghofer N. M151, T202, T317, W454, R615
 Schrader D. L. M104, W455*, R609, R613, F704, F705
 Schratz B. C. T342
 Schreiner B. R623
 Schröder C. T313, T329, W402, R644
 Schröder S. T302, T346, R625, R644
 Schröder S. E. T253
 Schroeder D. M. R641
 Schroeder J. F. T204
 Schroeder S. E. T253*, R615
 Schryvers D. R618
 Schubert G. T313
 Schubert M. T347
 Schubert W. T344
 Schuerger A. R642
 Schuerger A. C. M155, T311
 Schulte J. R504*
 Schultz P. H. T255*, T321, R619
 Schultz R. A. T327
 Schulz F. T204
 Schulz T. T321
 Schulzeck F. R615, R637
 Schurmeier L. T344
 Schuster B. T315
 Schutt J. W. R644
 Schwadron N. T318
 Schwadron N. A. T317
 Schwamb M. R628
 Schwamb M. E. F702
 Schwartz S. R. T203, T301, T302, T314, W401, R645
 Schwenzer S. P. M102, T255, T328, T330, T339, R552, R556, R632, R636, R639, R640
 Schwinger S. T204, T314, R620
 Scipioni F. M103, T305
 Scipioni S. T305
 Scott D. R. T338
 Scott E. R. D. R610, R612
 Scudder N. A. R632
 Scuderi L. A. T347, W452*, R627
 Scully J. R615
 Scully J. E. C. W454*, R615, R637
 Scwhadron N. A. T318
 Seabrook J. T203, T301
 Sedler M. A. R616
 Seeger C. H. T330, R624, R625
 Seelos F. R622, R623, F702
 Seelos F. P. T331, T343, R502, R622

- Seelos K. R642
 Seelos K. D. T331, T334, R621, R622, F702
 Sefton-Nash E. M151, T317, T339, T341, R505*, R622, R640, R643
 Seguin A. T318
 Seidel R. G. W. R632
 Seifert L. B. R607
 Seignovert B. R637
 Seiler S. R618
 Seimetz L. T315
 SEIS Commissioning Team T308
 Séjourné A. R627
 Sekiguchi T. T253
 Sekimoto S. T303
 Sekine Y. T202, T252, T302, T333, R624
 Semenov B. R638
 Semjonova L. F. T303
 Semprich J. M102*, R551
 Senges G. R606
 Senshu H. T253, T302
 Senshu S. T302
 Senske D. A. R637, R645
 Seo H. R614
 Sephton M. A. W451
 Serabyn E. R642
 Serebryanskiy A. R614
 Serla J. K. R623
 Sessa A. M. T331, R622, R634
 Setera J. R501
 Sethares L. T346
 Seu R. F702
 Sevy J. M. T334
 Seybold C. C. T342
 Seymour A. R555
 Seymour J. D. T252
 Shaddad M. H. W406, R617, F704
 Shah U. T338, T347
 Shahar A. R553
 Shakun A. M154
 Shaner A. T335
 Shang H. R607
 Sharkey B. R555
 Sharkey B. N. L. R503
 Sharma S. R618
 Sharma S. K. T345, T346
 Sharp T. T255
 Sharp T. G. R616, R620, F704
 Sharp Z. D. T251, R553*, R605
 Shaulis B. R604
 Shea T. R604
 Shearer C. K. T251, T308, T328, W403*, R501, R605
 Sheffer A. A. T321
 Sheikh D. R616
 Shelton D. T339
 Shen G. T205, T315
 Sheppard R. Y. T330
 Sheridan S. T347
 Sherlock S. C. R632
 Sherwood Lollar B. T313
- Sheu S. T303
 Shevade A. V. T337
 Shevchenko V. T314
 Shi E. B. R626, R634
 Shibuya T. T302, R619, R624
 Shih C.-Y. R605
 Shikar A. T347
 Shimada T. T253
 Shimaki Y. T253, T302
 Shimizu K. M104*
 Shimoda T. T336
 Shin H. R606
 Shin J. T339
 Shirai K. T253, T316
 Shirai N. T302, R604
 Shiraishi H. T206, T316, T336, T339
 Shirley K. A. R620
 Shirley M. M151
 Shiryayev A. A. T303
 Shizugami M. T253
 Shkolyar S. R642
 Shkuratov Y. T314
 Shober P. M. R555*
 Shoemaker C. S. T255
 Shoemaker E. S. R631
 Sholes S. F. R623
 Shollenberger Q. R. R504*
 Shornikov S. I. R610
 Showalter M. W453
 Showalter M. R. M103, M153*, F705
 Shukla A. D. R634
 Shukla S. R603
 Shupla C. T335
 Shuster D. L. T313
 Shusterman M. L. T335
 Si J. R620
 Siebach K. L. M102, T330, W453, R624, R633
 Siebert J. T251, R619
 Siegler M. M151, M152, T307, T309, T338, F701
 Siegler M. A. M151, M152, T203, T317, R602
 Sietins J. M. M101
 Sikder A. M. T321
 Silber E. R645
 Silber E. A. R621
 Siljeström S. T341, W451
 Sillitoe-Kukas S. T328, R618
 Silvestro S. T256*
 Sim C. K. W405, R603
 Simioni E. R623, F702
 Simkus D. N. W451*, R606
 Simon A. W453
 Simon A. A. T203*, T301
 Simon J. R620
 Simon J. I. R551, R610, R616
 Simon S. B. M104, T304, W455, R551*, R610
 Simpson E. N. R620
 Simpson S. R645
 Simpson S. L. T255*, T320
- Sims M. F703*
 Simurda C. M. R630, R631
 Sindoni G. T323, R631
 Singer K. N. M103*, M153, T305, T306
 Singh P. R622, R627
 Singh V. T254*
 Singletary S. J. T328
 Sinha P. F702*
 Sio C. K. R501
 Sipiera P. P. T303
 Siran S. T335
 Sirbescu M. R618
 Siron G. W455
 Sisson T. R631
 Sitnikova A. T335, T348
 Sivaraman B. T302
 Siwabessy A. T204
 Siyed Z. T318
 Sizemore H. G. T252, T341, W454, R615, R628, R637, F702
 Skerritt J. T345
 Skiba C. J. T347
 Skinner J. A. R633, R638
 Skinner L. A. R633
 Skjetne H. L. T306
 Sklute E. C. T321, T331, R626, R632
 Sklyanskiy E. T309
 Skok J. R. R627
 Slack K. A. T343
 Sladkova K. T344
 Slank R. A. T252*
 Slater G. F. R642
 Slavín J. A. T205
 Slavney S. R638
 Slick L. R. R503
 Slivicki S. J. T320
 Slodzian G. W406
 Smal E. T347
 Small J. T203, T301
 Small Body Mapping Tool Team R612
 Smedley A. R. D. R644
 Smirnov A. T347
 Smith A. T328
 Smith B. R627
 Smith C. L. M154*, M155, T313, T332, T341, F704
 Smith D. E. T338, T342, R603
 Smith H. D. M155*
 Smith I. B. T341, W452*, R554, R628, F702
 Smith L. R. R609
 Smith M. D. T329
 Smith P. T301
 Smith P. H. T203
 Smith R. T316
 Smith R. J. T330, R632
 Smith R. L. T335, R609
 Smith W. T328
 Smith Hackler A. T335
 Smrekar S. E. M152, T307, T308, T309, T337, W404*, W453

Smythe W. D. T344
 Snape J. F. T251*, R551
 Sneed c. J. T340
 Sneed J. W. R621
 Snodgrass C. T323
 Snyder K. R635
 Soare R. J. T202*, T332
 Soares C. E. T345
 Sobol P. E. F705
 Sobron P. T339, T346
 Socki R. T304
 Soderblom J. M. M105, T326, T336,
 T343, R555
 Soderlund K. M. T204, T325,
 W453*
 Sohn M. T319
 Solberger D. T309
 Soldini S. T253
 Soldovieri F. F702
 Soler C. Q. R614
 Soliman T. R640
 Solomon S. C. W453*
 Solomonidou A. M105
 Son D. T339
 Søndergaard A. S. T321
 Sonnett S. R614
 Sonzogni C. R618
 Sood R. R631
 Soós Á. T303
 Sopoco R. R621
 Sorek-Abramovich R. T347
 Sori M. M. W454, R553, R615,
 R628, F701, F702*
 Sorice C. T309
 Sossi P. T251, R618
 Sotin C. M105, M154, T343, T344,
 R637
 Sotirelis T. T338
 Soto A. M155, T339, T341, T343,
 R645
 Soto M. R636
 Sotzen K. S. T336
 Soucek O. T344
 Souza-Feliciano A. C. R555*
 Spagnuolo M. G. T334
 Spahr D. R606
 Spahr T. R555, R614
 Spathis V. R621
 Spaulding D. K. R619
 Spedding C. P. T347
 Spence H. E. T317, T318
 Spencer J. R. M103*, M153, T305,
 T335, T344, R607, R631,
 F705
 Speyerer E. M151
 Speyerer E. J. M101*, T315, W403,
 R603
 Spicuzza M. J. R504, F705
 Spiers E. T343
 Spiga A. M152, T308, T309, F702
 Spiga D. T346
 Spilde M. N. T303
 Spitale J. T324

Spitzer F. F704*
 Spohn T. M152*, T307, T309, T310,
 R555
 Spray J. G. T255, T328, R552, R620,
 R621, R624, F703
 Spring J. T336
 Springmann A. R503
 Sproewitz T. M152
 Squire J. P. T344
 Squyres S. W. T336, R555
 Srivastava A. R643
 Sruthi U. W404*
 Stabbins R. B. T346
 Stacey K. T320, R630
 Stachurski F. R502*
 Stack K. W402
 Stack K. M. T330, R502*, R624
 Stack Morgan K. T331
 Staehler S. C. T310
 Stahl S. E. T301
 Stahler S. M152, T308, T309, T336,
 T344
 Stalport F. W451
 Stamenkovic V. M155*, R628
 Standley I. M. M152, T308
 Stangarone C. T319, F703*
 Staniszewski Z. K. T342
 Stanley S. M152
 Stansberry J. A. M103, M153, T305
 Stansbery E. K. T341
 Stark A. T319, T325
 Starr M. T330
 Starr M. S. R624, R625
 Starr R. T330
 Starr R. D. T319
 Starrfield S. R607
 Statella T. R614
 Steakley K. E. T313
 Steckloff J. K. W454*, R612
 Steele A. W451, R642
 Steele L. J. M154
 Steenstra E. S. T314, T319, R553*,
 R606, R618
 Stefanov W. L. R645
 Steffl A. J. T305
 Stein N. T252, T344, R624
 Stein N. T. W454*
 Stein T. C. T330, R638, R640
 Steinbrugge G. R628
 Steinbrügge G. T325, T344, R623,
 R628
 Stellmach S. T201
 Stephan K. T253, R621
 Stephan T. R504
 Stephant A. T328, R501, R551*
 Stephen N. R. T303
 Stern J. R636
 Stern J. C. W402, W451, R624
 Stern S. A. M103*, M153, T305,
 T306, T335, W453, R607,
 R641, F705
 Stevanovic J. T308
 Stevens A. H. W451

Stevenson D. T344
 Stevenson D. J. T325
 Stewart S. T. T251, R505*, R619
 Stewart Z. R633
 Stickle A. M. T312, T316, T318,
 T336, T338, R613, R621
 Stillman D. E. T202, T252*, R628
 Stirling L. A. T347
 Stockli D. F. R620
 Stockstill-cahill K. R. R503, T205*
 Stockton A. W451
 Stofan E. R. T336
 Stöffler D. T255
 Stojic A. T319
 Stoker C. R. R643
 Stokke A. R. T303
 Stolper E. F701
 Stolper E. M. W454
 Stone H. T311
 Stone J. R639
 Stone K. J. T339
 Stonehill L. C. T344
 Stooke P. T314
 Stooke P. J. R602
 Stopar J. R554, R602
 Stopar J. D. T316, F701*
 Storms S. A. T344
 Storrar R. D. T332
 Stott A. M152, T308
 Stott A. E. M152, T308
 Stowell H. H. T320
 Strait M. M. R619
 Straif M. M. R617
 Strauss B. E. R501*
 Streiffert B. A. R641
 Stromberg J. R633
 Strong K. T313
 Stroud R. M. R504, R606, R607
 Strycker P. D. M151
 Stryk T. M103
 Studer-Ellis G. L. T327
 Sturkell E. T255
 Stutzmann E. M152, T308, T309
 Stu Webb R551*, R605
 Su M. R614
 Suarez S. T320
 Suarez S. E. T328
 Such P. T346, R606
 Suda K. R619
 Suda M. R630
 Suga H. T328
 Sugita S. T203, T252, T253*, T301,
 T302, W401
 Sugita S. S. T253
 Sugiyama T. T253, T302
 Sukhatme K. G. T342
 Suko K. T253, T302
 Sullivan D. L. T330
 Sullivan P. T343
 Sullivan R. T329, T334, W453, R625
 Sultana R. R613
 Sumino H. R620
 Summers M. E. T305

- Summons R. E. R643
 Sumner D. Y. R624
 Sun C. R618, R635
 Sun L. R602, R611
 Sun M. T327
 Sun T. T328
 Sun V. Z. T330, W405, R502*, R552, R624, R640
 Sun X. T342, R603
 Sun Y. R611
 Sunaoshi T. T304
 Sunshine J. M. F704
 Susko D. R631
 Susorney H. T203*, T301, W401, R505
 Suter P. F. R637
 Sutin B. M. T344
 Sutter B. T252, W402*, R624, R634, R640
 Sutton S. T202, T301, T343, T344, W451, R632, R638
 Sutton S. R. T304, R551, R606, R613
 Sutton S. S. R623, F702
 Suzuki H. T253, T301, T302, T341, W401
 Svedhem H. R643
 Svensson M. J. O. T320
 Svetsov V. V. R612
 Swartz J. M. W452
 Swayze G. A. R622
 Swiat A. K. R633
 Swisher C. S. III R618
 Swiss Space Center T348
 Sykes M. V. R615
 Sýkora I. T328
 Sylvest M. E. T202, T333, R629
 Synowicki R. A. R608
 Szabó M. T335, R610
 Szalay J. R. T344, R607
 Szopa C. T336, T344, W451, R636, R643
 Sztakovics J. R612
 Szumila I. R620
 Szymanski E. D. R627
 Szyszko M. T255
 Tabata H. T252*
 Tabata M. T347, R644
 Tachibana S. T253, T302, T341
 Tackley P. W404
 Tafla L. T. R606
 Tagle T. R612
 Taguchi M. T253
 Tailby N. D. T255
 Tait A. W. T329, R644
 Tait K. R604
 Tait K. T. M101, M102, T328
 Tai Udovicic C. J. R638
 Takac M. T. R619
 Takagi Y. T253
 Takahara P. M. T336
 Takahashi Y. T203, T301, T328, T333
 Takai K. R619
 Takano Y. T302, T341
 Takashima T. T342
 Takato N. T253, T302
 Takei Y. T253
 Takeichi Y. T328
 Takenouchi A. R501, R620
 Takigawa A. T336
 Takir D. T253, T302, T318, R503*, R613
 Takita J. T253, R639
 Tallarida N. T344
 Tamblyn P. M103
 Tampari L. K. T341
 Tan G. W451
 Tan J. S. W. W451*
 Tan S. R624
 Tanaka H. T302, R611
 Tanaka S. T253, T302, T314, T316, R639
 Tanbakouei S. R642
 Tang G. Q. T303
 Tang H. R553, R605
 Tang Y. R555
 Tansock J. T336
 Tao R. T205
 Tao Y. R623
 Tapella R. K. R641
 Tarduno J. A. R605
 Tarnas J. T338
 Tarnas J. D. T313, T331, R502*, R628
 Tartese R. F701*
 Tasoff P. R642
 Tate C. G. T330
 Tatsumi E. T253, T301, T302, W401
 Tatsumi E. T. T253
 Tatum K. R503
 Tatzel M. W455
 Tazuin B. T204, T308
 Taylor G. T339
 Taylor G. J. W405, R551, R604
 Taylor M. R614
 Taylor P. A. R555, R603, R612
 Taylor P. T. R602
 Taylor S. T317, R504*, R607
 Taylor S. E. T316
 Tazawa S. T253
 Teanby N. A. M152, T308, T309
 Tebolt M. T202*, T332
 Teffeteller H. R601
 Tegler S. C. M105, T326
 Teichert Z. G. R616
 Teinturier S. R643
 Tekeuchi H. T253
 Telus M. T344
 Templeton A. T343
 ten Kate I. L. T313
 Tenner T. J. R504
 Tennyson J. T346
 Ten Pierick J. M152, T308
 Teodoro L. T201*, R613
 Teodoro L. F. T312
 Tepper J. H. R605
 Terada K. T344
 Terada K. T. T317
 Terao J. R611
 Terazono J. T335
 Terrell D. M103
 Terui F. T253, T302
 Tessalina S. R610
 Tessenyi M. T346
 Tesson P.-A. T333, R623, R630, R631
 Tewksbury B. J. R645
 Thampi S. V. T313
 Thangjam G. W454, R615
 Tharimena S. T310, T344
 Theinat A. K. R603, R635
 Thelen A. R615
 Thesniya P. M. R602
 Thiessen F. R551*
 Thomas A. T347
 Thomas A. B. R605, R639
 Thomas C. R645
 Thomas C. A. T203, R613
 Thomas M. F. T252
 Thomas N. T252, T343, T344, R622, R623, R625, F702
 Thomas N. H. T328, T331, W402*, R633
 Thomas P. C. R614
 Thomas-Keprta K. L. R607
 Thomas-Keprta K. T. T347
 Thompson A. T344
 Thompson D. T343
 Thompson K. T339, T341, T345
 Thompson L. T330, R552, R620
 Thompson L. M. T252, T313, T328, T330, R552*, R624
 Thompson M. S. T304, T319, W403, W405*, R611
 Thompson R. A. R645
 Thompson T. J. T317, T318
 Thompson T. W. T318
 Thomson B. J. T316, T318, W405, R601, R603, R622, R631, R638, R639
 Thomson F. R638
 Thomson L. T252
 Thornburg J. T346
 Thorpe M. T. T330, R552, R633
 Thorpe R. S. T336
 Throop H. B. M103, M153, T305
 Thuillet F. T203
 Tian W. R601
 Tian Z. T303, T325, R605
 Tibuzzi M. T308
 Tice M. M. R642, R643
 Tiedeken M. T319
 Tiedeken S. T335
 Tielke J. R620
 Tikoo S. M. T338, R501, R605
 Tillier S. M152, T308
 Timmons M. R645
 Timms N. E. T303, R607, F703
 Tinetti G. T346

Tinker C. R. R502*
 Tipton M. T343
 Tirsch D. R622, R634
 Tiscareno M. S. R645
 Tissot F. L. H. W455, R606, R610
 Titus T. N. T334, T341, R615
 Tober B. S. R630
 Tobie G. T344
 Togashi S. R604
 Toigo A. D. T252
 Tokano T. T336
 Togle L. T338
 Tolbert M. A. T252
 Tolometti G. T320, T347, R645
 Tolometti G. D. T206, T339, R637
 Tolpekin V. A. R603
 Tomioka N. T302
 Tomiya A. R604
 Tomkins A. G. T303
 Tomlinson A. J. T255
 Tomokatsu M. T302
 Toner J. D. T252, R634
 Toner K. W404, R601
 Toplis M. J. W454, R631
 Torcivia M. A. T320, R604
 Torii M. R617
 Tornabene H. A. F704*
 Tornabene L. L. T328, T347, R621,
 R622, R623, R645
 Tornaberne L. L. R554
 Torrano Z. A. W455*
 Torre-Fdez I. R604, R626
 Torrence M. H. R603
 Torres A. T315
 Torres J. M152
 Tosca N. J. R556
 Tosi F. T323, R631
 Tosi N. M152, T204, T310
 Toth G. R601
 Touqan M. R636
 Towner M. C. R555, R644
 Townsend J. P. T308
 Toyoda M. T344
 Trafton L. W454
 Trafton L. M. T324, T325
 Trail D. R551, R605, R620
 Trainer M. G. T336, W402
 Trakinski V. T335
 Tran K. T. T311
 Tran V. D. T341
 Trang D. T203, W401, W405, R601,
 R611
 Trappitsch R. T303, R504, R606
 Trauthan F. T253
 Trautman M. R. T309
 Trautman M. T. R640
 Trautner R. T339
 Trautner V. T319
 Traxler C. T341
 Trebi-Ollennu A. T309
 Treffkorn J. R504
 Treiman A. H. M102, T328, T330,
 W453, R551*, R601

Tremblay C. T346
 Tremblay M. M. R604
 Trevino R. C. T342
 TREX SSERVI Team R635
 Trident Team T344
 Trigo-Rodriguez J. M. R642
 Trilling D. E. R613
 Trimby P. W. M102, T303, T328,
 R610
 Tripa C. E. R608
 Trokhimovskiy A. M154
 Tromp J. M152
 Trowbridge A. J. M101*, R621
 Truitt A. R. R619
 Trumel H. T255
 Tsai C. R602, R612
 Tsai V. C. T344
 Tsang C. T337
 Tsang C. S. R606
 Tschauner O. R613, R620, R626,
 R633
 Tsigaridis K. F701
 Tsuchiya T. T302
 Tsuchiyama A. T347
 Tsuda Y. T253, T302
 Tsukizaki R. T253
 Tsumura K. T253, T344
 Tsuno K. R553, R618, R631
 Tsuruta S. T253
 Tu S. R626
 Tu V. T330, R552, R636
 Tu V. M. R626
 Tucker E. S. R606
 Tucker O. J. T318
 Tulyakov S. R623, F702
 Turayev Y. R614
 Turenne N. R633, R634
 Turner L. R616
 Turner M. L. R624
 Turner S. M. R. R552*
 Turrin B. R501
 Turrin B. D. R604, R618
 Turrini D. W453
 Turtle E. T344, R645
 Turtle E. P. M154, T334, T336,
 T343, W453, R637
 Tutorow S. T304
 Tyler R. H. R641
 Tyler Y. D. T339, T343
 Uchida Y. T316
 Uckert K. T338
 Udry A. M102*, T328, R617
 Uemura C. U. R627
 Uesugi K. T302
 Uesugi M. T302
 Ulamec S. T342, T344
 Ulmer B. T319
 Umstätter Ph. M. J. R610
 Umurhan O. M. M103, M153, T305,
 T326, R555, R609, F705*
 Unterborn C. T312
 Urakawa S. R614
 Urbassek H. M. R610

Ure A. T321
 Urquhart M. L. T335
 Urso R. R625
 Usabal G. S. R622
 Ushikubo T. T304, W455*, R504
 Ustunisik G. K. M102
 Usui F. R555*
 Usui T. T341
 Usui T. U. R627
 Utasi Z. R645
 Utt K. L. W405*
 Vaccaro E. T340
 Vacher L. G. M104*
 Vaci Z. T303, R617
 Vaessen G. C. T348
 Vago J. L. T308, T317, R622, R643
 Väisänen T. R611
 Valdez C. S. J. T325
 Valencia S. N. M101, R551*
 Valenzuela M. T255
 Valle P. T347
 van Amerom F. H. W. W451
 Van Beek J. R644
 van Bloois S. J. T348
 Vanbommel S. J. T330, T252, T313,
 T328, T330, W402, R552,
 R624, R625, R638
 Vance G. R504
 Vance S. D. M155, T201, T310,
 T344, R645
 Vandaele A. C. M154
 van der Bogert C. H. M101, T204,
 T206, T314, T317, T319,
 R637
 Vander Kaaden K. E. T205*, T319,
 T347, R617
 Vanderliek D. M. R501*
 van der Meer F. D. T331, R502
 Vandermeulen M. T347
 van der Sanden G. A. R611
 VanderVelde D. W451
 van Driel M. M152, T204, T308,
 T309, T310T309
 van Gasselt S. R638
 Van Gorp B. T343
 van Haaster F. R618
 Vanhaecke F. R606
 Vaniman D. T. T252, T330, W402,
 R552
 Van Malderen S. J. M. R606
 van Mulligen R. R618
 Van Orman J. A. M104
 van Ruitenbeek F. J. A. T331, R502
 van Soest M. C. T314, R619
 van Verre W. R644
 Van Volkenburg T. T345
 Van wal S. T203
 van Westrenen W. T251, T314,
 T319, R553, R602, R606,
 R618
 Vanyó J. R612
 Varatharajan I. T302, T319, T331,
 T337, R637

- Varghese P. W454
 Varghese P. L. T324
 Varghese P. V. T325
 Vasavada A. T252, T330, T333
 Vasconcelos M. A. R. T320
 Vatsal V. T338, T347
 Vaz D. A. T256
 Veach T. J. T339, T343
 Veeder G. J. R641
 Veillet C. T314
 Velbel M. A. T303, T304, R633, R644
 Venditti F. C. F. R612
 Veneranda M. R634, R643
 Venkatadri T. K. M101*
 Vento D. M. R601
 Ventura K. T321
 Vepachedu V. T312
 Verbiscer A. M103, M153, T305, T335, R607, F705
 Verchovsky A. B. T303, R606
 Verdier N. M152, T308
 Verdier-Paoletti M. J. R607
 Verhagen C. T320
 Verheij R. S. T342
 Verlander T. M105
 Vermeesch P. T334
 Vermesse H. W406
 Vernazza P. R613
 Verosub K. L. T303
 Vertesi J. R645
 Veryovkin I. V. R608
 Veto M. T346
 Videen G. R611
 Vides C. R612
 Vijayan S. T302
 Vilas F. T253, T302, R613
 Villa-Rodriguez F. T335
 Villarreal M. N. R615
 Vincent J-B. T253, T302, R555
 Vincent M. A. T305
 Vinogradoff V. W454
 Viola D. T332, T345
 Violet M. T336
 Virkki A. K. T318, R555, R612
 Virmontois C. T345
 Visaya B. T347
 Visser R. R606, R644
 Vithanage M. V. R632
 Vittori R. T308
 Viudez-Moreira D. T 308, T309, M152
 Viviano C. W452, R622, R642
 Viviano C. E. M102, T331, R556*, R622
 Vizi P. G. T335
 Vocado L. T323
 Voelker M. R627
 Vogel N. R608
 Vogt D. S. T346, R625
 Voight J. R632
 Voigt J. R. C. R631
 Vollmer C. R609
 Volp J. T314
- Vona M. A. R640
 Vondrak R. R. W403
 Vorburger A. T319
 Vostrukhin A. T330
 Voytek M. R642
 Vrettos C. T309
 Vrubleviskis J. T340
 Vu T. H. M105
 VU Amsterdam Igluna Team T348
 VUSE Igluna Team T311
 Vye-Brown C. R630
 Wada K. T253, T302
 Wada T. T253
 Wade B. D. R633
 Wadhwa M. T328, T341, W455, R553, R616, F705
 Wagner N. L. T306
 Wagner R. T253
 Wagner R. J. W401, R621
 Wagner R. V. T338, T347, R603, R637, F701
 Wagstaff K. L. T330, T343
 Wahlund J.-E. T342
 Waite J. H. T201
 Waite J. H. Jr. W453*
 Wajer P. R623
 Wakabayashi N. T335
 Wakita S. R503*
 Walker C. C. T254, T344
 Walker J. D. R555*, R639
 Walker R. R633
 Walker R. J. R553*, R618, F704
 Wall S. T326
 Wallace J. K. R642
 Wallace P. R606
 Wallace S. L. T301
 Wallace S. M. R613
 Walroth R. T337, T339, T341
 Walroth R. C. T345
 Walsh K. J. T203*, T301, T338, T342, W401, R611, R645
 Walsworth R. L. R609
 Walter I. T319, T337
 Walter S. H. G. R640
 Walter T. R. M101
 Walton E. T255, T328
 Wang A. T339, T344, R605, R634
 Wang A. T256*, R626
 Wang C.-Y. T310
 Wang G. W. T311
 Wang H. M104
 Wang J. T206, T334, R607, R638
 Wang J. T. M101*, T316
 Wang K. T256, T303, W455, R605, R626
 Wang L. T205, R601
 Wang Q. R633
 Wang S. R626
 Wang S. J. R620
 Wang T. T342
 Wang W. G. T344
 Wang X. T317, R626
 Wang Y. T317, R639
- Wang Z. C. R611
 Wani S. C. T347
 Wanske A. T348
 Ward L. M. M155
 Warner B. D. R612
 Warner N. M152, T309
 Warner N. Z. T342
 Warren A. O. M154*
 Warren P. R616
 Warren T. M152, T308, T339
 Warriner H. E. T346
 Wasser M. T335, R632
 Wasserman L. H. M103
 Wasson J. T. R618
 Watanabe J. T335
 Watanabe S. T203, T253*, T301, T302, W401
 Waters-Tormey C. R616
 Watkins R. M. R604
 Watkins R. N. M101, T314, T317
 Watters T. R602
 Watters T. R. T204, T314, T332
 Watts L. A. R501
 Way M. J. T312, R601, F701
 Weaver E. F705
 Weaver H. A. M103*, M153, T305, T306, T335, W453, R607, R641, F705
 Webb A. A. G. R601
 Webb E. R617
 Weber I. T319
 Weber R. M152, T308, T338, T346
 Weber R. C. T310, W403*, R602
 Webster C. R. T313, T341
 Weert A. M. P. T342, R632
 Wegel D. C. T336
 Wegmann K. W. T327, R627
 Wehbe R. T343
 Weider S. Z. T319
 Weikusat C. T321
 Weinberg J. D. T342
 Weiner R. H. T341
 Weirich J. T203, T301, T317, R639
 Weisberg M. K. T303, W455*, R604, R610
 Weiss B. P. T338, T339, R553, R609, R617, R621
 Weissman G. W452
 Weitz C. M152, T309, W402*
 Weld K. R. R641
 Weller B. T303
 Weller L. A. R641
 Weller M. B. T204*
 Wellington D. W402, R505, R552, R644
 Wellington D. F. R552, R624, R625, R634, R644
 Welten K. C. R501, R608
 Wentworth S. J. T252
 Weppelman G. T347
 Werner S. R643
 Werner S. C. T316, W404, R621, R634

Werynski A. R645
 Wessen A. S. R645
 West J. R635
 West R. A. T313
 West S. T. T344, R628
 Westall F. T255, R643
 Westaway R. T321
 Westlake J. T338, T344
 Westphal A. J. T303, T342, R504,
 R607, R608, R614
 Westphal L. K. T. R608
 WG on Cartographic Coord. and
 Rotational Elements I. A.
 U. R638
 Whelley N. T335, R632
 Whelley P. R632
 Whelley P. L. T347, R554*
 Whipple K. X. T332
 Whitaker M. L. R620, F703
 Whitaker T. J. R606
 White A. A. R634
 White L. R501, R604
 White L. F. M101*, T328
 White M. R602
 White O. L. M103, T305, T306,
 R554, F705
 White V. T335, T343
 Whitehouse M. M101, R501, R604
 Whitehouse M. J. T251, R551, F703
 Whitley R. J. T347
 Whitten J. L. T327, T338, W404*,
 R601, F701
 Whittington A. G. R631
 Whitworth A. J. T303
 Whizin A. D. R606
 Whyte L. R643
 Wickramasinghe R. C. R608
 Widemann T. T337
 Widmer J. M. R628
 Widmer-Schnidrig R. M152, T308
 Wieczorek M. M152, T308, T316,
 T338, T339, R555
 Wieczorek M. A. M152, T204, T205,
 T307
 Wieler R. R608, R618
 Wielicki M. D. T320, R620
 Wiemer R. T308
 Wiens E. R633
 Wiens R. C. T252, T313, T328, T330,
 T333, T341, T345, T346,
 W402, W452, R552, R608,
 R624, R625, R627, R633,
 R634, R644
 Wiesehöfer T. T201
 Wilbur Z. E. R617
 Wilburn G. R503
 Wilcoski A. X. F702*
 Wilhelm B. R552
 Wilhelm B. J. T313, T330, R624,
 R625
 Wilhelm M. B. R643
 Williams D. A. R615
 Wilkinson M. J. R645

Williams A. T252, W402, R643
 Williams D. A. T327, T342, W454,
 R554, R614, R619, R631,
 R637, R638, R641
 Williams D. R. R602
 Williams J. T252
 Williams J. J. T324
 Williams J. M. T313
 Williams J.-P. M151*, T202, T313,
 T317, R611
 Williams N. M152, T309, R640
 Williams N. R. T256, T309
 Williams R. R643
 Williams R. M. R643
 Williams R. M. E. T330, W452, R627
 Williamson P. R. T339
 Williams J.-P. T316
 Williard P. T325
 Willis K. T335
 Willis P. A. R643
 Wilner D. J. F705
 Wilner J. T338
 Wilson B. J. T328
 Wilson C. M154, T336
 Wilson C. F. W453
 Wilson D. T343
 Wilson E. T337
 Wilson E. H. T313
 Wilson J. R644
 Wilson J. K. T317, T318
 Wilson J. T. M151*
 Wilson L. T313, T317, T338, R554*,
 R602, R630, R631
 Wilson S. M152, T309
 Wilson S. A. T309, R627
 Wimmer K. R617
 Wimmer-Schweingruber R. F. T315
 Wimpenny J. B. N. R501
 Wing B. R. T335
 Wingate M. T. D. F703
 Winhold A. T316
 Winkler B. R606
 Winter A. B. R640
 Wippermann T. M152, T309
 Wirick S. R607
 Wisniewski L. M152
 Witasse O. R505
 Witek P. R623
 Wittmann A. T255
 Wizenberg T. T313
 Wogelius R. T319
 Wöhler C. T331, W405, R623, R631
 Wohlfarth K. T331, W405*, R623
 Wojcicka N. M152, T308
 Wójcicka N. T308
 Wolf E. T. F701
 Wolff M. J. T331
 Wong C. F. T318
 Wong G. M. R624
 Wong T. T201*
 Woo J. M. Y. R621
 Wood C. A. T314, T326
 Wood I. G. T323

Wood K. M. R633
 Wooden D. R612
 Woods M. R640
 Wookey J. M152, T308, T309
 Woolum D. S. R608
 Wordsworth R. D. T313, T332
 Worsham E. A. R617
 Wozniakiewicz P. J. R644
 Wray J. T334, R623
 Wray J. J. T331, W402, R622, R629
 Wren P. F. R612
 Wright E. R555, R614, R638
 Wright I. P. T347
 Wright J. T205*, R637
 Wroblewski F. W. R601
 Wu B. R623, R639
 Wu N. R617
 Wu Q. T340
 Wu T.-D. W406
 Wu Y. Z. R611
 Wu Z. R626
 Wuennemann K. T255, R505
 Wulf G. T255, T320
 Wünnemann K. T206, T314, T320,
 R620
 Wurz P. T344
 Wylie M. T346
 Wyrick D. Y. T327, W454, R615
 Xiang C. R610
 Xiao H. T319
 Xiao L. T204, T206*, T334, R605,
 R633
 Xiao Z. T317, T334
 Xiao Z. Y. T206
 Xie M. R501
 Xie Z. T321, R620
 Ximenes S. R606
 Xin Y. Q. R626
 Xin-Chen L. T321
 Xing Z. X. R614
 Xiong Y. Y. T339, R604
 Xu H. T308
 Xu K. J. Jr. T314
 Xu L. T303, T338
 Xu T. Y. R611
 Xu Y. T334, R633
 Xu Z. T315
 Xue Z. Q. R605
 Yabuta H. T253, T302, T328, T344,
 T347, F703
 Yada T. T302, T347
 Yair Y. T347
 Yakovlev G. A. R620
 Yamada K. T336
 Yamada M. T253, T301, T302, T342,
 W401
 Yamada R. T253, T302, T316, T336,
 R602
 Yamagishi A. T347, R643
 Yamaguchi A. T253, T302, T304,
 T328, R604, R616, R618
 Yamaguchi T. T253, T302
 Yamaguchi Y. T302

- Yamakawi T. T336
 Yamamoto Y. T302
 Yamamoto K. T253, T302, T347
 Yamamoto M. T338, R639
 Yamamoto S. T347
 Yamamoto Y. T253, T302, R602
 Yamasaki T. R639
 Yamashita K. R503
 Yamashita N. T346, W454, R615, R639
 Yamashita S. T253
 Yamazaki A. T341
 Yamguchi A. F704
 Yan Y. C. T256, R626
 Yanagisawa M. T316
 Yang J. T205
 Yang L. R610
 Yang S. M102*
 Yang Y. R611
 Yano H. T253, T302, T344, T347, R619
 Yant M. R632
 Yant M. H. T342
 Yao P. W. T315
 Yasanayake C. N. T317, R501
 Yasutake M. T304, F704*
 Yawar Z. T330, T334
 Yazdani A. M155*
 Ye C. T331, R632, R634
 Yelle R. T313
 Yen A. T337, T341, R552
 Yen A. S. T252*, T313, T328, T330, W402, R552, R624
 Yen C. J.-K. W402*
 Yi E. R635
 Yim H.-S. R614
 Yin A. T325, T327
 Yin F. R620
 Yin J. J. T344
 Yin Q.-Z. T303, R609, R617, F704
 Yingst A. T328, T334
 Yingst R. A. T336, R625, R637
 Yogata K. T302
 Yokley Z. W. T342
 Yokochi R. W455
 Yokoi N. R501
 Yokota S. T317, T344
 Yokota Y. T253*, T301, T302, W401, R631
 Yokoyama T. M104, R616, F705*
 Yonetoku D. T344
 Yoon J.-N. R614
 Yoshida F. T253, T302, T316, T342, T344, R614
 Yoshikawa K. T253
 Yoshikawa M. T253, T302, T335, T344, W401
 Yoshinaga Y. T341
 Yoshioka K. T253, T301, T302, W401
- Yoshitake M. T302
 Young D. A. R623, R628
 Young E. D. T312, R553*, F704
 Young J. F703
 Young J. M. W406*, R632
 Young K. R635
 Young K. E. T347, R632, R645
 Young L. A. M103, M153, T305, T306, W453, R641
 Young P. R504
 Ytsma C. R625
 Yu A. T339, T346
 Yu J. T315
 Yu L. L. R555
 Yu S. T204*
 Yu X. M105*, T334
 Yu Y. T307
 Yuan B. T315
 Yuan Y. T321
 Yue Z. T315
 Yung Y. M154
 Yurimoto H. T302, T344, R608, F701
 Zacny K. T318, T323, T336, T337, T338, T339, T341, T343, T346
 Zacny K. A. T336
 Zagai M. T347
 Zahnle K. J. T312
 Zaidi S. G. T322
 Zajacz Z. R617
 Zaklynsky A. T335
 Zalewska N. E. R642
 Zalewski N. W404
 Zaman M. R626
 Zambrano-Marin L. F. R612
 Zamora C. A. T324
 Zanda B. M102, T328, R618
 Zanetti M. T347, R628
 Zangari A. M. M103*, M153, T305
 Zarate E. T343
 Zareh S. K. G. R642
 Zashirinsky A. R643
 Zasova L. T337
 Zastrow A. M. R502*
 Zega T. J. T304, T336, W405, R504*, R606, R607, R610, R611, R613
 Zeigler R. T335, T339, T340, R638, R639
 Zeigler R. A. T340, R501*, R605, R617, R639, R645
 Zeilhofer M. F. R621
 Zeitlin C. T330
 Zelkó Z. R644
 Zellner N. E. R605
 Zellner N. E. B. T316, R645
 Zemcov M. T344
 Zeng H. Z. T303
 Zeng X. T315
 Zent A. P. R628
- Zhai G. T310
 Zhang Chi. R606
 Zhang F. R631, R633
 Zhang G. L. T339, R604
 Zhang H. T344, R611
 Zhang J. T206, T303, T315, R602
 Zhang J. S. T308, T310
 Zhang Mingming. R606
 Zhang N. T251
 Zhang S. T315, F705
 Zhang X. T339, T342, R502, R636, R604
 Zhang Y. R605, R632, F701*
 Zhang Z. T318
 Zhao C. T303
 Zhao J. T206, T334
 Zhao M. T315
 Zhao X. R501, R551
 Zhao Y. R602
 Zhao Y.-Y. S. R626
 Zhao Z. T338
 Zharkova A. Yu. T205
 Zheng Y.-C. T316, T317
 Zhong F. R631
 Zhou D. R626
 Zhou F. T330, R638
 Zhou J. T345
 Zhou Q. T339, R604
 Zhou W.-Y. T308
 Zhu C. W405
 Zhu K. T327, R618, F705*
 Zhu X. Y. T339, R604
 Zhu Z. F705
 Ziegelman E. A. R645
 Ziegler K. M104, T303, R617, F704
 Ziethe R. R623
 Zimbelman J. R. T334
 Zimmerer M. J. R645
 Zimmerman W. K. T323
 Zimmermann C. R623
 Zimmermann L. R501
 Zipfel J. T303
 Zirnstein E. T305
 Ziurys L. M. R504
 Zolensky M. E. M104, T253, T302, T304, T342, W406, W451*, R617, F704
 Zolotov M. Yu. W454*
 Zorzano M.-P. T330
 Zou X.-D. T203, T301
 Zou Y. T303, T315, T338
 Zube N. G. R618
 Zuber M. T. T342, W403*, R603
 Zuccarello L. R632
 Zuckerman B. T312
 Zuluaga J. T312
 Zuo S. T321, R620
 Zweifel P. M152, T308

Codes correspond to session codes used in the program where the first letter indicates the day (M for Monday, T for Tuesday, etc.). The three-digit number indicates the session code and DOES NOT reference a poster location.